



World Journal of Gastroenterology®



Supported by NSFC
2005-2006

Volume 11 Number 19
May 21, 2005



National Journal Award
2005

Contents

REVIEW

- 2851 Roles of histamine and its receptors in allergic and inflammatory bowel diseases
Xie H, He SH

VIRAL HEPATITIS

- 2858 Enhancement of humoral immune responses to HBsAg by heat shock protein gp96 and its N-terminal fragment in mice
Li HT, Yan JB, Li J, Zhou MH, Zhu XD, Zhang YX, Tien P
- 2864 Hydrophobicity of reactive site loop of SCCA1 affects its binding to hepatitis B virus
Chen M, Cheng T, Xu CY, Wu T, Ou SH, Zhang T, Zhang J, Xia NS
- 2869 Presence and integration of HBV DNA in mouse oocytes
Huang TH, Zhang QJ, Xie QD, Zeng LP, Zeng XF
- 2874 Multigene tracking of quasispecies in viral persistence and clearance of hepatitis C virus
Chen S, Wang YM
- 2885 Generation of the regulatory protein rtTA transgenic mice
Xu K, Deng XY, Yue Y, Guo ZM, Huang B, Hong X, Xiao D, Chen XG
- 2892 Multicenter clinical study on Fuzhenghuayu capsule against liver fibrosis due to chronic hepatitis B
Liu P, Hu YY, Liu C, Xu LM, Liu CH, Sun KW, Hu DC, Yin YK, Zhou XQ, Wan MB, Cai X, Zhang ZQ, Ye J, Zhou RX, He J, Tang BZ

BASIC RESEARCH

- 2900 Six-year follow-up of pancreatic β cell function in adults with latent autoimmune diabetes
Yang L, Zhou ZG, Huang G, Ouyang LL, Li X, Yan X
- 2906 Nestin-positive progenitor cells isolated from human fetal pancreas have phenotypic markers identical to mesenchymal stem cells
Zhang L, Hong TP, Hu J, Liu YN, Wu YH, Li LS
- 2912 Effect of vector-expressed shRNAs on hTERT expression
Guo Y, Liu J, Li YH, Song TB, Wu J, Zheng CX, Xue CF
- 2916 Effects of extracellular iron concentration on calcium absorption and relationship between Ca^{2+} and cell apoptosis in Caco-2 cells
Wang L, Li Q, Duan XL, Chang YZ
- 2922 Tetrandrine inhibits activation of rat hepatic stellate cells *in vitro* via transforming growth factor- β signaling
Chen YW, Wu JX, Chen YW, Li DG, Lu HM
- 2927 Cytotoxic effect of a non-peptidic small molecular inhibitor of the p53-HDM2 interaction on tumor cells
Li WD, Wang MJ, Ding F, Yin DL, Liu ZH
- 2932 Expressed genes in regenerating rat liver after partial hepatectomy
Xu CS, Chang CF, Yuan JY, Li WQ, Han HP, Yang KJ, Zhao LF, Li YC, Zhang HY, Rahman S, Zhang JB

Contents

BASIC RESEARCH	2941	Effects of emodin and double blood supplies on liver regeneration of reduced size graft liver in rat model <i>Meng KW, Lv Y, Yu L, Wu SL, Pan CE</i>
CLINICAL RESEARCH	2945	Diagnosis of biliary strictures after liver transplantation: Which is the best tool? <i>Zoepef T, Maldonado-Lopez EJ, Hilgard P, Dechêne A, Malago M, Broelsch CE, Schlaak J, Gerken G</i>
BRIEF REPORTS	2949	Expression of bcl-2 protein in chronic hepatitis C: Effect of interferon alpha 2b with ribavirin therapy <i>Anatol P, Danuta P, Janusz D, Bozena P</i>
	2953	Computed tomography findings in fatal cases of enormous hepatic portal venous gas <i>Chan SC, Wan YL, Cheung YC, Ng SH, Wong AMC, Ng KK</i>
	2956	Relationship between proliferative activity of cancer cells and clinicopathological factors in patients with esophageal squamous cell carcinoma <i>Huang JX, Yan W, Song ZX, Qian RY, Chen P, Salminen E, Toppari J</i>
	2960	Phage displaying peptides mimic schistosoma antigenic epitopes selected by rat natural antibodies and protective immunity induced by their immunization in mice <i>Wang M, Yi XY, Li XP, Zhou DM, Larry M, Zeng XF</i>
	2967	Chinese medicine compound Changtong oral liquid on postoperative intestinal adhesions <i>Yang XX, Shi HP, Hou LB</i>
	2971	Clinical features of probable severe acute respiratory syndrome in Beijing <i>Lu HY, Xu XY, Lei Y, Wu YF, Chen BW, Xiao F, Xie GQ, Han DM</i>
	2975	Syndecan-1 and E-cadherin expression in differentiated type of early gastric cancer <i>Huang MF, Zhu YQ, Chen ZF, Xiao J, Huang X, Xiong YY, Yang GF</i>
	2981	Combined human growth hormone and lactulose for prevention and treatment of multiple organ dysfunction in patients with severe chronic hepatitis B <i>Ding HG, Shan J, Zhang B, Ma HB, Zhou L, Jin R, Tan YF, He LX</i>
	2984	Protective effect of <i>fufanghuangqiduogan</i> against acute liver injury in mice <i>Gui SY, Wei W, Wang H, Wu L, Sun WY, Wu CY</i>
	2990	Docetaxel shows radiosensitization in human hepatocellular carcinoma cells <i>Geng CX, Zeng ZC, Wang JY, Xuan SY, Lin CM</i>
	2994	Protective effect of L-arginine preconditioning on ischemia and reperfusion injury associated with rat small bowel transplantation <i>Cao B, Li N, Wang Y, Li JS</i>
	2998	Mutations of p53 gene exons 4-8 in human esophageal cancer <i>Li LY, Tang JT, Jia LQ, Li PW</i>
	3002	Recurrent acute pancreatitis and its relative factors <i>Zhang W, Shan HC, Gu Y</i>
	3005	Mild hypothermia protects liver against ischemia and reperfusion injury <i>Wang CY, Ni Y, Liu Y, Huang ZH, Zhang MJ, Zhan YQ, Gao HB</i>
CASE REPORT	3008	The right hepatic artery syndrome <i>Miyashita K, Shiraki K, Ito T, Taoka H, Nakano T</i>

<div> <div>World Journal of Gastroenterology®</div> <div>Volume 11 Number 19 May 21, 2005</div> </div>	
Contents	
ACKNOWLEDGMENTS	3010 Acknowledgments to reviewers for this issue
APPENDIX	<div>1A Meetings</div> <div>2A Instructions to authors</div> <div>4A <i>World Journal of Gastroenterology</i> standard of quantities and units</div>
FLYLEAF	I-V Editorial Board
INSIDE FRONT COVER	ISI journal citation reports 2003-GASTROENTEROLOGY AND HEPATOLOGY
INSIDE BACK COVER	15 th World Congress of the International Association of Surgeons and Gastroenterologists
Editorial Coordinator for this issue: Anitha Kumaran	
<p><i>World Journal of Gastroenterology</i> (<i>World J Gastroenterol</i> , <i>WJG</i>), a leading international journal in gastroenterology and hepatology, has an established reputation for publishing first class research on esophageal cancer, gastric cancer, liver cancer, viral hepatitis, colorectal cancer, and <i>Helicobacter pylori</i> infection, providing a forum for both clinicians and scientists, and has been indexed and abstracted in Index Medicus, MEDLINE, PubMed, Chemical Abstracts, EMBASE, Abstracts Journals, Nature Clinical Practice Gastroenterology and Hepatology, CAB Abstracts and Global Health. Impact factor of ISI JCR during 2000-2003 is 0.993, 1.445, 2.532 and 3.318 respectively. <i>WJG</i> is a weekly journal published jointly by The <i>WJG</i> Press and Elsevier Inc. The publication date is on 7th, 14th, 21st, and 28th every month. The <i>WJG</i> is supported by The National Natural Science Foundation of China, No. 30224801 and No.30424812, which was founded with a name of <i>China National Journal of New Gastroenterology</i> on October 1,1995, and renamed as <i>WJG</i> on January 25, 1998.</p>	
HONORARY EDITORS-IN-CHIEF Ke-Ji Chen, <i>Beijing</i> Dai -Ming Fan, <i>Xi'an</i> Zhi-Qiang Huang, <i>Beijing</i> Nicholas F LaRusso, <i>Rochester</i> Jie-Shou Li, <i>Nanjing</i> Geng-Tao Liu, <i>Beijing</i> Fa-Zu Qiu, <i>Wuhan</i> Eamonn M Quigley, <i>Cork</i> David S Rampton, <i>London</i> Rudi Schmid, <i>California</i> Nicholas Joseph Talley, <i>Rochester</i> Zhao-You Tang, <i>Shanghai</i> Guido NJ Tytgat, <i>Amsterdam</i> Meng-Chao Wu, <i>Shanghai</i> Xian-Zhong Wu, <i>Tianjin</i> Hui Zhuang, <i>Beijing</i> Jia-Yu Xu, <i>Shanghai</i>	EDITORIAL BOARD See full details flyleaf I-V DEPUTY EDITOR Michelle Gabbe, Xian-Lin Wang ASSOCIATE MANAGING EDITORS Jian-Zhong Zhang, Shi-Yu Guo EDITORIAL OFFICE MANAGER Jing-Yun Ma EDITORIAL ASSISTANT Juan Li TECHNICAL EDITORS Meng Li, Shao-Hua Li, Xi Li, Hu Wang PROOFREADERS Hong Li, Wen-Jian Mei, Shi-Yu Guo PUBLISHED JOINTLY BY The WJG Press and Elsevier Inc PRINTING GROUP Printed in Beijing on acid-free paper by Beijing Xexin Printing House COPYRIGHT © 2005 Published jointly by The WJG Press and Elsevier Inc. All rights reserved; no part of this publication may be reproduced, stored in a retrieval system, or transmitted in any form or by any means, electronic, mechanical, photocopying, recording, or otherwise without the prior permission of
PRESIDENT AND EDITOR-IN-CHIEF Lian-Sheng Ma, <i>Beijing</i> EDITOR-IN-CHIEF Bo- Rong Pan, <i>Xi'an</i> ASSOCIATE EDITORS-IN-CHIEF Bruno Annibale, <i>Roma</i> Henri Bismuth, <i>Villesauv</i> Jordi Bruix, <i>Barcelona</i> Roger William Chapman, <i>Oxford</i> Alexander L Gerbes, <i>Munich</i> Shou-Dong Lee, <i>Taipei</i> Walter Edwin Longo, <i>New Haven</i> You-Yong Lu, <i>Beijing</i> Masao Omata, <i>Tokyo</i> Harry H-X Xia, <i>Hong Kong</i>	The <i>WJG</i> Press and Elsevier Inc. Author are required to grant <i>WJG</i> an exclusive licence to publish. Print ISSN 1007-9327 CN 14-1219/R. SPECIAL STATEMENT All articles published in this journal represent the viewpoints of the authors except where indicated otherwise. EDITORIAL OFFICE Editor: <i>World Journal of Gastroenterology</i> , The WJG Press, Apartment 1066 Yishou Garden, 58 North Langxinzhuang Road, PO Box 2345, Beijing 100023, China Telephone: +86-(0)10-85381901-1023 Fax: +86-10-85381893 E-mail: wjg@wjgnet.com http://www.wjgnet.com Public Relationship Manager Shi-Yu Guo The WJG Press, Apartment 1066 Yishou Garden, 58 North Langxinzhuang Road, PO Box 2345, Beijing 100023, China Telephone: +86-(0)10-85381901-1023 Fax: +86-10-85381893 E-mail: s.y.guo@wjgnet.com http://www.wjgnet.com SUBSCRIPTION INFORMATION Foreign Elsevier (Singapore) Pte Ltd, 3 Killiney Road #08-01, Winsland House I, Singapore 239519 Telephone: +65-6349 0200 Fax: +65-6733 1817
	E-mail: r.garcia@elsevier.com http://asia.elsevierhealth.com Institutional Rates Print-2005 rates: USD1 500.00 Personal Rates Print-2005 rates: USD700.00 Domestic Local Post Offices Code No. BM 82-261 Author Reprints The WJG Press, Apartment 1066 Yishou Garden, 58 North Langxinzhuang Road, PO Box 2345, Beijing 100023, China Telephone: +86-(0)10-85381901-1023 Fax: +86-10-85381893 E-mail: wjg@wjgnet.com http://www.wjgnet.com ADVERTISING Rosalia Da Carcia Elsevier Science Journals Marketing & Society Relations Health Science Asia 3 Killiney Road #08-01, Winsland House 1 Singapore 239519 Telephone: +65-6349 0200 Fax: +65-6733 1817 E-mail: r.garcia@elsevier.com http://asia.elsevierhealth.com INSTRUCTIONS TO AUTHORS Full instructions are available online at http://www.wjgnet.com/wjg/help/ instructions.jsp If you do not have web access please contact the editorial office.

World Journal of Gastroenterology®

Editorial Board

2004-2006



Published by The WJG Press and Elsevier Inc., PO Box 2345, Beijing 100023, China
Fax: +86-(0)10-85381893 E-mail: wjg@wjgnet.com <http://www.wjgnet.com>

HONORARY EDITORS-IN-CHIEF

Ke-Ji Chen, *Beijing*
Dai-Ming Fan, *Xi'an*
Zhi-Qiang Huang, *Beijing*
Nicholas F LaRusso, *Rochester*
Jie-Shou Li, *Nanjing*
Geng-Tao Liu, *Beijing*
Fa-Zu Qiu, *Wuhan*
Eamonn M Quigley, *Cork*
David S Rampton, *London*
Rudi Schmid, *California*
Nicholas Joseph Talley, *Rochester*
Zhao-You Tang, *Shanghai*
Guido NJ Tytgat, *Amsterdam*
Meng-Chao Wu, *Shanghai*
Xian-Zhong Wu, *Tianjin*
Hui Zhuang, *Beijing*
Jia-Yu Xu, *Shanghai*

PRESIDENT AND EDITOR-IN-CHIEF

Lian-Sheng Ma, *Beijing*

EDITOR-IN-CHIEF

Bo-Rong Pan, *Xi'an*

ASSOCIATE EDITORS-IN-CHIEF

Bruno Annibale, *Roma*
Henri Bismuth, *Villesuif*
Jordi Bruix, *Barcelona*

Roger William Chapman, *Oxford*
Alexander L Gerbes, *Munich*
Shou-Dong Lee, *Taipei*
Walter Edwin Longo, *New Haven*
You-Yong Lu, *Beijing*
Masao Omata, *Tokyo*
Harry H-X Xia, *Hong Kong*

MEMBERS OF THE EDITORIAL BOARD



Albania
Bashkim Resuli, *Tirana*



Algeria
Hocine Asselah, *Algiers*



Argentina
Julio Horacio Carri, *Córdoba*



Australia
Darrell HG Crawford, *Brisbane*
Robert JL Fraser, *Daw Park*
Yik-Hong Ho, *Townsville*
Gerald J Holtmann, *Adelaide*
Michael Horowitz, *Adelaide*

www.wjgnet.com

Riordan SM, *Sydney*
IC Roberts-Thomson, *Adelaide*
James Toouli, *Adelaide*



Austria
Dragosics BA, *Vienna*
Peter Ferenci, *Vienna*
Alfred Gangl, *Vienna*
Michael Trauner, *Graz*
Harald Vogelsang, *Vienna*



Belarus
Yury K Marakhouski, *Minsk*



Belgium
Geerts AEC, *Brussels*
Cremer MC, *Brussels*
Yves J Horsmans, *Brussels*
Yvan Vandenplas, *Brussels*
Eddie Wisse, *Keerbergen*



Brazil
Heitor Rosa, *Goiania*

**Bulgaria**Zahariy Alexandrov Krastev, *Sofia***Canada**Wang-Xue Chen, *Ottawa*
Richard N Fedorak, *Edmonton*
Hugh James Freeman, *Vancouver*
Samuel S Lee, *Calgary*
Philip Martin Sherman, *Toronto*
Alan BR Thomson, *Edmonton*
Eric M Yoshida, *Vancouver***Egypt**Abdel-Rahman El-Zayadi, *Giza***Finland**Pentti Sipponen, *Espoo***Greece**Arvanitakis C, *Thessaloniki*
Elias A Kouroumalis, *Heraklion***China**Francis KL Chan, *Hong Kong*
Xiao-Ping Chen, *Wuhan*
Jun Cheng, *Beijing*
Chi-Hin Cho, *Hong Kong*
Zong-Jie Cui, *Beijing*
Da-Jun Deng, *Beijing*
Er-Dan Dong, *Beijing*
Sheung-Tat Fan, *Hong Kong*
Xue-Gong Fan, *Changsha*
Jin Gu, *Beijing*
De-Wu Han, *Taiyuan*
Shao-Heng He, *Shantou*
Fu-Lian Hu, *Beijing*
Wayne HC Hu, *Hong Kong*
Ching Lung Lai, *Hong Kong*
Kam Chuen Lai, *Hong Kong*
Wai-Keung Leung, *Hong Kong*
Zhi-Hua Liu, *Beijing*
Ai- Ping Lu, *Beijing*
Jing-Yun Ma, *Beijing*
Lun-Xiu Qin, *Shanghai*
Yu-Gang Song, *Guangzhou*
Peng Shang, *Xi'an*
Qin Su, *Beijing*
Yuan Wang, *Shanghai*
Benjamin Wong, *Hong Kong*
Wai-Man Wong, *Hong Kong*
Hong Xiao, *Shanghai*
Dong-Liang Yang, *Wuhan*
Xue-Biao Yao, *Hefei*
Yuan Yuan, *Shenyang*
Man-Fung Yuen, *Hong Kong*
Jian-Zhong Zhang, *Beijing*
Zhi-Rong Zhang, *Chengdu*
Xiao-Hang Zhao, *Beijing*
Shu Zheng, *Hangzhou***France**Charles Paul Balabaud, *Bordeaux*
Jacques Belghiti, *Clichy*
Pierre Brissot, *Rennes*
Franck Carbonnel, *Besancon*
Bruno Clément, *Rennes*
Jacques Cosnes, *Paris*
Francoise Degos, *Clichy*
Francoise Lunel Fabian, *Angers*
Gérard Feldmann, *Paris*
Jean Fioramonti, *Toulouse*
Rene Lambert, *Lyon*
Didier Lebrech, *Clichy*
Francis Mégraud, *Bordeaux*
Richard Moreau, *Clichy*
Jose Sahel, *Marseille*
Jean-Yves Scoazec, *Lyon*
Jean-Pierre Henri Zarski, *Grenoble***Hungary**Simon A László, *Szekszárd*
János Papp, *Budapest***Iceland**Hallgrímur Gudjonsson, *Reykjavik***India**Sujit Kumar Bhattacharya, *Kolkata*
Chawla YK, *Chandigarh*
Radha Dhiman K, *Chandigarh*
Sri Prakash Misra, *Allahabad*
Kartar Singh, *Lucknow***Iran**Reza Malekzadeh, *Tehran***Israel**Abraham Rami Eliakim, *Haifa*
Yaron Niv, *Pardesia***Italy**Giovanni Addolorato, *Roma*
Alfredo Alberti, *Padova*
Annese V, *San Giovanni Rotondo*
Giovanni Barbara, *Bologna*
Gabrio Bassotti, *Perugia*
Franco Bazzoli, *Bologna*
Adolfo Francesco Attili, *Roma*
Antonio Benedetti, *Ancona*
Giovanni Cammarota, *Roma*
Antonino Cavallari, *Bologna*
Dario Conte, *Milano*
Gino Roberto Corazza, *Pavia*
Guido Costamagua, *Roma*
Antonio Craxi, *Palermo*
Fabio Farinati, *Padua*
Giovanni Gasbarrini, *Roma*
Paolo Gentilini, *Florence*
Eduardo G Giannini, *Genoa***Costa Rica**Edgar M Izquierdo, *San José***Croatia**Marko Duvnjak, *Zagreb***Denmark**Flemming Burcharth, *Herlev*
Peter Bytzer, *Copenhagen*
Hans Gregersen, *Aalborg***Germany**HD Allescher, *Garmisch-Partenkirchen*
Rudolf Arnold, *Marburg*
Hubert Blum, *Freiburg*
Peter Born, *Muchen*
Heinz J Buhr, *Berlin*
Haussinger Dieter, *Düsseldorf*
Dietrich CF, *Bad Mergentheim*
Wolfram W Domschke, *Muenster*
Ulrich Robert Fölsch, *Kiel*
Peter R Galle, *Mainz*
Burkhard Göke, *Munich*
Axel M Gressner, *Aachen*
Eckhart Georg Hahn, *Erlangen*
Werner Hohenberger, *Erlangen*
RG Jakobs, *Ludwigshafen*
Joachim Labenz, *Siegen*
Ansgar W Lohse, *Hamburg*
Peter Malfertheiner, *Magdeburg*
Andrea Dinah May, *Wiesbaden*
Stephan Miehke, *Dresden*
Gustav Paumgartner, *Munich*
Ulrich Ks Peitz, *Magdeburg*
Giuliano Ramadori, *Göttingen*
Tilman Sauerbruch, *Bonn*
Hans Seifert, *Oldenburg*
J Ruediger Siewert, *Munich*
Manfred V Singer, *Mannheim*

Paolo Gionchetti, *Bologna*
 Roberto De Giorgio, *Bologna*
 Mario Guslandi, *Milano*
 Giovanni Maconi, *Milan*
 Giulio Marchesini, *Bologna*
 Giuseppe Montalto, *Palermo*
 Luisi Pagliaro, *Palermo*
 Fabrizio R Parente, *Milan*
 Perri F, *San Giovanni Rotondo*
 Raffaele Pezzilli, *Bologna*
 Pilotto A, *San Giovanni Rotondo*
 Massimo Pinzani, *Firenze*
 Gabriele Bianchi Porro, *Milano*
 Piero Portincasa, *Bari*
 Giacomo Laffi, *Firenze*
 Enrico Roda, *Bologna*
 Massimo Rugge, *Padova*
 Vincenzo Savarino, *Genova*
 Vincenzo Stanghellini, *Bologna*
 Calogero Surrenti, *Florence*
 Roberto Testa, *Genoa*
 Dino Vaira, *Bologna*

Junji Kato, *Sapporo*
 Mototsugu Kato, *Sapporo*
 Shinzo Kato, *Tokyo*
 Sunao Kawano, *Osaka*
 Yoshikazu Kinoshita, *Izumo*
 Masaki Kitajima, *Tokyo*
 Tsuneo Kitamura, *Chiba*
 Seigo Kitano, *Oita*
 Hironori Koga, *Kurume*
 Satoshi Kondo, *Sapporo*
 Shoji Kubo, *Osaka*
 Shigeki Kuriyama, *Kagawa*
 Masato Kusunoki, *Mie*
 Takashi Maeda, *Fukuoka*
 Shin Maeda, *Tokyo*
 Osamu Matsui, *Kanazawa*
 Yasushi Matsuzaki, *Tsukuba*
 Hiroto Miwa, *Hyogo*
 Masashi Mizokami, *Nagoya*
 Motowo Mizuno, *Hiroshima*
 Morito Monden, *Suita*
 Hisataka S Moriwaki, *Gifu*
 Yoshiharu Motoo, *Kanazawa*
 Akihiro Munakata, *Hirosaki*
 Kazunari Murakami, *Oita*
 Kunihiko Murase, *Tusima*
 Masato Nagino, *Nagoya*
 Yuji Naito, *Kyoto*
 Hisato Nakajima, *Tokyo*
 Hiroki Nakamura, *Yamaguchi*
 Shotaro Nakamura, *Fukuoka*
 Akimasa Nakao, *Nagoya*
 Mikio Nishioka, *Niihama*
 Susumu Ohmada, *Maebashi*
 Masayuki Ohta, *Oita*
 Tetsuo Ohta, *Kanazawa*
 Susumu Okabe, *Kyoto*
 Katsuhisa Omagari, *Nagasaki*
 Saburo Onishi, *Nankoku*
 Morikazu Onji, *Ehime*
 Hiromitsu Saisho, *Chiba*
 Hidetsugu Saito, *Tokyo*
 Takafumi Saito, *Yamagata*
 Isao Sakaida, *Yamaguchi*
 Michie Sakamoto, *Tokyo*
 Iwao Sasaki, *Sendai*
 Motoko Sasaki, *Kanazawa*
 Chifumi Sato, *Tokyo*
 Shuichi Seki, *Osaka*
 Hiroshi Shimada, *Yokohama*
 Mitsuo Shimada, *Tokushima*
 Hiroaki Shimizu, *Chiba*
 Tooru Shimosegawa, *Sendai*
 Tadashi Shimoyama, *Hirosaki*
 Ken Shirabe, *Iizuka City*
 Yoshio Shirai, *Niigata*
 Katsuya Shiraki, *Mie*
 Yasushi Shiratori, *Okayama*
 Yasuhiko Sugawara, *Tokyo*
 Toshiro Sugiyama, *Toyama*
 Kazuyuki Suzuki, *Morioka*
 Hidekazu Suzuki, *Tokyo*
 Tadatoshiki Takayama, *Tokyo*
 Tadashi Takeda, *Osaka*

Koji Takeuchi, *Kyoto*
 Kiichi Tamada, *Tochigi*
 Akira Tanaka, *Kyoto*
 Eiji Tanaka, *Matsumoto*
 Noriaki Tanaka, *Okayama*
 Shinji Tanaka, *Hiroshima*
 Kyuichi Tanikawa, *Kurume*
 Tadashi Terada, *Shizuoka*
 Akira Terano, *Shimotsugagun*
 Kazunari Tominaga, *Osaka*
 Hidenori Toyoda, *Ogaki*
 Akihito Tsubota, *Chiba*
 Shingo Tsuji, *Osaka*
 Takato Ueno, *Kurume*
 Shinichi Wada, *Tochigi*
 Hiroyuki Watanabe, *Kanazawa*
 Sumio Watanabe, *Akita*
 Toshio Watanabe, *Osaka*
 Yuji Watanabe, *Ehime*
 Chun-Yang Wen, *Nagasaki*
 Koji Yamaguchi, *Fukuoka*
 Takayuki Yamamoto, *Yokkaichi*
 Takashi Yao, *Fukuoka*
 Hiroshi Yoshida, *Tokyo*
 Masashi Yoshida, *Tokyo*
 Norimasa Yoshida, *Kyoto*
 Kentaro Yoshika, *Toyooka*
 Masahide Yoshikawa, *Kashiwara*



Japan

Kyoichi Adachi, *Izumo*
 Takashi Aikou, *Kagoshima*
 Taiji Akamatsu, *Matsumoto*
 Takafumi Ando, *Nagoya*
 Akira Andoh, *Otsu*
 Taku Aoki, *Tokyo*
 Masahiro Arai, *Tokyo*
 Tetsuo Arakawa, *Osaka*
 Yasuji Arase, *Tokyo*
 Masahiro Asaka, *Sapporo*
 Hitoshi Asakura, *Tokyo*
 Yutaka Atomi, *Tokyo*
 Takeshi Azuma, *Fukui*
 Nobuyuki Enomoto, *Yamanashi*
 Kazuma Fujimoto, *Saga*
 Toshio Fujioka, *Oita*
 Yoshihide Fujiyama, *Otsu*
 Hiroyuki Hanai, *Hamamatsu*
 Kazuhiro Hanazaki, *Nagano*
 Naohiko Harada, *Fukuoka*
 Makoto Hashizume, *Fukuoka*
 Tetsuo Hayakawa, *Nagoya*
 Kazuhide Higuchi, *Osaka*
 Ichiro Hirata, *Osaka*
 Keiji Hirata, *Kitakyushu*
 Takafumi Ichida, *Shizuoka*
 Kenji Ikeda, *Tokyo*
 Kohzoh Imai, *Sapporo*
 Fumio Imazeki, *Chiba*
 Masayasu Inoue, *Osaka*
 Hiromi Ishibashi, *Nagasaki*
 Shunji Ishihara, *Izumo*
 Toru Ishikawa, *Niigata*
 Kei Ito, *Sendai*
 Masayoshi Ito, *Tokyo*
 Hiroaki Itoh, *Akita*
 Hiroshi Kaneko, *Aichi-Gun*
 Shuichi Kaneko, *Kanazawa*
 Takashi Kanematsu, *Nagasaki*



Lithuania

Sasa Markovic, *Japljeva*



Macedonia

Vladimir Cirko Serafimovski, *Skopje*



Malaysia

Andrew Seng Boon Chua, *Ipoh*
 Jayaram Menon, *Sabah*
 Khean-Lee Goh, *Kuala Lumpur*



Monaco

Patrick Rampal, *Monaco*



Netherlands

Louis MA Akkermans, *Utrecht*
 Karel Van Erpecum, *Utrecht*
 Albert K Groen, *Amsterdam*
 Dirk Joan Gouma, *Amsterdam*
 Jan BMJ Jansen, *Nijmegen*
 Evan Anthony Jones, *Abcoude*
 Ernst Johan Kuipers, *Rotterdam*
 Chris JJ Mulder, *Amsterdam*
 Michael Müller, *Wageningen*

Pena AS, *Amsterdam*
Andreas Smout, *Utrecht*
RW Stockbrugger, *Maastricht*
GP Vanberge-Henegouwen,
Utrecht



New Zealand

Ian David Wallace, *Auckland*



Norway

Trond Berg, *Oslo*
Helge Lyder Waldum, *Trondheim*



Pakistan

Muhammad S Khokhar, *Lahore*



Philippines

Eulenia Rasco Nolasco, *Manila*



Poland

Tomasz Brzozowski, *Cracow*
Andrzej Nowak, *Katowice*



Portugal

Miguel Carneiro De Moura, *Lisbon*



Russia

Vladimir T Ivashkin, *Moscow*
Leonid Lazebnik, *Moscow*
Vasily I Reshetnyak, *Moscow*



Singapore

Bow Ho, *Kent Ridge*
Francis Seow-Choen, *Singapore*



Slovakia

Anton Vavrecka, *Bratislava*



South Africa

Michael C Kew, *Parktown*



South Korea

Jin-Hong Kim, *Suwon*
Myung-Hwan Kim, *Seoul*
Yun-Soo Kim, *Seoul*
Yung-Il Min, *Seoul*

Jae-Gahb Park, *Seoul*
Dong Wan Seo, *Seoul*



Spain

Abraldes JG, *Barcelona*
Fernando Azpiroz, *Barcelona*
Ramon Bataller, *Barcelona*
Josep M Bordas, *Barcelona*
Maria Buti, *Barcelon*
Xavier Calvet, *Sabadell*
Antoni Castells, *Barcelona*
Manuel Daz-Rubio, *Madrid*
Juan C Garcia-Pagán, *Barcelona*
Genover JB, *Barcelona*
Javier P Gisbert, *Madrid*
Jaime Guardia, *Barcelona*
Angel Lanas, *Zaragoza*
Ricardo Moreno-Otero, *Madrid*
Julian Panes, *Barcelona*
Miguel Perez-Mateo, *Alicante*
Josep M Pique, *Barcelona*
Jesus Prieto, *Pamplona*
Luis Rodrigo, *Oviedo*



Sri Lanka

Janaka De Silva, *Ragama*



Swaziland

Gerd Kullak-Ublick, *Zurich*



Sweden

Lars Christer Olbe, *Molndal*
Curt Einarsson, *Huddinge*
Lars R Lundell, *Stockholm*
Xiao-Feng Sun, *Linkoping*



Switzerland

Christoph Beglinger, *Basel*
Michael W Fried, *Zurich*
Bruno Stieger, *Zurich*
Arthur Zimmermann, *Berne*



Turkey

Yusuf Bayraktar, *Ankara*
Figen Gurakan, *Ankara*
Cihan Yurdaydin, *Ankara*



United Kingdom

Axon ATR, *Leeds*
Paul Jonathan Ciclitira, *London*
Amar Paul Dhillon, *London*



United States

Firas H Ac-Kawas, *Washington*
Gianfranco D Alpini, *Temple*
Paul Angulo, *Rochester*
Jamie S Barkin, *Miami Beach*
Todd Baron, *Rochester*
Kim Elaine Barrett, *San Diego*
Jennifer D Black, *Buffalo*
Xu Cao, *Birmingham*
David L Carr-Locke, *Boston*
Marc F Catalano, *Milwaukee*
Xian-Ming Chen, *Rochester*
James M Church, *Cleveland*
Vincent Coghlan, *Beaverton*
James R Connor, *Hershey*
Pelayo Correa, *New Orleans*
John Cuppoletti, *Cincinnati*
Peter V Danenberg, *Los Angeles*
Kiron Moy Das, *New Brunswick*
Hala El-Zimaity, *Houston*
Ronnie Fass, *Tucson*
Emma E Furth, *Pennsylvania*
John Geibel, *New Haven*
Graham DY, *Houston*
Joel S Greenberger, *Pittsburgh*
Anna S Gukovskaya, *Los Angeles*
Gavin Harewood, *Rochester*
Atif Iqbal, *Omaha*
Hajime Isomoto, *Rochester*
Dennis M Jensen, *Los Angeles*
Leonard R Johnson, *Memphis*
Peter James Kahrilas, *Chicago*
Anthony Nicholas Kallou, *Baltimore*
Neil Kaplowitz, *Los Angeles*
Emmet B Keefe, *Palo Alto*
Joseph B Kirsner, *Chicago*
Burton I Korelitz, *New York*
Robert J Korst, *New York*
Richard A Kozarek, *Seattle*
Shiu-Ming Kuo, *Buffalo*
Frederick H Leibach, *Augusta*
Andreas Leodolter, *La Jolla*
Ming Li, *New Orleans*
Lenard M Lichtenberger, *Houston*
Gary R Lichtenstein, *Philadelphia*
Josep M Llovet, *New York*
Martin Lipkin, *New York*

Robin G Lorenz, *Birmingham*
 James David Luketich, *Pittsburgh*
 Henry Thomson Lynch, *Omaha*
 Paul Martiw, *New York*
 Richard W McCallum, *Kansas City*
 Timothy H Moran, *Baltimore*
 Hiroshi Nakagawa, *Philadelphia*
 Douglas B Neison, *Minneapolis*
 Juan J Nogueras, *Weston*
 Curtis T Okamoto, *Los Angeles*
 Pankaj Jay Pasricha, *Galveston*
 Zhiheng Pei, *New York*
 Pitchumoni CS, *New Brunswick*
 Satish Rao, *Iowa City*
 Adrian Reuben, *Charleston*

Victor E Reyes, *Galveston*
 Richard E Sampliner, *Tucson*
 Vijay H Shah, *Rochester*
 Stuart Sherman, *Indianapolis*
 Stuart Jon Spechler, *Dallas*
 Michael Steer, *Boston*
 Gary D Stoner, *Columbus*
 Rakesh Kumar Tandon, *New Delhi*
 Tchou-Wong KM, *New York*
 Paul Joseph Thuluvath, *Baltimore*
 Swan Nio Thung, *New York*
 Travagli RA, *Baton Rouge-La*
 Triadafilopoulos G, *Stanford*
 David Hoffman Vanthiel, *Mequon*
 Jian-Ying Wang, *Baltimore*

Kenneth Ke-Ning Wang, *Rochester*
 Judy Van De Water, *Davis*
 Steven David Wexner, *Weston*
 Russell Harold Wiesner, *Rochester*
 Keith Tucker Wilson, *Baltimore*
 George Y Wu, *Farmington*
 Jian Wu, *Sacramento*
 Chung Shu Yang, *Piscataway*
 David Yule, *Rochester*
 Michael Zenilman, *Brooklyn*



Yugoslavia

Jovanovic DM, *Sremska Kamenica*

Manuscript reviewers of *World Journal of Gastroenterology*

Yogesh K Chawla, *Chandigarh*
 Chiung-Yu Chen, *Tainan*
 Gran-Hum Chen, *Taichung*
 Li-Fang Chou, *Taipei*
 Jennifer E Hardingham, *Woodville*
 Ming-Liang He, *Hong Kong*
 Li-Sung Hsu, *Taichung*
 Guang-Cun Huang, *Shanghai*
 Shinn-Jang Hwang, *Taipei*
 Jia-Horng Kao, *Taipei*
 Aydin Karabacakoglu, *Konya*
 Sherif M Karam, *Al-Ain*
 Tadashi Kondo, *Tsukiji*
 Jong-Soo Lee, *Nam-yang-ju*
 Lein-Ray Mo, *Tainan*
 Kpozehouen P Randolph, *Shanghai*
 Bin Ren, *Boston*
 Tetsuji Sawada, *Osaka*
 Cheng-Shyong Wu, *Cha-Yi*
 Ming-Shiang Wu, *Taipei*
 Wei-Guo Zhu, *Beijing*

Roles of histamine and its receptors in allergic and inflammatory bowel diseases

Hua Xie, Shao-Heng He

Hua Xie, Shao-Heng He, Allergy and Inflammation Research Institute, Shantou University Medical College, Shantou 515031, Guangdong Province, China

Supported by the Li Ka Shing Foundation, Hong Kong, China, No. C0200001; the Planned Science and Technology Project of Guangdong Province, China, No. 2003B31502

Correspondence to: Professor Shao-Heng He, Allergy and Inflammation Research Institute, Shantou University Medical College, 22 Xin-Ling Road, Shantou 515031, Guangdong Province, China. shoahenghe@hotmail.com

Telephone: +86-754-8900405 Fax: +86-754-8900192

Received: 2004-04-30 Accepted: 2004-07-15

Abstract

Mast cell has a long history of being recognized as an important mediator-secreting cell in allergic diseases, and has been discovered to be involved in IBD in last two decades. Histamine is a major mediator in allergic diseases, and has multiple effects that are mediated by specific surface receptors on target cells. Four types of histamine receptors have now been recognized pharmacologically and the first three are located in the gut. The ability of histamine receptor antagonists to inhibit mast cell degranulation suggests that they might be developed as a group of mast cell stabilizers. Recently, a series of experiments with dispersed colon mast cells suggested that there should be at least two pathways in man for mast cells to amplify their own activation-degranulation signals in an autocrine or paracrine manner. In a word, histamine is an important mediator in allergic diseases and IBD, its antagonists may be developed as a group of mast cell stabilizers to treat these diseases.

© 2005 The WJG Press and Elsevier Inc. All rights reserved.

Key words: Allergic diseases; Immunoglobulin

Xie H, He SH. Roles of histamine and its receptors in allergic and inflammatory bowel diseases. *World J Gastroenterol* 2005; 11(19): 2851-2857

<http://www.wjgnet.com/1007-9327/11/2851.asp>

INTRODUCTION

Allergic diseases including allergic asthma, allergic rhinitis, food allergy, drug allergy, and allergic atopic eczema/dermatitis syndrome, *etc.* are a group of common disorders which are regarded to be mediated by immunoglobulin (Ig) E. People at all ages in countries throughout the world suffer from

these diseases. The prevalence of allergy has shown an increase in the last few years. At present it affects about 30-40% of world population and has become one of the three key diseases in the 21st century.

Since last two decades, inflammation has been known as the main pathophysiological characteristics of allergy. Mast cells are major participants of allergic reactions, and their activation may be all that is sufficient and necessary for the rapid development of microvascular leakage and tissue edema in sensitized subjects exposed to allergen. Mast cell is a key source of potent mediators of allergic inflammation including histamine, neutral proteinases, proteoglycans, prostaglandin D₂, leukotriene C₄ and certain cytokines^[1]. Among them, histamine is the first mediator implicated in the pathophysiological changes of asthma when it was found to mimic several features of the disease, and James received the Nobel Prize for medicine in 1988 for his outstanding achievements in histamine research. Recently, some novel findings concerning histamine, mast cell and allergy or IBD have been reported and are summarized herein.

THE ROLES OF MAST CELLS IN ALLERGIC DISEASES

Mast cell has a long history of being recognized as an important mediator-secreting cell in allergic diseases. It has a high capacity to release an array of both preformed and newly generated mediators in response to environmental stimuli, especially allergen exposure. Cross linkage of IgE bound to high affinity receptors on mast cells not only results in the rapid release of autacoid mediators, but also the sustained synthesis and release of cytokines, chemokines and growth factors.

Mature mast cells are ubiquitous in human tissues and can thus participate in the processes of inflammation at different sites. Systemic anaphylaxis, a life-threatening disease, involves mast cell activation in multiple organs. In bronchial asthma, a disease characterized by widespread but potentially reversible bronchial obstruction, there are increased numbers of mast cells and a greater degree of continuous mast cell degranulation in bronchoalveolar lavage fluid from asthmatics compared with normal controls. Increased mast cell numbers and evidence for continuous degranulation of mast cells have been observed also in nasal lavage fluid and the nasal epithelium of the patients with allergic rhinitis.

Recent population surveys have estimated rates of prevalence of perceived food hypersensitivity of 12-20% in adults though this rate varied largely across different

countries (e.g., Spain, 4.6%; Australia, 19.1%) despite a common standardized methodology^[2]. Intestinal mast cells, as well as eosinophils, have been shown to be involved in the pathogenesis of food-allergy-related enteropathy.

Adverse drug reactions are common, but only 6-10% are immunologically mediated^[3]. Although allergic drug reactions are just one type of adverse reactions to medications, they are clinically very important because of the morbidity and mortality they cause. Allergic drug reactions may result in anaphylaxis, urticaria, bronchospasm and angioedema. During these reactions, allergic drugs cause direct histamine release from mast cells.

THE ROLES OF HISTAMINE IN ALLERGIC DISEASE

Since its discovery in 1911, histamine has been recognized as a major mediator in allergic diseases. Histamine is a primary amine synthesized from histidine in the Golgi apparatus, from where it is transported to the granule for storage in ionic association with the acidic residues of the glycosaminoglycans side chains of heparin and with proteinases. The histamine content of mast cells dispersed from human lung and skin is similar at 2-5 pg/cell, and the histamine stored ranges from 10 to 12 µg/g in both tissues. Following mast cell activation, histamine is rapidly dissociated from the granule matrix by exchange with sodium ions in the extracellular environment. Proteoglycans comprise the major supporting matrix of the mast cell granule with the sulfate groups binding to histamine, proteinases and acid hydrolases. As only mast cells and basophils contain histamine in man (apart from histaminergic nerve), and there are few basophils in human tissues, histamine can be used as a marker of mast cell degranulation.

The allergic process is believed to consist of two phases: early and late. The early phase reaction is mainly induced by histamine released from mast cells. Histamine is a potent vasoactive agent, bronchial smooth muscle constrictor, and stimulant of nociceptive itch nerves. In addition to its known effects on glands, vessels and sensory nerves, recent data have provided further evidence of histamine's proinflammatory actions^[4]. Histamine binding specific cell receptors produces clinical allergic symptoms. This mediator also activates neutrophils and eosinophils as well as being a chemoattractant for these cells^[5]. Histamine increases IL-8 level and evokes leukocyte rolling on endothelial cells. Thus histamine participates in both early and late-phase allergic responses.

ROLES OF HISTAMINE IN PATHOGENESIS OF IBD

Using segmental jejunal perfusion system with a two-balloon, six-channel small tube, Knutson and colleagues found that the histamine secretion rate was increased in patients with Crohn's disease compared with normal controls, and the secretion of histamine was related to disease activity, indicating strongly that degranulation of mast cells was involved in active Crohn's disease^[6]. The highly elevated mucosal histamine levels were also observed in allergic enteropathy and ulcerative colitis^[7]. Moreover, enhanced

histamine metabolism was found in collagenous colitis and food allergy^[8], and increased level of *N*-methylhistamine, a stable metabolite of the mast cell mediator histamine, was detected in the urine of patients with active Crohn's disease or ulcerative colitis^[9,10]. Since increased level of *N*-methylhistamine was significantly correlated to clinical disease activity, the above findings further strongly suggest the active involvement of histamine in the pathogenesis of these diseases.

Interestingly, mast cells originated from the resected colon of active Crohn's disease or ulcerative colitis were able to release more histamine than those from normal colon when being stimulated with an antigen, colon-derived murine epithelial cell-associated compounds^[11]. Similarly, cultured colorectal endoscopic samples from patients with IBD secreted more histamine towards substance P alone or substance P with anti-IgE than the samples from normal control subjects under the same stimulation^[12]. In a guinea pig model of intestinal inflammation induced by cow's milk proteins and trinitrobenzene sulfonic acid, both IgE titers and histamine levels were higher than normal control animals^[13].

As a proinflammatory mediator, histamine is selectively located in the granules of human mast cells and basophils and released from these cells upon degranulation. To date, a total of three histamine receptors H₁, H₂ and H₃ have been discovered in human gut^[14,15]. It proves that there are some specific targets that histamine can work on in intestinal tract. Histamine was found to cause a transient concentration-dependent increase in short-circuit current, a measure of total ion transport across the epithelial tissue in the gut^[16]. This could be due to that histamine interacts with H₁ receptors to increase the secretion of Na and Cl ions from epithelium^[17]. The finding that H₁-receptor antagonist pyrilamine was able to inhibit anti-IgE induced histamine release and ion transport^[18] suggested further that histamine is a crucial mediator responsible for diarrhea in IBD and food allergy. The ability of SR140333, a potent NK₁ antagonist in reducing mucosal ion transport, was most likely due to its inhibitory actions on histamine release from colon mast cells^[19].

HISTAMINE RECEPTORS

Histamine has multiple effects that are mediated by specific surface receptors on target cells. Four types of histamine receptors have now been recognized pharmacologically. Histamine receptors were first differentiated into H₁ and H₂ by Ash and Schild in 1966, when it was found that some responses to histamine were blocked by low doses of mepyramine (pyrilamine), whereas others were insensitive. A third histamine receptor subtype, termed H₃, was cloned in 1999 by Lovenberg and co-workers^[20] and the fourth histamine receptor subtype, termed H₄, was first reported in 2000 by Oda and co-workers^[21].

H₁ receptors

H₁ receptors have been cloned from cows, rats, guinea pigs and humans. The published sequences suggest that there are surprisingly large differences among species. H₁ receptors mediate most of the effects of histamine that are relevant to asthma. The cardinal features of asthma include smooth muscle spasm, mucosal edema, inflammation and mucous

secretion. It has been demonstrated that at least two of these features, bronchospasm and mucosal edema, can be caused by H₁-receptor stimulation. Northern analysis has demonstrated that there is a high level of expression of H₁ receptor messenger ribonucleic acid in lung.

Ocular allergy presents unsolved mysteries in molecular and cellular mechanisms, the recent understanding of the key role of the T helper type 2 cytokines, adhesion molecules and chemokines may provide future avenues for pharmacological targeting of releasable inflammatory mediators. More potent topical mast cell stabilizers and H₁ receptor antagonists have become commercially available for the management of the prevalent and benign forms of allergic conjunctivitis^[22]. Immunostimulatory DNA sequences present an innovative and promising route for the treatment of ocular allergy, but clinical studies are needed to demonstrate their efficacy in humans.

Bphs controls Bordetella pertussis toxin (PTX)-induced vasoactive amine sensitization elicited by histamine (VAASH) and has an established role in autoimmunity. Ma and co-workers^[23] reported that congenic mapping links Bphs to the histamine H₁ receptor gene (Hrh1/H₁R) and that H₁R differs at three amino acid residues in VAASH-susceptible and -resistant mice. Hrh1-/- mice are protected from VAASH, which can be restored by genetic complementation with a susceptible Bphs/Hrh1 allele, and experimental allergic encephalomyelitis and autoimmune orchitis due to immune deviation. Thus, natural alleles of Hrh1 control both the autoimmune T cells and vascular responses regulated by histamine after PTX sensitization.

H₂ receptors

H₂ receptors have been cloned from dogs and humans. Although H₂ receptors are present in the airway, their clinical relevance is unclear, because H₂ receptor antagonists have few measurable effects on airway function. Histamine stimulates an increase in cyclic AMP levels in lung fragments that is blocked by H₂ receptor antagonists, indicating that H₂ receptors are positively coupled to adenylyl cyclase in lung.

Atopic diseases such as allergic rhinitis and asthma are characterized by increases in Th2 cells and serum IgE antibodies. The binding of allergens to IgE on mast cells triggers the release of several mediators, of which histamine is the most prevalent. Mazzoni and co-workers reported that histamine, together with a maturation signal, acts directly upon immature dendritic cells (DCs), which express H₁ and H₂, two active histamine receptors. Histamine, acting upon the H₂ receptor for a short period of time, increased IL-10 production and reduced IL-12 secretion. As a result, histamine-matured DCs polarized naive CD4(+) T cells toward a Th2 phenotype, as compared with DCs that had matured in the absence of histamine. The Th2 cells favor IgE production, leading to increased histamine secretion by mast cells, thus creating a positive feedback loop that could contribute to the severity of atopic diseases^[24].

H₃ receptors

The identification of H₃ receptor cDNA allowed several groups to reveal the complexity of the histamine-mediated systems. Comparison of the cDNA with available genome

databases revealed that the gene encoding H₃ receptor is located on chromosome 20 and contains at least two introns. In rats, H₃ receptors consist of at least three functional isoforms, referred to as H_{3A}, H_{3B} and H_{3C}, which vary in the length of their third intracellular loop (I3) (136 104 and 88 amino acids respectively). In humans, H₃ receptor isoforms have been cloned, including one with an 80-amino-acid deletion of I3. Moreover, another isoform has been identified, in which the 80-amino-acid deletion is accompanied by an additional 8 amino acids at the C-terminal tail. Using reverse transcription polymerase chain reaction, the human isoforms have been found to be differentially expressed in various brain areas. The 80-amino-acid sequence located at the C-terminal portion of I3 plays an essential role in H₃ agonist-mediated signal transduction. The existence of multiple H₃ isoforms with different signal transduction capabilities suggests that H₃-mediated biological functions might be tightly regulated through alternative splicing mechanisms. Otherwise, histamine H₃ receptor activation inhibits neurogenic sympathetic vasoconstriction in porcine nasal mucosa, suggesting that histamine H₃ receptors may play a role in the regulation of vascular tone and nasal patency in allergic nasal congestive disease^[25].

H₄ receptors

The discovery of the histamine H₄ receptor adds a new chapter to the histamine story. The H₄ receptor is a G protein-coupled receptor and is most closely related to the H₃ receptor, sharing 58% identity in the transmembrane regions. The gene encoding the H₄ receptor was discovered initially in a search of the GenBank databases as sequence fragments retrieved in a partially sequenced human genomic contig mapped to chromosome 18^[26]. About the histamine-binding site of H₄ receptor, Shin reported that Asp94 (3.32) in transmembrane region (TM) 3 and Glu182 (5.46) in TM5 are critically involved in histamine binding. Asp94 probably serves as a counter-anion to the cationic amino group of histamine, whereas Glu182 (5.46) interacts with the N(τ) nitrogen atom of the histamine imidazole ring via an ion pair. These results resemble those for the analogous residues in the H₁ histamine receptor but contrast with findings regarding the H₂ histamine receptor. It indicates that although histamine seems to bind to the H₄ receptor in a fashion similar to that predicted for the other histamine receptor subtypes, there are also important differences that can probably be exploited for the discovery of novel H₄-selective compounds^[27]. H₄ receptor exhibits a very restricted localization, expression is primarily found in intestinal tissue, spleen, thymus and immune active cells, such as T cells, mast cells, neutrophils and eosinophils. It suggests an important role for the H₄ receptor in the regulation of immune function and offers novel therapeutic potentials for histamine receptor ligands in allergic and inflammatory diseases^[28].

THE EFFECTS OF HISTAMINE RECEPTOR ANTAGONISTS ON HISTAMINE RELEASE FROM MAST CELLS

Today, according to action on different receptors, the histamine

receptor agonists (Table 1) and antagonists (Table 2) are classified into four subtypes, respectively. Among H₁ receptor antagonists, the first generation antihistamines have considerable sedative effects caused by their ability to cross the blood-brain barrier. The second generation of antihistamines to emerge in the market is devoid of these sedative effects. The third generation antihistamines, metabolites of the earlier drugs, have demonstrated no cardiac effects of the parent drugs and are at least potent^[29].

Table 1 Agonists of histamine receptors

Receptor subtype	Agonists
H ₁	Dimethylhistaprodifen ^[30] , methylhistaprodifen ^[30] , histaprodifen ^[30,31] , histamine-trifluoromethyl-toluidine ^[32] , 2-thiazolyethylamine ^[33] , 2-(3-trifluoromethylphenyl) histamine ^[34] , 2-phenylhistamines ^[31] , 2-pyridylethylamine ^[35]
H ₂	Dimaprit ^[30,34]
H ₃	Imetit ^[32] , alpha-methylhistamine ^[33,34]
H ₄	Clobenpropit ^[32] , imetit ^[32]

Table 2 Antagonists of histamine receptors

Receptor subtype	Antagonists
H ₁	First-generation Azatadine, clemastine, chlorpheniramine (chlorphenamine maleate), diphenhydramine, dexchlorpheniramine, hydroxyzine, mepyramine (pyrilamine), promethazine, terfenadine (teldane), triprolidine ^[35-37] Second-generation Acrivastine ^[37,38] , astemizole (hismanal) ^[38] , azelastine ^[38] , cetirizine (virilx, zirtek, zyrtec) ^[39-41] , chlorpheniramine ^[42,43] , desloratadine ^[44,45] , ebastine ^[37,44] , emedastine ^[37] , epinastine ^[41,46] , homochlorcyclizine ^[47] , ketotifen ^[41,48] , levocabastine ^[46] , loratadine (claritin, clarityne) ^[41,44,49] , olopatadine ^[41,50] , mequitazine ^[47] , mizolastine ^[47] , pseudoephedrine ^[51,52] , rupatadine ^[53,54] , tripeleannamine (pyribenzamin) ^[55] Third-generation Fexofenadine ^[37,44,56] , levocetirizine ^[37,39]
H ₂	First-generation Cimetidine ^[57] , metiamide ^[58] Second-generation Ranitidine (1979) ^[59] , omeprazole (1982) ^[60] Third-generation Famotidine ^[61] , ebrotidine ^[62] , lafutidine ^[63,64] , niperotidine ^[60] , nizatidine ^[60] , potentidine ^[65] , roxatidine ^[60] , zolantidine ^[58]
H ₃	A-304121 ^[66] , A-317920 ^[66] , 4-(aminoalkoxy) benzylamines ^[67] , ciproxifan ^[66] , clobenpropit ^[68] , D-alanine-piperazine-amides ^[69] , imidazopyridine ^[70] , indole ^[70] , indolizine ^[70] , 4'-[(NR1R2-1-yl)]-propoxy-biaryl-4-carboxamides ^[70] , pyrazolopyridine ^[71] , 1-(4-(phenoxy-methyl)benzyl) piperidines ^[72] , SCH 79687 ^[73] , thioperamide ^[68,74]
H ₄	JNJ 777120 ^[75,76] , thioperamide ^[77]

Among them, H₁ receptor antagonists loratadine and terfenadine were able to inhibit IgE-induced histamine release from human mast cells^[78], which may at least partially

explain their potent antiallergic activity^[79]. However, the extent of H₁ receptor antagonists binding to mast cells is quite different. Wescott *et al*^[80], reported tripeleannamine > pyrilamine > diphenhydramine in binding H₁ receptor.

Fexofenadine, an effective H₁ antihistamine, is the active metabolite of terfenadine, but they had different effects on histamine and tryptase release from mast cells. Terfenadine inhibited release of histamine and tryptase from mast cells during the early allergic response, whereas fexofenadine did not^[81].

In combination with H₁ antihistamines, H₂ antihistamines famotidine, ranitidine or cimetidine suppressed effectively the chronic swelling. It is deduced that simultaneous blockage of both histamine H₁ and H₂ receptors may be necessary for sufficient inhibition of the microvascular permeability increase in some kinds of anaphylactic reactions, and that histamine, mainly interacting with H₂ receptors, may play an important role in activation of a certain phase of chronic inflammation where mast cell degranulation is involved^[82]. Metiamide, one H₂ receptor antagonist, can reduce the histamine release from secreting mast cells in mast-cell mediated angiogenesis^[83]. H₃ antagonists, thioperamide and clobenpropit combined with H₁ antihistamine loratadine, not the H₂ antagonist ranitidine, reduced nasal congestion^[84] in mast cell-deficient mice, indicating that its action was not associated with mast cell degranulation^[85].

THE HYPOTHESIS OF SELF-AMPLIFICATION MECHANISM OF MAST CELL DEGRANULATION

Tryptase has been proved to be a unique marker of mast cell degranulation *in vitro* as it is more selective than histamine to mast cells. Inhibitors of tryptase^[86,87] and chymase^[88] have been discovered to possess the ability to inhibit histamine or tryptase release from human skin, tonsil, synovial^[89] and colon mast cells^[90], suggesting that they are likely to be developed as a novel class of mast cell stabilizers. Recently, a series of experiments with dispersed colon mast cells suggested that there should be at least two pathways in man for mast cells to amplify their own activation-degranulation signals in an autocrine or paracrine manner, which may partially explain the phenomena that when a sensitized individual contacts allergen only once the local allergic response in the involved tissue or organ may last for days or weeks. These findings included that both anti-IgE and calcium ionophore were able to induce significant release of tryptase and histamine from colon mast cells, histamine is a potent activator of human colon mast cells and the agonists of PAR-2 and trypsin are potent secretagogues of human colon mast cells. Since tryptase was reported to be able to activate human mast cells^[86] and H₁ receptor antagonists terfenadine and cetirizine^[78] were capable of inhibiting mast cell activation, the hypothesis of mast cell degranulation self-amplification mechanisms is that mast cell secretagogues induce mast cell degranulation, and release of histamine, which then stimulates the adjacent mast cells or positively feedbacks to further stimulate its host mast cells through H₁ receptors, whereas released tryptase acts similarly to histamine, but through its receptor PAR-2 on mast cells.

REFERENCES

- 1 **Parikh SA**, Cho SH, Oh CK. Preformed enzymes in mast cell granules and their potential role in allergic rhinitis. *Curr Allergy Asthma Rep* 2003; **3**: 266-272
- 2 **Crespo JF**, Rodriguez J. Food allergy in adulthood. *Allergy* 2003; **58**: 98-113
- 3 **Gruchalla RS**. 10. Drug allergy. *J Allergy Clin Immunol* 2003; **111**: S548-S559
- 4 **Repka-Ramirez MS**, Baraniuk JN. Histamine in health and disease. *Clin Allergy Immunol* 2002; **17**: 1-25
- 5 **He S**, Peng Q, Walls AF. Potent induction of a neutrophil and eosinophil-rich infiltrate *in vivo* by human mast cell tryptase: selective enhancement of eosinophil recruitment by histamine. *J Immunol* 1997; **159**: 6216-6225
- 6 **Knutson L**, Ahrenstedt O, Odling B, Hallgren R. The jejunal secretion of histamine is increased in active Crohn's disease. *Gastroenterology* 1990; **98**: 849-854
- 7 **Raithel M**, Matek M, Baenkler HW, Jorde W, Hahn EG. Mucosal histamine content and histamine secretion in Crohn's disease, ulcerative colitis and allergic enteropathy. *Int Arch Allergy Immunol* 1995; **108**: 127-133
- 8 **Schwab D**, Hahn EG, Raithel M. Enhanced histamine metabolism: a comparative analysis of collagenous colitis and food allergy with respect to the role of diet and NSAID use. *Inflamm Res* 2003; **52**: 142-147
- 9 **Winterkamp S**, Weidenhiller M, Otte P, Stolper J, Schwab D, Hahn EG, Raithel M. Urinary excretion of N-methylhistamine as a marker of disease activity in inflammatory bowel disease. *Am J Gastroenterol* 2002; **97**: 3071-3077
- 10 **Weidenhiller M**, Raithel M, Winterkamp S, Otte P, Stolper J, Hahn EG. Methylhistamine in Crohn's disease (CD): increased production and elevated urine excretion correlates with disease activity. *Inflamm Res* 2000; **49** Suppl 1: S35-S36
- 11 **Fox CC**, Lichtenstein LM, Roche JK. Intestinal mast cell responses in idiopathic inflammatory bowel disease. Histamine release from human intestinal mast cells in response to gut epithelial proteins. *Dig Dis Sci* 1993; **38**: 1105-1112
- 12 **Raithel M**, Schneider HT, Hahn EG. Effect of substance P on histamine secretion from gut mucosa in inflammatory bowel disease. *Scand J Gastroenterol* 1999; **34**: 496-503
- 13 **Fargeas MJ**, Theodorou V, More J, Wal JM, Fioramonti J, Bueno L. Boosted systemic immune and local responsiveness after intestinal inflammation in orally sensitized guinea pigs. *Gastroenterology* 1995; **109**: 53-62
- 14 **Bertaccini G**, Coruzzi G. An update on histamine H3 receptors and gastrointestinal functions. *Dig Dis Sci* 1995; **40**: 2052-2063
- 15 **Rangachari PK**. Histamine: mercurial messenger in the gut. *Am J Physiol* 1992; **262**: G1-13
- 16 **Homaidan FR**, Tripodi J, Zhao L, Burakoff R. Regulation of ion transport by histamine in mouse cecum. *Eur J Pharmacol* 1997; **331**: 199-204
- 17 **Traynor TR**, Brown DR, O'Grady SM. Effects of inflammatory mediators on electrolyte transport across the porcine distal colon epithelium. *J Pharmacol Exp Ther* 1993; **264**: 61-66
- 18 **Crowe SE**, Luthra GK, Perdue MH. Mast cell mediated ion transport in intestine from patients with and without inflammatory bowel disease. *Gut* 1997; **41**: 785-792
- 19 **Moriarty D**, Goldhill J, Selve N, O'Donoghue DP, Baird AW. Human colonic anti-secretory activity of the potent NK(1) antagonist, SR140333: assessment of potential anti-diarrhoeal activity in food allergy and inflammatory bowel disease. *Br J Pharmacol* 2001; **133**: 1346-1354
- 20 **Lovenberg TW**, Roland BL, Wilson SJ, Jiang X, Pyati J, Huvar A, Jackson MR, Erlander MG. Cloning and functional expression of the human histamine H3 receptor. *Mol Pharmacol* 1999; **55**: 1101-1107
- 21 **Oda T**, Morikawa N, Saito Y, Masuho Y, Matsumoto S. Molecular cloning and characterization of a novel type of histamine receptor preferentially expressed in leukocytes. *J Biol Chem* 2000; **275**: 36781-36786
- 22 **Solomon A**, Pe'er J, Levi-Schaffer F. Advances in ocular allergy: basic mechanisms, clinical patterns and new therapies. *Curr Opin Allergy Clin Immunol* 2001; **1**: 477-482
- 23 **Ma RZ**, Gao J, Meeker ND, Fillmore PD, Tung KS, Watanabe T, Zachary JF, Offner H, Blankenhorn EP, Teuscher C. Identification of Bphs, an autoimmune disease locus, as histamine receptor H1. *Science* 2002; **297**: 620-623
- 24 **Mazzoni A**, Young HA, Spitzer JH, Visintin A, Segal DM. Histamine regulates cytokine production in maturing dendritic cells, resulting in altered T cell polarization. *J Clin Invest* 2001; **108**: 1865-1873
- 25 **Varty LM**, Hey JA. Histamine H3 receptor activation inhibits neurogenic sympathetic vasoconstriction in porcine nasal mucosa. *Eur J Pharmacol* 2002; **452**: 339-345
- 26 **Nguyen T**, Shapiro DA, George SR, Setola V, Lee DK, Cheng R, Rauser L, Lee SP, Lynch KR, Roth BL, O'Dowd BF. Discovery of a novel member of the histamine receptor family. *Mol Pharmacol* 2001; **59**: 427-433
- 27 **Shin N**, Coates E, Murgolo NJ, Morse KL, Bayne M, Strader CD, Monsma FJ. Molecular modeling and site-specific mutagenesis of the histamine-binding site of the histamine H4 receptor. *Mol Pharmacol* 2002; **62**: 38-47
- 28 **Leurs R**, Watanabe T, Timmerman H. Histamine receptors are finally 'coming out'. *TRENDS Pharmacol Sci* 2001; **22**: 337-339
- 29 **Oppenheimer JJ**, Casale TB. Next generation antihistamines: therapeutic rationale, accomplishments and advances. *Expert Opin Investig Drugs* 2002; **11**: 807-817
- 30 **Schlicker E**, Kozłowska H, Kwolek G, Malinowska B, Kramer K, Pertz HH, Elz S, Schunack W. Novel histaprodifen analogues as potent histamine H1-receptor agonists in the pithed and in the anaesthetized rat. *Naunyn Schmiedeberg Arch Pharmacol* 2001; **364**: 14-20
- 31 **Seifert R**, Wenzel-Seifert K, Burckstummer T, Pertz HH, Schunack W, Dove S, Buschauer A, Elz S. Multiple differences in agonist and antagonist pharmacology between human and guinea pig histamine H1-receptor. *J Pharmacol Exp Ther* 2003; **305**: 1104-1115
- 32 **Bell JK**, McQueen DS, Rees JL. Involvement of histamine H4 and H1 receptors in scratching induced by histamine receptor agonists in Balb C mice. *Br J Pharmacol* 2004; **142**: 374-380
- 33 **Lamberti C**, Ipponi A, Bartolini A, Schunack W, Malmberg-Aiello P. Antidepressant-like effects of endogenous histamine and of two histamine H1 receptor agonists in the mouse forced swim test. *Br J Pharmacol* 1998; **123**: 1331-1336
- 34 **Lecklin A**, Etu-Seppala P, Stark H, Tuomisto L. Effects of intracerebroventricularly infused histamine and selective H1, H2 and H3 agonists on food and water intake and urine flow in Wistar rats. *Brain Res* 1998; **793**: 279-288
- 35 **Leurs R**, Smit MJ, Meeder R, Ter Laak AM, Timmerman H. Lysine200 located in the fifth transmembrane domain of the histamine H1 receptor interacts with histamine but not with all H1 agonists. *Biochem Biophys Res Commun* 1995; **214**: 110-117
- 36 **Assanase P**, Naclerio RM. Antiallergic anti-inflammatory effects of H1-antihistamines in humans. *Clin Allergy Immunol* 2002; **17**: 101-139
- 37 **Verster JC**, Volkerts ER. Antihistamines and driving ability: evidence from on-the-road driving studies during normal traffic. *Ann Allergy Asthma Immunol* 2004; **92**: 294-303; quiz 303-355, 355
- 38 **Aaronson DW**. Comparative efficacy of H1 antihistamines. *Ann Allergy* 1991; **67**: 541-547
- 39 **Tillement JP**, Testa B, Bree F. Compared pharmacological characteristics in humans of racemic cetirizine and levocetirizine, two histamine H1-receptor antagonists. *Biochem Pharmacol* 2003; **66**: 1123-1126
- 40 **Christophe B**, Carlier B, Gillard M, Chatelain P, Peck M, Massingham R. Histamine H1 receptor antagonism by cetirizine in isolated guinea pig tissues: influence of receptor reserve and dissociation kinetics. *Eur J Pharmacol* 2003; **470**: 87-94
- 41 **Nishiga M**, Fujii Y, Konishi M, Hossen MA. Effects of sec-

- ond-generation histamine H1 receptor antagonists on the active avoidance response in rats. *Clin Exp Pharmacol Physiol* 2003; **30**: 60-63
- 42 **Aslanian R**, Mutahi Mw, Shih NY, Piwinski JJ, West R, Williams SM, She S, Wu RL, Hey JA. Identification of a dual histamine H1/H3 receptor ligand based on the H1 antagonist chlorpheniramine. *Bioorg Med Chem Lett* 2003; **13**: 1959-1961
- 43 **Sharma A**, Hamelin BA. Classic histamine H1 receptor antagonists: a critical review of their metabolic and pharmacokinetic fate from a bird's eye view. *Curr Drug Metab* 2003; **4**: 105-129
- 44 **Gelfand EW**, Appajosyula S, Meeves S. Anti-inflammatory activity of H1-receptor antagonists: review of recent experimental research. *Curr Med Res Opin* 2004; **20**: 73-81
- 45 **Monroe EW**. Desloratidine for the treatment of chronic urticaria. *Skin Therapy Lett* 2002; **7**: 1-2, 5
- 46 **Whitcup SM**, Bradford R, Lue J, Schiffman RM, Abelson MB. Efficacy and tolerability of ophthalmic epinastine: a randomized, double-masked, parallel-group, active- and vehicle-controlled environmental trial in patients with seasonal allergic conjunctivitis. *Clin Ther* 2004; **26**: 29-34
- 47 **Suzuki A**, Yasui-Furukori N, Mihara K, Kondo T, Furukori H, Inoue Y, Kaneko S, Otani K. Histamine H1-receptor antagonists, promethazine and homochlorcyclizine, increase the steady-state plasma concentrations of haloperidol and reduced haloperidol. *Ther Drug Monit* 2003; **25**: 192-196
- 48 **Kidd M**, McKenzie SH, Steven I, Cooper C, Lanz R. Efficacy and safety of ketotifen eye drops in the treatment of seasonal allergic conjunctivitis. *Br J Ophthalmol* 2003; **87**: 1206-1211
- 49 **Nelson HS**. Prospects for antihistamines in the treatment of asthma. *J Allergy Clin Immunol* 2003; **112**: S96-100
- 50 **Brockman HL**, Momsen MM, Knudtson JR, Miller ST, Graff G, Yanni JM. Interactions of olopatadine and selected antihistamines with model and natural membranes. *Ocul Immunol Inflamm* 2003; **11**: 247-268
- 51 **Mahgoub H**, Gazy AA, El-Yazbi FA, El-Sayed MA, Youssef RM. Spectrophotometric determination of binary mixtures of pseudoephedrine with some histamine H1-receptor antagonists using derivative ratio spectrum method. *J Pharm Biomed Anal* 2003; **31**: 801-809
- 52 **Meltzer EO**, Casale TB, Gold MS, O'Connor R, Reitberg D, del Rio E, Weiler JM, Weiler K. Efficacy and safety of clemastine-pseudoephedrine- acetaminophen versus pseudoephedrine-acetaminophen in the treatment of seasonal allergic rhinitis in a 1-day, placebo-controlled park study. *Ann Allergy Asthma Immunol* 2003; **90**: 79-86
- 53 **Salmun LM**. Antihistamines in late-phase clinical development for allergic disease. *Expert Opin Investig Drugs* 2002; **11**: 259-273
- 54 **Izquierdo I**, Merlos M, Garcia-Rafanell J. Rupatadine: a new selective histamine H1 receptor and platelet-activating factor (PAF) antagonist. A review of pharmacological profile and clinical management of allergic rhinitis. *Drugs Today (Barc)* 2003; **39**: 451-468
- 55 **Manohar M**, Goetz TE, Humphrey S, Depuy T. H1-receptor antagonist, tripeleminamine, does not affect arterial hypoxemia in exercising Thoroughbreds. *J Appl Physiol* (1985) 2002; **92**: 1515-1523
- 56 **Simpson K**, Jarvis B. Fexofenadine: a review of its use in the management of seasonal allergic rhinitis and chronic idiopathic urticaria. *Drugs* 2000; **59**: 301-321
- 57 **Yamaura K**, Yonekawa T, Nakamura T, Yano S, Ueno K. The histamine H2-receptor antagonist, cimetidine, inhibits the articular osteopenia in rats with adjuvant-induced arthritis by suppressing the osteoclast differentiation induced by histamine. *J Pharmacol Sci* 2003; **92**: 43-49
- 58 **Scaccianoce S**, Lombardo K, Nicolai R, Affricano D, Angelucci L. Studies on the involvement of histamine in the hypothalamic-pituitary-adrenal axis activation induced by nerve growth factor. *Life Sci* 2000; **67**: 3143-3152
- 59 **Vannay A**, Fekete A, Muller V, Strehlau J, Viklicky O, Veres T, Reusz G, Tulassay T, Szabo AJ. Effects of histamine and the h2 receptor antagonist ranitidine on ischemia-induced acute renal failure: involvement of IL-6 and vascular endothelial growth factor. *Kidney Blood Press Res* 2004; **27**: 105-113
- 60 **Mannino S**, Troncon MG, Wallander MA, Cattaruzzi C, Romano F, Agostinis L, Marighi PE, Walker A. Ocular disorders in users of H2 antagonists and of omeprazole. *Pharmacoepidemiol Drug Saf* 1998; **7**: 233-241
- 61 **Mozdarani H**. Radioprotective properties of histamine H2 receptor antagonists: present and future prospects. *J Radiat Res* 2003; **44**: 145-149
- 62 **Arroyo MT**, Lanás A, Sainz R. Prevention and healing of experimental indomethacin-induced gastric lesions: effects of ebrotidine, omeprazole and ranitidine. *Eur J Gastroenterol Hepatol* 2000; **12**: 313-318
- 63 **Isomoto H**, Inoue K, Furusu H, Nishiyama H, Shikuwa S, Omagari K, Mizuta Y, Murase K, Murata I, Kohno S. Lafutidine, a novel histamine H2-receptor antagonist, vs lansoprazole in combination with amoxicillin and clarithromycin for eradication of *Helicobacter pylori*. *Helicobacter* 2003; **8**: 111-119
- 64 **Sato H**, Kawashima K, Yuki M, Kazumori H, Rumi MA, Ortega-Cava CF, Ishihara S, Kinoshita Y. Lafutidine, a novel histamine H2-receptor antagonist, increases serum calcitonin gene-related peptide in rats after water immersion-restraint stress. *J Lab Clin Med* 2003; **141**: 102-105
- 65 **Li L**, Kracht J, Peng S, Bernhardt G, Elz S, Buschauer A. Synthesis and pharmacological activity of fluorescent histamine H2 receptor antagonists related to potentidine. *Bioorg Med Chem Lett* 2003; **13**: 1717-1720
- 66 **Esbenshade TA**, Krueger KM, Miller TR, Kang CH, Denny LI, Witte DG, Yao BB, Fox GB, Faghih R, Bennani YL, Williams M, Hancock AA. Two novel and selective nonimidazole histamine H3 receptor antagonists A-304121 and A-317920: I. *In vitro* pharmacological effects. *J Pharmacol Exp Ther* 2003; **305**: 887-896
- 67 **Apodaca R**, Dvorak CA, Xiao W, Barbier AJ, Boggs JD, Wilson SJ, Lovenberg TW, Carruthers NI. A new class of diamine-based human histamine H3 receptor antagonists: 4-(aminoalkoxy)benzylamines. *J Med Chem* 2003; **46**: 3938-3944
- 68 **Munzar P**, Tanda G, Justinova Z, Goldberg SR. Histamine h3 receptor antagonists potentiate methamphetamine self-administration and methamphetamine-induced accumbal dopamine release. *Neuropsychopharmacology* 2004; **29**: 705-717
- 69 **Faghih R**, Phelan K, Esbenshade TA, Miller TR, Kang CH, Krueger KM, Yao BB, Fox GB, Bennani YL, Hancock AA. D-alanine piperazine-amides: novel non-imidazole antagonists of the histamine H3 receptor. *Inflamm Res* 2003; **52** Suppl 1: S47-S48
- 70 **Faghih R**, Dwight W, Pan JB, Fox GB, Krueger KM, Esbenshade TA, McVey JM, Marsh K, Bennani YL, Hancock AA. Synthesis and SAR of aminoalkoxy-biaryl-4-carboxamides: novel and selective histamine H3 receptor antagonists. *Bioorg Med Chem Lett* 2003; **13**: 1325-1328
- 71 **Chai W**, Breitenbucher JG, Kwok A, Li X, Wong V, Carruthers NI, Lovenberg TW, Mazur C, Wilson SJ, Axe FU, Jones TK. Non-imidazole heterocyclic histamine H3 receptor antagonists. *Bioorg Med Chem Lett* 2003; **13**: 1767-1770
- 72 **Miko T**, Ligneau X, Pertz HH, Ganellin CR, Arrang JM, Schwartz JC, Schunack W, Stark H. Novel nonimidazole histamine H3 receptor antagonists: 1-(4-(phenoxymethyl)benzyl)piperidines and related compounds. *J Med Chem* 2003; **46**: 1523-1530
- 73 **McLeod RL**, Rizzo CA, West RE, Aslanian R, McCormick K, Bryant M, Hsieh Y, Korfmaier W, Mingo GG, Varty L, Williams SM, Shih NY, Egan RW, Hey JA. Pharmacological characterization of the novel histamine H3-receptor antagonist N-(3,5-dichlorophenyl)-N'-[[4-(1H-imidazol-4-ylmethyl)phenyl]-methyl]-urea (SCH 79687). *J Pharmacol Exp Ther* 2003; **305**: 1037-1044
- 74 **Liedtke S**, Flau K, Kathmann M, Schlicker E, Stark H, Meier G, Schunack W. Replacement of imidazole by a piperidine moiety differentially affects the potency of histamine H3-

- receptor antagonists. *Naunyn Schmiedebergs Arch Pharmacol* 2003; **367**: 43-50
- 75 **Thurmond RL**, Desai PJ, Dunford PJ, Fung-Leung WP, Hofstra CL, Jiang W, Nguyen S, Riley JP, Sun S, Williams KN, Edwards JP, Karlsson L. A potent and selective histamine H4 receptor antagonist with anti-inflammatory properties. *J Pharmacol Exp Ther* 2004; **309**: 404-413
- 76 **Jablonowski JA**, Grice CA, Chai W, Dvorak CA, Venable JD, Kwok AK, Ly KS, Wei J, Baker SM, Desai PJ, Jiang W, Wilson SJ, Thurmond RL, Karlsson L, Edwards JP, Lovenberg TW, Carruthers NI. The first potent and selective non-imidazole human histamine H4 receptor antagonists. *J Med Chem* 2003; **46**: 3957-3960
- 77 **Hofstra CL**, Desai PJ, Thurmond RL, Fung-Leung WP. Histamine H4 receptor mediates chemotaxis and calcium mobilization of mast cells. *J Pharmacol Exp Ther* 2003; **305**: 1212-1221
- 78 **Okayama Y**, Benyon RC, Lowman MA, Church MK. *In vitro* effects of H1-antihistamines on histamine and PGD2 release from mast cells of human lung, tonsil, and skin. *Allergy* 1994; **49**: 246-253
- 79 **Sugimoto Y**, Umakoshi K, Nojiri N, Kamei C. Effects of histamine H1 receptor antagonists on compound 48/80-induced scratching behavior in mice. *Eur J Pharmacol* 1998; **351**: 1-5
- 80 **Wescott SL**, Hunt WA, Kaliner M. Histamine H-1 receptors on rat peritoneal mast cells. *Life Sci* 1982; **31**: 1911-1919
- 81 **Allocco FT**, Votypka V, deTineo M, Naclerio RM, Baroody FM. Effects of fexofenadine on the early response to nasal allergen challenge. *Ann Allergy Asthma Immunol* 2002; **89**: 578-584
- 82 **Kaneta S**, Yanaguimoto H, Kagaya J, Ishizuki S, Fujihira E. Effects of H2-antihistamines in murine models of immediate hypersensitivity and chronic inflammation. *Res Commun Chem Pathol Pharmacol* 1993; **79**: 167-184
- 83 **Sorbo J**, Jakobsson A, Norrby K. Mast-cell histamine is angiogenic through receptors for histamine1 and histamine2. *Int J Exp Pathol* 1994; **75**: 43-50
- 84 **McLeod RL**, Mingo GG, Herczku C, DeGennaro-Culver F, Kreutner W, Egan RW, Hey JA. Combined histamine H1 and H3 receptor blockade produces nasal decongestion in an experimental model of nasal congestion. *Am J Rhinol* 1999; **13**: 391-399
- 85 **Hossen MA**, Sugimoto Y, Kayasuga R, Kamei C. Involvement of histamine H3 receptors in scratching behaviour in mast cell-deficient mice. *Br J Dermatol* 2003; **149**: 17-22
- 86 **He S**, Gaça MD, Walls AF. A role for tryptase in the activation of human mast cells: modulation of histamine release by tryptase and inhibitors of tryptase. *J Pharmacol Exp Ther* 1998; **286**: 289-297
- 87 **He S**, McEuen AR, Blewett SA, Li P, Buckley MG, Leufkens P, Walls AF. The inhibition of mast cell activation by neutrophil lactoferrin: uptake by mast cells and interaction with tryptase, chymase and cathepsin G. *Biochem Pharmacol* 2003; **65**: 1007-1015
- 88 **He S**, Gaça MD, McEuen AR, Walls AF. Inhibitors of chymase as mast cell-stabilizing agents: contribution of chymase in the activation of human mast cells. *J Pharmacol Exp Ther* 1999; **291**: 517-523
- 89 **He S**, Gaca MD, Walls AF. The activation of synovial mast cells: modulation of histamine release by tryptase and chymase and their inhibitors. *Eur J Pharmacol* 2001; **412**: 223-229
- 90 **He SH**, Xie H. Modulation of histamine release from human colon mast cells by protease inhibitors. *World J Gastroenterol* 2004; **10**: 337-341

• VIRAL HEPATITIS •

Enhancement of humoral immune responses to HBsAg by heat shock protein gp96 and its N-terminal fragment in mice

Hong-Tao Li, Jia-Bin Yan, Jing Li, Ming-Hai Zhou, Xiao-Dong Zhu, Yu-Xia Zhang, Po Tien

Hong-Tao Li, Jia-Bin Yan, Ming-Hai Zhou, Xiao-Dong Zhu, Yu-Xia Zhang, Po Tien, Department of Molecular Virology, Institute of Microbiology, Graduate School of the Chinese Academy of Sciences, Beijing 100080, China

Jing Li, Hepatitis B Department, National Vaccine and Serum Institute, Beijing 100024, China

Supported by the Major State Basic Research Development Program of China, Program 973, Grant No. 2001CB510001

Correspondence to: Professor Po Tien, Department of Molecular Virology, Institute of Microbiology, Chinese Academy of Sciences, Zhongguancun Beiyitiao, Beijing 100080, China. tienpo@sun.im.ac.cn
Telephone: +86-10-62554247 Fax: +86-10-62622101

Received: 2004-06-11 Accepted: 2004-06-29

against HBV infection.

© 2005 The WJG Press and Elsevier Inc. All rights reserved.

Key words: Heat shock protein; gp96 N-terminal fragment; HBV; Hepatitis B virus surface antigen (HBsAg); Vaccine

Li HT, Yan JB, Li J, Zhou MH, Zhu XD, Zhang YX, Tien P. Enhancement of humoral immune responses to HBsAg by heat shock protein gp96 and its N-terminal fragment in mice. *World J Gastroenterol* 2005; 11(19): 2858-2863

<http://www.wjgnet.com/1007-9327/11/2858.asp>

Abstract

AIM: Most studies on the immune effect of gp96 were focused on its enhancement of CTLs. It is interesting to know whether gp96 could influence the humoral immune response, and whether the recombinant N-terminal fragment of gp96 could substitute native gp96 to stimulate the immune system.

METHODS: gp96 isolated from livers of normal mice and its N-terminal fragment (amino acid 22-355) expressed in *E. coli* were used for immunization of BALB/c mice. Eight groups of mice received one of the following regimens subcutaneously in 100 μ L phosphate buffered saline (PBS) at an interval of 3 wk. Group 1: PBS only; group 2: gp96 only; group 3: N-terminal fragment only; group 4: HBsAg only; group 5: HBsAg+gp96; group 6: HBsAg+N-terminal fragment; group 7: HBsAg+incomplete Freud's adjuvant; group 8: HBsAg+N-terminal fragment (95 °C heated for 30 min). Serum anti-HBsAg antibody levels were assayed by ELISA. CTL responses in splenocytes were analyzed by ELISPOT after the last vaccination.

RESULTS: The average titer of serum anti-HBsAg antibody in the mice immunized with HBsAg together with gp96 or its N-terminal fragment were much higher than those immunized with HBsAg alone detected by ELISA. The cellular immune response of the mice immunized with HBsAg together with gp96 or its N-terminal fragment was not different with those immunized with HBsAg alone measured by ELISPOT assay.

CONCLUSION: gp96 or its N-terminal fragment greatly improved humoral immune response induced by HBsAg, but failed to enhance the CTL response, which demonstrated the potential of using gp96 or its N-terminal fragment as a possible adjuvant to augment humoral immune response

INTRODUCTION

Heat shock protein gp96 (HSP gp96; glucose-regulated protein, GRP94), as a member of HSP90 family, is one of the most abundant proteins in cells, which displays various roles besides protein folding and assembly^[1,2]. But most attractive feature of gp96 is its contributions to immune system^[3]. The phenomena that gp96 isolated from tumors or virus-infected cells elicit specific CTLs against their origins are widely observed^[4-10]. It is believed that gp96 is capable of channeling antigenic peptides to MHC class I presentation pathway of antigen presenting cell (APC) by acting as ligand of CD91^[11-14]. The immunologic processes activated in response to tumor antigen negative sources of GRP94/gp96 are currently presumed to be associated with the stimulation of CD11b (+) and CD11c (+) APCs and activation of the bystander CD4 (+) T cell Th1 cytokine production^[15]. Autologous vaccines based on general properties of gp96 have been widely studied, but there exists obvious limitations including quantity of gp96 for therapy, which are strictly limited by the size of the resected tumor mass^[16]. Moreover, only half of the treated patients vaccinated with gp96 derived from autologous tumor induced an antitumor response in phase I/II clinical trials^[17]. Hence, a novel HSP-mediated universally applicable vaccine is still in need. Ideal therapeutic vaccines for infectious diseases and cancer might elicit not only the cellular response but also the humoral response. However, the studies so far on the immune effect of gp96 were mainly focused on its enhancement of CTLs, hereby we wanted to check whether the gp96 derived from normal tissue could influence humoral immune response and act as a regular adjuvant. However, it was hard for such a big molecule expressed in *E. coli* by our experimental practice, so gp96 purified from normal tissue was used as the source of the protein.

The N-terminal domain (amino acids 1-263), homologous

to the proteolytic fragment of HSP90, was regarded as the nucleotide-binding domain^[18], followed by acidic residues (amino acids 264-344). The first 355 amino acids of GRP94 were found to be peptide-binding sites, capable of binding a number of peptides^[19,20]. Furthermore, it is reported that the N-terminal peptide binding domain fragment could suppress tumor growth like that of the full gp96^[21]. In order to check the idea of using recombinant N-terminal fragment as analog of gp96, and investigate its immune effect, we expressed the N-terminal fragment of gp96 in pGEX-6p1 vector in *E. coli*. After co-immunization with gp96 or the N-terminal fragment and HBsAg, the humoral and cellular immune responses in mice were compared with those of administration HBsAg alone. Some concern that the immune responses induced by recombinant HSPs produced in *E. coli* might result from the effects of lipopolysaccharide (LPS) contaminated during the preparation^[22]. Therefore, necessary measures were taken to avoid the possible influence by endotoxin.

MATERIALS AND METHODS

Recombinant HBsAg

Nonglycosylated HBsAg, subtypes adw, containing the small HBsAg (S) protein of HBV derived from the *Saccharomyces cerevisiae* host strain 2150-2-3 carrying pHBS56-GAP347/33 plasmid containing S-gene encoding HBsAg was obtained from Dr. Chin-Yuan Guo (Beijing Tiantan Biological Products Co., Ltd). Briefly, the harvested fermentation product of the yeast was homogenized to release HBsAg, the ruptured yeast cells were microfiltered and ultrafiltered to remove large debris and small molecule contaminants, the HBsAg particles was further purified by silica adsorption and butyl-agarose hydrophobic interaction chromatography consequently. The purity and pyrogen were tested by high performance size exclusion liquid chromatography on TSK G4000SW column and Limulus Amebocyte Lysate for endotoxin detection reagent (Chinese Horseshoe Crab Reagent Manufactory), which are higher than 99.0% and lower than 10 EU/mL respectively.

gp96 expressed in *E. coli* and purification of gp96 from normal liver tissue

The gene encoding murine gp96 was donated by Professor Srivastava (GenBank Accession No. gi: 6755862). The gene encoding amino acids 22-802 of gp96 was amplified by PCR and cloned into *E. coli* expression vector pET30a (Novagen) by two restriction enzyme sites of *Bam*HI and *Xho*I. A stopcodon was introduced immediately before the *Xho*I site. This cloning strategy yielded fusion proteins, in which there are extra 50 amino acids in total at the N-terminus of gp96. The recombinant plasmids of pET30a-gp96 were transformed into *E. coli* strain BL21 (DE3). Bacterial cells were harvested and lysed by sonication in phosphate buffered saline (PBS). The clarified supernatants were applied on Ni-chelated Sepharose affinity column (Pharmacia). The column then was washed by PBS and eluted with imidazole (100 mmol/L). The eluted material was applied to POROS 20QE column (4.6-100 mm, PE Biosystem, Foster City, CA, USA) on an AKTA fast protein liquid chromatography

(FPLC) Workstation with a 300-800 mmol/L NaCl gradient. Fractions (1 mL) were collected and analyzed by 10% SDS-PAGE.

Native gp96 was purified as described previously^[23]. Healthy mouse liver tissues were suspended in 30 mmol/L sodium bicarbonate. The lysate was centrifuged to remove nuclei and other debris. The supernatant was precipitated with ammonium sulfate (50-70%). The solubilized precipitation was applied to a ConA-Sepharose column (Pharmacia Biotech, Uppsala, Sweden). The column was eluted with buffer containing 10% α -methylmanno pyranoside (Sigma). The eluted material was applied to POROS 20QE column on a AKTA FPLC Workstation with a 300-800 mmol/L NaCl gradient. Fractions (1 mL) were collected and analyzed by 10% SDS-PAGE. The resultant protein was applied to a Gel filtration Superdex G200 on a AKTA FPLC Workstation. The identity of the gp96 protein was confirmed by Western blot using anti-gp96 monoclonal antibody (NeoMarkers, Fremont, USA).

Expression and purification of the N-terminal fragment of gp96

The N-terminal fragment (NTF) of gp96 (from 22aa to 355aa) was cloned into the *Bam*HI and *Xho*I sites of GST fusion expression vector pGEX-6p-1 (Pharmacia), containing PreScission protease cleavage site (Sigma). The positive plasmids were verified by direct DNA sequencing. *E. coli* strain BL21 (DE3) transformed with the recombinant pGEX-6p-1 plasmid was grown at 37 °C in 2× YTA medium before induction with 1 mmol/L IPTG for 4 h at 37 °C. Bacterial cells were harvested and lysed by sonication in PBS. The clarified supernatants of the lysate were passed through a glutathione±Sepharose 4B column. The GST fusion protein-bound column was washed with PBS and eluted with reduced glutathione. After cleavage the free GST and the protease were removed by passage through the glutathione±Sepharose 4B column again. The resultant protein was applied to a Gel filtration Superdex G75 on AKTA FPLC Workstation. SDS-PAGE and Western blot were used to identify the protein. The quantities of proteins were estimated by protein concentration test kit (BioRad). Additionally, all material for protein preparations were treated prior to use, to remove possible contaminants of endotoxin. All buffers were made in pyrogen-free water.

Immunization in mice

Female Balb/c mice were obtained from the Animal Research Center of Medical Department in Peking University (Beijing, China). Eight groups of mice were immunized with one of the following regiments in 100 μ L PBS: (1) PBS; (2) 10 μ g NTF only; (3) 10 μ g gp96 only; (4) HBsAg alone; (5) mixture of 10 μ g NTF and 10 μ g HBsAg; (6) mixture of 10 μ g gp96 and 10 μ g HBsAg; (7) 10 μ g of HBsAg emulsified in incomplete Freud's adjuvant (IFA); (8) mixture of 10 μ g NTF (heated at 95 °C for 30 min) and 10 μ g HBsAg. All groups contained at least 8 mice. All injections were done subcutaneously at 0, 3 and 6 wk.

HBsAg-specific antibody assay

Sera samples were collected from all mice by tail bleeding at different times and the presence of HBsAg-specific

antibody was analyzed by ELISA. The ELISA kits for the HBsAg-specific antibody detection were purchased from Sino-American BioTechnology Co., China and operated following the manufacturer's instructions 2 wk after the last immunization to compare the *A* values from different groups. HBsAg-specific IgG serum Abs were determined by an end-point dilution ELISA assay. Micro-ELISA plates (costar; Corning Incorporated, NY, USA) were coated with 150 ng recombinant HBsAg particles per well in 50 μ L 0.1 mol/L sodium carbonate buffer (pH 9.5) at 4 °C. Serial dilutions of the sera in loading buffer (PBS supplemented with 3% BSA and 2% Tween 20) were added to the antigen-coated wells. Serum Abs were incubated for 2 h at 37 °C before four washes with PBS supplemented with 0.05% Tween 20. Bound serum Abs were detected using HRP-conjugated goat anti-mouse IgG Ab (catalog no. 214-1 806; KPL, USA) before incubation with substrate *o*-phenylenediamine (Sigma) in PBS. The reaction was stopped by 1 M H₂SO₄, and determined at 450 nm. End-point titers were defined as the highest serum dilution that resulted in an absorbance value three times greater than that of negative control sera (derived from PBS immunized BALb/c mice).

CTL assay

Spleen cells of mice were segregated 2 wk after the last immunization and the CTL activities were measured by ELISPOT assay, which was performed according to the instruction of the murine IFN- γ ELISPOT kit (Diacor, France). Briefly, 96-well polyvinylidene difluoride-backed plates were precoated with 15 μ g/mL anti-IFN- γ mAb overnight at 4 °C. Plates were blocked for 1 h at 37 °C. Purified splenocytes were dispensed at predetermined density in duplicate wells. Ten micromole per liter of peptide (WYWGPSLYSI, GL Biochem, Shanghai) was used to stimulate the cells^[24]. The plates were incubated at 37 °C for 18-40 h. After washing, the plates were then incubated for another 1.5 h at 37 °C after addition of the biotinylated anti-IFN- γ antibody. A 1:1 000 dilution of streptavidin-alkaline phosphatase conjugate was then added into the wells and incubated for 1 h after which the chromogenic alkaline phosphatase substrate was added. After 30 min, the colorimetric reaction was terminated by washing with tap water. After drying, the spots were counted.

Statistical analysis

The statistical significance of the difference between two groups were determined by the two-tailed Student's *t* test and was set to *P*<0.05.

RESULTS

Expression and purification of gp96

gp96 were expressed as fusion protein with an extra 50 amino acids at their N-terminus derived from the expression vector pET30a, including the 6 \times his-tag and two protease cleavage sites (thrombin and enterokinase). The expressed proteins were purified with Ni-chelated affinity column. In the step of the purification on the POROS 20QE column, gp96 was eluted within a wide range of salt concentration (400-700 mmol/L NaCl). The product contained mostly degraded fragments of gp96 or its aggregations identified by 10%SDS-PAGE (Figure 1A). The purity of resultant proteins could not meet the demand of immunization. So we resorted to purify the gp96 from the normal tissue.

Approximately 20-30 mg of apparently homogeneous preparations of gp96 were obtained from each gram of wet weight of the healthy murine livers by our method^[23]. Unlike the recombinant gp96, all peak fractions in the wide range contained apparently homogeneous gp96. The purity of gp96 preparations were determined by 10% SDS-PAGE (Figure 1B). Fractions containing gp96 were pooled and further purified on a gel-filtration Superdex G200 column (Figure 1C). Using the purification procedures mentioned above, we routinely obtained gp96 of over 95% purity as judged by SDS-PAGE and Western blot (Figure 1D).

N-terminal fragment of gp96 was expressed as soluble proteins

E.coli is widely useful to produce target proteins for its high production and convenient manipulation, but the full-length gp96 molecule may be too big to produce in BL21 cells. Although the gp96 N-terminal fragment could stimulate maturation of APC and suppress tumor growth was reported, whether the fragment can generate immune effects is unknown^[21]. In order to investigate the idea of using recombinant N-terminal fragment as analog of gp96 and address its immune effect, the N-terminal fragment of gp96, NTF (22-355 aa) was cloned into pGEX-6p1 expression

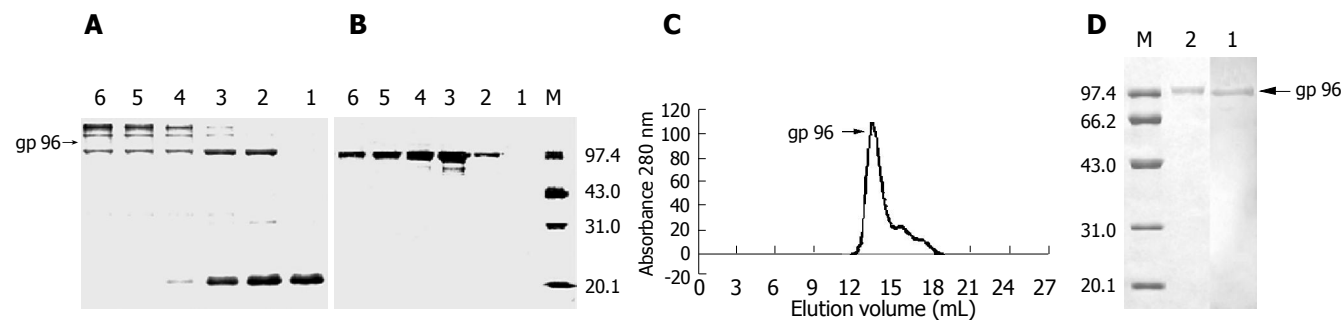


Figure 1 Gp96 expressed in *E.coli* and purification from normal murine livers. **A** and **B**: Elutions of gp96 from POROS 20QE column with 300-800 mmol/L NaCl were detected by SDS-PAGE. The gp96 expressed in *E.coli*. **A**: or purified from mice livers; **B**: were collected as 1 mL fractions during the purification on POROS 20QE column and a total of six individual fractions (lanes 1-6) were run

on the SDS-PAGE gel with Coomassie blue staining afterwards; **C**: Gel-filtration analysis of gp96 purified from mice livers. The protein samples are run on Superdex G200 column; **D**: Proteins collected from the peak of gel filtration were run on 10% SDS-PAGE and Western blot are shown on the right.

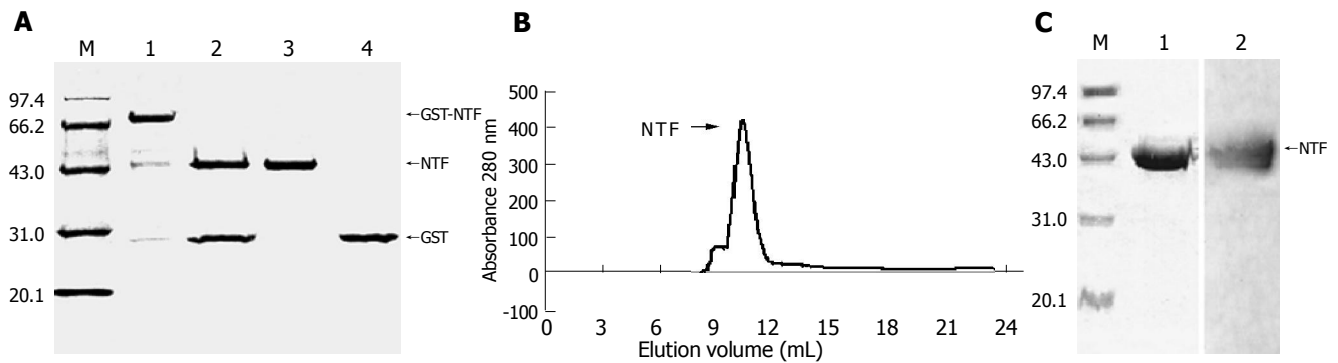


Figure 2 Expression and purification of the N-terminal fragment of gp96 in the GST fusion expression system. **A:** The resulting protein N-terminal fragment of gp96 (named after NTF) was separated from the digestion product on a glutathione-Sepharose 4B column to remove GST and GST-3C protease. Lane 1, 10% SDS-PAGE of GST-NTF eluted by reduced glutathione; lane 2, NTF after GST-3C protease digestion (16 h, 5 °C); lane 3, NTF after removing GST

and GST-3C protease; lane 4, purified GST as control; M, protein molecular weight markers as indicated in kilo Daltons; **B:** Gel-filtration analysis of NTF protein. NTF protein subjected to Superdex G75 gel-filtration; **C:** The proteins from the peak run on 10% SDS-PAGE and Western blot. The standard proteins are superimposed in both A and C.

vector, mainly expressed as fusion proteins to GST in supernatant of bacteria BL21 cells lysate (Figure 2A). The gel-filtration Superdex G75 column was applied for further purification after removing GST (Figure 2B). The resultant proteins were analyzed by Coomassie blue staining to be at least 95% pure (Figure 2C) and immunoblotted with an anti-gp96 monoclonal antibody (Figure 2C). NTF was recognized by the monoclonal antibody consistent with the previous report^[25]. Comparing with the recombinant gp96, NTF was more stable and purer.

Gp96 and its N-terminal fragment can enhance the humoral response to HBsAg

The *A* values of anti-HBsAg antibody from different groups were compared at day 63 after three doses of immunization (Figure 3A). Mice were immunized with HBsAg emulsified in IFA and PBS as positive and negative control respectively (Figure 1A: groups 1 and 7). NTF alone or gp96 alone had no effect on the antibody production (Figure 1A: groups 2 and 3). A strong anti-HBsAg response was observed in mice after three doses of immunization with the mixture of HBsAg and NTF, gp96 or IFA (groups 5, 6 and 7). The highest *A* value was from the mice immunized with HBsAg and NTF (group 5). The values of antibody were not significantly different between the groups immunized with HBsAg plus NTF (group 5) or gp96 (group 6) compared to those of HBsAg plus IFA (group 7) ($P>0.05$). However, the values of anti-HBsAg were significantly correlated with the mice immunized with or without the assistance of adjuvant to HBsAg ($P<0.05$).

In order to investigate whether the levels of anti-HBsAg were correlated with the time after immunization, and to examine the detailed difference between the mice immunized with HBsAg and those immunized with HBsAg and NTF or gp96, the end-point dilution was used to compare the anti-HBsAg IgG 2 wk after each vaccination (Figure 3B). There was no significant difference in anti-HBsAg antibody level between groups immunized with HBsAg alone and those immunized with HBsAg plus heated NTF, which demonstrated that the LPS contamination had no influence on the results (Figure 3A: groups 4 and 8). Therefore, we

added the mice immunized with HBsAg plus heated NTF to the group of mice immunized with HBsAg alone in the following tests. Significant difference was observed between the mice immunized with HBsAg plus heated NTF and those immunized with HBsAg plus NTF or gp96 after two doses of immunization (Figure 3B) ($P<0.05$). The highest end-point dilution titers were achieved in mice after three doses of immunization with HBsAg plus NTF or gp96 (Figure 3B), which were 5-10 fold higher than those with HBsAg plus heated NTF. The above results showed that gp96 and its N-terminal fragment enhanced the humoral response to HBsAg.

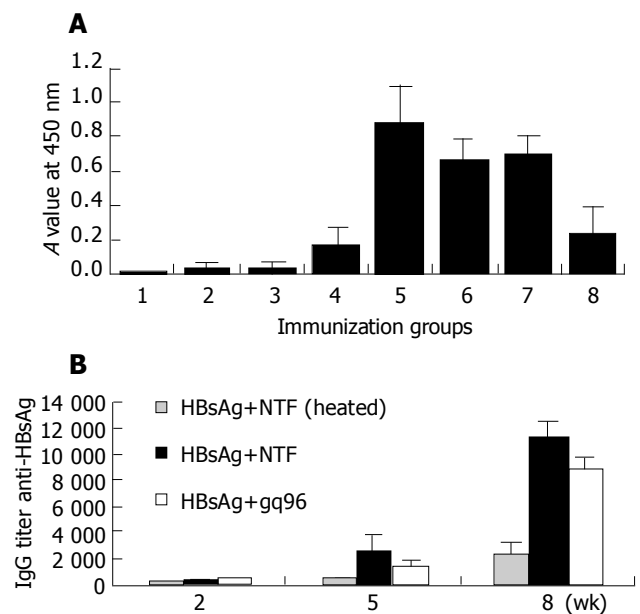


Figure 3 Induced humoral immune response in Balb/c mice. **A:** Groups (eight mice per group) of Balb/c mice were immunized with different gradient: group 1, PBS only; group 2, 10 µg gp96 only; group 3, 10 µg NTF only; group 4, 10 µg HBsAg only; group 5, 10 µg HBsAg+10 µg NTF; group 6, 10 µg HBsAg+10 µg gp96; group 7, 10 µg HBsAg+IFA; group 8, 10 µg HBsAg+10 µg NTF (95 °C heated for 30 min) at d 0 (day of first vaccination). At d 21, and 42 mice were re-immunized with the same material. At d 63 anti-HBsAg antibodies from different groups were compared using the value at 450 nm absorbance. The values of antibody were expressed as geometry mean \pm SD; **B:** Sera from the mice immunized with HBsAg plus heated NTF, HBsAg plus NTF or gp96 (groups 5, 6 and 8) were collected on d 14, 35 and 64 from first vaccination and stored at -20 °C and titers at different dilution were tested at the same time.

Gp96 and its N-terminal fragment failed to enhance the CTL response to HBsAg

Whether the CTLs could be obtained when the two proteins were simply mixed but not covalently bonded^[26] were examined. The number of spot forming cells (SFCs) representing the IFN- γ secreted CTLs, in splenocytes in response to the HBsAg epitope WYWGPSLYSI *in vitro* was measured by ELISPOT. Splenocytes stimulated with ConA served as the positive control. Splenocytes from mice immunized with HBsAg with gp96 or a mixture of HBsAg and NTF produced the same level of SFCs in response to stimulation with the peptide (Figure 4). While there were differences between the mice immunized with PBS and those with HBsAg plus adjuvant, there were no significant differences between mice immunized with HBsAg plus heated NTF and those with HBsAg plus gp96 or NTF (Figure 4). It is conceivable that this lack of immune enhancement effect was likely due to inability for gp96 to chaperone large exogenous antigen into MHC class I pathway of APC.

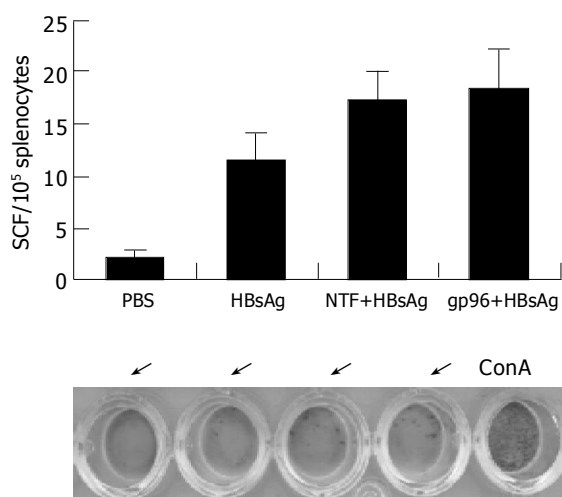


Figure 4 T-cell response of splenocytes of immunized Balb/c mice. Mice immunized with PBS, HBsAg plus heated NTF, HBsAg plus NTF or gp96 (the same groups as groups 5, 6, and 8 respectively in Figure 3) were killed on d 63 and the splenocytes were collected for ELISPOT assay with 10⁵ cells per well. The number of SFCs was calculated. The photograph of the representative wells from different groups is shown below the statistics.

DISCUSSION

During the process of studies on tumor transplantation and rejection, two important groups of proteins were found: MHC proteins and HSPs. HSPs appeared earlier in evolution, more conservative in structure and more abundant in the cells^[27]. As a member of HSPs, gp96 has similar biological characteristics to protein chaperones. The most attractive function of gp96 with respect to medicinal applications is its immune role upon both the innate and adaptive immune systems^[28]. Previously the main interests towards gp96 were the focus on its peptide chaperone and its involvement in the pathway of MHC class I to enhance CTL responses. Recently reports have disclosed the effect of gp96 upon the pathway of MHC class II^[29-31]. Our results illustrate for

the first time its enhancement of the humoral response to protein antigen HBsAg, which provides evidence that gp96 can influence the antibody production. The reason that gp96 is enhancing humoral response might be due to (1) stimulation of APC to increase the efficiency of processing exogenous antigen and presenting peptides to MHC class II molecules; (2) activation of bystander CD4⁺ T cells; (3) functions directly as a Th2-specific costimulatory molecule. A protein vaccine can potentially boost immune response, but without suitable adjuvant, soluble proteins can only elicit a weak immune response^[32,33]. Gp96 could act as a potent adjuvant to increase humoral responses by this study. Whether the covalently linked gp96 and HBsAg can elevate both the antibody and CTL specific to HBsAg needs further investigation.

In the world, the number of individuals infected by HBV is over 400 million. About 60% of the world's 530 000 cases of liver cancer per year are caused by viral hepatitis B infection^[34]. Interferon and nucleoside analogs are still the most effective drugs to treat chronic hepatitis B. However, cessation of treatment usually leads to a rapid relapse of disease, and long-term treatment often results in the selection of drugs resistant viral variants^[35]. Therapeutic vaccines have been proposed to break the established T-cell tolerance in chronically infected patients^[36,37]. Recently it was suggested that continuous stimulation of dendritic cells (DCs) by ligands of Toll-like receptors was needed to overcome CD4⁺CD25⁺ T cell-mediated suppression and mature DCs alone were not sufficient to break CD8 tolerance^[38]. Immunotherapeutic vaccines based on gp96 conceived in our lab maybe an optimal candidate to break the established T-cell tolerance because gp96 can act as ligand of pattern recognition receptors^[39]. However, the whole-length of gp96 was poorly expressed in *E.coli* and the product after purification was produced in unacceptably low amounts and was unstable, which limited its applications. Our results showed that the N-terminal fragment of gp96 expressed very well in *E.coli* with more production and higher quality, and owned the same effect as the full-length gp96 to increase the antibody to HBsAg. Further studies on the N-terminal fragment of gp96 and the HBV infection will bring us more knowledge for better usage of this fragment to fight against HBV infection.

ACKNOWLEDGMENTS

We are grateful to Dr. Gordon Laity for helping in the preparation of this manuscript, Dr. Song-Dong Meng for critical reading of the manuscript, Fu-Lian Liao for technical assistance, Professor Pramod K. Srivastava for providing the mouse gp96 clone, Professor Wei-Feng Chen of Peking University and Professor Xue-Tao Cao of the Second Military Medical University for help in various stages of the project, and Wei-Hua Zhuang for graphic preparation.

REFERENCES

- Morimoto RI. Regulation of the heat shock transcriptional response: cross talk between a family of heat shock factors, molecular chaperones, and negative regulators. *Genes Dev* 1998; **12**: 3788-3796
- Feder ME, Hofmann GE. Heat-shock proteins, molecular

- chaperones, and the stress response: evolutionary and ecological physiology. *Annu Rev Physiol* 1999; **61**: 243-282
- 3 **Srivastava P.** Roles of heat-shock proteins in innate and adaptive immunity. *Nat Rev Immunol* 2002; **2**: 185-194
 - 4 **Rivoltini L**, Castelli C, Carrabba M, Mazzaferro V, Pilla L, Huber V, Coppa J, Gallino G, Scheibenbogen C, Squarcina P, Cova A, Camerini R, Lewis JJ, Srivastava PK, Parmiani G. Human tumor-derived heat shock protein 96 mediates *in vitro* activation and *in vivo* expansion of melanoma- and colon carcinoma-specific T cells. *J Immunol* 2003; **171**: 3467-3474
 - 5 **Srivastava PK.** Purification of heat shock protein-peptide complexes for use in vaccination against cancers and intracellular pathogens. *Methods* 1997; **12**: 165-171
 - 6 **Graner MW**, Zeng Y, Feng H, Katsanis E. Tumor-derived chaperone-rich cell lysates are effective therapeutic vaccines against a variety of cancers. *Cancer Immunol Immunother* 2003; **52**: 226-234
 - 7 **Mazzaferro V**, Coppa J, Carrabba MG, Rivoltini L, Schiavo M, Regalia E, Mariani L, Camerini T, Marchiano A, Andreola S, Camerini R, Corsi M, Lewis JJ, Srivastava PK, Parmiani G. Vaccination with autologous tumor-derived heat-shock protein gp96 after liver resection for metastatic colorectal cancer. *Clin Cancer Res* 2003; **9**: 3235-3245
 - 8 **Janetzki S**, Palla D, Rosenhauer V, Lochs H, Lewis JJ, Srivastava PK. Immunization of cancer patients with autologous cancer-derived heat shock protein gp96 preparations: a pilot study. *Int J Cancer* 2000; **88**: 232-238
 - 9 **Tamura Y**, Peng P, Liu K, Dao U, Srivastava PK. Immunotherapy of tumors with autologous tumor-derived heat shock protein preparations. *Science* 1997; **278**: 117-120
 - 10 **Manjili MH**, Wang XY, Park J, Facciponte JG, Repasky EA, Subjeck JR. Immunotherapy of cancer using heat shock proteins. *Front Biosci* 2002; **7**: 7d43-d52
 - 11 **Basu S**, Binder RJ, Ramalingam T, Srivastava PK. CD91 is a common receptor for heat shock proteins gp96, hsp90, hsp70, and calreticulin. *Immunity* 2001; **14**: 303-313
 - 12 **Binder RJ**, Han DK, Srivastava PK. CD91: a receptor for heat shock protein gp96. *Nat Immunol* 2000; **1**: 151-155
 - 13 **Binder RJ**, Srivastava PK. Essential role of CD91 in re-presentation of gp96-chaperoned peptides. *Proc Natl Acad Sci USA* 2004; **101**: 6128-6133
 - 14 **Meng SD**, Gao T, Gao GF, Tien P. HBV-specific peptide associated with heat-shock protein gp96. *Lancet* 2001; **357**: 528-529
 - 15 **Baker-LePain JC**, Sarzotti M, Nicchitta CV. Glucose-regulated protein 94/glycoprotein 96 elicits bystander activation of CD4+ T cell Th1 cytokine production *in vivo*. *J Immunol* 2004; **172**: 4195-4203
 - 16 **Gordon NF**, Clark BL. The challenges of bringing autologous HSP-based vaccines to commercial reality. *Methods* 2004; **32**: 63-69
 - 17 **Castelli C**, Rivoltini L, Rini F, Belli F, Testori A, Maio M, Mazzaferro V, Coppa J, Srivastava PK, Parmiani G. Heat shock proteins: biological functions and clinical application as personalized vaccines for human cancer. *Cancer Immunol Immunother* 2004; **53**: 227-233
 - 18 **Prodromou C**, Roe SM, O'Brien R, Ladbury JE, Piper PW, Pearl LH. Identification and structural characterization of the ATP/ADP-binding site in the Hsp90 molecular chaperone. *Cell* 1997; **90**: 65-75
 - 19 **Vogen S**, Gidalevitz T, Biswas C, Simen BB, Stein E, Gulmen F, Argon Y. Radicicol-sensitive peptide binding to the N-terminal portion of GRP94. *J Biol Chem* 2002; **277**: 40742-40750
 - 20 **Gidalevitz T**, Biswas C, Ding H, Schneidman-Duhovny D, Wolfson HJ, Stevens F, Radford S, Argon Y. Identification of the N-terminal peptide binding site of glucose-regulated protein 94. *J Biol Chem* 2004; **279**: 16543-16552
 - 21 **Baker-LePain JC**, Sarzotti M, Fields TA, Li CY, Nicchitta CV. GRP94 (gp96) and GRP94 N-terminal geldanamycin binding domain elicit tissue nonrestricted tumor suppression. *J Exp Med* 2002; **196**: 1447-1459
 - 22 **Reed RC**, Berwin B, Baker JP, Nicchitta CV. GRP94/gp96 elicits ERK activation in murine macrophages. A role for endotoxin contamination in NF-kappa B activation and nitric oxide production. *J Biol Chem* 2003; **278**: 31853-31860
 - 23 **Meng SD**, Song J, Rao Z, Tien P, Gao GF. Three-step purification of gp96 from human liver tumor tissues suitable for isolation of gp96-bound peptides. *J Immunol Methods* 2002; **264**: 29-35
 - 24 **Falk K**, Rotzschke O, Stevanovic S, Jung G, Rammensee HG. Allele-specific motifs revealed by sequencing of self-peptides eluted from MHC molecules. *Nature* 1991; **351**: 290-296
 - 25 **Sargan DR**, Tsai MJ, O'Malley BW. hsp108, a novel heat shock inducible protein of chicken. *Biochemistry* 1986; **25**: 6252-6258
 - 26 **Suzue K**, Zhou X, Eisen HN, Young RA. Heat shock fusion proteins as vehicles for antigen delivery into the major histocompatibility complex class I presentation pathway. *Proc Natl Acad Sci USA* 1997; **94**: 13146-13151
 - 27 **Li Z**, Menoret A, Srivastava P. Roles of heat-shock proteins in antigen presentation and cross-presentation. *Curr Opin Immunol* 2002; **14**: 45-51
 - 28 **Srivastava P.** Roles of heat-shock proteins in innate and adaptive immunity. *Nat Rev Immunol* 2002; **2**: 185-194
 - 29 **Baker-LePain JC**, Sarzotti M, Nicchitta CV. Glucose-regulated protein 94/glycoprotein 96 elicits bystander activation of CD4+ T cell Th1 cytokine production *in vivo*. *J Immunol* 2004; **172**: 4195-4203
 - 30 **Doody AD**, Kovalchin JT, Mihalyo MA, Hagymasi AT, Drake CG, Adler AJ. Glycoprotein 96 can chaperone both MHC class I- and class II-restricted epitopes for *in vivo* presentation, but selectively primes CD8+ T cell effector function. *J Immunol* 2004; **172**: 6087-6092
 - 31 **Banerjee PP**, Vinay DS, Mathew A, Raje M, Parekh V, Prasad DV, Kumar A, Mitra D, Mishra GC. Evidence that glycoprotein 96 (B2), a stress protein, functions as a Th2-specific costimulatory molecule. *J Immunol* 2002; **169**: 3507-3518
 - 32 **Hansson M**, Nygren PA, Stahl S. Design and production of recombinant subunit vaccines. *Biotechnol Appl Biochem* 2000; **32**(Pt 2): 95-107
 - 33 **Liljeqvist S**, Stahl S. Production of recombinant subunit vaccines: protein immunogens, live delivery systems and nucleic acid vaccines. *J Biotechnol* 1999; **73**: 1-33
 - 34 **Lai CL**, Ratzliff V, Yuen MF, Poynard T. Viral hepatitis B. *Lancet* 2003; **362**: 2089-2094
 - 35 **Liaw YF**. Therapy of chronic hepatitis B: current challenges and opportunities. *J Viral Hepat* 2002; **9**: 393-399
 - 36 **Soemohardjo S**. New options in the treatment of chronic hepatitis. *Adv Exp Med Biol* 2003; **531**: 191-198
 - 37 **Pol S**, Driss F, Michel ML, Nalpas B, Berthelot P, Brechot C. Specific vaccine therapy in chronic hepatitis B infection. *Lancet* 1994; **344**: 342
 - 38 **Yang Y**, Huang CT, Huang X, Pardoll DM. Persistent Toll-like receptor signals are required for reversal of regulatory T cell-mediated CD8 tolerance. *Nat Immunol* 2004; **5**: 508-515
 - 39 **Vabulas RM**, Braedel S, Hilf N, Singh-Jasuja H, Herter S, Ahmad-Nejad P, Kirschning CJ, Da Costa C, Rammensee HG, Wagner H, Schild H. The endoplasmic reticulum-resident heat shock protein Gp96 activates dendritic cells via the Toll-like receptor 2/4 pathway. *J Biol Chem* 2002; **277**: 20847-20853

Hydrophobicity of reactive site loop of SCCA1 affects its binding to hepatitis B virus

Min Chen, Tong Cheng, Chen-Yu Xu, Ting Wu, Shan-Hai Ou, Tao Zhang, Jun Zhang, Ning-Shao Xia

Min Chen, Tong Cheng, Chen-Yu Xu, Ting Wu, Shan-Hai Ou, Tao Zhang, Jun Zhang, Ning-Shao Xia, Fujian Research Center of Medical Molecular Virology, Key Laboratory of Cell Biology and Tumor Cell Engineering of Ministry of Education, Xiamen University, Xiamen 361005, Fujian Province, China

Supported by the Cross-Century Talent Training Program of Ministry of Education, China

Correspondence to: Ning-Shao Xia, Key Laboratory of Cell Biology and Tumor Cell Engineering of Ministry of Education, Xiamen University, Xiamen 361005, Fujian Province, China. nsxia@jingxian.xmu.edu.cn

Telephone: +86-592-2184110 Fax: +86-592-2184110

Received: 2004-06-07 Accepted: 2004-06-29

Xia NS. Hydrophobicity of reactive site loop of SCCA1 affects its binding to hepatitis B virus. *World J Gastroenterol* 2005; 11(19): 2864-2868

<http://www.wjgnet.com/1007-9327/11/2864.asp>

Abstract

AIM: To investigate the role of SCCA2 and other SCCA1 molecules in the process of hepatitis B virus (HBV) binding to mammalian cells.

METHODS: SCCA1 and SCCA2 were isolated from HepG2. Binding protein (BP) genes were obtained through PCR. Recombinant baculoviruses expressing SCCA1, SCCA2, BP, and different mutants were constructed and utilized to infect mammalian cells to investigate the binding ability of infected cells to HBV.

RESULTS: A SCCA1 gene (A1) was isolated from HepG2, but it appeared to lack the binding ability of infected cells to HBV. Two mutants, A1-BP and BP-A1, were constructed by interchanging the carboxyl terminal of A1 and BP. Cells expressing A1-BP showed an increased virus binding capacity, but not BP-A1. Comparison of A1 sequence with the sequence of BP indicated the presence of only three amino acid changes in the carboxyl terminal, two of them were found in the reactive site loop (RSL) of SCCA1. Primary structure assay revealed that the hydrophobicity of BP and AJ515706 in this domain was strong, but A1 was relatively weak. Changing the aa349 of A1 from low hydrophobic glutamic acid to high hydrophobic valine enhanced HBV binding. In contrast, HBV binding was reduced by changing the aa349 of BP from valine to glutamic acid.

CONCLUSION: The results suggest that the hydrophobicity of RSL of SCCA1 may play an important role in HBV binding to cells.

© 2005 The WJG Press and Elsevier Inc. All rights reserved.

Key words: Hepatitis B virus; BP; SCCA1; SCCA2

Chen M, Cheng T, Xu CY, Wu T, Ou SH, Zhang T, Zhang J,

INTRODUCTION

Hepatitis B virus (HBV) is able to infect only humans or higher primates and shows a strong tropism for liver parenchymal cells. These characteristics and the lack of cell lines that support productive HBV replication *in vitro* have impeded the identification of HBV receptors. A number of receptor candidates for HBV have been reported, including receptors for immunoglobulin A (IgA), human interleukin-6 and annexin V. But these results are controversial, and no conclusive and convincing biological data could be obtained to fully demonstrate the functional role of these proteins in HBV binding and internalization^[1]. Studies using synthetic preS1(21-47) peptides and corresponding antibodies to prevent HBV attachment to HepG2 have identified the preS1 of the L protein as one of the important sites possibly involved in HBV infection^[2-4]. A recent candidate for HBV cellular receptors is HBV-binding proteins (BP), isolated from the plasma membranes of HepG2 by using a tetravalent derivative of the preS1(21-47) sequence^[5]. HepG2 cells after transfection of BP cDNA showed an increased virus binding capacity, while Chinese hamster ovary cells, which normally do not bind to HBV, acquired susceptibility to HBV binding after transfection. BPs encode for a protein of 390 amino acids. Comparison of BP sequence with the sequence of SCCA1, a member of serpin superfamily cloned by Suminami *et al*^[6], indicated the presence of only three amino acid changes (aa351, aa357 and aa389). BP is also a member of SCCA1. The serpin is a superfamily of structurally well-conserved protein presented in plants, animals, fungi, viruses, and involved in regulating of a variety of biological events^[7]. When De Falcon *et al*^[8], isolated HBV-BP from HepG2, 12 independent recombinant clones were sequenced, showing that the sequences corresponding to SCCA1, SCCA2, and HBV-BP were equally represented. SCCA2, another member of serpin, is found to be 91% close to SCCA1. Recently, Moore *et al*^[9], isolated another SCCA1 from HepG2, presenting four amino acid substitutions to BP, and confirmed that transfection of this SCCA1 into mammalian cells resulted in increased HBV binding. But the function of SCCA2 is still not known. In order to understand the role of SCCA2 and other SCCA1 in the process of HBV binding to mammalian cells, recombinant baculoviruses expressing SCCA1, SCCA2, BP, and different mutants were constructed

and the binding ability of infected cells to HBV was investigated using infected mammalian cells.

MATERIALS AND METHODS

Cloning and sequencing of SCCA1, SCCA2, and BP

Primers were synthesized according to the sequences of BPs (Table 1) by Shanghai Boya Company. Total RNA was purified from HepG2 cells using TRIzol (Invitrogen). Reverse transcription was primed using BP2. cDNA was used in a nested PCR reaction to amplified target genes (the external pair of primers were BP1 and BP2, and the internal pair of primers were BP3 and BP4). Cycling for both reactions was performed as follows: at 94 °C for 50 s, 25 cycles at 94 °C for 50 s, at 50–58 °C for 50 s, at 72 °C for 1 min, followed by 1 cycle at 72 °C for 10 min. Products of the same length to the target genes were amplified when annealing temperature ranged between 50 °C and 58 °C. PCR-amplified products under different annealing temperatures were recovered respectively using a gel extract kit (Shanghai Huashun Company) and used directly in ligation with pMD18-T (Dalian Takara Company). Sequencing was performed by Shanghai Boya Company. Sequences were compared with published sequences in GenBank™, and submitted to GenBank™. The product at 56 °C was one SCCA1 (named A1, accession number AY245781). The product at 52 °C was one SCCA2 (named A2, accession number AY245782). Comparison of A1 sequence with BP sequence indicated only five amino acid changes (aa185, aa202, aa349, aa351, aa389). Then A1 was mutated through PCR to obtain the same BP^[5] reported. Inserted genes were confirmed by sequencing.

Table 1 Sequences of primers

Primer	Sequence
BP1	5'-CAC AGG AGT TCC AGA TCA CAT CGA G-3'
BP2	5'-CTG GAA GAA AAA GTA CAT TTA TAT GTG GGC-3'
BP3	5'-CCG CTA GCT CACCAT GAA TTC ACT CAG-3'
BP4	5'-CCG TCG ACT CTA CGG GGA TGA GAA TCT-3'
BpF	5'-GGA TCC ATG AAT TCA CTC AGT G-3'
BPr	5'-CTC GAG CTA CGG GGG TGA GAA TC-3'
EgF1	5'-GAT ATC ATG GTG AGC AAG GGC G-3'
EgF2	5'-GTC GAC TTA CTT GTA CAG CTC GTCC-3'

Construction of recombinant donor plasmids: pFB-A1, pFB-A2, pFB-BP, and pFB-EGFP

A1, A2, and BP were used as templates for a pair of primers (BpF and BPr, Table 1). The amplified products were inserted into the donor plasmid pFastBac1 (Invitrogen) to construct pFB-A1 and pFB-A2 and pFB-BP (Figure 1). EGFP gene was amplified from pEGFP (Clontech) using primers EgF1 and EgF2. The obtained fragments were cloned into pFastBacDual (Invitrogen) to generate pFBD-EGFP (Figure 1). The sequences of the inserts were confirmed by sequencing.

Generation of recombinant baculoviruses^[9]

Recombinant donor plasmids were transformed into DH10Bac competent cells (Invitrogen). Then the transformed cells were plated on LB plates containing X-gal (Sigma), IPTG

(Sigma), gentamycin, kanamycin, and tetracycline for selection of white colonies. The white colonies were cultured in liquid LB containing the same three antibiotics, and the transposed bacmids were extracted by alkaline lysis. There were complementary sequences of M13 primer flanking the LacZ gene of bacmids. The length of PCR-amplified products using M13 primer was used to confirm the transposition. Cycling for both reactions was performed as follows: at 94 °C for 50 s, 30 cycles at 94 °C for 50 s, at 55 °C for 50 s, at 72 °C for 3 min, followed by 1 cycle at 72 °C for 10 min.

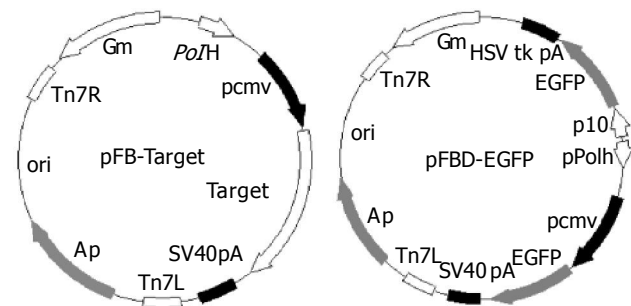


Figure 1 Map of pFB-targets (target is A1, A2 or BP respectively) and pFBD-EGFP.

The resultant bacmids were then used to transfect Sf9 (Invitrogen) cells by using liposome reagent (Cellfectin, Invitrogen) to produce recombinant baculoviruses BacA1, BacA2, BacBP, and BacEGFP. Supernatant of cell culture containing recombinant baculoviruses was collected after 4 d and used to reinfect Sf9 cells to obtain baculoviruses with a higher titer.

Harvest and plaque assay of baculoviruses

Sf9 cells about 80% confluence were seeded in a six-well plate, and incubated at 28 °C for 1 d. Baculoviruses were added to each well of six-well plates at serial dilution and 2 mL 0.8% low-melting agarose (Sigma) prepared using Grace's medium (Invitrogen) was overlaid after 1 h. The plate was stored at 28 °C for 5 d, and the plaques stained with 1% neutral red were counted.

Gene transfer to mammalian cells using recombinant baculoviruses

About 5×10^4 mammalian cells were seeded in each well of a 24-well plate. The medium was removed after 12 h at 37 °C, and 500 μ L Sf9 culture supernatant containing recombinant baculoviruses was added. New medium was used after 8 h at 37 °C and cultured for 48 h.

HBV binding assay and HBV DNA harvest

About 5×10^4 mammalian cells were seeded in each well of a 24-well plate. The medium was removed after 16 h at 37 °C, and washed once with D-hanks. To each well, 200 μ L Dane's particles (2×10^7 /well, Beijing Institute of Biological Products) was added and diluted with an appropriate growth medium of mammalian cells and the cells were incubated at 37 °C in a CO₂ incubator for 4 h. The entire medium was aspirated

off and washed twice with PBS and the cells were collected into an Eppendorf tube. Total HBV DNA was harvested using protease K after separation of cell nuclei and plasma.

Fluorescence PCR analysis

HBV DNA was analyzed using a HBV fluorescence PCR diagnostic kit (Xiamen Xingchuang Company). Cycling was performed in a Roton-gene real-time 2000 PCR system as follows: at 94 °C for 180 s, 50 cycles at 94 °C for 1 s, at 53 °C for 20 s. The data were analyzed and exported by fluorescence PCR analysis software.

Hydrophobicity of primary structure of target genes

Kyte-Doolittle method included in protean program of DNASTAR software was used to analyze hydrophobicity. The average length of amino acid residues used was by default, nine residues. The horizontal line represented the site of amino acids, and the vertical line represented the hydrophobicity index. Positive index meant amino acids were hydrophobic, and negative meant hydrophilic. The larger the absolute value, the stronger the hydrophobicity.

RESULTS

HBV binding to HepG2 cells and WI-38 cells

The following cell lines were used to study the binding to HBV: HepG2, WI-38, BNL 1ME A.7R.1, and CHO. Cells were incubated with an appropriate medium containing Dane's particles. Cell-associated HBV DNA was harvested after being washed with PBS and quantified using real-time fluorescence PCR (Table 2). HepG2 cells could bind to HBV in some degree, and some non-specific bindings to viruses were found in other non-tropic cell lines. WI-38 cells were observed to have a comparatively higher efficiency of report gene transfer and expression^[10]. So WI-38 cells were selected as target cells in following research.

HBV infection to WI-38 cells expressed different target proteins

Recombinant baculoviruses (BacA1, BacA2, BacBP, and

BacEGFP) infected WI-38 cells, respectively. Dane's particles were added to the cells after 48 h. HBV DNA was extracted after 4 h and quantified (Figure 2). We observed no increase in cell-associated virus DNA in cells infected with BacA1 and BacA2, a significant increase in cells infected with BacBP ($P < 0.05$) compared with mock infected cells (infected with BacEGFP) and uninfected cells (blank control), suggesting that expression of BP could make WI-38 acquire susceptibility to HBV binding, but not A1 and A2.

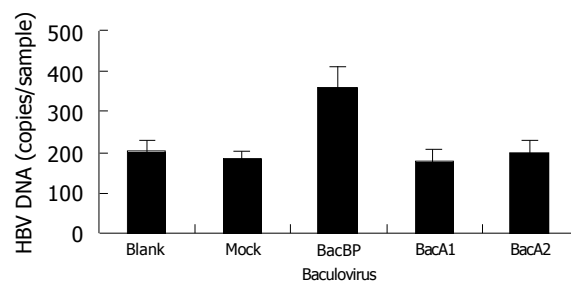


Figure 2 HBV binding to WI-38 cells infected with different recombinant baculoviruses; blank: uninfected cells; mock: BacEGFP infected cells.

SCCA1 protein sequence comparison

The expression of A1 could not enhance HBV binding to cells. Moore *et al*^[8], reported that they isolated a SCCA1 gene (GenBankTM accession number AJ515706) from HepG2 cells by PCR and transfection of this SCCA1 into mammalian cells (both hepatocyte-derived and of non-hepatocyte origin) resulted in increased HBV binding. Site-directed mutagenesis in RSL was utilized to create two AJ515706 gene mutants, P3 and P14. There was no significant difference in binding between the wild type SCCA1 and either RSL mutant. Thus, except A1, the other four SCCA1 protein (BP, AJ515706, P3, P14) expression could increase cell binding to HBV. Based on the sequence comparison (Table 3), amino acid changes of A1 at aa185, aa202, aa349 and aa351 were specific.

Construction of chimeric mutants of BP and A1 and their binding to HBV

The function of serpin involved exposure of the reactive site loop (RSL) to the active site of proteinases^[7]. In order to understand the amino acid changes involved in HBV binding ability, two chimeric mutants, BP-A1 and A1-BP, were constructed by interchanging the fragments of BP and A1 after aa342 (Figure 3).

Then, recombinant baculoviruses containing BP-A1 and A1-BP were generated and infected WI-38 cells were used

Table 2 Comparison of the relative binding to HBV in different cell lines

Cell line	Source	HBV DNA (copies/sample)
HepG2	Human/hepatocellular carcinoma	263 382±16 302
WI-38	Human/lung fibroblast	186 215±15 236
BNL 1ME A.7R.1	Mice/liver	169 221±13 489
CHO	Mice/ovary	105 400±25 076

Table 3 Amino acid sequence differences among five SCCA1 proteins

Amino acid residue	16	47	105	185	202	341	349	351	352	389
BP	F	D	N	Q	P	A	V	A	F	P
AJ515706	S	N	T	Q	P	A	V	A	F	S
P3	S	N	T	Q	P	A	V	A	A	S
P14	S	N	T	Q	P	R	V	A	F	S
A1	F	D	N	R	S	A	E	G	F	S

to investigate their functions in HBV binding (Figure 4). It showed that cells expressing A1-BP could bind to HBV, but BP-A1 could not. Apparently, the susceptibility of SCCA1 to HBV was significantly affected by amino acid changes after aa342.



Figure 3 Construction of chimeric mutants of BP and A1.

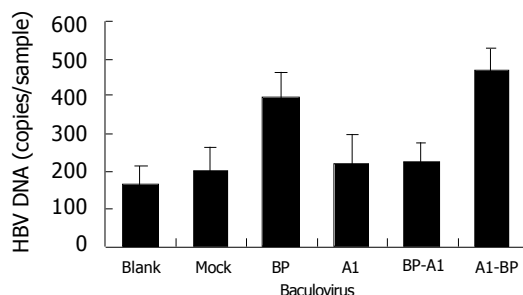


Figure 4 HBV binding to WI-38 cells expressing chimeric mutants of BP and A1. Blank: uninfected cells; mock: BacEGFP infected cells.

Hydrophobicity/hydrophilicity analysis of primary structure of several SCCA1 protein

Comparison of hydrophobicity/hydrophilicity of five SCCA1 proteins (BP, AJ515706, P3, P14, and A1) found that the four proteins with HBV binding ability displayed a relatively high hydrophobicity, and the peak value of hydrophobicity of these proteins was above 2.0. But the peak value of A1, the protein without HBV binding ability, was just 1.07 (Figure 5).

aa349 site-directed mutagenesis of BP and A1 affected HBV binding ability

A1 differed from all the other four proteins for the presence of two residue mutations, V349E and A351G between aa344 and aa354. Notably, at aa349 of A1, it was a low hydrophobic glutamine residue, but not a high hydrophobic valine residue. It was assumed that the hydrophobicity between aa344 and aa354 might have played a role in the process of SCCA1 binding to HBV. To elucidate this hypothesis, we constructed BP_{V349E} and A1_{E349V} utilizing the site-directed mutagenesis method at the aa349 of BP and A1, and found that a deletion mutant BP_{N342} deleted the fragments after BP aa342 (Figure 6). The hydrophobicity of BP_{V349E} between aa344 and aa354 was markedly reduced, but A1_{E349V} was reverse (Figure 5). Recombinant baculoviruses of these mutants were constructed

and infected WI-38 cells were used to analyze the binding of cells to HBV. The results revealed that the expression of A1_{E349V} could enhance cell binding to HBV, but BP_{V349E} could not, suggesting that aa349 was of pivotal importance to the function of SCCA1 (Figure 7). Surprisingly, in the case of BP_{N342} expression, some virus-cell binding ability still remained, implying that the binding of BP to HBV might involve several sites, or aa344-aa354 region was not directly involved in the binding. But the altered hydrophobicity of this region might indirectly lead to conformational changes of HBV binding sites.

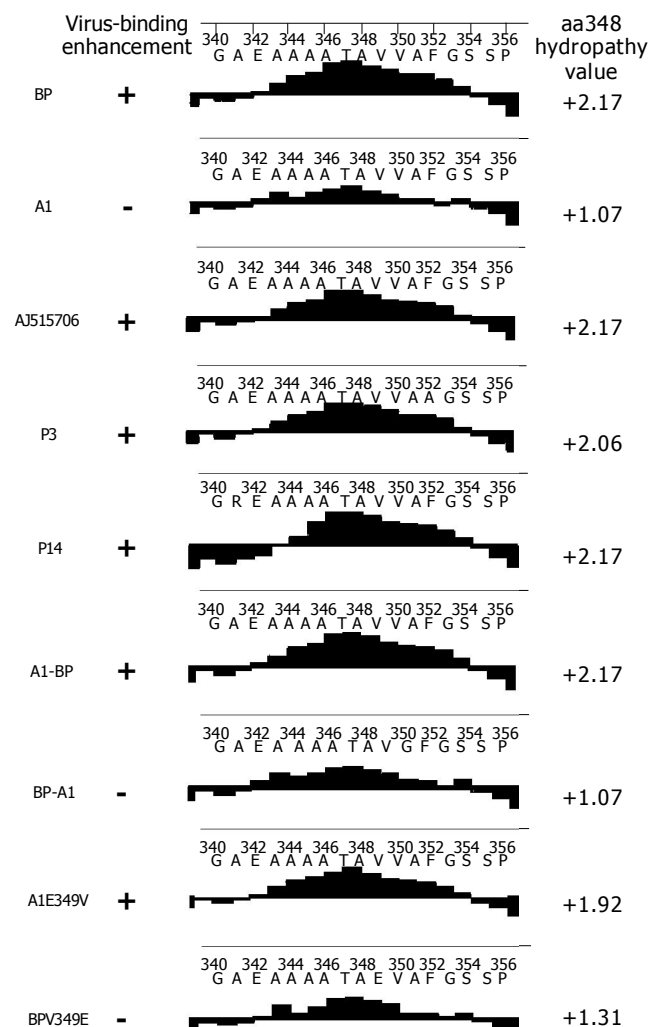


Figure 5 Hydrophobicity analysis of several SCCA1 proteins.

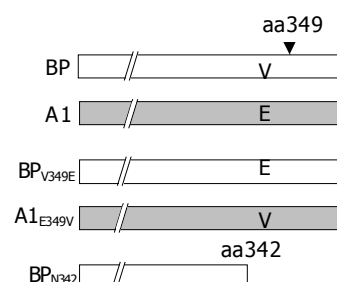


Figure 6 Construction of different SCCA1 mutants.

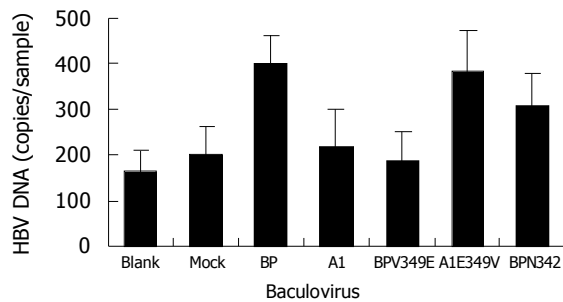


Figure 7 HBV binding to WI-38 cells expressing site-mutants of BP and A1. Blank: uninfected cells; mock: BacEGFP infected cells.

DISCUSSION

BP and AJ515706 are two SCCA1 genes isolated from HepG2 by De Falco *et al*^[5], and Moore *et al*^[8]. Mammalian cells expressing both genes showed an increased HBV binding capacity. But in this study, A1 isolated from HepG2 did not show the same capacity. A2, a SCCA2, which was found to be 91% homologous to SCCA1, also lacked this capacity.

BP, AJ515706 and A1 are of a high sequence homology, but they only have 4-7 different amino acids (Table 3). In order to understand which amino changes were related to HBV binding capacity, two mosaics, BP-A1 and A1-BP, were constructed by interchanging the fragments of BP and A1 at downstream aa342. The results showed that cells expressing A1-BP could bind to HBV, but BP-A1 could not. It seems that the changes of three amino acids between A1 and BP after aa342 were important in the binding to HBV. Two of the amino acid changes (aa349 and aa351) reside in RSL. The hydrophobicity of A1 in RSL was relatively mild, but that of BP and AJ515706 was strong. We created two mutants, A1_{E349V} and BP_{V349E}, by site-directed mutagenesis at the aa349 of BP and A1. The mild hydrophobic glutamic acid of A1 was changed into high hydrophobic valine. Correspondingly, valine of BP was changed into glutamic acid. Cells expressing A1_{E349V} acquired HBV binding ability, but BP_{V349E} lost it. The results revealed that there was an important correlation between hydrophobicity of SCCA1 RSL and HBV binding capacity. The decreased hydrophobicity in this region would lead to the reduction in levels of bound viruses.

In the hydrophobic conformation, DHBV particles were able to bind to liposome and intact cells^[11]. The strong hydrophobicity of BP and AJ515706 in RSL might help them to form stable complexes with HBV or some components of cells, increase attachment to and entry in cells.

Serpin is a conformation-dependent protein. The relationship between structure and function is very special. Until now, this has not been fully understood. The RSL of serpin not only plays an important role in the inhibitory activity of serpin, but also affects the whole conformation of serpin. The binding to ligands and the reciprocity between proteins

can occur at any site of serpin. The conformational changes on RSL may influence other regions of serpin interacting with HBV. So, the RSL and its hydrophobicity are important in the process of cell binding to HBV, but other regions on BP may also interact with HBV. In this study, the result of BP_{N342} might favor this explanation. Expression of BP_{N342} and deletion mutants of RSL, did not result in abrogation of enhanced virus binding to infected WI-38, suggesting the complicated effect of serpin structure.

HepG2 is a cell line from hepatocellular carcinoma. The surface components of each cell are not totally identical. Some different SCCA1 genes were isolated from HepG2 using the similar methods by De Falco *et al*^[5], and Moore *et al*^[8]. These SCCA1 genes have a high sequence homology, but their functions in HBV binding differ markedly. In the normal hepatocytes, are there different SCCA1 genes that express simultaneously? Does the expression of different SCCA1 have a relationship with the susceptibility of cells to HBV and the cytopathological changes after HBV infection? Further research on these problems may contribute to understanding the mechanism of interaction between hepatocytes and HBV.

REFERENCES

- 1 **Chen M**, Zhang J, Chen MC, Xia NS. Progress in HBV receptor research. *Bingdu Xuebao* 2002; **18**: 185-193
- 2 **Neurath AR**, Kent SB, Strick N, Parker K. Identification and chemical synthesis of a host cell receptor binding site on hepatitis B virus. *Cell* 1986; **46**: 429-436
- 3 **Qiao M**, Macnaughton TB, Gowans EJ. Adsorption and penetration of hepatitis B virus in a nonpermissive cell line. *Virology* 1994; **201**: 356-363
- 4 **Pontisso P**, Ruvoletto MG, Tiribelli C, Gerlich WH, Ruol A, Alberti A. The preS1 domain of hepatitis B virus and IgA cross-react in their binding to the hepatocyte surface. *J Gen Virol* 1992; **73**(Pt 8): 2041-2045
- 5 **De Falco S**, Ruvoletto MG, Verdoliva A, Ruvo M, Raucci A, Marino M, Senatore S, Cassani G, Alberti A, Pontisso P, Fassina G. Cloning and expression of a novel hepatitis B virus-binding protein from HepG2 cells. *J Biol Chem* 2001; **276**: 36613-36623
- 6 **Suminami Y**, Kishi F, Sekiguchi K, Kato H. Squamous cell carcinoma antigen is a new member of the serine protease inhibitors. *Biochem Biophys Res Commun* 1991; **181**: 51-58
- 7 **Gettins PG**. Serpin structure, mechanism, and function. *Chem Rev* 2002; **102**: 4751-4804
- 8 **Moore PL**, Ong S, Harrison TJ. Squamous cell carcinoma antigen1-mediated binding of hepatitis B virus to hepatocytes does not involve the hepatic serpin clearance system. *J Biol Chem* 2003; **278**: 46709-46717
- 9 **Duisit G**, Saleun S, Douthe S, Barsoum J, Chadeuf G, Moullier P. Baculovirus vector requires electrostatic interactions including heparan sulfate for efficient gene transfer in mammalian cells. *J Gene Med* 1999; **1**: 93-102
- 10 **Xu CY**, Cheng T, Lu WX, Chen M, Wu T, Wang YB, Zhang J, Xia NS. Mammalian gene-transfer and expression efficiencies of baculovirus bacV-CMV-EGFP. *Shengwu Gongcheng Xuebao* 2004; **20**: 73-77
- 11 **Grgacic EV**, Schaller H. A metastable form of the large envelope protein of duck hepatitis B virus: low-pH release results in a transition to a hydrophobic, potentially fusogenic conformation. *J Virol* 2000; **74**: 5116-5122

Presence and integration of HBV DNA in mouse oocytes

Tian-Hua Huang, Qing-Jian Zhang, Qing-Dong Xie, Li-Ping Zeng, Xi-Fan Zeng

Tian-Hua Huang, Qing-Jian Zhang, Qing-Dong Xie, Xi-Fan Zeng, Research Center of Reproductive Medicine, Shantou University Medical College, Shantou 515041, Guangdong Province, China

Li-Ping Zeng, Department of Gynecology and Obstetrics of the First Affiliated Hospital, Shantou University Medical College, Shantou 515041, Guangdong Province, China

Supported by the National Natural Science Foundation of China, No. 39970374

Correspondence to: Professor Tian-Hua Huang, Research Center of Reproductive Medicine, Shantou University Medical College, 22 Xinling Road, Shantou 515041, Guangdong Province, China. thhuang@stu.edu.cn

Telephone: +86-754-8900845 Fax: +86-754-8900845

Received: 2004-02-27 Accepted: 2004-04-20

Abstract

AIM: Hepatitis B is a worldwide public health problem. To explore the feasibility of hepatitis B virus (HBV) vertical transmission via oocytes, the presence and integration of HBV DNA in mouse oocytes were studied.

METHODS: Genomic DNA was isolated and metaphases were prepared, respectively from mouse oocytes cocultured with pBR322-HBV DNA plasmids. PCR, Southern blot, dot hybridization and fluorescence *in situ* hybridization (FISH) were performed to explore the existence and integration of HBV DNA in oocytes.

RESULTS: PCR detected positive bands in the tested samples, and then Southern blot revealed clear hybridization signals in PCR products. Final washing solutions were collected for dot hybridization and no signal for HBV DNA was observed, which excluded the possibility that contamination of washing solutions gave rise to positive results of PCR and Southern blot. FISH demonstrated that 36 of 1 000 metaphases presented positive signals.

CONCLUSION: HBV DNA sequences are able to pass through the zona and oolemma to enter into oocytes and to integrate into their chromosomes. HBV DNA sequences might be brought into embryo via oocytes as vectors when they are fertilized with normal spermatozoa.

© 2005 The WJG Press and Elsevier Inc. All rights reserved.

Key words: HBV DNA; Transmission; Mouse oocyte; Integration; Chromosomes

Huang TH, Zhang QJ, Xie QD, Zeng LP, Zeng XF. Presence and integration of HBV DNA in mouse oocytes. *World J Gastroenterol* 2005; 11(19): 2869-2873

<http://www.wjgnet.com/1007-9327/11/2869.asp>

INTRODUCTION

Hepatitis B is a worldwide public health problem. In Far-East Asia and tropical Africa, chronic carriers of hepatitis B virus (HBV) represent 10% or more of population^[1]. Both chronic hepatitis B and hepatitis C are prevalent among the 12 million Asians and Pacific Islanders living in the USA^[2]. It is still a potential risk for public health as a result of immigration from countries with a high prevalence of HBV infection although there is a low incidence rate among the indigenous population in North America and Scandinavian countries^[3-5]. Chronic active hepatitis and liver cirrhosis are major causes of mortality^[1,6]. Moreover, epidemiological studies have clearly shown the importance of HBV in hepatocellular carcinoma (HCC). In China, 500 000 to one million new cases appear every year^[1] and 73% of patients with chronic hepatitis and 78% and 71% of those with cirrhosis and HCC, respectively, are HBsAg positive^[7]. Therefore, studies on transmission of HBV are of substantial importance in virology as well as in public health.

The transmission routes of HBV through blood transfusion^[8,9]; body fluids including serum, saliva, vaginal secretions, breast milk, and semen^[10-14]; intrauterine infection^[15,16]; cell, tissue, and organ transplantation^[17,18] and others including hemodialysis units and intravenous drug injection^[19-23] have been documented. Hadchouel *et al*^[24], using molecular hybridization, confirmed the presence of integrated HBV DNA sequences in spermatozoa from two of three patients with HBV infection. They assumed that the presence of integrated sequences in spermatozoa suggested the possibility of true vertical transmission of HBV via the germ line. Using interspecific *in vitro* fertilization between zona-free hamster ova and spermatozoa from nine patients with HBV infection, we prepared human sperm metaphases for fluorescence *in situ* hybridization (FISH) with the biotin-labeled full length HBV DNA probe. The specific fluorescent signal spots for HBV DNA were seen in sperm chromosomes of one patient with chronic persistent hepatitis. Our results suggest that there is evidence that HBV DNA can integrate into human sperm chromosomes and that human sperms with HBV DNA sequences can normally complete the fertilization with oocytes and zygotes can develop to the first cleavage. The above studies provided some evidence for the feasibility of HBV vertical transmission via spermatozoa. Zhong *et al*^[25] analyzed HBV nucleotide sequences isolated from three sets of mother/child pairs and found that the nucleotide and deduced amino acid sequences were absolutely identical between the mother and children in two of three families. Their results suggested the vertical transmission linkage of HBV between the mother and children. An interesting question is that whether HBV

vertically transmits from mother to offspring via oocytes. To answer this question, the presence and integration of HBV DNA in oocytes should be confirmed. This is the purpose of our present study.

MATERIALS AND METHODS

Preparation of mouse oocytes

Mature female mice were induced to superovulate by intramuscular injection of 0.2 IU/g body weight of pregnant mare serum gonadotropin (PMSG, Ningbo Hormone Products Co., Ltd, China) into the inguinal region on d 1 of estrous cycle followed by administration of 0.2 IU/g body weight of human chorionic gonadotropin (HCG, Ningbo Hormone Products Co., Ltd) after 48-58 h. Superovulated oocytes were collected from ampullar region of oviducts 16 h after HCG injection and freed from cumulus cells by gently pipetting in 0.1% hyaluronidase and then washed thrice in modified TYH medium (mTYH)^[26]. The oocytes were divided into two groups. Group A was transferred into mTYH containing 0.2 µg/mL pBR322-HBV DNA plasmids and group B into HBV DNA-free mTYH. The oocytes of two groups were kept in a CO₂ incubator (37 °C, 50 mL/L CO₂ in air) for 2 h and then washed with mTYH eight times. The oocytes and washing solutions of the last three times were collected respectively.

Labeling of HBV DNA probe for Southern blot and dot hybridization

Recombinant plasmids, pBR322-HBV containing full length (3.2 kb) HBV genomic DNA, were taken to be amplified according to the routine PCR method. The PCR products, 591-bp HBV DNA fragments containing HBx coding region, were labeled with biotin using random primer biotin labeling of DNA (NEB® Phototope® Kit). Unincorporated nucleotides were separated by cold ethanol precipitation method.

Labeling of HBV DNA probe for FISH

Recombinant plasmids, pBR322-HBV containing full length (3.2 kb) HBV genomic DNA, were taken to be amplified according to the routine transformation method. The 3.2 kb HBV DNA probe was labeled with biotin-14-dATP by nick translation (BioNick DNA Labeling System, GIBCO BRL). Unincorporated nucleotides were separated by cold ethanol precipitation method.

DNA extraction

Cumulus-free oocytes from groups A and B were treated with 0.1% trypsin to remove the zona pellucida, then washed twice immediately in fresh mTYH. Genomic DNA was isolated from the zona-free oocytes through the digestion of lysis buffer, proteinase K and RNase I; the extraction of phenol-chloroform and the precipitation of ethanol.

Polymerase chain reaction (PCR)

The tested DNA samples were from group A oocytes in eight experiments. The positive and negative controls were from recombinant plasmids, pBR322-HBV and group B oocytes respectively.

Primers used for PCR amplification (Sangon Company, Shanghai, China) were as follows: P1 (up) (5'-gaactcctagcagc-ttggtt-3'); P2 (down) (5'-tgaacagtaggacatgaaca-3'). The expected size of the product was 591 bp and this fragment contained region X of HBV genome. A total of 50 µL reaction included 41.5 µL ddH₂O, 5 µL 10× buffer, 1 µL dNTPs (10 mmol/L), 0.5 µL primer 1 (100 pmol/L), 0.5 µL primer 2 (100 pmol/L), 0.5 µL Taq DNA polymerase (5 IU/5 µL), 1 µL DNA template (1 µg/µL). The thermocycling conditions were at 94 °C for 5 min, and 35 cycles each at 94 °C for 1 min, at 50 °C for 1 min, at 72 °C for 1 min, and finally at 72 °C for 10 min in a Peltier thermal cycler (PTC 100). The amplification products were visualized by staining with ethidium bromide, after electrophoresis on 1% agarose gel.

Southern blot hybridization

Each 15 µL amplification product from PCR assays was separated by electrophoresis on 1% agarose gel and blotted onto a nylon membrane (Schleicher & Schuell BioScience, Inc., USA). Southern blot analysis was carried out using biotin DNA labeling and detection kits (New England Biolabs, Inc., USA) with the biotin-labeled HBV DNA sequence containing HBx coding region as a probe.

Dot hybridization

The tested samples were from the solutions of the last three washings of group A in each experiment. All of the 24 tested samples in eight experiments were collected for dot hybridization. The positive and negative controls were from recombinant plasmids, pBR322-HBV and the washing solutions of group B respectively.

Each 2 µL of the samples of washing solution was subjected to denaturing in boiling water bath for 5 min and dotted onto a nylon membrane (Schleicher & Schuell BioScience, Inc.). The blots were dried and baked for 2 h at 80 °C. Dot hybridization was carried out using the biotin-labeled HBV DNA sequence containing HBx coding region as a probe. After an overnight hybridization at 68 °C, the blots were treated successively with SSC, sodium dodecyl sulfate, blocking reagent, streptokinase, alkaline phosphatase, CDP-star assay buffer, followed by the procedures of exposure, development and fixation, and analysis.

Preparation of oocyte metaphases

Oocyte metaphases were prepared using a gradual fixation air-dry method^[27]. In brief, oocytes were first exposed to a hypotonic solution containing 0.068 mol/L potassium chloride with 0.1% bovine serum albumin for about 30 min. The swollen oocytes were transferred to the bottom of a glass spot well pre-filled with fixative I (methanol:acetic acid:distilled water 5:1:3). When the color of oocytes changed from brown to white and subtransparent (after about 5-7 min), the oocytes were aspirated and then released gently onto the slide. Then fixative II (methanol:acetic acid 3:1) was dispensed carefully over the surface of the slide until it covered the oocytes. The slide was immersed in a Coplin jar containing fixative II for about 5 min or more. After that it was gently removed and placed in a Coplin jar

containing fixative III (methanol:acetic acid:distilled water 3:3:1) for 1 min. The slide was slowly removed and dried gradually with a stream of moist air.

FISH of oocyte chromosomes

FISH and detection of signals were performed with the procedures described previously.

RESULTS

PCR of the DNA from oocytes

The positive bands for HBV DNA in eight samples from group A oocytes were observed. A bright positive band was seen in the positive control and no band in the negative control was seen (Figure 1).

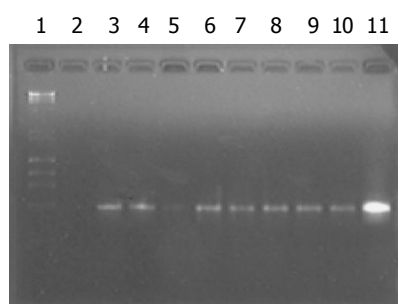


Figure 1 Electrophoresis of amplification products of DNA from mouse oocytes. Lane 1: markers; lane 2: negative control; lane 11: positive control; lanes 3-10: amplification products of DNA from group A oocytes in eight experiments.

Southern blot hybridization

Consistent with electrophoresis of amplification products, Southern blot analysis revealed that the hybridization signals for HBV DNA in each of eight samples from group A oocytes were observed. A strong signal was seen in the positive control and no signal was found in the negative control (Figure 2).

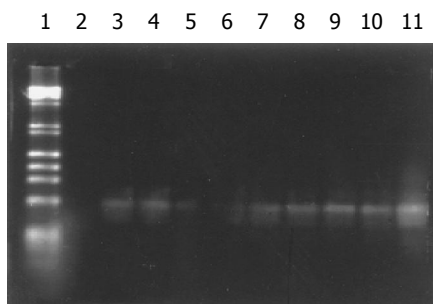


Figure 2 Southern blot results of amplification products of DNA from mouse oocytes. Lane 1: Markers; lane 2: negative control; lane 11: positive control; lanes 3-10: amplification products of DNA from group A oocytes in eight experiments.

Dot hybridization for washing solutions

No signal for HBV DNA was observed in all of the 24 tested samples. A strong signal was seen in the positive

control and no signal was observed in the negative control (Figure 3).

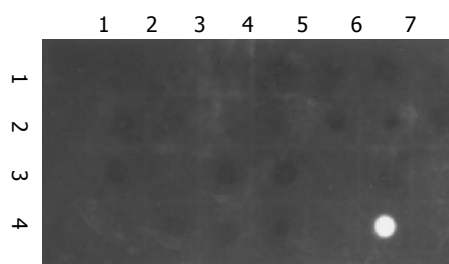


Figure 3 Dot hybridization for the washing solution. Dots (1,1): negative control; Dots (4,6): positive control; Dots (1,2) to (1,7), (2,1) to (2,7), (3,1) to (3,7), (4,1) to (4,4): the washing solution samples from group A in eight experiments.

FISH of oocyte chromosomes

Using specific whole length HBV DNA as a probe to perform FISH with oocyte chromosomes, 36 of 1 000 metaphases from group A oocytes presented positive signals for HBV DNA and no signal was found in 500 metaphases from group B oocytes (Figure 4).

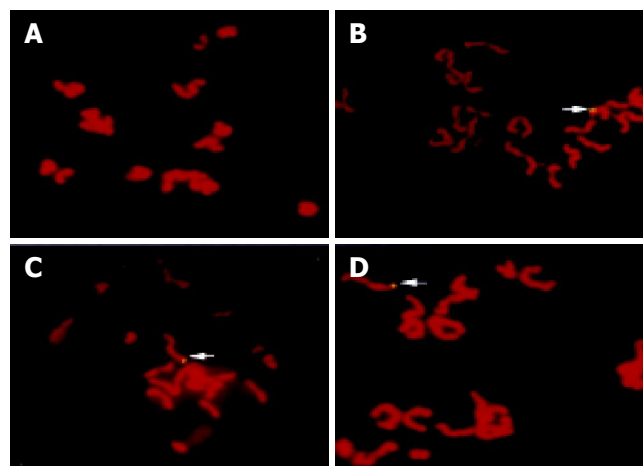


Figure 4 FISH results. **A**: No signal of HBV DNA integration in the metaphase from group B oocytes. **B-D**: Clear signals of HBV DNA integration in the metaphases from group A oocytes (arrow).

DISCUSSION

To confirm vertical transmission of HBV from mother to children via oocytes is an exciting program and of substantial importance. However, such studies have been hampered since neither experimental animals nor cell culture systems have been available. Thus it is very crucial to establish a model system for study on HBV transmission via oocytes. Zona pellucida is a glycoprotein coat surrounding the egg proper. It protects the fragile eggs and embryos from physical damage^[28]. Can zona become a barrier to the entry of HBV DNA sequence into the oocytes? This is a key question for establishing such a model system, which we primarily have to answer.

In our study, the PCR products were visualized after electrophoresis on 1% agarose gel. A bright specific band for HBV DNA and no specific band were detected in the positive and negative controls respectively. The specific bands for HBV DNA were observed in all the samples from group A oocytes that were cocultured with HBV DNA in eight experiments (Figure 1). Consistent with PCR results, Southern blot analysis revealed that the hybridization signals for HBV DNA in all the amplification products from group A oocytes were observed. A strong signal was seen in the positive control and no signal was found in the negative control (Figure 2). It was impossible that the contamination of washing solutions gave rise to such positive results of PCR and Southern blot in the tested oocytes because they were washed eight times in each experiment and dot hybridization showed negative results in the last three of eight washing solutions in our study (Figure 3). Two reasons might contribute to the positive results in the tested oocytes. One was that some samples contained HBV-plasmid DNA that stuck firmly to the zona surface, the other was that some samples contained HBV DNA fragments that passed through the zona and oolemma and entered into the oocytes. The latter has been confirmed by our FISH experiments, the former was not excluded.

Although HBV replication is restricted to a more or less stringent host cell range, it is clear that viral integration is not restricted to any particular organ but occurs in many tissues including host somatic cells and spermatozoa^[21,29-32]. However, so far no study on its integration into chromosomes of mammalian oocytes has been reported. We prepared metaphases of mouse oocytes cocultured with HBV DNA and performed FISH with a full length HBV DNA as a probe. Thirty-six of thousand metaphases presented positive signals and no FISH signal was detected in all the metaphases from 500 oocytes not cocultured with HBV DNA (Figure 4). This result indicated that the zona could not become a barrier to the entry of HBV DNA sequences into the oocytes and the oocytes cultured *in vitro* could passively take up exogenous DNA fragments. This result also indicated that HBV DNA fragments were able to enter into oocytes and integrate into their chromosomes. It is undoubted that HBV DNA sequences could be brought into embryos when the oocytes with the presence and integration of HBV DNA were fertilized with normal spermatozoa. So the *in vitro* culture system bringing HBV DNA into embryos via oocytes might be used as a model system for study on the exact vertical transmission of HBV via oocytes. Tsurimoto *et al*^[33] demonstrated that HBV genome in an integrated state could act as a template for viral gene expression and replication. It would provide direct evidence for HBV transmission via oocytes if we could demonstrate the replication and expression of such genes of HBV in embryonic cells.

Hepatotropism is a prominent feature of HBV infection. It has been reported that cell lines of nonhepatic origin do not independently support HBV replication^[34]. The reason why viral tropism was restricted to hepatocytes is largely unknown, although some investigations have indicated that HBV DNA methylation^[35,36], liver-enriched transcription factors^[37-39] and some receptors of hepatocytes^[40,41] contribute

to hepatotropism. Moreover, replication of HBV was found in transfected nonhepatic cells by ectopic expression of liver-enriched transcription factors^[42]. DNA methylation is a very important manner for cells to regulate the expression of host genes and viral genes entering into cells. These genes would be almost fully methylated in sperms and probably the female germ line^[43]. It was reported that DNA methylation patterns of the male and female pronuclei were erased in morula and early blastulae, when blastocysts formed, most of DNAs were demethylated. Following implantation, however, there was a surge of *de novo* methylation affecting the entire genome. During subsequent development, tissue-specific genes underwent programmed demethylation, which might cause their activation^[44]. Preimplantation embryonic cells are non-specialized cells that are different from hepatic cells as well as specialized nonhepatic cells. It might be helpful for exploring the mechanism of hepatotropism and HBV vertical transmission to study on the contribution of methylation of HBV DNA, individual and multiple liver-enriched transcription factors and some membrane receptors in preimplantation embryonic cells with HBV sequences brought via oocytes *in vitro* culture system. This would be our further study in the future projects.

ACKNOWLEDGMENTS

We are very grateful to Dr. Yi-Ping Hu, from the Second Military Medical University, for his kindness in providing us with the recombinant plasmid, pBR322-HBV.

REFERENCES

- 1 Tiollais P, Pourcel C, Dejean A. The hepatitis B virus. *Nature* 1985; **317**: 489-495
- 2 Nguyen MH, Keffe EB. Chronic hepatitis B and hepatitis C in Asian Americans. *Rev Gastroenterol Disord* 2003; **3**: 125-134
- 3 Gjørup IE, Skinhoj P, Bottiger B, Plesner AM. Changing epidemiology of HBV infection in Danish children. *J Infect* 2003; **47**: 231-235
- 4 Chu CJ, Keffe EB, Han SH, Perrillo RP, Min AD, Soldevila-Pico C, Carey W, Brown RS, Luketic VA, Terrault N, Lok AS. Hepatitis B virus genotypes in the United States: results of a nationwide study. *Gastroenterology* 2003; **125**: 444-451
- 5 Gjørup IE, Smith E, Borgwardt L, Skinhoj P. Twenty-year survey of the epidemiology of hepatitis B in Denmark: effect of immigration. *Scand J Infect Dis* 2003; **35**: 260-264
- 6 Sevinir B, Meral A, Gunay U, Ozkan T, Ozuysal S, Sinirtas M. Increased risk of chronic hepatitis in children with cancer. *Med Pediatr Oncol* 2003; **40**: 104-110
- 7 Merican I, Guan R, Amarapuka D, Alexander MJ, Chutaputti A, Chien RN, Hasnain SS, Leung N, Lesmana L, Phiet PH, Sjalfoellah Noer HM, Sollano J, Sun HS, Xu DZ. Chronic hepatitis B virus infection in Asian countries. *J Gastroenterol Hepatol* 2000; **15**: 1356-1361
- 8 Vrielink H, Reesink HW. Transfusion-transmissible infections. *Curr Opin Hematol* 1998; **5**: 396-405
- 9 Kleinman SH, Kuhns MC, Todd DS, Glynn SA, McNamara A, DiMarco A, Busch MP. Frequency of HBV DNA detection in US blood donors testing positive for the presence of anti-HBc: implications for transfusion transmission and donor screening. *Transfusion* 2003; **43**: 696-704
- 10 Scott RM, Snitbhan R, Bancroft WH, Alter HJ, Tingpalapong M. Experimental transmission of hepatitis B virus by semen and saliva. *J Infect Dis* 1980; **142**: 67-71
- 11 Darani M, Gerber M. Letter: Hepatitis-B antigen in vaginal secretions. *Lancet* 1974; **2**: 1008

- 12 **Linnemann CC**, Goldberg S. Letter: HBsAg in breast milk. *Lancet* 1974; **2**: 155
- 13 **Linnemann CC**, Goldberg S. Letter: Hepatitis-B antigen in saliva and semen. *Lancet* 1974; **1**: 320
- 14 **Meheus A**. Risk of hepatitis B in adolescence and young adulthood. *Vaccine* 1995; **13** Suppl 1: S31-S34
- 15 **Liu Y**, Zhang J, Zhang R, Li S, Kuang J, Chen M, Liu X. Relationship between the immunohistopathological changes of hepatitis B virus carrier mothers' placentas and fetal hepatitis B virus infection. *Zhonghua Fuchanke Zazhi* 2002; **37**: 278-280
- 16 **Xu DZ**, Yan YP, Choi BC, Xu JQ, Men K, Zhang JX, Liu ZH, Wang FS. Risk factors and mechanism of transplacental transmission of hepatitis B virus: a case-control study. *J Med Virol* 2002; **67**: 20-26
- 17 **Eastlund T**. Infectious disease transmission through cell, tissue, and organ transplantation: reducing the risk through donor selection. *Cell Transplant* 1995; **4**: 455-477
- 18 **Sugauchi F**, Orito E, Ohno T, Kato H, Suzuki T, Hashimoto T, Manabe T, Ueda R, Mizokami M. Liver transplantation-associated de novo hepatitis B virus infection: application of molecular evolutionary analysis. *Intervirology* 2002; **45**: 6-10
- 19 **Krekulova L**, Rehak V, da Silva Filho HP, Zavoral M, Riley LW. Genotypic distribution of hepatitis B virus in the Czech Republic: a possible association with modes of transmission and clinical outcome. *Eur J Gastroenterol Hepatol* 2003; **15**: 1183-1188
- 20 **Murakami H**, Kobayashi M, Zhu X, Li Y, Wakai S, Chiba Y. Risk of transmission of hepatitis B virus through childhood immunization in northwestern China. *Soc Sci Med* 2003; **57**: 1821-1832
- 21 **Otedo AE**, Mc'Ligeyo SO, Okoth FA, Kayima JK. Seroprevalence of hepatitis B and C in maintenance dialysis in a public hospital in a developing country. *S Afr Med J* 2003; **93**: 380-384
- 22 **Burdick RA**, Bragg-Gresham JL, Woods JD, Hedderwick SA, Kurokawa K, Combe C, Saito A, LaBrecque J, Port FK, Young EW. Patterns of hepatitis B prevalence and seroconversion in hemodialysis units from three continents: the DOPPS. *Kidney Int* 2003; **63**: 2222-2229
- 23 **Ansa VO**, Udoma EJ, Umoh MS, Anah MU. Occupational risk of infection by human immunodeficiency and hepatitis B viruses among health workers in south-eastern Nigeria. *East Afr Med J* 2002; **79**: 254-256
- 24 **Hadchouel M**, Scotto J, Huret JL, Molinie C, Villa E, Degos F, Brechot C. Presence of HBV DNA in spermatozoa: a possible vertical transmission of HBV via the germ line. *J Med Virol* 1985; **16**: 61-66
- 25 **Zhong M**, Hou J, Luo K. Identification of vertical transmission of hepatitis B virus from mother to children by direct sequencing a segment of surface gene of hepatitis B virus. *Zhonghua Yixue Zazhi* 1996; **76**: 194-196
- 26 **Tateno H**, Kamiguchi Y. *In vitro* fertilisation of Chinese hamster oocytes by spermatozoa that have undergone ionophore A23187-induced acrosome reaction, and their subsequent development into blastocysts. *Zygote* 1996; **4**: 93-99
- 27 **Kamiguchi Y**, Mikamo K. An improved, efficient method for analyzing human sperm chromosomes using zona-free hamster ova. *Am J Hum Genet* 1986; **38**: 724-740
- 28 **Yanagimachi R**. Mammalian fertilization In: Knobil E, Neill JD, editors. *The physiology of reproduction* Vol IV New York: Raven 1994: 229
- 29 **Naumova AK**, Kisselev LL. Biological consequences of interactions between hepatitis B virus and human nonhepatic cellular genomes. *Biomed Sci* 1990; **1**: 233-238
- 30 **Naumova AK**, Korenev VI, Leonov BV, Tsibinogin VV, Kiselev LL. DNA of the hepatitis B virus in human generative cells. *Genetika* 1986; **22**: 166-168
- 31 **Naumova AK**, Favorov MO, Keteladze ES, Nosikov VV, Kisselev LL. Nucleotide sequences in human chromosomal DNA from nonhepatic tissues homologous to the hepatitis B virus genome. *Gene* 1985; **35**: 19-25
- 32 **Xu X**. The possible role of sperm in family HBV infection. *Zhonghua Liuxingbingxue Zazhi* 1992; **13**: 337-339
- 33 **Tsurimoto T**, Fujiyama A, Matsubara K. Stable expression and replication of hepatitis B virus genome in an integrated state in a human hepatoma cell line transfected with the cloned viral DNA. *Proc Natl Acad Sci USA* 1987; **84**: 444-448
- 34 **Tang H**, McLachlan A. Transcriptional regulation of hepatitis B virus by nuclear hormone receptors is a critical determinant of viral tropism. *Proc Natl Acad Sci USA* 2001; **98**: 1841-1846
- 35 **Korba BE**, Wilson VL, Yoakum GH. Induction of hepatitis B virus core gene in human cells by cytosine demethylation in the promoter. *Science* 1985; **228**: 1103-1106
- 36 **Miller RH**, Robinson WS. Integrated hepatitis B virus DNA sequences specifying the major viral core polypeptide are methylated in PLC/PRF/5 cells. *Proc Natl Acad Sci USA* 1983; **80**: 2534-2538
- 37 **Miyoshi E**, Fujii J, Hayashi N, Ueda K, Towata T, Fusamoto H, Kamada T, Taniguchi N. Enhancement of hepatitis-B surface-antigen expression by 5-azacytidine in a hepatitis-B-virus-transfected cell line. *Int J Cancer* 1992; **52**: 137-140
- 38 **Zhang P**, McLachlan A. Differentiation-specific transcriptional regulation of the hepatitis B virus nucleocapsid gene in human hepatoma cell lines. *Virology* 1994; **202**: 430-440
- 39 **Johnson JL**, Raney AK, McLachlan A. Characterization of a functional hepatocyte nuclear factor 3 binding site in the hepatitis B virus nucleocapsid promoter. *Virology* 1995; **208**: 147-158
- 40 **Raney AK**, Johnson JL, Palmer CN, McLachlan A. Members of the nuclear receptor superfamily regulate transcription from the hepatitis B virus nucleocapsid promoter. *J Virol* 1997; **71**: 1058-1071
- 41 **Thung SN**, Gerber MA. Polyalbumin receptors: their role in the attachment of hepatitis B virus to hepatocytes. *Semin Liver Dis* 1984; **4**: 69-75
- 42 **Seifer M**, Heermann KH, Gerlich WH. Replication of hepatitis B virus in transfected nonhepatic cells. *Virology* 1990; **179**: 300-311
- 43 **Cedar H**. DNA methylation and gene activity. *Cell* 1988; **53**: 3-4
- 44 **Heby O**. DNA methylation and polyamines in embryonic development and cancer. *Int J Dev Biol* 1995; **39**: 737-757

Multigene tracking of quasispecies in viral persistence and clearance of hepatitis C virus

Song Chen, Yu-Ming Wang

Song Chen, Yu-Ming Wang, Department of Infectious Diseases, Southwest Hospital, Third Military Medical University, Chongqing 400038, China

Supported by the National Natural Science Foundation of China, No. 39870694

Correspondence to: Song Chen, MD, Department of Infectious Diseases, Southwest Hospital, Third Military Medical University, 30 Gaotanyan Zhengjie, Shapingba District, Chongqing 400038, China. cs196@medmail.com.cn

Telephone: +86-23-68753196

Received: 2004-04-06 Accepted: 2004-05-24

CONCLUSION: HCV persistence is associated with a complexity quasispecies and positive selection of HVR1 by the host immune system.

© 2005 The WJG Press and Elsevier Inc. All rights reserved.

Key words: Hepatitis C virus; Immune system

Chen S, Wang YM. Multigene tracking of quasispecies in viral persistence and clearance of hepatitis C virus. *World J Gastroenterol* 2005; 11(19): 2874-2884

<http://www.wjgnet.com/1007-9327/11/2874.asp>

Abstract

AIM: To investigate the evaluation of hepatitis C virus (HCV) quasispecies in the envelope region and its relationship with the outcome of acute hepatitis C.

METHODS: HCV quasispecies were characterized in specimens collected every 2-6 mo from a cohort of acutely HCV-infected subjects. We evaluated two individuals who spontaneously cleared viremia and three individuals with persistent viremia by cloning 33 1-kb amplicons that spanned E1 and the 5' half of E2, including hypervariable region 1 (HVR1). To assess the quasispecies complexity and to detect variants for sequencing, 33 cloned cDNAs representing each specimen were assessed by a combined method of analysis of a single-stranded conformational polymorphism and heteroduplex analysis. The rates of both synonymous and nonsynonymous substitutions for the E1, HVR1 and E2 regions outside HVR1 were analyzed.

RESULTS: Serum samples collected from chronic phase of infection had higher quasispecies complexity than those collected from acute phase of infection in all individuals examined. The genetic diversity (genetic distance) within HVR1 was consistently higher than that in the complete E1 (0.0322 ± 0.0068 vs -0.0020 ± 0.0014 , $P < 0.05$) and E2 regions outside HVR1 (0.0322 ± 0.0068 vs 0.0017 ± 0.0011 , $P < 0.05$) in individuals with persistent viremia, but did not change markedly over time in those with clearance of viremia. For individuals with persistent viremia, the rate of nonsynonymous substitutions within the HVR1 region ($2.76 \times 10^{-3} \pm 1.51 \times 10^{-3}$) predominated and gradually increased, as compared with that in the E1 and E2 regions outside HVR1 ($0.23 \times 10^{-3} \pm 0.15 \times 10^{-3}$, $0.50 \times 10^{-3} \pm 0.10 \times 10^{-3}$). By contrast, the rates of both nonsynonymous and synonymous substitutions for the E1 and E2 regions including HVR1 were consistently lower in individuals with clearance of viremia.

INTRODUCTION

Hepatitis C virus (HCV), a member of the *Flaviviridae* family, is the major cause of chronic liver disease worldwide^[1]. HCV is a positive-sense single-strand RNA virus with a genome that encodes one large polypeptide in which putative structural proteins are located at the N-terminal end, and the putative nonstructural proteins are located at the C-terminal end^[2]. One of the important characteristics of HCV is that its genome exhibits significant genetic heterogeneity as a result of the accumulation of mutations during viral replication. The genetic sequences of HCV variants are very heterogeneous, varying by more than 30% across the entire genome among the six major genotypes, 20% among subtypes, and up to 10% within a subtype^[3]. Analogous to other RNA viruses, HCV circulates in an infected individual as a population of close-related, yet heterogeneous, sequences: the quasispecies^[4-6]. The quasispecies distribution of HCV might have important biological consequences. It has been proposed that this genetic heterogeneity allows HCV to escape immune pressure and to establish chronic infection^[7-9]. Furthermore, the existence of a heterogeneous population of HCV may influence the outcome of antiviral therapy; and resistance to treatment might result from selection of minor viral populations during this therapy^[10]. Therefore, it is important to define accurately quasispecies populations of HCV.

Many analyses of viral quasispecies of HCV have been published. The majority of these studies have focused on the most variable part of the HCV genome, hypervariable region 1 (HVR1) of glycoprotein E2^[11-13]. Mutation of this region of the genome is believed to be associated with viral persistence via immune escape mechanisms^[14,15]. It is well known that genetic heterogeneity of HCV extends throughout the entire genome. However, it is still not known whether significant mutation occurred in other regions of

the HCV envelope genes during the chronic infection. In addition, most studies assessing the diversity of HCV quasispecies have been conducted by amplifying selected portions of the genome by PCR, isolating individual subgenomic fragments by a cloning product, and then characterizing the nucleotide sequence of each clone^[16-18]. Evaluating the diversity of HCV quasispecies in clinical samples often requires the sequencing of a large number of clones, but because of the effort and expense, published studies have obtained sequence information from a small number of colonies per subject.

Two recent developments enabled us to investigate genetic variation of the HCV envelope genes and its relationship with the outcome of acute hepatitis C. First, we identified and characterized the long-term virologic outcomes for five individuals with acute HCV infection. Second, we developed a method for efficiently and accurately characterizing the HCV quasispecies^[19-21]. In this study, these resources were used to examine viral complexity and distortion in amino acid sequences of subjects with persistent viremia *vs* those with clearance of viremia.

MATERIALS AND METHODS

Patients and samples

From November 1998 to January 2002, 284 current injection drug users (IDUs) totaling 125 HCV-infected individuals have been monitored in Chongqing. Five individuals were identified as HCV seroconverters when a sample tested positive for antibody to HCV following at least one negative result. After more than 3 years of semiannual follow-up subsequent to seroconversion, two distinct patterns of viremia were noted. For two subjects, HCV RNA was undetectable for a minimum of 2 years in at least two serum samples from each person. In contrast, for three subjects, HCV RNA remained detectable in the last sample tested. Clinical and virological backgrounds of the subjects studied are summarized in Table 1.

Detection of serum virological parameters

These samples were tested for antibodies to HCV (HCV EIA 2.0; Ortho Diagnostics Raritan, NJ) and, if these results were positive, by a strip immunoblot assay (RIBA HCV 2.0; Chiron Corporation, Emeryville, CA). HCV RNA was detected by a quantitative reverse transcriptase PCR (RT-PCR) assay (AMPLICOR HCV MONITO, Roche Diagnostic Systems, Branchburg, NJ), the linear range of which was determined to be 500-500 000 copies/mL of serum by our and other laboratories^[22,23]. Liver tests, including alanine aminotransferase (ALT) levels in serum, were performed at the first clinical examination and repeated during follow-up. Hepatitis B surface antigen, anti-HBc, anti-HBe and anti-HIV IgM were negative in all subjects detected by ELISA. HCV subtype was determined by the RT-PCR-restriction fragment length polymorphism analysis targeted to the 5' non-coding region of the HCV^[24].

Envelope region amplification

HCV RNA characterization was based on examination of 33 cloned cDNAs spanning the 1 025-nucleotide (nt) region thought to encode envelope protein E1 and a segment of E2, including HVR1. Total RNA was extracted from 100 µL serum using 500 µL of TRIzol LS Reagent (Life Technologies, Gaithersburg, MD) at room temperature, followed by chloroform extraction and isopropanol precipitation in the presence of 20 µg of glycogen (Boehringer Mannheim, Indianapolis, IN). The RNA pellet was washed with 75 mL/L ethanol and then air dried briefly and redissolved in 50 µL of diethyl pyrocarbonate-treated water with 10 mmol/L dithiothreitol (Promega, Madison, WI) and 5 U of RNasin ribonuclease inhibitor (Promega). After incubation at 65 °C for 5 min, 5 µL purified RNA was used to generate cDNA in a 20-µL reaction mixture at 37 °C for 1 h with 20 U of Moloney murine leukemia virus reverse transcriptase (Promega) and first-round PCR reverse primer.

The entire 20-µL cDNA synthesis reaction mixture was

Table 1 Molecular, biochemical, and serological characterization of five HCV primary infections

Subjects	Samples	Age (yr) /sex	Duration of infection (mo)	Genotype	Log ₁₀ [HCV RNA] ¹	HCV RNA	ALT level (nkat/L) ²	Result of ELISA
A	A1	30/M	0	3b	7.30	++++	1 833.70	-
	A2		6		6.20	+++	583.45	+
	A3		14		5.30	+++	616.79	+
B	B1	28/F	0	3b	7.50	++++	1 933.72	-
	B2		6		6.40	+++	1 150.23	+
	B3		12		6.90	+++	1 533.64	+
C	C1	33/M	0	1b	6.41	+++	683.47	+
	C2		24		5.25	+++	383.41	+
	C3		34		4.16	++	166.70	+
E	E1	20/M	0	1a	6.80	+++	4 017.47	-
	E2		3.5		4.20	++	766.82	+
	E3		9		0	-	583.45	+
	E4		24		0	-	400.08	-
F	F1	28/M	0	1b	6.00	++++	3 067.28	-
	F2		2		5.60	+++	1 066.88	+
	F3		7		0	-	666.80	+
	F4		18		0	-	483.43	-

¹Number of HCV RNA molecules per milliliter plasma. Time zero is the time where the first sample was available; others indicate are times after time zero. ²Normal value, <666.80 nkat/L.

used for the first-round PCR in a 25- μ L reaction mixture containing 0.75 U Expand HF polymerase mixture (Boehringer Mannheim), 1.5 mmol/L MgCl₂, 0.2 mmol/L concentration of deoxynucleoside triphosphates, and 500 μ mol/L concentrations of primers. The mixed oligonucleotides primers were used for RT-PCR (Table 1). Degenerate bases are indicated with standard codes of the International Union of Pure and Applied Chemistry. Nucleotide positions were numbered according to the HCV-J6 sequence. One microliter of the first-round reaction mixture was added to the second-round PCR, which had the same reagents as in the first round except for primers. Thermal-cycling conditions for the inner and outer reactions were pre-denaturation for 120 s at 94 °C, followed by 35 amplification cycles of 45 s at 94 °C, 45 s at 60 °C, and 120 s at 72 °C (during the last 25 cycles, the elongation time was increased by 20 s per cycle).

Cloning of cDNA and complexity analysis of 33 cloned cDNAs by gel shift

The 1-kb HCV cDNA product was ligated into vector pT-adv and used to transform *Escherichia coli* TOP 10F' competent cells (TA Cloning kit; CLONTECH Laboratories, Inc.). Transformants were detected according to the manufacturer's protocol, and cloning efficiency was >90%.

Then 80 g/L polyacrylamide gel electrophoresis was carried out with the addition of 150 g/L urea to increase the resolution. For each subject, the gel shift patterns of 33 cloned cDNAs were examined by amplifying a 470-bp sequence spanning E1 gene and 570-bp sequence including HVR1, responsively, and by a nonradioactive method that detected distinct variants within a sample by using a combination of heteroduplex analysis (HDA) and single-stranded conformational polymorphism (SSCP) on a single gel (SSCP+HDA)^[19]. Sequences obtained from the serial passage were analyzed by a divergent variant from the acute-phase sample from each subject. A clonotype is defined as two or more cloned cDNAs that have indistinguishable patterns of electrophoretic migration by SSCP+HDA. The complexity of the quasispecies was characterized by the clonotype ratio, calculated as the number of clonotypes divided by 33, the number of cloned cDNAs examined^[20]. The clonotype ratio therefore varied from 0.03 (homogenous) to 1.

Nucleotide sequencing

To examine each subject's quasispecies for signature sequences (motifs uniquely shared by a group of sequences) and for evaluations in the sensitivity of the SSCP+HDA method, a subset of cloned cDNAs was identified. For each subject, at least two cloned cDNAs were selected for sequencing based on gel shift patterns: one from the majority clonotype, another from each clonotype consisting of the cloned cDNAs with the largest heteroduplex gel shift. Sequences were positively determined from the M13 reverse primer and negatively from T7 promoter binding sites of plasmid clones by using a PRISM 377 DNA Sequencer (version 3.3; Applied Biosystems, Inc., Foster City, CA). Sequences were assembled by using the ESEE3s program, and primer sequences were removed prior to analysis.

Phylogenetic analysis

DNA distance matrices were calculated by using the DNADIST program, maximum-likelihood, with a transition-to-transversion ratio of 4.25^[25], and phylogenetic trees were generated by the Neighbor-joining program with random addition. Subtype reference sequences used for phylogenetic analysis had the following GenBank accession numbers: 1a, M62321; 1b, D10934; 2a, D00944; 2b, D10988; 3a, D17763; 4a, Y11604; 5a, Y13184; 6a, Y12083.

Nonsynonymous substitutions per potential nonsynonymous site (dN) and synonymous substitutions per potential synonymous site (dS) were calculated by the method of Nei and Gojobori^[26].

Statistical analysis

Quantitative values were compared using the Student's *t* test, the Kruskal-Wallis test or the analysis of the variance when necessary. *P* values lower than 0.05 were considered statistically significant. All statistical calculations were performed by using the SPSS for Windows, version 8.0 software package.

RESULTS

Clonotypes detected by SSCP+HDA method

The SSCP+HDA used in this investigation showed that each specimen contained a swarm of distinct but related variants represented by clonotypes. The number of clonotypes within the E1 region varied from 2 to 6 per sample, and within the E2/HVR1 region changed from 3 to 21 per sample. A subset of clonotypes always persisted in E1 during serial passages from each subject. In E2/HVR1 derived from five individuals, the subjects with self-limited viremia had the persistence of clonotypes during serial passages, whereas acute and chronic samples from persistent-infected cases shared no clonotype (Figure 1).

The quasispecies complexity was examined by assessing 33 cDNA clones from each specimen using the clonotype ratio of E2/HVR1. Serum samples collected from chronic phase of infection had higher quasispecies complexity than those collected from acute phase of infection (Figure 2), but no trends were observed as clonotype ratio values changed with the changes in circulating viral load (Figure 3).

Representative sequence analysis

Using SSCP+HDA to select representative cloned cDNAs, we identified 26 distinct cloned cDNAs for sequencing (Figure 4). The sequences of single variants from two subjects (A and B) were 1 022 bp and the sequences from two other subjects (C and F) were 1 021 bp, which had a 1-bp deletion, and those of subject E was 1 019 bp, which had a 3-bp deletion. To determine the genetic identity of cDNA clones of the same clonotype, two representative sequences representing the majority clonotype were compared for each specimen. No two-cloned cDNAs identified as being distinct by SSCP+HDA analysis had identical sequences, underscoring that the SSCP+HDA method was both highly sensitive and specific in detecting differences among cDNA clones, as previously reported. For each majority clonotype, which of the two sequences was free

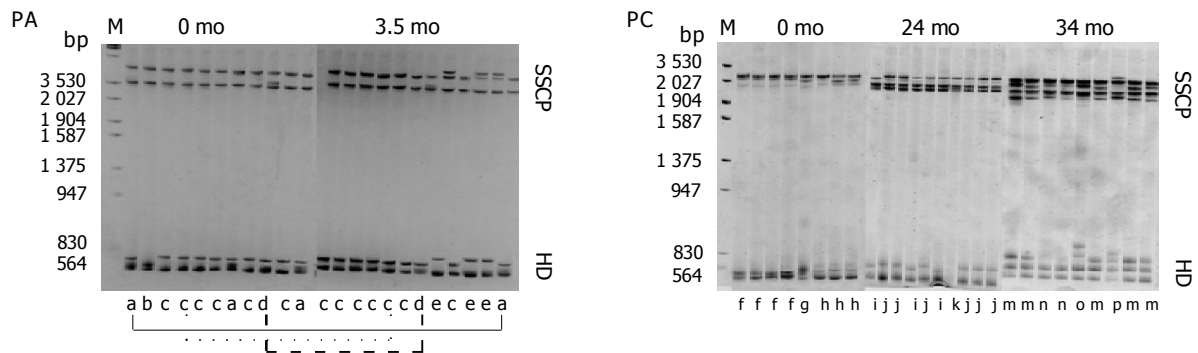


Figure 1 Analysis by SSCP+HDA of the E2 region (including the HVR1) of HCV in two HCV-positive IDUs. Clonotypes (groups of electrophoretically indistinguishable cloned cDNAs) were assigned sequential letter designations (a-p). As can be seen, the number of clonotypes in patient with clearance of viremia (PA) E did not differ significantly after antibody seroconversion compared

with the pre-antibody seroconversion sample, and the clonotypes composition remained largely unchanged during the follow-up. In contrast, the number of clonotypes increased in patient with persistent viremia (PC) C, and the clonotypes composition showed constant evolution during the follow-up.

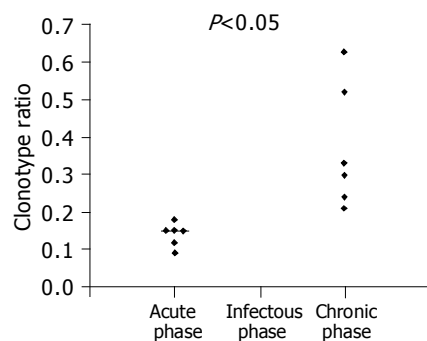


Figure 2 Clonotype ratio and outcome. Clonotype ratio values obtained for the samples from five individuals at each time point were calculated as described in Materials and methods.

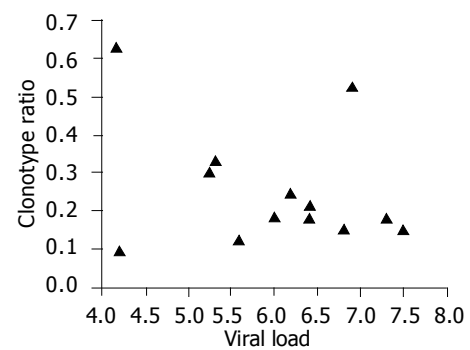


Figure 3 Correlation between HCV clonotype ratio and serum HCV RNA load. No correlation was found between them ($r = 0.2$).

of sporadic substitutions, one was used in all subsequent analyses to represent that clonotype (Table 2).

Figure 5 displays a dendrogram illustrating E2 sequence diversity in individuals from the two study groups. Sequences from each individual tended to cluster tightly, segregated away from clusters of sequences from other individuals in the same genotype.

Genetic evolution of viral quasispecies and outcome of acute infection

The genetic distances (genetic diversity) of the HCV

quasispecies were assessed by examining viral sequences spanning the envelope genes both within and outside the HVR1 for intrahost evolutionary analysis (Table 3). Results of these analyses revealed a difference in virus evolution according to the outcome of the disease. During serial passages, individuals who cleared viremia did not change significantly in the genetic diversity, whereas those with persistent viremia showed a marked increase in diversity. When the genetic diversity both in the complete E1 and the E2 regions outside HVR1, based on the analysis of 102 predicted amino acids, was analyzed, the viral diversity was

Table 2 Primers for amplification of E1 and E2 regions of HCV genome¹

Region	Designation	Sequence	5' to 3' polarity	Position of 5' base ²
C/E2	P1	GCAACAGGGAAYYTDCCCGGTGCTC	Outersense	837–862
	P2	TTCATCCASGTRCAVCCRAACCA	Outer antisense	2 020–1 998
	P3	CCATGTGCTCYTTYTCTATCTTC	Inner sense	855–874
	P4	GTITAAARCARTACACYGGRCCRCANAC	Inner antisense	1 882–1 857
C/E1	P3	CCATGTGCTCYTTYTCTATCTTC	Sense	855–874
	P5	GTRGGBGACCAGTTCATCATCAT	Antisense	1 333–1 311
E2	P6	GGGAYATGATGATGAAGTGGIC	Sense	1 306–1 327
	P4	GTITAAARCARTACACYGGRCCRCANAC	Antisense	1 882–1 857

¹Degenerate bases are indicated with standard codes of the international union of Pure and Applied Chemistry. ²Position of 5' base relative to the HCV genomic sequence of the HCV J6 strain.

Table 3 Comparison of changes in genetic diversity of viral strains in individuals with self-limited and persistent viremia¹

Patient group	Number of patients	Time points ²	Interval (wk)	Change in genetic diversity ($\times 10^{-2}$)		
				E1	HVR1	E2
Clearance	2	B vs A	3.75 \pm 0.35	0.08 \pm 0.20	0.30 \pm 0.71	-0.37 \pm 0.04
Persistence	3	B vs A	12.67 \pm 9.86	-0.20 \pm 0.14	3.22 \pm 0.68 ^a	0.17 \pm 0.11
		C vs A	20.0 \pm 12.16	0.06 \pm 0.23	4.10 \pm 2.35	0.21 \pm 0.39
		B vs C	7.33 \pm 3.03	-0.26 \pm 0.11	-0.89 \pm 1.81	0.15 \pm 0.71

¹Genetic diversity was assessed by using the DNADIST program, maximum-likelihood. The data are represented as mean \pm SE. Negative values indicate a reduction in genetic diversity of viral strains; positive values indicate an increase in genetic diversity of viral strains. ²The first time point (A) corresponds to the baseline, the second (B) and the third (C) after antibody seroconversion. ^a $P < 0.05$ time points B vs A of self-limited vs persistent viremia by unpaired Welch's t test.

Nucleotide sequences of envelope region at 3.5-mo serial samples from the subject E

E1.1	855	ATGTGCTCTTTCTCTATCTTCCTCTAGCCCTGCTTCTCGCTGACTGTGCCGCTTCAGCCTACCAAGTGCACACTCCACGGGGCTTTATCATG	951	(26)
E1.2		-----C-----		(4)
E2.1		-----C-----		(29)
E2.2		-----C-T-----		(3)
E1.1	952	TCACCAATGACTGCCCTAACTCGAGCATTGTGTACGAGCAGCTGATGCCATCTGCACACTCCGGGGTGCCTCCCTTGCCTTCGCGAGGGTAACAC	1 048	(26)
E1.2		-----		(4)
E2.1		-----		(29)
E2.2		-----		(3)
E1.1	1 049	CTCGAGGTGTTGGGTGGCGGTGACCCCCACGGTGGCCACCGGATGGCAAACCTCCCAACACGACGCTTCGACGTCACATCGATCTGCTTGTTCGGG	1 145	(26)
E1.2		-----		(4)
E2.1		-----		(29)
E2.2		-----		(3)
E1.1	1 146	AGTGCCACCTTCTGCTCGGCTCTTTACGTGGGGGACTTGTGCGGGTCCGCTCTTCTTGTGCGGTGAGCTGTTACCTTCTCTCCAGGCGCCACTGGA	1 242	(26)
E1.2		-----		(4)
E2.1		-----		(29)
E2.2		-----A-----		(3)
E1.1	1 243	CGACGCAAGACTGCAATTGTTCTATGTATCCCGCCATATAACGGGTGATCGCATGGCATGGGATGTGATGTAAGTGGTCCCTACGACGGCATT	1 339	(26)
E1.2		-----A-----		(4)
E2.1		-----		(29)
E2.2		-----A-----		(3)
E1.1	1 340	GGTAGTGGCTCAGCTGCTCCGATCCCAAGCCATCTTGGATATGATCGCTGGTGGCCACTGGGGAGTTCTAGCGGGCATAGCGTATTTCCTCATG	1 436	(26)
E1.2		-----		(4)
E2.1		-----		(29)
E2.2		-----		(3)
E1.1	1 437	GTGGGGAAGTGGGCGAAGGTCGTGGTGGTGTCTGCTATTTCGCCGGCGTGTACGCGGATACCTACGTCACCGGGGAAGTGGCGGCACACCGTAT	1 533	(26)
E1.2		-----G-----		(4)
E2.1		-----		(29)
E2.2		-----		(3)
E1.1	1 534	CGAGACTCAGCAGACTGCTCTACCGGGCGCAAAGCAGAATATCCAGCTGATCAACTCCAACGGCAGCTGGGACATCAATAGGACAGCCCTGAACATG	1 630	(26)
E1.2		--G-----G-----C-----		(4)
E2.1		--G-----G-----C-----		(29)
E2.2		--G-----C-----		(3)
E1.1	1 631	TAACGACAGCCTCAACACCGGCTGGATAGCAGGGCTCTTTTACCACTACAAATCAACTCTTCAGGCTGCCCGAGAGAATGGCCAGCTGTCATCTCT	1 727	(26)
E1.2		-----		(4)
E2.1		-----		(29)
E2.2		-----		(3)
E1.1	1 728	CTTACCGATTTTGCCAGGGCTGGGGCCCTATCGGGTACGCCAATGGAAGCGGCCCGACCATCGCCCTACTGCTGGCACTACCCCCAAGACCTT	1 824	(26)
E1.2		-----		(4)
E2.1		-----T-----		(29)
E2.2		-----		(3)
E1.1	1 825	GTGGTATTGTTCCGGCACAGAGTGTCTGTGGCCGGTGTACTGTTTAA	1 873	(26)
E1.2		-----G-----G-----		(4)
E2.1		-----G-----G-----		(29)
E2.2		-----G-----G-----		(3)

Nucleotide sequences of envelope region at 2-mo serial samples from the subject F

F1.1	855	ATGTGCTCTTTCTCTATCTTCCTTTAGCCTTGTCTATCTGTTTGACCAACCCAGCTTCCGCTTACGAAGTGCCTAACGTGTCGGGATATACCATG	951	(21)
F1.2		-----		(2)
F2.1		-----		(23)
F2.2		-----		(1)
F1.1	952	TCACGAACGACTGCTCCAACCTAAGCATTGTGTATGAGGCAGCGGACCTGATCATGCATACCCCTGGGTGCGTGCCCTGCGTTCCGGGAAGGCAACTC	1 048	(21)
F1.2		-----		(2)
F2.1		-----		(23)
F2.2		-----		(1)
F1.1	1 049	CTCCCGTTGCTGGGTAGCGCTCACTCCACGCTCGCGGCCAGGAACGCCACGATCCCACTGCGACAGTACGACGGCATGTGATCTGCTCGTTGGG	1 145	(21)
F1.2		-----		(2)
F2.1		-----		(23)
F2.2		-----		(1)
F1.1	1 146	GCGGCTGCTTCTCTTCCGCCATGTACGTGGGGGATCTCTGCGGATCTGTTTCTTGTCTCTCAGCTGTTACCTTCTCGCTCGCGGTATGAGA	1 242	(21)
F1.2		-----		(2)

Accession	Gene	Strain	Position	Sequence	Length	GC Content
F2.1				-----		(23)
F2.2				-----		(1)
F1.1	1	243	CAATACAGGACTGCAATTGCTCAATCTATCCCGCCACGTAACAGGTACCCGCATGGCTTGGGATATGATGATGAAGTGGTCGCCTACAACAGCTCT	1	339	(21)
F1.2			-----			(2)
F2.1			-----			(23)
F2.2			-----			(1)
F1.1	1	340	AGTGGTGTGCGAGTTACTCCGGATCCCTCAAGCCGTCATGGACATGGTGGTGGGGGCCACTGGGGAGTCTGGCGGGCCTTGCCCTACTATGCCATG	1	436	(21)
F1.2			--A-----			(2)
F2.1			-----			(23)
F2.2			--A--A-----			(1)
F1.1	1	437	TCCATGGTGGGGAATGGGCTAAGGTTTGATTGTGATGCTACTCTTCGCCGCGCTTGATGGGGATACCTACGCGTCTGGGGGGCGCAGGGCGCGT	1	533	(21)
F1.2			-----			(2)
F2.1			-----			(23)
F2.2			-----T-----			(1)
F1.1	1	534	CCACCCTCGGGTTACGTCCTCTTTACACCTGGGGCCTCTCAGAAGATCCAGCTTATAAATACCAATGGTAGCTGGCATATCAACAGGACTGCCCT	1	630	(21)
F1.2			-----			(2)
F2.1			-----			(23)
F2.2			-----C-----			(1)
F1.1	1	631	CAACTGCAATGACTCCCTCAATACTGGGTTTCTTGCCGCGCTGTTCTATACACACAGGTTCAACGCGTCCGGATGCGCAGAGCGCATG6CCAGCTGC	1	727	(21)
F1.2			G-----A-----			(2)
F2.1			G-----C-----			(23)
F2.2			G-----G-----			(1)
F1.1	1	728	CGCCCCATTGATACATTCGATCAGGGCTGGGGCCCCATCACTTATACTGAGCCAGATAGCTCGGACCAGAGGCCCTATTGCTGGCATACGCGCCTC	1	824	(21)
F1.2			-----T-----			(2)
F2.1			-----T-----			(23)
F2.2			-----T-----			(1)
F1.1	1	825	GAAAGTGGGCATCGTACCTGCGTCGTGCGGTCAGTGATTCTTTAA	1	875	(21)
F1.2			-----G-----			(2)
F2.1			-----G-----			(23)
F2.2			-----T-----G-----			(1)

Nucleotide sequences of envelope region at 14-mo serial samples from the subject A

Nucleotide sequences of envelope region at 27 kb serial samples from the subject 7		
A1.1	855	ATGTGCTCCTTTTCTATCTTCTCTCCTCGCTCTCTTCTCCTGCTTGACTTGCCCCGCGTCTGGTCTAGAGTACAGGAACACAGTCCGGCCATACATAC
A1.2		-----C-----
A2.1		-----
A2.2		-----
A3.1		-----
A3.2		-----C-----
A1.1	952	TTACCAACGACTGCTCTAACAAGAGCAATTGTGTATGAGGCCGACGATGTAATCTTGCACTACCCGGATGTGTGCCCTGCACCGCGACCGGCAACAA
A1.2		-----A-----
A2.1		-----T-----A-----C-----
A2.2		-----T-----A-----C-----
A3.1		-----G-----C-----
A3.2		-----T-----G-----A-----
A1.1	1 049	GACATCGTGCTGGACACCAAGTGTACCAACAGTGGCCGTGAGATATCCTGGCGCGACCACCGCATCGATCCGCGGTACAGTGGATATGCTGGTGGGC
A1.2		-----T-----T-----
A2.1		-----T-----
A2.2		-----T-----
A3.1		-----C-----
A3.2		-----T-----C-----T-----G-----T-----
A1.1	1 146	GCGGCCACGTTGTGCTCAGCACTATACGTCGGGGACCTCTGCGGGGCCGTGTTCTTGTGGGCAAGCATTACCTTCAGGCCCTCGCCGACACCGGA
A1.2		-----C-----
A2.1		-----A-----A-----C-----
A2.2		-----A-----C-----
A3.1		-----
A3.2		-----
A1.1	1 243	CTGTACAGACGTGCAACTGCTCAATCTACCCAGGCCACATTTTCAGGACATCGTATGGCGTGGGATATGATGATGAAGTGGTCTCCTGCAGTCGGGCT
A1.2		-----C-----
A2.1		-----C-----C-----A-----
A2.2		-----C-----C-----A-----
A3.1		-----C-----C-----A-----
A3.2		-----T-----C-----C-----A-----
A1.1	1 340	GTTAATATCACACTTAATGCGGTTGCCCAAACTTCTTTGACCTGGTGACAGGGGCCACTGGGCGGTAAATGGCAGGCCCTGCCTATTTTTCATG
A1.2		-----G-----C-----G-----
A2.1		-----G-----C-----T-----G-----C-----C-----
A2.2		-----G-----G-----T-----C-----T-----G-----C-----C-----
A3.1		-----G-----G-----T-----GT-----G-----C-----
A3.2		-----G-----T-----GT-----G-----C-----
A1.1	1 437	CAAGGTAACCGGGCCAAGGTCGGCATCGTGCTGATCATGTTCTCGGGAGTGGATCGGGGCAGTACACCACTGGTGGCTCCGCGGGCCGCACTGCTT
A1.2		-----T-----T-----
A2.1		-----T-----A-----A-----C-----C-----A-----T-----CA-----G-----
A2.2		-----G-----T-----A-----A-----C-----C-----A-----T-----CA-----A-----
A3.1		-----T-----T-----T-----A-----A-----C-----AA-----AT-----G-----
A3.2		-----T-----T-----T-----AC-----A-----G-----C-----AA-----T-----GG-----
A1.1	1 534	CCGGGCTTGTGGGCCGTGTTCTCCTCGGGCCCGCAACAGAACCTGCACCTAGTGAATTCCAACGGGTGCTGGCACATCAATAGCACTGCCCTGAATTG
A1.2		-----T-----
A2.1		-----T-----C-----TC-----AGC-----G-----G-----T-----C-----
A2.2		-----T-----A-----TG-----AGC-----G-----G-----T-----C-----
A3.1		-----A-----C-----A-----A-----G-----G-----G-----A-----T-----A-----C-----T-----
A3.2		-----A-----C-----A-----A-----G-----G-----G-----A-----T-----A-----C-----T-----

A3.2		-----C-----A--A-----G-----G--G-----A-T-----A-----C-----T-----	(2)
A1.1	1 631	CAACGATTCTTAAACACCGGGTTCATAGCAGGGCTCTTCTACTATCATAAGTTCAACTCCACGGGGTGCCAGATCGAATGTCCAGATGCAAGCCC	1 727 (27)
A1.2		-----	(1)
A2.1		--T-----C-----TA-----C-----CG-----C--G-----	(15)
A2.2		--T-----C-----TA-----C-----C-----C-----	(2)
A3.1		-----A-----T-----A-----C--C-----A--T--C-----C-----	(12)
A3.2		-----A-----T-----A-----C--C-----A--T--C-----C-----	(2)
A1.1	1 728	ATCACAGCTTTTCGAGCAGGGGTGGGGTTCCTGACAGATGTCAACGTGTCTGGTTCCAGTGAGGACAGACCATAATTGCTGGCACTACCCACCCAGGC	1 824 (27)
A1.2		-----	(1)
A2.1		-----A-----A--T-----A-----C-----A--	(15)
A2.2		-----A-----A--A-----A-----C-----A--	(2)
A3.1		-----A-----G-----A--A-----C-----	(12)
A3.2		-----A-----G-----A-----C-----	(2)
A1.1	1 825	CCTGCGAGACAGTCAAGGCACGAGTCTGCGGCCGGTGTACTGCTTTAA	1 876 (27)
A1.2		-----T--A-----	(1)
A2.1		-----A--C--G--C-----A-----	(15)
A2.2		-----A--C--G--C-----	(2)
A3.1		-----A--C--C--A--GTT-----A--T-----	(12)
A3.2		-----A--C--C--A--GTT-----A-----A-----	(2)

Nucleotide sequences of envelope region at 12-mo serial samples from the subject B

B1.1	855	ATGTGCTCTTTTCTATCTTCTCCTCGCTCTTCTCCTGCTTGACTTGCCCGCGTCTGGTCTGGAGCAGGAACGCGTCTGGCCTATACATAC	951 (21)
B1.2		-----A-----	(2)
B2.1		-----C-----C-----A-----	(19)
B2.2		-----C-----A-----	(2)
B3.1		-----T-----T-----A-----G--	(10)
B3.2		-----T-----T-----A-----A-----G--	(1)
B1.1	952	TTACTAATGACTGCTCTAACGGCAGCATTGTGTATGAGGCCGACGAGGTGATCTTGACCTACCCGGATGTGTGCCCTGCACCGCAACCGGCAACCA	1 048 (21)
B1.2		-----	(2)
B2.1		-----C-----G-----	(19)
B2.2		-----C-----G-----	(2)
B3.1		-----C--C--T-----T--G-----T-----	(10)
B3.2		-----C--C--T-----T--G-----T-----	(1)
B1.1	1 049	GACATCGTGTGGACACCAAGTGTACCAACAGTGGCCGTCAGGCATCTGCGCGACACCACCGCGTCGATCCGCAACCATGTGGATATGCTGGTGGGC	1 145 (21)
B1.2		A-----	(2)
B2.1		A-----A-----T-----G-----	(19)
B2.2		-----T-----G-----	(2)
B3.1		A-----C-----G--T-----T-----A--C-----T-----G-----	(10)
B3.2		A-----C-----G--T-----T-----T-----A--C-----T-----G-----	(1)
B1.1	1 146	GCAGCCACGTTGTGCTGTGCACTATACATCGGGGACCTCTGCGGGGCCGTGTTCTTGTTGGGACAAGCATTACCTTCAGGCCCCGCCGACACACGA	1 242 (21)
B1.2		-----CA-----	(2)
B2.1		-----CA-----G-----T-----G-----	(19)
B2.2		-----CA-----G-----T-----G-----	(10)
B3.2		-----CG-----G--T-----T-----T-----T-----G-----	(1)
B1.1	1 243	CTGTACAGACGTGCAACTGCTCAATTTACCCAGGCCACATTTTCAGGACATCGTATGCGCGTGGGACATGATGATGAAGTGTGCCCTGCAATCGGGCT	1 339 (21)
B1.2		-----CA-----	(2)
B2.1		-----A-----G-----	(19)
B2.2		-----A-----T-----	(2)
B3.1		-----T-----A-----T-----	(10)
B3.2		-----T-----A-----T-----	(1)
B1.1	1 340	GTTAATATCACACTTGATGCGGTTGCCCTCAAACCTTCTTTGACCTGGTCATAGGGGCCACTGGGGCGTGATGGCAGGCCTCGCTTACTTCTCTATG	1 436 (21)
B1.2		-----	(2)
B2.1		-----C-----A--C-----A--G-----C--T--T--C--	(19)
B2.2		-----C-----C-----A--G-----C--T--T--C--	(2)
B3.1		-----C-----C-----C--T-----C--	(10)
B3.2		-----C-----C-----C--T-----C--	(1)
B1.1	1 437	CAAGGCAACTGGGCCAAGTCTGCATCTGCTGATCATGTTCTCGGGAGTGGATGCGGGCACACACACCACCGCGGTGCCCGGCTTACTCTACTT	1 533 (21)
B1.2		-----A-----	(2)
B2.1		-----T-----G--G-----A--GT-----GT--T--CT-----CG--A--G--C--	(19)
B2.2		-----T-----G--G-----A--GT-----T--T--CT-----CG-----C--	(2)
B3.1		-----T-----G--G-----T-----AC--T-----G--A--CC-----CG--A--G--	(10)
B3.2		-----T-----G--G-----T-----AC--T-----A--C-----CG--A--G--	(1)
B1.1	1 534	CCGGGCTTGCGAGCCTGTTCACTCAGGGCCCCGAAACAGAACCTGCACTTGGTGAATTCTAACGGGTCTAGGCACATCAACAGCACTGCCCTGAGTTG	1 630 (21)
B1.2		-----C-----C-----T-----	(2)
B2.1		-----T--T-----T--C--C-----C-----T-----C-----G-----T-----A--	(19)
B2.2		-----T--T-----T--C--C-----C-----T-----C-----G-----T-----A--	(2)
B3.1		AA--A--A-----CTCA--C-----T-----A--	(10)
B3.2		AA--A--CA-----CTCA--C-----T-----A--	(1)
B1.1	1 631	CAATGATTCCCTAAACACCGGGTTCATAGCAGGGCTCATCTACCATCACAAGTTCAACTCCACGGGGTGCCAGCCCGAATGTCCAGTGTCAAGCCC	1 727 (21)
B1.2		-----	(2)
B2.1		-----C-----T-----T-----T-----T-----T-----	(19)
B2.2		-----C-----T-----T-----T-----T-----T-----	(2)
B3.1		-----C-----A-----T-----T-----T--C--T-----A--	(10)
B3.2		-----C-----A-----T-----T-----T--C--T-----A--	(1)
B1.1	1 728	ATCACTGCTTTCAAGCAGGGGTGGGGTTCCTGAAAGATGTCAACATATCTGGTCCCAGTGAAGACAGACCATACTGCTGGCACTACCCACCCAGAC	1 824 (21)
B1.2		-----	(2)
B2.1		-----A-----C-----G-----G-----G-----	(19)
B2.2		-----A-----C-----G-----G-----G-----	(2)
B3.1		-----A-----C-----G-----G-----G-----	(10)

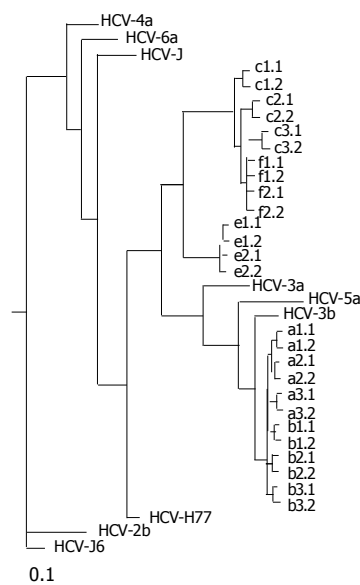


Figure 5 Unrooted tree showing the diversity of 384-nt E2 sequences from subjects. Letters represent individuals who cleared viremia (e and f) and those with persistent viremia (a-c), and lowercase numbers indicate the different clones obtained. The number and line at the bottom denote the proportion of nucleotides substituted for a given horizontal branch length. Dendrograms were produced using the Neighbor-joining program.

consistently lower than within HVR1 in individuals with persistent viremia. To investigate whether the different patterns of viral variation were due to positive selection, dN and dS both within and outside HVR1 were measured by comparing the sequences obtained at each time point from each subject with the sequence of the first time point (Figure 6). For individuals with persistent viremia, the mean number of dN within HVR1 predominated and gradually increased, compared to that in the E1 and E2 regions outside HVR1. However, these differences did not reach significance. By contrast, both dN and dS for the E1 and E2 regions including HVR1 was consistently lower in individuals with clearance of viremia. These data indicated that HCV persistence was associated with genetic evolution of the viral quasispecies and positive selection of HVR1 by the host immune system.

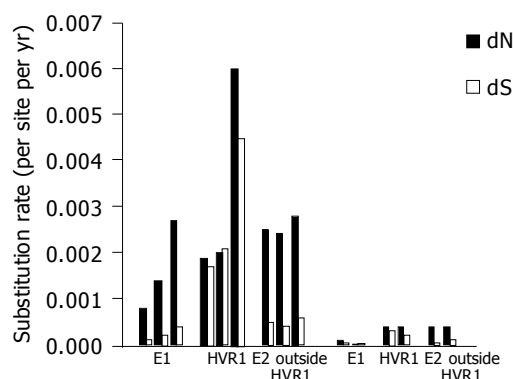


Figure 6 Nonsynonymous rate and synonymous rates of mutations for the E1, HVR1 and E2 regions outside HVR1 from five individuals.

DISCUSSION

This study, using PCR clones derived from two regions of the HCV envelope sequence E1, and E2/HVR1, which possessed different degrees of nucleotide sequence variability, showed that the SSCP+HDA might be applicable to the investigation of HCV genetic diversity at the intrahost level. Sequence differences in a relatively large number of clones from a subgenomic fragment (33 per sample) could be screened during a single procedure. Clones yielding differing gel migratory positions were rapidly identified to be processed further for nucleotide sequencing analyses if required. In each individual there was a major variant (most commonly observed) examined in E1, accompanied by minor variants, which were nearly always found in subsequent specimens in serial infection. The persistence of some variants through serial passage might indicate that E1 had functional constraints on genetic variation, such as RNA secondary structure or binding sites factors that regulated replication or translation^[20]. However, two different patterns of the evolution of quasispecies in E2 emerged during the acute phase of HCV infection: in subjects with clearance of viremia, the number of viral variants within quasispecies was reduced and the quasispecies composition remained largely unchanged during the follow-up, while in subjects with persistent viremia, the number of viral variants increased during persistent infection and quasispecies showed constant evolution thereafter, suggesting that the dynamics of viral quasispecies during HCV primary infection might contribute to the outcome of HCV infection. These data showed that the interplay between different HCV strains and hosts might result in different, perhaps unique, quasispecies compositions.

The assessment of quasispecies diversity, as opposed to complexity, requires sequencing procedures to be carried out. These are particularly necessary to define sequence changes in the minority variants. Sequencing of inserted E1 and E2/HVR1 clones derived from all five subjects showed that variation in sequences of the minority variants involved single-nucleotide substitutions from majority variant, accounting for the tight clustering of sequences seen in a dendrogram. These data were consistent with quasispecies evolution from a single HCV founder strain and again pointed to the rarity of multiple HCV carriage in IDUs^[27]. Despite the vulnerability of IDUs to HCV multiple transmission through a variety of unknown routes, we found no evidence of mixed HCV genotype infection, neither did we find higher quasispecies complexity nor genetic distance values in the first samples from the subjects with persistent viremia compared to the subjects with clearance of viremia. These findings demonstrated that the multiple HCV transmission events hypothesized to occur in IDUs, for various reasons, might not be associated with an increase in genetic complexity.

From a mechanistic perspective, variation with the HCV genome is assumed to be caused by random mutation and selection of variants, which are most fit to propagate in a given host. For example, in the immunocompetent host, antibodies directed against envelope gene product appear to play an important role in shaping quasispecies repertoires^[28-30]. However, in protein-coding regions, multiple forces affect the balance between fixation of silent

(synonymous) mutations *vs* those that alter amino acid sequence (nonsynonymous). Synonymous mutations are often thought to represent a molecular clock, independent of external pressure and expected to occur at a rate proportional to the organism's reproductive rate, whereas nonsynonymous mutations are selected by immune pressure^[31]. We also evaluated the E1, HVR1, and E2 regions outside HVR1 for synonymous and nonsynonymous substitutions. As shown in Figure 3, the rates of synonymous substitutions predominated and increased over time in the E1 and E2 regions. In contrast to the rates of substitutions found in the E1 and E2 regions outside HVR1, the rate of nonsynonymous substitutions predominated in the HVR1 region. A higher accumulation rate of nonsynonymous substitutions seen in individuals with persistent viremia was correlated with the greater genetic diversity, being consistent with a positive selection for change within HVR1. Published data from acute hepatitis C showed that viral genetic diversity in resolving patients was considerably less than in those who progressed to chronic disease, and crucially, that nonsynonymous substitutions in HVR1 were more common in rapid and slow progressors, compared with the resolving cases^[9]. The data of this study confirmed further that this region might be under selective pressure by the host immune system.

No correlation between the quasispecies complexity and serum viral RNA levels demonstrated in this study does not support the concept that viral quasispecies arise as a consequence of the limited fidelity of HCV replication. Although our data demonstrates the importance of immune pressure in the evolution of HCV quasispecies, selection of quasispecies in hepatocytes, both *in vivo* and *in vitro*, may result from the replication of a small subset of viruses due either to random sampling or to selection of only a few fit variants^[32,33]. Direct competition between virus strains, resulting in interference preventing simultaneous continuous infection by closely related variants, could also be possible.

In summary, the current study demonstrates the adaptation of the SSCP+HDA method for characterizing and tracking HCV quasispecies by analyzing multiple regions of the HCV genome in individuals with different outcomes of acute hepatitis C. This approach allows a larger number of patients and a larger proportion of the HCV genome to be analyzed than prior longitudinal studies of quasispecies diversity. We conclude that HCV persistence may be associated with a complexity of quasispecies and positive selection of HVR1 by the host immune system, and we postulate that both host and viral factors can play important roles in the pathogenesis of chronic hepatitis C in human populations. Further research is necessary to determine the extent to which the observed results are due to a different type of immune response in immunosuppressed patients compared with the immunocompetent host, a replicative advantage of quasispecies populations for certain HCV subgenotypes, and/or tropism of quasispecies variants for hepatic *vs* nonhepatic compartments.

REFERENCES

- 1 Di Bisceglie AM. Hepatitis C. *Lancet* 1998; **351**: 351-355
- 2 Grakoui A, Wychowski C, Lin C, Feinstone SM, Rice CM. Expression and identification of hepatitis C virus polyprotein cleavage products. *J Virol* 1993; **67**: 1385-1395
- 3 Smith DB, Simmonds P. Characteristics of nucleotide substitution in the hepatitis C virus genome: constraints on sequence change in coding regions at both ends of the genome. *J Mol Evol* 1997; **45**: 238-246
- 4 Kato N, Ootsuyama Y, Tanaka T, Nakagawa M, Nakazawa T, Muraio K, Ohkoshi S, Hijikata M, Shimotohno K. Marked sequence diversity in the putative envelope proteins of hepatitis C viruses. *Virus Res* 1992; **22**: 107-123
- 5 Martell M, Esteban JI, Quer J, Genesca J, Weiner A, Esteban R, Guardia J, Gomez J. Hepatitis C virus (HCV) circulates as a population of different but closely related genomes: quasispecies nature of HCV genome distribution. *J Virol* 1992; **66**: 3225-3229
- 6 Steinhauer DA, Holland JJ. Rapid evolution of RNA viruses. *Annu Rev Microbiol* 1987; **41**: 409-433
- 7 Weiner AJ, Geysen HM, Christopherson C, Hall JE, Mason TJ, Saracco G, Bonino F, Crawford K, Marion CD, Crawford KA. Evidence for immune selection of hepatitis C virus (HCV) putative envelope glycoprotein variants: potential role in chronic HCV infections. *Proc Natl Acad Sci USA* 1992; **89**: 3468-3472
- 8 Pawlotsky JM. Hepatitis C virus infection: virus/host interactions. *J Viral Hepat* 1998; **5 Suppl 1**: 3-8
- 9 Farci P, Shimoda A, Coiana A, Diaz G, Peddis G, Melpolder JC, Strazzera A, Chien DY, Munoz SJ, Balestrieri A, Purcell RH, Alter HJ. The outcome of acute hepatitis C predicted by the evolution of the viral quasispecies. *Science* 2000; **288**: 339-344
- 10 Farci P, Strazzera R, Alter HJ, Farci S, Degioannis D, Coiana A, Peddis G, Usai F, Serra G, Chessa L, Diaz G, Balestrieri A, Purcell RH. Early changes in hepatitis C viral quasispecies during interferon therapy predict the therapeutic outcome. *Proc Natl Acad Sci USA* 2002; **99**: 3081-3086
- 11 Kao JH, Chen PJ, Lai MY, Wang TH, Chen DS. Quasispecies of hepatitis C virus and genetic drift of the hypervariable region in chronic type C hepatitis. *J Infect Dis* 1995; **172**: 261-264
- 12 Kato N, Ootsuyama Y, Sekiya H, Ohkoshi S, Nakazawa T, Hijikata M, Shimotohno K. Genetic drift in hypervariable region 1 of the viral genome in persistent hepatitis C virus infection. *J Virol* 1994; **68**: 4776-4784
- 13 Manzin A, Solforosi L, Petrelli E, Macarri G, Tosone G, Piazza M, Clementi M. Evolution of hypervariable region 1 of hepatitis C virus in primary infection. *J Virol* 1998; **72**: 6271-6276
- 14 Farci P, Alter HJ, Wong DC, Miller RH, Govindarajan S, Engle R, Shapiro M, Purcell RH. Prevention of hepatitis C virus infection in chimpanzees after antibody-mediated *in vitro* neutralization. *Proc Natl Acad Sci USA* 1994; **91**: 7792-7796
- 15 Farci P, Shimoda A, Wong D, Cabezon T, De Gioannis D, Strazzera A, Shimizu Y, Shapiro M, Alter HJ, Purcell RH. Prevention of hepatitis C virus infection in chimpanzees by hyperimmune serum against the hypervariable region 1 of the envelope 2 protein. *Proc Natl Acad Sci USA* 1996; **93**: 15394-15399
- 16 Manzin A, Solforosi L, Petrelli E, Macarri G, Tosone G, Piazza M, Clementi M. Evolution of hypervariable region 1 of hepatitis C virus in primary infection. *J Virol* 1998; **72**: 6271-6276
- 17 McAllister J, Casino C, Davidson F, Power J, Lawlor E, Yap PL, Simmonds P, Smith DB. Long-term evolution of the hypervariable region of hepatitis C virus in a common-source-infected cohort. *J Virol* 1998; **72**: 4893-4905
- 18 Ni YH, Chang MH, Chen PJ, Lin HH, Hsu HY. Evolution of hepatitis C virus quasispecies in mothers and infants infected through mother-to-infant transmission. *J Hepatol* 1997; **26**: 967-974
- 19 Lee JH, Stripf T, Roth WK, Zeuzem S. Non-isotopic detection of hepatitis C virus quasispecies by single strand conformation polymorphism. *J Med Virol* 1997; **53**: 245-251
- 20 Kreis S, Whistler T. Rapid identification of measles virus

- strains by the heteroduplex mobility assay. *Virus Res* 1997; **47**: 197-203
- 21 **Maynard JH**, Upadhyaya M. High-throughput screening for the detection of unknown mutations: improved productivity using heteroduplex analysis. *Biotechniques* 1998; **25**: 648-651
- 22 **Wang YM**, Ray SC, Laeyendecker O, Ticehurst JR, Thomas DL. Assessment of hepatitis C virus sequence complexity by electrophoretic mobilities of both single- and double-stranded DNAs. *J Clin Microbiol* 1998; **36**: 2982-2989
- 23 **Ray SC**, Wang YM, Laeyendecker O, Ticehurst JR, Villano SA, Thomas DL. Acute hepatitis C virus structural gene sequences as predictors of persistent viremia: hypervariable region 1 as a decoy. *J Virol* 1999; **73**: 2938-2946
- 24 **Hadziyannis E**, Fried MW, Nolte FS. Evaluation of Two Methods for Quantitation of Hepatitis C Virus RNA. *Mol Diagn* 1997; **2**: 39-46
- 25 **Roth WK**, Lee JH, Ruster B, Zeuzem S. Comparison of two quantitative hepatitis C virus reverse transcriptase PCR assays. *J Clin Microbiol* 1996; **34**: 261-264
- 26 **Park YS**, Lee KO, Oh MJ, Chai YG. Distribution of genotypes in the 5' untranslated region of hepatitis C virus in Korea. *J Med Microbiol* 1998; **47**: 643-647
- 27 **Smith DB**, Simmonds P. Characteristics of nucleotide substitution in the hepatitis C virus genome: constraints on sequence change in coding regions at both ends of the genome. *J Mol Evol* 1997; **45**: 238-246
- 28 **Nei M**, Gojobori T. Simple methods for estimating the numbers of synonymous and nonsynonymous nucleotide substitutions. *Mol Biol Evol* 1986; **3**: 418-426
- 29 **Harris KA**, Teo CG. Diversity of hepatitis C virus quasispecies evaluated by denaturing gradient gel electrophoresis. *Clin Diagn Lab Immunol* 2001; **8**: 62-73
- 30 **Kato N**, Sekiya H, Ootsuyama Y, Nakazawa T, Hijikata M, Ohkoshi S, Shimotohno K. Humoral immune response to hypervariable region 1 of the putative envelope glycoprotein (gp70) of hepatitis C virus. *J Virol* 1993; **67**: 3923-3930
- 31 **Weiner AJ**, Geysen HM, Christopherson C, Hall JE, Mason TJ, Saracco G, Bonino F, Crawford K, Marion CD, Crawford KA. Evidence for immune selection of hepatitis C virus (HCV) putative envelope glycoprotein variants: potential role in chronic HCV infections. *Proc Natl Acad Sci USA* 1992; **89**: 3468-3472
- 32 **Yun Z**, Barkholt L, Sonnerborg A. Dynamic analysis of hepatitis C virus polymorphism in patients with orthotopic liver transplantation. *Transplantation* 1997; **64**: 170-172
- 33 **Rumin S**, Berthillon P, Tanaka E, Kiyosawa K, Traubaud MA, Bizollon T, Gouillat C, Gripon P, Guguen-Guillouzo C, Inchauspe G, Trepo C. Dynamic analysis of hepatitis C virus replication and quasispecies selection in long-term cultures of adult human hepatocytes infected *in vitro*. *J Gen Virol* 1999; **80** (Pt 11): 3007-3018

Science Editor Kumar M and Ma JY Language Editor Elsevier HK

Generation of the regulatory protein rtTA transgenic mice

Kang Xu, Xin-Yan Deng, Ying Yue, Zhong-Min Guo, Bing Huang, Xun Hong, Dong Xiao, Xi-Gu Chen

Kang Xu, Xin-Yan Deng, Ying Yue, Zhong-Min Guo, Bing Huang, Xun Hong, Dong Xiao, Xi-Gu Chen, Center of Experimental Animals, Sun Yat-Sen (Zhongshan) University, Guangzhou 510080, Guangdong Province, China

Kang Xu, The First Affiliated Hospital of Sun Yat-Sen University, Sun Yat-Sen (Zhongshan) University, Guangzhou 510080, Guangdong Province, China

Supported by the National Natural Science Foundation of China, No. 30271177 and No. 39870676; Guangdong Province Natural Science Foundation of China, No. 021903; Postdoctoral Fellowship Foundation of China

Co-correspondents: Dong Xiao

Correspondence to: Professor Xi-Gu Chen, Center of Experimental Animals, Sun Yat-Sen (Zhongshan) University, No. 74, Zhongshan Road 2, Guangzhou 510080, Guangdong Province, China. xiguchen@163.com

Telephone: +86-20-8733-1393 Fax: +86-20-8733-1230

Received: 2004-02-02 Accepted: 2004-04-05

Xu K, Deng XY, Yue Y, Guo ZM, Huang B, Hong X, Xiao D, Chen XG. Generation of the regulatory protein rtTA transgenic mice. *World J Gastroenterol* 2005; 11(19): 2885-2891

<http://www.wjgnet.com/1007-9327/11/2885.asp>

INTRODUCTION

Hepatitis C virus (HCV) infection is a global public health problem, with approximately 3% of the world population now infected; HCV infection is the major cause of post-transfusion non-A non-B hepatitis; persistent HCV infection often progresses to chronic hepatitis, liver cirrhosis, and hepatocellular carcinoma (HCC), usually more than a decade after initial infection^[1,2]. Thus, the development of adequate treatment and prophylactics for HCV infection has been important. Nonetheless, HCV is not infectious *in vivo* except in primates, a phenomenon that has resulted in the lack of a proper HCV culture system and inbred animal model, which has in turn hampered detailed analysis of viral life cycle and pathogenesis of HCV infection^[1,2]. Therefore, establishing *in vitro* and *in vivo* valuable models for human HCV infection is of great importance.

Since the first report of transgenic mice generated by injecting DNA into the pronucleus of one-cell mouse embryos, this technique has been immensely useful in creating model organisms for research purposes^[3]. A great number of transgenic mouse models created by conventional transgene technology for human viral hepatitis [e.g., hepatitis B virus (HBV) and HCV] have already been established and provided new insights into the pathogenesis of hepatitis and HCC^[4-7]. However, one biggest shortcoming of the consistent gene expression system is that the conventional transgene systems provide only "immune tolerant" mice for transgene products, e.g., viral antigen (s), that is to say, the transgenic animals for HBV or HCV are not immunocompetent for the transgene product (s). In the consistent gene expression system, once transferred into embryos, the target gene immediately begins to express viral protein (s) at the early stage of embryo development under the control of the promoter before the formation of immune system. During embryo development, immune cells are stimulated by viral antigen (s) to progressively develop maturation with concurrent "immune tolerance" to virus antigen (s), which makes hepatocyte injury uncertain. Thus, after birth the immune system of organisms cannot recognize the exotic identity of viral antigen (s) and not only in theory but also in fact the liver damage in transgenic mice is not ascertained. In human chronic hepatitis C, hepatocyte injury is not directly caused by HCV infection, but is a consequence of the destruction of infected hepatocytes by cytotoxic lymphocytes^[8].

Abstract

AIM: To translate Tet-on system into a conditional mouse model, in which hepatitis B or C virus (HBV or HCV) gene could be spatiotemporally expressed to overcome "immune tolerance" formed during the embryonic development and "immune escape" against hepatitis virus antigen(s), an effector mouse, carrying the reverse tetracycline-responsive transcriptional activator (rtTA) gene under the tight control of liver-specific human apoE promoter, is required to be generated.

METHODS: To address this end, rtTA fragment amplified by PCR was effectively inserted into the vector of pLiv.7 containing apoE promoter to create the rtTA expressing vector, i.e., pApoE-rtTA. ApoE-rtTA transgenic fragment (-6.9 kb) released from pApoE-rtTA was transferred into mice by pronucleus injection, followed by obtaining one transgene (+) founder animal from microinjection through PCR and Southern blot analysis.

RESULTS: rtTA transgene which could be transmitted to subsequent generation (F1) derived from founder was expressed in a liver-specific fashion.

CONCLUSION: Taken together, these findings demonstrate that rtTA transgenic mice, in which rtTA expression is appropriately targeted to the murine liver, are successfully produced, which lays a solid foundation to 'off-on-off' regulate expression of target gene (s) (e.g., HBV and/or HCV) in transgenic mice mediated by Tet-on system.

© 2005 The WJG Press and Elsevier Inc. All rights reserved.

Key words: Hepatitis virus; Tet-on system; Transgenic mice; Liver-specific human apoE promoter

In fact, the immune system plays pivotal roles in pathogenesis of HCV infection^[9-15]. The traditional HBV and HCV transgenic mice were assayed to find that antigen gene (s) could express normally, but obviously pathologic changes are not observed in the liver and the serum alanine aminotransferase levels were basically normal, indirectly suggesting that the immune system plays a rather important part in hepatitis pathogenesis^[4-7]. So this kind of HCV or HBV transgenic mice is not extremely ideal models suitable for investigating host immune response against HBV or HCV infection and pathogenesis of HBV or HCV infection.

One expected goal of transgene technology is conditional control of target gene, e.g., viral gene (s), expression in a specific tissue/organ during a particular stage of development to mimic viral infections in humans. Therefore, by integrating with the conventional transgene technology, the inducible expression systems for temporal, spatial, and cell-specific control of gene expression in mice provide an approach to tide over the limitation of the stable expression system described above and may be employed to generate immunocompetent transgenic mice with hepatitis B or C.

Heretofore, among the inducible overexpression transgenic systems, the tetracycline-inducible systems, as a reliable excellent tool for stringently reversible (on \leftrightarrow off; 'off-on-off' or 'on-off-on' regulation is more attractive when verifying the function of a given gene, and would be valuable for stage-specific serial gene regulation in developmental studies), temporal and spatial control of transgene expression, have been successfully and most frequently used in transgenic mouse modeling^[16-18]. There are two basic variants: one is the tTA (tetracycline-controlled transactivator) system ("Tet-Off" system)^[19] and the other is rtTA (reverse tTA) system ("Tet-On" system)^[20]. Based on the characteristics of two systems that work through the opposite mechanism, if a gene is to be kept inactive most of the time and turned on only occasionally, Tet-on system appears to be more appropriate.

Therefore, to well elucidate host immune response against HBV or HCV infection and pathogenesis of HBV or HCV infection, we plan to employ Tet-on system to establish a binary transgenic mouse model in which the conditional expression of HBV or HCV transgene can be tightly regulated in the liver by administration of doxycycline (Dox). To use this system *in vivo*, it is necessary to generate two sets of transgenic animals. One mouse line expresses the activator rtTA under the control of a liver-specific promoter that targets rtTA expression at the liver. Another set of transgenic animals, in which HBV or HCV transgene expression is under the control of the target sequence for rtTA, harbors the "acceptor" transgenic construct, i.e., TRE-PminCMV-HBV or TRE-PminCMV-HCV. Mating two strains of mice will and should result in the birth of bi-transgenic offspring, allowing *in vivo* reversible and spatiotemporal control of HBV or HCV transgene expression through addition or without addition of Dox to the food or drinking water of the double-transgenic mice.

The rtTA system has been used successfully in numerous transgenic animal models with a variety of transgenes targeted at various tissues and organs; in Tet-regulated transgenic mice, tissue specificity of target gene expression

is conferred by the promoter driving rtTA expression, in other words, defining the site of expression of rtTA determines the site of transgene expression, because the **minimal promoter** (e.g., tetO-PminCMV in responsive element) itself confers no tissue specificity^[16-18,21]. Unfortunately, there is lack of one transgenic mouse line expressing rtTA in a liver-specific manner (<http://www.zmg.unimainz.de/tetmouse/>)^[16-18,21]. Thus, this study was undertaken to generate the transgenic mice expressing regulatory protein rtTA under the control of a liver-specific apoE promoter to lay a solid base for spatiotemporal expression of HBV and/or HCV in transgenic mouse modeling.

MATERIALS AND METHODS

Plasmid construction

For liver-specific expression of rtTA *in vivo*, the transgenic construct ApoE-rtTA, containing rtTA under the control of the liver-specific apoE promoter, was constructed (Figure 2). rtTA fragment (774-1 781) was amplified by PCR using pTet-on DNA (Clontech), which encodes the regulatory protein rtTA, as template and the rtTA specific primers corresponded to the plasmid pTet-on with the suitable restriction sites *KpnI* and *HpaI* incorporated into the forward and reverse primers, respectively. The primers specific for rtTA were rtTA forward primer (rtTA-FP): 5'-CCGGGGTACC ATG TCT AGA TTA GAT AAA AGT-3' and rtTA reverse primer (rtTA-RP): 5'-TATAGTTAAC CTA CCC ACC GTA CTC GTC-3' (added restriction sites of *KpnI* and *HpaI* were underlined sequentially). PCR reaction conditions were: 30 cycles of 94 °C for 50 s, 58 °C for 50 s, and 72 °C for 1 min 30 s. PCR product (1 008 bp) of amplified rtTA was first cloned into pMD18-T (T-vector; Takara) by T/A cloning to give pMD18-T-rtTA, and thereafter sequenced with general sequencing primers M13-47/RV-M (Takara). After confirmed to be identical to the published rtTA sequences (Genbank accession no. U89930), rtTA fragment was released from pMD18-T-rtTA using *KpnI* and *HpaI*, and then directionally subcloned into the *KpnI* and *HpaI* sites in the polylinker of the expression vector pLiv.7 (9.3 kb) containing a liver-specific human apolipoprotein E promoter (apoE promoter)^[22], designated as pApoE-rtTA, followed by identification of PCR and enzyme digestion analysis.

Production of ApoE-rtTA transgenic mice

Transgenic mice were generated in F1 zygotes using standard pronuclear injection as previously described^[23]. The Kunming mouse line, supplied by Center of Experimental Animals, Zhongshan University, was used as the source of embryos for the micromanipulation and subsequent breeding trials. All transgenic lines were created on the Kunming mouse background. For microinjection, the -6.9-kb fragment of transgene ApoE-rtTA (Figure 2) was separated free from the vector backbone of pApoE-rtTA by *NotI* and *SpeI* double digestion. The injected fragments of ApoE-rtTA were isolated and purified using the QIA quick gel extraction kit (Qiagen), diluted to a final concentration of 2 µg/mL DNA injection buffer (10 mmol/L Tris/0.1 mmol/L EDTA, pH 7.4), and microinjected into the pronuclei of one cell-

stage fertilized embryos [Kunming mouse (♀) × Kunming mouse (♂)]. Then 20–25 injected DNA fertilized eggs that survived microinjection were implanted into the oviducts of one pseudopregnant recipient Kunming mouse as described^[23] 2–3 h after injection or on the next day. Potential transgenic founder animals were weaned at 3 wk of age, and identified by screening mouse tail genomic DNA prepared with standard protocols^[24] for the presence of ApoE-rtTA transgene using PCR, and confirmed by standard Southern blotting analysis with horseradish peroxidase (HRP)-labeled rtTA DNA as a probe.

Polymerase chain reaction (PCR) analysis for genotyping

PCR was performed on tail genomic DNA preparations to screen which mice had ApoE-rtTA integrated into their genome. Amplification reactions for genotype animals used the oligonucleotide pairs rtTA-FP/rtTA-RP (see above) specific for rtTA coding region (see Figure 2 for their positions) to amplify a 1-kb fragment. Reaction conditions were: 30 cycles of 94 °C for 50 s, 62 °C for 50 s, and 72 °C for 1 min 30 s. The positive control for each PCR reaction used 100 ng of ApoE-rtTA construct DNA. Genomic DNA from wild-type mice was amplified as a reaction control (e.g., negative control). DNA samples were considered positive for a particular transgene, if a band of the predicted size in the test sample was present with no amplification occurring in the control sample.

Southern blot analysis for genotyping

The north2south[®] direct HRP labeling and detection kit (Pierce) is a complete system for labeling and chemiluminescent detection of nucleic acids in Northern and Southern blot applications. This one-step labeling and hybridization system combined with a novel enhanced luminol substrate for HRP ensures rapid and consistent results with sensitivity equal to or exceeding ³²P.

To further confirm presence of ApoE-rtTA in the transgenic mouse genome, Southern blots were performed by standard techniques^[24] and following the manufacturer's instructions of north2south[®] direct HRP labeling and detection kit. Briefly, 10 µg of tail genomic DNA from PCR-positive pups was digested overnight with *Pst*I, fractionated by electrophoresis through 0.8% agarose gels in Tris-borate-EDTA (TBE) buffer (90 mmol/L Tris-borate, 2 mmol/L EDTA, pH 8.0), transferred onto a positively charged nylon membrane (Schleicher & Schuell, Keene, NH), which was not fixed with UV crosslinking, by alkaline transfer, and subjected to prehybridization and hybridization with probe (see Figure 2 for its position) of 1-kb HRP-labeled *Kpn*I–*Hpa*I fragment from pApoE-rtTA synthesized according to the protocol of probe labeling in kit. After stringent washes, the membranes were then subjected to chemiluminescence analysis with a commercial north2south[®] direct HRP labeling and detection kit. The chemiluminescence-treated membranes were then exposed to X-ray film (X-Omat AR-5, Eastman Kodak Company, Rochester, NY), usually for 1–10 min at room temperature. Genomic DNA from normal Kunming mice was used as a negative control, while a 3.9-kb fragment excised from the 6.9-kb transgenic ApoE-rtTA by *Pst*I digestion was employed as the positive control for Southern blots.

Mouse propagation and transmission

At 6–8 wk of age, founder mice were backcrossed with normal Kunming mice to generate F1. The genotypes of the founder progeny were analyzed for inheritance of the transgene by PCR performed using the rtTA-FP/RP primers (see above for details) and genomic DNA isolated from tail biopsy samples of 4-wk founder progeny. The PCR protocols for rtTA were noted above.

Analysis of reverse transcription-PCR (RT-PCR)

RNA extraction The isolation of total RNA from the different tissues of 5–6-mo old F1 PCR-positive offspring of founder (s), and non-transgenic littermates of F1 PCR-positive transgenic pups and normal mice as negative controls was performed using the RNeasy Mini Kit (Qiagen) following the manufacturer's recommendations. Purified RNA was eluted in a final volume of 50 µL DNA-free water and aliquots were stored at –80 °C with 2 µL of RNasin.

RT-PCR

RT-PCR is thought to be the most sensitive method for the detection of RNA, but contamination of DNA originated from animal genome results in false positivities. In this study, we used one-step mRNA selective PCR kit (Version 1.1) (TaKaRa) that could only detect target mRNA distinguished from genomic DNA of host cells, by using dNTP analogs^[25,26]. The dNTP/analog were incorporated into cDNA formed with mRNA as a template at the reverse transcription (RT) step. The cDNA/mRNA hybrid was denatured at about 85 °C, but genomic DNA was not. The dNTP/analog incorporated into cDNA was selectively amplified at the next PCR step. Using this system, there is the possibility that only target mRNA is detected, even if there is contamination by genomic DNA.

A specific system for the amplification of mRNA used was one-step mRNA selective PCR kit (version 1.1) (TaKaRa). RT-PCR was carried out as recommended by the manufacturer (Takara) with minor modifications. Briefly, it was carried out in a volume of 50 µL including 25 µL 2× mRNA selective PCR buffer I, 10 µL 25 mmol/L MgCl₂, 5 µL 1 mmol/L dNTP/analog mixture each, 1 µL RNase inhibitor (40 U/mL), 1 µL AMV reverse transcriptase XL (5 U/mL), 1 µL AMV-optimized *Taq* (5 U/mL). In the reaction volume of 50 µL, 1 µg total RNA was used to synthesize the single-stranded cDNA with AMV reverse transcriptase XL (Takara) in one-step RT-PCR. The oligonucleotide primers used for RT-PCR were rtTA-FP/RP primers (see above for details) (PCR product size: 1 kb). RT-PCR amplification was carried out as follows: 30 min at 50 °C for RT, denaturation for 5 min at 85 °C and then a succession of 35 cycles as follows: 1 min at 85 °C, 1 min at 58 °C, 90 s at 72 °C, and a final extension at 72 °C for 10 min.

The integrity of each tissue RNA sample was checked by RT-PCR with primers for the human β-actin gene, used as an internal standard (sense: 5'-GAT ATC GCT GCG CTG GTC GT -3' and antisense: 5'-CGG AAC CGC TCG TTG CCA AT -3'), which produced a 758-bp fragment. For the detection of β-actin mRNA, 30 cycles of one-step RT-PCR were carried out (30 min at 50 °C for RT, and then a succession of 30 cycles as follows: 85 °C for 1 min,

62 °C for 1 min, and 72 °C for 1 min).

Equal quantities (-1 µg) of total RNA were tested in each reaction of RT-PCR. The negative control reactions including reagent control without reverse transcriptase to ensure that RT-PCR was RNA-dependent, negative control I (total RNA from the normal Kunming mouse), and negative control II (total RNA from the non-transgenic littermates of F1 PCR-positive offspring derived from founder (s)) were performed simultaneously under identical conditions. All experiments were performed in triplicate.

RESULTS

Construction of regulatory protein rtTA expression vector

To express rtTA in a liver-specific fashion *in vivo*, we constructed a fusion gene of the apoE promoter (3.0 kb), which targeted expression of rtTA transgene at the murine liver, and rtTA gene (1 008 bp) (Figure 2) to prepare the rtTA expression vector, i.e., pApoE-rtTA.

rtTA fragment (-1 kb) was amplified by PCR (data not shown), subsequently inserted into pMD18-T (T-vector) to prepare pMD18-T-rtTA screened from many clones by PCR (data not shown), and thereafter sequenced (data not shown). After confirming its sequence, rtTA fragment was removed from pMD18-T-rtTA using *KpnI* and *HpaI*, isolated and purified (Figure 1), and then directionally subcloned into *KpnI* and *HpaI* sites of the expression vector pLiv.7 (8.3 kb) linearized with *KpnI* and *HpaI* (Figure 1) to generate pApoE-rtTA. The desired recombinant pApoE-rtTA (9.3 kb) would also be confirmed by electrophoresis map of enzyme digestion (Figure 1) and by sequencing of the sequence in the frame of ApoE-rtTA transgene (data not shown). The expected pApoE-rtTA would release two fragments of -1 and 8.3 kb after digested by *KpnI* and *HpaI* (Figure 1). In addition, two predicted fragments, -6.9 kb ApoE-rtTA transgene and 2.4 kb vector backbone, were excised from pApoE-rtTA with *NotI* and *SpeI* (Figure 1).

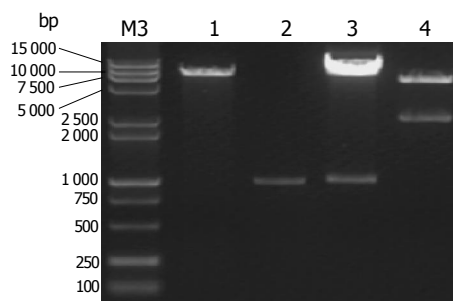


Figure 1 Identification of pApoE-rtTA. Lane M3: DL2 000 + DL15 000 (TaKaRa); Lane 1: pLiv.7 cut by *KpnI* and *HpaI*; Lane 2: purified rtTA fragment; Lane 3: pApoE-rtTA cut by *KpnI* and *HpaI*; Lane 4: pApoE-rtTA digested by *NotI* and *SpeI*.

Generation and genotyping of ApoE-rtTA transgenic mice

For microinjection, a -6.9-kb fragment of ApoE-rtTA transgene was excised from pApoE-rtTA with *NotI* and *SpeI*, isolated and purified (data not shown). The structure and components of ApoE-rtTA transgene construct are fully demonstrated in Figure 2. For the liver-specific rtTA

expression, the construct ApoE-rtTA was generated to express target gene under the control of the liver-specific apoE promoter. A 6.9-kb transgenic construct used for microinjection was released from pApoE-rtTA via digestion with *NotI* and *SpeI*. The transgenic construct contains the human apoE regulatory region (3.0 kb), i.e., an apoE promoter for liver-specific expression of gene, followed by an apoE intron (0.9 kb), and human apoE gene poly(A) signal (apoE pA, 254 bp) and a liver element (1.7 kb) ensuring efficient transgene transcription in the liver. The 1 008-bp rtTA fragment [encoding the regulatory protein rtTA with the indicated translation initiation (ATG) and termination (TAG) sites] was inserted just after the intron, followed by the downstream regulatory sequence of human apoE pA and a liver element. The restriction sites are: H, *HpaI*; K, *KpnI*; M, *MluI*; P, *PstI*; N, *NotI*; S, *SpeI*; X, *XbaI*. The restriction enzyme(s) used in Southern blot hybridization are shown in boldface. The positions of the hybridization rtTA probe (black bar) and predicted size of fragment detected by the probe of HRP-labeled rtTA fragment (-1 kb), the primers specific for the rtTA used in PCR amplification (small arrows) and expected size of the PCR products are indicated. For Southern blot analysis, the genomic DNA samples were digested with *PstI*; as the probe, -1 kb *HpaI*-*KpnI* fragment of ApoE-rtTA construct was used. At the bottom of diagram, the fragment size of the individual sequence in the transgenic construct is shown. The construct map is not drawn to the scale.

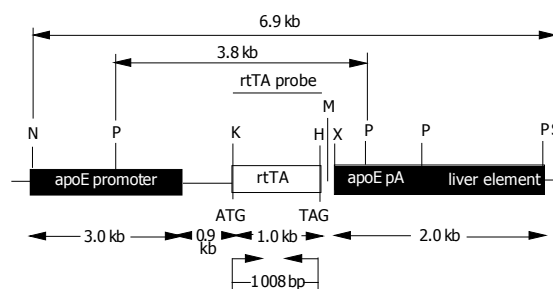


Figure 2 Schematic illustration of the ApoE-rtTA transgenic construct used to generate ApoE-rtTA transgenic mice.

The -6.9 kb ApoE-rtTA was transferred into mice by pronucleus injection. Of 357 embryos transferred to recipient females, 55 embryos developed to term. Among 55 potential founders PCR analysis revealed two positivites (Figure 3A), i.e., C1 and A1, but Southern blot analysis showed one positivity (e.g., C1) (Figure 3B), carrying ApoE-rtTA transgene. Therefore, one founder animal was attained. Fifty-five offspring were individually analyzed by PCR for the genomic integration of transgene with tail biopsy-derived DNA of the potential transgenic founder mice and rtTA primers shown in Figure 2. The results were compared with those obtained with DNA from a negative control (NC) wild-type mouse (lane NC) and positive control (PC) ApoE-rtTA DNA (lane PC). Lanes 1-5, the genomic DNA of the representative five animals were analyzed out of 55 F0 pups born in PCR reaction, the data on the rest of non-

transgenic littermates were not shown. The molecular weight of amplified rtTA fragment band was ascertained as ~1 kb calculated by the amplified band in lane PC and by the migration of standard DNA molecular weight markers [DL2 000 DNA marker (2 000, 1 000, 750, 500, 250, 100 bp) (TaKaRa)] (lane M1), size markers are shown to the left. The arrow indicates the positions of PCR products amplified by the primers shown in Figure 2. Lanes 3 (C1) and 5 (A1) show the amplified 1 008-bp band. Genomic DNA (10 µg) from PCR positive founder mice (e.g., C1 and A1) and a negative control (NC) normal mouse (lane NC) was digested with *Pst*I and used for Southern analysis with an rtTA probe shown in Figure 2. A 3.8-kb fragment (Figure 2) isolated from transgenic ApoE-rtTA construct by *Pst*I digestion was used as a positive control (lane PC). Desired fragment size detected by rtTA probe, as calculated by the hybridized band in lane PC and the relative positions of fragments of known size in bp [M4: λ - *Eco*TI14 I digest Marker (TaKaRa)] (data not shown), was indicated at the right of the blot. This is a representative Southern blot from three separate experiments that yielded similar results.

In addition, to determine whether the transgene ApoE-rtTA was passed to the next generation, founder (C1) was back-crossed to the parental mouse strain to give F1 generation. PCR analysis of F1 offspring (8), derived from founder C1, showed that the percentage of transgenic animals in the progeny was 37.5% (3/8) (Figure 3C). PCR analysis was performed to examine the possibility that the foreign transgene ApoE-rtTA was transmitted from founder C1 to subsequent generation (F1, eight littermates) from the mating of founder C1 (♀) and normal Kunming mouse. Lanes 1-8, genomic DNA from F1 offspring derived from mating mentioned above. Lanes 3, 4 and 7 demonstrated the 767-bp specific band amplified from genomic DNA of F1 offspring. Thus these data demonstrated that founder C1 would transmit the foreign transgene to subsequent generation.

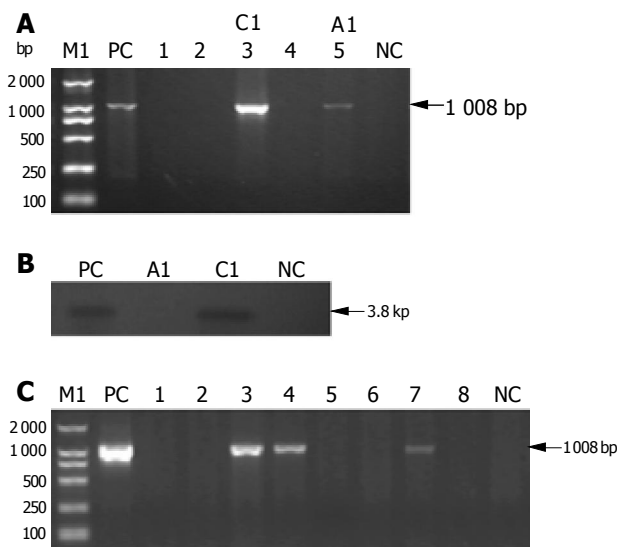


Figure 3 Mouse genotyping for the potential ApoE-rtTA transgenic founders (A and B) and subsequent generation(s) (C). **A:** Diagnostic PCR results for the presence and absence of ApoE-rtTA gene from genomic DNA of the potential transgenic founders; **B:** Southern blot analysis for detection of integrated ApoE-rtTA transgene within founder mouse genome; **C:** Genotyping for the subsequent generation (F1) derived from transgenic founder C1.

Expression of regulatory protein rtTA in transgenic mice

The regulatory sequence of the human apoE gene was used to achieve liver-specific expression of rtTA in one set of transgenic mice. RT-PCR of whole liver RNA was used to evaluate rtTA gene expression in the transgenic mice. rtTA mRNA was readily detected in total liver RNA from one F1 transgenic (+) animal derived from founder C1 (Figure 4A), and not detected in liver RNA from non-transgenic (-) littermate control (Figure 4A) and normal animal control (data not shown). A typical analysis of the PCR products by agarose gel electrophoresis from a positive-control ApoE-rtTA plasmid DNA (lane PC), RNA from one transgenic F1 offspring from founder C1 (lane 1), and RNA from a non-transgenic littermate (lane NC) is shown, while the result from RNA of a normal Kunming mouse is not indicated. β -actin served as an internal control to check the integrity of each tissue RNA sample and normalize for the quantity of input total RNA. Data were representative of three independent RT-PCRs that yielded similar results. Female offspring (F1) of founder C1 was surveyed for transgene (rtTA) expression in the different tissues by RT-PCR. A typical analysis of the RT-PCR products by agarose gel electrophoresis from RNA of brain (lane 1), heart (lane 2), lung (lane 3), kidney (lane 4), spleen (lane 5), muscle (lane 6), intestine (lane 7), stomach (lane 8), eye (lane 9), liver (lane 10), gonad (lane 11) and a non-transgenic littermates (lane NC) is shown. Results from reagent control (lane 12) and a positive-control ApoE-rtTA plasmid DNA (lane PC) are also indicated, while the result from RNA of a normal Kunming mouse is not shown. Furthermore, the transgenic animals were phenotypically similar to their non-transgenic (-) littermates and normal animals, and did not exhibit a detectable histologic change in the liver (data not shown). The results apparently suggested that rtTA gene integrated into the genome of one line from founder C1 could be normally expressed in the liver of transgenic mice.

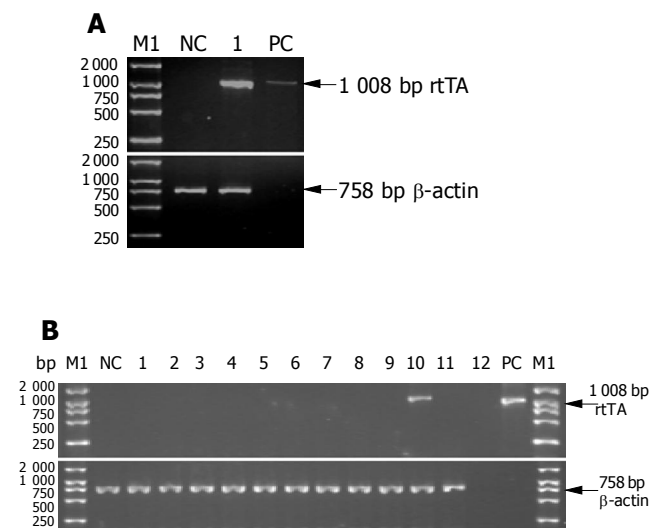


Figure 4 mRNA expression in ApoE-rtTA transgenic mice. **A:** RT-PCR analysis was performed to examine expression of rtTA in transgenic mouse liver; **B:** Tissue-specificity of rtTA transgene expression in transgenic animals.

To confirm the tissue-specificity of transgene expression, an initial survey of transgene expression in a variety of tissues was performed on one mouse line from C1 by RT-PCR. RNA isolated from brain, heart, lung, kidney, spleen, muscle, intestine, stomach, eye and gonad of a female progeny (F1) from C1 did not demonstrate rtTA expression by RT-PCR, suggesting that the transgene expression was tightly restricted to the liver (Figure 4B).

Together, these findings demonstrate that apoE promoter appropriately drives rtTA expression in the murine liver.

DISCUSSION

Recent advances in molecular biology have enabled examination of the function of genes of interest by raising stable cell lines or transgenic animals with consistent gene expression^[16-18]. However, if the transgene is harmful or disadvantageous for cell growth or embryogenesis, the resultant cell lines or animals may be already genetically changed to tolerate the effects of the transgene products because the transgene behaves as a self antigen, inducing negative selection of reactive T cells in the thymus^[16-18]. Therefore, the immunologic response to the transgene cannot be easily studied without special manipulation. This is particularly obvious in models of autoimmune or viral disease. To circumvent these problems, it is necessary to develop a system by which the expression of a transgene can be induced at desired time points and otherwise be kept completely silent for an extended period of time. Such a model may also allow a viral or self-antigen to escape the thymic selection process so the immunologic response can be studied. Using conditional gene expression technology, it is possible to override such restrictions mentioned above to achieve temporal and tissue-specific manipulation of gene expression *in vivo*. Conditional gene expression *in vivo* has been achieved using a variety of model systems^[16-18]. One of them takes advantage of the Cre/*lox* P recombination system by which a transgene can be activated in a tissue-specific and time-dependent manner; however, this system requires the exogenous delivery of Cre gene (usually by Cre transgenic mice or an adeno- or retrovirus), and the induction is irreversible, that is to say, these strategies of transgene regulation can only be carried out once, i.e., 'off to on' or 'on to off', when manipulated by Cre alone; however, sequential gene regulation such as a 'off-on-off' or 'on-off-on' strategy may be a valuable tool, especially in time-course experiments, to obtain further functional information^[16-18,27,28]. The Tet-on/Tet-off expression systems, which are the most widely used inducible regulation system as a reliable excellent tool for stringent reversible, temporal and spatial control of transgene expression, are another choice to overcome the limitation(s) *in vivo*^[19,20].

The availability of the Tet-on/Tet-off systems raises questions concerning under which conditions one should be preferred over the other. Based on the characteristics of two systems, the Tet-on system seems more appropriate for this project if a transgene is to be kept inactive most of the time and turned on only occasionally^[19,20]. Though this system and other rtTA-based systems face the disadvantage, i.e., basal transgene leak *in vivo*, several approaches have been developed to effectively avoid this limitation^[21,29].

In this study, the liver-specific promoter systems were employed to drive the viral proteins expression at the physiologically relevant site of hepatocytes. Presently the liver-specific promoters mainly include human serum albumin (Alb) promoter^[9,30], MUP promoter (mouse major urinary protein promoter)^[9,12], hSAP promoter (human serum amyloid P component promoter)^[31], and apoE promoter (human apolipoprotein E promoter)^[22,32-34]. In our laboratory, the vector of pLiv.7, containing apoE promoter, is used as the basic vector backbone to prepare the transgenic construct. Actually, when the target gene(s) is/are placed downstream of the human apoE promoter/intron for a liver-specific expression manner of gene, and upstream of the apoE polyadenylation sequences/liver element, which has been shown to ensure the high expression of target gene (Figure 2)^[22,32-34], high-level expression of target gene (s) in transgenic mouse liver without interfering with mouse development has been often seen^[22,32-34]. These points on the characteristics of the pLiv.7 and apoE promoter were also verified by the present study.

In Tet-on regulated transgenic mice, tissue specificity of target gene expression was conferred by the promoter driving rtTA expression^[16-18]. Thus, rtTA expression in transgenic mouse liver was controlled by apoE promoter, which in turn determined the site(s) of HBV and/or HCV transgene expression in double-transgenic mice.

Studies on the fate of foreign DNA introduced into an established mammalian genome are of considerably general interest. In almost all instances, transgenic DNA is stably maintained once it has integrated into the genome; even when there are multiple copies if DNA integrated in a tandem head-to-tail array, the transgenic DNA is transmitted stably from one generation to the next without genomic rearrangements and without deletions^[35,36]. However, examples of transgenic families with genetic instability under selective pressure have been identified^[37]. The tyrosinase transgenic families have all displayed stable Southern hybridization patterns, and those families with stable pigmentation have maintained a uniform pigmentation intensity over more than 10 generations of mating^[37]. Because alterations of the integration site would be expected to change both tyrosinase expression and pigmentation, these results imply that genetic instability is very rare for these transgenic inserts^[37]. In the rtTA transgenic mice, the rtTA transgene have been already stably carried over from founder to its progeny (F1).

In summary, in the present study, we successfully generate the effector transgenic mice, e.g., ApoE-rtTA transgenic mice, in which rtTA expression can be tightly targeted at the murine liver.

ACKNOWLEDGMENTS

We express our deepest gratitude to Dr. C.Y. Fan (Department of Pathology and Otolaryngology, University of Arkansas for Medical Sciences, USA) for his unstinting advice and technical guidance in making transgenic mice, for his supportive and friendly attitude toward this project, and for the reagents. We are also indebted to the expert technical assistance of JY Han, HH Zhang, GG Qiu, Y Ma, YL Lin, WG Huang, FY Chen, FR Ni, JY Xie and JH

Wang at Center of Experimental Animal, Zhongshan University, and H Tang at the Third Military Medical University, Chongqing, China.

REFERENCES

- 1 **Moradpour D**, Cerny A, Heim MH, Blum HE. Hepatitis C: an update. *Swiss Med Wkly* 2001; **131**: 291-298
- 2 **Rosenberg S**. Recent advances in the molecular biology of hepatitis C virus. *J Mol Biol* 2001; **313**: 451-464
- 3 **Gordon JW**, Scangos GA, Plotkin DJ, Barbosa JA, Ruddle FH. Genetic transformation of mouse embryos by microinjection of purified DNA. *Proc Natl Acad Sci USA* 1980; **77**: 7380-7384
- 4 **Akbar SK**, Onji M. Hepatitis B virus (HBV)-transgenic mice as an investigative tool to study immunopathology during HBV infection. *Int J Exp Pathol* 1998; **79**: 279-291
- 5 **Feitelson MA**, Larkin JD. New animal models of hepatitis B and C. *ILAR J* 2001; **42**: 127-138
- 6 **Koike K**. Hepatocarcinogenesis in hepatitis viral infection: lessons from transgenic mouse studies. *J Gastroenterol* 2002; **37** Suppl 13: 55-64
- 7 **Milich DR**. Transgenic technology and the study of hepatitis viruses: a review of what we have learned. *Can J Gastroenterol* 2000; **14**: 781-787
- 8 **Fausto N**. A mouse model for hepatitis C virus infection? *Nat Med* 2001; **7**: 890-891
- 9 **Kawamura T**, Furusaka A, Koziel MJ, Chung RT, Wang TC, Schmidt EV, Liang TJ. Transgenic expression of hepatitis C virus structural proteins in the mouse. *Hepatology* 1997; **25**: 1014-1021
- 10 **Moriya K**, Fujie H, Shintani Y, Yotsuyanagi H, Tsutsumi T, Ishibashi K, Matsuura Y, Kimura S, Miyamura T, Koike K. The core protein of hepatitis C virus induces hepatocellular carcinoma in transgenic mice. *Nat Med* 1998; **4**: 1065-1067
- 11 **Moriya K**, Yotsuyanagi H, Shintani Y, Fujie H, Ishibashi K, Matsuura Y, Miyamura T, Koike K. Hepatitis C virus core protein induces hepatic steatosis in transgenic mice. *J Gen Virol* 1997; **78**(Pt 7): 1527-1531
- 12 **Pasquinelli C**, Shoenberger JM, Chung J, Chang KM, Guidotti LG, Selby M, Berger K, Lesniewski R, Houghton M, Chisari FV. Hepatitis C virus core and E2 protein expression in transgenic mice. *Hepatology* 1997; **25**: 719-727
- 13 **Soguero C**, Joo M, Chianese-Bullock KA, Nguyen DT, Tung K, Hahn YS. Hepatitis C virus core protein leads to immune suppression and liver damage in a transgenic murine model. *J Virol* 2002; **76**: 9345-9354
- 14 **Wakita T**, Taya C, Katsume A, Kato J, Yonekawa H, Kanegae Y, Saito I, Hayashi Y, Koike M, Kohara M. Efficient conditional transgene expression in hepatitis C virus cDNA transgenic mice mediated by the Cre/loxP system. *J Biol Chem* 1998; **273**: 9001-9006
- 15 **Wakita T**, Katsume A, Kato J, Taya C, Yonekawa H, Kanegae Y, Saito I, Hayashi Y, Koike M, Miyamoto M, Hiasa Y, Kohara M. Possible role of cytotoxic T cells in acute liver injury in hepatitis C virus cDNA transgenic mice mediated by Cre/loxP system. *J Med Virol* 2000; **62**: 308-317
- 16 **Lewandoski M**. Conditional control of gene expression in the mouse. *Nat Rev Genet* 2001; **2**: 743-755
- 17 **Ryding AD**, Sharp MG, Mullins JJ. Conditional transgenic technologies. *J Endocrinol* 2001; **171**: 1-14
- 18 **van der Weyden L**, Adams DJ, Bradley A. Tools for targeted manipulation of the mouse genome. *Physiol Genomics* 2002; **11**: 133-164
- 19 **Gossen M**, Bujard H. Tight control of gene expression in mammalian cells by tetracycline-responsive promoters. *Proc Natl Acad Sci USA* 1992; **89**: 5547-5551
- 20 **Gossen M**, Freundlieb S, Bender G, Muller G, Hillen W, Bujard H. Transcriptional activation by tetracyclines in mammalian cells. *Science* 1995; **268**: 1766-1769
- 21 **Zhu Z**, Zheng T, Lee CG, Homer RJ, Elias JA. Tetracycline-controlled transcriptional regulation systems: advances and application in transgenic animal modeling. *Semin Cell Dev Biol* 2002; **13**: 121-128
- 22 **Allan CM**, Taylor S, Taylor JM. Two hepatic enhancers, HCR.1 and HCR.2, coordinate the liver expression of the entire human apolipoprotein E/C-I/C-IV/C-II gene cluster. *J Biol Chem* 1997; **272**: 29113-29119
- 23 **Nagy A**, Gertsenstein M, Vintersten K, Behringer R. Manipulating the Mouse Embryo: A Laboratory Manual. 3rd ed. New York: Cold Spring Harbor Press 2003: 1-600
- 24 **Sambrook JE**, Fritsch F, Maniatis T. Molecular Cloning: A Laboratory Manual. 3rd ed. New York: Cold Spring Harbor Laboratory Press 2001: 1-800
- 25 **Andre-Garnier E**, Robillard N, Costa-Mattioli M, Besse B, Billaudel S, Imbert-Marcille BM. A one-step RT-PCR and a flow cytometry method as two specific tools for direct evaluation of human herpesvirus-6 replication. *J Virol Methods* 2003; **108**: 213-222
- 26 **Mizutani T**, Nishino Y, Kariwa H, Takashima I. Reverse transcription-nested polymerase chain reaction for detecting p40 RNA of Borna disease virus, without risk of plasmid contamination. *J Vet Med Sci* 1999; **61**: 77-80
- 27 **Nagy A**. Cre recombinase: the universal reagent for genome tailoring. *Genesis* 2000; **26**: 99-109
- 28 **Sauer B**. Inducible gene targeting in mice using the Cre/lox system. *Methods* 1998; **14**: 381-392
- 29 **Zhu Z**, Ma B, Homer RJ, Zheng T, Elias JA. Use of the tetracycline-controlled transcriptional silencer (tTs) to eliminate transgene leak in inducible overexpression transgenic mice. *J Biol Chem* 2001; **276**: 25222-25229
- 30 **Kato T**, Ahmed M, Yamamoto T, Takahashi H, Oohara M, Ikeda T, Aida Y, Katsuki M, Arakawa Y, Shikata T, Esumi M. Inactivation of hepatitis C virus cDNA transgene by hypermethylation in transgenic mice. *Arch Virol* 1996; **141**: 951-958
- 31 **Matsuda J**, Suzuki M, Nozaki C, Shinya N, Tashiro K, Mizuno K, Uchinuno Y, Yamamura K. Transgenic mouse expressing a full-length hepatitis C virus cDNA. *Jpn J Cancer Res* 1998; **89**: 150-158
- 32 **Fan J**, Wang J, Bensadoun A, Lauer SJ, Dang Q, Mahley RW, Taylor JM. Overexpression of hepatic lipase in transgenic rabbits leads to a marked reduction of plasma high density lipoproteins and intermediate density lipoproteins. *Proc Natl Acad Sci USA* 1994; **91**: 8724-8728
- 33 **Majumder M**, Ghosh AK, Steele R, Zhou XY, Phillips NJ, Ray R, Ray RB. Hepatitis C virus NS5A protein impairs TNF-mediated hepatic apoptosis, but not by an anti-FAS antibody, in transgenic mice. *Virology* 2002; **294**: 94-105
- 34 **Yamanaka S**, Balestra ME, Ferrell LD, Fan J, Arnold KS, Taylor S, Taylor JM, Innerarity TL. Apolipoprotein B mRNA-editing protein induces hepatocellular carcinoma and dysplasia in transgenic animals. *Proc Natl Acad Sci USA* 1995; **92**: 8483-8487
- 35 **Jackson IJ**, Abbott CM. Mouse Genetics and Transgenics: A Practical Approach. London: Oxford University Press 2000: 1-350
- 36 **Tymms MJ**, Kola I. Gene knockout protocols. Totowa: Humana Press Inc 2001: 1-370
- 37 **Overbeek PA**. Factors affecting transgenic animal production. In: Pinkert CA, ed. Transgenic Animal Technology: A Laboratory Handbook. San Diego: Academic Press Inc 1994: 69-114

• VIRAL HEPATITIS •

Multicenter clinical study on Fuzhenghuayu capsule against liver fibrosis due to chronic hepatitis B

Ping Liu, Yi-Yang Hu, Cheng Liu, Lie-Ming Xu, Cheng-Hai Liu, Ke-Wei Sun, De-Chang Hu, You-Kuan Yin, Xia-Qiu Zhou, Mo-Bin Wan, Xiong Cai, Zhi-Qing Zhang, Jun Ye, Ren-Xing Zhou, Jia He, Bao-Zhang Tang

Ping Liu, Yi-Yang Hu, Cheng Liu, Lie-Ming Xu, Cheng-Hai Liu, Institute of Liver Disease, Shanghai University of Traditional Chinese Medicine, Shanghai 201203, China

Ke-Wei Sun, the Affiliated Hospital, Hunan College of TCM, Changsha 410000, Hunan Province, China

De-Chang Hu, You-Kuan Yin, Zhongshan Hospital, Fudan University, Shanghai 200032, China

Xia-Qiu Zhou, Ruijin Hospital, Shanghai Second Medical University, Shanghai 200025, China

Mo-Bin Wan, Changhai Hospital, Shanghai 200423, China

Xiong Cai, Shanghai Changzheng Hospital, Shanghai 200236, China

Zhi-Qing Zhang, the 4th People Hospital of Huaian City, Huaian 232000, Jiangsu Province, China

Jun Ye, the Central Hospital of Putuo District, Shanghai 200062, China

Ren-Xing Zhou, Shanghai Modern Technique Co., Ltd for TCM, Shanghai 200037, China

Jia He, Shanghai Second Military Medical University, Shanghai 200233, China

Bao-Zhang Tang, the Affiliated Hospital, Yunnan College of TCM, Yunnan 650000, Kunming Province, China

Supported by the Main Research Project of Shanghai Municipal Fund for Medical Development

Correspondence to: Professor Ping Liu, Institute of Liver Diseases, Shanghai University of Traditional Chinese Medicine, Shanghai 201203, China. liuliver@online.sh.cn

Telephone: +86-21-5132-2059 Fax: +86-21-5132-2445

Received: 2003-07-12 Accepted: 2003-12-22

Abstract

AIM: To study the efficacy and safety of Fuzhenghuayu capsule (FZHY capsule, a capsule for strengthening body resistance to remove blood stasis) against liver fibrosis due to chronic hepatitis B.

METHODS: Multicenter, randomized, double blinded and parallel control experiment was conducted in patients (aged from 18 to 65 years) with liver fibrosis due to chronic hepatitis B. Hepatic histologic changes and HBV markers were examined at wk 0 and 24 during treatment. Serologic parameters (HA, LM, P-III-P, IV-C) were determined and B ultrasound examination of the spleen and liver was performed at wk 0, 12 and 24. Liver function (liver function and serologic parameters for liver fibrosis) was observed at wk 0, 6, 12, 18 and 24. Blood and urine routine test, renal function and ECG were examined before and after treatment.

RESULTS: There was no significant difference between experimental group (110 cases) and control group (106

cases) in demographic features, vital signs, course of illness, history for drug anaphylaxis and previous therapy, liver function, serologic parameters for liver fibrosis, liver histologic examination (99 cases in experimental group, 96 cases in control group), HBV markers, and renal function. According to the criteria for liver fibrosis staging, mean score of fibrotic stage(s) in experimental group after treatment (1.80) decreased significantly compared to the previous treatment (2.33, $P < 0.05$), but there was no significant difference in mean score of fibrotic stage(s) (2.11 and 2.14 respectively). There was a significant difference in reverse rate between experimental group (52%) and control group (23.3%) in liver biopsy. With marked effect on decreasing the mean value of inflammatory activity and score of inflammation ($P < 0.05$), Fuzhenghuayu capsule had rather good effects on inhibiting inflammatory activity and was superior to that of Heluoshugan capsule. Compared to that of pretreatment, there was a significant decrease in HA, LM, P-III-P and IV-C content in experimental group after 12 and 24 wk of treatment. The difference in HA, LM, P-III-P and IV-C content between 12 and 24 wk of treatment and pretreatment in experimental group was significantly greater than that in control group ($P < 0.01-0.05$). The effect, defined as two of four parameters lowering more than 30% of the baseline, was 72.7% in experimental group and 27.4% in control group ($P < 0.01$). Obvious improvement in serum Alb, ALT, AST and GGT was seen in two groups. Compared to that of control group, marked improvement in GGT and Alb was seen in experimental group ($P < 0.05$). The effective rate of improvement in serum ALT was 72.7% in experimental group and 59.4% in control group. No significant difference was seen in blood and urine routine and ECG before and after treatment. There was also no significant difference in stable rate in ALT and serologic parameters for liver fibrosis between experimental group and control group after 12 wk of withdrawal.

CONCLUSION: Fuzhenghuayu capsule has good therapeutic effects on alleviating liver fibrosis due to chronic hepatitis B without any adverse effect and is superior to that of Heluoshugan capsule.

© 2005 The WJG Press and Elsevier Inc. All rights reserved.

Key words: Chronic hepatitis B; Fuzhenghuayu capsule

Liu P, Hu YY, Liu C, Xu LM, Liu CH, Sun KW, Hu DC, Yin YK, Zhou XQ, Wan MB, Cai X, Zhang ZQ, Ye J, Zhou RX, He J,

Tang BZ. Multicenter clinical study on Fuzhenghuayu capsule against liver fibrosis due to chronic hepatitis B. *World J Gastroenterol* 2005; 11(19): 2892-2899
<http://www.wjgnet.com/1007-9327/11/2892.asp>

INTRODUCTION

Liver fibrosis, characterized by overproduction and deposition of extracellular matrix in liver tissue, is a healing response to chronic injuries, and through which, chronic hepatitis develops into cirrhosis. Nowadays prevention and reverse of liver fibrosis are a rather important therapeutic strategy, since we still lack the special and effective therapy for primary diseases with liver fibrosis. In the past 20 years, based on the pathogenesis of chronic hepatitis as a dual deficiency of Qi and Yin, static blood blocking vessels and pestilent damp-heat lingering, we composed Fuzhenghuayu recipe directed by the therapeutic method of invigorating blood transforming stasis and boosting essence supplementing deficiency. The previous clinical trials revealed that the recipe could significantly improve clinical symptoms in patients with liver fibrosis due to chronic hepatitis B, improve liver functions, decrease portal pressure and effectively reverse tissue fibrosis^[1]. Also, it has been shown that the recipe could enhance serum albumin level in patients with post-hepatitis cirrhosis, improve serum fibrotic markers and adjust immune function^[2]. In this study, we conducted a multicenter, randomized, double blinded and parallel control experiment on 216 patients with liver fibrosis due to chronic hepatitis B (110 cases in experimental group, 106 in control group, among them 99 cases in experimental and 96 in control group received histologic diagnosis) in five centers to confirm the efficacy and safety of Fuzhenghuayu recipe against liver fibrosis due to chronic hepatitis B.

MATERIALS AND METHODS

Trial design

Multicenter, randomized, double blinded and parallel control (Heluoshugan capsule) clinical experiment was conducted to investigate the efficacy and safety of Fuzhenghuayu capsule against liver fibrosis due to chronic hepatitis B. Volunteers were selected and enrolled for 24-wk observation. All endpoints were evaluated before and 6, 12, 18 and 24 wk after administration of Fuzhenghuayu capsule respectively.

Case selection

Patients were diagnosed as liver fibrosis due to chronic hepatitis B according to diagnostic standard as follows^[3]: (1) History with chronic hepatitis B ≥ 6 mo, abnormal ALT ≥ 10 -folds of normal level and TBil ≤ 54 $\mu\text{mol/L}$; (2) Serum markers for liver fibrosis, including hyaluronic acid (HA), laminin (LM), type III procollagen (P-III-P) and type IV collagen (IV-C) were \geq normal value $\pm 2\text{SD}$; (3) B ultrasound examination accorded with changes in chronic hepatitis, including increased dense, coarse and enhanced echo of liver; (4) Liver histologic examination accorded with diagnostic criteria for chronic hepatitis, including inflammatory grading degrees (G1-G4) and liver fibrosis staging scores (S1-S4); and (5) symptoms, including pain in hepatic region, fatigue,

poor appetite, abdominal distension, liver and spleen tumescence, facies hepatica, liver palm, and spider angioma.

Those satisfied the 1st item and the 2nd item, or the 1st item and the 4th item, or the two positive parameters in the 2nd item could be diagnosed as liver fibrosis due to chronic hepatitis B.

Subject inclusion criteria Patients satisfied diagnostic standard and simultaneously met the qualifications including age (range from 18 to 65 years, no sex limitation) and signing of informed consent form.

Subject exclusion criteria The patients were excluded under the following conditions: (1) TBil > 54 $\mu\text{mol/L}$, diagnosed as severe hepatitis B or had the tendency to develop fulminant chronic hepatitis B; (2) Complicated by serious cardiovascular, renal, endocrine, hematologic, nervous and mental disease; (3) Alcoholic, drug induced, infectious, inherited, immune and other viral liver diseases; (4) Women with pregnancy or during lactation; (5) Decompensated post-hepatitis cirrhosis; and (6) Received interferon- γ , antiviral or immunomodulator treatment in the latest 3 mo.

Subject withdrawal criteria Patients failed to follow instructions for administration and observation, or withdrew from therapy without medical reasons, or had incomplete data.

Experimental protocol

Case resource All cases were from inpatient and outpatient department, and various factors for outpatients should be controlled strictly to guarantee planned administration and observation.

Randomization methods Complete randomized principles were employed. Cases were numbered from the 1st to the 240th and divided randomly by SAS software into experimental and control groups. Cases were assigned to five centers according to the admission order.

Protocol for administration With specification of 1.6 g per capsule and Lot# 9912220002 and used as an experimental drug, consisted of *Cordyceps sinensis*, *Peach kernel*, *Salvia*, *Gynostemma*, etc., Fuzhenghuayu capsule was provided by Shanghai Sundise Medicine Technology Development Co. Ltd. With specification of 0.93 g per capsule and used as a control drug, Heluoshugan capsule consisted of *largehead atractylodes rhizome*, *white peony*, *nutgrass galingale rhizome*, *Chinese angelica*, *papaya*, *common burreed rhizome*, *zedoary*, *turtle shell*, *Dung beetle*, etc.

Experimental and control drugs were same in appearance, shape, size, color and luster, package and label, etc. Two drugs were numbered randomly and five capsules were taken orally once, thrice a day. After 24 wk of treatment, patients were followed up for 12 wk. Patients were forbidden to take any kind of medications that could affect therapeutic effect on liver fibrosis.

Blinding method

Blinding methods included double blind, results were disclosed blindly twice and medications were dispensed according to randomization charts.

Parameters observed

In this study, efficacy and safety assessment were performed.

Assessment of efficacy

Efficacy was assessed from the following aspects:

Primary parameters

Histologic examination Liver biopsy was conducted before and after treatment. Grade and stage scoring were conducted in accordance with “1995 viral hepatitis preventing and treating protocol”^[1] and “protocol for scoring activity and degree of fibrosis due to chronic hepatitis”^[2]. Liver tissues were embedded in paraffin and stained with HE, reticular fiber staining and collagen staining (VG) were microscopically observed by three pathologists respectively, then histologic diagnosis was established if at least two experts reached an agreement.

Serum markers for hepatic fibrosis Serum markers including HA, LM, P-III-P, and IV-C were measured before treatment, after 12 and 24 wk of treatment and at 12 wk of follow up. Serum samples were assayed with the same batch kit at the same clinical center. HA and LM were assayed by radioimmunoassay (RIA) with the kit from Institute of Naval Medicine, IV-C by ELISA with the kit produced by Shanghai Shigao Biotech Company and P-III-P by RIA with the kit from Orion Company (Finland).

Second parameters

B ultrasound examination and liver function B ultrasound examination and serum parameters of liver function, including AST, ALT, GGT and ALP activity, Alb and TBil/Dbil content determination, were performed before and after 12 and 24 wk of treatment, and at the end of 12 wk of follow up. Serum HBV markers, including HBeAg, HBeAb and HBcAg, were detected with RIA and ELISA, and HBV-DNA with dot blot or PCR.

Safety assessment

Clinical findings manifested as rash, fever, diarrhea, nausea and poor appetite due to administration were carefully evaluated. Blood and urine routine, renal function (BUN and Cr) and ECG were examined before and after treatment.

Requirements for observation and record

Personnel carrying out clinical test should have substantial clinical and research backgrounds in this field and at least intermediate professional title. Appointed technicians performed the laboratory assays. Except for routine examination, blood and liver tissue samples with the size of 0.2 cm×1.5 cm or five hepatic lobules should be obtained before and after treatment. Liver samples were fixed in 100 mL/L neutral formalin. Patients with 10-folds of ALT activity than the upper threshold of normal level after 4 wk of treatment should take enzyme-deactivating drugs, which had no effect on liver fibrosis until termination of treatment. Patients with high ALT levels (10-folds of the upper threshold of normal level) and high TBil contents (more than 85.5 μ mol/L) after 1.5 mo should withdraw from therapy and their treatment protocol should be modified.

Summarization of data

At the end of trial, all original data were submitted to statistical

experts for further analysis.

Criterion for short-term therapeutic effect Very effective after treatment, liver fibrotic stage decreased by two or more scores, two among the four serum fibrotic markers (IV-C, HA, LM and P-III-P) decreased by more than 30% of the values before treatment and serum ALT returned to normal. Effective: After treatment, liver fibrotic stage decreased by one score, two out of the four serum fibrotic markers (IV-C, HA, LM and P-III-P) decreased by more than 20% of the values before treatment and ALT lowered to 50% of the value before treatment. Ineffective: No obvious improvement was seen.

Criterion for assessing long-term therapeutic effect

After 12 wk of follow up, fibrotic markers, liver function and TCM syndromes were observed, long-term therapeutic effect was defined as stability or instability. Stability referred to the increase of fibrotic markers and serum ALT level being less than 20% at the end of treatment, while instability meant that the fibrotic markers and ALT levels increased more than 20% at the end of treatment.

Statistical analysis

Statistical analysis was performed with 6.12 SAS software. χ^2 test, *t* test and non-parametric statistical test were employed for comparison between two groups before experiment. For self-comparison in each group, variance and non-parametric statistical test were employed to compare therapeutic effect before and after administration in experimental and control groups. For comparison between two groups including comparison of efficacy and safety, central effect oriented variance analysis model (double factors) was employed for quantitative data and central effect-oriented CMH method was employed for classified data. Descriptive analysis was used for safety analysis.

Drugs in each group were known only after statistical analysis was finished.

RESULTS

General condition of the subjects

Enrolment and fulfilment The withdrawal rate of patients (six patients) was 2.7%, a total of 222 subjects were enrolled according to the protocol and among them 216 fulfilled the trial. All the subjects enrolled were eligible for the entry criteria.

Comparison between two groups before treatment

There was no significant difference between experimental group (110 cases) and control group (106 cases) in demographic features, vital signs, disease history and seriousness (liver function, serum fibrotic markers, liver histological examination, HBV markers, and ultrasound scores, *etc.*). Blood, and urine routine and ECG were normal in all subjects before treatment (Tables 1-4).

Histologic changes

Variation of inflammation and fibrosis in liver biopsy

A total of 195 cases received liver biopsy (99 in experimental group and 96 in control group) before treatment, among them 93 cases received the second biopsy after therapy (50 in trial group, 43 in control group). There was no difference

Table 1 General information in two groups before treatment (mean±SD)

Group	<i>n</i>	Sex M/F	Age (yr)	Marriage single/married	Weight (kg)	Previous treatment (case)	Treated with other drugs (case)
Experimental	110	95/15	37.7±9.2	21/89	64.30±8.25	11	26
Control	106	89/17	38.5±8.9	15/91	64.09±6.64	17	26
<i>P</i>		0.848	0.512	0.361	0.844	0.155	0.174

Table 2 Blood and renal routine and PT in two groups before treatment (mean±SD)

Group	<i>n</i>	RBC (10 ¹² /L)	Hemoglobin (g/L)	WBC (10 ⁹ /L)	Platelet (10 ⁹ /L)	BUN (mmol/L)	Cr (μmol/L)	PT (s)
Experimental	110	4.6±0.7	139.8±16.7	5.1±1.4	137.1±86.0	4.4±1.3	84.1±17.4	13.6±1.9
Control	106	4.5±0.7	138.9±16.5	5.0±1.4	117.8±48.1	4.7±1.6	86.9±21.0	13.5±1.7
<i>P</i>		0.499	0.761	0.499	0.054	0.193	0.441	0.168

PT: prothrombin time, BUN: blood urea nitrogen, Cr: creatinine.

in inflammation grade and fibrosis stage between two groups before treatment (Table 5). However, in experimental group, liver inflammation grades and fibrosis stage decreased markedly after treatment, whereas no obvious improvement was seen in control group.

Score of liver inflammation and fibrosis Half-quantitative scoring of inflammation activity and fibrosis in liver biopsy in 68 cases (37 cases in experimental group and 31 cases in control) was carried out. There was no difference in grading and staging scores between two groups before treatment (Tables 5 and 6). However, in experimental group, liver inflammation and fibrosis scores decreased markedly after treatment, but no obvious improvement was observed in control group (Tables 7 and 8).

Efficacy on histologic changes The total effective rate was 52% in experimental group and 23.2% in control group according to the set criteria (Table 9).

Changes of serum markers for liver fibrosis There was no significant difference in serum HA, LM, P-III-P and IV-C contents between two groups before treatment, while compared to previous treatment, HA, IV-C, LM and P-III-P decreased significantly in experimental group after treatment (Tables 10-1-3).

Effective rate for fibrosis The effective rate for liver fibrosis was significantly higher in experimental group (72.7%) than in control group (27.4%) ($P<0.01$) (Table 11).

Liver function parameters Experimental group, with a total effective rate of 72.7%, showed a better improvement

in liver function than control group with an effective rate of 59.4% ($\chi^2 = 4.263$, $P<0.05$) (Tables 12 and 13).

Changes in ultrasound examination before and after treatment There was no significant difference in B ultrasound scoring, liver size, diameter of stem hepatic portal vein, thickness of spleen, diameter of splenic vein and size of gallbladder in two groups. But compared to those before treatment, there was a significant decrease in hepatic portal vein (after 12 and 24 wk of treatment) in experimental group, diameter of spleen (after 12 wk of treatment in experimental group and 24 wk treatment in control group) and diameter of splenic vein (after 24 wk of treatment in experimental group and 12 and 24 wk of treatment in control group) ($P<0.05-0.01$) (Table 14).

Changes in serum viral markers The positive rates of HBsAg, HBeAg, HBc-IgM and HBV-DNA in experimental and control groups were 100%/100%, 43.64%/45.28%, 40.40%/36.46% and 34.55%/30.91% before treatment, and the negative reverse rates of the above markers were 4.55%/4.76%, 11.82%/11.43%, 11.1%/8.42% and 12.84%/13.33% after treatment. There was no significant difference between two groups before and after treatment.

Efficacy evaluation in follow up

One hundred and four patients were followed up for 12 wk after treatment and emphasis was on observing serum markers for liver fibrosis, ALT and TCM patterns. Results

Table 3 Inflammation grading and fibrosis staging of biopsies in two groups before treatment

Group	<i>n</i>	Inflammation (G)				Fibrosis (S)			
		1	2	3	4	1	2	3	4
Experimental	99	12	49	29	9	22	39	21	17
Control	96	22	39	27	8	33	31	20	12
<i>P</i>			0.277				0.121		

Table 4 Serum viral markers in two groups (cases) before treatment

Group	<i>n</i>	HBsAg	HBsAb	HBeAg	HBeAb	HBcAb	HBcAb-IM	HBV-DNA
Experimental	110	110	3	48	48	105	40	38
Control	106	106	2	48	56	100	35	37
<i>P</i>			1.000	0.891	0.220	0.765	0.659	1.000

Table 5 Comparison of inflammation activity (G) in two groups in liver biopsy

Group	n	Pretreatment					Post-treatment					P
		1	2	3	4	mean	1	2	3	4	mean	
Experimental	50	5	25	15	5	2.40	18	20	11	1	1.9	0.001
Control	43	10	19	12	2	2.14	11	17	10	5	2.21	0.583
P		0.277					0.004					

Table 6 Comparison of liver fibrosis staging (S) in two groups in liver biopsy

Group	n	Pretreatment						After treatment						P
		0	1	2	3	4	mean	0	1	2	3	4	mean	
Experimental	50	0	8	23	10	9	2.40	1	23	14	9	3	1.80	0.001
Control	43	0	11	20	7	5	2.14	2	8	22	4	7	2.14	1.000
P		0.121						0.001						

showed that serum ALT and some markers for liver fibrosis were stable, there was no significant difference between the two groups (Table 15).

Changes of safety parameters

Blood routine and renal function There was an increase in count of RBC, WBC and platelets in two groups after treatment. There was a significant difference in count of RBC in control group, content of Hb in experimental group and count of WBC in two groups after treatment ($P < 0.05$). There were changes in BUN in experimental group, Cr and PT after treatment in control group before and after treatment. However, all changes were within normal range and of no clinical significance.

Urine routine, ECG and α -fetoprotein (AFP) No abnormality was seen in urine routine, ECG and X-ray examination in two groups before and after treatment. There was a slight increase in serum AFP in some cases in the two groups. However, the change was in accordance with the characteristics of chronic hepatitis and of no clinical significance.

Adverse reaction No obvious adverse reaction was observed in experimental group, mild reaction (increased exhaust which disappeared after withdrawal) was seen in one case in control group and the adverse reaction rate was 0.9%.

DISCUSSION

Chronic hepatitis B is a common and prevalent disease

endangering people's health seriously in China^[4,5]. Liver fibrosis, through which chronic hepatitis B develops into cirrhosis, is a common pathologic process for almost all chronic liver diseases, so searching for new medications to prevent and reverse liver fibrosis is an urgent task for hepatologists.

Fuzhenghuayu capsule is a new medication formulated on the basic pathogenesis of liver fibrosis and cirrhosis-*body resistance weakness and stasis blocking vessels*. Previous studies^[6-9] have revealed that this medication has good effects on improving liver function and serum fibrotic parameters and cirrhosis, decreasing portal pressure, regulating immune function and amino acids balance. *In vitro* study showed that the underlying mechanism of the medication against liver fibrosis was to inhibit of stellate cell proliferation, collagen synthesis, lipid peroxidation, collagen and transforming growth factor- β 1 gene expression and improvement in matrix metalloproteinases activity.

In this study, a multicenter, randomized, double blinded and parallel control method was employed to observe the efficacy and safety of Fuzhenghuayu capsules on 216 cases of liver fibrosis due to chronic hepatitis B at five centers. In accordance with previous trials, a rather good reproducible result is expected.

Fuzhenghuayu capsule can effectively alleviate liver fibrosis in chronic hepatitis B

Liver biopsy examination is a gold standard for diagnosis

Table 7 Inflammation activity scoring in liver biopsy before and after treatment (mean \pm SD)

Group	n	Pretreatment	Post-treatment	P
Experimental	37	8.8 \pm 3.9	6.6 \pm 4.7	0.001
Control	31	7.3 \pm 4.1	7.4 \pm 4.1	0.978
P		0.185 (P_1)	0.036 (P_2)	

Table 8 Fibrosis scoring in liver biopsy before and after treatment (mean \pm SD)

Group	n	Pretreatment	Post-treatment	P
Experimental	37	8.1 \pm 5.6	6.0 \pm 5.4	0.001
Control	31	7.2 \pm 5.5	8.1 \pm 6.3	0.413
P		0.433 (P_1)	0.007 (P_2)	

Table 9 Efficacy in two groups in histologic changes of liver fibrosis

Group	n	Very effective cases (%)	Effective cases (%)	Ineffective cases (%)	P
Experimental	50	4 (8.0)	22 (44.0)	24 (48.0)	0.008
Control	43	1 (2.4)	9 (20.9)	33 (76.7)	

Table 10-1 Changes in serum HA, LM, P-III-P and IV-C contents (mean±SD)

Parameter	Group	n	Pretreatment	12 wk of treatment	24 wk of treatment
HA (μg/L)	Experimental	110	303.6±235.7	178.9±158.0 ^b	147.9±131.3 ^b
	Control	106	276.3±234.9	258.9±243.2 ^a	261.8±253.6 ^b
LM (μg/L)	Trial	110	137.0±84.6	127.5±92.7 ^a	122.4±96.5 ^b
	Control	106	134.1±98.6	128.4±55.7	121.2±48.9
P-III-P (μg/L)	Experimental	110	11.1±5.0	8.8±4.9 ^b	7.4±4.4 ^b
	Control	106	9.6±5.6	9.7±6.6	9.4±6.9
IV-C (μg/L)	Trial	110	119.1±132.5	74.5±88.4 ^b	64.5±82.5 ^b
	Control	106	91.8±76.7	71.4±57.8	62.4±54.7 ^b

^aP<0.05, ^bP<0.01 *vs* the same group.**Table 10-2** Difference in serum HA, LM, P-III-P and IV-C contents between two groups before and after treatment

Time points	Group	n	HA (μg/L)			LM (μg/L)		
			Median of difference	Standard deviation	Percent of difference	Median of difference	Standard deviation	Percent of difference
12-wk treatment	Experimental	110	-75.6 ^b	196.5	-36.3	-10.0 ^a	58.3	-8.1
	Control	106	-19.8	222.6	-12.8	3.0	102.2	2.0
24-wk treatment	Experimental	110	-96.1 ^b	201.5	-48.5	-17.0	69.3	-13.0
	Control	106	-26.0	254.6	-15.9	-4.5	108.0	-4.5

^aP<0.05, ^bP<0.01 *vs* control.**Table 10-3** Changes in serum P-III-P, IV-C contents between two groups before and after treatment

Time points	Group	n	P-III-P (μg/L)			IV-C (μg/L)		
			Median of differential	Standard deviation	Percent of difference	Median of difference	Standard deviation	Percent of difference
12-wk treatment	Experimental	110	-2.2 ^b	5.0	-20.1	-25.0 ^a	128.2	-39.3
	Control	106	-0.0	5.0	-1.3	-6.5	87.0	-9.1
24-wk treatment	Experimental	110	-2.9 ^b	4.6	-33.9	-33.0 ^a	139.1	-48.3
	Control	106	-0.3	5.5	-3.0	-14.0	80.4	-18.6

^aP<0.05, ^bP<0.01 *vs* control.

and evaluation of efficacy on liver fibrosis. In this study, liver biopsies showed that Fuzhenghuayu capsule was superior to Heluoshugan capsule in reversing liver fibrosis. Histologic examination also revealed that Fuzhenghuayu capsule had rather good effects on inhibiting hepatic inflammation. Superior to that in control group, a significant decrease in mean value of degree of inflammatory activity and inflammatory score was seen in experimental group after treatment. This reveals that Fuzhenghuayu capsule has good effects on alleviating inflammatory infiltration and/or hepatic cell necrosis.

Fuzhenghuayu capsule can significantly improve serum fibrotic markers in liver fibrosis due to chronic hepatitis B

It has been widely accepted that serum HA, LM, P-III-P and IV-C are useful markers to evaluate liver fibrosis,

especially serum HA and IV-C contents, so multi-parameter determination is advocated for diagnosing and evaluating liver fibrosis in clinic^[10-13]. In this study, there was no significant difference in serum HA, LM, P-III-P and IV-C contents between the two groups before treatment. All markers in experimental group showed a consistent and stepwise decrease after 12 and 24 wk of treatment, and before and after treatment, the difference in serum HA and IV-C contents in experimental group were obviously greater than that of control group.

The effective rate was 72.7% in experimental group and 27.4% in control group, indicating that there was a significant difference between the two groups. From this point of view, we conclude that Fuzhenghuayu capsule is superior to Heluoshugan capsule in inhibiting liver fibrosis due to chronic hepatitis B.

Table 11 Efficacy on liver fibrosis in two groups

Group	n	Very effective cases (%)	Effective cases (%)	Ineffective cases (%)	P
Experimental	110	80 (72.7)	2 (1.8)	28 (25.5)	0.001
Control	106	29 (27.4)	2 (1.9)	75 (70.7)	

Central effect-oriented CMH method was employed in comparison of efficacy between two groups, Q of statistics was Q_{CMH} .

Table 12 Changes in liver function of two groups before and after treatment (mean±SD)

Parameter	Group	Pretreatment	6 wk of treatment	12 wk of treatment	18 wk of treatment	24 wk of treatment
Alb (g/L)	Experimental	40.1±5.2	42.6±5.0 ^b	43.2±4.7 ^b	43.3±4.3 ^{bc}	43.5±5.7 ^{bc}
	Control	41.0±5.9	42.6±5.3 ^b	43.3±5.3 ^b	42.8±4.9 ^b	43.1±5.2 ^b
Glo (g/L)	Experimental	30.1±6.4	29.8±6.1	30.8±6.5	31.3±5.7	31.3±5.8
	Control	29.2±5.1	30.9±5.7 ^b	30.9±6.0 ^a	31.9±5.6 ^b	31.9±6.6 ^b
ALT (U/L)	Experimental	116.0±74.6	57.5±56.0 ^{bc}	50.9±39.0 ^{bc}	50.1±43.6 ^{bc}	49.4±41.2 ^{bc}
	Control	96.7±55.0	59.5±52.0 ^b	58.9±54.4 ^b	61.8±58.5 ^b	51.2±39.0 ^b
AST (U/L)	Experimental	78.4±59.3	55.5±47.7 ^b	54.2±47.4 ^b	46.2±29.2 ^{bc}	48.2±35.0 ^b
	Control	68.5±53.1	53.8±39.1 ^b	59.3±50.2 ^a	55.8±39.4 ^a	51.9±51.6 ^b
GGT (U/L)	Experimental	92.0±71.4	75.3±64.9 ^b	67.9±75.8 ^b	67.4±70.1 ^b	56.4±51.8 ^{bd}
	Control	86.8±68.6	68.6±52.9 ^b	67.7±59.9 ^b	70.4±48.0 ^a	67.3±58.2 ^b
ALP (U/L)	Experimental	100.6±38.2	96.4±47.3 ^a	100.3±52.2	97.9±47.1	93.5±38.8 ^a
	Control	95.1±41.9	97.0±43.6	93.1±42.1	91.1±36.5	92.9±41.5
TBil (μmol/L)	Experimental	17.8±7.9	15.8±5.9 ^b	15.9±6.4 ^b	15.5±9.5 ^{bc}	15.5±5.8 ^{bc}
	Control	16.9±8.4	16.4±8.2	17.1±8.6	18.5±12.1	18.5±13.5
DBil (μmol/L)	Experimental	5.9±5.5	4.7±3.0 ^b	4.6±3.0 ^{bc}	4.5±2.5 ^{bc}	4.6±2.7 ^{bd}
	Control	5.2±4.4	4.8±3.7	5.1±3.7	5.3±3.6	5.9±5.4

^aP<0.05, ^bP<0.01 vs the same group; ^cP<0.05, ^dP<0.01 vs difference between different time points value and previous treatment in two groups.

Table 13 Efficacy in ALT activity between two groups before and after treatment

Group	n	Effectual (%)	Effective (%)	Noneffective (%)	P
Experimental	110	64 (58.2)	16 (14.5)	30 (27.3)	0.105
Control	106	54 (50.9)	9 (8.5)	43 (40.6)	

In comparison of efficacy between two groups, central effect-oriented CMH method was employed. Q of statistics was Q_{CMH} .

Fuzhenghuayu capsule can significantly improve liver function in liver fibrosis due to chronic hepatitis B

Parameters of liver function improved significantly in both groups after treatment, indicating that both medications have protective effects on liver injury. Compared to those of pretreatment, there was a significant decrease in TBil and DBil in experimental group at different time points after

treatment. The difference in TBil and DBil between 18 and 24 wk of treatment and pretreatment in experimental group was significantly higher than that in control group. Comprehensively, compared to Heluoshugan capsule, we draw a conclusion that Fuzhenghuayu capsule has some advantages in improving liver function in patients with chronic hepatitis B.

Table 14 Changes in diameter of stem hepatic portal vein, thickness of spleen and diameter of splenic vein before and after treatment in two groups (mean±SD)

Parameters	Group	n	Pretreatment	12-wk treatment	24-wk treatment
Diameter of stem hepatic vein (mm)	Experimental	110	12.34±1.94	11.96±1.69 ^{bd}	12.03±1.61 ^a
	Control	106	12.30±1.75	12.37±1.76	12.06±1.51
Diameter of spleen (mm)	Experimental	110	42.77±9.23	41.10±8.11 ^b	41.77±7.88
	Control	106	42.45±9.94	42.12±9.90	41.32±8.28 ^a
Diameter of splenic vein (mm)	Experimental	110	7.57±1.86	7.41±1.84	7.28±1.52 ^a
	Control	106	7.67±1.94	7.43±1.80 ^a	7.39±2.00 ^a

^aP<0.05, ^bP<0.01 vs treatment, ^dP<0.01 vs different time point and pretreatment between groups.

Table 15 Comparison of stable rate (%) between two groups in follow up

Group	Stable cases/follow up cases (stable rate%)				
	HA	LM	P-III-P	IV-C	ALT
Experimental	18/29 (62.07)	29/34 (85.29)	14/29 (48.28)	30/34 (88.24)	49/50 (98.00)
Control	16/28 (57.14)	25/37 (67.57)	15/25 (60.00)	34/37 (91.89)	54/54 (100.00)
P	0.790	0.100	0.425	0.703	0.481

Fisher precise probability calculation was employed in comparison of stable rates between the two groups.

No obvious anti-virus effect of Fuzhenghuayu capsule was found. Based on the results available from serum parameters for liver fibrosis and ALT activity in follow-up cases, there was no obvious difference in stable rate 12 wk after withdrawal of the drug in two groups.

No change in laboratory examination and ECG after 24 wk of treatment was seen in two groups. No obvious adverse reaction was seen in experimental group. Digestive tract reaction disappeared after withdrawal of the drug was seen in one case only (0.9%) in control group. These indicate that both medications are rather safe.

In conclusion, Fuzhenghuayu capsule can effectively alleviate hepatic fibrosis and decrease serologic fibrotic parameters due to chronic hepatitis B. Since the reverse rate of Fuzhenghuayu capsule is higher than that of Heluoshugan capsule, the medication has excellent effects on reversing liver fibrosis. Thus, Fuzhenghuayu capsule is a safe and effective medication against liver fibrosis due to chronic hepatitis B.

REFERENCES

- 1 **Liu P**, Liu C, Chen GC, Hu YY, Xu LM, Lu P, Yang JL, Yan RM, Ji Q, Chu F. Effect of fuzheng huayu 319 capsule on serological parameters of fibrosis in treating chronic hepatitis B. *Zhongguo Zhongxiyi Jiehe Zazhi* 1996; **16**: 588-592
- 2 **Liu P**, Liu C, Hu YY. Effect of fuzheng huayu recipe in treating posthepatic cirrhosis. *Zhongguo Zhongxiyi Jiehe Zazhi* 1996; **16**: 459-462
- 3 **Zu WR**, Wang TL, Zhou TH, Zhang TH. Diagnosis, grading and staging for chronic hepatitis. *Chin J Dis* 1996; **16**: 277-281
- 4 **Anonymous**. Protocol for preventing and treating viral hepatitis (experimental implementation). *Chin J Inter Med* 1995; **34**: 788-791
- 5 **Wang TL**, Liu X, Zhou YP, He JW, Zhang J, Li NZ, Duan ZP, Wang BE. A semiquantitative scoring system for assessment of hepatic inflammation and fibrosis in chronic viral hepatitis. *Chin J Hepatol* 1998; **6**: 195-197
- 6 **Liu P**, Liu CH, Liu C, Xu LM. Serum Pharmacological effects of fuzheng huayu decoction on its cell proliferation and collagen synthesis in rats. *CJIM* 1998; **4**: 118-122
- 7 **She WN**, Hu DC, Zhou CH. Clinical study of ganping capsule in treating liver fibrosis in chronic hepatitis B. *Chin Hepatol* 2002; **7**: 254-255
- 8 **Liu P**, Liu C. Experimental study of the effect of fuzheng huayu 319 recipe on inhibiting liver fibrosis. Progress in pharmacological and clinical study of traditional Chinese medicine (Vol 4 edited by Zhou Jinhua Wang Jianhua). *Press Military Med* 1996: 314-321
- 9 **Liu C**, Wang X, Liu P. Serapharmacological effect of fuzheng huayu 319 Decoction on expression of type I collagen and transforming growth factor beta 1 in hepatic stellate cells. *Zhongguo Zhongxiyi Jiehe Zazhi* 1999; **19**: 412-414
- 10 **Liu P**, Wu DZ, Liu CH. Mechanism study on combination of Chinese herbs formula to support anti-pathogenic ability and dissipate blood stasis in promoting reversion of liver fibrosis. *Act Shanghai Univ TCM* 2002; **16**: 37-41
- 11 **Murawaki Y**, Ikuta Y, Koda M, Yamada S, Kawasaki H. Comparison of serum 7S fragment of type IV collagen and serum central triple-helix of type IV collagen for assessment of liver fibrosis in patients with chronic viral liver disease. *J Hepatol* 1996; **24**: 148-154
- 12 **Murawaki Y**, Ikuta Y, Koda M, Nishimura Y, Kawasaki H. Clinical significance of serum hyaluronan in patients with chronic viral liver disease. *J Gastroenterol Hepatol* 1996; **11**: 459-465
- 13 **Wang BE**. Diagnosis and evaluation of seriousness of liver fibrosis. *Chin J Hepatol* 1998; **6**: 193-194

• BASIC RESEARCH •

Six-year follow-up of pancreatic β cell function in adults with latent autoimmune diabetes

Lin Yang, Zhi-Guang Zhou, Gan Huang, Ling-Li Ouyang, Xia Li, Xiang Yan

Lin Yang, Zhi-Guang Zhou, Gan Huang, Xia Li, Xiang Yan, Institute of Metabolism and Endocrinology, the Second Xiangya Hospital, Central South University, Changsha 410011, Hunan Province, China

Ling-Li Ouyang, the First Affiliated Hospital, Guangxi Medical University, Nanning 530021, Guangxi Province, China

Lin Yang, Institute of Metabolism and Endocrinology, the Second Xiangya Hospital, Central South University, Changsha 410011, Hunan Province, China

Supported by the National Natural Science Foundation of China, No. 39370343, the National Ministry of Health Youth Talents Foundation, No. Q9420, and the Hunan Health Bureau Key Scientific Funds, No. 9736, 2001-Z04

Co-first-authors: Lin Yang and Zhi-Guang Zhou

Co-correspondents: Lin Yang

Correspondence to: Dr. Zhi-Guang Zhou, Institute of Metabolism and Endocrinology, the Second Xiangya Hospital, Central South University, Changsha 410011, Hunan Province, China. zhouzg@hotmail.com

Telephone: +86-731-5550254 Fax: +86-731-5533525

Received: 2004-06-24 Accepted: 2004-07-15

in LADA patients were correlated with GAD-Ab index, body mass index (BMI) and age at onset ($r_s = 0.408, -0.301$ and -0.523 respectively, $P < 0.05$). Moreover, GAD-Ab was the only risk factor for predicting β cell failure in LADA patients ($B = 1.455$, EXP (B) = 4.283, $P = 0.023$).

CONCLUSION: The decreasing rate of islet β cell function in LADA, being highly heterogeneous, is three times that of T2DM patients. The titer of GAD-Ab is an important predictor for the progression of islet β cell function, and age at onset and BMI could also act as the predictors.

© 2005 The WJG Press and Elsevier Inc. All rights reserved.

Key words: Latent autoimmune diabetes in adults; Type 2 diabetes; Islet β cell function; Glutamic acid decarboxylase antibody

Yang L, Zhou ZG, Huang G, Ouyang LL, Li X, Yan X. Six-year follow-up of pancreatic β cell function in adults with latent autoimmune diabetes. *World J Gastroenterol* 2005; 11(19): 2900-2905

<http://www.wjgnet.com/1007-9327/11/2900.asp>

Abstract

AIM: To investigate the characteristics of the progression of islet β cell function in Chinese latent autoimmune diabetes in adult (LADA) patients with glutamic acid decarboxylase antibody (GAD-Ab) positivity, and to explore the prognostic factors for β cell function.

METHODS: Forty-five LADA patients with GAD-Ab positivity screened from phenotypic type 2 diabetic (T2DM) patients and 45 T2DM patients without GAD-Ab matched as controls were followed-up every 6 mo. Sixteen patients in LADA1 and T2DM1 groups respectively have been followed-up for 6 years, while 29 patients in LADA2 and T2DM2 groups respectively for only 1.5 years. GAD-Ab was determined by radioligand assay, and C-peptides (CP) by radioimmune assay.

RESULTS: The percentage of patients whose fasting CP (FCP) decreased more than 50% compared with the baseline reached to 25.0% at 1.5th year in LADA1 group, and FCP level decreased (395.8 ± 71.5 vs 572.8 ± 72.3 pmol/L, $P < 0.05$) at 2.5th year and continuously went down to the end of follow-up. No significant changes of the above parameters were found in T2DM1 group. The average decreased percentages of FCP per year in LADA and T2DM patients were 15.8% (4.0-91.0%) and 5.2% (-3.5 to 35.5%, $P = 0.000$) respectively. The index of GAD-Ab was negatively correlated with the FCP in LADA patients ($r_s = -0.483$, $P = 0.000$). The decreased percentage of FCP per year

INTRODUCTION

Latent autoimmune diabetes in adults (LADA), screened from phenotypic type 2 diabetic (T2DM) patients by glutamic acid decarboxylase antibody (GAD-Ab) and characterized by slowly progressive islet β cell dysfunction, initially presents as non-insulin-dependent and easily misdiagnosed as T2DM^[1-4]. Studies have shown that islet β cell function of LADA patients decreases with different velocity until being insulin-dependent and some factors can predict the failure rate of islet function^[5-9]. However, the characteristics and risk factors of progression of β cell function in LADA remain unclear in Chinese. We measured GAD-Ab, as markers of autoimmunity, and fasting C-peptide (FCP), as a marker of β cell destruction in LADA patients and studied them prospectively for 6 years in order to unveil the unknown changes of β cell function in LADA patients. In this way we can offer suitable therapy including insulin or immune intervention for LADA at an early time to preserve their islet function.

MATERIALS AND METHODS

Subjects

We screened phenotypic T2DM, from endocrine ward and outpatient clinic in our hospital, with GAD-Ab. We would

diagnose a phenotypic T2DM as LADA according to the criteria^[10] of diagnosis of LADA as follows: (1) >25 year of age at onset; (2) no ketosis within half a year after diagnosis; (3) GAD-Ab positive. If the LADA patient still preserved some β cell function (defined as FCP>100 pmol/L), the patient would be enrolled in our follow-up study. From 1996 to 2001, we had screened 45 LADA patients, including 28 males and 17 females, with a mean age of 48.5 ± 11.6 years (range 28-68 years). Mean FCP and 2-h-postprandial C-peptide (CP) level was 546.1 ± 284.7 pmol/L ($111-1\ 194$ pmol/L) and $1\ 098.0 \pm 669.0$ pmol/L ($186.0-2\ 317.0$ pmol/L) respectively and median of GAD-Ab was 0.49 ± 0.08 (0.05-1.91) at the beginning of the follow-up. Twenty-seven patients received insulin therapy, 13 were given sulfonylurea and biguanide, 4 were given biguanide alone and 1 was on diet control. Six patients were with family history of T2DM. Meanwhile, 45 other T2DM patients (included 31 males and 14 females), with a mean age of 48.3 ± 10.2 years (range 26-68 years), with no history of ketosis or ketonic acidosis and was GAD-Ab negative were enrolled in this study as matched controls. Their mean FCP and 2-h-postprandial CP level were 753.0 ± 401.2 pmol/L ($270.7-2\ 356.6$ pmol/L) and $1\ 469.8 \pm 462.0$ pmol/L ($540.0-3\ 972.0$ pmol/L) respectively. Twenty-one of these patients received insulin therapy, 20 were given both sulfonylurea and biguanide, 4 were given biguanide alone. Five patients were with family history of T2DM. LADA and T2DM patients were followed every 6 mo (except the 24th mo). Fasting blood glucose, 2-h-postprandial glucose, HbA1c, FCP, 2hCP and GAD-Ab index were determined for all patients at each visitation. LADA1 ($n = 16$) and T2DM1 ($n = 16$) group patients had been followed for 72 mo (entered in 1996-1998), while LADA2 ($n = 29$) and T2DM2 ($n = 29$) for 18 mo (entered in 1999-2001). The patients with undetectable FCP/2hCP during the follow-up were excluded.

We established a healthy control group from epidemiological surveys in Changsha and sampled 188 healthy individuals to define the normal range of islet autoantibodies including GAD-Ab. One hundred and eighty-eight subjects were without family history of diabetes or autoimmune diseases (99 males and 89 females) with a mean age of 35.2 ± 13.5 years (range 1.5-68.0 years) and with normal fasting and postprandial blood glucose levels.

GAD-Ab and C-peptide radioimmune assay

GAD-Ab is determined by radioligand assays^[11,12] in our laboratory and the assay was evaluated in the 3rd Diabetes Autoantibody Standardization Program (DASP 2003) sponsored by the Immunology of Diabetes Society (IDS) with 82% sensitivity and 98% specificity. The GAD₆₅-Ab^[13] plasmid (kindly provided by Dr. W.A. Hagopian, Seattle, WA, USA) is used in coupled *in vitro* transcription and translation (TnT, Promega, Madison, WI, USA) in the presence of ³⁵S-methionine as previously described^[14]. A human serum with high levels of immunoprecipitating autoantibodies was used as index positive control, and healthy serum from screening is used as negative control. All samples are tested in duplicate. Results are expressed as a normalized index, which is calculated using the formula: index = (unknown sample CPM-index negative control CPM)/(index

positive control CPM-index negative control CPM). The inter-assay coefficients of variation were 7.1-10.8% ($n = 5$), and the intra-assay CV were 4.9-8.3% ($n = 5$) respectively. Based on the data from 188 healthy blood donors whose GAD-Ab indices ranged from -0.118 to 0.052, the cut-off for positivity was 0.052 (99.5 percentile).

CP was determined by radioimmune assay using a commercial kit (DePu Company, Germany). The inter-assay coefficients of variance were 9.1-15.0% ($n = 3$), and the intra-assay coefficients of variance were 3.7-8.6% ($n = 3$).

Statistical analyses

All data were expressed as mean \pm SD. All statistics were performed by using statistical procedure of social science (SPSS), including Student's *t* test, Mann-Whitney *U* test, ANOVA or Friedman test, Pearson or nonparametric correlation analyses, stepwise multiple linear regressions in multivariate analysis, survival and Cox stepwise regression analysis. *P* values less than 0.05 were considered significant.

RESULTS

Baseline data

Baseline characteristics of the subjects are summarized in Table 1. LADA and T2DM patients were matched with age, sex, age at onset, duration, body mass index (BMI) and HbA1c. Two-hour-postprandial CP was significantly lower in LADA1 than T2DM1 group ($P < 0.05$) and FCP and 2hCP were both lower in LADA2 than T2DM2 group ($P < 0.05$, $P < 0.01$).

Table 1 Baseline data of LADA1, two group and T2DM1, two group (mean \pm SD)

	LADA1	T2DM1	LADA2	T2DM2
Number	16	16	29	29
Sex (male/female)	11/5	12/4	18/11	19/10
Age (yr)	47.7 ± 11.2	47.0 ± 7.9	49.0 ± 12.0	52.2 ± 10.9
Age at onset (yr)	44.9 ± 10.5	44.2 ± 7.4	46.0 ± 11.1	49.9 ± 10.1
Duration (yr)	2.7 ± 0.9	2.8 ± 0.5	3.0 ± 0.6	2.2 ± 0.4
BMI (kg/m ²)	20.7 ± 2.9	21.8 ± 1.7	21.4 ± 3.3	22.5 ± 1.9
FBG (mmol/L)	14.5 ± 5.3	13.7 ± 1.7	14.2 ± 5.6	13.5 ± 3.1
HbA1c (%)	10.1 ± 0.6	9.9 ± 1.9	9.2 ± 2.2	8.6 ± 2.0
Family history (%)	18.8	12.5	10.3	10.3
Insulin therapy (%)	56.3 (9/16)	37.5 (6/16)	65.5 (19/29)	51.7 (15/29)
FCP (pmol/L)				
Postprandial-2-h	572.8 ± 72.3	714.6 ± 63.7	531.3 ± 53.2^b	772.7 ± 86.1
C-peptide (pmol/L)	885.1 ± 147.7^a	$1\ 196.7 \pm 104.2$	$1\ 240.0 \pm 140.5^b$	$1\ 659.9 \pm 188.5$

^a $P < 0.05$ vs T2DM group, ^b $P < 0.01$ vs T2DM group.

Serum C-peptide changes in LADA and T2DM patients during the follow-up

Patients in the LADA1 group were followed for 5 years (from 4 to 6 years), LADA2 for 1.3 years (from 0.5 to 1.5 years).

The change of absolute C-peptide in LADA1 patients

Figure 1 shows that FCP levels were not significantly different between LADA1 and T2DM1 patients at entry ($P > 0.05$). In the LADA1 patients, CP levels did not change significantly

during the 1st year of follow-up, but FCP declined from the 30th mo ($P < 0.05$). T2DM1 patients did not show any significant decrease during the follow-up period ($P > 0.05$).

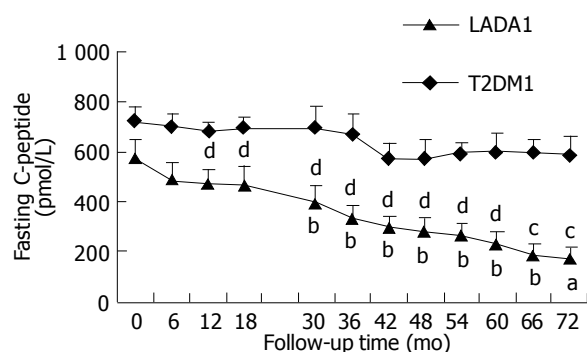


Figure 1 Changes of FCP level in LADA1 and T2DM1 patients during the 6-year follow-up time. Values are mean \pm SE of 16 patients respectively. The lower line shown here is representative of LADA patients and the upper one of T2DM group's. The FCP of LADA1, decreasing much quicker than that of T2DM1 patients, declined significantly from the 30th mo compared with the entry ($^aP < 0.05$, $^bP < 0.01$). And from the 12th mo, the difference of FCP between LADA1 and T2DM1 patients became significant until the end of follow-up time ($^cP < 0.05$, $^dP < 0.01$). Meanwhile T2DM1 group did not show any significant decrease during the follow-up period ($P > 0.05$).

The change of absolute C-peptide in LADA2 patients

The FCP, which was always lower in LADA2 than T2DM2 patients, did not change significantly, compared with their baseline data during their 1.5-year follow-up period in the two groups ($P > 0.01$ and 0.01).

The change of relative C-peptide value

The proportion of LADA1 patients with islet function decreased more than 50% (Figure 2) The proportion of LADA1 patients whose islet function decreased by larger than 50% went up with time. This proportion in FCP increased from 6.25% at the 6th mo to 25.0% at the 18th mo ($P < 0.05$) and reached to 93.8% at the 5.5th-6th year ($P < 0.01$). While in T2DM1 patients, only 30.0% at the 5.5th-6th year ($P < 0.05$).

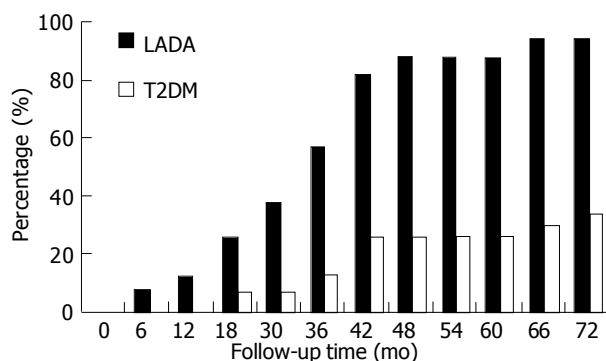


Figure 2 The percentage of patients whose FCP decreased more than 50% compared with the baseline during the follow-up time. Black bar graph representing the percentage of LADA patients, which showed us a much quicker increase from 6.25% at 6th mo to 25.0% at 18th mo until 93.8% at 72th mo. Meanwhile in the white bar of T2DM group, the percentage increased much slower and only to 30.0% at the end of follow-up.

The relation between complete β cell failure and duration (Figure 3) There were eight LADA patients who progressed complete β cell failure (undetectable FCP) for about 4.4 ± 1.9 years (2-6.8 years) after diagnosis until now. The frequency of β cell failure increased from 0 of 9 (0/9) patients at diagnosis to 8 of 11 (8/11) patients after 7 years. None of the T2DM patients developed complete β cell failure during the follow-up.

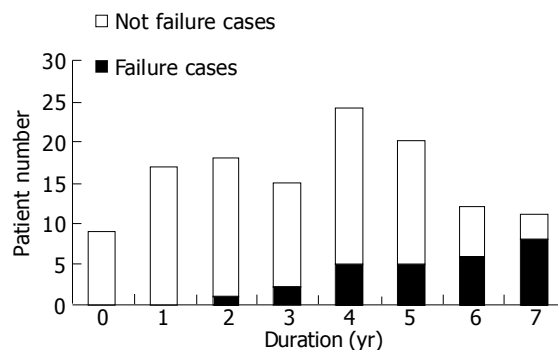


Figure 3 The failure of islet function during the follow-up in LADA patients. The number of patients with β cell failure increased from 0/9 (new onset) to 1/18 (2-year duration), 2/15 (3-year duration), 5/24 (4-year duration), 5/20 (5-year duration), 6/12 (6-year duration) and 8/11 (7-year duration). The average time for β cell failure was 4.4 ± 1.9 years.

Correlation analysis of islet β cell function in LADA patients

The relation between FCP and GAD-Ab index in LADA patients Baseline FCP levels of 45 LADA patients were negatively correlated with GAD-Ab index ($r = -0.483$, $P = 0.001$) (Figure 4), which indicated that the much higher titer of GAD-Ab that the LADA patient had, the more faster the failure of islet β cell function would occur.

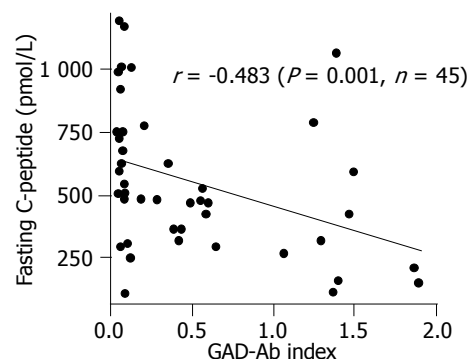


Figure 4 Correlation of FCP level and GAD-Ab index in LADA patients. The X-axis represented GAD-Ab index that ranged from 0.05 to 1.91 and the Y-axis showed the FCP that ranged from 111 to 1 194 pmol/L of 45 LADA patients at enrollment. The scatter diagram showed us that these two factors were negatively correlated ($r = -0.483$, $P = 0.001$), which meant that the LADA patients with much higher GAD-Ab titer would face more risk of islet function failure.

Correlation analysis of the average decreased percentages of FCP per year in LADA patients (Table 2) We could calculate the average decreased percentages of FCP per year in 45 LADA patients through dividing the decreased

Table 2 Correlation analysis of the average decreased percentages of FCP per year in LADA patients

	GAD-Ab Index	Age at onset (yr)	BMI (kg/m ²)	Sex (m/f)	Duration (yr)	Family history	FBG (mmol/L)	HbA1c (%)
Correlation efficient	0.408	-0.301	-0.523	0.19	-0.084	-0.198	0.132	-0.035
P	0.006	0.047	0.000	0.216	0.590	0.197	0.430	0.835

The correlations between variables at entry including GAD-Ab index, age at onset, BMI, sex, duration, family history, FBG, HbA1c and the average decreased percentages of FCP per year in LADA patients were analyzed. And GAD-Ab index, age at onset and BMI were found to be the three significant variables ($r = 0.408$, -0.301 and -0.523 , $P = 0.006$, 0.047 and 0.000).

value of FCP during the follow-up period with their initial FCP. As the follow-up times of LADA1 and LADA2 group were different, we further divided the above percentage with corresponding follow-up time for each patient. Then we got 15.8%/year (4.0-91.0%/year) as the average decreased percentage of FCP per year for LADA patients and 5.2%/year (-3.5 to 35.5%/year) for T2DM and their difference was significant ($P < 0.001$). We also analyzed the correlation between the variables at entry with the above percentage in LADA group and found that the decreased percentage of FCP per year were correlated with GAD-Ab index, BMI and age at onset ($r_s = 0.408$, -0.301 and -0.523 respectively, $P < 0.05$).

Multivariate analysis for β cell function in LADA patients A multiple stepwise regression analysis was used to identify the factors (age at onset, duration of disease, BMI, sex, HbA1c, FBS, family history and therapy protocol) to predict β cell failure in LADA patients. In analysis, duration of disease, GAD-Ab index, age at onset, and BMI by turns (according to their effects on FCP) were significant risk factors and the regression equation was as follows: $y = -3.390 \times \text{duration} - 3.153 \times \text{GAD-Ab index} + 2.834 \times \text{age at onset} + 2.264 \times \text{BMI}$ ($F = 8.978$, $P = 0.000$).

Survival analysis of β cell failure in LADA and T2DM patients (Figure 5) In order to further characterize the different prognosis of β cell function between LADA and T2DM patients, survival analysis was introduced to our study. We supposed the patient that developed β cell failure as “dead”, otherwise, as “survival” at different period of

duration of disease (called “survival time”). We found two significantly different survival curves in the two groups and the cumulative proportion of β cell failure increased from 0.074 at the 2nd year to 0.462 at the 8th year of duration in LADA patients that was gradually rising with the duration; however, that of T2DM remained unchangeable in the whole period.

Risk factor analysis for β cell failure with Cox stepwise regression model GAD-Ab titer, age at onset, sex, BMI, FBS and HbA1c of patients at the diagnosis were introduced as covariates with “survival time” (defined as “the time before β cell failure”) and Cox setpwise regression model was used to identify the risk factor for β cell failure in LADA patients. With forward stepwise method, most factors were excluded and GAD-Ab titer was the only variable that entered the equation ($B = 1.455$, $\text{EXP}(B) = 4.283$, $P = 0.023$), which meant that the odds of β cell failure will increase 4.283 times with the increase of the GAD-Ab titer.

DISCUSSION

There has been four prospective studies with follow-up time for more than 5 years on LADA patients, including Finland's 10-year study reported by Niskanen *et al*^[5], in 1995, UKPDS' 6-year by Turner *et al*^[15], in 1997, Goetz *et al*'s^[6], 5-year report on Americans in 2002 and 12-year study in Sweden by Borg *et al*^[7], in 2002. Among the above studies, only the latter two were focusing on the relationship between β cell function and islet autoantibodies. Compared with the above reports, although there were some disadvantages such as small sample, we could still find some priorities in the study which included (1) more frequent, which meant more accurate to reflect the tiny change of islet β cell function; (2) analyze β cell function with different parameters, such as the changes of FCP value and its proportion, the changes from overall and from individual separately, correlation, multivariate regression analysis, survival analysis and Cox regression analysis; (3) using new index to assess the change of islet function such as “the proportion of LADA patients with islet function decreased more than 50%” and “the average decreased percentage of FCP per year”.

We found that FCP and 2-h PCP of LADA patients declined slowly during the follow-up. Though T2DM patients also showed a decreasing trend, there were no significant changes. Borg *et al*^[7], reported that FCP of diabetics with GAD-Ab positivity decreased obviously, while those without GAD-Ab did not show any change during the 12-year prospective study, corresponding well with our results. We have observed that (1) the change of FCP value, which showed that FCP remained stable during the

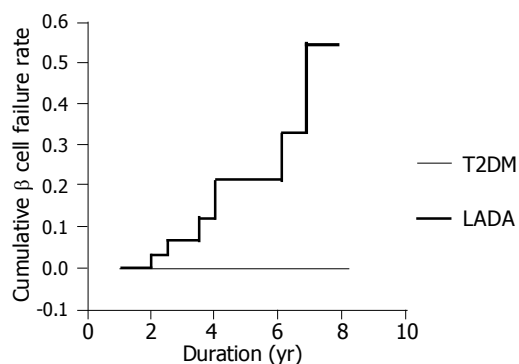


Figure 5 Survival analysis of the cumulative failure rates of islet β cell function in LADA and T2DM patients during the follow-up period. The X-axis represented the duration of diabetes and Y-axis meant the cumulative proportion of β cell failure in these patients. Patient that developed β cell failure would be supposed as “dead”, otherwise, as “survival” at different period of duration (called “survival time”). The dotted and the solid line represented LADA and T2DM patients respectively. The β cell failure cumulative rate increased from 0.074 at the 2nd year to 0.462 at the 8th year of duration in LADA patients; however, that of T2DM remained unchangeable in the whole period.

1.5th year of follow-up, but began to decrease at the 2.5th year in LADA1 group; (2) the proportion of LADA patients with islet function decreased more than 50%, which already reached to 37.5% at 1.5th year (equivalent 3-5 years after diagnosis) in LADA patients, and the difference was significant compared with the baseline, while the T2DM patients did not show such changes until the 5.5-6th year (equivalent 8-9 years after diagnosis). In a word, the declining of β cell function developed about 3-4 years earlier in LADA than in T2DM patients.

LADA patients also showed heterogeneous descending rates of β cell function in the study. Firstly, the FCP in some patients presented a linearly decreasing way and even decreased to lower than 121.0 pmol/L (decreased 63.2%) in half a year and some progressed slowly that FCP maintained 680.0 pmol/L with 9-year duration and decreased more than 50% (65.4%) compared with baseline until 12.5 years later. Secondly, "the average decreased percentages of FCP per year (%/yr)" was calculated to reflect the decreasing rate of islet function. FCP of 45 LADA patients decreased 15.8%/year averagely and with the quickest 91%/year, the slowest 5.2%/year. However, that of T2DM patients was 5.2%/year which amount to one-third (1/3) of LADA's and was similar with 4.5%/year in 6 years after diagnosis reported by UKPDS^[16]. Thirdly, undetectable FCP was defined as β cell failure^[7] and no one developed at entry, but the failure frequency increased to 1/18 at the 2nd year and to 8/11 at the 7th year. The fastest declining one needed only 2 years to lose insulin secretion function; nevertheless some patients still preserved β cell function even 15 years after diagnosis. The β cell failure in LADA patients experienced 4.4 ± 1.9 years averagely and no one failed in T2DM patients during our current study. In addition, β cell failure was supposed as "dead" (otherwise "survival") and then, we made a survival analysis in the two groups and found that β cell cumulative failure rate was rising with duration in LADA patients. In contrast, β cell failure did not occur with any T2DM patient at all times.

GAD-Ab, as the major immune marker for the diagnosis of LADA, and its predictive value for the failure of β cell function had been confirmed in many studies^[2,5-8,15,17-20]. Moreover, the predictive value was related with the titer of GAD-Ab^[7,8,15,17,19]. Borg *et al*^[7], and Gottsater *et al*^[17], found that GAD-Ab in high levels usually predicts much faster decrease of β cell function. The predictive value, highest with GAD-Ab titer more than 60 U, the second with titer from 20 to 60 U/L and worst with titer less than 20 U/L had been reported by UKPDS^[15]. While there were still some studies^[21] that suggested that GAD-Ab did not directly induce β cell failure. With GAD-Ab assay we identified the two groups of patients, and they showed completely different characteristics in the progression of β cell function, confirming the predictive value of GAD-Ab for islet function in LADA patients. We found that the initial GAD-Ab levels were negatively correlated with FCP, and antibody levels were positively associated with the average decreased percentages of FCP per year (%/yr). At last, the risk factor analysis of β cell failure in LADA with Cox stepwise regression model also revealed that GAD-Ab titer was the only factor responsible for β cell failure. All these suggested that GAD-

Ab, as the most classic marker for diagnosing LADA, also provided the most important predictive value for the loss or failure of β cell function. It suggested that stronger immune damage results in faster loss of islet β cell function. Of 16 LADA1 patients, 56.3% (9/16) used insulin at the beginning of follow-up, and the proportion rose to 90% (9/10) at the end of follow-up, while only 37.5% (6/16) used insulin in T2DM1 subjects at entry and 44.4% (4/9) turned to insulin dependency at the end of follow-up. This not only reflected some different characteristics of two groups in progression of islet beta-cell function, but also demonstrated the predictive value of GAD-Ab for insulin requirement in LADA patients^[6,12,17,18,22,23].

In this study, age at onset, BMI of LADA patients were negatively correlated with the average decreased percentages of FCP per year, which meant that much younger and thinner the patients were, much faster decrease of islet function would happen. It was similar with UKPDS and other reports^[15,17,21,24] that the patients with younger age and smaller BMI at onset may present a linear and fast failure of β cell function, otherwise much slower. But someone^[15] also pointed out that BMI was of no prognostic importance for islet function in LADA patients older than 45 years. Other factors including sex, family history, FBS and HbA1c did not show any significant relation with FCP in our study, which indicated that they were not key points for the β cell failure. To search for the major factors to predict islet function in LADA, a multiple regression analysis^[25-27] had been applied. We identified GAD-Ab, age at onset, BMI and duration of disease as the best predictors. Duration, which was not linearly related with β cell function, entered the regression equation and it suggested that duration could predict β cell function in coordination with other factors. This also indicated the importance of assessing islet function with all the parameters combined together. Nevertheless, Cox stepwise regression model suggested that, among the above factors, only GAD-Ab could truly predict β cell failure in LADA patients, which further testified that this antibody not only was an important marker for the diagnosis of LADA but its titer could also predict the progress and prognosis of islet β cell function in LADA patients.

As β cell function of LADA was in a relatively steady state at early 3-5 years after diagnosis and duration was the important predictor for the deterioration of islet function, immune interventions, including insulin therapy, should be carried out as early as possible, especially for the patients with high titer of GAD-Ab, lower BMI and younger age at onset to delay the failure of β cell function^[28-31].

ACKNOWLEDGMENTS

We thank Dr. William A. Hagopian (University of Washington, Seattle, WA) for kindly providing the human GAD65 cDNA, and Dr. Thomas Dyrberg (Novo, Bagsvaerd, Denmark) for technical assistance in autoantibodies assay.

REFERENCES

- 1 Tuomi T, Groop LC, Zimmet PZ, Rowley MJ, Knowles W, Mackay IR. Antibodies to glutamic acid decarboxylase reveal latent autoimmune diabetes mellitus in adults with a non-

- insulin-dependent onset of disease. *Diabetes* 1993; **42**: 359-362
- 2 **Hagopian WA**, Karlsen AE, Gottsater A, Landin-Olsson M, Grubin CE, Sundkvist G, Petersen JS, Boel E, Dyrberg T, Lernmark A. Quantitative assay using recombinant human islet glutamic acid decarboxylase (GAD65) shows that 64K autoantibody positivity at onset predicts diabetes type. *J Clin Invest* 1993; **91**: 368-374
- 3 **Gottsater A**, Landin-Olsson M, Fernlund P, Lernmark A, Sundkvist G. Beta-cell function in relation to islet cell antibodies during the first 3 yr after clinical diagnosis of diabetes in type II diabetic patients. *Diabetes Care* 1993; **16**: 902-910
- 4 **Tuomi T**, Carlsson A, Li H, Isomaa B, Miettinen A, Nilsson A, Nissen M, Ehrnstrom BO, Forsen B, Snickars B, Lahti K, Forsblom C, Saloranta C, Taskinen MR, Groop LC. Clinical and genetic characteristics of type 2 diabetes with and without GAD antibodies. *Diabetes* 1999; **48**: 150-157
- 5 **Niskanen LK**, Tuomi T, Karjalainen J, Groop LC, Uusitupa MI. GAD antibodies in NIDDM. Ten-year follow-up from the diagnosis. *Diabetes Care* 1995; **18**: 1557-1565
- 6 **Goetz FC**, Roel J, Jacobs DR, Barbosa J, Hannan P, Palmer J, Hagopian W. Declining beta-cell function in type 2 diabetes: 5-year follow-up and immunologic studies of the population of Wadena, MN. *Metabolism* 2002; **51**: 144-148
- 7 **Borg H**, Gottsater A, Fernlund P, Sundkvist G. A 12-year prospective study of the relationship between islet antibodies and beta-cell function at and after the diagnosis in patients with adult-onset diabetes. *Diabetes* 2002; **51**: 1754-1762
- 8 **Borg H**, Gottsater A, Landin-Olsson M, Fernlund P, Sundkvist G. High levels of antigen-specific islet antibodies predict future beta-cell failure in patients with onset of diabetes in adult age. *J Clin Endocrinol Metab* 2001; **86**: 3032-3038
- 9 **Zimmet PZ**, Tuomi T, Mackay IR, Rowley MJ, Knowles W, Cohen M, Lang DA. Latent autoimmune diabetes mellitus in adults (LADA): the role of antibodies to glutamic acid decarboxylase in diagnosis and prediction of insulin dependency. *Diabet Med* 1994; **11**: 299-303
- 10 **Zhou ZG**, Wu HW. Diagnosis and treatment of latent autoimmune diabetes in adults (LADA). *Zhonghua Neifenmi Daixie Zazhi* 1998; **14**: 1-2
- 11 **Petersen JS**, Hejnaes KR, Moody A, Karlsen AE, Marshall MO, Hoier-Madsen M, Boel E, Michelsen BK, Dyrberg T. Detection of GAD65 antibodies in diabetes and other autoimmune diseases using a simple radioligand assay. *Diabetes* 1994; **43**: 459-467
- 12 **Huang G**, Zhou ZG, Peng J, Yan X, Zhu XP, Yang L, Li X, Wang JP, Jiang TJ. Detection of GAD-Ab index in diabetic patients using ³⁵S-labeled recombinant human GAD₆₅ antigen. *Zhonghua Heyixue Zazhi* 2003; **23**: 82-86
- 13 **Falorni A**, Ortqvist E, Persson B, Lernmark A. Radioimmunoassays for glutamic acid decarboxylase (GAD65) and GAD65 autoantibodies using 35S or 3H recombinant human ligands. *J Immunol Methods* 1995; **186**: 89-99
- 14 **Woo W**, LaGasse JM, Zhou Z, Patel R, Palmer JP, Campus H, Hagopian WA. A novel high-throughput method for accurate, rapid, and economical measurement of multiple type 1 diabetes autoantibodies. *J Immunol Methods* 2000; **244**: 91-103
- 15 **Turner R**, Stratton I, Horton V, Manley S, Zimmet P, Mackay IR, Shattock M, Bottazzo GF, Holman R. UKPDS 25: autoantibodies to islet-cell cytoplasm and glutamic acid decarboxylase for prediction of insulin requirement in type 2 diabetes. UK Prospective Diabetes Study Group. *Lancet* 1997; **350**: 1288-1293
- 16 **U.K. prospective diabetes study 16**. Overview of 6 years' therapy of type II diabetes: a progressive disease. U.K. Prospective Diabetes Study Group. *Diabetes* 1995; **44**: 1249-1258
- 17 **Gottsater A**, Landin-Olsson M, Lernmark A, Fernlund P, Sundkvist G, Hagopian WA. Glutamate decarboxylase antibody levels predict rate of beta-cell decline in adult-onset diabetes. *Diabetes Res Clin Pract* 1995; **27**: 133-140
- 18 **Seissler J**, de Sonnaville JJ, Morgenthaler NG, Steinbrenner H, Glawe D, Khoo-Morgenthaler UY, Lan MS, Notkins AL, Heine RJ, Scherbaum WA. Immunological heterogeneity in type I diabetes: presence of distinct autoantibody patterns in patients with acute onset and slowly progressive disease. *Diabetologia* 1998; **41**: 891-897
- 19 **Torn C**, Landin-Olsson M, Lernmark A, Palmer JP, Arnqvist HJ, Blohme G, Lithner F, Littorin B, Nystrom L, Schersten B, Sundkvist G, Wibell L, Ostman J. Prognostic factors for the course of beta cell function in autoimmune diabetes. *J Clin Endocrinol Metab* 2000; **85**: 4619-4623
- 20 **Torn C**, Landin-Olsson M, Lernmark A, Schersten B, Ostman J, Arnqvist HJ, Bjork E, Blohme G, Bolinder J, Eriksson J, Littorin B, Nystrom L, Sundkvist G. Combinations of beta cell specific autoantibodies at diagnosis of diabetes in young adults reflects different courses of beta cell damage. *Autoimmunity* 2001; **33**: 115-120
- 21 **Rattarasarn C**, Diosdado MA. Clinical characteristics, and time course of pancreatic beta-cell function and glutamic acid decarboxylase antibodies in Thai patients with adult-onset Type 1 diabetes: distinction between patients of rapid- and slow-onset. *Horm Metab Res* 1999; **31**: 311-316
- 22 **Littorin B**, Sundkvist G, Hagopian W, Landin-Olsson M, Lernmark A, Ostman J, Arnqvist HJ, Blohme G, Bolinder J, Eriksson JW, Lithner F, Schersten B, Wibell L. Islet cell and glutamic acid decarboxylase antibodies present at diagnosis of diabetes predict the need for insulin treatment. A cohort study in young adults whose disease was initially labeled as type 2 or unclassifiable diabetes. *Diabetes Care* 1999; **22**: 409-412
- 23 **Falorni A**, Gambelunghe G, Forini F, Kassi G, Cosentino A, Candeloro P, Bolli GB, Brunetti P, Calcinaro F. Autoantibody recognition of COOH-terminal epitopes of GAD65 marks the risk for insulin requirement in adult-onset diabetes mellitus. *J Clin Endocrinol Metab* 2000; **85**: 309-316
- 24 **Decochez K**, Keymeulen B, Somers G, Dorchy H, De Leeuw IH, Mathieu C, Rottiers R, Winnock F, ver Elst K, Weets I, Kaufman L, Pipeleers DG, Rottiers R. Use of an islet cell antibody assay to identify type 1 diabetic patients with rapid decrease in C-peptide levels after clinical onset. Belgian Diabetes Registry. *Diabetes Care* 2000; **23**: 1072-1078
- 25 **Chiu KC**, Lee NP, Cohan P, Chuang LM. Beta cell function declines with age in glucose tolerant Caucasians. *Clin Endocrinol (Oxf)* 2000; **53**: 569-575
- 26 **Bonfanti R**, Bazzigaluppi E, Calori G, Riva MC, Viscardi M, Bognetti E, Meschi F, Bosi E, Chiumello G, Bonifacio E. Parameters associated with residual insulin secretion during the first year of disease in children and adolescents with Type 1 diabetes mellitus. *Diabet Med* 1998; **15**: 844-850
- 27 **Skyler JS**, Rabinovitch A. Cyclosporine in recent onset type I diabetes mellitus. Effects on islet beta cell function. Miami Cyclosporine Diabetes Study Group. *J Diabetes Complications* 1992; **6**: 77-88
- 28 **Pozzilli P**, Di Mario U. Autoimmune diabetes not requiring insulin at diagnosis (latent autoimmune diabetes of the adult): definition, characterization, and potential prevention. *Diabetes Care* 2001; **24**: 1460-1467
- 29 **Kobayashi T**, Nakanishi K, Murase T, Kosaka K. Small doses of subcutaneous insulin as a strategy for preventing slowly progressive beta-cell failure in islet cell antibody-positive patients with clinical features of NIDDM. *Diabetes* 1996; **45**: 622-626
- 30 **Kobayashi T**, Maruyama T, Shimada A, Kasuga A, Kanatsuka A, Takei I, Tanaka S, Yokoyama J. Insulin intervention to preserve beta cells in slowly progressive insulin-dependent (type 1) diabetes mellitus. *Ann N Y Acad Sci* 2002; **958**: 117-130
- 31 **Li X**, Zhou ZG, Huang G, Peng J, Yang L, Wang JP, Yang L. Rosiglitazone combined with insulin preserves Islet β Cell Function in LADA: A preliminary study. *Zhongguo Tangniaobing Zazhi* 2003; **11**: 242-246

• BASIC RESEARCH •

Nestin-positive progenitor cells isolated from human fetal pancreas have phenotypic markers identical to mesenchymal stem cells

Ling Zhang, Tian-Pei Hong, Jiang Hu, Yi-Nan Liu, Yong-Hua Wu, Ling-Song Li

Ling Zhang, Tian-Pei Hong, Yong-Hua Wu, Department of Endocrinology, Peking University Third Hospital, Beijing 100083, China

Jiang Hu, Yi-Nan Liu, Ling-Song Li, Stem Cell Research Center, Peking University Health Science Center, Beijing 100083, China

Supported by the National Natural Science Foundation of China, No. 30170443; Major State Basic Research Development Program of China, No. 2001CB510105 and "211" Project Foundation of Peking University

Co-correspondents: Ling-Song Li

Correspondence to: Dr. Tian-Pei Hong, Department of Endocrinology, Peking University Third Hospital, 49 Huayuanbeilu, Haidian District, Beijing 100083, China. tpho66@bjmu.edu.cn
Telephone: +86-10-62017691-8212 Fax: +86-10-62017700

Received: 2004-06-19 Accepted: 2004-07-22

CONCLUSION: Nestin-positive cells isolated from human fetal pancreas possess the characteristics of pancreatic progenitor cells since they have highly proliferative potential and the capability of differentiation into insulin-producing cells *in vitro*. Interestingly, the nestin-positive pancreatic progenitor cells share many phenotypic markers with mesenchymal stem cells derived from bone marrow.

© 2005 The WJG Press and Elsevier Inc. All rights reserved.

Key words: Fetus; Nestin; Pancreas; Stem cells

Zhang L, Hong TP, Hu J, Liu YN, Wu YH, Li LS. Nestin-positive progenitor cells isolated from human fetal pancreas have phenotypic markers identical to mesenchymal stem cells. *World J Gastroenterol* 2005; 11(19): 2906-2911
<http://www.wjgnet.com/1007-9327/11/2906.asp>

Abstract

AIM: To isolate nestin-positive progenitor cells from human fetal pancreas and to detect their surface markers and their capability of proliferation and differentiation into pancreatic islet endocrine cells *in vitro*.

METHODS: Islet-like cell clusters (ICCs) were isolated from human fetal pancreas by using collagenase digestion. The free-floating ICCs were handpicked and cultured in a new dish. After the ICCs developed into monolayer epithelium-like cells, they were passaged and induced for differentiation. Reverse transcription polymerase chain reaction (RT-PCR), immunofluorescence stain, fluorescence-activated cell sorting (FACS) and radioimmunoassay (RIA) were used to detect the expression of cell markers.

RESULTS: (1) The monolayer epithelium-like cells had highly proliferative potential and could be passaged more than 16 times *in vitro*; (2) RT-PCR analysis and immunofluorescence stain showed that these cells expressed both nestin and ABCG2, two of stem cell markers; (3) FACS analysis revealed that CD44, CD90 and CD147 were positive, whereas CD34, CD38, CD45, CD71, CD117, CD133 and HLA-DR were negative on the nestin-positive cells; (4) RT-PCR analysis showed that the mRNA expression of insulin, glucagon and pancreaticoduodenal homeobox gene-1 was detected, whereas the expression of nestin and neurogenin 3 disappeared in these cells treated with serum-free media supplemented with the cocktail of growth factors. Furthermore, the intracellular insulin content was detected by RIA after the induction culture.

INTRODUCTION

Pancreatic β -cell replacement therapy via islet transplantation has become a subject of intense interest again, because the recent success rate of the procedure is largely improved by using the Edmonton protocol. However, this successful new protocol utilizes the islets isolated from at least two human cadaveric pancreata^[1]. In order to make such a therapy available to more than a few of thousands of patients with diabetes, new sources of insulin-producing cells must be identified. Pancreatic stem cells have the capacity to expand and differentiate into pancreatic islet cells, and are therefore considered as the potential donor source for islet transplantation.

A definitive molecular marker of pancreatic stem cells remains obscure. One recent study demonstrated that nestin-positive cells resided in adult human and rat islets had the characteristics of stem cells and could be differentiated into pancreatic endocrine, exocrine and hepatic cell phenotypes *in vitro*^[2]. Therefore, it has been firstly proposed that nestin is a marker for pancreatic stem cells. Another more recent report showed that nestin-positive precursors derived from human fetal pancreas could differentiate into pancreatic endocrine cells, which displayed the ability to reverse hyperglycemia in diabetic mice^[3]. On the other hand, several other publications have recently suggested that nestin-positive cells in either adult or fetal pancreata were unable to generate pancreatic islet β -cells *in vitro*^[4-6]. This controversy

may reflect that nestin-positive pancreatic cells may be a heterogeneous cell population, or the protocol for inducing their differentiation must be optimized.

In this study, nestin-positive cells were isolated from human fetal pancreata, and then reverse transcription polymerase chain reaction (RT-PCR), immunofluorescence stain, fluorescence-activated cell sorting (FACS) and radioimmunoassay (RIA) were used to determine whether the nestin-positive pancreatic cells had the characteristics of stem cells.

MATERIALS AND METHODS

Isolation, culture and induction of pancreatic progenitor cells

Human fetal pancreata at 20th gestational weeks were provided by Department of Obstetrics and Gynecology, Peking University First Hospital after the termination of pregnancy. Informed consent for tissue donation was obtained by the procurement centers. In addition, our institutional review board had reviewed and approved the use of fetal tissue for these studies. The pancreata were received within 8 h after procurement and enzymatically digested as previously described^[7]. The digested tissue was washed twice in cold HBSS and placed on 100-mm bacteria Petri dishes in RPMI 1640 media (Hyclone, Logan, UT, USA) supplemented with 10% fetal bovine serum (Hyclone), 10 mmol/L HEPES, 1 mmol/L sodium pyruvate and 71.5 μ mol/L β -mercaptoethanol (Merck, Darmstadt, Germany). After incubation for 96 h, the floating islet-like cell clusters (ICCs) were pipetted out and cultured in new dishes with fresh media supplemented with 20 ng/mL basic fibroblast growth factor and 20 ng/mL epidermal growth factor (both from Invitrogen, Carlsbad, CA, USA). The ICCs attached to the bottom and a monolayer of epithelium-like cells started the outgrowth from the ICCs within 24 h. After confluence, the cells were repeatedly passaged. After about 80% confluence in the cells passaged 10 times, a serum-free medium supplemented with 100 pmol/L hepatocyte growth factor (Chemicon, Temecula, CA, USA), 2 nmol/L activin A (R&D Systems, Minneapolis, MN, USA), 500 pmol/L betacellulin, 10 nmol/L exendin-4 (glucagon-like peptide-1 analog) and 10 mmol/L nicotinamide (all three from Sigma, St. Louis, MO, USA) in a low-glucose concentration (5 mmol/L) was changed, and the cells were further cultured for another 6 d.

Immunofluorescence

The expanded pancreatic progenitor cells were grown on coverslips and processed as previously described^[8]. Briefly, the cells were fixed in 4% paraformaldehyde in PBS for 15 min at room temperature. The cells were rinsed with PBST (PBS with 0.5% Triton X-100) thrice and incubated in PBS containing 10% goat serum and 0.01% Triton X-100 for blocking, and then incubated overnight at 4 °C with mouse anti-human nestin monoclonal antibody (1:100; BD Transduction Laboratories, Lexington, KY, USA). After washing thrice with PBST, the cells were incubated with FITC-conjugated goat anti-mouse IgG (1:100; BD Transduction Laboratories) for 1 h at room temperature. Following three washes with PBS, the samples were mounted on slides and

examined with an Olympus BX51 fluorescence microscope (Olympus Optical, Tokyo, Japan) equipped with a Micro Color RGB-MS-C CCD camera (CRI, Woburn, MA, USA).

Identification of cell surface markers by FACS

2 \times 10⁵ of the cells passaged 10 times were resuspended in 100 μ L of PBS and incubated with FITC-conjugated CD34, CD38, CD45, CD90 and HLA-DR antibodies, and PE-conjugated CD44, CD71, CD117, CD133 and CD147 antibodies (all from BD Pharmingen, San Diego, CA, USA) for 30 min at 4 °C. After washing with PBS twice, the labeled cells were analyzed in a flow cytometer (Becton-Dickinson, San Jose, CA, USA).

RNA extraction and RT-PCR analysis

RNA was isolated from the cultured pancreatic progenitor cells using TRIzol (Gibco, Carlsbad, CA, USA) following the manufacturer's protocol. Single-stranded cDNA was prepared with the Superscript First-Strand System (Invitrogen) as described previously^[9]. The cDNAs were amplified by polymerase chain reaction (PCR). The PCR products were analyzed by 1% agarose gel electrophoresis. G₃PDH, nestin, ABCG2, pancreatic-duodenal homeobox gene-1 (PDX-1), insulin, and glucagon were amplified for 30, 40, 34, 35, 36 and 23 cycles, and the annealing temperatures were 50, 55, 56, 52, 62, and 59 °C, respectively. The annealing temperature of neurogenin 3 (Ngn3) was descended from 68 to 57 °C at 1 °C every cycle, and then the PCR reaction was run for 29 cycles. The sequences of primers were as follows: 5' ACC ACA GTC CAT GCC ATC AC 3' and 5' ATG TCG TTG TCC CAC CAC CT 3' for G₃PDH; 5' AGC GTT GGA ACA GAG GTT GGA 3' and 5' TGT TTC CTC CCA CCC TGT GTC T 3' for nestin; 5' GGC CTC AGG AAG ACT TAT GT 3' and 5' AAG GAG GTG GTG TAG CTG AT 3' for ABCG2; 5' AGA GCG AGT TGG CAC TGA G 3' and 5' CTG AGA AAG CCA GAC TGC C 3' for Ngn3; 5' CCC ATG GAT GAA GTC TAC C 3' and 5' GTC CTC CTC CTT TTT CCA C 3' for PDX-1; 5' GCC TTT GTG AAC CAA CAC CTG 3' and 5' GTT GCA GTA GTT CTC CAG CTG 3' for insulin; and 5' ATG AAC GAG GAC AAG CGC 3' and 5' TTC ACC AGC CAA GCA ATG 3' for glucagon.

Measurement of intracellular insulin content by RIA

For the determination of insulin content, insulin was extracted from the cells before and after induction following standard protocol^[10]. The cells were washed twice in PBS, and treated with acid ethanol (10% glacial acetic acid in absolute ethanol) overnight at 4 °C, followed by cell sonication. Total protein in the lysates was determined by Biophotometer (Eppendorf, Hamburg, Germany). Insulin was measured by using a solid-phase radioimmunoassay (RIA) kit (DPC, Los Angeles, CA, USA).

RESULTS

Nestin-positive progenitor cells isolated from human fetal pancreas

After a 96-h incubation, the free-floating ICCs were handpicked and placed into a new dish. Within 24 h, the

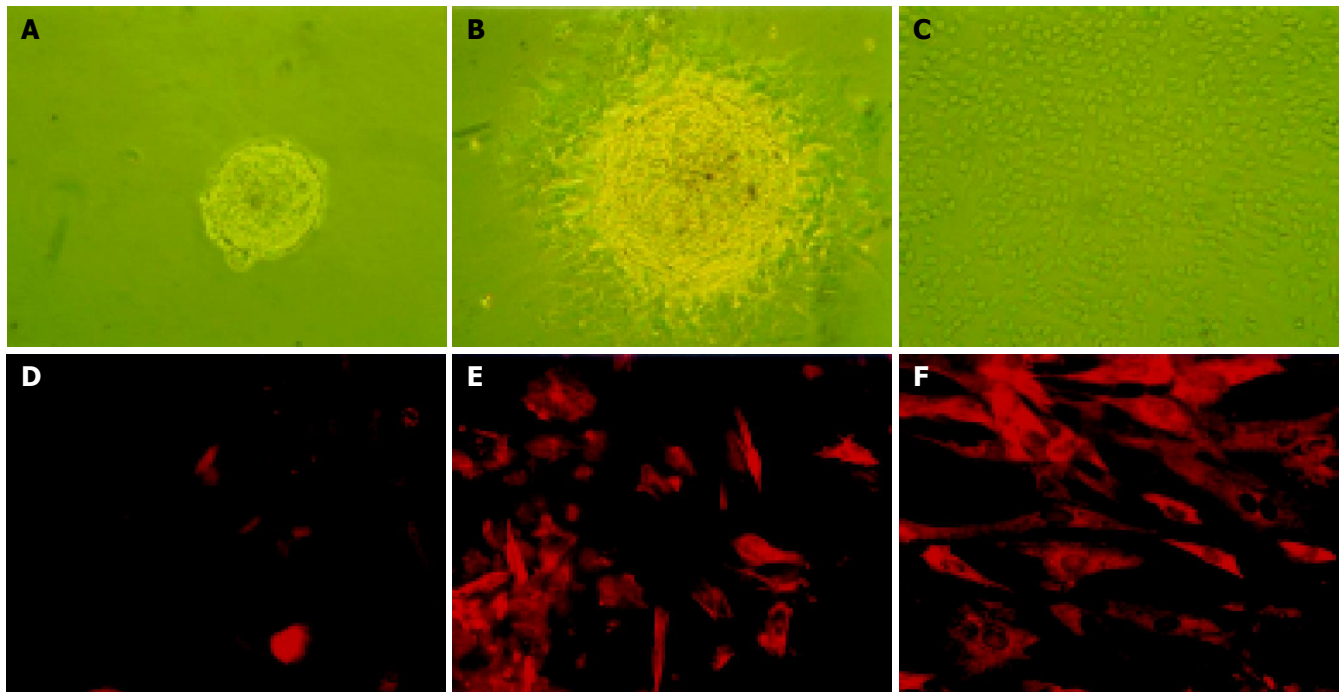


Figure 1 The culture (A-C) and immunofluorescence staining (D-F) of nestin-positive cells isolated from human fetal pancreas. **A:** The free-floating ICCs isolated from fetal human pancreas; **B:** After pipetted out and cultured in a new dish, the ICCs attached to the bottom and a monolayer of epithelium-like cells spread out; **C:** The epithelium-like cells making confluent sheet, the ICCs

disappeared structurally ($\times 100$); **D:** Negative control using mouse IgG to substitute the primary antibody; **E:** Nestin expressed in some of the epithelium-like cells spreading out from ICCs. **F:** Expression of nestin in most of the epithelium-like cells passaged 10 times ($\times 200$).

ICC attached to the bottom and epithelium-like cells spread out from the ICCs (Figures 1A-C). The cells were able to be passaged more than 16 times *in vitro*. To confirm the existence of nestin-positive cells, an immunofluorescence study was conducted in the cultured pancreatic cells. Nestin expression was detected in the monolayer cells that grew out from the ICCs and in those that passaged for 10 times (Figures 1D-F). RT-PCR showed that both nestin and ABCG2 were expressed in the passaged cells (Figure 2).

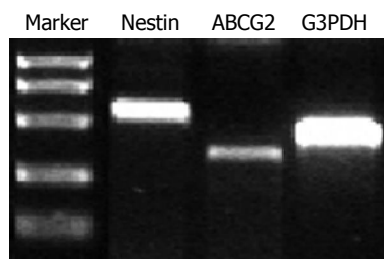


Figure 2 RT-PCR analysis of nestin (549 bp) and ABCG2 (342 bp) expression in the cultured cells. G₃PDH (452 bp) served as internal control.

Surface markers of the nestin-positive pancreatic progenitor cells

FACS analysis showed that CD44, CD90 and CD147 were positive, whereas CD34, CD38, CD45, CD71, CD 117, CD133 and HLA-DR were negative in the nestin-positive pancreatic progenitor cells (Figure 3), suggesting that the phenotype of these cells was identical to that of mesenchymal

stem cells derived from bone marrow.

In vitro differentiation of the nestin-positive pancreatic progenitor cells

To investigate the ability of the nestin-positive cells to differentiate into pancreatic islet endocrine cells, the nestin-positive cells were cultured in the serum-free media with the cocktail of several growth factors for 6 d. RT-PCR analysis showed that the mRNA expression of insulin, glucagon and PDX-1 appeared, whereas the expression of nestin and Ngn3 disappeared in these cells after the induction culture (Figure 4). Furthermore, the intracellular insulin protein content was detectable in the cells after the induction culture, but not in the cells before the induction culture (Figure 5).

DISCUSSION

The intermediate filament protein nestin has been identified as a marker for neural stem cells^[11,12]. A recent study showed that nestin-positive cells isolated from adult human and rat islets could be expanded and differentiated into pancreatic endocrine, exocrine and hepatic phenotypes *in vitro*, leading to the suggestion that they were multipotent tissue stem cells^[2]. Studies have also shown that ES cell-derived cultures enriched for nestin-expressing cells can be differentiated *in vitro* into cells that produce both insulin and glucagon^[10,13,14]. Furthermore, another paper demonstrated recently that nestin-positive precursors derived from human fetal pancreas were induced to differentiate into pancreatic endocrine cells that displayed the ability to reverse hyperglycemia in diabetic mice^[3]. These observations have led to the hypothesis

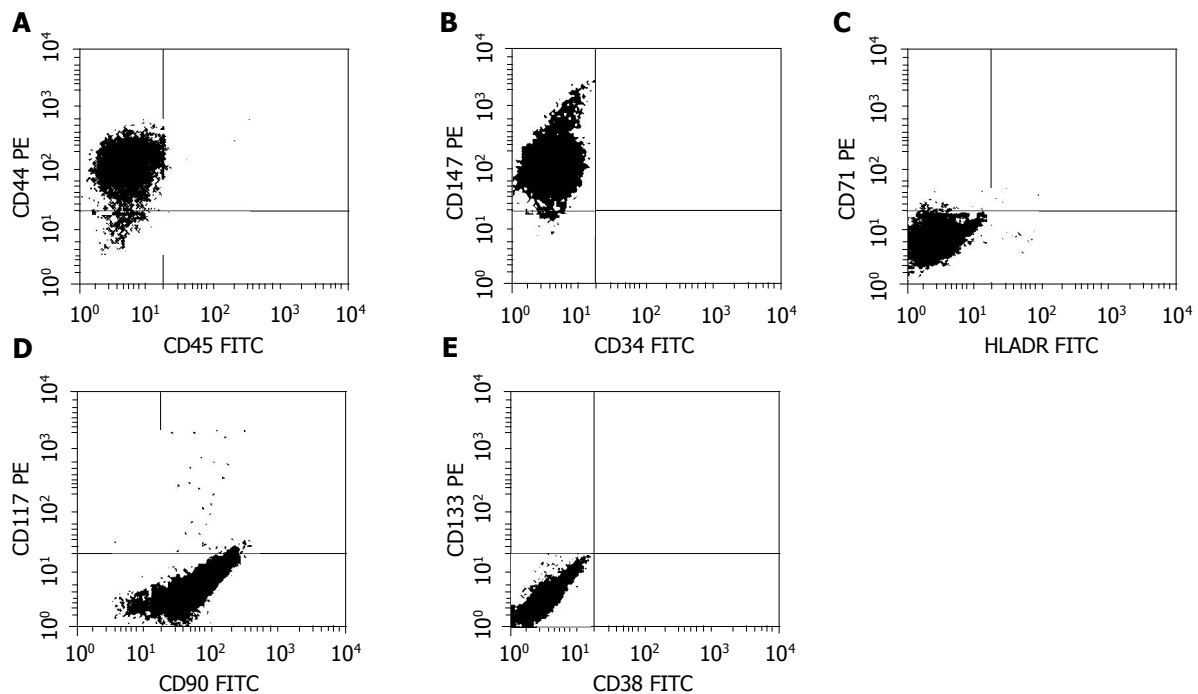


Figure 3 FACS analysis of the surface marker in the nestin-positive cells. The cells were labeled with FITC- or PE-conjugated antibodies and then analyzed in a flow cytometer. CD44, CD90 and CD147 were positive, whereas CD34,

CD38, CD45, CD71, CD117, CD133 and HLA-DR were negative in the cells, resembling the phenotype of mesenchymal stem cells.

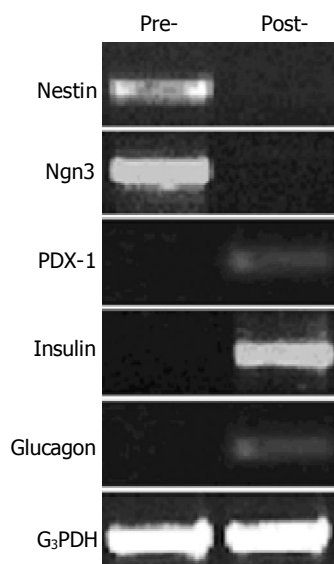


Figure 4 RT-PCR analysis of gene expression change in the nestin-positive cells before and after induction by using the primers for nestin (549 bp), Ngn3 (420 bp), PDX-1 (262 bp), insulin (261 bp), and glucagon (236 bp). G₃PDH were used as internal control (452 bp). Pre-, cells before induction; post-, cells after induction.

that nestin is a marker of pancreatic stem cells.

An important property of stem cells is their ability for self-renewal and differentiation into specific cell lineages. In the present study, we showed that nestin-positive cells isolated from human fetal pancreas had highly proliferative potential. These cells could be passaged more than 16 times *in vitro*. To determine whether the nestin-positive cells could differentiate into pancreatic endocrine cells, the cells were

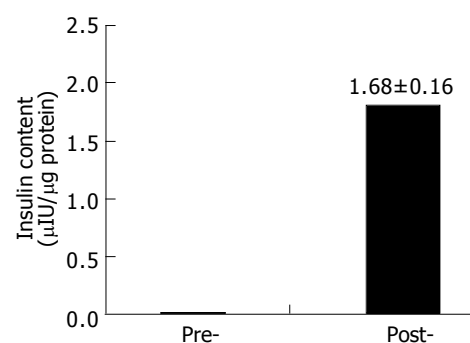


Figure 5 RIA detection of intra-cellular insulin content before and after induction. Data are the mean \pm SD of three separate experiments with the nestin-positive cells. Pre-, the cells before induction; post-, the cells after induction.

induced for differentiation after exposure to the serum-free media supplemented with the cocktail of growth factors. Our results revealed that the mRNA expression of pancreatic endocrine cell markers insulin, glucagon and PDX-1 was detected, whereas the expression of pancreatic progenitor cell markers nestin and Ngn3 disappeared in the cells after the induction. Moreover, the intracellular insulin protein content was also detectable in the cells after the induction. These results suggest that the nestin-positive pancreatic cells possess the characteristics of stem cells.

ABCG2 known as a member of ATP binding cassette (ABC) transporter superfamily, also called Bcrp1, can efflux the fluorescent dyes such as Hoechst 33342 from the cells termed as side population (SP) cells displaying low Hoechst fluorescence. SP cells were firstly isolated following Hoechst 33342 staining from murine hematopoietic stem cells, which was highly replicating and presented in the bone marrow of

all species examined^[15,16]. Soon after, it has been demonstrated that stem cells from skeletal muscle^[17,18], brain^[19], heart^[20], lung^[21] and possibly other tissues^[22,23], as well as ES cells^[23], can be identified by the SP phenotype. Therefore, the SP phenotype might represent a common molecular feature for stem cells possessing multi-organ plasticity^[23]. Meanwhile, the studies have shown that ABCG2 gene expression alone defines the SP phenotype and is a conserved feature of stem cells from a wide variety of sources^[23]. RT-PCR analysis in this study revealed that ABCG2 mRNA was expressed in the nestin-positive cells isolated from human fetal pancreas. These results further support that the nestin-positive cells have the characteristics of pancreatic stem cells.

Importantly, this study also showed that the nestin-positive pancreatic progenitor cells shared many phenotypic markers with mesenchymal stem cells derived from bone marrow. Mesenchymal stem cells of bone marrow origin are a kind of multipotential stem cells that can differentiate into adipocytic, chondrocytic or osteocytic lineages, neurons and functional hepatocyte-like cells under the appropriate induction condition^[24-26]. Several other studies reported that mesenchymal stem cells were isolated from postnatal murine muscle and brain, human first-trimester fetal blood and liver, human umbilical cord, and human trabecular bone^[27-30]. Therefore, it has been proposed that mesenchymal stem cells may be the universal stem cells akin to ES cells existing in multiple tissues, which take part in tissue repairs and regeneration and possess multi-organ plasticity. Interestingly, a recent paper shows that bone marrow harbors cells which have the capacity to differentiate into functionally competent pancreatic islet β -cells^[31].

In summary, the nestin-positive cells isolated from human fetal pancreas possess the characteristics of pancreatic progenitor cells since they have highly proliferative potential and the capability of differentiation into pancreatic endocrine cells *in vitro*. We show for the first time that these nestin-positive pancreatic progenitor cells share many phenotypic markers with mesenchymal stem cells derived from bone marrow.

ACKNOWLEDGMENTS

This work was supported by the grants from the National Natural Science Foundation of China (30170443), Major State Basic Research Development Program of China (2001CB510105) and "211" Project Foundation of Peking University. We are grateful to Ai-Li Lu and Lu Zhang for excellent technical assistance.

REFERENCES

- Shapiro AM, Lakey JR, Ryan EA, Korbutt GS, Toth E, Warnock GL, Kneteman NM, Rajotte RV. Islet transplantation in seven patients with type 1 diabetes mellitus using a glucocorticoid-free immunosuppressive regimen. *N Engl J Med* 2000; **343**: 230-238
- Zulewski H, Abraham EJ, Gerlach MJ, Daniel PB, Moritz W, Muller B, Vallejo M, Thomas MK, Habener JF. Multipotential nestin-positive stem cells isolated from adult pancreatic islets differentiate *ex vivo* into pancreatic endocrine, exocrine, and hepatic phenotypes. *Diabetes* 2001; **50**: 521-533
- Huang H, Tang X. Phenotypic determination and characterization of nestin-positive precursors derived from human fetal pancreas. *Lab Invest* 2003; **83**: 539-547
- Gao R, Ustinov J, Pulkkinen MA, Lundin K, Korsgren O, Otonkoski T. Characterization of endocrine progenitor cells and critical factors for their differentiation in human adult pancreatic cell culture. *Diabetes* 2003; **52**: 2007-2015
- Treutelaar MK, Skidmore JM, Dias-Leme CL, Hara M, Zhang L, Simeone D, Martin DM, Burant CF. Nestin-lineage cells contribute to the microvasculature but not endocrine cells of the islet. *Diabetes* 2003; **52**: 2503-2512
- Humphrey RK, Bucay N, Beattie GM, Lopez A, Messam CA, Cirulli V, Hayek A. Characterization and isolation of promoter-defined nestin-positive cells from the human fetal pancreas. *Diabetes* 2003; **52**: 2519-2525
- Otonkoski T, Beattie GM, Mally MI, Ricordi C, Hayek A. Nicotinamide is a potent inducer of endocrine differentiation in cultured human fetal pancreatic cells. *J Clin Invest* 1993; **92**: 1459-1466
- Beattie GM, Rubin JS, Mally MI, Otonkoski T, Hayek A. Regulation of proliferation and differentiation of human fetal pancreatic islet cells by extracellular matrix, hepatocyte growth factor, and cell-cell contact. *Diabetes* 1996; **45**: 1223-1228
- Hong TP, Andersen NA, Nielsen K, Karlens AE, Fantuzzi G, Eizirik DL, Dinarello CA, Mandrup-Poulsen T. Interleukin-18 mRNA, but not interleukin-18 receptor mRNA, is constitutively expressed in islet beta-cells and up-regulated by interferon-gamma. *Eur Cytokine Netw* 2000; **11**: 193-205
- Lumelsky N, Blondel O, Laeng P, Velasco I, Ravin R, McKay R. Differentiation of embryonic stem cells to insulin-secreting structures similar to pancreatic islets. *Science* 2001; **292**: 1389-1394
- Lendahl U, Zimmerman LB, McKay RD. CNS stem cells express a new class of intermediate filament protein. *Cell* 1990; **60**: 585-595
- Dahlstrand J, Zimmerman LB, McKay RD, Lendahl U. Characterization of the human nestin gene reveals a close evolutionary relationship to neurofilaments. *J Cell Sci* 1992; **103**(Pt 2): 589-597
- Hori Y, Rulifson IC, Tsai BC, Heit JJ, Cahoy JD, Kim SK. Growth inhibitors promote differentiation of insulin-producing tissue from embryonic stem cells. *Proc Natl Acad Sci USA* 2002; **99**: 16105-16110
- Blyszczuk P, Czyz J, Kania G, Wagner M, Roll U, St-Onge L, Wobus AM. Expression of Pax4 in embryonic stem cells promotes differentiation of nestin-positive progenitor and insulin-producing cells. *Proc Natl Acad Sci USA* 2003; **100**: 998-1003
- Goodell MA, Brose K, Paradis G, Conner AS, Mulligan RC. Isolation and functional properties of murine hematopoietic stem cells that are replicating *in vivo*. *J Exp Med* 1996; **183**: 1797-1806
- Goodell MA, Rosenzweig M, Kim H, Marks DF, DeMaria M, Paradis G, Grupp SA, Sieff CA, Mulligan RC, Johnson RP. Dye efflux studies suggest that hematopoietic stem cells expressing low or undetectable levels of CD34 antigen exist in multiple species. *Nat Med* 1997; **3**: 1337-1345
- Jackson KA, Mi T, Goodell MA. Hematopoietic potential of stem cells isolated from murine skeletal muscle. *Proc Natl Acad Sci USA* 1999; **96**: 14482-14486
- Gussoni E, Soneoka Y, Strickland CD, Buzney EA, Khan MK, Flint AF, Kunkel LM, Mulligan RC. Dystrophin expression in the mdx mouse restored by stem cell transplantation. *Nature* 1999; **401**: 390-394
- Hulspar R, Quesenberry PJ. Characterization of neurosphere cell phenotypes by flow cytometry. *Cytometry* 2000; **40**: 245-250
- Hierlihy AM, Seale P, Lobe CG, Rudnicki MA, Megeney LA. The post-natal heart contains a myocardial stem cell population. *FEBS Lett* 2002; **530**: 239-243
- Summer R, Kotton DN, Sun X, Ma B, Fitzsimmons K, Fine A. Side population cells and Bcrp1 expression in lung. *Am J*

- Physiol Lung Cell Mol Physiol* 2003; **285**: L97-104
- 22 **Asakura A**, Rudnicki MA. Side population cells from diverse adult tissues are capable of *in vitro* hematopoietic differentiation. *Exp Hematol* 2002; **30**: 1339-1345
- 23 **Zhou S**, Schuetz JD, Bunting KD, Colapietro AM, Sampath J, Morris JJ, Lagutina I, Grosveld GC, Osawa M, Nakauchi H, Sorrentino BP. The ABC transporter Bcrp1/ABCG2 is expressed in a wide variety of stem cells and is a molecular determinant of the side-population phenotype. *Nat Med* 2001; **7**: 1028-1034
- 24 **Pittenger MF**, Mackay AM, Beck SC, Jaiswal RK, Douglas R, Mosca JD, Moorman MA, Simonetti DW, Craig S, Marshak DR. Multilineage potential of adult human mesenchymal stem cells. *Science* 1999; **284**: 143-147
- 25 **Pittenger MF**, Mosca JD, McIntosh KR. Human mesenchymal stem cells: progenitor cells for cartilage, bone, fat and stroma. *Curr Top Microbiol Immunol* 2000; **251**: 3-11
- 26 **Schwartz RE**, Reyes M, Koodie L, Jiang Y, Blackstad M, Lund T, Lenvik T, Johnson S, Hu WS, Verfaillie CM. Multipotent adult progenitor cells from bone marrow differentiate into functional hepatocyte-like cells. *J Clin Invest* 2002; **109**: 1291-1302
- 27 **Jiang Y**, Vaessen B, Lenvik T, Blackstad M, Reyes M, Verfaillie CM. Multipotent progenitor cells can be isolated from postnatal murine bone marrow, muscle, and brain. *Exp Hematol* 2002; **30**: 896-904
- 28 **Campagnoli C**, Roberts IA, Kumar S, Bennett PR, Bellantuono I, Fisk NM. Identification of mesenchymal stem/progenitor cells in human first-trimester fetal blood, liver, and bone marrow. *Blood* 2001; **98**: 2396-2402
- 29 **Romanov YA**, Svintsitskaya VA, Smirnov VN. Searching for alternative sources of postnatal human mesenchymal stem cells: candidate MSC-like cells from umbilical cord. *Stem Cells* 2003; **21**: 105-110
- 30 **Sottile V**, Halleux C, Bassilana F, Keller H, Seuwen K. Stem cell characteristics of human trabecular bone-derived cells. *Bone* 2002; **30**: 699-704
- 31 **Ianus A**, Holz GG, Theise ND, Hussain MA. *In vivo* derivation of glucose-competent pancreatic endocrine cells from bone marrow without evidence of cell fusion. *J Clin Invest* 2003; **111**: 843-850

Science Editor Guo SY Language Editor Elsevier HK

• BASIC RESEARCH •

Effect of vector-expressed shRNAs on hTERT expression

Ying Guo, Jun Liu, Ying-Hui Li, Tian-Bao Song, Jing Wu, Cai-Xia Zheng, Cai-Fang Xue

Ying Guo, Jing Wu, Cai-Xia Zheng, Department of Obstetrics and Gynecology, Second Hospital of Xi'an Jiaotong University, Xi'an 710001, Shaanxi Province, China

Jun Liu, Ying-Hui Li, Cai-Fang Xue, Department of Etiology, Fourth Military Medical University, Xi'an 710033, Shaanxi Province, China

Tian-Bao Song, Department of Histology and Embryology, Medical School of Xi'an Jiaotong University, Xi'an 710061, Shaanxi Province, China

Supported by the Shaanxi Province Natural Science Foundation, No. 2003C217

Correspondence to: Dr. Jun Liu, Department of Etiology, Fourth Military Medical University, Xi'an 710033, Shaanxi Province, China. etiology@fmmu.edu.cn

Telephone: +86-29-83374536 Fax: +86-29-83374594

Received: 2004-06-29 Accepted: 2004-07-22

Abstract

AIM: To study the effect of short hairpin RNAs (shRNAs) expressed from DNA vector on hTERT expression.

METHODS: Oligonucleotides coding for four shRNAs against hTERT were cloned into a mammalian shRNA expression vector pUC18U6 to form pUC18U6ht1-4, which were then introduced into HepG2 cells by using liposome-mediated transfection. HepG2 cells transfected by pUC18U6 and pUC18U6GFPsir, which expressed shRNA against green fluorescent protein (GFP), were used as controls. hTERT mRNA in the transfected cells were quantified by using real-time fluorescent RT-PCR.

RESULTS: Among the four shRNAs against hTERT, two decreased the hTERT mRNA level. Compared with the controls, pUC18U6ht which expressed the two shRNAs reduced hTERT mRNA by 39% and 49% ($P < 0.05$).

CONCLUSION: hTERT expression is inhibited by the shRNAs expressed from the DNA vector.

© 2005 The WJG Press and Elsevier Inc. All rights reserved.

Key words: RNA interference; Short hairpin RNA; Telomerase

Guo Y, Liu J, Li YH, Song TB, Wu J, Zheng CX, Xue CF. Effect of vector-expressed shRNAs on hTERT expression. *World J Gastroenterol* 2005; 11(19): 2912-2915
<http://www.wjgnet.com/1007-9327/11/2912.asp>

INTRODUCTION

Telomeres are the ends of eukaryotic linear chromosomes.

Consisting of tandem repeats of G-rich nucleotides and associated proteins, telomeres protect chromosomes from degradation, fusion, and recombination and are therefore important for maintaining genomic stability^[1,2]. In most normal somatic cells, telomeres shorten with each cycle of cell division due to a so-called "end-replication problem"^[3]. When telomeres reach a critical short length, cell arrest/apoptosis will ensue, which is called cell senescence. However, for immortal cells, such as germ cells and cancer cells, telomeres maintain their length stable generally through the action of a cellular reverse transcriptase-telomerase^[2,4-6]. Telomerase is a ribonucleoprotein and, using RNA subunit as a template, the catalytic subunit of telomerase (telomerase reverse transcriptase, TERT) adds telomeric hexanucleotide repeats onto chromosome ends, thus compensating for telomeric loss accompanying each cell division. Eighty-five percent of all cancers are telomerase positive, while for most normal somatic cells, telomerase activity is absent or very low^[7,8]. Furthermore, recent studies have demonstrated that reactivation of telomerase is a key step in tumorigenesis^[9]. Therefore, telomerase is considered to be an ideal target for cancer therapy, and many strategies have been developed to inhibit telomerase, such as antisense nucleotides, ribozymes, dominant-negative proteins and small synthetic molecules^[10-13].

RNA interference (RNAi) is a potent gene silencing mechanism conserved in all eukaryotes, in which double-stranded RNAs suppress the expression of cognate genes by inducing degradation of mRNAs or blocking mRNAs translation^[14-16]. In mammalian cells, double-stranded RNAs inducing RNAi must be short in length (<30 bp) so that they will not activate nonspecific interferon reaction. These short interfering RNAs (siRNAs) can be produced by four different ways: chemical synthesis, *in vitro* transcription, enzymatic digestion of dsRNAs and transfection of DNA vectors encoding siRNAs or short hairpin RNAs (shRNAs), which are converted to siRNAs in cells. Among the four ways, transfection of DNA vectors has some advantages such as low cost, lasting expression of siRNA, easiness of preparation, making it the preferential method when using siRNAs in the treatment of diseases.

As a first step to explore the possibility of using RNAi in cancer therapy, we transfected HepG2 cells, a tumor cell line, with DNA vectors which can express shRNAs against human telomerase reverse transcriptase (hTERT), and then by quantifying mRNA of hTERT with real-time fluorescent RT-PCR, we selected two shRNAs which could inhibit the expression of hTERT.

MATERIALS AND METHODS

Cell culture

Human hepatoblastoma HepG2 cell line was cultured in

Dulbecco's modified Eagle's medium (Gibco Life Technologies, Grand Island, NY, USA) supplemented with 100 mL/L fetal calf serum (Sijiqing Biotech Company, Hangzhou, China).

Construction of hTERT-shRNAs expression vectors

pUC18U6 is a vector which can express siRNA in mammalian cells (Figure 1A). Eight oligodeoxyribonucleotides encoding four shRNAs against hTERT were designed according to the principles proposed in Ref. 19 and synthesized by Bioasia Company (Shanghai). The sequences of these eight oligodeoxyribonucleotides and their target sites on hTERT mRNA are shown in Table 1. To construct hTERT-shRNAs expression vectors, 400 nmol/L for each of the two corresponding oligodeoxyribonucleotides encoding a shRNA were mixed together, heated at 100 °C for 5 min, and cooled gradually to room temperature to anneal. pUC18U6 was digested with *Kpn*I, blunt-ended with T4 DNA polymerase, then digested with *Eco*RI, purified and ligated with the annealed oligodeoxyribonucleotides. The ligation mixtures were transformed into competent *E. coli*. The recombinant plasmids-pUC18U6ht1, pUC18U6ht2, pUC18U6ht3, and pUC18U6ht4 were then purified from transformed *E. coli*, and verified by *Hind*III/*Xho*I digestion analysis and automated DNA sequencing. The construction of a control vector, pUC18U-6GFPsir, which expressed a siRNA against green fluorescent protein (GFP), was reported previously.

Transfection

Twenty-four hours before transfection, HepG2 cells were seeded onto the culture plate at a density of 2×10^8 /L. Lipofectamine™ 2000 reagent (Invitrogen, Carlsbad, CA, USA) was used for the transfection of HepG2 cells by pUC18U6ht1, pUC18U6ht2, pUC18U6ht3, pUC18U6ht4 and control vector pUC18U6 and pUC18U6GFPsir according to the manufacturer's protocol. All transfections were performed in triplicates. pEGFP-N3 (Clontech, Palo Alto, CA, USA) which can express GFP was transfected in the same way as transfection efficiency control.

Quantification of hTERT mRNA by real-time fluorescent RT-PCR

The establishment of the real-time fluorescent RT-PCR method for quantification of hTERT mRNA has been reported elsewhere^[18]. The method has a good sensitivity, specificity, and reproducibility. For example, the correlation coefficient of the calibration curve was 1.00, and the mean coefficient

of variation of the assay was 7.1%. After the validity of the method was confirmed, it was used in this study to quantify hTERT mRNA. Briefly, 48 h after the transfection, total RNA was isolated from transfected HepG2 cells by using Trizol® reagent (Invitrogen) according to the manufacturer's protocol. Isolated total RNA was first reverse transcribed into cDNA using random primers and SuperScript™ II reverse transcriptase (Invitrogen). Then cDNA was used as a template in real-time fluorescent PCR. The sequences of the primers were as follows: P1: 5'TCACCTCACC-CACGCGA3'; P2: 5'CAGCCATACTCAGGGACACCTC3'. The sequence of Taqman-MGB probe was 5'CTTCCTC-AGGACCCTGGT3'. P1 and P2 were designed in different exons of hTERT gene, exon 10 and exon 11, respectively, so that only mRNA of functional hTERT but not genomic DNA would be amplified in PCR. The primers and the probe were synthesized by Shanghai Genecore BioTechnologies (Shanghai). All PCR reactions were performed and analyzed using an ABI Prism 7700 Sequence Detection System (Applied Biosystems, Foster City, CA, USA). For each sample, mRNA for human β -actin (hBA) was also quantified as the endogenous RNA control to which hTERT mRNA level was normalized. The primers and probe for hBA were provided by Shanghai Genecore BioTechnologies (Shanghai). Experiments were performed with triplicates for each cDNA sample.

Statistical analysis

One-way ANOVA was used for data analysis. Differences were considered significant when $P < 0.05$.

RESULTS

Construction of hTERT-shRNAs expression vectors

Since there was no *Xho*I site in pUC18U6, a parental vector which was suitable to express siRNA in mammalian cells, we designed the spacer in shRNA to be *Xho*I site (CTCGAG). Therefore, the recombinant vectors pUC18U6ht1-4 which contained the shRNAs coding sequences should yield new 310-bp fragments compared with pUC18U6 after being digested with *Xho*I and *Hind*III (Figure 1B), and this was verified by agarose gel analysis (Figure 2). These recombinant vectors were then automatically sequenced, but only pUC18U6ht4 could be successfully sequenced, showing that shRNA encoding cassette was correctly cloned into the vector. For pUC18U6ht1-3, the sequences of the inserts could

Table 1 Sequences of oligonucleotides used in the research

shRNA	Sequences of oligonucleotides	Target site on hTERT mRNA (GenBank accession no. NM_003219)
1	F: 5'ttctgctgactggctgctgctgagcatcagccagtcaggaactttttg3' R: 5'aattcaaaaagttctgctgactggctgctgctgagcatcagccagtcaggaa3'	1 682-1 702nt
2	F: 5'agtgtctgagcaagttgctgagcaactgtctccagacactctttttg3' R: 5'aattcaaaaaagagtgtctgagcaagttgctgagcaactgtctccagacact3'	1 787-1 807nt
3	F: 5'catggactacgtctgggactcagtgagtcacacgacgtagtcattgctttttg3' R: 5'aattcaaaaaagcatggactacgtctgggactcagtgagtcacacgacgtagtcattg3'	1 958-1 978nt
4	F: 5'agccagctctctacctgctcagcaaggtagagacgtggctctttttg3' R: 5'aattcaaaaaagaccagctctctacctgctcagcaaggtagagacgtggct3'	2 333-2 353nt

shRNA encoding cassettes 1-4 were formed by annealing two corresponding oligonucleotides, respectively. F stands for forward and R for reverse. The underlined bases are spacer region and recognition site for *Xho*I. nt: nucleotide.

not be reliably obtained, possibly due to strong secondary structure formed by the hairpin sequences (see Discussion).

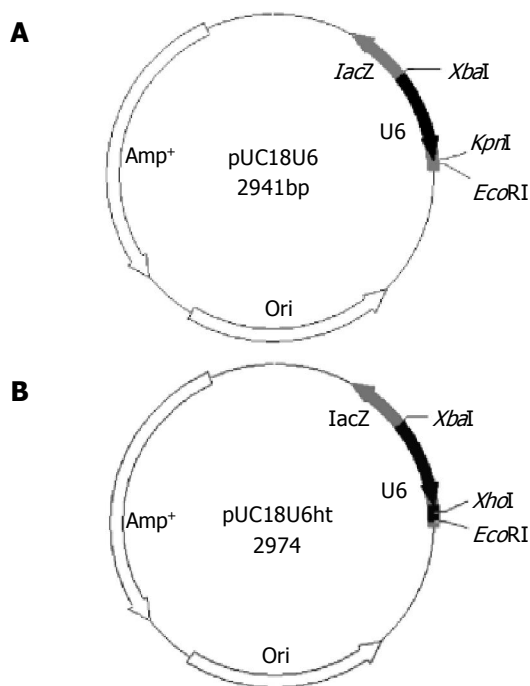


Figure 1 Maps of pUC18U6 and pUC18U6ht. **A:** pUC18U6. **B:** pUC18U6ht.

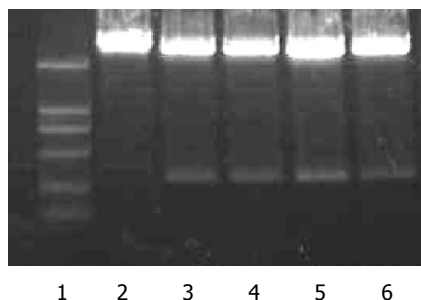


Figure 2 Restriction digestion analysis of recombinant vector pUC18U6ht. 1: DNA marker (2 000, 1 000, 750, 500, 250, 100 bp from top to bottom); 2: pUC18U6; 3-6: pUC18U6ht1-4, respectively.

Effect of shRNA expressed by pUC18U6ht on hTERT mRNA

pUC18U6ht1-4 were transfected into HepG2 cells by using liposome. As controls, parental vector pUC18U6 and pUC18U6GFPsir expressing shRNA against GFP were also introduced into HepG2 cells by liposome transfection. Forty-eight hours after the transfection, total cellular RNA was isolated from transfected cells and hTERT mRNA was quantified by real-time fluorescent RT-PCR as described in Materials and methods. As shown in Figure 3, transfection of all pUC18U6ht1-4 reduced hTERT mRNA level, but only the reduction caused by pUC18U6ht1 and pUC18U6ht2 was statistically significant as compared with the controls ($P < 0.05$). Normalized hTERT mRNA levels of HepG2 cells transfected by pUC18U6ht1 and pUC18U6ht2 were reduced by 39% and 49%, respectively, as compared with

that of HepG2 cells transfected by pUC18U6. This suggested that shRNA expressed by pUC18U6ht1 and pUC18U6ht2 suppressed the expression of hTERT, and this suppression was specific because transfection of pUC18U6GFPsir, which expressed siRNA against GFP, had no effect on hTERT mRNA.

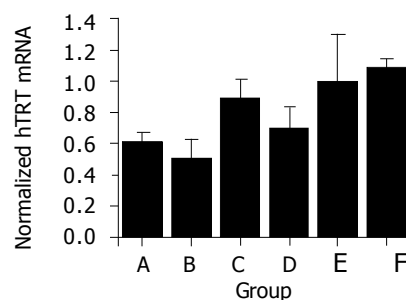


Figure 3 Normalized hTERT mRNA of transfected HepG2 cells. Groups A-F represent HepG2 cells transfected by pUC18U6ht1, pUC18U6ht2, pUC18U6ht3, pUC18U6ht4, pUC18U6, and pUC18U6GFPsir, respectively ($n = 3$ for each group). Normalized hTERT mRNA levels of HepG2 cells transfected by pUC18U6ht1 and pUC18U6ht2 were reduced by 39% and 49%, respectively, as compared with that of HepG2 cells transfected by pUC18U6.

DISCUSSION

Due to its high efficiency and specificity, RNAi is now being widely used as a method to knockdown target gene, to study gene function or to be used in experimental treatment of some diseases^[19-23]. As the first step to explore RNAi in the treatment of tumor, in present study we constructed four recombinant DNA vectors which could express shRNAs against hTERT. The parental vector used in this study, pUC18U6, was constructed by us and could drive the expression of shRNA in mammalian cells under the action of U6 promoter. shRNAs transcribed in the cells could be processed by Dicer, a key enzyme in RNAi, to yield siRNAs, which would guide degradation of cognate mRNA^[14-16,24,25]. A diagnostic *Xba*I/*Hind*III restriction enzyme analysis indicated that the four recombinant DNA vectors were constructed successfully. However, automated DNA sequencing could only verify the insert sequence in one vector, pUC18U6ht4, but failed in the other three. Devroe and Silver reported that they had encountered the same difficulty, which may be caused by the strong secondary structure formed by hairpin sequence^[26]. This problem might be overcome by inclusion of a longer non-palindromic loop sequence instead of the *Xba*I sequence, or by placing one or two mismatched nucleotides in the sense strand of the hairpin^[26,27].

We then tested whether the expressed shRNAs could inhibit hTERT expression by quantifying hTERT mRNA using quantitative real-time fluorescent RT-PCR. Real-time fluorescent PCR is a simple, sensitive, specific and precise method to quantitate nucleic acids over a vast dynamic range^[28]. Due to these advantages, real-time fluorescent PCR has been widely used in both basic research and clinical diagnosis to measure the quantity of nucleic acids. Real-time fluorescent RT-PCR has been reported in quantifying hTERT mRNA level in human tumors, and has shown to have several advantages over conventional assay to measure telomerase activity-telomeric repeat amplification protocol, such as sensitivity,

reproducibility, precision, and quantifiability^[29-31]. The results of quantitative real-time fluorescent RT-PCR showed that two out of four shRNAs used in the present study reduced hTERT mRNA level by 39% and 49%, respectively. Considering the transfection efficiency for transient transfection (about 50% in our study), the results of our research indicated that the two shRNAs expressed from DNA vector efficiently degraded hTERT mRNA. Further studies are needed to verify if these two shRNAs can also reduce hTERT protein level efficiently and lead to growth arrest and/or apoptosis of tumor cells *in vitro* and *in vivo*.

One problem in using siRNA to knockdown gene expression is target sequence selection. siRNAs target at different sites of the same gene can vary from strong to no inhibition of the gene expression. The mechanism of this selection is not well known. Therefore, it is still an empirical matter to design the most effective siRNAs, although some principles have been put forward and some softwares were invented to facilitate the selection process^[17,32,33]. In present study, four target sites were chosen according to these criteria, but only half of them turned out to be effective. Interestingly, two recent reports showed that siRNAs against other two sites respectively could also suppress hTERT expression^[8]. Further studies are needed to systemically evaluate the efficacy of siRNAs against different target sites of hTERT to pick out the most effective siRNAs in knocking down hTERT expression.

In summary, we demonstrated that two shRNAs expressed from DNA vectors could suppress hTERT expression. The results of our study provide basis for future research to utilize RNAi in tumor treatment.

REFERENCES

- Blackburn EH. Switching and signaling at the telomere. *Cell* 2001; **106**: 661-673
- Chan SR, Blackburn EH. Telomeres and telomerase. *Philos Trans R Soc Lond B Biol Sci* 2004; **359**: 109-121
- Harley CB, Futcher AB, Greider CW. Telomeres shorten during ageing of human fibroblasts. *Nature* 1990; **345**: 458-460
- Cech TR. Beginning to understand the end of the chromosome. *Cell* 2004; **116**: 273-279
- Janknecht R. On the road to immortality: hTERT upregulation in cancer cells. *FEBS Lett* 2004; **564**: 9-13
- Shay JW, Roninson IB. Hallmarks of senescence in carcinogenesis and cancer therapy. *Oncogene* 2004; **23**: 2919-2933
- Shay JW, Bacchetti S. A survey of telomerase activity in human cancer. *Eur J Cancer* 1997; **33**: 787-791
- Masutomi K, Yu EY, Khurts S, Ben-Porath I, Currier JL, Metz GB, Brooks MW, Kaneko S, Murakami S, DeCaprio JA, Weinberg RA, Stewart SA, Hahn WC. Telomerase maintains telomere structure in normal human cells. *Cell* 2003; **114**: 241-253
- Blasco MA, Hahn WC. Evolving views of telomerase and cancer. *Trends Cell Biol* 2003; **13**: 289-294
- Shammas MA, Koley H, Beer DG, Li C, Goyal RK, Munshi NC. Growth arrest, apoptosis, and telomere shortening of Barrett's-associated adenocarcinoma cells by a telomerase inhibitor. *Gastroenterology* 2004; **126**: 1337-1346
- Saretzki G, Ludwig A, von Zglinicki T, Runnebaum IB. Ribozyme-mediated telomerase inhibition induces immediate cell loss but not telomere shortening in ovarian cancer cells. *Cancer Gene Ther* 2001; **8**: 827-834
- Kraemer K, Fuessel S, Schmidt U, Kotzsch M, Schwenzer B, Wirth MP, Meyer A. Antisense-mediated hTERT inhibition specifically reduces the growth of human bladder cancer cells. *Clin Cancer Res* 2003; **9**: 3794-3800
- Nakajima A, Tauchi T, Sashida G, Sumi M, Abe K, Yamamoto K, Ohyashiki JH, Ohyashiki K. Telomerase inhibition enhances apoptosis in human acute leukemia cells: possibility of antitelomerase therapy. *Leukemia* 2003; **17**: 560-567
- Dykxhoorn DM, Novina CD, Sharp PA. Killing the messenger: short RNAs that silence gene expression. *Nat Rev Mol Cell Biol* 2003; **4**: 457-467
- Downward J. RNA interference. *BMJ* 2004; **328**: 1245-1248
- Agrawal N, Dasaradhi PV, Mohammed A, Malhotra P, Bhatnagar RK, Mukherjee SK. RNA interference: biology, mechanism, and applications. *Microbiol Mol Biol Rev* 2003; **67**: 657-685
- Elbashir SM, Harborth J, Weber K, Tuschl T. Analysis of gene function in somatic mammalian cells using small interfering RNAs. *Methods* 2002; **26**: 199-213
- Guo Y, Liu J, Xue CF, Wu J, Song TB. Quantitation of human telomerase reverse transcriptase mRNA with real-time fluorescent RT-PCR. *XiBao Yu FenZi MianYiXue ZaZhi* 2004; **20**: 618-620
- Aoki H, Satoh M, Mitsuzuka K, Ito A, Saito S, Funato T, Endoh M, Takahashi T, Arai Y. Inhibition of motility and invasiveness of renal cell carcinoma induced by short interfering RNA transfection of beta1,4GalNAc transferase. *FEBS Lett* 2004; **567**: 203-208
- Cho YY, Bode AM, Mizuno H, Choi BY, Choi HS, Dong Z. A novel role for mixed-lineage kinase-like mitogen-activated protein triple kinase alpha in neoplastic cell transformation and tumor development. *Cancer Res* 2004; **64**: 3855-3864
- Takei Y, Kadomatsu K, Yuzawa Y, Matsuo S, Muramatsu T. A small interfering RNA targeting vascular endothelial growth factor as cancer therapeutics. *Cancer Res* 2004; **64**: 3365-3370
- Jacque JM, Triques K, Stevenson M. Modulation of HIV-1 replication by RNA interference. *Nature* 2002; **418**: 435-438
- McCaffrey AP, Nakai H, Pandey K, Huang Z, Salazar FH, Xu H, Wieland SF, Marion PL, Kay MA. Inhibition of hepatitis B virus in mice by RNA interference. *Nat Biotechnol* 2003; **21**: 639-644
- Lee YS, Nakahara K, Pham JW, Kim K, He Z, Sontheimer EJ, Carthew RW. Distinct roles for Drosophila Dicer-1 and Dicer-2 in the siRNA/miRNA silencing pathways. *Cell* 2004; **117**: 69-81
- Pham JW, Pellino JL, Lee YS, Carthew RW, Sontheimer EJ. A Dicer-2-dependent 80s complex cleaves targeted mRNAs during RNAi in Drosophila. *Cell* 2004; **117**: 83-94
- Devroe E, Silver PA. Retrovirus-delivered siRNA. *BMC Biotechnol* 2002; **2**: 15
- Yu JY, Taylor J, DeRuiter SL, Vojtek AB, Turner DL. Simultaneous inhibition of GSK3alpha and GSK3beta using hairpin siRNA expression vectors. *Mol Ther* 2003; **7**: 228-236
- Klein D. Quantification using real-time PCR technology: applications and limitations. *Trends Mol Med* 2002; **8**: 257-260
- Bieche I, Nogues C, Paradis V, Olivi M, Bedossa P, Lidereau R, Vidaud M. Quantitation of hTERT gene expression in sporadic breast tumors with a real-time reverse transcription-polymerase chain reaction assay. *Clin Cancer Res* 2000; **6**: 452-459
- Tchirkov A, Rolhion C, Kemeny JL, Irthum B, Puget S, Khalil T, Chinot O, Kwiatkowski F, Perissel B, Vago P, Verrelle P. Clinical implications of quantitative real-time RT-PCR analysis of hTERT gene expression in human gliomas. *Br J Cancer* 2003; **88**: 516-520
- Lehner R, Enomoto T, McGregor JA, Shroyer AL, Haugen BR, Pugazhenth U, Shroyer KR. Quantitative analysis of telomerase hTERT mRNA and telomerase activity in endometrioid adenocarcinoma and in normal endometrium. *Gynecol Oncol* 2002; **84**: 120-125
- Chalk AM, Wahlestedt C, Sonnhhammer EL. Improved and automated prediction of effective siRNA. *Biochem Biophys Res Commun* 2004; **319**: 264-274
- Reynolds A, Leake D, Boese Q, Scaringe S, Marshall WS, Khvorovova A. Rational siRNA design for RNA interference. *Nat Biotechnol* 2004; **22**: 326-330

• BASIC RESEARCH •

Effects of extracellular iron concentration on calcium absorption and relationship between Ca^{2+} and cell apoptosis in Caco-2 cells

Li Wang, Qing Li, Xiang-Lin Duan, Yan-Zhong Chang

Li Wang, Qing Li, Xiang-Lin Duan, Yan-Zhong Chang, The Key Laboratory of Animal Physiology, Biochemistry and Molecular Biology of Hebei Province, Life Science College, Hebei Normal University, Shijiazhuang 050016, Hebei Province, China
Supported by the Natural Science Foundation of Hebei Province, No. 303158; Education Department Foundation of Hebei Province, No. 2002136

Correspondence to: Professor Xiang-Lin Duan, Life Science College, Hebei Normal University, Shijiazhuang 050016, Hebei Province, China. duanxianglin@mail.hebtu.edu.cn

Telephone: +86-311-6269480 Fax: +86-311-6268313

Received: 2004-05-25 Accepted: 2004-07-22

Abstract

AIM: To determine the method of growing small intestinal epithelial cells in short-term primary culture and to investigate the effect of extracellular iron concentration ($[\text{Fe}^{3+}]$) on calcium absorption and the relationship between the rising intracellular calcium concentration ($[\text{Ca}^{2+}]_i$) and cell apoptosis in human intestinal epithelial Caco-2 cells.

METHODS: Primary culture was used for growing small intestinal epithelial cells. $[\text{Ca}^{2+}]_i$ was detected by a confocal laser scanning microscope. The changes in $[\text{Ca}^{2+}]_i$ were represented by fluorescence intensity (FI). The apoptosis was evaluated by flow cytometry.

RESULTS: Isolation of epithelial cells and preservation of its three-dimensional integrity were achieved using the digestion technique of a mixture of collagenase XI and dispase I. Purification of the epithelial cells was facilitated by using a simple differential sedimentation method. The results showed that proliferation of normal gut epithelium *in vitro* was initially dependent upon the maintenance of structural integrity of the tissue. If 0.25% trypsin was used for digestion, the cells were severely damaged and very difficult to stick to the Petri dish for growing. The Fe^{3+} chelating agent desferrioxamine (100, 200 and 300 $\mu\text{mol/L}$) increased the FI of Caco-2 cells from 27.50 ± 13.18 (control, $n = 150$) to 35.71 ± 13.99 ($n = 150$, $P < 0.01$), 72.19 ± 35.40 ($n = 150$, $P < 0.01$) and 211.34 ± 29.03 ($n = 150$, $P < 0.01$) in a concentration-dependent manner. There was a significant decrease in the FI of Caco-2 cells treated by ferric ammonium citrate (FAC, a Fe^{3+} donor; 10, 50 and 100 $\mu\text{mol/L}$). The FI value of Caco-2 cells treated by FAC was 185.85 ± 33.77 ($n = 150$, $P < 0.01$), 122.73 ± 58.47 ($n = 150$, $P < 0.01$), and 53.29 ± 19.82 ($n = 150$, $P < 0.01$), respectively, suggesting that calcium absorption was influenced by $[\text{Fe}^{3+}]$. Calcium ionophore A_{23187} (0.1, 1.0 and 10 $\mu\text{mol/L}$) increased the FI of Caco-2 cells from 40.45 ± 13.95 (control, $n = 150$) to

45.19 ± 21.95 ($n = 150$, $P < 0.01$), 89.87 ± 43.29 ($n = 150$, $P < 0.01$) and 104.64 ± 51.07 ($n = 150$, $P < 0.01$) in a concentration-dependent manner. The positive apoptotic cell number of the Caco-2 cells after being treated with A_{23187} increased from 0.32% to 0.69%, 0.90% and 1.10%, indicating that the increase in the positive apoptotic cell number was positively correlated with $[\text{Ca}^{2+}]_i$.

CONCLUSION: Ca^{2+} absorbability is increased with the decrease of extracellular iron concentration Fe^{3+} and hindered with the increase of Fe^{3+} consistence out of them. Furthermore, increase of $[\text{Ca}^{2+}]_i$ can induce apoptosis in Caco-2 cells.

© 2005 The WJG Press and Elsevier Inc. All rights reserved.

Key words: Iron calcium absorption; Cell apoptosis; Caco-2 cells

Wang L, Li Q, Duan XL, Chang YZ. Effects of extracellular iron concentration on calcium absorption and relationship between Ca^{2+} and cell apoptosis in Caco-2 cells. *World J Gastroenterol* 2005; 11(19): 2916-2921

<http://www.wjgnet.com/1007-9327/11/2916.asp>

INTRODUCTION

Calcium is one of the most important and necessary element which maintains the physiological function. When the absorption of calcium is obstructed, many diseases are induced, such as hypertension, hyperkinesias, colorectal carcinoma, cardiovascular disease and osteoporosis, *etc.* The iron is one of the most common metals existing in our environment. In the last decade, a number of studies^[1,2] suggested that the ferric absorption was inhibited by calcium. However, little is known about the effect of iron concentration change on calcium absorption. The purpose of the present study was to investigate the effect of extracellular iron concentration ($[\text{Fe}^{3+}]$) on calcium absorption, and to study the effect of rising intracellular calcium concentration ($[\text{Ca}^{2+}]_i$) on the apoptosis of Caco-2 cells.

MATERIALS AND METHODS

Materials

All chemicals were of analytical grade. Dulbecco's modified Eagle's medium (DMEM) and fetal calf serum (FCS) were purchased from Gibco. FDA, A_{23187} and Fluo-3/AM were purchased from the Laboratory of Molecular Cell Biology of Hebei Normal University. Desferrioxamine (DFO), ferric

ammonium citrate (FAC) and A_{23187} were dissolved in Ca^{2+} / Mg^{2+} -free phosphate-buffered saline containing 0.40 g KCl, 0.06 g KH_2PO_4 , 8 g NaCl, 0.35 g NaHCO_3 , and 0.09 g $\text{Na}_2\text{HPO}_4 \cdot 7\text{H}_2\text{O}$ in 1-L liquid.

Cell preparation

Caco-2 cells, from cell store room of Shanghai Cell Academic Institution of CAS, were cultured in DMEM supplemented with 10% fetal bovine serum. Culture medium was changed every 2–3 d. The 20–30th generation of Caco-2 cells cultured for 3 d at 37 °C was digested with trypsin and the cell concentration was fixed to about $1 \times 10^6/\text{mL}$, they were then seeded in six-well plates and continuously cultured. The culture liquid was made up of ϕ (FCS) = 10%, DMEM ϕ (high sugar) = 85%, double antibiotics in which the final concentration of penicillin was 100 IU/mL and that of streptomycin was 100 $\mu\text{g}/\text{mL}$.

Fluo3-AM loading

The Caco-2 cells were incubated with Fluo3-AM working solution containing 0.03% Pluronic F-127 (the final concentration of Fluo3-AM was 20 $\mu\text{mol}/\text{L}$) at 37 °C for 40 min. After incubation, the cells were washed thrice at 25 °C with Ca^{2+} / Mg^{2+} -free phosphate-buffered saline to remove extracellular Fluo3-AM.

Measurement of $[\text{Ca}^{2+}]_i$

After Fluo3-AM loading, the cells were mounted on the small pool of Teflon printed slice, and covered with cover glass. Only the cells with rod shaped and visible striations were used for experiments. The fluorescence signals were detected with a confocal laser scanning system (Biorad lasersharpe MRA2, Oxfordshire, UK), which was equipped with a Nikon E-600 eclipse microscope. An argon laser was used to excite Fluo3 at 488 nm and emit at 530 nm. $[\text{Ca}^{2+}]_i$ changes were represented with fluorescence intensity (FI).

Experimental protocols

The experiments consisted of three groups: (1) Effect of DFO on intracellular calcium concentration ($[\text{Ca}^{2+}]_i$): FI was measured after 100, 200 and 300 $\mu\text{mol}/\text{L}$ DFO were added to normal phosphate-buffered saline containing Ca^{2+} and Mg^{2+} for 20 min ($n = 150$). Ca^{2+} / Mg^{2+} -free phosphate-buffered saline was used as a control ($n = 150$). (2) Effect of FAC on $[\text{Ca}^{2+}]_i$: FI was measured after 10, 50 and 100 $\mu\text{mol}/\text{L}$ FAC were added to normal phosphate-buffered saline containing Ca^{2+} and Mg^{2+} for 20 min ($n = 150$). Ca^{2+} / Mg^{2+} -free phosphate-buffered saline was used as a control ($n = 150$). (3) Effect of calcium ionophore A_{23187} on $[\text{Ca}^{2+}]_i$: FI was measured after 0.1, 1.0, and 10 $\mu\text{mol}/\text{L}$ A_{23187} were added to normal phosphate-buffered saline containing Ca^{2+} and Mg^{2+} for 20 min ($n = 150$). Ca^{2+} / Mg^{2+} -free phosphate-buffered saline was used as a control ($n = 150$).

FCM examination method

The Caco-2 cells of the 20–30th generation were planted to plastic culture flasks after being digested by trypsin and the number of the cells was $1 \times 10^6/\text{mL}$, and cultured for 3 d. The nutrition liquid for growth was discarded after the cells developed into a confluent monolayer, and the course of medi-

cation was the same as the previous one. PBS (0.01 mol/L) was added to the cells after they were digested, the cells were then centrifuged and the supernatant fluid was discarded. The cells were fixed with cold ethanol of 70%, and then stored at -4 °C overnight for flow cytometry (FCM) analysis.

Data processing

The cells were dealt with confocal assistant software, and 150 cells were disposed for each sample. The data were analyzed with ANOVA and LSD examination by STAT software, and the examination results were expressed as mean \pm SD.

The coherence examination of χ^2 -test was used for the test of apoptotic percentage, and the test method of $df = 1$ and $f > 5$ for two groups was used. The calculating formula was $\chi^2 = \sum (f_o - f_e)^2 / f_e$, where practice frequency is denoted with f_o , theoretical frequency is denoted with f_e , and the summation is denoted with Σ . The test level of χ^2 -test was $\alpha = 0.05$, and $P < 0.05$ was considered statistically significant.

RESULTS

Primary culture of epithelial cells

The intestinal mucosa suspension after being digested was constituted of recess epithelial cells observed under an inverted microscope. The cell livability was more than 95.7% digested by the mixture of collagenase IX and neutral proteinase I after trypan blue staining. There were undispersed epithelial cells and elastic fiber in the discarded depositions (Figure 1A). Primary cultured cells of intestinal mucosa were adhered after 24–48 h and then converged into groups of cell colonies after 4–6 d (Figure 1B), and the cells joined into pieces after 10–12 d. They were monolayer and polygon cells and pavement-like (Figure 1C). Cell borderlines were clear and not overlapped. The cytoplasm was abundant and their nuclei were round and olivary, the chromatin in the nuclei was very sparse with 1–2 nucleoli. There were few smooth muscle cells, fibroblasts and glial cells when observed under the microscope. The cells cultured in this experiment were not subcultured.

The cell keratin was the characteristic antigen ingredient of epithelial tissue. The antibody of cell keratin marked with biotin was used in this experiment to show qualitatively the rat intestinal epithelial cells. The immunocytochemistry result showed that the intestinal epithelial cells were positive brown (Figure 1D), and that the negative group was not stained (Figure 1E).

Effect of DFO on $[\text{Ca}^{2+}]_i$

Fe^{3+} was chelated by adding different concentrations of DFO into the culture liquid. DFO (100, 200 and 300 $\mu\text{mol}/\text{L}$) increased $[\text{Ca}^{2+}]_i$ of Caco-2 cells in a concentration-dependent manner. The FI value of Caco-2 cells was 35.71 ± 13.99 ($n = 150$, $P < 0.01$), 72.19 ± 35.40 ($n = 150$, $P < 0.01$) and 211.34 ± 29.03 ($n = 150$, $P < 0.01$), respectively. The FI value of control was 27.50 ± 13.18 (control, $n = 150$). There was a significant difference among the treatments ($P < 0.01$, Figure 2A). It showed that the transportation of Ca^{2+} into the cells was increased with the decrease of Fe^{3+} concentration in the cells.

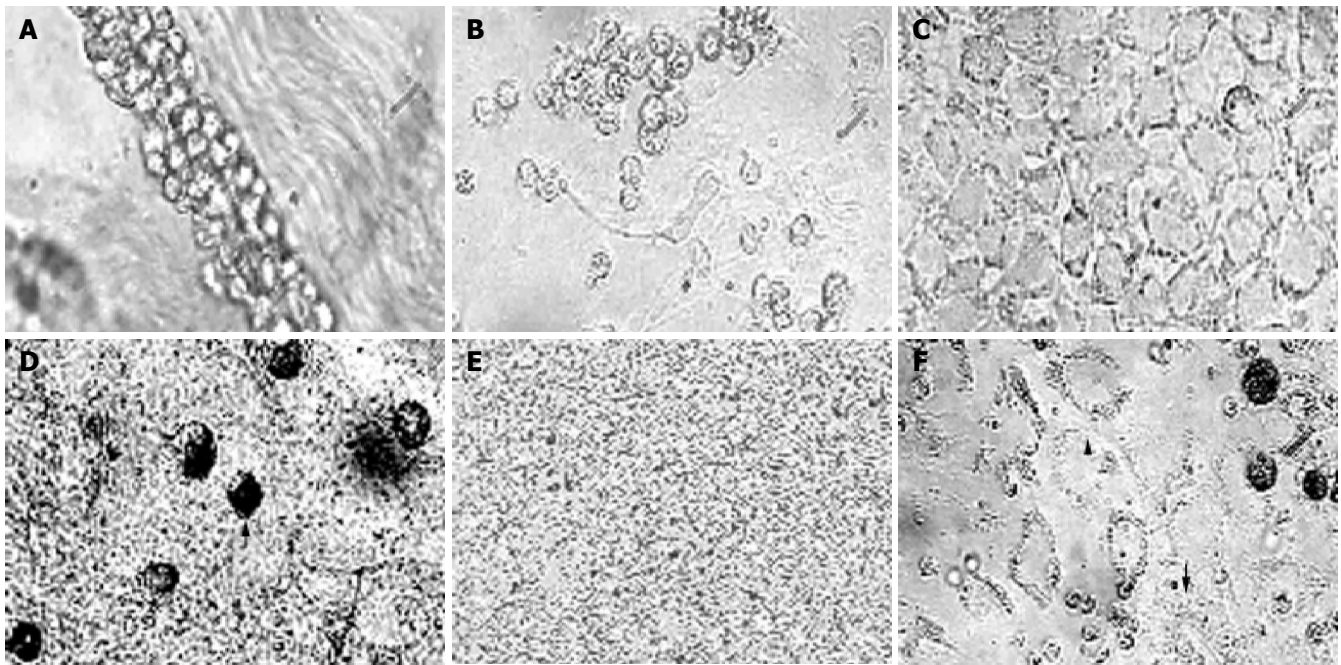


Figure 1 Epithelial cells in primary culture. **A:** Ingredients in the sediment after centrifugation ($\times 200$); **B:** colonies formed in cells cultured for 6 d ($\times 100$); **C:** pavement-like cells formed in cells cultured for 9 d ($\times 200$); **D:** immune positive

cells (\uparrow) ($\times 400$); **E:** no staining in negative group ($\times 100$); **F:** cell movement, adherent cells (\blacktriangle) and just adherent cells (\downarrow) ($\times 100$).

Effect of ferric ammonium citrate (FAC) on $[Ca^{2+}]_i$

Fe^{3+} was increased by adding different concentrations of Fe^{3+} donor FAC into the culture liquid. The FI value of Caco-2 cells was examined, the result showed that FAC (10, 50 and 100 $\mu\text{mol/L}$) decreased the FI from 44.43 ± 14.14 (control, $n = 150$) to 185.85 ± 33.77 ($n = 150$, $P < 0.01$), 122.73 ± 58.47 ($n = 150$, $P < 0.01$), and 53.29 ± 19.82 ($n = 150$, $P < 0.01$), respectively. There was a significant difference among the treatments ($P < 0.01$, Figure 2B). It showed that the transportation of Ca^{2+} into the cells could be induced by the slight increase of $[Fe^{3+}]$, but the transportation of Ca^{2+} into the cells was hindered with the continuous increase of $[Fe^{3+}]$ in the cells.

Effect of calcium ionophore A_{23187} on $[Ca^{2+}]_i$

The cell livability was examined with FDA, and its final concentration was 10 mg/L. FDA could be decomposed and take on green fluorescence when it enters the live cells, but it cannot be decomposed when it enters the dead cells and take on fluorescence. The live nature of cells was observed by confocal laser scanning microscope, and the cell livability was more than 90%.

The FI of blank control without A_{23187} and Fluo-3/AM was very feeble (25.47 ± 6.48 , $n = 150$), and that of negative control without A_{23187} was relatively feeble (40.45 ± 13.95 , $n = 150$). The FI of negative control was obviously stronger than that of blank control ($P < 0.01$). Calcium ionophore A_{23187} (0.1, 1.0 and 10 $\mu\text{mol/L}$) increased the FI of Caco-2 cells from 40.45 ± 13.95 (control, $n = 150$) to 45.19 ± 21.95 ($n = 150$, $P < 0.01$), 89.87 ± 43.29 ($n = 150$, $P < 0.01$) and 104.64 ± 51.07 ($n = 150$, $P < 0.01$) in a concentration-dependent manner. There was a significant difference among the treatments ($P < 0.01$, Figure 2C).

Effect of $[Ca^{2+}]_i$ on the apoptosis of Caco-2 cells

There was a sub-duple body apex, namely apoptotic apex, in front of the G_0/G_1 phase cells of all groups in the PI fluorescent histograms examined with FCM. The result showed that the positive apoptotic rate of control was 0.32%, and the AP apex was very low. The apoptotic percentage of each treatment was 0.69%, 0.90% and 1.10%, respectively. The cell apoptotic percentage of treatment group with A_{23187} (0.1 $\mu\text{mol/L}$) was obviously higher than that of negative control ($P < 0.01$) examined with χ^2 -test. The cell apoptotic percentage of treatment group with A_{23187} (10 $\mu\text{mol/L}$) was also not obviously different from that of treatment group with A_{23187} (1 $\mu\text{mol/L}$) ($P > 0.05$). But the cell apoptotic percentage of treatment group with A_{23187} (10 $\mu\text{mol/L}$) was obviously increased compared to that of treatment with A_{23187} (0.1 $\mu\text{mol/L}$) ($P < 0.01$), suggesting that the cell apoptotic percentage was related with the increase of Ca^{2+} concentration in Caco-2 cells, that is to say, the increase of Ca^{2+} concentration in the Caco-2 cells was positively correlated to its apoptosis.

DISCUSSION

Iron is one of the most abundant micronutrients. Excessive iron also has cell toxicity and induces cell damnification. So there are rigid regulating mechanisms in the body to keep the balance of iron metabolism. Duodenum and jejunum are the main place of iron absorption and the hinge position in regulating the balance of iron metabolism. It is known that iron in the enteric cavity is carried into the small intestine epithelia by divalent metal transporter 1 in its membrane with Fe^{2+} formation. It is commonly considered that calcium hinders iron absorption^[1-5]. Iron absorption was hindered by adding $CaCl_2$ and this function was in a dose-dependent

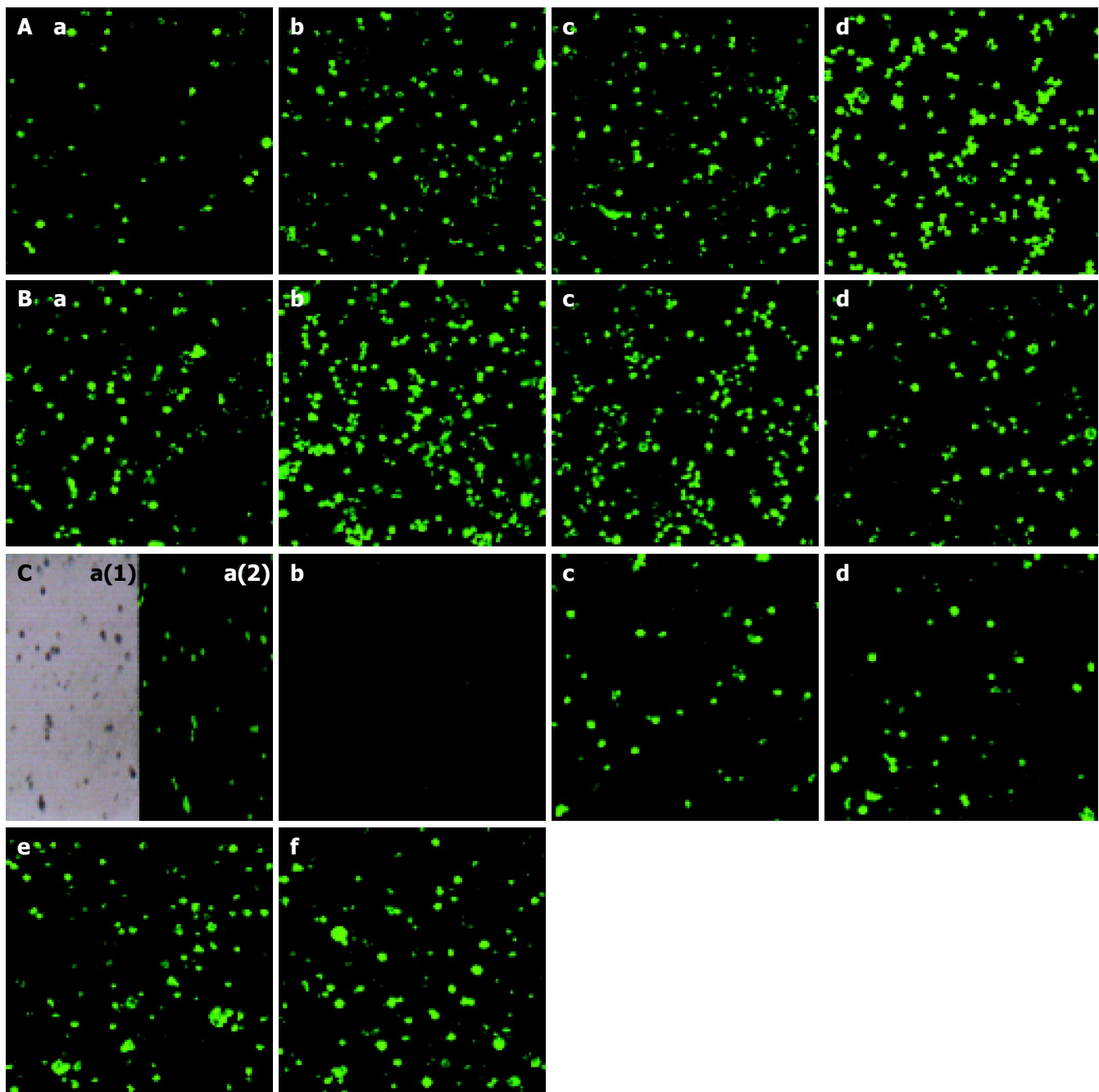


Figure 2 Effect of different concentrations of DFO (A), FAC (B), and A_{23187} (C) on Ca^{2+} concentration in Caco-2 cells. **A:** 1a: Control, $\times 200$; 1b: the final consistence of DFO was $100 \mu\text{mol/L}$, $\times 200$; 1c: the final consistence of DFO was $200 \mu\text{mol/L}$, $\times 200$; 1d: the final consistence of DFO was $300 \mu\text{mol/L}$, $\times 200$. **B:** 2a: control, $\times 200$; 2b: the final consistence of FAC was $10 \mu\text{mol/L}$, $\times 200$; 2c: the final consistence of FAC was $50 \mu\text{mol/L}$, $\times 200$; 2d: the final

consistence of FAC was $100 \mu\text{mol/L}$, $\times 200$. **C:** 3a (1) the photograph of transmission light, showing the place of cells, $\times 200$; (2) the photograph of fluorescence, showing the active cells, $\times 200$; 3b: blank control, $\times 200$; 3c: negative control, $\times 200$; 3d: the final consistence of A_{23187} was $0.1 \mu\text{mol/L}$, $\times 200$; 3e: the final consistence of A_{23187} was $1.0 \mu\text{mol/L}$, $\times 200$; 3f: the final consistence of A_{23187} was $10 \mu\text{mol/L}$, $\times 200$.

manner by separating rat gastrointestinal loop and observing the iron absorption after the rat was supplied with different doses of calcium (CaCl_2)^[6-10]. At present, the mechanism of reciprocity between calcium and iron has not yet been elucidated. Although the absorption methods of heme iron and nonheme iron were different, their absorption was also hindered by calcium. Hallberg *et al.*^[6], thought that the same transport carrier was used by calcium and iron, and there existed competition and inhibition between them in the transport process from mucous membrane cells to blood plasma. This track of nonheme iron was the same to heme

iron. There were only few reports on the calcium absorption under the effect of iron. Calcium absorption was not influenced by the increase of Fe^{3+} concentration, but it was increased by iron only in the instance of the ratio of 20 to 1 of iron to calcium under the effect of different Fe^{3+} in the brush border vesicle^[11-16]. In the present study, we demonstrated that the Fe^{3+} chelating agent DFO increased the Ca^{2+} concentration of Caco-2 cells in a concentration-dependent manner and the FAC decreased the Ca^{2+} concentration of Caco-2 cells, suggesting that calcium absorption is influenced by $[\text{Fe}^{3+}]$. But the idiographic

mechanism of calcium absorption increased by a low dose of Fe^{3+} and inhibited by a high dose of Fe^{3+} remains to be further established.

In the present study, calcium ionophore A_{23187} increased the Ca^{2+} concentration of Caco-2 cells in a concentration-dependent manner. Ca^{2+} being the important second messenger in cells is the signal of subsistence and death, and almost all physiological activities are regulated by Ca^{2+} , for instance, flop of heart, secretion of hormone and transfer and reserve of information in cerebrum. The foundation at the start of life and the process of cells developing into special type cells are touched and controlled by Ca^{2+} , and cell physiological activity is regulated by Ca^{2+} , and then finally cell apoptosis is ongoing under the function of Ca^{2+} . Intracellular calcium concentration is commonly between 0.1 and 10 mmol/L, while extracellular calcium concentration is about 0.1 $\mu\text{mol/L}$. It is the concentration difference that becomes the base of the physiological function of Ca^{2+} . The concentration of dissociating Ca^{2+} in cell cytoplasts is the pivotal factor to regulate various responses, and there are different kinds of calcium-regulating mechanism to keep its balance. Some studies showed that the transitory increase of Ca^{2+} concentration in cells could be reduced by ATP which can stimulate cells^[17-22]. Biological function can be regulated by mobilization of Ca^{2+} in cells including temporary reaction of muscle constriction, nerve conduction and cell secretion, etc., and permanent reaction of cell differentiation and proliferation. All in all, cell function is regulated by Ca^{2+} , and it could pass the stimulating signals of excitomotors onto the enzyme reaction system and functional protein^[23-26].

Excessive $[\text{Ca}^{2+}]_i$ is harmful to cells. Many damaging factors such as insufficient oxygen, toxin, oxidative stress, defective blood perfusion, blood poisoning, ionizing radiation and enteritis can induce the rising of intracellular calcium, which results in cell apoptosis. A_{23187} is a moving ionic carrier which carries bivalent positive ions of Ca^{2+} , Mg^{2+} , etc. into cells and two H^+ s are carried out of cells at the same time. Ca^{2+} can step into cell cytoplasts immediately if A_{23187} is added into live cell culture liquid. Therefore, A_{23187} is widely used to increase the extranuclear dissociated Ca^{2+} concentration in cells. The extranuclear Ca^{2+} concentration can be immediately increased by calcium carrier of A_{23187} when touched with cells, and then the endogeneity endoprotease, which can make DNA rupture among the nucleosomes into segments between 180 and 200 bp or its diploid segments taking on ladder atlas in the gel electrophoresis, is aroused and cell apoptosis is increased. Inhibition of oxidative phosphorylation process in mitochondria, decrease of mitochondrial membrane electric potential and ATP content in tissues, activation of phosphatidase and proteinase and irreversible cell damage have been induced by calcium overload^[27-32].

REFERENCES

- 1 Cook JD, Dassenko SA, Whittaker P. Calcium supplementation: effect on iron absorption. *Am J Clin Nutr* 1991; **53**: 106-111
- 2 Reddy MB, Cook JD. Effect of calcium intake on nonheme-iron absorption from a complete diet. *Am J Clin Nutr* 1997; **65**: 1820-1825
- 3 Monsen ER, Cook JD. Food iron absorption in human subjects. IV. The effects of calcium and phosphate salts on the absorption

- of nonheme iron. *Am J Clin Nutr* 1976; **29**: 1142-1148
- 4 Hurrell RF, Reddy MB, Juillerat MA, Cook JD. Degradation of phytic acid in cereal porridges improves iron absorption by human subjects. *Am J Clin Nutr* 2003; **77**: 1213-1219
- 5 Cook JD, Reddy MB. Effect of ascorbic acid intake on nonheme-iron absorption from a complete diet. *Am J Clin Nutr* 2001; **73**: 93-98
- 6 Hallberg L, Brune M, Erlandsson M, Sandberg AS, Rossander-Hulten L. Calcium: effect of different amounts on nonheme- and heme-iron absorption in humans. *Am J Clin Nutr* 1991; **53**: 112-119
- 7 Merritt JE, Rink TJ. Regulation of cytosolic free calcium in fura-2-loaded rat parotid acinar cells. *J Biol Chem* 1987; **262**: 17362-17369
- 8 Chen JT, Chen RM, Lin YL, Chang HC, Lin YH, Chen TL, Chen TG. Confocal laser scanning microscopy: I. An overview of principle and practice in biomedical research. *Acta Anaesthesiol Taiwan* 2004; **42**: 33-40
- 9 Turnlund JR, Smith RG, Kretsch MJ, Keyes WR, Shah AG. Milk's effect on the bioavailability of iron from cereal-based diets in young women by use of *in vitro* and *in vivo* methods. *Am J Clin Nutr* 1990; **52**: 373-378
- 10 Gleerup A, Rossander-Hulten L, Gramatkovski E, Hallberg L. Iron absorption from the whole diet: comparison of the effect of two different distributions of daily calcium intake. *Am J Clin Nutr* 1995; **61**: 97-104
- 11 Roth-Bassell HA, Clydesdale FM. The influence of zinc, magnesium, and iron on calcium uptake in brush border membrane vesicles. *J Am Coll Nutr* 1991; **10**: 44-49
- 12 Berner LA, Clydesdale FM, Douglass JS. Fortification contributed greatly to vitamin and mineral intakes in the United States, 1989-1991. *J Nutr* 2001; **131**: 2177-2183
- 13 Roughead ZK, Zito CA, Hunt JR. Initial uptake and absorption of nonheme iron and absorption of heme iron in humans are unaffected by the addition of calcium as cheese to a meal with high iron bioavailability. *Am J Clin Nutr* 2002; **76**: 419-425
- 14 Wauben IP, Atkinson SA. Calcium does not inhibit iron absorption or alter iron status in infant piglets adapted to a high calcium diet. *J Nutr* 1999; **129**: 707-711
- 15 Hebbert D, Morgan EH. Calmodulin antagonists inhibit and phorbol esters enhance transferrin endocytosis and iron uptake by immature erythroid cells. *Blood* 1985; **65**: 758-763
- 16 Lonnerdal B. Effects of milk and milk components on calcium, magnesium, and trace element absorption during infancy. *Physiol Rev* 1997; **77**: 643-669
- 17 Shimohama S, Fujimoto S, Matsushima H, Takenawa T, Taniguchi T, Perry G, Whitehouse PJ, Kimura J. Alteration of phospholipase C-delta protein level and specific activity in Alzheimer's disease. *J Neurochem* 1995; **64**: 2629-2634
- 18 Kazilek CJ, Merkle CJ, Chandler DE. Hyperosmotic inhibition of calcium signals and exocytosis in rabbit neutrophils. *Am J Physiol* 1988; **254**: C709-C718
- 19 Fendyur A, Kaiserman I, Kasinetz L, Rahamimoff R. The burst of mitochondrial diseases: neurons and calcium. *Isr Med Assoc J* 2004; **6**: 356-359
- 20 Grewal SS, Fass DM, Yao H, Ellig CL, Goodman RH, Stork PJ. Calcium and cAMP signals differentially regulate cAMP-responsive element-binding protein function via a Rap1-extracellular signal-regulated kinase pathway. *J Biol Chem* 2000; **275**: 34433-34441
- 21 Gorczynska E, Handelsman DJ. The role of calcium in follicle-stimulating hormone signal transduction in Sertoli cells. *J Biol Chem* 1991; **266**: 23739-23744
- 22 Hudson PL, Pedersen WA, Saltsman WS, Liscovitch M, MacLaughlin DT, Donahoe PK, Blusztajn JK. Modulation by sphingolipids of calcium signals evoked by epidermal growth factor. *J Biol Chem* 1994; **269**: 21885-21890
- 23 Smeland E, Bremnes RM, Fuskevag OM, Aarbakke J. The effect of calcium channel blockers and calcium on methotrexate accumulation in rat hepatocytes. *Anticancer Res* 1995; **15**: 1221-1225
- 24 Baker AJ, Longuemare MC, Brandes R, Weiner MW. Intracel-

- lular tetanic calcium signals are reduced in fatigue of whole skeletal muscle. *Am J Physiol* 1993; **264**: C577-C582
- 25 **Moore TM**, Chetham PM, Kelly JJ, Stevens T. Signal transduction and regulation of lung endothelial cell permeability. Interaction between calcium and cAMP. *Am J Physiol* 1998; **275**: L203-L222
- 26 **Lane PJ**, Ledbetter JA, McConnell FM, Draves K, Deans J, Schieven GL, Clark EA. The role of tyrosine phosphorylation in signal transduction through surface Ig in human B cells. Inhibition of tyrosine phosphorylation prevents intracellular calcium release. *J Immunol* 1991; **146**: 715-722
- 27 **Bellomo G**, Perotti M, Taddei F, Mirabelli F, Finardi G, Nicotera P, Orrenius S. Tumor necrosis factor alpha induces apoptosis in mammary adenocarcinoma cells by an increase in intranuclear free Ca²⁺ concentration and DNA fragmentation. *Cancer Res* 1992; **52**: 1342-1346
- 28 **Atsma DE**, Bastiaanse EM, Van der Valk L, Van der Laarse A. Low external pH limits cell death of energy-depleted cardiomyocytes by attenuation of Ca²⁺ overload. *Am J Physiol* 1996; **270**: H2149-H2156
- 29 **Atsma DE**, Bastiaanse EM, Jerzewski A, Van der Valk LJ, Van der Laarse A. Role of calcium-activated neutral protease (calpain) in cell death in cultured neonatal rat cardiomyocytes during metabolic inhibition. *Circ Res* 1995; **76**: 1071-1078
- 30 **Mailland M**, Waelchli R, Ruat M, Boddeke HG, Seuwen K. Stimulation of cell proliferation by calcium and a calcimimetic compound. *Endocrinology* 1997; **138**: 3601-3605
- 31 **Bostick RM**, Fosdick L, Wood JR, Grambsch P, Grandits GA, Lillemoe TJ, Louis TA, Potter JD. Calcium and colorectal epithelial cell proliferation in sporadic adenoma patients: a randomized, double-blinded, placebo-controlled clinical trial. *J Natl Cancer Inst* 1995; **87**: 1307-1315
- 32 **Bostick RM**, Boldt M, Darif M, Wood JR, Overn P, Potter JD. Calcium and colorectal epithelial cell proliferation in ulcerative colitis. *Cancer Epidemiol Biomarkers Prev* 1997; **6**: 1021-1027

• BASIC RESEARCH •

Tetrandrine inhibits activation of rat hepatic stellate cells *in vitro* via transforming growth factor- β signaling

Yuan-Wen Chen, Jian-Xin Wu, Ying-Wei Chen, Ding-Guo Li, Han-Ming Lu

Yuan-Wen Chen, Jian-Xin Wu, Ying-Wei Chen, Ding-Guo Li, Han-Ming Lu, Digestive Disease Laboratory, Xinhua Hospital, Shanghai Second Medical University, Shanghai 200092, China
Supported by the College Science and Technology Developing Foundation of Shanghai, No. 02BK14

Correspondence to: Dr. Jian-Xin Wu, Digestive Disease Laboratory, Xinhua Hospital, Shanghai Second Medical University, 1665 Kongjiang Road, Shanghai 200092, China. wjxgp@sh163.net
Telephone: +86-21-65790000-3362 Fax: +86-21-55571294
Received: 2004-05-25 Accepted: 2004-06-24

Abstract

AIM: To investigate the effect of various concentrations of tetrandrine on activation of quiescent rat hepatic stellate cells (HSCs) and transforming growth factor- β (TGF- β) signaling *in vitro*.

METHODS: HSCs were isolated from rats by *in situ* perfusion of liver and 18% Nycodenz gradient centrifugation, and primarily cultured on uncoated plastic plates for 24 h with DMEM containing 20% fetal bovine serum (FBS/DMEM) before the culture medium was substituted with 2% FBS/DMEM for another 24 h. Then, the HSCs were cultured in 2% FBS/DMEM with tetrandrine (0.25, 0.5, 1, 2 mg/L, respectively). Cell morphological features were observed under an inverted microscope, smooth muscle- α -actin (α -SMA) was detected by immunocytochemistry and image analysis system, laminin (LN) and type III procollagen (PCIII) in supernatants were determined by radioimmunoassay. TGF- β_1 mRNA, Smad 7 mRNA and Smad 7 protein were analyzed with RT-PCR and Western blotting, respectively.

RESULTS: Tetrandrine at the concentrations of 0.25-2 mg/L prevented morphological transformation of HSC from the quiescent state to the activated one, while α -SMA, LN and PCIII expressions were inhibited. As estimated by gray values, the expression of α -SMA in tetrandrine groups (0.25, 0.5, 1, 2 mg/L) was reduced from 21.3% to 42.2% (control: 0.67, tetrandrine groups: 0.82, 0.85, 0.96, or 0.96, respectively, which were statistically different from the control, $P < 0.01$), and the difference was more significant in tetrandrine at 1 and 2 mg/L. The content of LN in supernatants was significantly decreased in tetrandrine groups to 58.5%, 69.1%, 65.8% or 60.0% that of the control respectively, and that of PCIII to 84.6%, 81.5%, 75.7% or 80.7% respectively ($P < 0.05$ vs control), with no significant difference among tetrandrine groups. RT-PCR showed that TGF- β_1 mRNA expression was reduced by tetrandrine treatments from 56.56% to 87.90% in

comparison with the control, while Smad 7 mRNA was increased 1.4-4.8 times. The TGF- β_1 mRNA and Smad 7 mRNA expression was in a significant negative correlation ($r = -0.755$, $P < 0.01$), and both were significantly correlated with α -SMA protein expression ($r = -0.938$, $P < 0.01$; $r = 0.938$, $P < 0.01$, respectively). The up-regulation of Smad 7 protein by tetrandrine (1 mg/L) was confirmed by Western blotting as well.

CONCLUSION: Tetrandrine has a direct inhibiting effect on the activation of rat HSCs in culture. It up-regulates the expression of Smad 7 which in turn blocks TGF- β_1 expression and signaling.

© 2005 The WJG Press and Elsevier Inc. All rights reserved.

Key words: Tetrandrine; Hepatic stellate cell; Transforming growth factor- β ; Smad 7; Liver fibrosis; Signal transduction

Chen YW, Wu JX, Chen YW, Li DG, Lu HM. Tetrandrine inhibits activation of rat hepatic stellate cells *in vitro* via transforming growth factor- β signaling. *World J Gastroenterol* 2005; 11(19): 2922-2926

<http://www.wjgnet.com/1007-9327/11/2922.asp>

INTRODUCTION

Hepatic stellate cells (HSCs) belonging to the nonparenchymal cell type in Disse space undergo morphological and biochemical transformation, which is quite a complex process of activation and evolution, into myofibroblasts in various liver injuries. The activated HSCs are the main source of extra cellular matrix (ECM). Many profibrogenic cytokines^[1,2] can activate HSCs, and among them the transforming growth factor- β_1 (TGF- β_1) is the master factor for promoting HSC activation, ECM synthesis, and excretion of other profibrogenic factors^[3-5]. Abnormally elevated TGF- β_1 level and altered intercellular signaling bear a close relation to persistent HSC activation and higher function^[4-7].

Both experimental and clinical research have shown that tetrandrine, a bisbenzyl isoquinoline alkaloid derived from *Stephania tetrandra* S. Moore, a traditional Chinese herb medicine, could exert an anti-inflammation effect on injured liver, attenuate ECM deposition, and inhibit hepatic fibrosis. In order to further investigate the possible mechanism involved, we examined the effects of various dosages of tetrandrine on HSCs and also the expression of laminin (LN), type III procollagen (PCIII), smooth muscle- α -actin (α -SMA), TGF- β_1 and its downstream signal transduction

components, Smad 7, to elucidate the influence of tetrandrine on activation of HSCs and TGF- β_1 signaling.

MATERIALS AND METHODS

Animals

Male Sprague-Dawley rats weighing 400–500 g were purchased from Shanghai Laboratory Animal Center, Chinese Academy of Sciences. They received normal chow and water ad libitum.

Tetrandrine solution

Tetrandrine (molecular formula $C_{38}H_{42}N_2O_6$) purchased from Shanxi Huike Botanical Development Co., Ltd, was dissolved in ethanol at 1 mg/mL, diluted and added to the culture medium. The final concentration of ethanol was lower than 0.2%.

Main reagents

DMEM was purchased from Gibco. Nycodenz, pronase E, type IV collagenase and mouse α -SMA monoclonal antibody were purchased from Sigma. Two-step immunocytochemistry detection reagent was purchased from Antibody Diagnostica Inc. LN and PCIII radioimmunoassay kits were purchased from the Institute of Naval Medicine, Shanghai. TRIzol reagent, Moloney murine leukemia virus reverse transcriptase (M-MLV) and rabbit Smad 7 polyclonal antibody were purchased from Invitrogen, Promega, and Santa Cruz, respectively.

Isolation and cultivation of HSCs

HSCs were isolated and cultured as described by Friedman and Roll^[8] with some modifications. Briefly, the rats were anesthetized with an intraperitoneal injection of pentobarbital. After cannulation into the portal vein, the liver was perfused with calcium-free balanced salt solution, salt solution containing 0.5 mg/mL collagenase, salt solution containing 0.5 mg/mL collagenase and 1 mg/mL pronase E in turn respectively. Then the liver was taken out, cut into small pieces and incubated in solution containing 0.5 mg/mL collagenase. After being washed by repeated suspension and centrifugation, HSCs were purified by density gradient centrifugation with 18% Nycodenz. HSCs were collected from the top layer, washed and suspended in DMEM supplemented with 20% fetal bovine serum (FBS) at a density of 1×10^6 cell/mL, and seeded on uncoated 24- and 6-well plastic plates at 1×10^5 /cm² supplemented with 20% FBS/DMEM for 24 h. Then HSCs were subjected to tetrandrine treatment after cultivation in 2% FBS/DMEM for another 24 h. More than 90% of isolated HSCs were viable as assessed by trypan blue exclusion and consisted of more than 90% of HSCs as determined by direct cell counting under a phase-contrast microscope and intrinsic vitamin A autofluorescence^[9].

Immunocytochemistry analysis of α -SMA

HSCs were cultured on 24-well plates without or with tetrandrine (0.25, 0.5, 1, 2 mg/L). After being incubated for 3 d, the supernatant was collected and preserved at -20 °C

for further assay. Cells were fixed with ethanol/acetic acid, and α -SMA antibody, horse radish peroxidase-conjugated secondary antibody and diaminobenzidine were added sequentially according to the standard protocol. Semi-quantitative assessment of protein expression was performed using a pathological image analysis system. The expression of α -SMA was estimated by gray value.

Measurement of TGF- β_1 and Smad 7 mRNA

HSCs were seeded on 6-well plates and treated as above. Total RNA was extracted with TRIzol reagent. For RT-PCR, 1 μ g total RNA was reverse transcribed with M-MLV according to manufacturer's instructions. cDNAs were amplified using specific sets of primers for TGF- β_1 (ggactctccacctgcaagac, ccccagaatcatcgagac) and Smad 7 (ctgtgttgctgtgaatcttac, gctgtaggcctttcatagt). The PCR procedure for TGF- β_1 consisted of 30 cycles of denaturation at 94 °C for 30 s, annealing at 53 °C for 30 s, extension at 72 °C for 30 s, with initial denaturation of sample cDNAs at 94 °C for 5 min before PCR and additional extension period of 10 min after the last cycle. A touch down PCR procedure was performed for Smad 7 cDNA amplification. After denaturation at 94 °C for 5 min, 10 cycles were run with an initial annealing temperature at 58 °C, which was 0.5 °C lower after each cycle before 25 cycles of denaturation at 94 °C for 40 s, annealing at 53 °C for 40 s, extension at 72 °C for 40 s, and additional extension period of 10 min after the last cycle. In parallel, PCR reactions were performed with primers coding for the housekeeping gene, *GAPDH*, to control for equal amounts of template cDNAs. Five microliters of 20 μ L total PCR reaction was analyzed in a 20 mg/g agarose gel with a 100-bp DNA marker. Densitometric analysis of PCR products was performed by the computer software, SmartViewer (Shanghai Furi Science and Technology), and standardized by the *GAPDH*.

Western blotting analysis of Smad 7

HSCs, which were cultured on 6-well plates with or without tetrandrine (1 mg/L) for 3 d, were washed twice with Hanks' balanced salt solution and lysed directly in SDS loading buffer. Cell lysates (5 μ g of protein) were subjected to SDS-polyacrylamide gel electrophoresis on a 0.1 g/g gel and then transferred to a nitrocellulose membrane. The membrane was incubated with antibody to Smad 7 (diluted 1:500) at 4 °C for 12 h. After being vigorously washed, the membrane was incubated with horse radish peroxidase-conjugated secondary antibody (diluted 1:2 000). The membrane blot was developed with diaminobenzidine.

LN and PCIII content

LN and PCIII in supernatant were measured with radioimmunoassay kits according to manufacturer's instructions.

Statistical analysis

All data were expressed as mean \pm SD. Statistical significance for the difference between the groups was assessed using one-way ANOVA test. $P < 0.05$ was considered statistically significant.

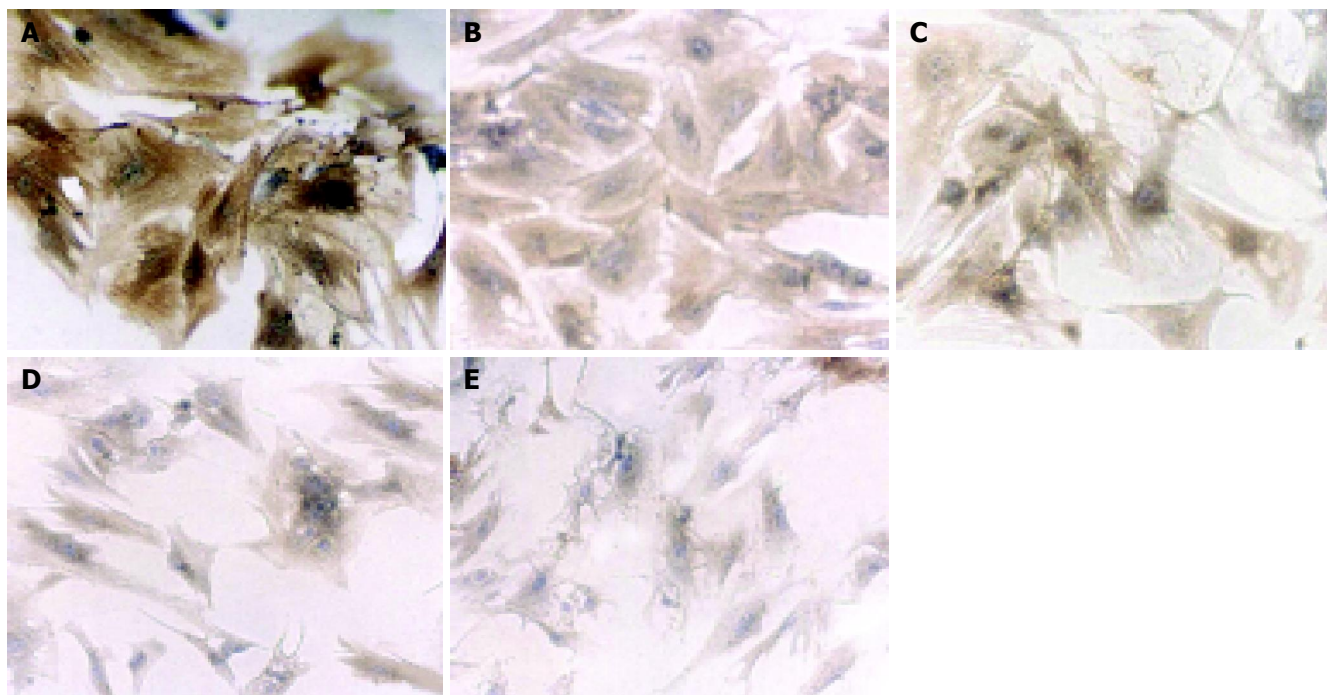


Figure 1 Immunocytochemistry analysis of α -SMA of HSCs subjected to different treatment of tetrandrine (magnification $\times 200$). **A:** control; **B:** tetrandrine

0.25 mg/L; **C:** tetrandrine 0.5 mg/L; **D:** tetrandrine 1 mg/L; **E:** tetrandrine 2 mg/L.

RESULTS

Changes of HSC morphology

HSCs cultured for 5 d exhibited flattened and membranous processes, representing a myofibroblastic morphology (Figure 1 A), while those treated with tetrandrine (0.25, 0.5, 1, 2 mg/L) showed a more slender, spindle stellate cell shape (Figures 1B-E), which was similar to the appearance of quiescent HSCs.

α -SMA expression of culture-activated HSCs

In the control group, HSCs cultured for 5 d were strongly positive for α -SMA (Figure 1A), which was weaker in tetrandrine-treated groups in varying degrees according to the doses used (Figures 1B-E). Image analysis showed a statistical difference between the control and tetrandrine groups ($P < 0.01$), and the difference was more significant in tetrandrine at 1 and 2 mg/L (Figure 2).

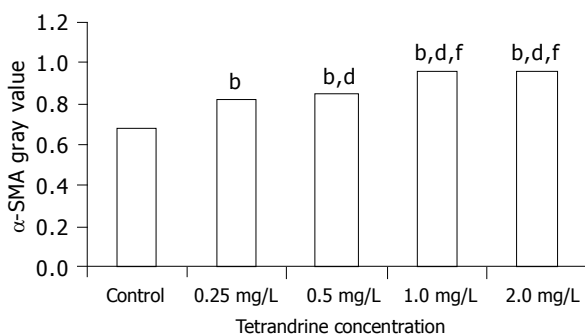


Figure 2 Expression of α -SMA in culture-activated HSCs. ^b $P < 0.01$ vs control group. ^d $P < 0.01$ vs tetrandrine 0.25 mg/L group. ^f $P < 0.01$ vs tetrandrine 0.25, 0.5 mg/L groups.

TGF- β_1 and Smad 7 mRNA expression

TGF- β_1 mRNA expression of HSCs was suppressed from 56.56% to 87.90% in tetrandrine groups (0.25, 0.5, 1, 2 mg/L) when compared with that of the control ($P < 0.01$), while the up-regulated Smad 7 mRNA expression in tetrandrine groups reached 2.4-5.8 times that of the control. A dosage-dependent effect was observed at 0.25-1 mg/L ($P < 0.01$), but no difference at 1 and 2 mg/L was demonstrated ($F = 0.394$, $P = 0.564$) (Table 1 and Figure 3). TGF- β_1 and Smad 7 mRNA expressions showed a clear negative correlation ($r = -0.755$, $P < 0.01$), and both were significantly correlated with α -SMA protein expression ($r = -0.938$, $P < 0.01$; $r = 0.938$, $P < 0.01$, respectively).

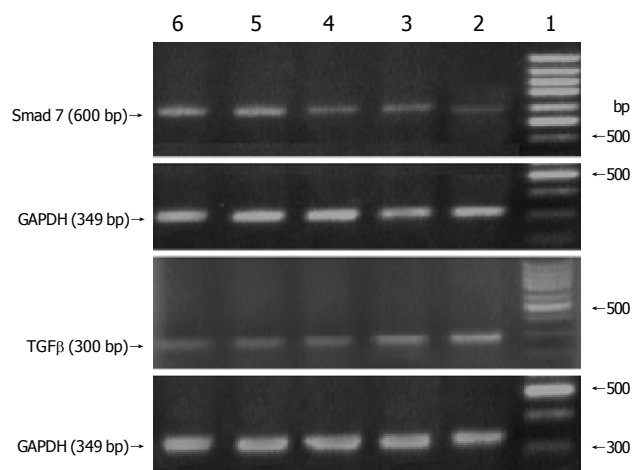


Figure 3 RT-PCR determination of Smad 7 and TGF- β_1 mRNA expressions. Lane 1: 100-bp marker, lane 2: control group, lanes 3-6: treatment with tetrandrine at 0.25, 0.5, 1.0, 2.0 mg/L, respectively.

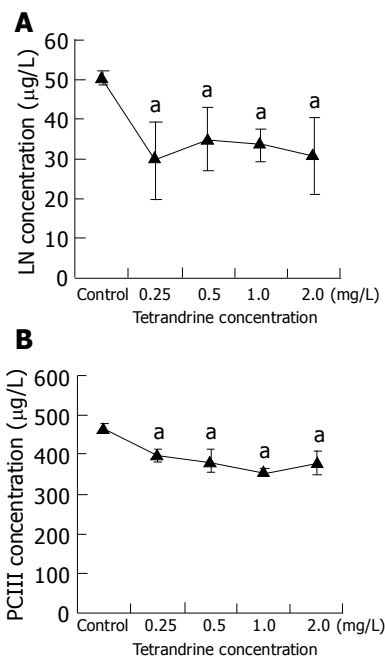
Table 1 Densitometric analysis of PCR products of each group (mean \pm SD)

Group	A_S/A_G	A_T/A_G
Control	11.5 \pm 0.5	78.5 \pm 0.4
Tet-0.25	27.3 \pm 0.3 ^a	34.1 \pm 0.3 ^a
Tet-0.5	25.9 \pm 0.2 ^{a,c}	12.6 \pm 0.3 ^{a,c}
Tet-1.0	67.0 \pm 1.0 ^{a,c,e}	9.5 \pm 0.3 ^{a,c,e}
Tet-2.0	67.4 \pm 0.2 ^{a,c,e}	9.5 \pm 0.1 ^{a,c,e}

^a $P < 0.05$ vs control group. ^c $P < 0.05$ vs Tet-0.25 group. ^e $P < 0.05$ vs Tet-0.25, Tet-0.5 groups. A_S/A_G : Ratio of the densities of Smad 7 to that of GAPDH (%). A_T/A_G : Ratio of the densities of TGF- β_1 to that of GAPDH (%).

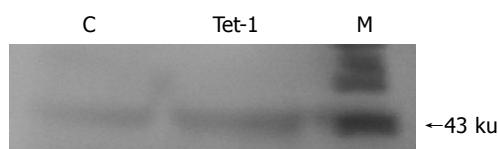
LN and PCIII excretion of culture-activated HSCs

Compared with the control group, the content of LN in HSC culture medium was reduced in tetrandrine groups (0.25, 0.5, 1, 2 mg/L) to 58.5%, 69.1%, 65.8% or 60.0%, respectively ($P < 0.05$), and that of PCIII to 84.6%, 81.5%, 75.7% or 80.7%, respectively ($P < 0.05$), whereas there was no difference among the groups with various concentrations of tetrandrine (Figure 4).

**Figure 4** Radioimmunoassay of LN and PCIII. ^a $P < 0.05$ vs control group.

Expression of Smad 7 of culture-activated HSCs

Immunoblot analysis indicated that HSCs after 5 d of culture expressed Smad 7, which was markedly increased by tetrandrine (1 mg/L) treatment. This was consistent with RT-PCR results (Figure 5).

**Figure 5** Immunoblot analysis for Smad 7. C: control group, Tet-1: treatment with tetrandrine at 1 mg/L, M: protein marker.

DISCUSSION

Tetrandrine is a bisbenzyl isoquinolone alkaloid extracted from *Stephania tetrandra* S. Moore, a traditional Chinese herb medicine. With the progression of basic researches and clinical experiments in recent years, tetrandrine has been demonstrated to be effective in anti-inflammation, immunomodulation, reversion of cardiac and vascular remodeling, inhibition of pulmonary vessels and airway smooth muscle contraction, suppression of tumor proliferation and multi-drug resistance, and so on^[10-12]. Anti-fibrogenesis have long been an important field. Over the years, more experimental animal and clinical studies have shown that tetrandrine has anti-fibrogenic actions, such as inhibition of inflammatory reaction of injured liver, attenuation of ECM deposition, decrease in serum PCIII and LN levels, and inhibiting proliferation and collagen synthesis of fibroblasts or HSCs induced by platelet-derived growth factor. Some earlier studies showed a direct inhibiting effect of tetrandrine on the proliferation of vascular smooth muscle cells and pulmonary fibroblasts^[13,14]. More recently, Lee *et al.*^[15], showed that tetrandrine inhibited tissue inhibitor of metalloproteinase expression and thus attenuate liver fibrosis, while the study of Park *et al.*^[16], revealed that α -SMA, the marker of activated HSCs, was significantly reduced when primary cultured HSCs were treated with tetrandrine (10 mg/L), and much higher concentrations of tetrandrine induced apoptosis in HSCs^[17]. However, little is known how tetrandrine affects HSC activation, the key process in the progression of liver fibrosis, and the possible mechanism involved. It is true when it comes to a lower concentration of tetrandrine of less than 10 mg/L. This seems to be more important when realizing its cytotoxicity. In this study, using the most popular cell model of HSC activation^[2], we disclosed that tetrandrine could suppress the morphological transformation of HSCs from the quiescent type to activated one, and decrease the expression of α -SMA. Likewise, the production of LN and PCIII and expression of TGF- β_1 mRNA were diminished. Our results strongly demonstrated the direct inhibiting effect of tetrandrine on HSC activation and transformation to myofibroblast. Additionally, our data revealed the influence of tetrandrine on inhibitory signaling molecule (Smad 7) for TGF- β . All the findings enriched our knowledge of the anti-fibrogenic mechanism of tetrandrine.

In the course of liver fibrosis, activated HSCs are the most important source of TGF- β_1 , which in turn induces and accelerates the activation of quiescent HSCs in an autocrine and paracrine manner, promotes ECM production, and results in progression of liver fibrosis. It has been widely accepted that TGF- β_1 is the most potent profibrogenic mediator in liver fibrosis^[2-4], and thus to inhibit TGF- β_1 function is of great importance and effective in anti-fibrogenic strategy^[4,18-20]. The signals of TGF- β mainly go through its receptors and downstream Smad proteins to HSCs^[21]. Smads, including Smad 1-Smad 8, are the intercellular components of the signal pathway of TGF- β superfamily. Smads interact with type I and type II TGF- β receptors and directly or indirectly transduce or modulate TGF- β signals into nuclei^[5,6]. It has been reported that the balance between Smads may be the key issue in maintaining

normal TGF- β functions^[5,21], and Smad 7 is the main negative feedback regulator of TGF- β signaling in HSCs^[6]. However, in activated HSCs, TGF- β -induced Smad 7 expression was diminished in an unknown way and this was thought to be strongly associated with the overwhelming profibrogenic action of TGF- β following liver injury. Therefore, an attempt to up-regulate Smad 7 expression might be a promising way to reduce TGF- β excretion, restore normal signal regulation, and inhibit HSC activation with resulting abnormal functions.

Our study indicated that the activation of HSCs was significantly inhibited by tetrandrine, as shown by the delayed morphologic transformation, diminution of α -SMA and TGF- β_1 mRNA expression, decrease in LN and PCIII production, increase in Smad 7 expression. Statistical analysis showed a close correlation among the changes of α -SMA, TGF- β_1 mRNA and Smad 7. These data suggested that tetrandrine inhibited activation of HSCs via down-regulation of TGF- β_1 expression. However, this may not be the only mechanism, for it might be the result of inhibition of HSC activation via some other pathways instead of TGF- β_1 signaling^[22]. Smad 7, both at mRNA and protein levels, was remarkably increased in comparison with lowered TGF- β_1 , suggesting that Smad 7 plays an important role in HSC inactivation, in addition to the result of diminution of TGF- β_1 . Tetrandrine may inhibit activation of HSCs by up-regulation of Smad 7 with resulting blockage of TGF- β gene transcription. This view is supported by recently reported findings that up-regulation of Smad 7 or blockage of TGF- β_1 signaling resulted in inhibition of HSC activation^[23,24].

HSC activation is a complicated process, which is even true when it comes to *in vivo* studies. The reasons why the feedback regulation of TGF- β signaling in normal liver cell is maintained and why such a regulation is lost in the pathological process of liver fibrosis are still not fully understood at present. Although in this study we revealed that tetrandrine could influence TGF- β_1 and its signaling through Smads, more efforts should be made to further investigate the mechanisms involved and the interaction with other factors in their signal transduction pathways.

REFERENCES

- 1 **Reeves HL**, Friedman SL. Activation of hepatic stellate cells—a key issue in liver fibrosis. *Front Biosci* 2002; **7**: d808-d826
- 2 **Friedman SL**. Molecular regulation of hepatic fibrosis, an integrated cellular response to tissue injury. *J Biol Chem* 2000; **275**: 2247-2250
- 3 **Gressner AM**, Weiskirchen R, Breitkopf K, Dooley S. Roles of TGF-beta in hepatic fibrosis. *Front Biosci* 2002; **7**: d793-d807
- 4 **Shek FW**, Benyon RC. How can transforming growth factor beta be targeted usefully to combat liver fibrosis? *Eur J Gastroenterol Hepatol* 2004; **16**: 123-126
- 5 **Bauer M**, Schuppan D. TGFbeta1 in liver fibrosis: time to change paradigms? *FEBS Lett* 2001; **502**: 1-3
- 6 **Nakao A**, Afrakhte M, Moren A, Nakayama T, Christian JL, Heuchel R, Itoh S, Kawabata M, Heldin NE, Heldin CH, ten Dijke P. Identification of Smad7, a TGFbeta-inducible antagonist of TGF-beta signalling. *Nature* 1997; **389**: 631-635
- 7 **Dooley S**, Streckert M, Delvoux B, Gressner AM. Expression of Smads during *in vitro* transdifferentiation of hepatic stellate cells to myofibroblasts. *Biochem Biophys Res Commun* 2001; **283**: 554-562
- 8 **Friedman SL**, Roll FJ. Isolation and culture of hepatic lipocytes, Kupffer cells, and sinusoidal endothelial cells by density gradient centrifugation with Stractan. *Anal Biochem* 1987; **161**: 207-218
- 9 **Uyama N**, Shimahara Y, Okuyama H, Kawada N, Kamo S, Ikeda K, Yamaoka Y. Carbenoxolone inhibits DNA synthesis and collagen gene expression in rat hepatic stellate cells in culture. *J Hepatol* 2003; **39**: 749-755
- 10 **Lai JH**. Immunomodulatory effects and mechanisms of plant alkaloid tetrandrine in autoimmune diseases. *Acta Pharmacol Sin* 2002; **23**: 1093-1101
- 11 **Xie QM**, Tang HF, Chen JQ, Bian RL. Pharmacological actions of tetrandrine in inflammatory pulmonary diseases. *Acta Pharmacol Sin* 2002; **23**: 1107-1113
- 12 **Wang G**, Lemos JR, Iadecola C. Herbal alkaloid tetrandrine: from an ion channel blocker to inhibitor of tumor proliferation. *Trends Pharmacol Sci* 2004; **25**: 120-123
- 13 **Zhang JX**, Pegoli W, Clemens MG. Endothelin-1 induces direct constriction of hepatic sinusoids. *Am J Physiol* 1994; **266**: G624-G632
- 14 **Reist RH**, Dey RD, Durham JP, Rojanasakul Y, Castranova V. Inhibition of proliferative activity of pulmonary fibroblasts by tetrandrine. *Toxicol Appl Pharmacol* 1993; **122**: 70-76
- 15 **Lee SH**, Nan JX, Sohn DH. Tetrandrine prevents tissue inhibitor of metalloproteinase-1 messenger RNA expression in rat liver fibrosis. *Pharmacol Toxicol* 2001; **89**: 214-216
- 16 **Park PH**, Nan JX, Park EJ, Kang HC, Kim JY, Ko G, Sohn DH. Effect of tetrandrine on experimental hepatic fibrosis induced by bile duct ligation and scission in rats. *Pharmacol Toxicol* 2000; **87**: 261-268
- 17 **Zhao YZ**, Kim JY, Park EJ, Lee SH, Woo SW, Ko G, Sohn DH. Tetrandrine induces apoptosis in hepatic stellate cells. *Phytother Res* 2004; **18**: 306-309
- 18 **Ueno H**, Sakamoto T, Nakamura T, Qi Z, Astuchi N, Takeshita A, Shimizu K, Ohashi H. A soluble transforming growth factor beta receptor expressed in muscle prevents liver fibrogenesis and dysfunction in rats. *Hum Gene Ther* 2000; **11**: 33-42
- 19 **Isono M**, Soda M, Inoue A, Akiyoshi H, Sato K. Reverse transformation of hepatic myofibroblast-like cells by TGFbeta1/LAP. *Biochem Biophys Res Commun* 2003; **311**: 959-965
- 20 **Xu XB**, He ZP, Liang ZQ, Leng XS. Obstruction of TGF-beta1 signal transduction by anti-Smad4 gene can therapy experimental liver fibrosis in the rat. *Zhonghua Ganzhangbing Zazhi* 2004; **12**: 263-266
- 21 **Bissell DM**, Roulot D, George J. Transforming growth factor beta and the liver. *Hepatology* 2001; **34**: 859-867
- 22 **Fang LH**, Zhang YH, Ma JJ, Du GH, Ku BS, Yao HY, Yun YP, Kim TJ. Inhibitory effects of tetrandrine on the serum- and platelet-derived growth factor-BB-induced proliferation of rat aortic smooth muscle cells through inhibition of cell cycle progression, DNA synthesis, ERK1/2 activation and c-fos expression. *Atherosclerosis* 2004; **174**: 215-223
- 23 **Dooley S**, Hamzavi J, Breitkopf K, Wiercinska E, Said HM, Lorenzen J, Ten Dijke P, Gressner AM. Smad7 prevents activation of hepatic stellate cells and liver fibrosis in rats. *Gastroenterology* 2003; **125**: 178-191
- 24 **Zhao JF**, Liu CH, Hu YY, Xu LM, Liu P, Liu C. Effect of salvianolic acid B on Smad3 expression in hepatic stellate cells. *Hepatobiliary Pancreat Dis Int* 2004; **3**: 102-105

• BASIC RESEARCH •

Cytotoxic effect of a non-peptidic small molecular inhibitor of the p53-HDM2 interaction on tumor cells

Wen-Dong Li, Mi-Juan Wang, Fang Ding, Da-Li Yin, Zhi-Hua Liu

Wen-Dong Li, Fang Ding, Zhi-Hua Liu, National Laboratory of Molecular Oncology, Cancer Institute, Peking Union Medical College and Chinese Academy of Medical Sciences, Beijing 100021, China

Mi-Juan Wang, Da-Li Yin, Institute of Materia Medica, Peking Union Medical College and Chinese Academy of Medical Sciences, Beijing 100021, China

Supported by the China Key Program on Basic Research, G1998051102 and G1998051021, National Science Foundation of China, 39870862

Correspondence to: Zhi-Hua Liu, Professor, National Laboratory of Molecular Oncology, Cancer Institute, Peking Union Medical College and Chinese Academy of Medical Sciences, Beijing 100021, China. liuzh@pubem.cicams.ac.cn

Telephone: +86-10-67723789 Fax: +86-10-67723789

Received: 2004-05-27 Accepted: 2004-06-17

Abstract

AIM: To investigate if non-peptidic small molecular inhibitors of the p53-HDM2 interaction could restore p53 function and kill tumor cells.

METHODS: A series of non-peptidic small HDM2 inhibitors were designed by computer-aided model and synthesized by chemical method. Syl-155 was one of these inhibitors. Cytotoxic effect of syl-155 on three tumor cell lines with various states of p53, HT1080 (wild-type p53), KYSE510 (mutant p53), MG63 (p53 deficiency) was evaluated by MTT assay, Western blot and flow cytometry.

RESULTS: Syl-155 stimulated the accumulation of p53 and p21 protein in HT1080 cells expressing wild-type p53, but not in KYSE510 and MG63 cells. Consequently, syl-155 induced cell cycle arrest and apoptosis in HT1080 cells.

CONCLUSION: Non-peptidic small molecular inhibitors of the p53-HDM2 interaction show promise in treatment of tumors expressing wild-type p53.

© 2005 The WJG Press and Elsevier Inc. All rights reserved.

Key words: Non-peptidic small molecular weight inhibitors; Cytotoxic effect; p53; Cancer therapy; HDM2

Li WD, Wang MJ, Ding F, Yin DL, Liu ZH. Cytotoxic effect of a non-peptidic small molecular inhibitor of the p53-HDM2 interaction on tumor cells. *World J Gastroenterol* 2005; 11(19): 2927-2931

<http://www.wjgnet.com/1007-9327/11/2927.asp>

INTRODUCTION

HDM2 protein regulates the activity of p53 protein in at least three different ways^[1]. First, HDM2 inhibits the transcription activity of p53 protein by binding to its transactivation domain^[2]. Second, HDM2 protein modulates nucleo-cytoplasmic shuffling of p53 protein as a shuffle protein^[3]. Third, it promotes the degradation of p53 protein as an E3 ubiquitin ligase^[4,5]. HDM2 overexpression inactivates p53 protein in 5-10% of human cancers. Since the p53-HDM2 interaction was elucidated by Kussie *et al*^[6], inhibition of this interaction has been of interest for the study of cancer therapy^[7-10]. The feasibility of this strategy has been verified by many inhibitors such as modified thioredoxin protein^[11], anti-MDM2 monoclonal antibody 3G5^[12], peptidic inhibitor fused to the glutathione S-transferase protein^[13], anti-sense oligonucleotide resistant to HDM2^[14], HDM2 alternatively spliced products^[15], chalcone and its derivatives^[16], chlorofusin^[17,18] and octamer synthetic peptide^[19,20]. These inhibitors above inhibit p53-HDM2 interaction, increase p53 accumulation and cause cell cycle arrest or apoptosis in various tumor cells.

Based on the clarification of the crystal structure of p53-HDM2 complex^[6], we have obtained a series of non-peptidic small HDM2 inhibitors designed by computer-aided model and synthesized by chemical method. These inhibitors have been proved to release p53 through competing with the binding site of p53 and HDM2 by ELISA and some results were shown previously^[21]. Syl-155 is one of these inhibitors (data not shown). In this report, we investigate whether syl-155 could rescue p53 function from the p53-HDM2 interaction and evaluate its activities in tumor cells with various states of p53.

MATERIALS AND METHODS

Cell lines

Human fibrosarcoma cell line HT1080 expressing wild-type p53 protein, human esophageal squamous cancer cell line KYSE510 expressing mutant p53 protein and human osteosarcoma osteoblast-like cell line MG63 which was p53-negative^[22] express HDM2 were used in this study. Human embryo lung fibroblast (HELFL) cell line was used as control. HT1080 and MG63 were purchased from cell center, Wuhan University, China; KYSE510 was a gift from Dr. Shimada Y, First Department of Surgery, Faculty of Medicine, Kyoto University, Japan; HELFL was a gift from Institute of Material Medica, CAMS, China.

Non-peptidic small molecular HDM2 inhibitor

Non-peptidic small molecular HDM2 inhibitors were

synthesized chemically by Yin *et al.*, in Institute of Material Medica, CAMS^[21]. These inhibitors could prevent the interaction of HDM2 and p53 proteins through competing with p53 for binding to HDM2. Syl-155 was one of these inhibitors. DMSO was used as assistant solvent for these inhibitors. In this study, the final concentration of DMSO was 0.2 mL/L in cultures. Control cells also received 0.2 mL/L DMSO (<4 mL/L) which had no effect on cell proliferation or viability^[23].

MTT assay for determination of cell viability and growth

The MTT assay was carried out as described previously^[24] with some modifications. HT1080, KYSE510, MG63 and HELF cells were seeded in seven 96-well plates, and each well contained 1.2×10^3 cells. Triplicate wells were used for each experimental condition. Absorbance was measured in a bio-kinetics reader (Bio-Tek Instruments Inc., Winooski, VT) at a wavelength of 490 nm. The means were obtained on each of 7 d and used to draw a curve of cell proliferation. The viability rates (VR) on the third day were calculated as follows:

$$\text{VR (\%)} = \frac{\text{Total absorbance in tested group (3 d)}}{\text{Total absorbance in control (3 d)}} \times 100\%$$

Flow cytometry assay

HT1080, KYSE510 and MG63 cells were harvested at various time points after treatment with 10 $\mu\text{g/mL}$ syl-155 for up to 72 h, stained with 50 $\mu\text{g/mL}$ PI (Calbiochem, San Diego, CA, USA), and analyzed by a FACSCalibur flow cytometer (Becton Dickson, Mountain View, CA, USA) using CELLQUEST software. The position of the cells with sub-G₁ DNA content was indicative of apoptosis^[25].

Western blot assay

HT1080, KYSE510 and MG63 cells were harvested at various time points after treatment with 10 $\mu\text{g/mL}$ syl-155 for up to 120 h. Whole cell lysates were prepared using cell lysis buffer (100 $\mu\text{g/mL}$ PMSF, 2 $\mu\text{g/mL}$ aprotinin, 2 $\mu\text{g/mL}$ leupeptin, 1 mL/L NP-40 in cold PBS), and then protein was extracted for Western blot. Western blot analysis was

performed as described previously^[26]. HDM2, p53 and p21 proteins were detected by mouse monoclonal antibodies D-12, DO-1 and F-5 (Santa Cruz Biotechnology, Santa Cruz, CA) as primary antibodies, respectively. β -actin was used as internal control.

RESULTS

Viability of tumor cells detected by MTT

A series of non-peptidic small molecular HDM2 inhibitors were synthesized. Based on the IC₅₀ (<10 $\mu\text{g/mL}$) calculated by MTT assay (data not shown), syl-155, one of these non-peptidic small molecular HDM2 inhibitors, was chosen for further studies. Cell viability assay by MTT showed that syl-155 could cause cell death in HT1080 cells while its cytotoxic effect on KYSE510, MG63 and HELF cells were not obvious (Table 1).

Table 1 Results of cell viability assay (%)¹

	HT1080	KYSE510	MG63	HELF
Syl-155	40.79	80.61	85.59	87.59
Syc-40	91.23	88.65	90.70	92.51

¹The percentage shown was the VR of three tumor cell lines and one normal cell line after treatment with non-peptidic small compound (syl-155) or negative control compound (syc-40)^[21] for 3 d at the concentration of 10 $\mu\text{g/mL}$. The results were shown as the mean value of three different experiments.

Changes of cell growth curves by syl-155

HT1080, KYSE510 and MG63 cell lines were treated with syl-155 at various concentrations for 1-6 d, and the cell viability was determined as described above by MTT assay. Syl-155 inhibited the growth of the three cell lines in a dose-and time-dependent manner (Figure 1). With the prolongation of treatment time, the growth of HT1080 cells treated with syl-155 at concentrations 2.5, 5.0 and 10 $\mu\text{g/mL}$ was slower than that of KYSE510 and MG63 cells treated with the same concentration of syl-155 compared with the negative control within 6 d. HT1080 cells incubated with 10 $\mu\text{g/mL}$ of syl-155 grew slower than that incubated with 2.5 or 5.0 $\mu\text{g/mL}$ of syl-155. Syl-155

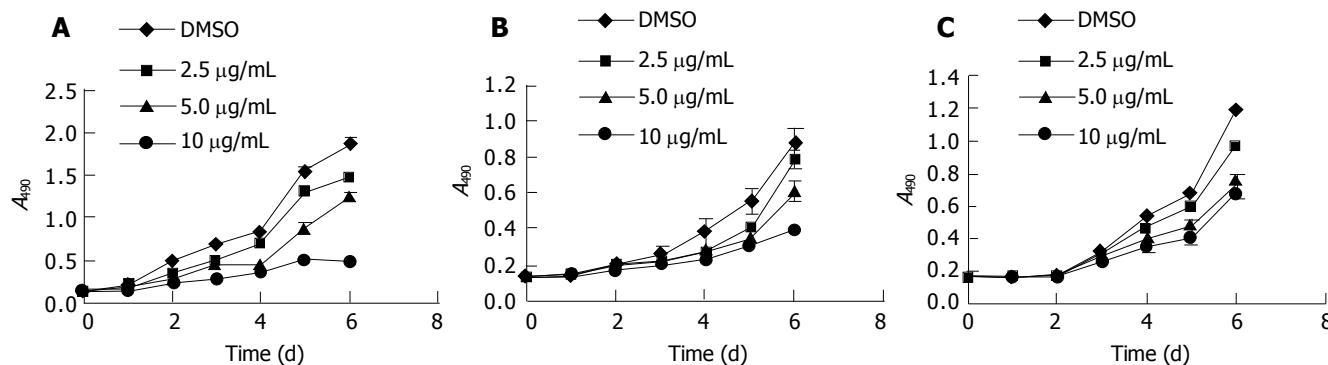


Figure 1 Time- and dose-dependent effect of syl-155 on the cell growth of the three tumor cell lines. All the three cell lines were treated with either syl-155 at different concentrations (2.5, 5.0, 10 $\mu\text{g/mL}$) or 0.2 mL/L DMSO. MTT method was employed at the indicated time for analyses of cell growth. The experiments

were performed in triplicate, and similar results were obtained from three independent experiments. The data were expressed as mean \pm SD. A: HT1080; B: KYSE510; C: MG63.

at 10 $\mu\text{g}/\text{mL}$ had an inhibitory effect of more than 50% on tumor cell growth 3 d after treatment. The inhibitory rate in the next 3 d was 57.86%, 67.54% and 74.98%, respectively, after treatment with 10 $\mu\text{g}/\text{mL}$ of syl-155.

Expression of HDM2, p53 and p21 protein induced by syl-155

Previous studies indicate that inhibition of the interaction between p53 and p21 protein can prevent HDM2 degrading p53, which leads to accumulation of p53 and induce apoptosis. In HT1080 cells, 12 h after syl-155 administration, the protein level of p53 increased. At 24 h, p53 protein reached a higher level. Then the protein level of p53 decreased but maintained a higher level than the basal level. At 120 h, p53 protein rose and reached a much higher level than ever before. The p21 protein level also slowly rose (Figure 2A), whereas no accumulation of p53 or p21 protein was observed in tumor cell lines KYSE510 (Figure 2B) and MG63 (data not shown). Syl-155 had no effect on the levels of p53 and p21 proteins in both p53-negative or p53-mutant cells.

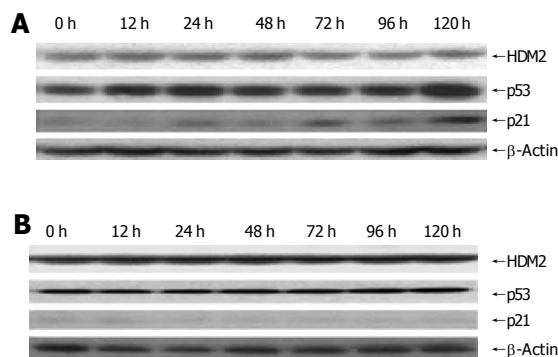


Figure 2 Expression of HDM2, p53 and p21 proteins in HT1080 cells (A) and KYSE510 cells (B) induced by syl-155. The HT1080 cells were harvested at the indicated time after treatment with 10 $\mu\text{g}/\text{mL}$ syl-155, and then protein was extracted for Western blot. HDM2, p53, p21 and β -actin proteins were detected using mouse monoclonal antibodies DO-1, D-12, DO-1, F-5 and anti- β -actin antibody as primary antibodies, respectively.

Syl-155 induced apoptosis of HT1080 cells

The inhibitory effect of syl-155 on cell proliferation was stronger in HT1080 cells than in KYSE510 or MG63 cells. Western blot results showed that syl-155 induced accumulation of p53 and p21 proteins in HT1080 cells but not in KYSE510 and MG63 cells. The question was raised as to whether syl-155 could induce cell cycle arrest or apoptosis of HT1080 cells through the accumulation of p53 protein by preventing HDM2 from degrading it. Therefore flow cytometry was employed for the investigation. HT1080, KYSE510 and MG63 cells were treated with 10 $\mu\text{g}/\text{mL}$ syl-155 for 0-72 h, stained with PI, and analyzed by flow cytometry. The cells with sub- G_1 DNA content were apoptotic cells confirmed by annexin V-FITC binding assay (data not shown). Syl-155 induced more apoptosis of HT1080 cells than DMSO while less apoptosis of KYSE510 and MG63 cells was found (Figure 3). The syl-155-induced apoptosis of HT1080 cells increased in a time-dependent manner (Figure 4).

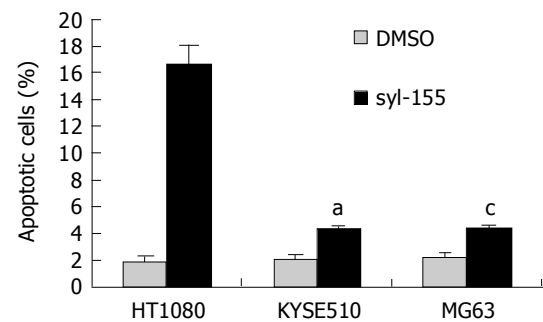


Figure 3 Syl-155-induced apoptosis of tumor cells. All the three cell lines were incubated with 0.2 mL/L DMSO or 10 $\mu\text{g}/\text{mL}$ syl-155 for 3 d, stained with PI, and analyzed by flow cytometry to quantitate cells with a subdiploid DNA content. The data were expressed as mean \pm SD, ^a $P < 0.05$ vs HT1080 group, ^c $P < 0.05$ vs HT1080 group.

Syl-155 induced G_1 arrest in HT1080 cells

HT1080 cells were incubated with 0.02% DMSO or 10 $\mu\text{g}/\text{mL}$ syl-155 for 0-72 h, stained with PI, and analyzed by flow cytometry to quantitate cells in the different phases of cell cycle. The results showed that syl-155 induced an increased cell cycle arrest at G_0/G_1 phase in HT1080 cells (Table 2).

Table 2 Changes in cell cycle distribution (%)¹

	Negative control	DMSO	Syl-155		
			24 h	48 h	72 h
G_0/G_1	54.1	49.8	60.6	60.0	63.5
S	34.1	37.1	30.4	23.9	27.6
G_2/M	11.8	13.1	9.0	16.1	8.9

¹The percentage shown is the distribution of cell cycle in HT1080 cells.

DISCUSSION

The function of p53 is inactivated during the development of most human tumors^[27,28]. The main mechanism of p53 inactivation is due to p53 gene mutation which occurs in more than 50% human tumors. Another important mechanism is that p53 protein interacts with other proteins which either promote p53 protein degradation or inhibit its ability to transactivate its downstream genes involved in cell cycle arrest or apoptosis^[29]. HDM2 is an oncoprotein that mainly binds to p53 protein functioning as E3 ubiquitin ligase and promotes its proteolysis through a ubiquitination degradation pathway by the 26S proteasome^[3-5,30]. Furthermore, HDM2 is a target of the transcriptional factor p53. Therefore, there is an autoregulatory negative feedback loop between p53 and HDM2 protein^[31]. In normal cells, HDM2 maintains p53 protein at low levels. HDM2 can also inactivate p53 by masking the transactivation domain of p53 so that the downstream genes of p53 such as p21 cannot be transcribed^[32]. HDM2 overexpression can result in excessive inactivation of p53, diminishing its tumor suppression function. HDM2 can affect cell cycle, apoptosis and tumorigenesis by interacting with other proteins, including retinoblastoma 1 and ribosomal protein L5.

HDM2 is amplified in 7% of human tumors, 40-60% of osteosarcomas and approximately 30% of soft tissue

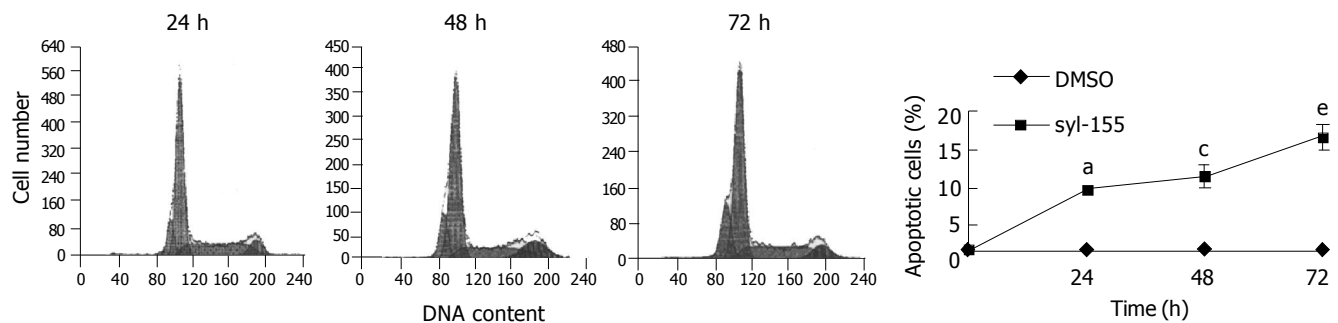


Figure 4 Syl-155-induced apoptosis of HT1080 cells. Time course analysis for the occurrence of apoptosis induced by syl-155. HT1080 cells were treated with 10 μ g/mL syl-155 for 0-72 h, stained with PI, and analyzed by flow cytometry

to quantitate cells with a subdiploid DNA content. The data were expressed as mean \pm SD, * P <0.05 vs DMSO group, ^a P <0.05 vs DMSO group, ^c P <0.05 vs DMSO group.

sarcomas^[33,34]. The inactivation of p53 through the binding to HDM2 is of particular interest in a therapeutic point of view, as the function of p53 protein could be potentially restored by disrupting the interaction of p53 with HDM2. So it has become very significant to seek inhibitors of p53-HDM2 interaction.

The feasibility of this strategy has been verified by previous studies. These inhibitors include HDM2 alternatively spliced products^[15], GST fusion protein^[13], monoclonal antibody^[12], synthetic peptides^[11,19,20], chalcone and its derivatives^[16], chlorofusin^[17,18], and anti-sense oligonucleotide^[14]. All these inhibitors can cause p53 accumulation and activate the function of p53 as tumor suppressor in tumor cells. Usually non-peptidic small molecules have higher permeability into cells, and can be synthesized with a lower cost. It is interesting to note whether non-peptidic small molecules can substitute for these inhibitors. Computer-aided design based on the crystal structures makes it possible to screen and choose effective compound on a large scale. Elucidation of the crystal structure of p53-HDM2 complex^[6] provides a basis for seeking non-peptidic small molecule HDM2 inhibitors. In the study, we synthesized a series of non-peptidic small molecule HDM2 inhibitors by computer-aided design based on the crystal structure of p53-HDM2 complex. MTT assay initially screened these compounds, and one (syl-155) of them was chosen for further study.

We studied the effect of syl-155-activated p53 pathway on three tumor cell lines with various status of p53. In HT1080 cell line expressing wild type p53, syl-155 induced the accumulation of p53 protein, which consequently increased the levels of p21. However, like AP^[35], syl-155 had no effect on p21 levels in both p53-negative or p53-mutant cells. p53-mutant protein was also not affected after treatment with syl-155 in KYSE510 cells expressing mutated p53. Therefore, we can conclude that syl-155 only inhibits p53-HDM2 interaction in cells carrying wild-type p53 protein and elevates p21 protein levels by stimulating the accumulation of wild-type p53 protein. Wild-type p53 protein is a labile protein and its cellular level is mainly regulated by the rate of its proteosomal degradation. p53 degradation is mediated by two alternative pathways that either depend on HDM2 and ubiquitin or they are independent of both. The latter pathway is regulated by NAD(P)H and quinone oxidoreductase 1 (NQO1)^[36]. This can explain why p53 protein level decreases after reaching a higher level, which correlates with the

changes of p21 protein level.

In cell assay, syl-155 affected proliferation of the three cell lines in a dose- and time-dependent manner. The growth of HT1080 cells treated with syl-155 was slower than that of KYSE510 and MG63 cells. The syl-155-mediated inhibition of tumor cell proliferation may be the consequence of an induction of apoptosis or cell cycle arrest. In our experiment, syl-155 induced more apoptosis of HT1080 cells than of KYSE510 and MG63 cells. Syl-155 also induces G₁ arrest of HT1080 cells. Syl-155 induced cell cycle arrest and apoptosis in HT1080 cells which is consistent with the accumulation of p53 and p21 protein. Syl-155 only stimulates the p53 pathway in cells expressing wild-type p53. In combination with MTT assay, syl-155 is more toxic to tumor cells expressing wild-type p53. The more the cell expresses HDM2, the more it is susceptible to AP-mediated apoptosis^[20]. In summary, drugs for inhibiting the p53-HDM2 interaction show promise in treatment of tumors expressing wild-type p53.

ACKNOWLEDGMENTS

We are indebted to Dr. Li-Yong Zhang of Institute of Bioinformatics, Department of Automation, Tsinghua University, Beijing 100084, China for his help with image management.

REFERENCES

- 1 Freedman DA, Wu L, Levine AJ. Functions of the MDM2 oncoprotein. *Cell Mol Life Sci* 1999; **55**: 96-107
- 2 Picksley SM, Lane DP. The p53-mdm2 autoregulatory feedback loop: a paradigm for the regulation of growth control by p53? *Bioessays* 1993; **15**: 689-690
- 3 Roth J, Dobbelstein M, Freedman DA, Shenk T, Levine AJ. Nucleo-cytoplasmic shuttling of the hdm2 oncoprotein regulates the levels of the p53 protein via a pathway used by the human immunodeficiency virus rev protein. *EMBO J* 1998; **17**: 554-564
- 4 Haupt Y, Maya R, Kazaz A, Oren M. Mdm2 promotes the rapid degradation of p53. *Nature* 1997; **387**: 296-299
- 5 Kubbutat MH, Jones SN, Vousden KH. Regulation of p53 stability by Mdm2. *Nature* 1997; **387**: 299-303
- 6 Kussie PH, Gorina S, Marechal V, Elenbaas B, Moreau J, Levine AJ, Pavletich NP. Structure of the MDM2 oncoprotein bound to the p53 tumor suppressor transactivation domain. *Science* 1996; **274**: 948-953
- 7 Chene P. Inhibition of the p53-MDM2 interaction: targeting a protein-protein interface. *Mol Cancer Res* 2004; **2**: 20-28

- 8 **Moll UM**, Petrenko O. The MDM2-p53 interaction. *Mol Cancer Res* 2003; **1**: 1001-1008
- 9 **Zheleva DI**, Lane DP, Fischer PM. The p53-Mdm2 pathway: targets for the development of new anticancer therapeutics. *Mini Rev Med Chem* 2003; **3**: 257-270
- 10 **Chene P**. Inhibiting the p53-MDM2 interaction: an important target for cancer therapy. *Nat Rev Cancer* 2003; **3**: 102-109
- 11 **Bottger A**, Bottger V, Sparks A, Liu WL, Howard SF, Lane DP. Design of a synthetic Mdm2-binding mini protein that activates the p53 response *in vivo*. *Curr Biol* 1997; **7**: 860-869
- 12 **Blaydes JP**, Gire V, Rowson JM, Wynford-Thomas D. Tolerance of high levels of wild-type p53 in transformed epithelial cells dependent on auto-regulation by mdm-2. *Oncogene* 1997; **14**: 1859-1868
- 13 **Wasylyk C**, Salvi R, Argentini M, Dureuil C, Delumeau I, Abecassis J, Debussche L, Wasylyk B. p53 mediated death of cells overexpressing MDM2 by an inhibitor of MDM2 interaction with p53. *Oncogene* 1999; **18**: 1921-1934
- 14 **Chen L**, Agrawal S, Zhou W, Zhang R, Chen J. Synergistic activation of p53 by inhibition of MDM2 expression and DNA damage. *Proc Natl Acad Sci USA* 1998; **95**: 195-200
- 15 **Evans SC**, Viswanathan M, Grier JD, Narayana M, El-Naggar AK, Lozano G. An alternatively spliced HDM2 product increases p53 activity by inhibiting HDM2. *Oncogene* 2001; **20**: 4041-4049
- 16 **Stoll R**, Renner C, Hansen S, Palme S, Klein C, Belling A, Zeslawski W, Kamionka M, Rehm T, Muhlhahn P, Schumacher R, Hesse F, Kaluza B, Voelter W, Engh RA, Holak TA. Chalcone derivatives antagonize interactions between the human oncoprotein MDM2 and p53. *Biochemistry* 2001; **40**: 336-344
- 17 **Duncan SJ**, Gruschow S, Williams DH, McNicholas C, Purewal R, Hajek M, Gerlitz M, Martin S, Wrigley SK, Moore M. Isolation and structure elucidation of Chlorofusin, a novel p53-MDM2 antagonist from a *Fusarium* sp. *J Am Chem Soc* 2001; **123**: 554-560
- 18 **Duncan SJ**, Cooper MA, Williams DH. Binding of an inhibitor of the p53/MDM2 interaction to MDM2. *Chem Commun (Camb)* 2003; **3**: 316-317
- 19 **Chene P**, Fuchs J, Bohn J, Garcia-Echeverria C, Furet P, Fabbro D. A small synthetic peptide, which inhibits the p53-hdm2 interaction, stimulates the p53 pathway in tumour cell lines. *J Mol Biol* 2000; **299**: 245-253
- 20 **Chene P**, Fuchs J, Carena I, Furet P, Garcia-Echeverria C. Study of the cytotoxic effect of a peptidic inhibitor of the p53-hdm2 interaction in tumor cells. *FEBS Lett* 2002; **529**: 293-297
- 21 **Zhao J**, Wang M, Chen J, Luo A, Wang X, Wu M, Yin D, Liu Z. The initial evaluation of non-peptidic small-molecule HDM2 inhibitors based on p53-HDM2 complex structure. *Cancer Lett* 2002; **183**: 69-77
- 22 **Chandar N**, Billig B, McMaster J, Novak J. Inactivation of p53 gene in human and murine osteosarcoma cells. *Br J Cancer* 1992; **65**: 208-214
- 23 **Longthorne VL**, Williams GT. Caspase activity is required for commitment to Fas-mediated apoptosis. *EMBO J* 1997; **16**: 3805-3812
- 24 **Mosmann T**. Rapid colorimetric assay for cellular growth and survival: application to proliferation and cytotoxicity assays. *J Immunol Methods* 1983; **65**: 55-63
- 25 **Haupt Y**, Rowan S, Shaulian E, Vousden KH, Oren M. Induction of apoptosis in HeLa cells by trans-activation-deficient p53. *Genes Dev* 1995; **9**: 2170-2183
- 26 **Ueda S**, Nakamura H, Masutani H, Sasada T, Yonehara S, Takabayashi A, Yamaoka Y, Yodoi J. Redox regulation of caspase-3(-like) protease activity: regulatory roles of thioredoxin and cytochrome c. *J Immunol* 1998; **161**: 6689-6695
- 27 **Levine AJ**, Momand J, Finlay CA. The p53 tumour suppressor gene. *Nature* 1991; **351**: 453-456
- 28 **Nigro JM**, Baker SJ, Preisinger AC, Jessup JM, Hostetter R, Cleary K, Bigner SH, Davidson N, Baylin S, Devilee P. Mutations in the p53 gene occur in diverse human tumour types. *Nature* 1989; **342**: 705-708
- 29 **Lane DP**. p53 and human cancers. *Br Med Bull* 1994; **50**: 582-599
- 30 **Freedman DA**, Levine AJ. Nuclear export is required for degradation of endogenous p53 by MDM2 and human papillomavirus E6. *Mol Cell Biol* 1998; **18**: 7288-7293
- 31 **Wu X**, Bayle JH, Olson D, Levine AJ. The p53-mdm-2 autoregulatory feedback loop. *Genes Dev* 1993; **7**: 1126-1132
- 32 **Oliner JD**, Pietenpol JA, Thiagalingam S, Gyuris J, Kinzler KW, Vogelstein B. Oncoprotein MDM2 conceals the activation domain of tumour suppressor p53. *Nature* 1993; **362**: 857-860
- 33 **Velculescu VE**, Zhang L, Vogelstein B, Kinzler KW. Serial analysis of gene expression. *Science* 1995; **270**: 484-487
- 34 **Collins FS**, Patrinos A, Jordan E, Chakravarti A, Gesteland R, Walters L. New goals for the U.S. Human Genome Project: 1998-2003. *Science* 1998; **282**: 682-689
- 35 **Garcia-Echeverria C**, Chene P, Blommers MJ, Furet P. Discovery of potent antagonists of the interaction between human double minute 2 and tumor suppressor p53. *J Med Chem* 2000; **43**: 3205-3208
- 36 **Asher G**, Lotem J, Tsvetkov P, Reiss V, Sachs L, Shaul Y. P53 hot-spot mutants are resistant to ubiquitin-independent degradation by increased binding to NAD(P)H: quinone oxidoreductase 1. *Proc Natl Acad Sci USA* 2003; **100**: 15065-15070

• BASIC RESEARCH •

Expressed genes in regenerating rat liver after partial hepatectomy

Cun-Shuan Xu, Cui-Fang Chang, Jin-Yun Yuan, Wen-Qiang Li, Hong-Peng Han, Ke-Jin Yang, Li-Feng Zhao, Yu-Chang Li, Hui-Yong Zhang, Salman Rahman, Jing-Bo Zhang

Cun-Shuan Xu, Cui-Fang Chang, Jin-Yun Yuan, Hong-Peng Han, Ke-Jin Yang, Li-Feng Zhao, College of Life Science, Henan Normal University, Xinxiang 453007, Henan Province, China
Salman Rahman, Homophilia Research Center, London University, London SE17EH, UK
Wen-Qiang Li, Yu-Chang Li, Hui-Yong Zhang, Jing-Bo Zhang, Key Laboratory for Cell Differentiation Regulation, Xinxiang 453007, Henan Province, China
Supported by the National Natural Science Foundation of China, No. 30270673
Correspondence to: Professor Cun-Shuan Xu, College of Life Science, Henan Normal University, Xinxiang 453007, Henan Province, China. xucs@x263.net.cn
Telephone: +86-373-3326001 Fax: +86-373-3326524
Received: 2004-06-08 Accepted: 2004-08-05

© 2005 The WJG Press and Elsevier Inc. All rights reserved.

Key words: Subtracted cDNA libraries; Complementary DNA microarray; Liver regeneration; Partial hepatectomy; Cluster analysis

Xu CS, Chang CF, Yuan JY, Li WQ, Han HP, Yang KJ, Zhao LF, Li YC, Zhang HY, Rahman S, Zhang JB. Expressed genes in regenerating rat liver after partial hepatectomy. *World J Gastroenterol* 2005; 11(19): 2932-2940
<http://www.wjgnet.com/1007-9327/11/2932.asp>

Abstract

AIM: To reveal the liver regeneration (LR) and its control as well as the occurrence of liver disease and to study the gene expression profiles of 551 genes after partial hepatectomy (PH) in regenerating rat livers.

METHODS: Five hundred and fifty-one expressed sequence tags screened by suppression subtractive hybridization were made into an in-house cDNA microarray, and the expressive genes and their expressive profiles in regenerating rat livers were analyzed by microarray and bioinformatics.

RESULTS: Three hundred of the analyzed 551 genes were up- or downregulated more than twofolds at one or more time points during LR. Most of the genes were up- or downregulated 2-5 folds, but the highest reached 90 folds of the control. One hundred and thirty-nine of them showed upregulation, 135 displayed downregulation, and up or down expression of 26 genes revealed a dependence on regenerating livers. The genes expressed in 24-h regenerating livers were much more than those in the others. Cluster analysis and generalization analysis showed that there were at least six distinct temporal patterns of gene expression in the regenerating livers, that is, genes were expressed in the immediate early phase, early phase, intermediate phase, early-late phase, late phase, terminal phase.

CONCLUSION: In LR, the number of down-regulated genes was almost similar to that of the upregulated genes; the successively altered genes were more than the rapidly transient genes. The temporal patterns of gene expression were similar 2 and 4 h, 12 and 16 h, 48 and 96 h, 72 and 144 h after PH. Microarray combined with suppressive subtractive hybridization can effectively identify the genes related to LR.

INTRODUCTION

In the healthy adult rat liver, most of the hepatocytes lie in G₀ phase, and their cell division index is very low (about one ten thousandth)^[1-5]. However, metabolism of hepatocytes is quickly altered after partial hepatectomy (PH)^[6-10]. Activation of hepatocytes in G₀ phase occurs about 2 h after PH, and they progress to G₁ phase about 6 h after PH. Then, the cells enter into S phase of cell cycle in 12 h. DNA synthesis occurs in the early 6 h (12-17 h) of S phase, and then DNA is synthesized 18-30 h after PH, which reaches a maximum at 24 h. The G₂ phase of cell cycle lies in the subsequent 2-4 h (31-34 h after PH). After that, hepatocytes go on dividing, and the peak of cell division is at 36 h after PH. The next cycle of hepatocytes is in the following 36-66 h after PH^[11,12]. The re-differentiation of liver cells and the re-building of regenerated livers are in 72-144 h after PH. Many experiments have confirmed that a cell cycle of hepatocytes lasts for about 30 h, but that of other cells distinguishes from them^[13]. Briefly, cells in the residual liver would be activated to proliferate, re-differentiate and rebuild their structure and function after PH. In different phases of liver regeneration (LR), the physiological and biochemical actions of different kinds of cells of the liver are different. The categories and amounts of the expressed genes in them are various^[14,15]. To learn the molecular mechanism of LR, it is essential to highlight how many genes are related to it. Therefore, this paper reports that 300 genes have been successfully identified to correlate with LR by combing microarray in combination with suppression subtractive hybridization.

MATERIALS AND METHODS

Partial hepatectomy of rats

Healthy SD rats weighing 200±20 g were obtained from the Experimental Animal Center of Henan Normal University. Following the method of Higgins and

Anderson^[16], 70% of the rat liver was removed under sterile conditions.

Regenerating liver preparation and RNA isolation

The regenerating livers of four rats (male:female = 1:1) were taken 2, 4, 8, 12, 16, 24, 36, 48, 72, 96 and 144 h after PH. The livers were rinsed in cold PBS and immersed in a -80 °C refrigerator for RNA extraction. Total RNA was isolated from frozen livers according to the manual of TRIzol kit of Invitrogen. In brief, 50-100 mg liver was homogenized in 1 mL TRIzol reagent containing phenol and guanidinium isothiocyanate/cationic detergent, followed by phenol-chloroform extraction and isopropyl alcohol precipitation. The quantity and integrity of total RNA were examined by an ultraviolet spectrometer and denaturing formaldehyde agarose electrophoresis by ethidium bromide staining.

Subtracted cDNA library construction and screening

cDNA subtracted libraries were generated from total RNA by PCR-Select™ cDNA subtraction kit (Clontech) following the manufacturer's instructions. Briefly, total RNA was transcribed into double cDNA strands and digested with restriction enzymes, followed by subtracted hybridization with drivers and testers. Finally, differential expression sequence tags were performed to construct subtracted cDNA libraries with suppression PCR.

Sequence analysis

Base sequence assay of ESTs was carried out according to the current protocols in molecular biology. All sequences were determined on both strands. Comparison analysis of the selected sequences was conducted with the DNAMAN and the National Center for Biotechnology Information (www.ncbi.nlm.nih.gov) GenBank database^[17].

cDNA microarray construction

cDNA fragments amplified by PCR with nested PCR primer1 and primer2 and purified by NaAc/isopropyl alcohol were spotted onto glass slides (BioStar) with the help of the ProSys-5510A spotting machine. Then the gene chips were ready by hydrating and blocking and drying. A total of 1 152 elements (double spot chip) including 50 control system genes (8 negative control, 12 void control, 30 internal control) and 551 target genes to be studied comprised 8 submatrixes (12*12) occupying 9 mm×18 mm (BioStar). Then the gene chips were ready by hydrating, blocking and drying.

Fluorescence-labeled cDNA preparation

RNA prepared from rat livers before PH was ready for a reference for all cDNA microarray analyses. Total denatured RNA was reverse transcribed with cy3-conjugated dCTP (control group) and cy5-conjugated dCTP (test group) (Amersham-Pharmacia Biotech) using MMLV reverse transcriptase (Promega) with oligo(dT) primers. After bath incubation for 2 h, labeled buffers I and II were subsequently added to the reaction. The control group and test group were mixed symmetrically and stored avoiding light for application^[17].

Hybridization and scanning

Glass slides were prehybridized at 42 °C for 5-6 h in hybridization buffer containing freshly cooked salmon sperm DNA. The labeled denatured probes were hybridized against cDNA microarray and incubated overnight (16-18 h) at 42 °C. The slides were then washed twice with 2× SSC containing 0.5% SDS for 5 min at room temperature, then with 0.2× SSC containing 0.5% SDS at 60 °C for 10 min, and finally with 0.2× SSC at 60 °C for 10 min. The slides were exposed to a photographer. Hybridized images were scanned by a fluorescence laser-scanning device, GenePix4000A. At least, two hybridizations were performed at each time point. In addition, a semiquantitative inspection of the hybridization results was performed for green signals (downregulation), yellow signals (no obvious regulation), and red signals (upregulation)^[17].

Data analysis

cy3 and cy5 signal intensities were quantified by GenePixPro 3.0 software. Subsequently, we normalized the obtained numerical data with classical linear regression techniques. In brief, quantified cy3 and cy5 signal intensities were obtained when foreground signal intensities were deducted by background signal intensities and cy5 signal intensities were replaced by 200 when they were <200. When R_i ($R_i = \text{cy5}/\text{cy3}$) was between 0.1 and 10, R_i was taken as logarithms to generate R_i' [$\log(R_i)$] and ND was taken by EXP (R_i') (averaged R_i'). The modified cy3^* was generated by ND multiplying cy3 and was replaced by 200 when it was <200. The ratio was expressed by $\text{cy5}/\text{cy3}^*$. Therefore, we selected the genes, whose ratio was more than 2 or less than 0.5 representing a twofold difference in expression level. To analyze the selected gene expression data, we performed GeneMaths cluster analysis and hierarchical clustering to appraise the number of groups. Whole analyses were executed using Microsoft Excel and GeneSpring^[11,17].

RESULTS

The analysis of gene expression spectrum showed that, of the 551 elements made in microarray, the expression intensity of 300 genes increased or decreased at least more than twofolds at one time point after PH. Their sequence analysis showed that 152 were unreported genes, and 133 genes were significantly reported. Of which 49 were upregulated in regenerating rat livers, 74 were downregulated, and 10 were either up- or downregulated in different phases of LR. Following biochemical actions, the 133 elements were categorized into 24 groups (Table 1).

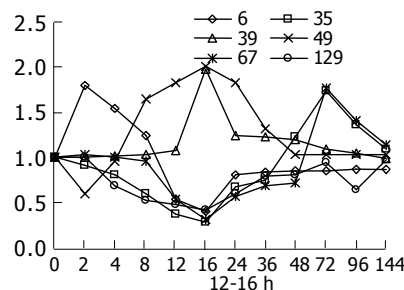
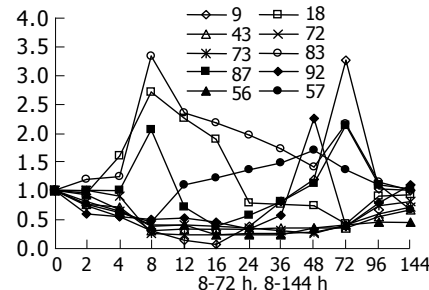
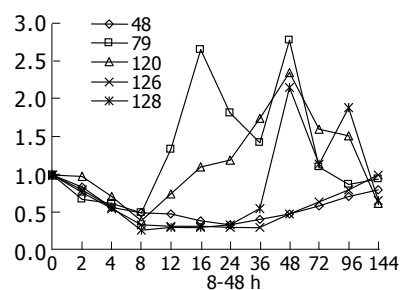
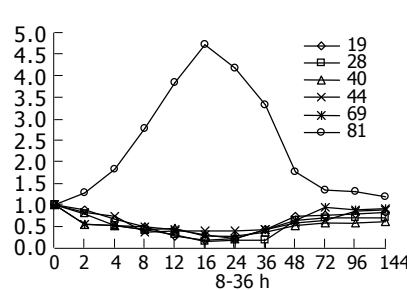
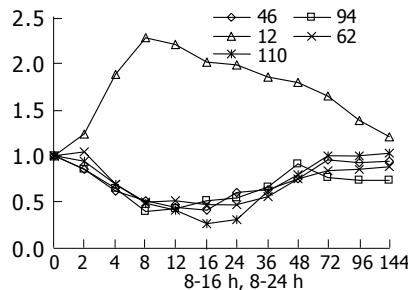
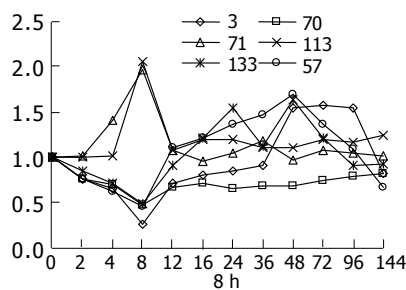
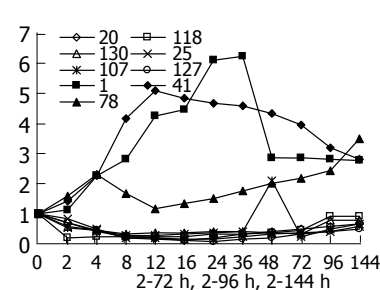
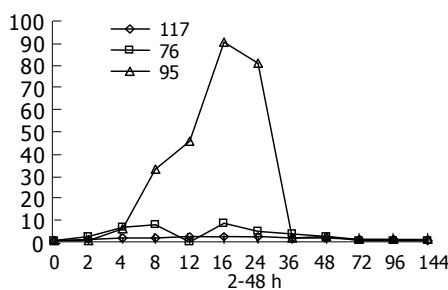
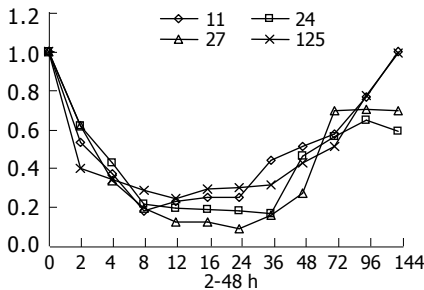
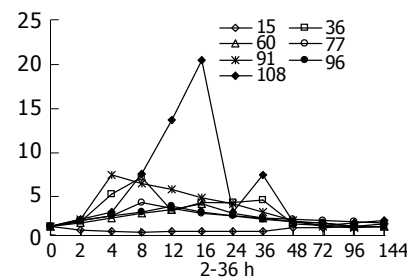
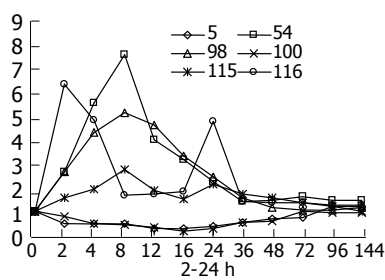
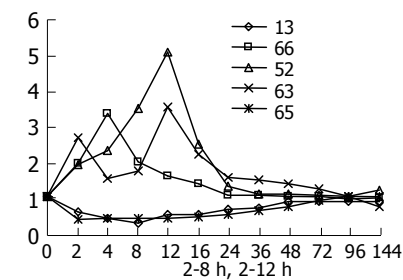
Analysis of their expression in the regenerating livers at different time points after PH showed that, in the priming phase of LR, the expression of 34 genes was rapidly altered within 6 h and then recovered gradually to the control levels in 48-72 h after PH. In the cell cycle progression phase of 8-36 h after PH, the expression of 86 genes was altered markedly. In the terminal phase of LR over 72 h after PH, the expression of 13 genes was altered distinctly (Figure 1).

Clustering analysis of genes expressed at 12 time points after PH showed that the 300 elements altered at least more than twofolds in density at one time point (Figure 2A), and

Table 1 Genes altered at least by more than twofold intensity at one time point after PH

No.	Gene description	Fold difference	No.	Gene description	Fold difference
Stress response			69	Angiopoietin-like 3	0.2
1	Alpha-1 major acute phase protein	6.2	70	Ring1 and YY1 binding protein	0.5
2	Acute-phase protein alpha-1-inhibitor 3	0.2	71	Chromatin remodeling factor	2.0
3	Clusterin (Clu)	0.3	Hemoglobins		
4	C-reactive protein, petaxin related	2.2	72	Hemoglobin beta chain (Hbb)	0.3
Glycometabolism			Immunological proteins		
5	Isocitrate dehydrogenase 1 (Idh1)	0.3	73	Immunoglobulin C kappa	0.2
6	Glycerol 3-phosphate dehydrogenase (Gpd3)	0.4	74	Achaete-scute complex homolog-like 1 (Ascl1)	0.4
7	Aldolase B	0.3	75	Complement component 1	0.3
8	Enolase 1	4.0	76	Complement component 5	8.8
9	Small subunit of RuBPCase	3.3, 0.1	77	JE/MCP-1	4.0
Fatty and stearoyl metabolism			78	Class III Fc-gamma receptor	3.5
10	Acyl-CoA desaturase	0.4	Chaperonins		
11	3-alpha-hydroxysteroid dehydrogenase	0.2	79	70 ku heat shock protein (Hspa5)	2.8, 0.5
12	Bile acid CoA ligase	2.3	80	DnaJ (Hsp40)	2.5
13	Methylmalonate semialdehyde dehydrogenase	0.3	Cytoskeletons		
14	Prostaglandin D2 synthase 2 (Ptgds2)	3.0	81	Actin gamma	4.7
15	Cytochrome P450 cholesterol 7-alpha-hydroxylase (P450 VII)	2.3, 0.5	82	Karyopherin (importin) alpha 2	0.4
16	Malonyl-CoA decarboxylase	0.3	83	Clathrin, heavy polypeptide (Cltc)	3.3
17	NAD(P)-dependent steroid dehydrogenase	0.4	Ribosomal proteins		
Oxidation and reduction response			84	Ribosomal protein L28 (Rpl28)	2.2
18	Acyl-coA oxidase (RATACO1)	2.7, 0.4	85	Ribosomal protein L41 (Rpl41)	2.1
19	Cytochrome b5 (Cyb5)	0.2	86	Ribosomal protein S19	2.5
20	Flavin-containing monooxygenase 1 (Fmo1)	0.1	Marker proteins		
21	Paraoxonase 1 (Pon1)	0.2	87	Probable surface antigen protein	2.1, 0.4
22	Selenium-dependent glutathione peroxidase	0.4	88	Surfeit 1 (Surf1)	2.5
23	Peroxisomal sarcosine oxidase (PSO)	0.3	89	Alpha globin	0.3
24	P450 arachidonic acid epoxidase (cyp 2C23)	0.2	90	Pregnancy-zone protein (Pzp)	2.4
25	Cytochrome P450	0.2	91	Adipose differentiation-related protein	7.3
26	Cytochrome P450 15-beta (Cyp2c12)	0.2	92	Subchromosomal-transferable fragment 4	2.3, 0.3
27	Cytochrome P450 2E1	0.1	93	Cocoa protein	4.9
28	Cytochrome P450, 2c39 (Cyp2c39)	0.1	94	Amyloid P-component (Sap)	0.4
29	Cytochrome P450, 7a1 (Cyp7a1)	2.0	95	Amyloid alpha-5 protein	0.2
30	Cytochrome P450 (PNCN inducible, Cyp3A1)	0.2	Amino acid enzymes		
31	Cytochrome b	0.5	96	Arginase 1 (Arg1)	0.4
Regulation proteins			97	2-hydroxyphytanoyl-CoA lyase (Hpcl2)	90.5
32	G-protein, beta polypeptide 2 (Gnb2l1)	2.4	98	Cytosolic aspartate aminotransferase	5.3
33	Interferon-induced protein with tetratricopeptide repeats 3	0.2	Nuclearase		
34	Protein RAKb	0.2	99	Mitochondrial adenine nucleotidase	2.0
Glycoproteins			100	Rnase A family 4	0.2
35	Selenoprotein P (Sepp1)	0.3	101	Rnase H	0.4
36	Myelin-associated glycoprotein (L-MAG)	7.0	Proteolytic enzymes		
37	Alpha-1-B glycoprotein (A1bg)	0.1	102	Caspase 1 (Casp1)	2.6
38	Histidine-rich glycoprotein (Hrg)	0.1	103	Cathepsin C (Ctsc)	0.4
39	Mannosylalpha-1, 6-glycoprotein beta-1, 2-N-acetylglucosaminyltransferase (Mgat2)	2.0	104	Cathepsin D (Ctsd)	0.3
40	UDP-glucuronosyltransferase 2B3 (Udpgt)	0.3	105	Neutrophil collagenase (Mmp8)	0.2
41	Fibrinogen gamma polypeptide (Fgg)	5.1	106	Coagulation factor 2 (F2)	0.2
42	TRAM1	3.3, 0.4	Proteinase inhibitors		
Lipid-proteins			107	Alpha-1 microglobulin/bikunin (Ambp)	2.1, 0.2
43	Apolipoprotein C-II	0.3	108	Alpha-2-macroglobulin (A2m)	21.3
44	Apolipoprotein M (Apom)	0.4	109	Alpha-trypsin inhibitor, heavy chain 4	0.2
45	Fatty acid binding protein 1 (Fabp1)	0.3	110	Leuserpin-2 (Serpind1)	0.2
46	Retinol-binding protein (PRBP)	0.4	111	Serine protease inhibitor 1	5.0
47	Solute carrier family 20 (phosphate transporter) member 1 (Slc20a1)	0.4	Phosphorylases		
48	Transferrin-related protein (TTN)	0.3	112	Thymidylate kinase (dTMP kinase)	3.0
Nucleolar proteins			113	Mss4 protein	2.1
49	P53	2.0	114	CDK110	0.5
50	Damage-specific DNA binding protein 1 (Ddb1)	0.3	Phosphatases		
51	Nucleolar protein family A, member 2	3.9	115	Carbamyl phosphate synthetase I	2.9
52	Nuclear protein 1 (Nupr1)	5.1	116	Phosphodiesterase 1 (Enpp1)	6.6
53	AP1 gamma subunit binding protein 1	2.3	117	Phosphatidylserine-specific phospholipase A1	2.8
Receptors			118	Protein phosphatase 1 (GL-subunit)	0.2
			119	UTP-glucose-1-phosphatase	0.4
			Synthase		

54 Interleukin 1 receptor, type 1 (Il1r1)	7.9	120 H ⁺ -ATP synthase alpha subunit (Atp5a1)	2.4, 0.4
55 Golgi SNAP receptor complex member 1 (Gosr1)	0.4	121 Bifunctional aminoacyl-tRNA synthetase	0.4
56 Nuclear receptor subfamily 0, member 2 (Nr0b2)	0.2	122 ATP synthase subunit 8	2.2
57 Lysosomal-associated protein transmembrane 4A	0.5	123 Glutaryl-prolyl-tRNA synthetase (Eprs)	4.5
58 ATP-binding cassette, sub-family B	0.4	124 Fatty acid elongase 1 (rELO1)	0.2
59 ATP-binding cassette, sub-family C	0.2	125 RNA cyclase	0.2
Factors		Transferases	
60 Eukaryotic translation initiation factor 4A1	3.8	126 Carnitine O-octanoyltransferase (Crot)	0.3
61 Eukaryotic release factor 3	2.0	127 Glutathione S-transferase, alpha 1 (Gsta1)	0.1
62 Insulin-like growth factor I	0.5	128 Glutathione S-transferase, type 3 (Gstm3)	2.2, 0.3
63 Early growth response factor 1 (Egr1)	3.6	129 Microsomal glutathione S-transferase 1 (Mgst1)	0.4
64 Neuropeptide Y (Npy)	18.2	130 Sulfotransferase K2	0.3
65 NF-E2-related factor 2 (Nfe2l2)	0.4	131 Sialyltransferase 1 (Siat1)	2.6
66 Pre-B-cell colony-enhancing factor (Pbef)	3.5	132 UDP-glucuronosyltransferase member	50.3
67 Amphoterin	0.3	(Ugt2b5)	0.5
68 Angiogenin	0.2	133 Protein disulfide isomerase-related protein	



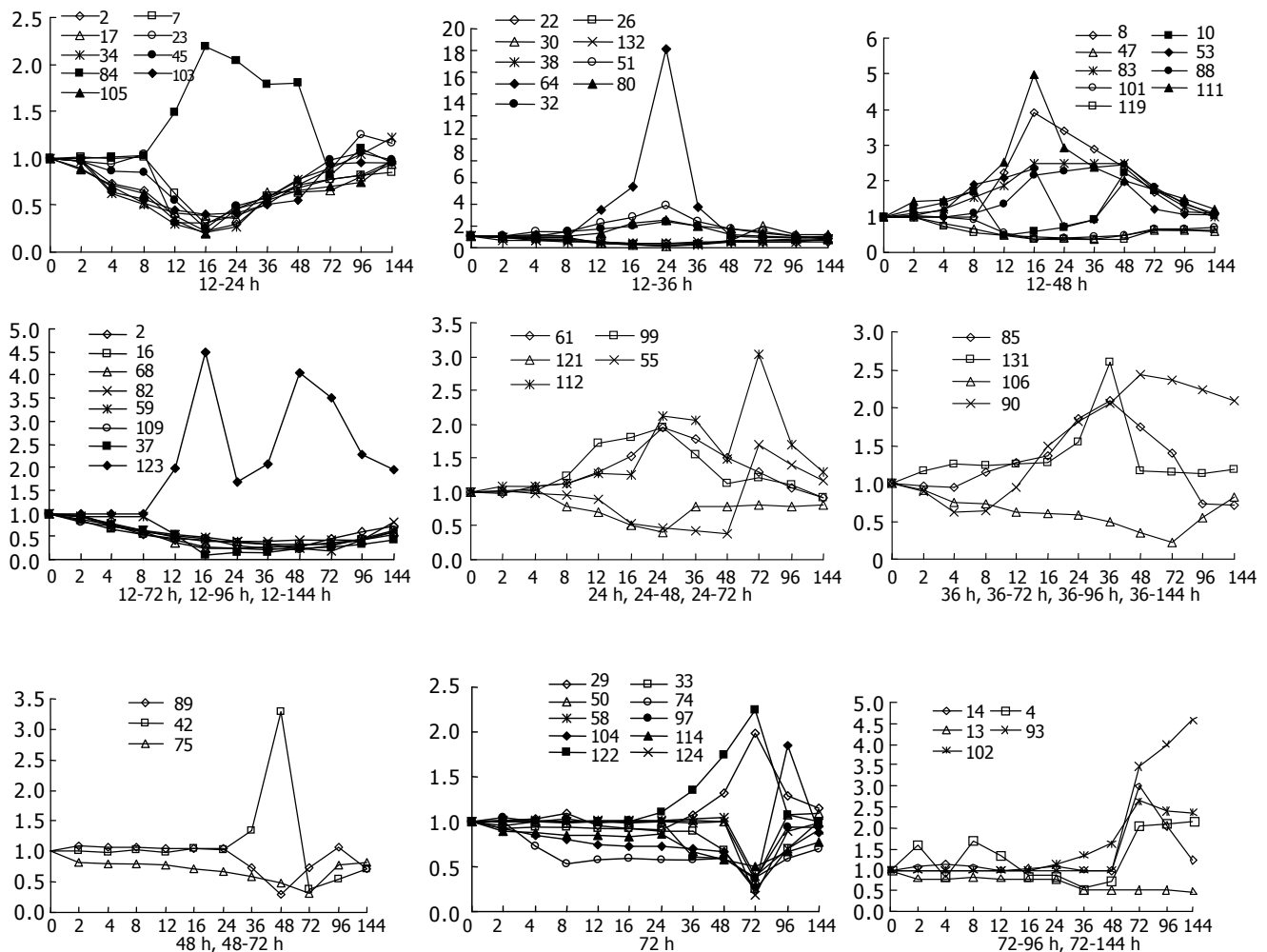


Figure 1 Gene expression differences at different time points after PH. The 133 elements were categorized into 21 temporal patterns following the induction of

suppressed time points.

that the most similar patterns of gene expression were located next to each other and placed in a major branch of the dendrogram. Twelve and sixteen hours 48 and 96 h, 72 and 144 h patterns were clustered as separate groups in major branches, indicating that these time points shared common expression profiles of genes (Figure 2B). Thirty-four genes

were induced to express in 2-4 h and reached a maximum in 8-24 h, but a smaller peak of gene expression appeared at 72 h after PH. To facilitate the visualization and interpretation of the gene expression program in these data, we used the method of GeneMaths to order genes of similarities in their expression patterns and displayed them

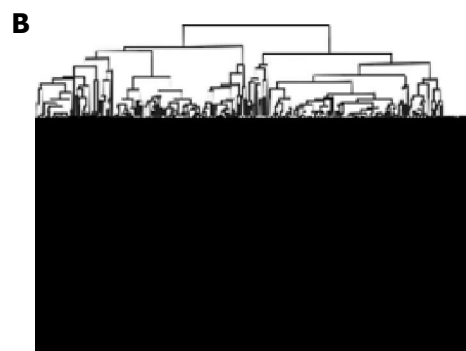
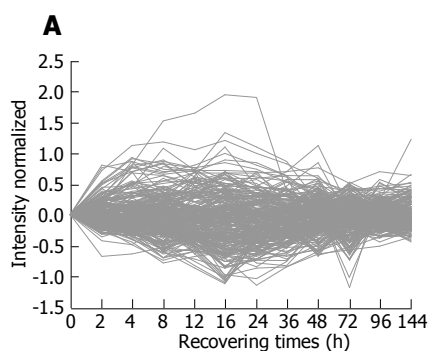


Figure 2 Hierarchical cluster analysis of 300 elements. **A:** Cluster of distribution trend. Three hundred elements differing by at least more than twofold intensity at one time point were identified; **B:** Cluster of hierarchical relativeity. A hierarchical

cluster of 11 time points showed that 12 and 16 h, 48 and 96 h as well as 72 and 144 h patterns were clustered together as separate groups in major branches.

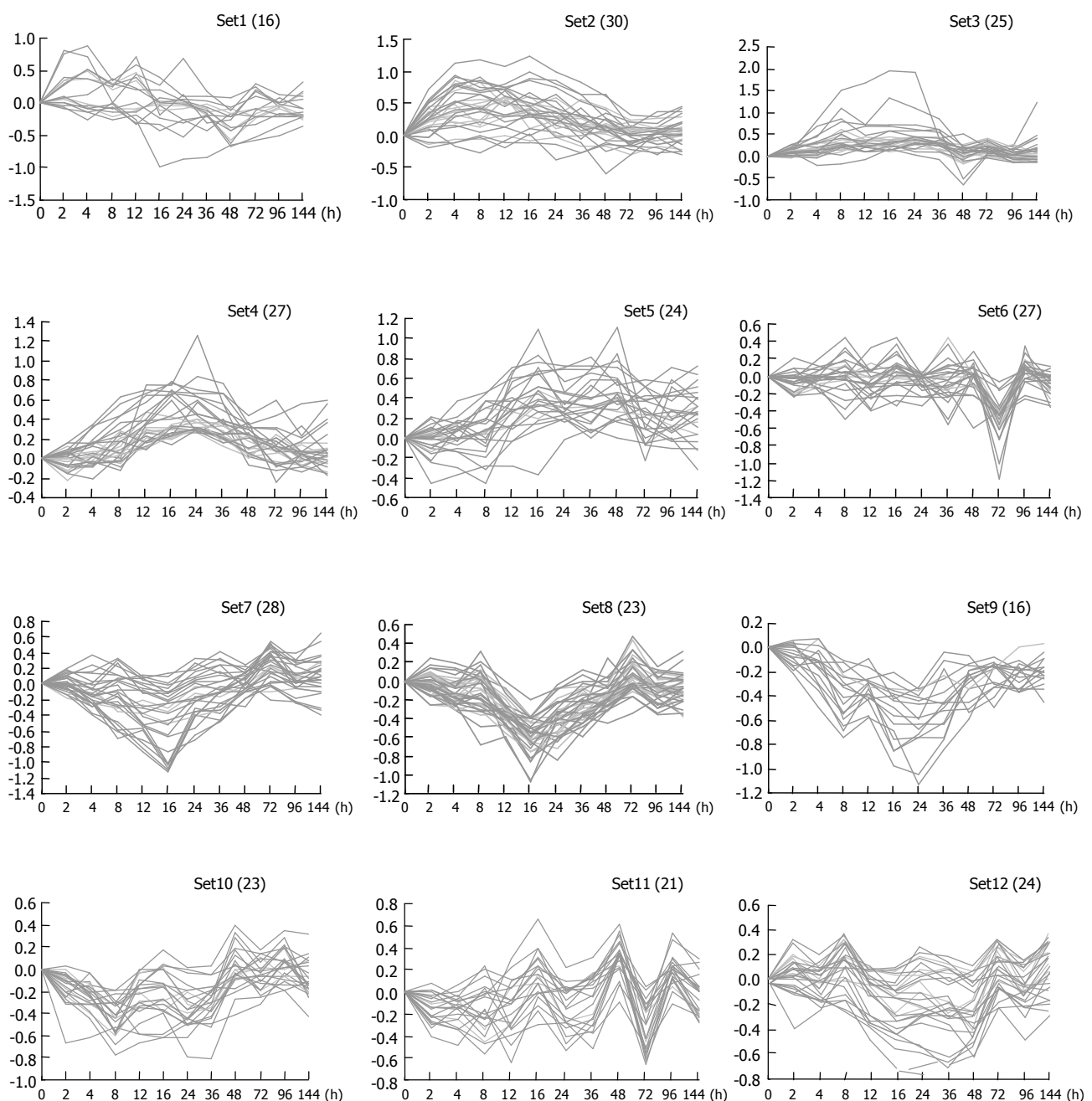


Figure 3 Cluster analysis of differentially expressed genes identified by cDNA microarray-based gene expression profiling. These genes were classified into

12 clusters by GeneMaths.

in a compact graphical format (Figure 3). Based on the expressed characteristics of genes in LR and following the review of Michalopoulos and Defrances, the selected elements were categorized into six distinct temporal patterns of expression: the genes of rapid induction which were expressed in the immediate early phase of 2-6 h after PH, the genes of early induction in the early phase of 8-16 h, the genes of middle induction in the intermediate phase of 16-24 h, the genes of early-late induction in the early-late phase of 24-36 h, the genes of late induction in the late phase of 36-72 h, and the genes of consistent repression in the terminal phase of 72-144 h.

It was found that expression of the 133 genes in the regenerating livers was quite different. Seventy-four of them decreased 2-10 folds, 49 of them were increased to 2-5 folds, 9 genes to 5-10 folds, 3 genes to over 10 folds, and the maximum to over 90 folds (Figure 4).

DISCUSSION

Genes of rapid induction expression

In the immediate early phase of LR (2-6 h after PH), liver damage occurred in inflammation response, hepatocytes in G_0 phase were activated, and then progressed to G_1 phase.

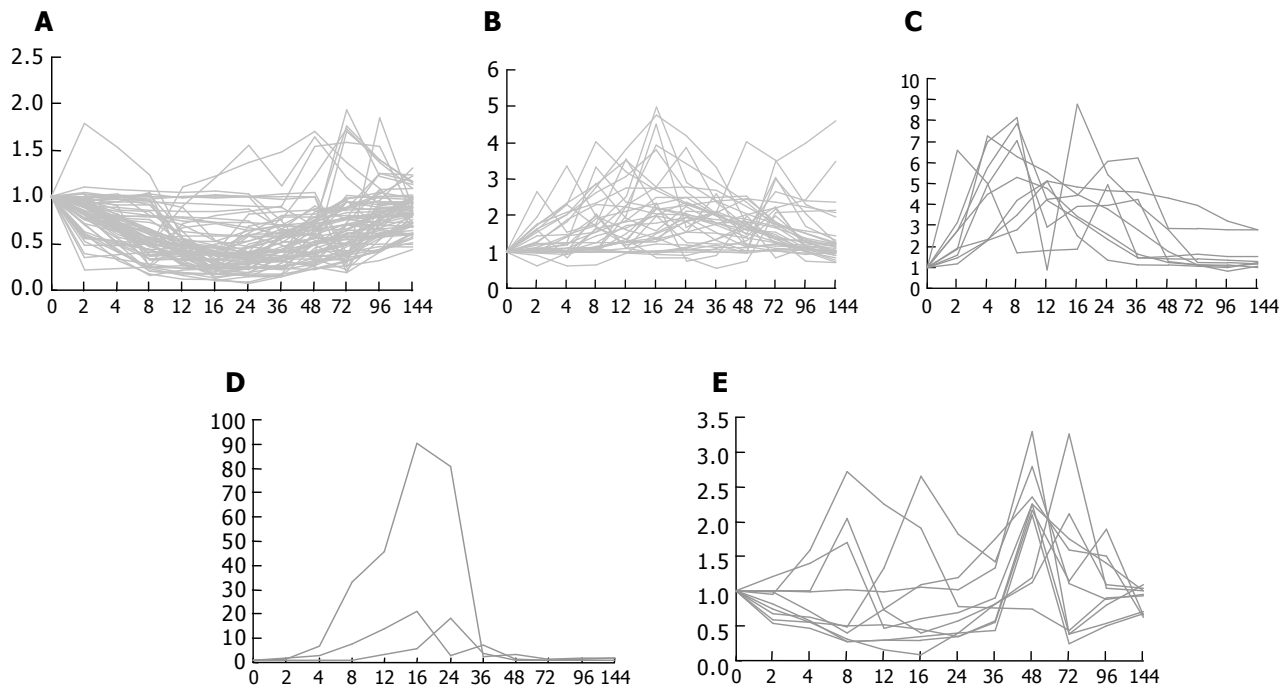


Figure 4 Expression of different genes in LR. **A:** Seventy-four downregulated genes; **B:** thirty-seven upregulated genes whose fold changes were 2-5; **C:** nine

upregulated genes whose fold changes were 5-10; **D:** three up-regulated genes whose fold changes were above 10; **E:** ten up- and downregulated genes.

Thirty-four genes, except the previous reported genes, were consistently and rapidly induced to express, 19 of them were upregulated and 15 downregulated. Among the genes, NF-E2-related factor 2 (Nfe2l2), isocitrate dehydrogenase, JE/MCP-1, and complement component 5 were advantageous to block oxidative injuries and to prevent the occurrence of inflammation of the residual liver after PH. Pre-B-cell colony-enhancing factor (PBEF), nuclear protein 1 (Nupr1), early growth response factor 1 (Egr1) were upexpressed, which probably play an important role in activating hepatocytes to start DNA synthesis^[18]. The expression of isozymes of aspartate aminotransferase and phosphodiesterase 1 (Enpp1) was induced, which supply purine and adenosine for DNA synthesis^[19]. The proteins of providing energy for LR such as adipose differentiation-related protein and phosphatidylserine-specific phospholipase A1 and proteins associated with inflammation response and cell apoptosis such as α -1 major acute phase protein, fibrinogen gamma polypeptide (Fgg), kininogen and class III Fc-gamma receptor were also included, which play important parts in preventing the occurrence of inflammation and the startup of LR in the immediate early phase.

Initiated genes in the early phase of LR

In the early phase of LR (8-16 h after PH), livers damaged stress response and hepatocytes were prepared to synthesize DNA. The expression of 31 genes was altered at 8 h after PH. Among them, 11 were upregulated and 20 downregulated, of which, 5 genes reached expression peak at 8 h after PH. Myelin-associated glycoprotein (MAG) was induced, which is important for nerve system regeneration in LR^[20]. The stress-inducible 70-ku protein (Hsp70) and protein disulfide isomerase-related protein were expressed, which promote

protein folding correctly and degradation of harmful proteins in LR. Serum amyloid P component and clusterin were repressed in 8-16 h after PH, which can decrease accumulation of false or toxic proteins in neurocytes, and are useful in protecting neonatal livers^[21]. Plasma retinol-binding protein, bile acid CoA ligase (BAL), insulin-like growth factor-I (IGF-I), ApoM, angiopoietin-like protein 3 (Angptl3) and lysosomal-associated protein transmembrane-4 beta (LAPTM4B) were increased as well in this phase. Plasma retinol-binding protein could transport retinol and vitamin A, whose increase in 8-16 h after PH showed that retinol and vitamin A were essential to hormone synthesis in LR^[22]. BAL could facilitate adsorption of amino acids by catalyzing conjugation of bile acids with amino acids^[23]. IGF-I was found to be involved in the liver and brain growth and development of embryos^[24]. Its downregulation in 8-24 h after PH indicated that cell cycle was in the phase of DNA synthesis. The reduction of ApoM in 8-24 h after PH was supposed to promote lipolysis and to provide energy for LR. Angptl3 is a hepatic secretory factor, which could activate lipolysis in adipocytes by response to the liver X receptor^[25]. LAPTM4B, a novel gene was upregulated in hepatic carcinoma, whose N-terminus is essential for the survival of cells^[26]. The downregulation of LAPTM4B may be related to refraining cell necrosis in LR.

Genes expression started in the intermediate phase of LR

In the intermediate phase of LR (16-24 h after PH), hepatocytes synthesized DNA. It was confirmed that 41 genes were expressed at 12 h after PH. The increase of mitochondrial glycerol 3-phosphate dehydrogenase (mGPDH) at 12 h was assumed to provide enough ATP for DNA synthesis. NAD(P)H steroid dehydrogenase (Nsdhl), hepatic

cytochrome P450 cholesterol 7 α -hydroxylase (CYP7) and ATP-binding cassette were induced in this time, which may play a role in the conversion of lanosterol into cholesterol^[27,28]. L28 is a component of 70S ribosome, whose upregulation in 12-24 h after PH was supposed to help 70S ribosome conformation and to accelerate protein synthesis. Activator protein 1 (AP1)-like elements and P53 were increased, which probably prevent injured liver from apoptosis and necrosis^[29]. The proteins associated with protein fold such as cathepsin C (Ctsc), dipeptidyl aminopeptidase I (Dpap1), Hsp40 and hsp70 (p73/p72) were also up expressed, which are essential to form the correct structure of proteins.

Genes expression started in the early-late phase of LR

In the early-late phase of LR (24-36 h after PH), hepatocytes must complete all the activations of later S phase, G₂ phase and M phase. It was checked that seven genes were started to express at 24 h after PH. Five of them were upregulated and two were downregulated, of which, the restrain of bifunctional aminoacyl-tRNA synthetase was up expressed at 24 h after PH, which may play a pivotal role in separating the subunits of the eukaryotic tRNA synthetase complex in LR. Furthermore, eukaryotic release factor 3 incorporated in a complete scheme for translation termination of proteins, whose induction may be advantageous to release essential proteins to exert functions. The mRNA level of sialyltransferase was increased at 36 h, suggesting that liver releases large amounts of sialyltransferase to mediate recovery of liver functions after PH.

Genes expression in the late phase of LR

In the late phase of LR (24-36 h after PH), hepatocytes went through the second cell cycle, and other cells began to divide. It was found that seven genes were induced to express at 36 h after PH. Of them, coagulation factor 2 inhibitor was upregulated, which facilitates blood circulation in the regenerating liver. The pregnancy-zone protein (Pzp) was induced, which accelerates hepatocyte division and mediate cell differentiation in LR. Complement component 1 was increased in 48-72 h after PH, which protects against the outer intruders in the injured liver.

Genes expression started in the terminal phase of LR

In the terminal phase of LR (72-144 h after PH), structure and function of the regenerating liver were recovered. It was found that 15 genes were induced in 48-144 h after PH. Of them, galactose-specific genes such as membrane-bound C-reactive protein were increased, demonstrating that galactose is necessary in terminal phase of LR. Cathepsin D was decreased, suggesting that cell migration was suppressed^[30]. CDK110 was upregulated at 72 h after PH, which mediates cell differentiation in LR. Flavanol cocoa was continuously induced in LR, which can prevent the regenerated liver from early alcohol-induced liver injury^[31].

In summary, we have screened 576 genes from subtracted cDNA libraries and made an in-house cDNA microarray. These genes were highly and specifically expressed in the liver. Using the chips, we performed a large-scale analysis of gene expression in LR and found that the expressions of 133 reported and 167 unreported genes were altered

more than twofolds at one or more time points. Cluster analysis showed gene expression patterns at 2 and 4 h, 12 and 16 h, 48 and 96 h as well as 72 and 144 h after PH had strong correlations respectively. The 133 reported genes could be categorized into six distinct temporal patterns of induction and were involved in 24 groups of proteins. Their actions in LR were discussed. However, to elucidate the mechanism of LR, further research is needed.

ACKNOWLEDGEMENTS

The authors thank BioStar for providing microarray.

REFERENCES

- 1 Michalopoulos GK, DeFrances MC. Liver regeneration. *Science* 1997; **276**: 60-66
- 2 Fausto N. Liver regeneration. *J Hepatol* 2000; **32**: 19-31
- 3 Zimmermann A. Liver regeneration: the emergence of new pathways. *Med Sci Monit* 2002; **8**: RA53-RA63
- 4 Taub R. Liver regeneration 4: transcriptional control of liver regeneration. *FASEB J* 1996; **10**: 413-427
- 5 Nagy P, Bisgaard HC, Schnur J, Thorgeirsson SS. Studies on hepatic gene expression in different liver regenerative models. *Biochem Biophys Res Commun* 2000; **272**: 591-595
- 6 Gressner AM. Cytokines and cellular crosstalk involved in the activation of fat-storing cells. *J Hepatol* 1995; **22**: 28-36
- 7 Cressman DE, Diamond RH, Taub R. Rapid activation of the Stat3 transcription complex in liver regeneration. *Hepatology* 1995; **21**: 1443-1449
- 8 FitzGerald MJ, Webber EM, Donovan JR, Fausto N. Rapid DNA binding by nuclear factor kappa B in hepatocytes at the start of liver regeneration. *Cell Growth Differ* 1995; **6**: 417-427
- 9 Hsu JC, Laz T, Mohn KL, Taub R. Identification of LRF-1, a leucine-zipper protein that is rapidly and highly induced in regenerating liver. *Proc Natl Acad Sci USA* 1991; **88**: 3511-3515
- 10 Enami Y, Kato H, Murakami M, Fujioka T, Aoki T, Niiya T, Murai N, Ohtsuka K, Kusano M. Anti-transforming growth factor-beta1 antibody transiently enhances DNA synthesis during liver regeneration after partial hepatectomy in rats. *J Hepatobiliary Pancreat Surg* 2001; **8**: 250-258
- 11 Sato Y, Igarashi Y, Hakamata Y, Murakami T, Kaneko T, Takahashi M, Seo N, Kobayashi E. Establishment of Alb-DsRed2 transgenic rat for liver regeneration research. *Biochem Biophys Res Commun* 2003; **311**: 478-481
- 12 Fukuhara Y, Hirasawa A, Li XK, Kawasaki M, Fujino M, Funesima N, Katsuma S, Shiojima S, Yamada M, Okuyama T, Suzuki S, Tsujimoto G. Gene expression profile in the regenerating rat liver after partial hepatectomy. *J Hepatol* 2003; **38**: 784-792
- 13 Xu CS, Lu AL, Xia M, Li XY, Li YH, Zhao XY. The effect of heat shock before rat partial hepatectomy on HSC70/HSP68, expression and phosphatase activities. *Shiyan Shengwu Xuebao* 2000; **33**: 1-11
- 14 Jensen SA. Liver gene regulation in rats following both 70 or 90% hepatectomy and endotoxin treatment. *J Gastroenterol Hepatol* 2001; **16**: 525-530
- 15 Su AI, Guidotti LG, Pezacki JP, Chisari FV, Schultz PG. Gene expression during the priming phase of liver regeneration after partial hepatectomy in mice. *Natl Acad Sci USA* 2002; **99**: 11181-11186
- 16 Higgins GM, Anderson RM. Experimental pathology of the liver I. Restoration of the liver of white rat following partial surgical removal. *Arch Pathol* 1931; **12**: 186-202
- 17 Yang GP, Ross DT, Kuang WW, Brown PO, Weigel RJ. Combining SSH and cDNA microarrays for rapid identification of differentially expressed genes. *Nucleic Acids Res* 1999; **27**: 1517-1523
- 18 Ognjanovic S, Bao S, Yamamoto SY, Garibay-Tupas J, Samal

- B, Bryant-Greenwood GD. Genomic organization of the gene coding for human pre-B-cell colony enhancing factor and expression in human fetal membranes. *J Mol Endocrinol* 2001; **26**: 107-117
- 19 **Kamimoto Y**, Horiuchi S, Tanase S, Morino Y. Plasma clearance of intravenously injected aspartate aminotransferase isozymes: evidence for preferential uptake by sinusoidal liver cells. *Hepatology* 1985; **5**: 367-375
- 20 **Ito H**, Ishida H, Collins BE, Fromholt SE, Schnaar RL, Kiso M. Systematic synthesis and MAG-binding activity of novel sulfated GM1b analogues as mimics of Chol-1 (alpha-series) gangliosides: highly active ligands for neural siglecs. *Carbohydr Res* 2003; **338**: 1621-1639
- 21 **Hind CR**, Collins PM, Pepys MB. Calcium-dependent aggregation of human serum amyloid P component. Inhibition by the cyclic 4,6-pyruvate acetal of galactose. *Biochim Biophys Acta* 1984; **802**: 148-150
- 22 **Soprano DR**, Pickett CB, Smith JE, Goodman DS. Biosynthesis of plasma retinol-binding protein in liver as a larger molecular weight precursor. *J Biol Chem* 1981; **256**: 8256-8258
- 23 **Falany CN**, Xie X, Wheeler JB, Wang J, Smith M, He D, Barnes S. Molecular cloning and expression of rat liver bile acid CoA ligase. *J Lipid Res* 2002; **43**: 2062-2071
- 24 **Santos A**, Yusta B, Fernandez-moreno MD, Blazquez E. Expression of insulin-like growth factor-I (IGF-I) receptor gene in rat brain and liver during development and in regenerating adult rat liver. *Mol Cell Endocrinol* 1994; **101**: 85-93
- 25 **Shimamura M**, Matsuda M, Kobayashi S, Ando Y, Ono M, Koishi R, Furukawa H, Makishima M, Shimomura I. Angiotensin-like protein 3, a hepatic secretory factor, activates lipolysis in adipocytes. *Biochem Biophys Res Commun* 2003; **301**: 604-609
- 26 **Shao GZ**, Zhou RL, Zhang QY, Zhang Y, Liu JJ, Rui JA, Wei X, Ye DX. Molecular cloning and characterization of LAPTM4B, a novel gene upregulated in hepatocellular carcinoma. *Oncogene* 2003; **22**: 5060-5069
- 27 **Ohashi M**, Mizushima N, Kabeya Y, Yoshimori T. Localization of mammalian NAD(P)H steroid dehydrogenase-like protein on lipid droplets. *J Biol Chem* 2003; **278**: 36819-36829
- 28 **Hoekstra M**, Kruijt JK, Van Eck M, Van Berkel TJ. Specific gene expression of ATP-binding cassette transporters and nuclear hormone receptors in rat liver parenchymal, endothelial, and Kupffer cells. *J Biol Chem* 2003; **278**: 25448-25453
- 29 **Miro F**, Lelong JC, Pancetti F, Roher N, Duthu A, Plana M, Bourdon JC, Bachs O, May E, Itarte E. Tumour suppressor protein p53 released by nuclease digestion increases at the onset of rat liver regeneration. *J Hepatol* 1999; **31**: 306-314
- 30 **Bond JS**, Aronson NN. Endocytosis and degradation of native, cathepsin D-degraded, and glutathione-inactivated aldolase by perfused rat liver. *Arch Biochem Biophys* 1983; **227**: 367-372
- 31 **McKim SE**, Konno A, Gabele E, Uesugi T, Froh M, Sies H, Thurman RG, Arteel GE. Cocoa extract protects against early alcohol-induced liver injury in the rat. *Arch Biochem Biophys* 2002; **406**: 40-46

• BASIC RESEARCH •

Effects of emodin and double blood supplies on liver regeneration of reduced size graft liver in rat model

Ke-Wei Meng, Yi Lv, Liang Yu, Sheng-Li Wu, Cheng-En Pan

Ke-Wei Meng, Yi Lv, Liang Yu, Sheng-Li Wu, Cheng-En Pan, Department of Hepatobiliary Surgery, First Hospital of Xi'an Jiaotong University, Xi'an 710061, Shaanxi Province, China
Correspondence to: Dr. Ke-Wei Meng, Department of Hepatobiliary Surgery, First Hospital of Xi'an Jiaotong University, Xi'an 710061, Shaanxi Province, China. doctormkw@126.com
Telephone: +86-29-85274736 Fax: +86-29-85274736
Received: 2004-07-28 Accepted: 2004-09-09

Abstract

AIM: To study the influences of emodin and reconstruction of double blood supplies on liver regeneration of reduced size graft liver in rat model.

METHODS: A total of 45 SD-SD rat reduced size liver transplantation models were randomly divided into three groups (A-C). The conventional reduced size liver transplantation was performed on rats in group A, while the hepatic artery blood supply was restored in groups B and C. The emodin (1.5 mg/kg/d) was given by intraperitoneal route in group C only. The recipients were killed on the seventh day after the operation. The proliferative cell nuclear antigen (PCNA), TBil and ALT of serum were detected, and the pathological changes of liver cell were observed.

RESULTS: The numbers of the rats that survived in A, B, and C group on the seventh day after operation were 14, 13, 13, respectively. The levels of TBil ($31.5 \pm 5.2 \mu\text{mol/L}$, $23.2 \pm 3.1 \mu\text{mol/L}$ vs $38.6 \pm 6.8 \mu\text{mol/L}$), and ALT ($5351 \pm 1050 \text{ nKat}$, $1300 \pm 900 \text{ nKat}$ vs $5779 \pm 1202 \text{ nKat}$) in serum in groups B and C were lower than those in group A ($P < 0.05$), while the expression of PCNA in groups B or C was higher than that in group A ($22.0 \pm 3.5\%$, $28.2 \pm 4.2\%$ vs $18.6 \pm 3.2\%$, $P < 0.05$). The deeper staining nuclei, double nuclei, multi-nuclei and much glycogen were observed in liver cells of groups B and C, especially in group C, while fewer were found in liver cells of group A.

CONCLUSION: The reconstruction of arterial blood supply is very important for rat liver regeneration after reduced size liver transplantation. Emodin has the effect of promoting liver regeneration and improving liver function in rats after reduced size transplantation. The possible mechanism is improving proliferation of liver cell and protecting liver cells from injury.

Meng KW, Lv Y, Yu L, Wu SL, Pan CE. Effects of emodin and double blood supplies on liver regeneration of reduced size graft liver in rat model. *World J Gastroenterol* 2005; 11 (19): 2941-2944

<http://www.wjgnet.com/1007-9327/11/2941.asp>

INTRODUCTION

It is well-known recently that clinic liver transplantation has been the most effective method to treat liver disease in terminal stage. However, due to the deficiency of the donor, more surgical methods were applied for liver transplantation, for example, vivid liver transplantation and resized liver transplantation. In vivid liver transplantation and resized liver transplantation, it is very important that the donor and recipient match each other, and liver regeneration of the new liver is also a focus of study. Liver regeneration may be affected co-operatively not only by humoral factors such as hormones, growth factors and growth inhibitory factors, but also by the immune system^[1-7].

Emodin is extracted from Chinese herb and more properties of it are being found^[8,9]. The reported biological effects of emodin include antitumor, antibacterial and anti-inflammatory activities^[10-13]. Experiments have demonstrated that the hepatic lesion induced by CCl_4 could be decreased by emodin by ameliorating cellular regeneration activities and protecting liver function^[14,15].

In the present study we established the rat resized liver transplantation model with restored arterial blood supply to evaluate the effects of emodin and double blood supplies on liver regeneration.

MATERIALS AND METHODS

Animals and reagents

Emodin was presented by Huaian Reilei preparation Co., LTD (Jiangshu, China), dissolved and sterilized in dimethyl sulfoxide (DMSO) first and then diluted to the required working concentrations in RPMI 1640 (Gibco, USA) containing 100 mL/L calf serum (Sijiqing Co., Hangzhou, China). Male SD rats, 9-10 wk old, weighing $220 \pm 280 \text{ g}$, were purchased from the Animal Center of Xi'an Jiaotong University. Proliferative cell nuclear antigen (PCNA) ABC ultra-sensitive immunostaining kit was purchased from Boshide Biotechnology Developing Co. (Wuhan, China).

Effect of emodin and double blood supplies on liver regeneration in rat model

All the 45 SD rats were fasted for 24 h before operation, but had free access to tap water. Then they were divided

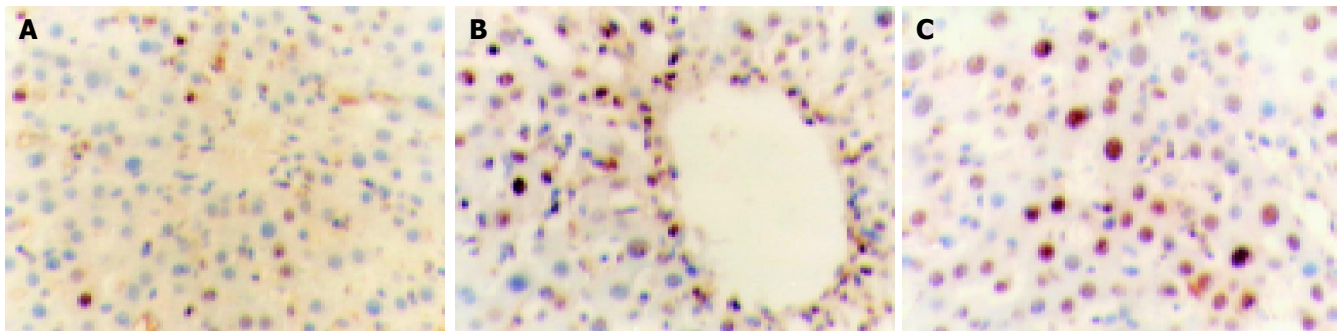


Figure 1 PCNA in transplanted rat liver SABC, $\times 400$. Group A: $18.6 \pm 3.2\%$ vs

group B: $22 \pm 3.5\%$ vs group C: $28.2 \pm 4.2\%$.

into three groups randomly: groups A-C. In group A, reduced size liver transplantation was performed on the rats by using cuff method^[8], with the left lobe of liver resected which accounts for the 30% of total liver weight; in groups B and C, reduced size liver transplantation was performed on the rats and hepatic arteries were anastomosed by sleeve method^[16], while only group C was given emodin (1.5 mg/kg/d) by intraperitoneal route for 7 d. All the recipient rats were killed on the 7th d after transplantation and a 3-5-mL blood sample was obtained from the right ventricles. These blood samples were centrifuged immediately at 3 000 r/min at room temperature for 5 min and the serum samples were assayed by Olympus AV800 auto-analyses instrument for the detection of serum total bilirubin (TBil) and alanine aminotransferase (ALT).

PCNA expression in rat's allograft liver tissue

The allograft liver tissues taken from group A, B and C were 100 mL/L formalin-fixed, paraffin-embedded and cut into 4 μ m thick sections for staining. PBS of 0.01 mol/L was used to substitute for primary antibody for negative control, while a breast cancerous tissue expressing PCNA was used for positive control. The working concentration of antibody was 1:100. The staining procedures used were as described in ABC immunostaining kit. The sections were examined twice on different days by the same pathologist and the distribution of positively stained cells was evaluated semi-quantitatively by calculating the percentage of positive cells in 100 cells in five nonoverlapping microscopic high-power fields.

Histopathologic and ultra structural examination

The allograft liver tissues taken from group A-C were 100 mL/L formalin-fixed, paraffin-embedded and cut into 4 μ m thick sections for HE staining, while some samples were cut into small pieces of 1 mm³ on ice and fixed in glutaral for electron microscopic observation.

Statistical analysis

All values were expressed in the mean \pm SD. SPSS statistics software was used to evaluate the statistical significance of the differences among the three groups with Student's *t* test. When $P < 0.05$, it is considered significant.

RESULTS

Survivals and liver function

The numbers of survivals on the 7th d after transplantation

in groups A-C were 14, 13, and 13, respectively. The levels of TBil and ALT in serum in groups B and C were lower than those in group A ($P < 0.05$), and the levels of TBil and ALT in serum in group C was still lower than those in group B ($P < 0.05$, Table 1).

Table 1 Levels of ALT and TBIL in the rat's serum on the 7th d after transplantation

Liver transplantation	<i>n</i>	ALT (nKat/L)	TBil (μ mol/L)
A: reduced size	14	5 779 \pm 1 202	38.6 \pm 6.8
B: reduced size +double blood supplies	13	5 351 \pm 1 050 ^a	31.5 \pm 5.2 ^a
C: reduced size +double blood supplies +emodin	13	1 300 \pm 900 ^{a,c}	23.2 \pm 3.1 ^{a,c}

^a $P < 0.05$ vs group A; ^c $P < 0.05$ vs group B.

PCNA expression in rat's allograft liver tissue

The expression of PACN in B or C groups was higher than that in A group ($P < 0.05$), and the expression of PACN in C group was higher than that in B groups ($P < 0.05$). The positive cells percentage in the groups A-C was $18.6 \pm 3.2\%$, $22 \pm 3.5\%$, and $28.2 \pm 4.2\%$, respectively (Figure 1).

Histopathologic and ultra structural examination

The deeper staining nuclei, double nuclei, multi-nuclei and much glycogen were observed in liver cells of groups B and C, especially in group C, while fewer were found in liver cells of group A (Figures 2 and 3).

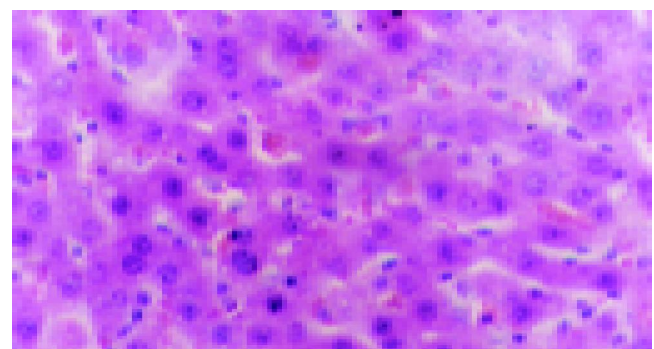


Figure 2 HE staining: the deeper staining nuclei and double nuclei in group C, HE $\times 400$.

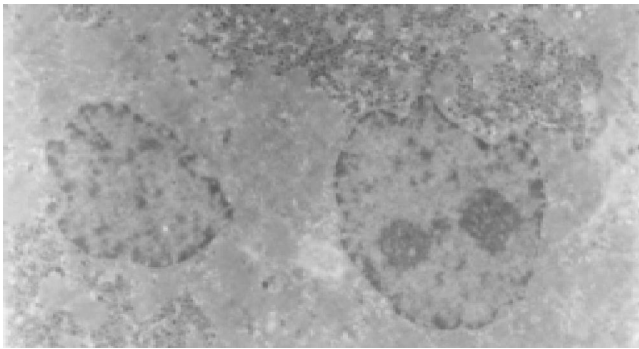


Figure 3 Double nuclei and much glycogen of hepatocyte in group C, TCM×1 500.

DISCUSSION

It is well known that the activity of liver regeneration is very strong. The synthesis of DNA of the liver cell could be found in 12-16 h after 2/3 liver was resected, and this regeneration process could be completed in 6-8 d^[17]. Liver regeneration is a special and complicated process, which could be affected by many factors, for example, insulin, estrogen, and thyroxine. There are many problems in the liver regeneration after transplantation remained to be explored, and rat liver transplantation model, especially reduced size liver transplantation, is an ideal model for the study of these problems. Recent studies have shown that the liver of rat demonstrated strong activity of regeneration after liver transplantation or partial liver resection. Compared with liver after partial liver resection, the proliferation peak of liver cells after liver transplantation or partial liver transplantation occurred late, but the proliferation cycle is longer. The possible reasons are the injuries due to operative procedure or ischemia-reperfusion, or the modulation of cytokines and hormones produced by recipient's immune system^[4].

At present, the most common orthotopic rat liver transplantation model was performed by the cuff technique without hepatic artery reconstruction. However, the effects of hepatic artery on the regeneration of liver cells are obvious. Therefore, the liver transplantation model with double blood supplies mostly accords with the physiological demand of experimental animals. In our study the rat reduced size liver transplantation model was applied with double blood supplies to study the liver cell regeneration. The advantages of the model are as follows: (1) There are double blood supplies in the grafted liver, whose micro-environment is more similar to that of human liver graft than the traditional liver transplantation model; (2) Because the transplantation is a homogenic transplantation, there is no more involvement of immunity factors, so the factors of research were easy to be controlled.

Proliferating cell nuclear antigen (PCNA) is a popular marker to assess the activities of liver cell regeneration. The molecular mass of PCNA is 36 ku and PCNA consisted of 261 amino acids. PCNA exists and is synthesized in the nucleus, and it is required for DNA replication and repair. In quiescent cells the level of PCNA is very low, while it is higher in proliferated and transformed cells^[18-29]. In this

study we found that PCNA exists in the liver of all three groups. This means that the cell proliferation after reduced size liver transplantation is active. Compared with group A, the expressions of PCNA in groups B and C are much higher ($P<0.05$), and compared with group B, the expression of PCNA in group C is still much higher too ($P<0.05$). The histopathologic and electron microscopic examination showed that the deeper staining nuclei, double nuclei, multi-nuclei and much glycogen were observed in liver cells of groups B and C, especially in group C, while fewer was found in liver cells of group A. Besides, the levels of ALT and TBil in the rat's serum on the 7th d after transplantation in groups B and C were lower than that in group A ($P<0.05$), and the levels of TBil and ALT in serum in group C was still lower than those in group B ($P<0.05$). All these results showed that restoring liver artery is very important in liver cell regeneration.

Emodin, whose molecular mass is 270.23 ku, is extracted from Chinese herb and more properties of it are being found^[8,9]. The reported biological effects of emodin include antitumor, antibacterial and anti-inflammatory activities^[10-13]. Experiments have demonstrated that the hepatic lesion induced by CCl₄ could be decreased by emodin by ameliorating cellular regeneration activities and protecting liver function^[14,15]. In our experiment, the lower levels of TBil and ALT in serum in group C, and more cell regeneration in the group C than those in groups A and B were found ($P<0.05$). These results are consistent with others which support that emodin has the effects of promoting cellular regeneration and restoring liver function.

On the whole, the reconstruction of arterial blood supply is very important to rat liver regeneration after reduced size transplantation. Emodin has the effect of promoting liver regeneration and improving liver function in rat after reduced size transplantation. However, the molecular mechanism of emodin still remains to be studied.

REFERENCES

1. Liu L, Sakaguchi T, Cui X, Shirai Y, Nishimaki T, Hatakeyama K. Liver regeneration enhanced by orally administered ursodesoxycholic acid is mediated by immunosuppression in partially hepatectomized rats. *Am J Chin Med* 2002; **30**: 119-126
2. Polimeno L, Margiotta M, Marangi L, Lisowsky T, Azzarone A, Ierardi E, Frassanito MA, Francavilla R, Francavilla A. Molecular mechanisms of augmenter of liver regeneration as immunoregulator: its effect on interferon-gamma expression in rat liver. *Dig Liver Dis* 2000; **32**: 217-225
3. Saitou Y, Shiraki K, Yamaguchi Y, Nakano T, Mizuno S, Uemoto S. Serum vascular endothelial growth factor-receptor 1 during liver regeneration. *J Hepatol* 2004; **41**: 170-171
4. Markiewski MM, Mastellos D, Tudoran R, DeAngelis RA, Strey CW, Franchini S, Wetsel RA, Erdei A, Lambris JD. C3a and C3b activation products of the third component of complement (C3) are critical for normal liver recovery after toxic injury. *J Immunol* 2004; **173**: 747-754
5. Hirao A, Yamasaki M, Chujo H, Koyanagi N, Kanouchi H, Yasuda S, Matsuo A, Nishida E, Rikimaru T, Tsujita E, Shimada M, Maehara Y, Tachibana H, Yamada K. Effect of dietary conjugated linoleic acid on liver regeneration after a partial hepatectomy in rats. *J Nutr Sci Vitaminol (Tokyo)* 2004; **50**: 9-12
6. Di Stefano G, Derenzini M, Kratz F, Lanza M, Fiume L. Liver-targeted doxorubicin: effects on rat regenerating

- hepatocytes. *Liver Int* 2004; **24**: 246-252
- 7 **Delman KA**, Zager JS, Bhargava A, Petrowsky H, Malhotra S, Ebricht ML, Bennett JJ, Gusani NJ, Kooby DA, Roberts GD, Fong Y. Effect of murine liver cell proliferation on herpes viral behavior: implications for oncolytic viral therapy. *Hepatology* 2004; **39**: 1525-1532
- 8 **Alves DS**, Perez-Fons L, Estepa A, Micol V. Membrane-related effects underlying the biological activity of the anthraquinones emodin and barbaloin. *Biochem Pharmacol* 2004; **68**: 549-561
- 9 **Micsenyi A**, Tan X, Sneddon T, Luo JH, Michalopoulos GK, Monga SP. Beta-catenin is temporally regulated during normal liver development. *Gastroenterology* 2004; **126**: 1134-1146
- 10 **Srinivas G**, Anto RJ, Srinivas P, Vidhyalakshmi S, Senan VP, Karunakaran D. Emodin induces apoptosis of human cervical cancer cells through poly (ADP-ribose) polymerase cleavage and activation of caspase-9. *Eur J Pharmacol* 2003; **473**: 117-125
- 11 **Kuo YC**, Meng HC, Tsai WJ. Regulation of cell proliferation, inflammatory cytokine production and calcium mobilization in primary human T lymphocytes by emodin from *Polygonum hypoleucum* Ohwi. *Inflamm Res* 2001; **50**: 73-82
- 12 **Fabriciova G**, Sanchez-Cortes S, Garcia-Ramos JV, Miskovsky P. Surface-enhanced Raman spectroscopy study of the interaction of the antitumoral drug emodin with human serum albumin. *Biopolymers* 2004; **74**: 125-130
- 13 **Liu Y**, Shan HL, Sun HL, He SZ, Yang BF. Effects of emodin on the intracellular calcium concentration ($[Ca^{2+}]_i$) and L-type calcium current of the single ventricular myocytes from guinea pig. *Yaoxue Xuebao* 2004; **39**: 5-8
- 14 **Chiu PY**, Mak DH, Poon MK, Ko KM. *In vivo* antioxidant action of a lignan-enriched extract of Schisandra fruit and an anthraquinone-containing extract of *Polygonum* root in comparison with schisandrin B and emodin. *Planta Med* 2002; **68**: 951-956
- 15 **Zhan Y**, Li D, Wei H. Effect of emodin on development of hepatic fibrosis in rats. *Zhongguo Zhongxiyi Jiehe Zazhi* 2000; **20**: 276-278
- 16 **Bahr W**, Rosbänder R, Gutwald R, Scholz C. Vascular anastomosis using a biodegradable device with a heat-shrinking sleeve: a preliminary report. *J Oral Maxillofac Surg* 1998; **56**: 1404-1409
- 17 **Fausto N**. Liver regeneration. *J Hepatol* 2000; **32**: 19-31
- 18 **Fernandez-Martinez A**, Callejas NA, Casado M, Bosca L, Martin-Sanz P. Thioacetamide-induced liver regeneration involves the expression of cyclooxygenase 2 and nitric oxide synthase 2 in hepatocytes. *J Hepatol* 2004; **40**: 963-970
- 19 **Tsutsumi R**, Kamohara Y, Eguchi S, Azuma T, Fujioka H, Okudaira S, Yanaga K, Kanematsu T. Selective suppression of initial cytokine response facilitates liver regeneration after extensive hepatectomy in rats. *Hepatogastroenterology* 2004; **51**: 701-704
- 20 **Gupta S**, Adhami VM, Subbarayan M, MacLennan GT, Lewin JS, Hafeli UO, Fu P, Mukhtar H. Suppression of prostate carcinogenesis by dietary supplementation of celecoxib in transgenic adenocarcinoma of the mouse prostate model. *Cancer Res* 2004; **64**: 3334-3343
- 21 **Roncales M**, Achon M, Manzarbeitia F, Maestro de las Casas C, Ramirez C, Varela-Moreiras G, Perez-Miguelsanz J. Folic acid supplementation for 4 weeks affects liver morphology in aged rats. *J Nutr* 2004; **134**: 1130-1133
- 22 **Nanashima A**, Yano H, Yamaguchi H, Tanaka K, Shibasaki S, Sumida Y, Sawai T, Shindou H, Nakagoe T. Immunohistochemical analysis of tumor biological factors in hepatocellular carcinoma: relationship to clinicopathological factors and prognosis after hepatic resection. *J Gastroenterol* 2004; **39**: 148-154
- 23 **Zhang Y**, Fan XG, Tian XF, Huang Y. Influence of *H pylori* on cyclinD1 and PCNA mRNA expression in HepG2 cell line. *Shijie Huaren Xiaohua Zazhi* 2004; **12**: 93-96
- 24 **Jia KD**, Shi SX, Ruan YB. Relationship between expression of survivin gene and proliferation of hepatocytes in liver cirrhosis and hepatocellular carcinoma. *Shijie Huaren Xiaohua Zazhi* 2004; **12**: 550-554
- 25 **Niu ZS**, Zhang ZC. Correlation of AgNORs, DNA contents and PCNA expression with liver cirrhosis, hyperplastic nodules and hepatocellular carcinoma. *Shijie Huaren Xiaohua Zazhi* 2004; **12**: 555-558
- 26 **Wu YQ**, Wang MW, Wu BY, You WD, Zhu QF. Expression of apoptosis-related proteins and proliferating cell nuclear antigen during stomach canceration. *Shijie Huaren Xiaohua Zazhi* 2004; **12**: 770-773
- 27 **Feng Y**, Zhao L, Zhang AH, Liu KD, Liu LC, Wang YH, Yin JQ, Yang BH. Expression of PCNA and nm23-H1/NDPK in Hepatocellular Carcinoma following transcatheter arterial chemoembolization therapy. *Shijie Huaren Xiaohua Zazhi* 2003; **11**: 912-915
- 28 **Yuji J**, Masaki T, Yoshida S, Kita Y, Feng H, Uchida N, Yoshiji H, Kitanaka A, Watanabe S, Kurokohchi K, Kuriyama S. Identification of p46 Shc expressed in the nuclei of hepatocytes with high proliferating activity: Study of regenerating rat liver. *Int J Mol Med* 2004; **13**: 721-728
- 29 **Micsenyi A**, Tan X, Sneddon T, Luo JH, Michalopoulos GK, Monga SP. Beta-catenin is temporally regulated during normal liver development. *Gastroenterology* 2004; **126**: 1134-1146

• CLINICAL RESEARCH •

Diagnosis of biliary strictures after liver transplantation: Which is the best tool?

Thomas Zoepf, Evelyn J. Maldonado-Lopez, Philip Hilgard, Alexander Dechêne, Massimo Malago, Christoph E. Broelsch, Joerg Schlaak, Guido Gerken

Thomas Zoepf, Evelyn J. Maldonado-Lopez, Philip Hilgard, Alexander Dechêne, Massimo Malago, Christoph E. Broelsch, Joerg Schlaak, Guido Gerken, Department of Gastroenterology and Hepatology, University Hospital of Essen

Thomas Zoepf, Evelyn J. Maldonado-Lopez, Philip Hilgard, Alexander Dechêne, Joerg Schlaak, Guido Gerken, Department of General Surgery and Transplantation, University Hospital of Essen: Massimo Malago, Christoph E. Broelsch

Correspondence to: Thomas Zoepf, MD, Department of Gastroenterology and Hepatology, University Hospital Essen, Hufelandstr. 55, D-45147 Essen, Germany. thomas.zoepf@uni-essen.de
Telephone: +49-201-723 3610 Fax: +49-201-723 5745

Received: 2004-09-22 Accepted: 2004-09-30

might further improve the diagnostic impact of this method.

© 2005 The WJG Press and Elsevier Inc. All rights reserved.

Key words: ERCP; Liver transplantation; Biliary strictures; Endoscopy; Therapy; Ultrasound; MRCP; Diagnosis

Zoepf T, Maldonado-Lopez EJ, Hilgard P, Dechêne A, Malago M, Broelsch CE, Schlaak J, Gerken G. Diagnosis of biliary strictures after liver transplantation: Which is the best tool? *World J Gastroenterol* 2005; 11(19): 2945-2948
<http://www.wjgnet.com/1007-9327/11/2945.asp>

Abstract

AIM: To evaluate the diagnostic value of different indirect methods like biochemical parameters, ultrasound (US) analysis, CT-scan and MRI/MRCP in comparison with endoscopic retrograde cholangiography (ERC), for diagnosis of biliary complications after liver transplantation.

METHODS: In 75 patients after liver transplantation, who received ERC due to suspected biliary complications, the result of the cholangiography was compared to the results of indirect imaging methods performed prior to ERC. The cholangiography showed no biliary stenosis (NoST) in 25 patients, AST in 27 and ITBL in 23 patients.

RESULTS: Biliary congestion as a result of AST was detected with a sensitivity of 68.4% in US analysis (specificity 91%), of 71% in MRI (specificity 25%) and of 40% in CT (specificity 57.1%). In ITBL, biliary congestion was detected with a sensitivity of 58.8% in the US, 88.9% in MRI and of 83.3% in CT. However, as anastomotic or ischemic stenoses were the underlying cause of biliary congestion, the sensitivity of detection was very low. In MRI detected the dominant stenosis at a correct localization in 22% and CT in 10%, while US failed completely. The biochemical parameters, showed no significant difference in bilirubin (median 5.7; 4.1; 2.5 mg/dL), alkaline phosphatase (median 360; 339; 527 U/L) or gamma glutamyl transferase (median 277; 220; 239 U/L) levels between NoST, AST and ITBL.

CONCLUSION: Our data confirm that indirect imaging methods to date cannot replace direct cholangiography for diagnosis of post transplant biliary stenoses. However MRI may have the potential to complement or precede imaging by cholangiography. Optimized MRCP-processing

INTRODUCTION

Biliary tract complications after liver transplantation occur with a reported incidence of up to 34% and show a mortality of 5%^[1-5]. The leading etiological factors are ischemic type biliary lesions (ITBL) and anastomotic strictures (AST) of duct-to-duct anastomosis, which may lead to malfunction and loss of the graft^[6-10]. In addition leaks or stones in the biliary tract have to be considered^[1,5,6]. There are several reports of successful endoscopic treatment of post transplant biliary stenoses (PTBS)^[5-10]. However, the exact diagnosis and localization of PTBS prior to ERC is difficult. This may be due to several reasons: (1) Dilatation of the biliary system in transplanted livers may develop slower, (2) the biliary system may be filled with epithelial cast, which cannot be visualized by indirect imaging, (3) elevated liver enzymes and cholestasis parameters may be due to graft rejection or recurrence of the underlying pretransplant liver disease.

Therefore, the aim of this study was to evaluate the diagnostic value of different indirect methods such as biochemical parameters, ultrasound (US) analysis, CT-scan and MRI/MRCP in comparison with direct endoscopic retrograde cholangiography (ERC), which is still the gold standard for diagnosis of biliary complications after liver transplantation.

MATERIALS AND METHODS

Seventy-five patients (39 male, 36 female, median age 51 years [range 20-66 years]) received ERC due to suspected biliary complications after liver transplantation. In all patients liver biopsy was obtained prior to ERC for exclusion of graft rejection.

Biochemical cholestasis parameters like serum bilirubin level, alkaline phosphatase and gamma glutamyl transferase

were determined at the time of indication for ERC. For analysis, cholestasis parameters, US reports, magnetic resonance imaging and computed tomography scan reports as well as ERC reports were put into a computer database (Access 2000, Microsoft Inc.).

According to the results of direct biliary imaging by ERC, patients were divided into three groups: Group A with no apparent stenosis of the biliary tract, classified as no stenosis (NoST); group B with a short stenosis in the anastomotic region, classified as AST; and group C with one or multiple non-AST of the biliary tract, classified as ITBL. ITBL was subdivided into three groups as proposed by Hintze^[5] with regard to the localization of stenoses: Type I extrahepatic lesion, Type II intrahepatic lesion, Type III extra- and intrahepatic lesions.

Statistical analysis

Statistical analysis was performed with SPSS for Windows® release 11.0.1 (SPSS Inc.). For statistical analysis of qualitative characteristics, we used χ^2 or Fisher's exact test, when appropriate. To evaluate the effect of continuous variables we used the Mann-Whitney *U* test.

RESULTS

ERC showed no biliary stenosis (NoST) in 25 patients, AST in 27 and ITBL in 23 patients. The three groups showed no significant differences in age and gender with the exception of a predominance of women. There was a significant difference with regard to the underlying liver disease, as acute liver failure (ALF) was found significantly more often in ITBL patients (Table 1 and Figure 1).

US were available in 88% of patients with NoST and in 74% of patients with AST or ITBL, respectively. MRI of the liver was performed in 16% of NoST, in 26% of AST and in 48% of ITBL patients. A CT-scan was available in 28% of NoST, in 19% of AST and in 26% of ITBL patients (Figure 2).

Biliary congestion as a result of AST was detected with a sensitivity of 68.4% in US analysis (specificity 91%), 71.4% in MRI (specificity 25%) and 40% in CT (specificity

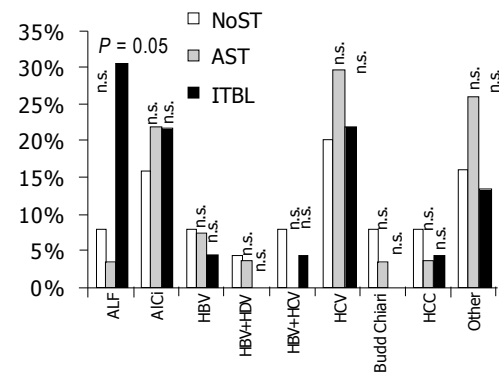


Figure 1 Differences in underlying liver disease prior to transplantation. NoST = no apparent biliary stenosis in ERC. AST = anastomotic stricture in ERC. ITBL = ischemic type biliary lesions in ERC. ALF = acute liver failure; ALCi = alcoholic liver cirrhosis; HBV = chronic hepatitis B virus infection; HDV = chronic hepatitis D virus superinfection; HCV = chronic hepatitis C virus infection; HCC = hepatocellular carcinoma; n.s. = not significant.

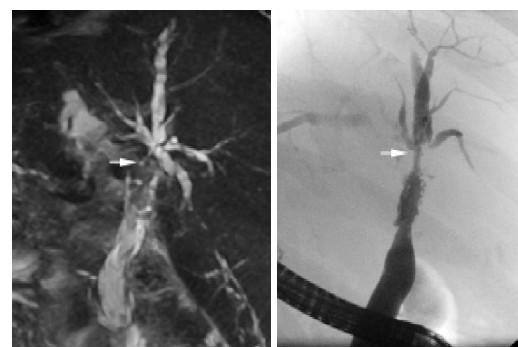


Figure 2 Comparison of ERC and MRC in posttransplant biliary stenosis. ITBL type III with hilar stenosis (arrow) and multiple peripheral duct stenoses. Left: MRC, right: ERC. The dominant hilar stenosis (arrow) is seen with both methods. The peripheral stenoses are better seen in ERC.

Table 1 Patient characteristics

	NoST	AST	ITBL
<i>n</i>	25	27	23
m/f	16/9	11/16 (<i>P</i> = 0.08 ¹)	13/10 (<i>P</i> = 0.40 ¹)
Median age (yr)	50 yr [33-63]	54 yr [33-65] (<i>P</i> = 0.09)	49 yr [27-63] (<i>P</i> = 0.94)
Type of LTx	OLTx = 17/25 LDLTx = 5/25 Split = 3/25	OLTx = 17/27 (<i>P</i> = 0.46 ¹) LDLTx = 7/27 (<i>P</i> = 0.43 ¹) Split = 3/27 (<i>P</i> = 0.70 ¹)	OLTx = 20/23 (<i>P</i> = 0.11 ¹) LDLTx = 3/23 (<i>P</i> = 0.40 ¹) Split = 0/23 (<i>P</i> = 0.13 ¹)

NoST = no apparent biliary stenosis in ERC. AST = anastomotic stricture in ERC. ITBL = ischemic type biliary lesions in ERC. OLTx = orthotopic liver transplantation; LDLTx = Living donor liver transplantation. ¹Fisher's exact test.

57.1%). In ITBL, biliary congestion was detected with a sensitivity of 58.8% in US, 88.9% in MRI and of 83.3% in CT. However, as anastomotic or ischemic stenoses were the underlying cause of biliary congestion, the sensitivity and specificity as well as the correct localization of stenoses was very low. In AST MRI detected the dominant stenosis in 38.9% and CT in 10%, while US failed completely. In ITBL, MRI localized stenoses correctly in 22%, whereas US or CT failed (Table 3).

The presence of biliary stones were regularly detected in patients without stenosis with all indirect diagnostic methods but interestingly, they could almost never be visualized in patients with underlying anastomotic or ischemic type stenoses (Table 3).

Regarding the biochemical parameters, there was no significant difference in bilirubin (median 5.7; 4.1; 2.5 mg/dL), alkaline phosphatase (median 360; 339; 527 U/L) or gamma glutamyl transferase (median 277; 220; 239 U/L) levels between NoST, AST and ITBL (Table 2).

DISCUSSION

Biliary strictures after liver transplantation are a diagnostic and therapeutic challenge. They occur in up to 34% of

Table 2 Impact of biochemical cholestasis parameters on diagnosis of post-transplant biliary strictures¹

	NoST	AST	ITBL
Serum bilirubin (mg/dL)	5.7 (0.8-30)	4.1 (0.7-9.5) <i>P</i> = 0.179 ²	2.5 (0.5-23.7) <i>P</i> = 0.245 ²
Alkaline phosphatase (U/L)	360 (157-1206)	339 (72-2185) <i>P</i> = 0.56 ²	527 (288-2256) <i>P</i> = 0.239 ²
Gamma glutamyl transferase (U/L)	277 (64-832)	220 (33-1580) <i>P</i> = 0.06 ²	239 (65-849) <i>P</i> = 0.669 ²

¹Data given as median and (range); ²Mann-Whitney test.

patients receiving liver transplantation^[1-5]. Usually they appear 3-5 mo after transplantation and therefore easy direct imaging via post surgical t-tube is not possible.

Elevation of liver enzymes in patients after liver transplantation are caused by a variety of reasons, such as graft rejection, recurrence of the underlying liver disease, biliary strictures and/or biliary stones. As endoscopic retrograde or percutaneous transhepatic cholangiography for diagnostic reasons are invasive and technically often challenging, it would be desirable to have another easy diagnostic tool for differentiation between these causes of cholestasis. Therefore, the aim of this study was to evaluate the diagnostic value of these different indirect methods in comparison with (ERC), which is the gold standard for diagnosis of biliary complications after liver transplantation.

It is reported, that the level of alkaline phosphatase may be a diagnostic feature of ischemic biliary strictures^[5]. We could not find any statistically significant difference of alkaline phosphatase, gamma glutamyl transferase or bilirubin serum level in patients with anastomotic or ischemic type biliary strictures compared to patients with a normal biliary system. Therefore biochemical liver function tests may provide a hint for the existence of PTBS but do not contribute to prove the case for or disclose the kind of PTBS.

In the ITBL group our study demonstrated a significantly higher proportion of patients with ALF than in both other groups as the underlying cause for transplantation. The reason therefore remains to be resolved. Several pathog-enetic reasons such as thrombosis of the hepatic artery, cytomegaly virus infection, hepatitis C infection, *etc.* have been suggested as a cause of ITBL, however ALF as a risk factor for ITBL has not yet been demonstrated^[12]. Further studies will have to clarify that issue.

In contrast to patients without transplantation, US is reported to have a low sensitivity (close to 50%) for the diagnosis of posttransplant biliary congestion and strictures^[13-15]. In contrast, Hussaini *et al*^[6], reported a high negative predictive value of 95% for transabdominal US in the diagnosis of biliary tract complications, when statistically adjusted for the low prevalence rate of biliary complications in their post liver transplant patients. They assume that a normal ultrasonography makes the presence of biliary complications unlikely. In contrast, we observed a considerable proportion of patients with normal US despite of substantial bile duct stenosis. The specific localization of stenosis could not be visualized by ultrasonography. This may be due to the fact, that the post transplant bile ducts are often filled with epithelial cast, which could mask the true biliary diameter. Other authors presume that acute occlusion may not result in a prompt dilatation of the prestenotic bile ducts^[13-15].

It is reported, that helical CT, which is often used to examine suspected vascular disease, can also demonstrate associated biliary complications^[17], although exact data are not available. In our study, CT-scan was able to detect biliary congestion in 40% of AST and in 83% of ITBL with a specificity of 71%. The specific site of stenosis could be detected in 10% of patients.

Sensitivity and specificity of MR-imaging of post-transplant biliary complications is reported to be high^[18-22]. For instance, Borasci *et al*^[18], reported a sensitivity of 93%, specificity of 92%, a positive predictive value of 86% and a negative

Table 3 Impact of indirect imaging tools on diagnosis of posttransplant biliary strictures

	Sensitivity (%)	Specificity (%)	PPV (%)	NPV (%)
US-biliary congestion all	63.9	91.0	92.0	60.6
-biliary congestion AST	68.4	91.0	86.7	76.9
-biliary congestion ITBL	58.8	91.0	83.3	74.1
US-biliary stenosis	0	0	0	0
US-concomitant biliary stones all	22.0	97.0	66.7	82.5
-stones AST	0	97	0	91.7
-stones ITBL	0	97	0	94
CT-biliary congestion all	63.6	57.1	70.0	50.0
-biliary congestion AST	40.0	57.1	40.0	57.1
-biliary congestion ITBL	83.3	57.1	62.5	80.0
CT-biliary stenosis	10	0	0	43.75
CT-concomitant biliary stones	0	0	0	0
MR-biliary congestion all	83.3	25.0	83.3	25.0
-biliary congestion AST	71.4	25.0	62.5	33.3
-biliary congestion ITBL	88.9	25.0	72.7	50.0
MR-biliary stenosis	38.9	75	87.5	21.4
MR-correct localisation of stenosis	22	75	80	17.6
MR-concomitant biliary stones all	33.0	94	50	89
-stones AST	0	94		
-stones ITBL	0	94		

PPV, positive predictive value; NPV, negative predictive value.

predictive value of 96% in detecting post-LTx biliary complications. Unfortunately most of the other MR-imaging studies did not compare MRI with direct cholangiography. In view of our data, the results of all these studies appear questionable^[19-23].

Using MR-Imaging (MRI) in combination with MR-cholangiography (MRC) in our study sensitivity of correct diagnosis was highest regarding all indirect techniques. MRC techniques vary considerably from study to study and so, most studies are not comparable. There are novel computation modes under evaluation, which might improve the diagnostic impact of MRC in PTBS.

Therefore, to date MRC seems to be the most promising indirect tool for the diagnosis of biliary congestion in post liver transplant patients, but sensitivity of the specific type and pattern of stenoses still remains poor. However, with further improvement MRC may become a valuable tool before endoscopic intervention.

In conclusion, our data confirm that indirect imaging methods to date cannot replace direct cholangiography for diagnosis of PTBS. However MRI may have the potential to complement or precede imaging by cholangiography. Optimized MRC-processing might further improve the diagnostic impact of this method.

REFERENCES

- Li S, Stratta RJ, Langnas AN, Wood RP, Marujo W, Shaw BW. Diffuse biliary tract injury after orthotopic liver transplantation. *Am J Surg* 1992; **164**: 536-540
- Gholson CF, Zibari G, McDonald JC. Endoscopic diagnosis and management of biliary complications following orthotopic liver transplantation. *Dig Dis Sci* 1996; **41**: 1045-1053
- Greif F, Bronsther OL, Van Thiel DH, Casavilla A, Iwatsuki S, Tzakis A, Todo S, Fung JJ, Starzl TE. The incidence, timing and management of biliary tract complications after orthotopic liver transplantation. *Ann Surg* 1994; **219**: 40-45
- Sossenheimer M, Slivka A, Carr-Locke D. Management of extrahepatic biliary disease after orthotopic liver transplantation: review of the literature and results of a multicenter survey. *Endoscopy* 1996; **28**: 565-571
- Hintze RE, Abou-Rebyeh H, Adler A, Veltzke W, Langrehr J, Wiedenmann B, Neuhaus P. Endoscopic therapy of ischemia-type biliary lesions in patients following orthotopic liver transplantation. *Z Gastroenterol* 1999; **37**: 13-20
- Hintze RE, Adler A, Veltzke W, Abou-Rebyeh H, Felix R, Neuhaus P. Endoscopic management of biliary complications after orthotopic liver transplantation. *Hepatogastroenterology* 1997; **44**: 258-262
- Rerknimitr R, Sherman S, Fogel EL, Kalayci C, Lumeng L, Chalasani N, Kwo P, Lehman GA. Biliary tract complications after orthotopic liver transplantation with choledochocholedochostomy anastomosis: endoscopic findings and results of therapy. *Gastrointest Endosc* 2002; **55**: 224-231
- Thuluvath PJ, Atassi T, Lee J. An endoscopic approach to biliary complications following orthotopic liver transplantation. *Liver Int* 2003; **23**: 156-162
- Morelli J, Mulcahy HE, Willner IR, Cunningham JT, Draganov P. Long-term outcomes for patients with post-liver transplant anastomotic biliary strictures treated by endoscopic stent placement. *Gastrointest Endosc* 2003; **58**: 374-379
- Pfau PR, Kochman ML, Lewis JD, Long WB, Lucey MR, Olthoff K, Shaked A, Ginsberg GG. Endoscopic management of postoperative biliary complications in orthotopic liver transplantation. *Gastrointest Endosc* 2000; **52**: 55-63
- Mosca S, Militerno G, Guardascione MA, Amitrano L, Picciotto FP, Cuomo O. Late biliary tract complications after orthotopic liver transplantation: diagnostic and therapeutic role of endoscopic retrograde cholangiopancreatography. *J Gastroenterol Hepatol* 2000; **15**: 654-660
- Guichelaar MM, Benson JT, Malinchoc M, Krom RA, Wiesner RH, Charlton MR. Risk factors for and clinical course of non-anastomotic biliary strictures after liver transplantation. *Am J Transplant* 2003; **3**: 885-890
- Shaw AS, Ryan SM, Beese RC, Sidhu PS. Ultrasound of non-vascular complications in the post liver transplant patient. *Clin Radiol* 2003; **58**: 672-680
- Zemel G, Zajko AB, Skolnick ML, Bron KM, Campbell WL. The role of sonography and transhepatic cholangiography in the diagnosis of biliary complications after liver transplantation. *AJR Am J Roentgenol* 1988; **151**: 943-946
- Kok T, Van der Sluis A, Klein JP, Van der Jagt EJ, Peeters PM, Slooff MJ, Bijleveld CM, Haagsma EB. Ultrasound and cholangiography for the diagnosis of biliary complications after orthotopic liver transplantation: a comparative study. *J Clin Ultrasound* 1996; **24**: 103-115
- Hussaini SH, Sheridan MB, Davies M. The predictive value of transabdominal ultrasonography in the diagnosis of biliary tract complications after orthotopic liver transplantation. *Gut* 1999; **45**: 900-903
- Quiroga S, Sebastia MC, Margarit C, Castells L, Boye R, Alvarez-Castells A. Complications of orthotopic liver transplantation: spectrum of findings with helical CT. *Radiographics* 2001; **21**: 1085-1102
- Boraschi P, Braccini G, Gigoni R, Sartoni G, Neri E, Filippini F, Mosca F, Bartolozzi C. Detection of biliary complications after orthotopic liver transplantation with MR cholangiography. *Magn Reson Imaging* 2001; **19**: 1097-1105
- Linhares MM, Gonzalez AM, Goldman SM, Coelho RD, Sato NY, Moura RM, Silva MH, Lanzoni VP, Salzedas A, Serra CB, Succi T, D'Ippolito G, Szejnfeld J, Trivino T. Magnetic resonance cholangiography in the diagnosis of biliary complications after orthotopic liver transplantation. *Transplant Proc* 2004; **36**: 947-948
- Fulcher AS, Turner MA. Orthotopic liver transplantation: evaluation with MR cholangiography. *Radiology* 1999; **211**: 715-722
- Meersschaut V, Mortelet KJ, Troisi R, Van Vlierberghe H, De Vos M, Defreyne L, de Hemptinne B, Kunnen M. Value of MR cholangiography in the evaluation of postoperative biliary complications following orthotopic liver transplantation. *Eur Radiol* 2000; **10**: 1576-1581
- Laghi A, Pavone P, Catalano C, Rossi M, Panebianco V, Alfani D, Passariello R. MR cholangiography of late biliary complications after liver transplantation. *AJR Am J Roentgenol* 1999; **172**: 1541-1546
- Ito K, Siegelman ES, Stolpen AH, Mitchell DG. MR imaging of complications after liver transplantation. *AJR Am J Roentgenol* 2000; **175**: 1145-1149

• BRIEF REPORTS •

Expression of bcl-2 protein in chronic hepatitis C: Effect of interferon alpha 2b with ribavirin therapy

Panasiuk Anatol, Prokopowicz Danuta, Dzieciol Janusz, Panasiuk Bozena

Panasiuk Anatol, Prokopowicz Danuta, Panasiuk Bozena, Department of Infectious Diseases, Medical University of Bialystok, Zurawia Str., 14, 15-540 Bialystok, Poland
Dzieciol Janusz, Department of Human Anatomy, Medical University of Bialystok, Zurawia Str., 14, 15-540 Bialystok, Poland
Correspondence to: Associate Professor Panasiuk Anatol, M.D., Department of Infectious Diseases, Medical University of Bialystok, Zurawia Str, 14, 15-540 Bialystok, Poland. apanasiuk@wp.pl
Telephone: +48-85-7416-921 Fax: +48-85-7416-921
Received: 2004-02-20 Accepted: 2004-04-13

Abstract

AIM: Mechanisms responsible for persistence of HCV infection and liver damage in chronic hepatitis C are not clear. Apoptosis is an important form of host immune response against viral infections. Anti-apoptotic protein bcl-2 expression on liver tissue as well as the influence of interferon alpha 2b (IFN α 2b) and ribavirin (RBV) were analyzed in patients with chronic hepatitis C.

METHODS: In 30 patients with chronic hepatitis C (responders - R and non-responders - NR) treated with IFN α 2b+RBV, protein bcl-2 was determined in hepatocytes and in liver associated lymphocytes before and after the treatment.

RESULTS: The treatment diminished bcl-2 protein accumulation in liver cells in patients with hepatitis C ($P < 0.05$). Before and after the therapy, we detected bcl-2 protein in R in 87 \pm 15% and 83 \pm 20% of hepatocytes and in 28 \pm 18% and 26 \pm 10% of liver-associated lymphocytes, respectively. In NR, the values before treatment decreased from 94 \pm 32% to 88 \pm 21% of hepatocytes and 39 \pm 29% to 28 \pm 12% of lymphocytes with bcl-2 expression. There was no statistical correlation between bcl-2 expression on liver tissue with inflammatory activity, fibrosis and biochemical parameters before and after the treatment.

CONCLUSION: IFN α 2b+RBV treatment, by bcl-2 protein expression decrease, enables apoptosis of hepatocytes and associated liver lymphocytes, which in turn eliminate hepatitis C viruses.

© 2005 The WJG Press and Elsevier Inc. All rights reserved.

Key words: Bcl-2; Chronic hepatitis C; Interferon alpha; Ribavirin; Hepatitis C virus

Anatol P, Danuta P, Janusz D, Bozena P. Expression of bcl-2 protein in chronic hepatitis C: Effect of interferon alpha 2b

with ribavirin therapy. *World J Gastroenterol* 2005; 11(19): 2949-2952

<http://www.wjgnet.com/1007-9327/11/2949.asp>

INTRODUCTION

Hepatitis C virus is a major frequent agent of chronic liver inflammation. Many aspects play an important role in pathogenesis of HCV infection, e.g., viral genotype, virus-host interactions, local and systemic immune reactions and expression of viral proteins. Hepatitis C virus has cytopathic and viropathic features and induces T lymphocyte cytotoxicity by causing their selective accumulation in the liver. Hepatitis C virus has structural and non-structural proteins, which play a role in replication and production of cellular promoters^[1,2]. Several viral proteins interfere with cellular functions, which are involved in the immune response, cell proliferation and apoptosis in the liver^[3-5].

Apoptosis is an important mechanism limiting viral replication in infected cells. Many viruses produce a variety of mechanisms to neutralize IFN secretion and block genes participating in apoptosis^[6]. Hepatitis C virus has the features of both induction and inhibition of hepatocyte apoptosis. Apoptosis induction upon HCV infection may contribute to liver inflammation, while inhibition of apoptosis may result in HCV persistence and oncogenesis. Modulation of apoptosis by HCV core protein is possible by death receptors, such as Fas, TNF, and lymphotoxin B. The HCV NS3 and NS5A proteins have anti-apoptotic effects^[7,8]. Apoptosis is a result of proapoptotic factor activation (bax, FADD Fas-associated death domain-containing protein, TNFRF1, Fas/CD95) and anti-apoptotic inhibition (bcl-2). The activation of caspase-8 (determined as proapoptotic - b.i.d.) influences the release of cytochrome C from mitochondria and secondary activation of cytoplasmic caspase 9 and 3. Bcl-2 regulates apoptosis through the influence on mitochondrial membrane channel proteins and that decides the amount of released cytochrome C to the cytoplasm^[9-11]. In hepatitis C, apoptosis of parenchymal (hepatocytes) and non-parenchymal cells occurs. The increase of apoptosis of circulating activated T lymphocytes in hepatitis C was observed^[12]. Lack of correlation between caspase activity and the stage of inflammatory changes in the liver is probably caused by this phenomenon. Viral infections are capable of limiting or blocking cell apoptosis in which they reproduce themselves. Core protein among HCV proteins has a crucial role in protecting the cells from apoptosis mediated by anti-Fas and TNF-alpha.

Cytotoxic T lymphocytes induce apoptosis of cells infected with viruses. There is a strict relation between infiltrating lymphocytes and hepatocyte apoptosis. It is suggested that apoptosis is mediated by the host immune system^[8]. Infected hepatocytes show increased Fas expression. In liver inflammatory areas, the increase in Fas ligand expression occurs, which correlates with the stage of hepatitis C^[13]. This is a consequence of T lymphocyte induction after the contact with viral antigen on presented hepatocytes^[14]. Besides Fas-FasL pathway, there is another way through the release of granzyme B/perforin induction of apoptosis in infected cells^[15].

Interferon alpha synthesized by most cell types is a cytokine of multiple properties, e.g., antiviral, immunomodulatory, and antiproliferative properties^[16]. Detailed mechanisms of IFN activity remain elusive. It is assumed that antiviral effect of IFN is possible by induction of apoptosis of infected hepatocytes. The role of IFN in apoptosis and antiviral host defense lies in inducing a number of cellular genes. Hepatitis C virus NS5 and E2 proteins inhibit antiviral activity of IFN by inhibition of IFN signaling pathways and antiviral protein production, e.g., threonine protein kinase^[17].

It seems that hepatocyte apoptosis plays a crucial role in hepatitis C pathogenesis and antiviral activity of interferon alpha may be the effect of apoptosis induction. Therefore, we examined the correlation between liver cell damage and bcl-2 expression on the liver in patients with chronic hepatitis C before and after the treatment with IFN α 2b and RBV.

MATERIALS AND METHODS

Patients

Examinations were conducted in 30 patients, aged 38 ± 13.6 years (14 women and 16 men), with chronic hepatitis C. Chronic hepatitis C lasting for 2.4 ± 1.7 years was confirmed by the presence of anti-HCV antibodies, HCV-RNA in blood serum with elevated alanine aminotransferase in all patients. Patients with liver cirrhosis were excluded from the study. HCV-RNA in sera and biochemical parameters were examined at the end of the treatment and after 6 mo. Patients were divided into responders (R) and non-responders (NR) according to their sustained response to a course of IFN α 2b (3 MU thrice weekly for 48 wk, Rebetrin, Schering-Plough Corporation, USA) with ribavirin (RBV, 1.2 g/d/48 wk, Rebetrin, Schering-Plough Corporation) treatment. Blind liver biopsies were performed using the Hepafix system (Braun, Melsungen, Germany) before the treatment and 6 mo after the therapy. Histopathological inflammatory activity (grading, scales 0-4) and fibrosis (staging, scores 0-4) were evaluated in accordance with the classification of chronic viral hepatitis according to Scheuer classification^[18]. Ethical approval for research was obtained from Local Ethics committee in Medical University.

Methods

Liver tissues obtained from biopsy were placed in 4% formalin buffered solution (24 h), after that they were fixed and paraffin embedded. Five-micrometers of thick sections were routinely stained with hematoxylin-eosin and immunostained by using monoclonal antibodies (isotope IgG1, kappa, clone

DO-7, Dako, Denmark). Primary antibodies were used by the dilution according to the producer's instructions (1:50). A LSAB+HRP kit (Dako, Denmark) with DAB (Dako, Denmark) and chromogen was used as a detective set. The positive reaction was expressed by red-brown color of the cytoplasm for bcl-2. Under a microscope we calculated hepatocytes and lymphocyte percentage (the amount of cells with positive reaction in ratio to 100 cells) containing bcl-2 protein in five fields of vision ($\times 400$) of one slide. Intensity of accumulation of bcl-2 protein in cellular cytoplasm was also evaluated. Intensive immunohistochemical reaction of specific antibodies to bcl-2 protein was determined as grade 1, moderate reaction as grade 2 with high granular intensity of bcl-2 protein accumulation.

Statistical analysis

Results were presented as mean \pm SD. Statistical analysis was performed using Student's *t*-test for pairs, χ^2 test, and Spearman's test.

RESULTS

The clinical characteristics of patients are presented in Table 1. After the treatment, we observed improved inflammatory activity and fibrosis in liver tissue. In four patients we noted progressive liver damage IFN α 2b+RBV therapy diminished accumulation of bcl-2 proteins in all patients with hepatitis C (Table 2). Before the treatment, bcl-2 protein was detected in $92 \pm 12\%$ of hepatocytes and in $37 \pm 26\%$ of liver-associated lymphocytes in all patients. In responders, bcl-2 expression on hepatocytes was $87 \pm 15\%$ and $28 \pm 18\%$, respectively. In patients with successful therapy we observed the lowest percentage of hepatocytes and lymphocytes containing bcl-2 protein before and after the treatment. There were no statistically significant differences in bcl-2 expression on the liver between responders and non-responders.

Together with inflammatory activity (portal, periportal) and liver fibrosis, we noted increased percentages of hepatocytes and liver associated lymphocytes containing bcl-2 protein. However, we did not observe any statistical correlation between bcl-2 expression and histological changes in the liver in patients who revealed both worsening and improvement of inflammatory activity and fibrosis. There was no correlation between bcl-2 expression on hepatocytes

Table 1 Clinical characteristics of patients with chronic hepatitis C (mean \pm SD)

Woman/man (n)	14/16	
Age (yr)	38.0 ± 13.6	
Duration of HCV infection (yr)	2.4 ± 1.7	
	Before treatment	After treatment
ALT/AST (U/L)	$80 \pm 61/78 \pm 46$	$53 \pm 56/65 \pm 41$
ALP/GGT (U/L)	$89 \pm 22/62 \pm 41$	$79 \pm 21/55 \pm 26$
Albumin/gamma globulin (g/dL)	$3.7 \pm 0.4/1.2 \pm 0.3$	$3.9 \pm 0.9/1.3 \pm 0.5$
HCV-RNA positive (n)	30	20
Inflammatory activity (grading), score ¹		
Periportal: 1/2/3/4 (n)	6/8/16/0	10/4/16/0
Intralobular: 1/2/3/4 (n)	18/12/0/0	16/14/0/0
Fibrosis (staging), score: 1/2/3/4 (n)	20/8/2/0	16/12/2/0

¹According to Scheuer classification (1991).

Table 2 Expression of bcl-2 protein on hepatocytes and lymphocytes in liver tissue before and after treatment with IFN α 2b and RBV (mean \pm SD)

Chronic hepatitis C, total, <i>n</i> = 30	Before treatment	After treatment	<i>P</i>
Hepatocytes (%)	92 \pm 12	87 \pm 11	<0.05
Liver-associated lymphocytes (%)	37 \pm 26	27 \pm 21	NS
Responders, <i>n</i> = 10			
Hepatocytes (%)	87 \pm 15	83 \pm 20	NS
Liver-associated lymphocytes	28 \pm 18	26 \pm 10	NS
Non-responders, <i>n</i> = 20			
Hepatocytes (%)	94 \pm 32	88 \pm 21	<0.05
Liver-associated lymphocytes (%)	39 \pm 29	28 \pm 12	NS

and lymphocytes, and activity of alanine aminotransferase before and after the treatment. Analyzing the intensity of bcl-2 accumulation in cells, we observed a high granular accumulation of bcl-2 proteins in hepatocytes and in liver associated lymphocytes in hepatitis C patients (Table 3). The treatment achieved the decrease in bcl-2 positive cell percentage and the density of protein in cells. There was no statistically significant difference between responders and non-responders concerning bcl-2 accumulation before and after the treatment. A statistical correlation between bcl-2 intensity on lymphocytes and liver fibrosis was observed in responders ($r = 0.7$, $P < 0.01$) after IFN α 2b+RBV treatment.

DISCUSSION

The results proved that the initiation of apoptosis in chronic hepatitis C led to HCV elimination. All patients treated with IFN α 2b+RBV showed a significant reduction in bcl-2 accumulation in hepatocytes and lymphocytes. It proves that IFN α 2b+RBV could affect bcl-2 concentrations in the liver, and stimulate apoptosis of hepatocytes and lymphocytes. Whether it is a direct effect of antiviral drugs on bcl-2 or a result of HCV elimination is unknown. Immunohistopathological study revealed that apoptosis was much inhibited in non-responders than in responders before the treatment. In NR, bcl-2 expression was also decreased, although to a less extent than in responders, under the influence of IFN α 2b+RBV therapy.

HCV proteins could modulate apoptosis of hepatocytes by indirect or direct mechanisms^[3,19]. Mechanisms of immune-mediated apoptosis in the liver are the most probable. Degree of liver apoptosis correlates positively with histological inflammatory activity and with level of infiltrating CD8 T cells. Apoptosis is regulated by products of various gene expressing bcl-2 inhibitors (bcl-2, bcl-xl, mcl-10) and apoptosis promoters (so called "killers" bax, bak, bok, bad, which contain domains of BH1, BH2, BH3)^[9]. The bcl-2 proto-oncogene is localized in the inner mitochondrial membrane of cells and blocks programmed cell death. Over-expression of *bcl-2* gene could lead to apoptosis inhibition and enable cell survival. Sensitivity of cells to factors inducing apoptosis may also be regulated by pro- and anti-apoptotic protein ratio.

Calabrese *et al*^[8], showed that apoptotic index of hepatocytes in liver tissue ranged from 0.01% to 0.54%, and presented a positive correlation between histological

Table 3 Intensity of bcl-2 protein expression on hepatocytes and liver lymphocytes in patients with chronic hepatitis C during IFN α 2b and RBV therapy

Intensity of accumulation	Bcl-2 in hepatocytes (%)		Bcl-2 in liver lymphocytes (%)	
	Before	After	Before	After
High granular (<i>n</i>)	21	9	15	13
Moderate (<i>n</i>)	9	21	15	17
χ^2 test	$P > 0.1$		$P > 0.5$	

activity and value of CD8 cells in liver tissue. However, the relation between apoptosis intensity and aminotransferase level as well as HCV viremia and genotype was not observed. Apoptosis could also occur without elevated transaminases. There was no correlation between biochemical activity and liver cell injury. Our study did not show any statistical significance between bcl-2 protein expression and histological activity and liver fibrosis.

Rubbia-Brandt *et al*^[20], revealed that 50% of patients with hepatitis C had apoptotic hepatocytes, 52% Fas receptor expression, and 30% tumor necrosis factor receptors (TNFR). Fas- and TNFR-positive hepatocytes did not correlate with the value of intrahepatic CD8+ T cells, the grading and staging of liver diseases, or the serum or liver HCV-RNA levels^[20]. Many factors, such as HCV NS proteins, could decide bcl-2 expression. Hepatitis C virus core protein could bind to a domain of lymphotoxin B receptor (LTBR), which is a member of the tumor necrosis factor receptor family^[21]. It was reported that LTB receptor was involved in lymph node development^[22]. Thus, it should be assumed that HCV core protein plays a potential role in induction of host immune mechanisms. It seems that hepatitis C virus may cause both necrosis and apoptosis of hepatocytes.

HCV-specific T cells migrate to the liver and recognize viral antigens and affect the expression of Fas ligand, which enables transmission of apoptotic death signals with induction of apoptosis. Fas antigen is a cell surface protein that mediates apoptosis in hepatitis C. Hayashi and Mita^[23] observed a high prevalence of Fas expression mainly in the cytoplasm of hepatocytes and in infiltrating lymphocytes in liver tissues with severe inflammation. Inflammatory cells could secrete cytokines (mainly TNF α), inducing apoptosis through surface receptors^[24]. Ray *et al*^[25], suggested that HCV core protein inhibited TNF α -mediated apoptosis and might enhance HCV replication with persistent infection. Pharmacological inhibition of apoptosis may favor chronic HCV infection and even intensify its replication. Persistent infection of HCV might be a result of suppression of Fas- and TNF- α -mediated cell death and inhibition of apoptosis of liver cells^[20,26].

HCV infection could induce caspase activation, which correlates closely with the inflammatory response. HCV proteins could inhibit the activation of caspases-9 and 3/7 and release of cytochrome C from mitochondria. Bcl-2 protein could inhibit apoptosis of infected cells in a caspase-dependent manner. Caspase activation and apoptosis did not correlate with biochemical activity (aminotransferase levels), viral load, and genotype^[4]. It is possible that apoptosis occurs not only in hepatocytes, but also in other cells.

Furthermore, the release of transaminases was lower from apoptotic cells than from necrotic cells. It could explain the progression of liver diseases in asymptomatic patients with HCV infection and normal values of transaminases^[7]. It is believed that caspase activity monitoring may be an index of liver injury and efficacy of antiviral therapy (IFN alpha, RBV).

It seems that apoptosis is a principal process leading to HCV elimination. But activation of this process is not clear. Antiviral treatment is a potent signal to apoptosis activation but future research is required.

REFERENCES

- 1 Ray RB, Lagging LM, Meyer K, Steele R, Ray R. Transcriptional regulation of cellular and viral promoters by the hepatitis C virus core protein. *Virus Res* 1995; **37**: 209-220
- 2 Reyes GR. The nonstructural NS5A protein of hepatitis C virus: an expanding, multifunctional role in enhancing hepatitis C virus pathogenesis. *J Biomed Sci* 2002; **9**: 187-197
- 3 Bantel H, Schulze-Osthoff K. Apoptosis in hepatitis C virus infection. *Cell Death Differ* 2003; **10** Suppl 1: S48-S58
- 4 Kountouras J, Zavos C, Chatzopoulos D. Apoptosis in hepatitis C. *J Viral Hepat* 2003; **10**: 335-342
- 5 Pavio N, Lai MM. The hepatitis C virus persistence: how to evade the immune system? *J Biosci* 2003; **28**: 287-304
- 6 Teodoro JG, Branton PE. Regulation of apoptosis by viral gene products. *J Virol* 1997; **71**: 1739-1746
- 7 Bantel H, Lugering A, Poremba C, Lugering N, Held J, Domschke W, Schulze-Osthoff K. Caspase activation correlates with the degree of inflammatory liver injury in chronic hepatitis C virus infection. *Hepatology* 2001; **34**: 758-767
- 8 Calabrese F, Pontisso P, Pettenazzo E, Benvegnu L, Vario A, Chemello L, Alberti A, Valente M. Liver cell apoptosis in chronic hepatitis C correlates with histological but not biochemical activity or serum HCV-RNA levels. *Hepatology* 2000; **31**: 1153-1159
- 9 Gross A, McDonnell JM, Korsmeyer SJ. BCL-2 family members and the mitochondria in apoptosis. *Genes Dev* 1999; **13**: 1899-1911
- 10 Kroemer G. The proto-oncogene Bcl-2 and its role in regulating apoptosis. *Nat Med* 1997; **3**: 614-620
- 11 Luo X, Budihardjo I, Zou H, Slaughter C, Wang X. Bid, a Bcl2 interacting protein, mediates cytochrome c release from mitochondria in response to activation of cell surface death receptors. *Cell* 1998; **94**: 481-490
- 12 Botarelli P, Brunetto MR, Minutello MA, Calvo P, Unutmaz D, Weiner AJ, Choo QL, Shuster JR, Kuo G, Bonino F. T-lymphocyte response to hepatitis C virus in different clinical courses of infection. *Gastroenterology* 1993; **104**: 580-587
- 13 Jarmay K, Karascony G, Ozsvar Z, Nagy I, Lonovics J, Schaff Z. Assessment of histological features in chronic hepatitis C. *Hepatogastroenterology* 2002; **49**: 239-243
- 14 Toubi E, Kessel A, Goldstein L, Slobodin G, Sabo E, Shmuel Z, Zuckerman E. Enhanced peripheral T-cell apoptosis in chronic hepatitis C virus infection: association with liver disease severity. *J Hepatol* 2001; **35**: 774-780
- 15 Lau JY, Xie X, Lai MM, Wu PC. Apoptosis and viral hepatitis. *Semin Liver Dis* 1998; **18**: 169-176
- 16 Stark GR, Kerr IM, Williams BR, Silverman RH, Schreiber RD. How cells respond to interferons. *Annu Rev Biochem* 1998; **67**: 227-264
- 17 Taylor DR, Shi ST, Romano PR, Barber GN, Lai MM. Inhibition of the interferon-inducible protein kinase PKR by HCV E2 protein. *Science* 1999; **285**: 107-110
- 18 Scheuer PJ. Classification of chronic viral hepatitis: a need for reassessment. *J Hepatol* 1991; **13**: 372-374
- 19 Patel T, Steer CJ, Gores GJ. Apoptosis and the liver: A mechanism of disease, growth regulation, and carcinogenesis. *Hepatology* 1999; **30**: 811-815
- 20 Rubbia-Brandt L, Taylor S, Gindre P, Quadri R, Abid K, Spahr L, Negro F. Lack of *in vivo* blockade of Fas- and TNFR1-mediated hepatocyte apoptosis by the hepatitis C virus. *J Pathol* 2002; **197**: 617-623
- 21 Matsumoto M, Hsieh TY, Zhu N, VanArsdale T, Hwang SB, Jeng KS, Gorbalenya AE, Lo SY, Ou JH, Ware CF, Lai MM. Hepatitis C virus core protein interacts with the cytoplasmic tail of lymphotoxin-beta receptor. *J Virol* 1997; **71**: 1301-1309
- 22 Rennert PD, Browning JL, Mebius R, Mackay F, Hochman PS. Surface lymphotoxin alpha/beta complex is required for the development of peripheral lymphoid organs. *J Exp Med* 1996; **184**: 1999-2006
- 23 Hayashi N, Mita E. Fas system and apoptosis in viral hepatitis. *J Gastroenterol Hepatol* 1997; **12**: S223-S226
- 24 Nasir A, Arora HS, Kaiser HE. Apoptosis and pathogenesis of viral hepatitis C-an update. *In Vivo* 2000; **14**: 297-300
- 25 Ray RB, Meyer K, Steele R, Shrivastava A, Aggarwal BB, Ray R. Inhibition of tumor necrosis factor (TNF-alpha)-mediated apoptosis by hepatitis C virus core protein. *J Biol Chem* 1998; **273**: 2256-2259
- 26 Marusawa H, Hijikata M, Chiba T, Shimotohno K. Hepatitis C virus core protein inhibits Fas- and tumor necrosis factor alpha-mediated apoptosis via NF-kappaB activation. *J Virol* 1999; **73**: 4713-4720

• BRIEF REPORTS •

Computed tomography findings in fatal cases of enormous hepatic portal venous gas

Siu-Cheung Chan, Yung-Liang Wan, Yun-Chung Cheung, Shu-Hang Ng, Alex Mun-Ching Wong, Koon-Kwan Ng

Siu-Cheung Chan, Yung-Liang Wan, Yun-Chung Cheung, Shu-Hang Ng, Alex Mun-Ching Wong, Koon-Kwan Ng, Department of Diagnostic Radiology, Chang Gung Memorial Hospital, Linko Medical Center and Keelung Hospital, Taoyuan, Taiwan, China

Correspondence to: Yun-Chung Cheung, MD, First Department of Diagnostic Radiology, Chang Gung Memorial Hospital at Lin-Kou, 5 Fu-Hsing Street, Tao Yuan Hsien, Taiwan, China. chan3015@ms27.hinet.net

Telephone: +886-3-3281200-2575 Fax: +886-3-2702023

Received: 2004-07-12 Accepted: 2004-08-31

Abstract

AIM: To assess the computed tomography (CT) findings in the patients with hepatic portal venous gas (HPVG) who presented with a short fatal clinical course in our hospital in order to demonstrate if there was any sign for prediction.

METHODS: Between January 1997 and December 2000, CT scan of the abdomen was performed on 949 patients with acute abdominal pain in our emergency department. Five patients were found having HPVG. The CT images and clinical presentations of all these five patients were reviewed.

RESULTS: In reviewing the CT findings of the cases, HPVG in bilateral hepatic lobes, abnormal gas in the superior mesenteric veins, small bowel intramural gas, and bowel distension were observed in all patients. Dry gas in multiple branches of the mesenteric vein was also revealed in all cases. All the patients expired due to irreversible septic shock within 48 h after their initial clinical presentation in emergency room. Two patients had acute pancreatitis with grade D and E Balthazar classification and they expired within 24 h due to progressing septic shock under aggressive medical treatment and life support. Two patients with underlying end stage renal disease expired within 48 h even though emergent surgical intervention was undertaken. The excited bowels revealed severe ischemic change. One patient expired only a few hours after the CT examination.

CONCLUSION: HPVG is a diagnostic clue in patients with acute abdominal conditions, and CT is the most specific diagnostic tool for its evaluation. The dry mesenteric veins are the suggestive fatal sign, especially for the deteriorating patients, with the direct effect on gastrointestinal perfusion.

© 2005 The WJG Press and Elsevier Inc. All rights reserved.

Key words: Hepatic portal vein; Intestines; Ischemia;

Computed tomography

Chan SC, Wan YL, Cheung YC, Ng SH, Wong AMC, Ng KK. Computed tomography findings in fatal cases of enormous hepatic portal venous gas. *World J Gastroenterol* 2005; 11 (19): 2953-2955

<http://www.wjgnet.com/1007-9327/11/2953.asp>

INTRODUCTION

Hepatic portal vein gas (HPVG) is an uncommon feature of acute abdomen. Its radiological findings were first described in children with necrotizing enteritis in 1955^[1] followed by the first publication of HPVG in an adult in 1960^[2]. HPVG was associated with necrotic bowel (72%), ulcerative colitis (8%), intra-abdominal abscess (6%), small bowel obstruction (3%), and gastric ulcer (3%)^[3]. Recognition of HPVG in acute abdomen is important because of high mortality despite intense, conservative medical treatment or urgent surgery^[3]. The clinical outcomes of the acute abdomen with HPVG vary.

Radiological signs of abnormal air density in the hepatic region, either with or without gastrointestinal disturbance, are diagnostic clues for such urgent conditions. HPVG can be identified on plain radiography, computed tomography (CT) and ultrasound. Among these imaging modalities, CT is the most sensitive and specific for detecting HPVG and for demonstrating associated intra-abdominal disorders and coexisting abnormal air. Features of pneumatosis intestinalis are most frequently observed, accounting of 50-75% of cases^[4]. Demonstration of associated intra-abdominal conditions is essential for planning treatment. On the other hand, prediction of fatalities helps to avoid ineffective aggressive procedures. We reviewed five fatal cases of enormous HPVG. These patients died within 2 d after initial presentation at the emergency room, despite intense medical treatment. We reviewed these cases in order to better understand the clinical course and CT findings of HPVG.

MATERIALS AND METHODS

We searched the hospital records for emergency abdominopelvic CT studies from January 1997 to December 2000 and found 949 patients with acute abdomen. CT was performed using a helical CT scanner (HiSpeed CT/I; GE Medical Systems, Milwaukee, WI, USA). All examinations were standardized with an axial section thickness of 10 mm from the liver dome to the pelvic floor after oral intake of 600 mL of 4% iohalamate meglumine (Conray 60, Mallinck-



Figure 1 Contrast-enhanced abdominal CT at celiac axis level shows evidence of HPVG.

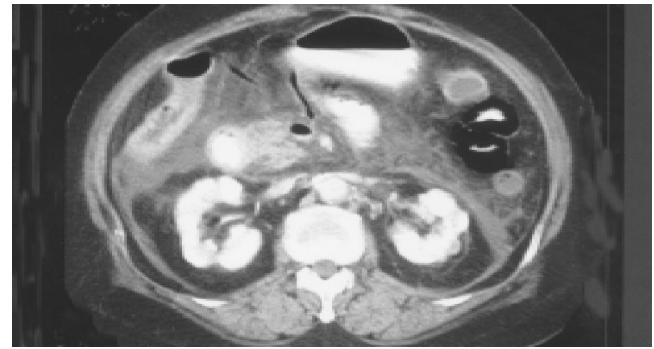


Figure 2 Contrast-enhanced abdominal CT at renal hilar level shows tubular dry gases (arrow) and air-fluid level (arrowhead) within the mesenteric veins. Pneumatosis intestinalis and inflammation fluid collection in the left pararenal space indicating that pancreatitis is also observed.

rodt Canada Incorporated, Quebec, Canada). The enhancement technique and scanning time were the same for all patients, with the total dosage of 100 mL 60% iohalamate meglumine (Conray 60, Mallinckrodt Canada Incorporated, Quebec, Canada) at a 2 mL/s injection rate. All images were reviewed by two radiologists (Chan SC, Cheung YC) to identify cases of HPVG and to determine the associated CT findings, including coexisting abnormal air and intra-abdominal conditions. Medical records were reviewed to determine clinical courses and outcomes.

RESULTS

Five patients (two men and three women) with ages ranging from 50 to 90 years were found having HPVG. All five patients complained of an acute abdomen at their initial presentation in our emergency room. They all presented with severe abdominal pain and leukocytosis. Of them, two patients had elevated serum amylase (646 and 213 U/L, respectively) levels that were suggestive of acute pancreatitis. These five patients also had chronic diseases such as hypertension, alcoholism and diabetes mellitus (Table 1). Upon emergency CT, HPVG in bilateral hepatic lobes (Figure 1), abnormal gas in the superior mesenteric veins, small bowel intramural gas, and bowel distension were observed in all cases. Additionally, multiple branches of the mesenteric vein that appeared with dry gas were visualized in all patients (Figure 2). Of them, colonic intramural gas was also visible in two patients.

One patient had pneumoperitoneum.

Two patients underwent emergency exploratory laparotomy after CT examination. The 65-year-old female patient had end-stage renal disease and under regular hemodialysis was found to have extensive ischemic bowel disease from the Treitz ligament to the ileocecal valve, with more than 1 000 mL of turbid ascites fluid. Only surgical open and close was done. She expired within 12 h due to irreversible septic shock. Another case of a 90-year-old male patient had the chronic renal insufficiency and after surgery, 40 cm of small bowel gangrene was found. The necrotic bowel was resected, but his clinical condition worsened because of infection and multiple organ failure; he expired within 48 h after surgery due to irreversible septic shock. The two patients with suspected pancreatitis had Balthazar classifications D and E disease, respectively, on CT imaging. Even though these four patients were given intense medical treatment with antibiotics and life support, they expired within 24 h after initial clinical presentation due to rapidly progressing septic shock. The remaining patient expired a few hours after CT due to irreversible septic shock.

DISCUSSION

The pathogenesis of HPVG is not fully understood. Two theories, mechanical and bacterial, have been proposed. The

Table 1 Summary of the patients with portal venous gas

Patient	Age (yr)	Sex	HPVG	SMV gas	Intramural gas		Metabolic acidosis	Bowel distention	Clinical manifestations	Underlying disease	Prognosis
					Small bowel	Colon					
1	90	M	+	+	+	-	-	+	Segmental small bowel ischemia	Chronic renal insufficiency, hypertension	Expired within 72 h after operation
2	71	F	+	+	+	-	+	+	Acute pancreatitis	Hypertension, DM	Expired within 24 h
3	72	F	+	+	+	-	+	+	Rapid progression of septic shock	Ischemia heart disease, gouty arthritis	Expired within 24 h
4	50	M	+	+	+	+	+	+	Acute pancreatitis	Alcoholism, DM	Expired within 24 h
5	65	F	+	+	+	+	-	+	Long segmental small bowel ischemia	ESRD, DM, hypertension	Expired within 12 h after operation

mechanical theory proposes that gas dissects into the bowel wall from either the intestinal lumen or the lung^[5]. Mucosal damage and bowel distention are important factors in this theory. Mucosal damage allows intraluminal gas to enter the venous system. About 85% of patients with HPVG have mucosal ulceration with bowel distention and increased intramural pressure^[5]. The bacterial theory proposes that gas-forming bacilli enter the submucosa through mucosal rents and produce gas within the intestinal wall and then enter into the portal vein^[5].

In cases of ischemic bowel distention with mucosal damage, mucosal damage allows gas to enter the mesenteric vessels directly^[6,7]. Bowel distention and ischemia can also produce minimal mucosal disruption that allows intraluminal gas to become intravascular^[8]. To our knowledge, HPVG is a rare complication of acute pancreatitis, first reported in 1961^[9]. In 1997, Faberman and Mayo-Smith reported three more cases and proposed that HPVG was caused by the breakdown of intestinal mucosa by pancreatic enzymes or mucosal disruption that induced intestinal ischemia^[10]. They demonstrated that pancreatitis with HPVG may not have as fulminant a course as previously thought. However, two of our patients with apparent pancreatitis died within 24 h after diagnosis. This situation may suggest that the clinical outcome of acute pancreatitis with HPVG is variable.

Long-term chronic diseases decrease the immune function and tolerance capability of the HPVG patients, which might lead to fatality^[11]. Among our five patients, one had chronic renal insufficiency and another had end-stage renal disease. In addition, the remaining patients had diabetes mellitus, hypertension, ischemic heart disease, or alcoholism (Table 1). Patients with chronic renal failure have greatly increased numbers of microbial flora, both anaerobes and aerobes, in the small intestine or during hemodialysis. According to their medical records, the patients had been examined and treated for long-term infections. These patients all took long-term medication to control their deteriorating underlying conditions. For this reason, we suppose that the disruption of the small bowel mucosa was related to the effects of long-term medications or to deteriorating health conditions that could have promoted HPVG formation^[12].

Evidence-based signs of HPVG are comparatively more important than understanding the mechanism of HPVG formation. The CT features of all five of our patients included bowel distention, gas in the superior mesenteric vein and pneumatosis intestinalis. Nonetheless, the CT findings do

not indicate the proposed mechanism of HPVG formation. CT findings of air-fluid levels and dry gas within the mesenteric veins were common signs; however, sign of mesenteric venous dry gas in our cases indicated the subsequent occurrence of gastrointestinal ischemia secondary to the venous air blockage. These signs may prospectively relate to the impending death, if the condition is irreversible.

Regardless of the CT diagnosis of HPVG, CT also provides greater detail of patients' intra-abdominal conditions. The CT features of superior mesenteric vein gas, bowel distention, pneumatosis intestinalis or pneumoperitoneum were commonly found. Signs of dry gas in multiple branches of the mesenteric veins may suggest a fatal course inducing with progressing bowel ischemia, especially among patients with deteriorating chronic systemic diseases in our cases.

REFERENCES

- 1 **Wolfe JN**, Evans WA. Gas in the portal veins of the liver in infants; a roentgenographic demonstration with postmortem anatomical correlation. *Am J Roentgenol Radium Ther Nucl Med* 1955; **74**: 486-488
- 2 **Susman N**, Senturia HR. Gas embolization of the portal venous system. *Am J Roentgenol Radium Ther Nucl Med* 1960; **83**: 847-850
- 3 **Liebman PR**, Patten MT, Manny J, Benfield JR, Hechtman HB. Hepatic--portal venous gas in adults: etiology, pathophysiology and clinical significance. *Ann Surg* 1978; **187**: 281-287
- 4 **Sebastia C**, Quiroga S, Espin E, Boye R, Alvarez-Castells A, Armengol M. Portomesenteric vein gas: pathologic mechanisms, CT findings, and prognosis. *Radiographics* 2000; **20**: 1213-1224; discussion 1224-1226
- 5 **Yamamuro M**, Ponsky JL. Hepatic portal venous gas: report of a case. *Surg Today* 2000; **30**: 647-650
- 6 **Federle MP**, Chun G, Jeffrey RB, Rayor R. Computed tomographic findings in bowel infarction. *AJR Am J Roentgenol* 1984; **142**: 91-95
- 7 **Smerud MJ**, Johnson CD, Stephens DH. Diagnosis of bowel infarction: a comparison of plain films and CT scans in 23 cases. *AJR Am J Roentgenol* 1990; **154**: 99-103
- 8 **Gosink BB**. Intrahepatic gas: differential diagnosis. *AJR Am J Roentgenol* 1981; **137**: 763-767
- 9 **Wiot JF**, Felson B. Gas in the portal venous system. *Am J Roentgenol Radium Ther Nucl Med* 1961; **86**: 920-929
- 10 **Faberman RS**, Mayo-Smith WW. Outcome of 17 patients with portal venous gas detected by CT. *AJR Am J Roentgenol* 1997; **169**: 1535-1538
- 11 **Wolff GT**. Hepatic portal venous gas. *Am Fam Physician* 1982; **26**: 185-186
- 12 **Morimoto Y**, Yamakawa T, Tanaka Y, Hiranaka T, Kim M. Recurrent hepatic portal venous gas in a patient with hemodialysis-dependent chronic renal failure. *J Hepatobiliary Pancreat Surg* 2001; **8**: 274-278

• BRIEF REPORTS •

Relationship between proliferative activity of cancer cells and clinicopathological factors in patients with esophageal squamous cell carcinoma

Jun-Xing Huang, Wei Yan, Zheng-Xiang Song, Rong-Yu Qian, Ping Chen, Eeva Salminen, Jorma Toppari

Jun-Xing Huang, Zheng-Xiang Song, Rong-Yu Qian, Ping Chen, Department of Oncology and Pathology, The People's Hospital of Taizhou, Taizhou Medical School, Yangzhou University, Taizhou 225300, Jiangsu Province, China

Wei Yan, Department of Physiology and Cell Biology, University of Nevada, Reno Room 111, Anderson Building/352 1664 South Virginia Street, Reno, NV 89557, USA

Eeva Salminen, Department of Oncology, Turku University Hospital, Turku, Finland

Jorma Toppari, Department of Pediatrics and Physiology, University of Turku, FIN-20520 Turku, Finland

Supported by the Key Medical Talent Foundation of Jiangsu Province, China, No. 2001-34 and 2002-15

Correspondence to: Dr. Jun-Xing Huang, Department of Oncology and Pathology, The People's Hospital of Taizhou, Taizhou 225300, Jiangsu Province, China. huangjunxing@yahoo.com.cn

Telephone: +86-523-6606300 Fax: +86-523-6225199

Received: 2004-06-15 Accepted: 2004-07-22

may be understood by immunohistochemistry of Ki-67 and cyclin A in Chinese patients with esophageal SCC. These cell cycle markers may serve as an indicator of cancer cell proliferation rate. The overexpression of cell cycle markers Ki-67 and cyclin A suggests the poor SCC differentiation in patients with esophageal carcinoma.

© 2005 The WJG Press and Elsevier Inc. All rights reserved.

Key words: Proliferative activity; Esophageal neoplasms; Ki-67; Cyclin A

Huang JX, Yan W, Song ZX, Qian RY, Chen P, Salminen E, Toppari J. Relationship between proliferative activity of cancer cells and clinicopathological factors in patients with esophageal squamous cell carcinoma. *World J Gastroenterol* 2005; 11(19): 2956-2959

<http://www.wjgnet.com/1007-9327/11/2956.asp>

Abstract

AIM: To assess whether the molecular markers of malignant tumors could improve the understanding of tumor characteristics, and to observe the characteristics of expression of cell cycle markers Ki-67 and cyclin A in esophageal carcinoma and to analyze the relationship between proliferative activity of cancer cells and clinicopathological factors.

METHODS: Seventy of surgically resected esophageal squamous cell carcinoma (SCC) were examined by immunohistochemistry utilizing commercially available antibodies. Nuclear staining was regarded as a positive result. At least 50 fields in each tumor and non-tumor section were evaluated at a medium power ($\times 200$) to determine the proportion of tumor cells and the staining intensity of nuclei in the entire sections.

RESULTS: Ki-67 and cyclin A were only expressed in base cells of normal esophageal mucosa. The positive immunostaining of nuclei of SCC was significantly higher than that in normal esophageal mucosa ($t = 13.32$ and $t = 7.52$, respectively, $P < 0.01$). The distribution of positively stained was more diffuse and stronger in poorly differentiated SCC. Both Ki-67 and cyclin A expressions were related to histological grades of tumors ($t = 3.5675$ and $t = 3.916$; $t = 2.13$, respectively, $P < 0.05$) but not to the sex and age of the patients, tumor size, lymphatic invasion, location, or stage grouping.

CONCLUSION: The proliferative activity of cancer cells

INTRODUCTION

Tumor cell cycle analysis has indicated that tumors with a higher proliferation rate show more aggressive clinical behaviors compared to tumors with a low proliferation rate^[1]. Immunostaining studies using antibodies that recognize the Ki-67 nuclear antigen, a marker of cell proliferation, have provided a reliable method to characterize malignant tumors^[1-3]. Ki-67 is present in all periods of the cell cycle except for G₀^[2]. Cyclin A is a cell cycle regulatory protein, which achieves its maximal level during the S and G₂ phases. It is regarded as a regulator of the transition to mitosis^[4].

Esophageal carcinoma is the sixth most common cancer in the world, and one of the most lethal tumors. Especially, there is a high morbidity and mortality for this disease in China, accounting for 54% of all new esophageal cancers in the world^[5]. Several studies have focused on cell cycle regulatory proteins in this cancer, trying to thoroughly elucidate its relation to clinicopathologic features and prognosis of esophageal carcinoma. Ikeda *et al*^[6], have found a significant correlation of Ki-67 expression to patient survival; Furihata *et al*^[7], reported that patients with cyclin A immunopositivity had a significantly poorer survival rate in esophageal squamous cell carcinoma (SCC). Several studies have demonstrated poor prognosis patients with down-regulation of p27 in this carcinoma^[8,9]. Nagasawa *et al*^[10], reported that immunohistochemical examination of cyclin D1 expression could provide important prognostic information

in univariate and multivariate analyses and might be necessary for determining therapeutic strategies for esophageal cancer. Other studies have found that the expression of cell cycle markers is associated with the response to chemoradiotherapy in esophageal SCC^[11,12], which is a very useful discovery for clinical oncology. However, study of cell cycle markers (Ki-67 and cyclin A) in esophageal SCC has not been reported in Chinese patients. In the present study, the expression of Ki-67 and cyclin A by immunostaining was found to be associated with the clinical characteristics of Chinese patients with esophageal cancer.

MATERIALS AND METHODS

Patients and specimens

Seventy patients (54 males and 16 females) with esophageal SCC underwent a surgical resection at the Department of Thoracic Surgery, People's Hospital of Taizhou (Taizhou Medical School, Yangzhou University) between May 1999 and December 2002. All patients were operated with subtotal or total esophagectomy and radical lymph node dissection. Histopathologic specimens were fixed in 10% buffered formalin, processed routinely, and embedded in paraffin. All specimens were obtained from patients who did not receive chemo- or radiotherapy prior to surgical resection. All hematoxylin-eosin stained sections were reviewed and re-examined by pathologists. The grade of tumor differentiation was determined according to the histologic classification of the World Health Organization^[13]. Tumors were staged according to the TNM classification of the esophagus^[14].

Antibodies

The following antibodies were used in this study: mouse monoclonal antibody anti-human Ki-67 (Novocastra Laboratories Ltd, Newcastle, UK), rabbit polyclonal antibody anti-human cyclin A (H-432) (Lab Vision Corporation, Fremount, CA). The final diluted concentrations (in TBS containing 1% BSA) were for anti-Ki-67 1:200 and for anti-cyclin A 1:250.

Immunohistochemical staining

The specimens with adjacent noncancerous esophageal mucosa were cut into 4–5- μ m-thick sections and mounted onto Superfrost Plus slides (Germany), deparaffinized with xylene, rehydrated with graded concentrations of ethanol. Endogenous peroxidase activity was blocked with 0.3% H₂O₂ in methanol. The slides were washed twice in TBS buffer (10 mmol/L Tris-HCl, 100 mmol/L NaCl, pH 7.5) for 5 min. Before application of the primary antibody, a microwave antigen retrieval technique was used (at 700 W for 15 min in 10 mmol/L sodium citrate solution, pH 6.0), after washing twice with TBS, an aliquot of 100 μ L blocking solution (TBS containing 1% BSA, 3% fetal calf serum, and 3% normal horse serum for mouse monoclonal antibody or 3% normal goat serum for rabbit polyclonal antibody) was applied to each section and incubated for 1 h at RT. Then, an aliquot of 100 μ L primary antibody was applied to each section and incubated at 4 °C overnight. After being washed thrice with TBS, the secondary antibody (biotinylated horse antimouse or goat antirabbit IgG, Vector Laboratories, Inc., Burlingame, CA) was applied for 30 min at RT. Immun-

ostaining was performed using the avidin-biotin-peroxidase complex technique (Vector Laboratories, Inc.). Immunoreactions were visualized with 0.0067% diaminobenzidine (Sigma) as the substrate with 0.03% hydrogen peroxide in 100 mmol/L Tris-HCl buffer for 3 min. The sections were lightly counterstained in Harris hematoxylin solution for microscopic examination. Simultaneously, each section was incubated with nonimmune mouse IgG or rabbit IgG instead of the primary antibody for an internal negative control.

The immunostained specimens were analyzed by two independent pathologists. Nuclear staining was regarded as a positive result. At least 50 fields in each tumor and non-tumor section were evaluated at a medium power ($\times 200$) to determine the proportion of tumor cells and the staining intensity of nuclei in the entire sections. The tumor cellularity was scored from 1 to 6 based on the proportion of tumor cells and the staining intensity was scored from 0 to 6 according to the intensity and staining pattern of the section. The staining index (SI) was calculated by multiplying the cellularity and staining scores as described previously^[15]. Finally, the SI for a section was calculated as the mean of the SIs of all fields examined in that section. To confirm the reproducibility of the result, all sections were scored twice: the highest score for each index and the highest score between the two observers were thus reported.

Statistical analysis

The mean follow-up period was too short (18 mo) to allow the comparison with the disease-free and the overall survival times of our patients. We performed statistical analysis to verify the possibility of an association between the different variables of the considered tumors (histological type and grading, evidence of metastasis, and Ki-67, cyclin A expression levels). The correlations between the expression of Ki-67, cyclin A proteins and the various clinicopathological factors considered were determined using the Student's *t* test at the 5% level.

RESULTS

Expression pattern of Ki-67 and cyclin A in normal human esophageal mucosa and in esophageal SCC

Without specific primary antibody to Ki-67 or cyclin A, no staining was observed in esophageal specimens (Figures 1A and E). Ki-67 and cyclin A were only expressed in base cells of normal esophageal mucosa (Figures 1B and F). The staining of Ki-67 was confined to the nuclei of cells, while the staining of cyclin A was concentrated mainly on the nuclei of cells, occasionally, the cytoplasm was also stained. Ki-67 immunostaining was also confined to the nuclei of neoplastic cells. Ki-67 staining was observed in well- and moderately differentiated esophageal SCC (Figure 1C), but it was more diffuse and stronger in poorly differentiated SCC (Figure 1D). The distribution of positively stained cyclin A was similar to that of Ki-67 staining (Figures 1G and H).

Ki-67 and cyclin A staining and clinicopathological factors

The correlations between the SIs of Ki-67, cyclin A and the clinicopathologic features of esophageal SCC are

summarized in Table 1. The SIs of Ki-67 and cyclin A did not significantly correlate with the sex and age of patients or with tumor stage, but were significantly higher in carcinomas than in normal tissues ($t = 13.32$ and $t = 7.52$, respectively, $P < 0.01$ for each protein).

Table 1 Relationship between Ki-67, cyclinA and clinicopathologic characteristics of esophageal SCC (mean \pm SD)

Factor	n	SI			
		Ki-67	P	Cyclin A	P
Sex					
M	54	23.5 \pm 5.9		13.9 \pm 6.3	
F	16	22.3 \pm 6.8	>0.05	12.0 \pm 6.1	>0.05
Age (yr)					
<60	29	23.1 \pm 6.2		13.8 \pm 6.9	
≥ 60	41	22.1 \pm 6.9	>0.05	12.5 \pm 6.3	>0.05
Histological grade					
Normal	20	3.9 \pm 2.1		2.8 \pm 1.2	
SCC	70	22.6 \pm 6.1	<0.01	13.1 \pm 6.2	<0.01
Well	26	21.0 \pm 6.5		11.5 \pm 6.5	
Moderate	24	20.3 \pm 5.9	<0.05	13.0 \pm 6.8	
Poor	20	27.4 \pm 5.1	<0.05	15.6 \pm 5.4	<0.05
Lymphatic invasion					
(-)	39	22.0 \pm 6.9		12.6 \pm 6.7	
(+)	31	24.2 \pm 5.2	>0.05	13.1 \pm 5.8	>0.05
Location					
Cervical	1	24.1		13.3	
Upper	8	23.4 \pm 6.2		12.7 \pm 4.9	
Middle	46	22.0 \pm 7.1		10.9 \pm 6.4	
Lower	15	22.3 \pm 4.9	>0.05	12.1 \pm 5.0	>0.05
Stage					
0	1	18.2		7.3	
I	15	22.9 \pm 6.5		14.0 \pm 6.8	
II	43	20.6 \pm 6.7		12.5 \pm 5.8	
III	7	23.5 \pm 5.9		12.8 \pm 5.5	
IV	4	24.8 \pm 6.2	>0.05	13.1 \pm 6.0	>0.05

Cervical: cervical esophagus; upper: upper intra-thoracic esophagus; middle: middle intra-thoracic esophagus; lower: lower intra-thoracic esophagus.

The Ki-67 SI ranged 7.7-34.5 (mean: 22.6 \pm 6.1). The index did not correlate significantly to the sex and age of patients, tumor size, lymph node metastasis, depth of invasion or tumor stage. However, the index was significantly higher in poorly differentiated SCC than in well- and moderately differentiated SCC ($t = 3.5675$ and $t = 3.916$, respectively, $P < 0.05$).

The cyclin A SI ranged 3.2-29.2 (mean: 13.1 \pm 6.2) and was not significantly related to the sex and age of patients, tumor size, lymph node metastasis, depth of invasion or tumor stage. Compared to Ki-67, the cyclin A SI correlated with tumor differentiation and was significantly higher in poorly differentiated SCC than in well-differentiated SCC ($t = 2.13$, $P < 0.05$).

DISCUSSION

The proliferative activity of esophageal SCC has been investigated by calculating the immunohistochemical index of cell proliferation using two cell cycle regulators, Ki-67 and cyclin A, as markers^[6-10]. Because Ki-67 is present in proliferating cells but not in cells in the G₀ phase, it may serve as an indicator of cancer cell proliferation rate. Our results suggested that the SI of Ki-67 correlated with differentiation of esophageal SCC but not with lymph node metastasis and stage of tumors. During the cell cycle progression, cyclin A is involved in the onset of DNA replication and is required for the G₂-M transition. Overexpression of cyclin A would, therefore, contribute to the high proliferative activity in cancer cells. In our study, the SI of cyclin A was higher in esophageal SCC than in normal tissues ($P < 0.01$), thus esophageal SCC exhibited overexpression of cyclin A. Several researchers have also demonstrated that the expression of cell cycle markers varies in esophageal precancerous lesions

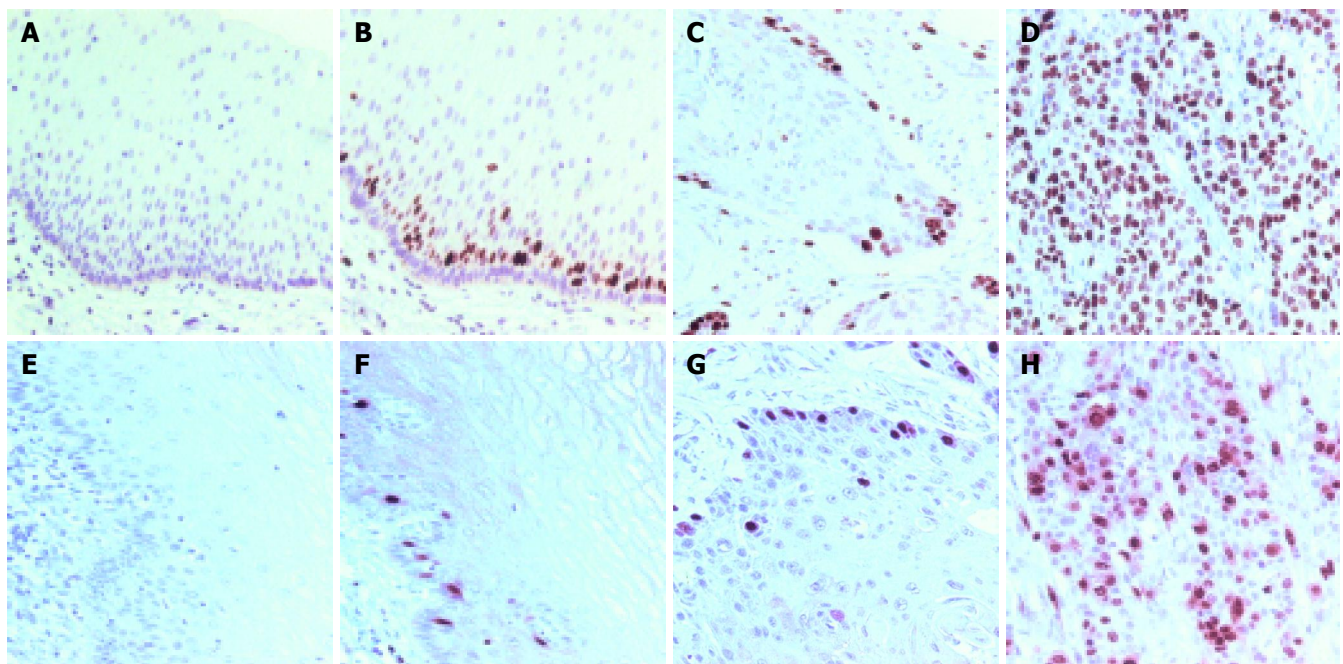


Figure 1 Ki-67 and cyclin A staining patterns in human normal esophageal mucosa and esophageal SCC. **A** and **E**: Negative control in normal esophageal mucosa; **B** and **F**: positive nuclear staining in normal esophageal mucosa; **C** and **G**: moderately differentiated SCC; **D** and **H**: poorly differentiated SCC.

Positive nuclear staining was located in base cells in normal mucosa. The diffuse and strong Ki-67 immunostaining in esophageal SCC and the higher SI of the poorly differentiated SCC were found compared with the other carcinomas. Counterstaining with hematoxylin, $\times 200$.

and cancer tissues, and these markers help distinguish high-grade dysplasia from mucosal invasive carcinoma^[16]. The SI of cyclin A was also significantly higher in poorly differentiated SCC than in well-differentiated SCC, suggesting that cyclin A may reflect the high proliferative activity of cancer cells. The observation is concordant to results reported by Furihata *et al*^[7], and Nozoe *et al*^[17].

In conclusion, cell cycle regulatory proteins Ki-67 and cyclin A are expressed in esophageal SCC and associated with some clinicopathological features of Chinese patients. These biologic markers may improve the characterization of esophageal SCC.

REFERENCES

- 1 **Tubiana M**, Courdi A. Cell proliferation kinetics in human solid tumors: relation to probability of metastatic dissemination and long-term survival. *Radiother Oncol* 1989; **15**: 1-18
- 2 **Gerdes J**, Lemke H, Baisch H, Wacker HH, Schwab U, Stein H. Cell cycle analysis of a cell proliferation-associated human nuclear antigen defined by the monoclonal antibody Ki-67. *J Immunol* 1984; **133**: 1710-1715
- 3 **Cattoretti G**, Becker MH, Key G, Duchrow M, Schluter C, Galle J, Gerdes J. Monoclonal antibodies against recombinant parts of the Ki-67 antigen (MIB 1 and MIB 3) detect proliferating cells in microwave-processed formalin-fixed paraffin sections. *J Pathol* 1992; **168**: 357-363
- 4 **Cordon-Cardo C**. Mutations of cell cycle regulators. Biological and clinical implications for human neoplasia. *Am J Pathol* 1995; **147**: 545-560
- 5 **Parkin DM**, Laara E, Muir CS. Estimates of the worldwide frequency of sixteen major cancers in 1980. *Int J Cancer* 1988; **41**: 184-197
- 6 **Ikeda G**, Isaji S, Chandra B, Watanabe M, Kawarada Y. Prognostic significance of biologic factors in squamous cell carcinoma of the esophagus. *Cancer* 1999; **86**: 1396-1405
- 7 **Furihata M**, Ishikawa T, Inoue A, Yoshikawa C, Sonobe H, Ohtsuki Y, Araki K, Ogoshi S. Determination of the prognostic significance of unscheduled cyclin A overexpression in patients with esophageal squamous cell carcinoma. *Clin Cancer Res* 1996; **2**: 1781-1785
- 8 **Shamma A**, Doki Y, Tsujinaka T, Shiozaki H, Inoue M, Yano M, Kawanishi K, Monden M. Loss of p27(KIP1) expression predicts poor prognosis in patients with esophageal squamous cell carcinoma. *Oncology* 2000; **58**: 152-158
- 9 **Ohashi Y**, Sasano H, Yamaki H, Shizawa S, Shineha R, Akaishi T, Satomi S, Nagura H. Cell cycle inhibitory protein p27 in esophageal squamous cell carcinoma. *Anticancer Res* 1999; **19**: 1843-1848
- 10 **Nagasawa S**, Onda M, Sasajima K, Makino H, Yamashita K, Takubo K, Miyashita M. Cyclin D1 overexpression as a prognostic factor in patients with esophageal carcinoma. *J Surg Oncol* 2001; **78**: 208-214
- 11 **Nakajima Y**, Miyake S, Tanaka K, Ogiya K, Toukairin Y, Kawada K, Nishikage T, Nagai K, Kawano T. The expressions of p21 and pRB may be good indicators for the sensitivity of esophageal squamous cell cancers to CPT-11: Cell proliferation activity correlates with the effect of CPT-11. *Cancer Sci* 2004; **95**: 464-468
- 12 **Takeuchi H**, Ozawa S, Ando N, Kitagawa Y, Ueda M, Kitajima M. Cell-cycle regulators and the Ki-67 labeling index can predict the response to chemoradiotherapy and the survival of patients with locally advanced squamous cell carcinoma of the esophagus. *Ann Surg Oncol* 2003; **10**: 792-800
- 13 **Sarbia M**, Bittinger F, Porschen R, Dutkowski P, Willers R, Gabbert HE. Prognostic value of histopathologic parameters of esophageal squamous cell carcinoma. *Cancer* 1995; **76**: 922-927
- 14 **Iizuka T**, Onoda T. TNM classification of carcinoma of the esophagus. *Gan To Kagaku Ryoho* 1997; **24**: 893-901
- 15 **King RJ**, Coffey AI, Gilbert J, Lewis K, Nash R, Millis R, Raju S, Taylor RW. Histochemical studies with a monoclonal antibody raised against a partially purified soluble estradiol receptor preparation from human myometrium. *Cancer Res* 1985; **45**: 5728-5733
- 16 **Ohbu M**, Kobayashi N, Okayasu I. Expression of cell cycle regulatory proteins in the multistep process of oesophageal carcinogenesis: stepwise over-expression of cyclin E and p53, reduction of p21(WAF1/CIP1) and dysregulation of cyclin D1 and p27(KIP1). *Histopathology* 2001; **39**: 589-596
- 17 **Nozoe T**, Korenaga D, Futatsugi M, Saeki H, Ohga T, Sugimachi K. Cyclin A expression in superficial squamous cell carcinoma of the esophagus and coexisting infiltrated lymphocyte follicle. *Cancer Lett* 2002; **188**: 221-229

• BRIEF REPORTS •

Phage displaying peptides mimic schistosoma antigenic epitopes selected by rat natural antibodies and protective immunity induced by their immunization in mice

Min Wang, Xin-Yuan Yi, Xian-Ping Li, Dong-Ming Zhou, McReynolds Larry, Xian-Fang Zeng

Min Wang, Xian-Ping Li, Department of Clinical Laboratory, The Second Xiangya Hospital of Central South University, Changsha 410011, Hunan Province, China

Xin-Yuan Yi, Xian-Fang Zeng, Dong-Ming Zhou, Department of Parasitology, Xiangya Medical College of Central South University, Changsha 410078, Hunan Province, China

McReynolds Larry, Molecular Parasitology Group, New England Biolabs, Inc., Beverly, MA 01915, USA

Supported by the WHO/TDR, No. 980255 and the Science Commission of Hunan Province, No. 00jzy2115

Co-first-authors: Min Wang and Xin-Yuan Yi

Co-correspondents: Xin-Yuan Yi

Correspondence to: Min Wang, Department of Clinical Laboratory, The Second Xiangya Hospital of Central South University, Changsha 410011, Hunan Province, China. wangmin0000@yahoo.com.cn

Telephone: +86-731-5550258

Received: 2004-06-28 Accepted: 2004-07-22

Abstract

AIM: To obtain the short peptides mimic antigenic epitopes selected by rat natural antibodies to schistosomes, and to explore their immunoprotection against schistosomiasis in mice.

METHODS: Adults worm antigens (AWA) were analyzed by sodium dodecyl sulfate-polyacrylamide gel electrophoresis (SDS-PAGE) and enzyme-linked transferred immunoblotting methods with normal SD rat sera (NRS). The killing effects on schistosomula with fresh and heat-inactivated sera from SD rats were observed. Then the purified IgG from sera of SD rats was used to biopanning a phage random peptide library and 20 randomly selected positive clones were detected by ELISA and 2 of them were sequenced. Sixty female mice were immunized thrice with positive phage clones (0, 2nd, 4th wk). Each mouse was challenged with 40 cercariae, and all mice were killed 42 d after challenge. The worms and the liver eggs were counted.

RESULTS: NRS could specifically react to the molecules of 75 000, 47 000, 34 500 and 23 000 of AWA. Sera from SD rats showed that the mortality rate of schistosomula was 76.2%, and when the sera were heat-inactivated *in vitro*, the mortality rate was decreased to 41.0% after being cultured for 48 h. The specific phages bound to IgG were enriched about 300-folds after three rounds of biopanning. Twenty clones were detected by ELISA, 19 of them bound to the specific IgG of rat sera. Immunization with these epitopes was carried out in mice. Compared with the control groups, the mixture of two mimic peptides

could induce 34.9% ($P = 0.000$) worm reduction and 67.6% ($P = 0.000$) total liver egg reduction in mice. Two different mimic peptides could respectively induce 31.0% ($P = 0.001$), 14.5% ($P = 0.074$) worm reduction and 61.2% ($P = 0.000$), 35.7% ($P = 0.000$) total liver egg reduction. The specific antibody could be induced by immunization of the mimic peptides, and the antibody titer in immunized mice reached more than 1:6 400 as detected by ELISA.

CONCLUSION: Specific peptides mimic antigenic molecules can be obtained by biopanning the phage random peptide library and a partially protective immunity against schistosome infection can be stimulated by these phage epitopes in mice.

© 2005 The WJG Press and Elsevier Inc. All rights reserved.

Key words: *Schistosome*; Phage peptide library; Epitope; Mimic peptide; Protective immunity; Vaccine

Wang M, Yi XY, Li XP, Zhou DM, Larry M, Zeng XF. Phage displaying peptides mimic schistosoma antigenic epitopes selected by rat natural antibodies and protective immunity induced by their immunization in mice. *World J Gastroenterol* 2005; 11(19): 2960-2966

<http://www.wjgnet.com/1007-9327/11/2960.asp>

INTRODUCTION

It is a major strategy to develop vaccines against schistosomiasis recommended by the World Health Organization^[1]. In recent years, studies on vaccines have progressed rapidly, and a series of vaccine candidates have been identified and tested against schistosome infection in experimental models^[2]. Nevertheless, these vaccines provide only 20-40% protection against the challenge of schistosoma cercariae. The protection so far achieved could not meet the need for control of this disease^[3-5]. So scientists now intend to use new techniques for developing anti-schistosomiasis vaccines. Phage displaying technique appears to be a very powerful and promising technique.

Schistosome has a very broad range of hosts including more than 40 kinds of mammals, but adaptability and permissibility of the parasite in various mammals are different. Chinese researchers have discovered that the growth and development of schistosomes in rats are slower than those in permissive hosts. According to the research

of Yu *et al.*^[6], the worms and egg-granulomas in rat livers were rarely observed when rats were challenged with *Schistosoma japonicum* (*S.j*) cercariae. The majority of eggs were unripe eggs and black dead eggs and the number of mean liver eggs per gram (LEPG) was 1 393.46, apparently less than that in the permissive host mouse. These results indicate that some factors are related to the natural resistance that existed in rats. Our previous research^[7] showed that the levels of IgG to adult worm antigens (AWA) and soluble egg antigens (SEA) in normal rat sera (NRS) and infected rat sera (IRS) were significantly higher than the corresponding levels observed in the uninfected mice sera. High levels of protection against schistosomes could be induced. Now the common understanding acknowledged is that rats are semi-permissive hosts of schistosomes that have been used as an experimental model for vaccine development.

The work described in this paper was performed to explore the immunological characteristics of natural resistance to *S.j* infection in rats, evaluate the killing effects on schistosomula *in vitro*, and determine whether individual peptides selected from a phage random peptide library of 12-mer by the NRS could induce the immune protection in mice. The results showed that the specific antibodies existed in rats, which play an important role in killing the larva, and the two peptides (P3, P5) selected from the library in this way can induce an antibody response, which confer a partial protection against infection in mice. These experimental data provide the basis for a peptide vaccine.

MATERIALS AND METHODS

Phage display peptide library

Phage library and host strain *E.coli* ER 2738 were a kind present from Professor Larry McReynolds in New England Biolabs, USA. The library, which was based on a combined library of random peptide 12-mer fused to a minor coat protein (pIII), consists of 2.7×10^9 electroporated sequences and the phage titer is 1.5×10^{12} pfu/mL.

Animals

All experimental animals were provided by the Animal Center, Central South University, Xiangya School of Medicine, including 10 SD female rats (300-350 g), 10 male mice (25-30 g) and 60 female mice (18-22 g) of Kunming strain and 4 male rabbits (1.5-2 kg).

Oncomelania hupensis

S.j cercariae were released from *Oncomelania hupensis* purchased from Hunan Institute of Parasitic Diseases, YueYang, China.

Reagents

All reagents and chemicals used in this study were of analytical grade or the best quality purchased from domestic and international companies.

Preparation of sera

The rats and 10 male mice were given 500 and 40 *S.j* cercariae respectively, killed 45 d after infection, and the infected sera (IRS and IMS) were collected. Normal rat

sera (NRS) and normal mice sera (NMS) were obtained before challenge infection. Rabbit sera pool (RS) was taken and heat-inactivated NRS were incubated at 56 °C for 30 min in an attempt to deplete the complements. All sera were filtered with a microcell filter (Φ 0.22 μ m) to eliminate RBC fragments and bacteria.

SDS-PAGE and Western blot

S.j AWA was separated by 10% sodium dodecylsulfate polyacrylamide gels (SDS-PAGE). After electrophoresis (20 mA for 2 h), the separated proteins were transferred onto a nitrocellulose membrane (120 mA for 2 h), and then the membrane was blocked with 3% non-fat milk. After that, nitrocellulose strips were incubated with 1:100 diluted NRS, IRS, NMS and IMS for 2 h at 37 °C respectively. The strips were cultured with horseradish peroxidase-labeled goat -anti-mouse IgG conjugates (1:3 000 dilution) for 2 h after being washed. Following washing, the strips were visualized by staining with 3,3'-diaminobenzidine and the molecular weight of tested proteins was calculated according to RF value of the marker.

Schistosomula

The cercariae released from *Oncomelania hupensis* were collected for 10 min on ice. After being spun for 5 min at 1 500 r/min, the supernatant was decanted. The pellet was washed and centrifuged thrice with Earle's culture medium containing 300 U/mL penicillin and 300 μ g/mL streptomycin. Then the cercariae were suspended in RPMI 1640 containing 35% heat-inactivated rabbit sera. The suspension was subsequently added to 24-well culture plates and the density was adjusted to 200 ± 20 cercariae/mL and maintained at 37 °C in a 5% atmosphere in 1 mL of RPMI 1640 culture medium (100 U/mL penicillin, 100 μ g/mL streptomycin).

Killing effect in vitro

Duplicate wells of a 24-well flat-bottomed microtiter plates were placed in RPMI 1640 containing NRS, heat-inactivated NRS, NMS and RS with a concentration of 10%. The number of dead and alive schistosomula was counted under a reverse microscope after *in vitro* culture for 24, 48 and 72 h. The mortality was calculated [the mortality (%) = (dead schistosomula/total schistosomula) \times 100%]. The judgment criteria of dead schistosomula were referred to Vadas *et al.*^[8]. The interior structure was vague, the tegument membrane was destroyed, and the inside substance was released as radiation, or the schistosomula was inactive with an obscure structure.

Biopanning of the phage peptide library

Serum pools were obtained from normal rats. The IgG from rat sera was purified by ammonium sulfate precipitation method (50-33-33%). Then the supernatant was dialyzed against phosphate-buffered saline (PBS, pH 7.2). Microtiter wells were coated overnight at 4 °C with 100 μ g/well of the purified IgG from NRS. The plates were then blocked with 3% nonfat milk for 2 h at 37 °C, washed five times with 0.05% Tween-20 in Tris-buffered saline (PBST). One hundred microliters of the diluted library containing 1.5×10^{11} pfu was added to the coated plates and incubated

at room temperature for 1 h. Following that, bound phages were subsequently eluted with 100 μ L of 0.2 mol/L glycine-HCl (pH 2.2) and neutralized with 1 mol/L Tris-HCl (pH 9.1). Then the eluted phages were amplified in host strain *E. coli* 2738 and purified by precipitation for about 4 h using 1/6 volume of PEG/NaCl. Another two rounds of affinity selection were carried out in the same way, but 1:200 and 1:400 sera dilution was used and added to 100 μ L of diluted phages from those of the last round. The percentage of enrichment of phage clones was calculated using the following formula: percentage enrichment of phage clones (%) = (eluted phages/added phages) \times 100%.

Amplifying and titting of phages

The eluted phages were added to the host strain ER2738 culture (A_{600} -0.5) and incubated at 37 $^{\circ}$ C with vigorous shaking for 4.5 h. The culture was transferred to a tube and spun at 10 000 *g* for 10 min at 4 $^{\circ}$ C. The supernatant was transferred and spun once again. Then the upper 80% of the supernatant was removed to a fresh tube and 1/6 volume of PEG/NaCl was added. Then the phages were allowed to precipitate at 4 $^{\circ}$ C overnight. The supernatant was spun and decanted at 12 000 *g* for 10 min. The suspended deposit was precipitated with PEG again. After being incubated on ice for 1 h and spun for 20 min, the supernatant was discarded and the pellet was suspended in 200 μ L TBS, 0.02% NaN_3 . After being micro-centrifuged for 1 min, remaining insoluble matter was pelleted, the supernatant contained the amplified phages. The amplified phages were diluted by a series of different titers. Ten microliters of each dilution was added to 200 μ L host strain culture, mixed and incubated for 20 min at 37 $^{\circ}$ C. Then cells were transferred to a culture tube containing 45 $^{\circ}$ C agarose, quickly vortexed and immediately poured onto pre-warmed LB plates. After being cooled, the plates were inverted and incubated for 16 h at 37 $^{\circ}$ C. The plates were inspected and the plaques on plates were counted. The phage titer was obtained.

Enzyme-linked immunosorbent assay (ELISA)

Ten microliters of eluted phages from the third round was added to 200 μ L of the host strain cultured overnight, and incubated for 20 min at 37 $^{\circ}$ C to finish transfection. Then the transfected cells were transferred to a culture tube with agarose, quickly vortexed and immediately poured onto a pre-warmed LB plate. After being cooled for 5 min, the plates were inverted and incubated overnight at 37 $^{\circ}$ C. On the 2nd d, 20 clones were randomly picked. Each selected clone was amplified, purified and tittered according to the procedure described above. The ELISA wells were coated with 2×10^{11} phage particles and then blocked with 3% nonfat milk. Afterwards 100 μ L of 1:200 diluted NRS was added and allowed to bind for 2 h at 37 $^{\circ}$ C. The wells were subsequently washed with PBS containing 0.05% Tween-20 (PBST). After goat anti-mouse IgG conjugated to HRP was added, specially bound antibodies were visualized by adding 3,3',5,5'-tetramethylbenzidine. The absorbance was determined at 595 nm. The original phage library was used as a negative control. Phage clones were considered positive when the *A* value was 2.1-fold higher

than that of the negative control.

DNA sequencing of selected phages

Two phage clones that showed *A* values higher than the others were precipitated with PEG/NaCl. Their single-strand DNA was prepared by phenol extraction. These two phages were automatically sequenced on the ABI PRISM 377 sequencer using the -28 g111 sequencing primer (5'-110 GTA TGG GAT TTT GCT AAA CAA C-3') from the phage display peptide library kit.

Immunization and challenge

Female Kunming mice were divided into five groups. The experimental groups (P5+P3 mixture group, P5 group, P3 group) were injected with 0.2 mL positive clones (containing 10^{13} phage particles) thrice (0, 2nd, 4th wk). Two control groups were injected with original phages or TBS buffer. Blood samples were collected by tail vein puncture before immunization and challenge. The antibody response induced was analyzed by ELISA. At the 5th wk, each mouse was percutaneously infected with 40 ± 1 *S.j.* cercariae. All mice were killed and perfused 45 d post-infection, and the worm and liver eggs were counted.

Statistical analysis

Significance testing was conducted by analysis of variance between experimental and control groups using one-way ANOVA of SPSS software. $P < 0.05$ was considered statistically significant. Results were presented as mean \pm SD.

RESULTS

Recognition of *S.j* AWA by NRS

NRS was tested for its recognition of AWA by Western blot (Figure 1). The results showed that NRS and IRS could recognize four bands of AWA. Their molecular weight was 75 000, 47 000, 34 500 and 23 000, respectively.

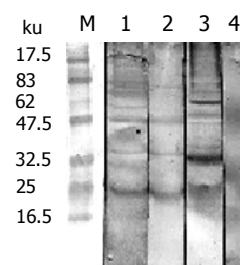


Figure 1 Immunological recognition bands of AWA in rat sera. M: Molecular weight standards; 1: IRS; 2: NRS; 3: IMS; 4: NMS.

Killing effects *in vitro*

Killing effects of different sera (NRS, heat-inactive NRS, NMS and RS) on schistosomula *in vitro* were studied in 24-, 48- and 72-h culture (Table 1). The mortality of larva after being cultivated for 48 and 72 h was not significantly different in each sera group. The mortality rates were 23% and 76.2% in NRS after 24- and 48-h cultivation, which showed that the killing effect of NRS was higher than those

of other sera. Nevertheless, when the NRS was heated at 56 °C for 30 min to inactivate the complement components, the mortality rates were 16.9% and 41.0%, respectively. The result implied that the complements and the antibodies of NRS had significant effects on killing the early phase schistosomula *in vitro*.

Table 1 Killing effect of different sera on schistosomula *in vitro*

Sera	Schistosomula (<i>n</i>)	Mortality (%)		
		24 h	48 h	72 h
NRS	206	23.0	76.2	86.4
Heat-inactive normal rat sera	234	16.9	41.0	43.6
NMS	240	6.4	23.8	30.0
RS	231	4.7	16.9	21.2

Analysis of enrichment

The percentages of phage enrichment after three rounds of biopanning are presented in Table 2. In the condition of decreasing IgG antibody concentration gradually, the specific phages bound to IgG were increased. The eluted phages increased from 1.65×10^{-6} to 5×10^{-4} , an enrichment of about 300-folds. The data reflected a successful affinity selection of phages that were ligands for particular antibodies.

Table 2 Percentage enrichment of phages by biopanning

Biopanning	Phages added	Phages washed	Yield (%)
1	1.5×10^{11}	2.47×10^5	1.65×10^{-6}
2	1.0×10^{11}	4.26×10^6	4.26×10^{-5}
3	1.0×10^{11}	5.00×10^7	5.00×10^{-4}

Identification of positive clones

Twenty randomly selected individual clones were tested for their binding to rat sera by ELISA. Original phages were used as negative controls. The results showed that natural antibodies from NRS recognized 19 randomly selected clones. The positive percentage was 95% (Figure 2).

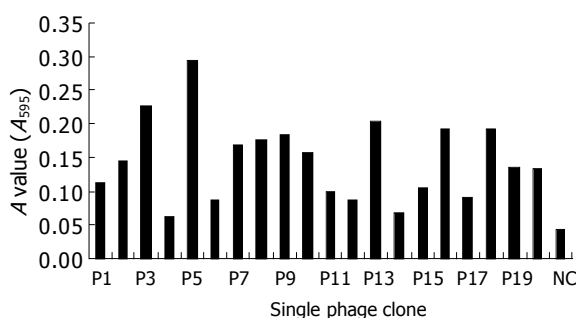


Figure 2 Detection of positive phage clones by ELISA. P1-P20: Twenty phage clones; NC: normal controls (original peptides).

Analysis of DNA sequences

The single-strand DNA from two positive phages named P3 and P5 was sequenced. The DNA sequences and the deduced amino acid (AA) sequences are listed in Table 3. We have fed the sequence data on the Internet and analyzed them using nucleotide blast software of NCBI. The results revealed that there was no significant similarity with other sequences (score <50).

Table 3 DNA and AA sequences of the positive phage clones (P3, P5)

Clone	DNA sequence	AA sequence
P3	AAACGGAGGCTGCGGCCAGT AGAGTGAGAATAGAA	KRRLRPSRVRIE
P5	AATATGCCTATTAGCATGAAG AGAGTGAGAATAGAA	NMPASMKRVRIE

Detection of antibodies after immunization with phages

Compared with control groups, the specific antibodies could be stimulated and detected by ELISA in mice after the third immunization with positive phage clones, and the titer of specific antibodies was $>1:6400$, significantly higher than that in control groups (Figure 3).

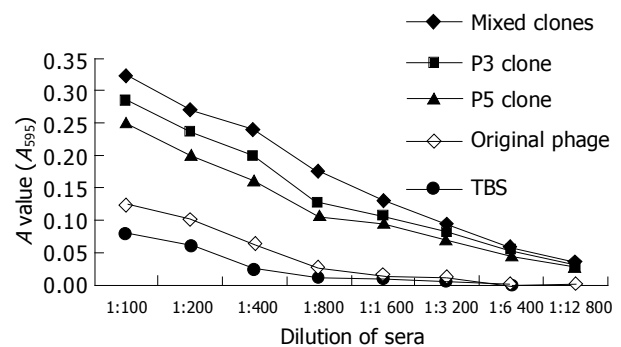


Figure 3 Antibody titer in sera of mice after the third immunization.

Protection against challenge with *S.j* cercariae

All mice were perfused and the number of worms and the number of liver eggs were counted 42 d after being challenged with 40 ± 1 *S.j* cercariae. Compared with the control groups, the group immunized with the mixture of two mimic peptides (P3+P5) showed 34.9% worm reduction and 67.6% total liver egg reduction. Two different groups immunized with P3 or P5 showed 31.0%, 14.5% worm reduction and 61.2%, 35.7% total liver egg reduction, respectively. Some immune protection could be seen in original phage controls, but there was no statistical significance between the two control groups (Tables 4 and 5).

DISCUSSION

Schistosomiasis is a serious parasitic disease with over 200 million people infected worldwide and causes about estimated 1 million deaths per year. In the past 50 years,

Table 4 Worm reduction in mice immunized with phage clones (mean±SD)

Groups	Mice (n)	Worms (n)	Worm reduction rates (%)	P
Mix phage (P3+P5) immunized	12	19.42±5.99	34.90	0.000 ^a
P3 immunized	12	20.58±5.36	31.01	0.001 ^a
P5 immunized	12	25.50±4.17	14.52	0.074
Original phage control	12	27.92±5.08	6.40	0.338
TBS control	12	29.83±2.92	–	–

^aP<0.05 vs TBS control group.**Table 5** Reduction in egg load in liver of mice immunized with phage clones (mean±SD)

Groups	Mice (n)	LEPG (×10 ⁴)	LEPG reduction rate (%)	P
Mix phage (P3+P5) immunized	12	0.890±0.063	67.62	0.000 ^a
P3 immunized	12	1.073±0.136	61.20	0.000 ^a
P5 immunized	12	1.769±0.063	35.65	0.000 ^a
Original phage control	12	2.255±0.142	17.97	0.013 ^a
TBS control	12	2.749±0.144	–	–

^aP<0.05 vs TBS control group.

though some control strategies have been successfully employed in some regions, the disease remains endemic in 76 developing countries and more than 600 million people are at risk of schistosoma infection. As investigated, the patients presented with a series of serious symptoms. Praziquantel, as a major drug for schistosomiasis, has been reported to develop resistance^[9-11]. Furthermore, re-infection occurs rapidly in endemic regions. So it is the most effective strategy to develop vaccine against schistosomiasis. Scientists have studied different types of schistosomiasis vaccines. Despite the progress achieved, a feasible anti-schistosomiasis vaccine for humans or livestock has not been found.

In contrast to mouse as a permissive host of schistosomes, rats could eliminate the primary schistosomes around 4 wk post-infection and subsequently developed protective immunity to re-infection. In rats with schistosomiasis, a predominant expression of Th2-type cytokine response at the mRNA level was shown after infection^[12]. The protective immune mechanism was related to a Th2 response^[12-14]. On d 4 and 7 post-infection, the morphology and size of schistosomula in the lung of rats were similar to those in mice, but there were strong inflammatory reactions around the schistosomula in the lung of rats. The inflammatory cells including eosinophils, neutrophils, macrophages and lymphocytes gathered around the larva and different levels of damage could be found on teguments. The inflammatory reactions in the lung of rats were significantly ameliorated on d 14 post-infection than before. These findings indicated that the immune response reacted mainly to the early-stage schistosomula^[12,15]. In this model, several other studies have revealed that the resistance is due to antibody-dependent cell-mediated cytotoxicity mechanism that plays an essential role in destructing the young schistosomula in rats^[16,17]. Passive transfer of sera from rats vaccinated with attenuated schistosoma cercariae conferred high levels of resistance against challenge. The worm reduction rate was up to 64%. Heat inactivation of sera at 56 °C for 3 h to deplete the IgE and complement components weakened the protective capacity^[12].

The specific IgG to AWA and SEA was increased after infection in rats^[6,7]. Passive transfer of NRS to mice, a reduction in worm burden and LEPC in transfer group were 19.1% and 46.4% compared with the control group^[7]. In the present study, we observed that the NRS could specifically react to four bands with molecular weights of AWA, which were 75 000, 47 000, 34 500 and 23 000. The killing effects of NRS were accessed. The mortality was

23% and 76.2% in NRS after 24- and 48-h cultivation, higher than those of other sera. Nevertheless, when the complement was depleted, the mortality decreased to 16.9% and 41.0%, respectively. These data showed that the natural antibodies to schistosomes existed in rats and might play an important role in killing young schistosomula.

Phage display library technique has become a new powerful tool. Filamentous bacteriophages display foreign peptides on their surfaces. The technique involves specific screening and affinity selection of certain phage displaying peptides that are ligands for a particular protein, and the selected phages could be applied to affinity from 10³- to 10⁸-folds according to the process of absorption, elution and amplification. Furthermore it was easy to identify the DNA sequences of specific phage peptides selected^[18]. Screening phage library could identify protein antigen epitopes^[19], study protein interaction^[20], search novel vaccines^[21] and develop drugs^[22]. Now the technique has been widely used in many fields including bacteria^[23], viruses^[24] and helminthes^[25]. For instance, Jolive-Reynaud *et al*^[26], screened a dodecapeptide library on phages with anti-NS3 mouse mAbs and human anti-HCV NS3 positive sera. Two peptides were selected since they were recognized specifically by the anti-NS3 mAbs and human sera from HCV-infected patients. Homology search showed that one shared AA similar to NS3 at residues 1 396-1 398 and the other had two AAs similar to nearby residues 1 376 and 1 378. Reproduced as synthetic dodecapeptides, the two mimotopes were recognized specifically by 12 and 22, respectively, out of 49 sera from HCV-infected patients. Other characteristics of the phages screened were that they could induce protection without the addition of any adjuvant. Because filamentous phages had the capability of activating CD₄⁺ helper T cells^[27], the phages were the ideal carrier of vaccines.

Due to the above characteristics, the technique has been used to develop vaccines against schistosomes in recent years. Arnon *et al*^[28], screened a phase 8-mer random peptide library with the protective mAb against *Schistosoma mansoni* (152-66-9B). Four epitopes were obtained. Subsequently synthetic relevant peptides (P28-P31) were prepared. The peptides except P31 were recognized by 152-66-9B. Sera from mice immunized with the peptides were tested by ELISA. The results showed that each was recognized by the respective homologous anti-sera as well as by sera from infected mice with comparable titers. Moreover, worm burden was reduced by an average of 42±3% as a result of immunization with the P30 in mice. Fu *et al*^[29], used the

purified polyclonal IgG against the *S.j* 22.6 ku antigen to screen a 12-mer phage library. The polyclonal antibody could recognize 16 clones that were randomly picked. The sera from mice immunized with six clones of them were proved to have biological activities by Western blot. Six clones were sequenced, four epitopes were then identified. One epitope (H₂) had three AA (III) sequences homologous to those of 22.6 ku. The mice immunized with the mixture of four peptide clones induced a significant worm reduction (39.5%) and total liver egg reduction (57.1%). Our previous studies also showed a protective immunity against schistosomiasis stimulated by mixed phage peptides in mice^[30,31].

The work described in this paper was designed to explore whether or not the mimic peptides recognized by rat natural antibodies could induce protective immunity against *S.j*. It should be known that B-cell response was particularly important in the course of schistosomiasis and has been used to identify potential vaccine candidates^[29,31]. Thus, the characteristics of natural antibodies in rats were tested. The results implied that natural antibodies which existed in rats had significant killing effects on schistosomula *in vitro* and the complement participated in the killing effects. A 12-mer phage random library was screened with the antibodies. It was hoped to determine that the mimic peptides could be identified in this way, and used to induce protective antibody response. Of the 20 randomly picked phage clones from a peptide library, 19 clones were shown to react specially with the NRS in ELISA and 2 clones (P3, P5) of them were bound at a higher level than the others. The two clones were analyzed to have partial homologous sequences (RVRIE). These data supported the views that these phages were able to mimic the binding properties of antigen epitopes. In a further study of the two clones, the mixed phages (P3+P5) and two individual phages (P3, P5) were used to immunize mice. Sera from mice immunized with phages had a higher binding than those immunized with the original peptides and TBS. The fact that high titers of antibodies were generated suggested that the immunization with these phages could result in the induction of protective responses. To test the phages for their protective effects, challenge experiment was performed. Significant protection was observed following immunization with the mixed phages that could induce 34.9% worm reduction and 67.6% total liver egg reduction in mice. This level of protection is similar to that of immunization with only P3 that induced 31.0% worm reduction and 61.2% total liver egg reduction, while the mice immunized with P5 induced only 14.5% worm reduction and 35.7% egg reduction. The results showed partial protection against challenge infection. Though the liver egg reduction rate that was 18.0% ($P = 0.013$) in original phage control group had a statistical significant compared with TBS control group, there was no actual significance in experiments. As far as the protective mechanism was concerned, the antibody in mice was tested. The titers of specific antibodies in mice immunized with phages were significantly higher than those in control groups (Figure 3). But there was an insignificant difference between the two groups immunized with individual phages P3 and P5. Because the antibody isotypes or cytokine expression was not detected, we could not better understand the protection.

Furthermore, though the two peptides had the core sequence, the protection induced was different. Whether the core sequence or the sequence alongside plays an important role has to be further studied. In a word, the results obtained demonstrated that the protective immunity could be induced by the selected phages without adjuvant.

In conclusion, natural antibodies to *S.j* that existed in rats play a critical role in killing schistosomula. The short peptides selected with NRS from a 12-mer random phage library have both antigenicity and immunogenicity and two peptides obtained have an identical core sequence. The selected phages stimulate a protective immunity against infection and fecundity of schistosomes. P3 phage clone, as a vaccine candidate, is worthy to be studied further.

REFERENCES

- 1 **Bergquist R**, Al-Sherbiny M, Barakat R, Olds R. Blueprint for schistosomiasis vaccine development. *Acta Trop* 2002; **82**: 183-192
- 2 **Capron A**, Capron M, Dombrowicz D, Riveau G. Vaccine strategies against schistosomiasis: from concepts to clinical trials. *Int Arch Allergy Immunol* 2001; **124**: 9-15
- 3 **McManus D**. The *Schistosoma japonicum* angle on vaccine research. *Parasitol Today* 2000; **16**: 357-358
- 4 **Yan YT**, Liu SX. Advances in the candidate vaccine antigens against *Schistosoma japonicum*. *Zhongguo Jishengchongxue Yu Jishengchongbing Zazhi* 2000; **18**: 115-119
- 5 **McManus DP**. A vaccine against Asian schistosomiasis: the story unfolds. *Int J Parasitol* 2000; **30**: 265-271
- 6 **Yu XC**, Wu GL, Wu YQ, Zhang YJ, Zhang ZH. Studies on the dynamic changes in specific antibodies isotope of IgG IgG2a IgG2c in sera from rats infected with *Schistosoma japonicum*. *Zhongguo Xuexichongbing Fangzhi Zazhi* 2000; **12**: 148-150
- 7 **Zhou DM**, Yi XY, Zeng XF, Wang M, Zhang SK. Preliminary study on the immunological characteristics of natural resistance in *Rat* to infection with *Schistosoma japonicum*. *Difangbing Tongbao* 2001; **16**: 25-28
- 8 **Vadas MA**, Butterworth AE, Sherry B, Dessein A, Hogan M, Bout D, David JR. Interactions between human eosinophils and schistosomula of *Schistosoma mansoni*. I. Stable and irreversible antibody-dependent adherence. *J Immunol* 1980; **124**: 1441-1448
- 9 **Ismail M**, Metwally A, Farghaly A, Bruce J, Tao LF, Bennett JL. Characterization of isolates of *Schistosoma mansoni* from Egyptian villagers that tolerate high doses of praziquantel. *Am J Trop Med Hyg* 1996; **55**: 214-218
- 10 **van Lieshout L**, Stelma FF, Guisse F, Falcao Ferreira ST, Polman K, van Dam GJ, Diakhate M, Sow S, Deelder A, Gryseels B. The contribution of host-related factors to low cure rates of praziquantel for the treatment of *Schistosoma mansoni* in Senegal. *Am J Trop Med Hyg* 1999; **61**: 760-765
- 11 **Gryseels B**, Mbaye A, De Vlas SJ, Stelma FF, Guisse F, Van Lieshout L, Faye D, Diop M, Ly A, Tchuem-Tchuente LA, Engels D, Polman K. Are poor responses to praziquantel for the treatment of *Schistosoma mansoni* infections in Senegal due to resistance? An overview of the evidence. *Trop Med Int Health* 2001; **6**: 864-873
- 12 **Cetre C**, Pierrot C, Cocude C, Lafitte S, Capron A, Capron M, Khalife J. Profiles of Th1 and Th2 cytokines after primary and secondary infection by *Schistosoma mansoni* in the semipermissive rat host. *Infect Immun* 1999; **67**: 2713-2719
- 13 **Gracie JA**, Bradley JA. Interleukin-12 induces interferon-gamma-dependent switching of IgG alloantibody subclass. *Eur J Immunol* 1996; **26**: 1217-1221
- 14 **Cetre C**, Cocude C, Pierrot C, Godin C, Capron A, Capron M, Khalife J. *In vivo* expression of cytokine mRNA in rats infected with *Schistosoma mansoni*. *Parasite Immunol* 1998; **20**: 135-142

- 15 **Zhou DM**, Zeng XF, Wang M, McReynold L, Yi XY. *Schistosoma japonicum*: preparation of peptides mimicking antigenic epitopes of attenuated cercariae using phage displayed random peptide library. *Zhongguo Renshou Gonghuanbing Zazhi* 2002; **18**: 73-75
- 16 **Moloney NA**, Webbe G. Antibody is responsible for the passive transfer of immunity to mice from rabbits, rats or mice vaccinated with attenuated *Schistosoma japonicum* cercariae. *Parasitology* 1990; **100** Pt 2: 235-239
- 17 **Khalife J**, Cetre C, Pierrot C, Capron M. Mechanisms of resistance to *S. mansoni* infection: the rat model. *Parasitol Int* 2000; **49**: 339-345
- 18 **Chappel JA**, He M, Kang AS. Modulation of antibody display on M13 filamentous phage. *J Immunol Methods* 1998; **221**: 25-34
- 19 **Fehrsen J**, du Plessis DH. Cross-reactive epitope mimics in a fragmented-genome phage display library derived from the rickettsia, *Cowdria ruminantium*. *Immunotechnology* 1999; **4**: 175-184
- 20 **Pedersen MV**, Kohler LB, Ditlevsen DK, Li S, Berezin V, Bock E. Neuritogenic and survival-promoting effects of the P2 peptide derived from a homophilic binding site in the neural cell adhesion molecule. *J Neurosci Res* 2004; **75**: 55-65
- 21 **Jeon SH**, Ben-Yedidia T, Arnon R. Intranasal immunization with synthetic recombinant vaccine containing multiple epitopes of influenza virus. *Vaccine* 2002; **20**: 2772-2780
- 22 **Stanojevic S**, Dimitrijevic M, Kovacevic-Jovanovic V, Miletic T, Vujic V, Radulovic J. Stress applied during primary immunization affects the secondary humoral immune response in the rat : involvement of opioid peptides. *Stress* 2003; **6**: 247-258
- 23 **Lesinski GB**, Smithson SL, Srivastava N, Chen D, Widera G, Westerink MA. A DNA vaccine encoding a peptide mimic of *Streptococcus pneumoniae* serotype 4 capsular polysaccharide induces specific anti-carbohydrate antibodies in Balb/c mice. *Vaccine* 2001; **19**: 1717-1726
- 24 **Misumi S**, Endo M, Mukai R, Tachibana K, Umeda M, Honda T, Takamune N, Shoji S. A novel cyclic peptide immunization strategy for preventing HIV-1/AIDS infection and progression. *J Biol Chem* 2003; **278**: 32335-32343
- 25 **Zhou DM**, Yi XY, Zeng XF, Wang M, McReynolds L. Immunity against *Schistosoma japonicum* induced by phage display peptides mimicking antigenic epitopes of *Trichinella spiralis*. *Zhongguo Jishengchongxue Yu Jishengchongbing Zazhi* 2001; **19**: 268-271
- 26 **Jolivet-Reynaud C**, Adida A, Michel S, Deleage G, Paranhos-Baccala G, Gonin V, Battail-Poirot N, Lacoux X, Rolland D. Characterization of mimotopes mimicking an immunodominant conformational epitope on the hepatitis C virus NS3 helicase. *J Med Virol* 2004; **72**: 385-395
- 27 **Grabowska AM**, Jennings R, Laing P, Darsley M, Jameson CL, Swift L, Irving WL. Immunisation with phage displaying peptides representing single epitopes of the glycoprotein G can give rise to partial protective immunity to HSV-2. *Virology* 2000; **269**: 47-53
- 28 **Arnon R**, Tarrab-Hazdai R, Steward M. A mimotope peptide-based vaccine against *Schistosoma mansoni*: synthesis and characterization. *Immunology* 2000; **101**: 555-562
- 29 **Fu XM**, Zhang ZS, Li CL, Wu HW, Su C, Ji MJ, Wang Y, Liu F, Wu GL. Studies on immunoprotection in mice after immunization with the epitopes of 22.6 kDa antigen of *Schistosoma japonicum*. *Zhongguo Xuexichongbing Fangzhi Zazhi* 2001; **13**: 86-89
- 30 **Ouyang L**, Yi X, Zeng X, Zhou J, Wang Q, McReynolds L. Partial protection induced by phage library-selected peptides mimicking epitopes of *Schistosoma japonicum*. *Chin Med J (Engl)* 2003; **116**: 138-141
- 31 **Wang M**, Yi XY, Zeng XF, Zhou DM, Yuan SS, Zhang SK, Zhang J. A short peptide mimicking epitopes of the membrane antigen of *Shistosoma japonicum* hepato-portal schistosomula using phage display techniques. *Zhonghua Weishengwuxue He Mianyixue Zazhi* 2003; **23**: 862-865

Chinese medicine compound Changtong oral liquid on postoperative intestinal adhesions

Xi-Xiao Yang, Han-Ping Shi, Lian-Bing Hou

Xi-Xiao Yang, Lian-Bing Hou, Department of Pharmacy, Nanfang Hospital, The First Military Medical University, Guangzhou 510515, Guangdong Province, China

Han-Ping Shi, Department of Surgery, Nanfang Hospital, The First Military Medical University, Guangzhou 510515, Guangdong Province, China

Supported by the National New Drug Foundation of China, No. 96-901-05-245

Co-correspondents: Xi-Xiao Yang

Correspondence to: Professor Lian-Bing Hou, Department of Pharmacy, Nanfang Hospital, The First Military Medical University, Guangzhou 510515, Guangdong Province, China. yaxx@263.net
Telephone: +86-20-61641888-87236 Fax: +86-20-87701797

Received: 2004-07-19 Accepted: 2005-03-16

activity of PAI and OHP content in abdominal wall in rabbits, compared with saline group. The result suggests that CT could effectively prevent adhesions without interfering wound healing.

© 2005 The WJG Press and Elsevier Inc. All rights reserved.

Key words: Chinese medicine compound; Postoperative intestinal adhesions

Yang XX, Shi HP, Hou LB. Chinese medicine compound Changtong oral liquid on postoperative intestinal adhesions. *World J Gastroenterol* 2005; 11(19): 2967-2970

<http://www.wjgnet.com/1007-9327/11/2967.asp>

Abstract

AIM: The aim of this study was to observe the effect of a Chinese medicine compound Changtong oral liquid (CT) on tissue plasminogen activity (t-PA), plasminogen activator inhibitor (PAI), TGF- β 1 and hydroxyproline (OHP).

METHODS: Two sets of animal experiments were performed in the present study. Forty New Zealand rabbits and 48 Sprague-Dawley (SD) rats were assigned randomly to one of the five groups: sham adhesion, adhesion with saline, adhesion with low dosage of the CT, adhesion with middle dosage of the CT and adhesion with high dosage of the CT. t-PA and PAI activity in plasma, OHP and TGF- β 1 expression in adhesion were investigated. Analysis of variance was used to test differences among groups.

RESULTS: CT treatment increased plasma t-PA activity in rabbits but decreased TGF- β 1 activity in rats. The data were expressed from low to high dose respectively as follows: t-PA, 46.1 ± 8.6 μ kat/L, 59.6 ± 10.1 μ kat/L, 64.0 ± 11.5 μ kat/L; TGF- β 1 $28 \pm 7.23\%$, $31 \pm 3.05\%$, $30 \pm 4.04\%$. There were significant differences compared with saline-treated animals (t-PA 26.4 ± 5.1 μ kat/L, TGF- β 1 $54 \pm 5.51\%$). OHP content in cecum of rabbits from middle and high but not low dose of CT lowered significantly as compared with saline-treated rabbits, 0.3641 ± 0.1373 , 0.3348 ± 0.0321 , 0.2757 ± 0.0497 mg/g vs 0.4183 ± 0.0883 mg/g of protein, $P > 0.05$, $P < 0.05$, $P < 0.05$ respectively. The rabbit plasma PAI activity and OHP content in abdominal wall had no difference in all groups.

CONCLUSION: CT treatment significantly enhanced t-PA activity in rabbits, but decreased TGF- β 1 content in rats, OHP content in cecum of rabbits, and failed to affect the

INTRODUCTION

Adhesions result from normal peritoneal wound healing response and develop in the first 5-7 d after injury. Adhesion formation and adhesion-free re-epithelialization are alternative pathways, both of which begin with coagulation which initiates a cascade of events resulting in the buildup of fibrin gel matrix. When unremoved, the fibrin gel matrix serves as the progenitor to adhesions by forming a band or bridge when two peritoneal surfaces coated with it are apposed. The band or bridge becomes the basis for the forming of an adhesion.

Intra-abdominal adhesion formation and reformation after surgery is a significant cause of morbidity. Postoperative adhesions, account for 40% of all cases of intestinal obstruction and 60-70% of these involve the small bowel^[1]. Currently, there is no ideal method of preventing adhesion formation. In terms of surgical technique, gentle tissue handling, the no-touch technique, meticulous hemostasis, copious irrigation, prevention of infection, avoidance of powdered gloves which can evoke a foreign body response in the peritoneum and prevention of extensive thermal injury have all been described as means of adhesion prevention. Multiple adjuvants to post-surgical adhesion prevention have also been evaluated. They include agents that prevent inflammation such as both steroidal and non-steroidal anti-inflammatory medications, agents that degrade fibrin such as recombinant tissue plasminogen activator and barrier methods involving the application of an absorbable material/solution/gel intraperitoneally to prevent the peritoneal surfaces from adhering together^[2]. Many Chinese medicines had been used to prevent adhesion. These include drugs for promoting blood circulation and removing blood stasis, such as safflower, *Radix Salviae Miltiorrhizae*, *Radix Angelicae Sinensis*, *Radix et Rhizoma rhei* and drugs for regulating Qi,

such as *Magnolia officinalis* Rehd. *Saussurea lappa* C. B. Clarke. Some Chinese medicine compound had also been used to prevent adhesion, such as Decoction of Simo, Minor decoction for purgation. Most of these drugs can be anti-inflammatory, promoting intestine peristalsis. Till recently, there was some lack of knowledge about how the Chinese medicine compound prevents adhesion at cellular and molecular level.

Changtong oral liquid (CT) is a Chinese medicine compound, which is included in *Radix Salviae Miltiorrhizae*, *Radix et Rhizoma rhei*, etc. In rat and rabbit models, we observed the effect that it prevents postoperative intestinal adhesion formation according to macroscopic adhesion grading^[2,12].

A better understanding of the mechanism of CT at the cellular and molecular level would undoubtedly help develop more effective treatment strategies. Many peritoneal fluid factors are associated with established peritoneal adhesion, such as tissue plasminogen activity (t-PA), plasminogen activator inhibitor (PAI), TGF- β ^[1], metalloproteinases^[4], interleukin-10^[5]. In this section, we study how CT adjusts the cellular events t-PA, PAI, TGF- β 1 and hydroxyproline (OHP)^[3], which is involved in the peritoneal healing.

MATERIALS AND METHODS

Animals

Specific pathogen-free Sprague-Dawley (SD) rats of both sexes, weighing 200-240 g, and New Zealand rabbits of both sexes, weighing 1.8-2.2 kg, were obtained from the animal center of The First Military Medical University. They were housed under barrier-sustained conditions and kept at 25 °C with 12-h light/dark cycles. The rats had free access to water and chow. All animals received care in compliance with the guidelines of China Ministry of Health

Reagents

TGF- β 1 antibody (1:100) was purchased from Santa Cruz Biotechnology Inc. (USA). S-P kit was purchased from Maixing Biotechnology Co., Ltd (Xiamen, China), t-PA kit was purchased from Department of Molecular Genetics, Fudan Medical College, PAI was purchased from Sun Biotechnology Co., Ltd (Shanghai, China).

Drug

CT was manufactured by Nanfang Hospital. Danshengsu [D(+)- β -(3,4-dihydroxyphenyl)lactic acid] contents is 0.4 g/L.

Experiment model

The model utilized in this experiment is postoperative intestinal adhesion on animals.

The SD rats and New Zealand rabbits were subjected to a laparotomy (trauma).

They were anesthetized with intraperitoneal sodium pentobarbital, and their cecum were isolated using aseptic techniques, exposed to air for 5 min, scratched chorion 10 times by scalpel, a drop of absolute alcohol dropped on the injury, clamped segmental artery by tweezers for 2 min, then put cecum in original site. A laparotomy was then performed on each animal and the abdominal cavity was closed with running 3-0 silk surgical sutures.

Experimental protocol

Forty New Zealand rabbits and 48 SD rats were assigned randomly to one of the five groups: sham adhesion, adhesion with saline, adhesion with low dosage of the CT, adhesion with intermediate dosage of the CT and adhesion with high dosage of the CT. Each animal was orally administered after operation.

Assay for TGF- β 1, t-PA, PAI and OHP

A blood sample of 2 mL was taken from the rabbits on the 3rd d after the operation. Chromogenic assay was used to identify the activity of t-PA and PAI in plasma. The animals were killed on the 7th d, a tissue sample of 1 g was taken from the abdominal incision line and adhesive segment. The expression of OHP was examined by spectrophotometric method. The expression of TGF- β 1 was examined by immunohistochemistry method.

Statistical analysis

All measurements are expressed as the mean \pm SD and were analyzed by one-way analysis of variance with the Student-Newman-Keuls multiple comparisons or *t*-test when comparing the differences between the means of four or two groups at the same time point. Probabilities less than 0.05 were considered to be statistically significant.

RESULTS

Effect of CT on t-PA, PAI

The t-PA content was significantly increased in three groups of the CT when compared with saline group ($P<0.001$). The t-PA content was significantly decreased in saline group when compared with sham adhesion group ($P<0.05$). There was no significant difference among the three groups of the CT. But the PAI content did not have variations in each group (Table 1).

Table 1 Effect of the CT on the t-PA, PAI in plasma of rabbits with adhesion (mean \pm SD)

Group	Dosage (g/kg)	Number	t-PA (μ kat/L)	PAI (μ kat/L)
Sham	-	8	38.3 \pm 11.4	12.5 \pm 0.8
Saline	-	8	26.4 \pm 5.1 ^b	12.5 \pm 2.4
CT	2.15	8	46.1 \pm 8.6 ^a	13.3 \pm 1.5
CT	4.30	8	59.6 \pm 10.1 ^a	10.8 \pm 1.8
CT	8.60	8	64.0 \pm 11.5 ^a	13.5 \pm 1.9

^a $P<0.05$ vs sham adhesion group, ^b $P<0.001$ vs saline group.

Effect of CT on TGF- β 1

The TGF- β 1 content was significantly decreased in three groups of the CT when compared with saline group ($P<0.001$). The TGF- β 1 content was significantly increased in saline group when compared with sham adhesion group ($P<0.001$). There were no significant differences among the three groups of the CT (Table 2).

Effect of CT on OHP

The OHP content in cecum was significantly decreased in

groups of middle and high dosage of the CT when compared with saline group ($P<0.05$ or 0.01). The OHP content in cecum was significantly increased in saline groups when compared with sham adhesion group ($P<0.001$). The OHP content in abdominal wall had no significant difference in groups of the CT when compared with saline group (Table 3).

Table 2 Effect of the CT on the expression of TGF- β 1 of rats with adhesion (mean \pm SD)

Group	Number	Dosage (g/kg)	Rate of positive reaction (%)
Sham	10		12 \pm 2.08
Saline	10		54 \pm 5.51 ^b
CT	10	4.3	28 \pm 7.23 ^d
CT	9	8.6	31 \pm 3.05 ^d
CT	9	17.2	30 \pm 4.04 ^d

^b $P<0.001$ vs saline group. ^d $P<0.001$ vs sham adhesion group.

Table 3 Effect of the CT on OHP in rabbits with adhesions (mean \pm SD)

Group	Dosage (g/kg)	Number	OHP (mg/g of protein)	
			Cecum	Abdominal wall
Sham	-	8	0.2056 \pm 0.0983	0.2373 \pm 0.1189
Saline	-	8	0.4183 \pm 0.0883 ^d	0.2527 \pm 0.1202
CT	2.15	8	0.3641 \pm 0.1373	0.2302 \pm 0.1577
CT	4.30	8	0.3348 \pm 0.0321 ^a	0.2784 \pm 0.2325
CT	8.60	8	0.2757 \pm 0.0497 ^b	0.1957 \pm 0.3721

^a $P<0.05$, ^b $P<0.01$ vs saline group, ^d $P<0.001$ vs sham adhesion group.

DISCUSSION

The peritoneal leukocytes, mesothelial cells, and macrophages are important cellular components of peritoneal healing^[1,6]. After injury to the peritoneum, there is increased vascular permeability in vessels supplying the damaged area, followed by an exudation of inflammatory cells, ultimately leading to the formation of a fibrin matrix. The fibrin matrix is gradually organized and replaced by tissue containing fibroblasts, macrophages, and giant cells. This fibrin matrix connects two injured peritoneal surfaces forming fibrin bands. These fibrin bands can be broken down by fibrinolysis into smaller molecules as fibrin degradation products. Under conditions of aberrant peritoneal healing, ischemia results in a reduction in fibrinolytic activity and thus persistence of the fibrin bands. The organization of the fibrin bands over time results in the persistence of the adhesions. The cell population changes with the maturity of the adhesion tissue, with the initial cell type at d 1-3 being mainly polymorphonuclear leukocytes and on d 5-7 being mainly fibroblasts. Adhesion tissue also contains nerve fibers and small vascular channels of endothelial cells. The role of the fibrinolysis in adhesion formation is to breakdown fibrin clots that are formed during the healing process. In the healthy mesothelial layer, t-PA and PAI protein were present, compared with the submesothelial layer, where only PAI-1 and not t-PA were present. Inflamed peritoneum, t-PA expression in the mesothelium was substantially reduced, whereas PAI-1 expression in the submesothelial layer was intensified. Expression of t-PA in

the mesothelium but not the submesothelium suggested that t-PA was responsible for the clearance of fibrin in the peritoneal cavity proper^[7]. CT can significantly increase the t-PA content in rabbit models. Maybe it is one of the reasons that CT prevents postoperative intestinal adhesion formation.

In peritoneal healing and adhesion formation, latent TGF- β is activated by plasmin in its active form, TGF- β not only interacts with the fibrinolytic system and extracellular matrix but also with many other cellular mediators involved in the process of adhesion formation^[8]. It is healthily found in platelets, macrophages, and wound fluid. It is a key factor in healthy wound healing and is also a potent inducer of tissue fibrosis in peritoneal wound healing. During the acute phase of the inflammatory response, peritoneal macrophages and/or mesothelial cells produce TGF- β . It can contribute to the synthesis of the extracellular matrix by stimulating fibroblastic cell production of collagen and fibronectin. TGF- β overexpression by the parietal peritoneum and the serosal surfaces of the pelvic organs as well as increased concentrations of TGF- β in the peritoneal fluid have been associated with an increased incidence of adhesion formation in both humans and animals. Krause^[9] utilized heterozygous mice to study that healthy TGF- β levels can modulate the injury response that regulates the extent of adhesion formation. The TGF- β 1 content was significantly decreased in CT groups, but the TGF- β 1 content was significantly increased in saline group when compared with sham adhesion group. Maybe it is another reason that CT prevents postoperative intestinal adhesion.

OHP content was considered to play a role in wound healing. Baykal^[3] and Ozogul^[10] used adhesion grading and tissue OHP levels to value adhesion severity, they found that there was linear correlation between adhesion degree and tissue OHP levels ($r = 0.86$, $P<0.001$; $r = 0.73$, $P = 0.00000$). Avsar^[11] found that OHP levels in the tissue were significantly lower in groups, which has low adhesion formation rate in rats. Ozogul^[10] considered that OHP levels showed significant correlation with adhesion severity. In our study, although CT decreases cecum OHP level, there was no significant difference in abdominal wall OHP content between the groups. CT plays a role in the prevention of adhesion formation without affecting wound healing.

ACKNOWLEDGMENT

We thank Professor Qing-He Wu, Dr. Xiang-Lu Rong at Department of Pharmacology, Guangzhou University of TCM, for their technical support.

REFERENCES

- 1 Cheong YC, Laird SM, Li TC, Shelton JB, Ledger WL, Cooke ID. Peritoneal healing and adhesion formation/reformation. *Hum Reprod Update* 2001; **7**: 556-566
- 2 Li HC, Wang MY, Hou LB, Luo R, Chen ZD, Shi HP. Prevention Effect of changtong oral liquid on postoperative intestinal adhesion formation in rats. *Di Yi Jun Yi Daxue Xuebao* 1999; **19**: 466
- 3 Baykal A, Onat D, Rasa K, Renda N, Sayek I. Effects of polyglycolic acid and polypropylene meshes on postoperative adhesion formation in mice. *World J Surg* 1997; **21**: 579-582; discussion 582-583
- 4 Koks CA, Groothuis PG, Slaats P, Dunselman GA, de Goeij AF, Evers JL. Matrix metalloproteinases and their tissue in-

- hibitors in antegradely shed menstruum and peritoneal fluid. *Fertil Steril* 2000; **73**: 604-612
- 5 **Holschneider CH**, Nejad F, Montz FJ. Immunomodulation with interleukin-10 and interleukin-4 compared with ketorolac tromethamine for prevention of postoperative adhesions in a murine model. *Fertil Steril* 1999; **71**: 67-73
- 6 **Haney AF**. Identification of macrophages at the site of peritoneal injury: evidence supporting a direct role for peritoneal macrophages in healing injured peritoneum. *Fertil Steril* 2000; **73**:988-995
- 7 **Ivarsson ML**, Holmdahl L, Falk P, Molne J, Risberg B. Characterization and fibrinolytic properties of mesothelial cells isolated from peritoneal lavage. *Scand J Clin Lab Invest* 1998; **58**: 195-203
- 8 **Cegini N**. The role of growth factors in peritoneal healing: transforming growth factor beta(TGF-beta). *Eur J Surg Suppl* 1997; **577**: 17-23
- 9 **Krause TJ**, Katz D, Wheeler CJ, Ebner S, McKinnon RD. Increased levels of surgical adhesions in TGFbeta1 heterozygous mice. *J Invest Surg* 1999; **12**: 31-38
- 10 **Ozogul Y**, Baykal A, Onat D, Renda N, Sayek I. An experimental study of the effect of aprotinin on intestinal adhesion formation. *Am J Surg* 1998; **175**: 137-141
- 11 **Avsar FM**, Sahin M, Aksoy F, Avsar AF, Akoz M, Hengirmen S, Bilici S. Effects of diphenhydramine HCl and methylprednisolone in the prevention of abdominal adhesions. *Am J Surg* 2001; **181**: 512-515
- 12 **Li X**, Hou L, Shan Y, Tong L, Chen Y. Effect of changtong oral liquids on the fibrinolytic activity of rabbits with experimental intestinal adhesion. *Zhongyao* 2002; **25**: 416-417

Science Editor Guo SY Language Editor Elsevier HK

• BRIEF REPORTS •

Clinical features of probable severe acute respiratory syndrome in Beijing

Hai-Ying Lu, Xiao-Yuan Xu, Yu Lei, Yang-Feng Wu, Bo-Wen Chen, Feng Xiao, Gao-Qiang Xie, De-Min Han

Hai-Ying Lu, Xiao-Yuan Xu, Department of Infectious Diseases, Peking University First Hospital, Beijing 100034, China
Yu Lei, Department of Hepatic Disease, Renmin Hospital of Fangxian, Fangxian 442100, Hubei Province, China
De-Min Han, Beijing TongRen Hospital, Beijing 100730, China
Yang-Feng Wu, Gao-Qiang Xie, Chinese Academy of Medical Sciences, Fu Wai Hospital, Beijing 100037, China
Bo-Wen Chen, Feng Xiao, Capital Institute of Pediatrics, Beijing 100020, China
Supported by the National High Technology Research and Development Program of China (863 Program), No. 2003AA208107
Correspondence to: Xiao-Yuan Xu
Correspondence to: De-min Han, Beijing TongRen Hospital, 2 ChongNei Street, DongCheng District, Beijing 100730, China. handemin@trhos.com
Received: 2004-07-09 Accepted: 2004-08-30

Abstract

AIM: To summarize clinical features of probable severe acute respiratory syndrome (SARS) in Beijing.

METHODS: Retrospective cases involving 801 patients admitted to hospitals in Beijing between March and June 2003, with a diagnosis of probable SARS, moderate type. The series of clinical manifestation, laboratory and radiograph data obtained from 801 cases were analyzed.

RESULTS: One to three days after the onset of SARS, the major clinical symptoms were fever (in 88.14% of patients), fatigue, headache, myalgia, arthralgia (25-36%), etc. The counts of WBC (in 22.56% of patients) lymphocyte (70.25%) and CD₃, CD₄, CD₈ positive T cells (70%) decreased. From 4-7 d, the unspecific symptoms became weak; however, the rates of low respiratory tract symptoms, such as cough (24.18%), sputum production (14.26%), chest distress (21.04%) and shortness of breath (9.23%) increased, so did the abnormal rates on chest radiograph or CT. The low counts of WBC, lymphocyte and CD₃, CD₄, CD₈ positive T cells touched bottom. From 8 to 16 d, the patients presented progressive cough (29.96%), sputum production (13.09%), chest distress (29.96%) and shortness of breath (35.34%). All patients had infiltrates on chest radiograph or CT, some even with multi-infiltrates. Two weeks later, patients' respiratory symptoms started to alleviate, the infiltrates on the lung began to absorb gradually, the counts of WBC, lymphocyte and CD₃, CD₄, CD₈ positive T cells were restored to normality.

CONCLUSION: The data reported here provide evidence that the course of SARS could be divided into four stages, namely the initial stage, progressive stage, fastigium

and convalescent stage.

© 2005 The WJG Press and Elsevier Inc. All rights reserved.

Key words: SARS; Clinical features; Clinical stage

Lu HY, Xu XY, Lei Y, Wu YF, Chen BW, Xiao F, Xie GQ, Han DM. Clinical features of probable severe acute respiratory syndrome in Beijing. *World J Gastroenterol* 2005; 11(19): 2971-2974
<http://www.wjgnet.com/1007-9327/11/2971.asp>

INTRODUCTION

A novel coronavirus^[1-3] has been identified as an etiologic agent for severe acute respiratory syndrome (SARS), which caused about 8 437 SARS cases in the world between December 2002 and October 2003. The previous reports^[4-7] described the clinical features of SARS, but there is little information available in literature about features of this illness in a large SARS population. In this paper, we will describe the characteristics of SARS during the whole course systematically, through investigation of the data derived from 801 cases of probable SARS.

MATERIALS AND METHODS

Patients

This study includes 801 cases of patients admitted to hospitals between March and June 2003 in Beijing. These cases are consistent with the criteria of WHO for a probable SARS, with fever, abnormality of chest radiograph or CT scan and history of exposure to an index patient suspected of SARS or to have had direct contact with an individual who became ill after exposure to a patient with SARS.

Methods

Clinical manifestation, laboratory and chest radiographic data were documented prospectively. Investigations included a complete blood count, CD₃, CD₄, CD₈ positive T cell, lymphocyte count, and serum biochemical measurements (including electrons, renal function and liver function, creatine kinase, creatine kinase MB and lactate dehydrogenase). After the patients were admitted to hospitals, the above examinations were performed every week during the entire course of this illness.

Statistical analysis

All analyses were performed using Statistica software. Data are expressed as mean±SD and percentage.

RESULTS

Our cohort comprised 801 cases of probable SARS, the mean age of the study population was 37.04 ± 15.64 years (range, 0.72-92.89 years), 412 cases (51.56%) were female, and 154 patients (9.23%) were medical personnel. Sixty-five patients (8.1%) had coexisting conditions, hypertension in 21 cases, hepatitis cirrhosis in 13 cases, diabetes mellitus in 9 cases and cardiovascular disease in 8 cases. The mean day of hospitalization was 29.02 ± 9.07 d, and that of the entire course was 32.79 ± 10.82 d. 64.17% of patients were admitted to hospital 1-3 d after onset of illness, 88.9%, 4-7 d, 93.51%, 8-11 d, 95.51%, 12-14 d, 95.76%, 15-21 d. In later days, the percentages gradually decreased.

Temperature

The range of patient's temperature on admission during 1-14 d after onset of illness was 38.11-38.36 °C. On d 1, 88.14% of patients had a documented fever, and 98.12% with a reported fever. The percentages of patients with fever declined to 40.31%, 15.13%, 5.07% and 6.02% on the 7th, 14th, 21st and 28th d respectively, the mean time taken for the patient's temperature to drop below 37.2 °C after admission was 5.69 ± 4.53 d.

Hypoxemia findings

The oxygen saturation (SaO₂) went down below 93% in 1.39-3.13% of patients, the mean of oxygen saturation was more than 96%. The partial arterial pressure of oxygen (PaO₂) was noted below 12.7 ± 3.4 kPa in 65.74% of patients (mean 12.4 ± 1.6 kPa) from the 1st to the 3rd d, then the percentage subsequently reduced. On the 4th wk, 40% of patients presented low PaO₂, and the mean of PaO₂ was 15.5 ± 2.4 kPa. The medians of low PaO₂ and SaO₂ occurred at the 3rd and 1st d respectively, and recovered to the normal levels in the later 8 and 9.5 d, respectively.

There were seven cases of patients who required noninvasive ventilation and one case with mechanical ventilation at the 1st-3rd d, and 18 cases with noninvasive ventilation at the 4th-7th d, 15 cases at the 8th-11th d, 7 cases at the 12th-14th d, and 3 cases at the 3rd wk.

Clinical features

At the 1st-3rd d, the predominant symptom was high fever, and other common symptoms were fatigue (in 33.85% of patients), headache (21.34%), myalgia (22.17%), sore throat (18.66%), arthralgia (16.01%), chills, rigors, or both (12.6%).

At d 4-7 above prodromal symptoms appeared less worsening, but the low respiratory tract symptoms appeared obvious, such as cough (in 24.28% of patients), sputum production (14.26%), chest distress (21.04%) and shortness of breath (9.23%). These respiratory symptoms deteriorated progressively and touched the peak at the periods from d 8-16 then alleviated gradually in the subsequent days.

The prodromal symptoms that usually persisted for 3-5 d are cough and sputum production, occurring at the 2nd and 3rd d, and disappeared later at d 13 and 7 respectively, chest distress and shortness of breath at d 7th and 5th, and recovered later in d 10 and 17.5 respectively. The positive rates of symptoms in our study cohort during the whole course are listed in Table 1.

Hematologic findings

In the early phase (1-3 d) of the course for SARS, the white blood cell count, lymphocyte cell count and its subtype cell count (CD4, CD3, CD8 positive cell) presented reduction, and touched bottom at the 4th to 7th d, then gradually went up to the normal levels at the 4th wk. The Table 2 shows the abnormal rates and means of hematology in our study cohort during the course.

Radiographic findings

At the 1st to 3rd d after onset of illness, 96.65% of patients had abnormal chest radiographs, most of them showed a unilateral one focal infiltrates, but some patients (11.45%) presented unilateral or bilateral multifocal involvement and had a dramatic worsening in the period from the 8th to 14th d. After that, the majority of patients had radiographic evidence of improvement in lung consolidation. There were, however, 17.35% and 10.24% of patients with abnormal chest radiograph at the 6th and 7th wk after onset of this illness, and 4.37% at the 8th wk. The abnormal change in SARS patients' chest CT scans also showed the same trend, but CT scan is more sensitive than X-ray examination. The abnormal rates of chest radiographs and CT in our study cohort during the course are presented in Table 3.

Biochemical findings

A substantial proportion of patients had several abnormal serum chemical values, which could occur early but progressively worsened at the 2nd and 3rd wk. 64.66% of patients had an elevated serum alanine aminotransferases levels (>40 IU/L, ALT), 44.34% of patients with an elevated serum AST levels

Table 1 Positive rates of symptoms in our study cohort (%)

Variable	1-3 d	4-7 d	8-11 d	12 d-	15 d-	22 d-	29 d-
Chill	12.6	9.34	4.32	2.4	1.43	0.31	0.57
Rigor	4.29	2.39	0.61	1.05	0.29	0	0.19
Fatigue	33.85	27.59	22.65	14.16	3.3	8.47	4.32
Headache	21.34	12.03	7.45	3.18	13.88	1.99	1.89
Arthralgia	16.01	9.64	5.31	3.53	2.87	2.31	2.29
Myalgia	22.17	13.23	7.63	5.38	4.3	2.92	1.52
Diarrhea	9.88	12.09	5	3.71	3.14	1.8	2.7
Cough	23.76	24.18	29.18	28.68	20.85	8.02	4.23
Sputum production	8.02	14.26	13.09	11.36	8.56	3.08	2.01
Chest distress	8.43	21.04	31.83	35.23	35.34	26.09	17.15
Breath shortness	8.24	9.23	15.65	20.35	18.01	7.12	5.01
Rales	6.2	4.78	5.08	4.65	3.12	1.25	1.01

Table 2 Abnormal rate (%) and value of hematology in our study cohort

Variable	1 d-	4 d-	8 d-	12 d-	15 d-	22 d-	29 d-
WBC							
Abnormal rate	22.56	38.93	16.45	8.44	6.44	6.81	8.66
Mean	5.15	4.75	7.46	4.75	8.42	8.22	7.33
SD	2.56	2.73	4.21	4.83	3.96	3.76	3.49
Lymphocyte							
Abnormal rate	70.25	78.81	58.9	45.21	39.29	25.8	29.94
Mean	1.11	1.19	1.50	1.70	1.75	1.87	1.74
SD	0.51	0.64	0.81	0.91	0.92	0.94	0.75
CD8							
Abnormal rate	68.42	80.33	75.81	67.35	51.58	48.15	35.42
Mean	307.23	244.14	306.19	318.28	453.06	534.37	511.31
SD	274.19	182.34	251.53	227.91	433.46	428.46	269.11
CD3							
Abnormal rate	68.42	87.1	82.26	71.43	60	54.43	49.94
Mean	690.97	568.03	711.48	787.24	1 068.9	1 184.5	1 148.3
SD	576.36	434.18	515.14	559.83	788.19	713.17	620.1
CD4							
Abnormal rate	69.05	84.38	72.58	60.78	48.42	44.44	36
Mean	367	295.28	377.66	430.92	582.21	656.78	670.32
SD	300.64	248.96	326.16	325.07	464.04	576.2	447.19

Table 3 Abnormal rates of chest radiographs in our study cohort

Variable	1 d-	4 d-	8 d-	12 d-	15 d-	22 d-	29 d-
Abnormal rate X-ray	96.65	94.3	97.04	80.68	74.96	64.98	56.37
Multifocal opacities X-ray	11.45	15.19	25.44	25.18	20.38	15.82	16.56
Abnormal rate CT	95.45	95.92	95.56	91.67	84.21	73.97	82
Multifocal opacities CT	21.88	28.21	42.5	37.5	24.14	20.31	20.19

(>45 IU/L), and 29.72% of patients with an elevated serum bilirubin levels. Serum urea (>7.85 mmol/L) and creatinine (>106.5 mmol/L) were elevated in 20.87% and 11.16% of patients respectively.

DISCUSSION

SARS is a new contagious and rapidly progressive infectious disease with substantial morbidity and mortality. SARS-CoV antibodies (IgM or IgG) cannot be tested until 10 d later after infection^[8-11]; and virus RNA (by RT-PCR) can be found in nasopharyngeal aspirates or blood samples of patients at the early stage of illness, but it is difficult to be used in all hospitals. So, in 2003, reliable, rapid and simple diagnostic test was not available for the diagnosis of SARS. The criteria for SARS relied on the definition by the World Health Organization (WHO), a probable case of SARS is an individual with fever [temperature >38 °C], low respiratory tract symptoms, and contact with a person believed to have had SARS or a history of travel to a region where there has been documented transmission of the illness, and present abnormality on chest radiograph. All our subjects matched with the above criteria. Though a worldwide SARS outbreak in 2003 was controlled, it is unfortunate that several cases of SARS have been reported in the early spring of 2004. Therefore, SARS is still a potential health crisis putting humans at danger. Then, a clear picture of clinical feature for SARS is very valuable to medical personnel to alert the possibility of SARS. In this study, our aim is to describe the characteristics of SARS in different periods of the course.

In the data derived from 801 probable SARS cases, at the initial stage of this illness (1-3 d), the predominated symptom was fever, accompanied with the prodromal symptoms due to the viremia. An important abnormality in routine blood count was to present lymphopenia, especially, the counts of CD3, CD4, CD8 positive T lymphocytes reduced dramatically. It has been proved^[12,13] that the mechanism of SARS is the SARS-CoV attacking the T lymphocyte and triggering the immune response, causing a series of pathogenic immune damage in tissue or organs of the infected patients. SARS presents predominantly with infiltrates on chest radiographs^[14-17]. In our study, the chest radiographic examination showed the infiltrates occurred early (in more than 90% of patients), which is different from the pneumonia caused by the bacteria and common virus.

In the later 4-7 d, the vast majority of patients persisted with high fever, but the prodromal symptoms appeared to be alleviated, the low respiratory tract symptom and abnormalities on chest radiographs began to deteriorate. The most specific feature in this period was that the lymphopenia, and low count of CD3, CD4, CD8 positive T lymphocytes had worsened. These data indicate that the immune response in body caused by SARS-CoV reaches the highest peak and starts to produce pathologic lesions in tissue and organs. We take the name of this period as progressive stage.

In the period from 8 to 16 d, the patients had progressive low respiratory symptoms, the air-space opacities in chest increased in size, extent and severity in majority of patients, some of them appeared to have diffuse opacification and required noninvasive ventilation, even the mechanical ventilation

owing to the respiratory failure. Some patients developed damage of liver, kidney or other organs. The lung biopsy specimen obtained at autopsy^[18,19] had shown diffuse alveolar damage with pulmonary congestion, edema and formation of hyaline membrane. So, this period is the most danger phase in the whole course of SARS, and is named as fastigium stage.

When the first 2 wk passed, the patients presented the normal temperature and hardly had the prodromal symptoms, with the exception of some patients having only fatigue. The counts of lymphocyte and its subtype cells (CD3, CD4, CD8) gradually increased, meaning the pathologic damage by immune response stopped. Patients showed an improvement of respiratory symptoms and in the air-space opacities. About 3 wk later, the symptoms almost disappeared, the counts of lymphocyte and its subtype cells turned back to the normal levels and body's immune function also returned to normal. The infiltrates in lung were gradually absorbed and disappeared. But we found occasionally patients (in 10.29-17.35% patients) still presented abnormal shadows on lung at the 6th and 7th wk after onset of illness. So, the convalescence of SARS in some patients may need a longer time to recover, about 3-4 wk, more ever, some of them could remain with interstitial fibrosis in lung.

In summary, at the early stage of SARS (1-3 d), the most common symptoms were fever and the prodromal symptoms. The low respiratory symptoms also occurred early with moderate hypoxemia, but usually lacking of rales. The majority of patients had the reducing counts of CD3 (+), CD4 (+) and CD8 (+) T cells, about one-third of the patients developed lymphopenia. Most patients presented infiltrates on chest radiograph, but about 20% and 10% of patients had normal results of chest X-ray and CT examination respectively on admission. At the progressive stage (4-7 d), the patients still had high fever, the low respiratory symptoms and inflammation in lung began to progress, almost all patients had abnormality on chest radiograph, the counts of CD3 (+), CD4 (+) and CD8 (+) T cells reached the lowest levels. The fastigium stage (8-16 d), patients may occur with serious chest distress and shortness of breath, some with cough and sputum produce, the air-space opacities on chest deteriorated quickly, some of them showed diffuse infiltrates and developed respiratory function failure, even ARDS. At the convalescent stage (17-28 d), patients' temperature were normal, symptoms almost disappeared, the counts of lymphocyte and its subtype cells increased to the normal values, and the infiltrates in lung were gradually absorbed and disappeared.

REFERENCES

- 1 **Peiris JS**, Lai ST, Poon LL, Guan Y, Yam LY, Lim W, Nicholls J, Yee WK, Yan WW, Cheung MT, Cheng VC, Chan KH, Tsang DN, Yung RW, Ng TK, Yuen KY. Coronavirus as a possible cause of severe acute respiratory syndrome. *Lancet* 2003; **361**: 1319-1325
- 2 **Ksiazek TG**, Erdman D, Goldsmith CS, Zaki SR, Peret T, Emery S, Tong S, Urbani C, Comer JA, Lim W, Rollin PE, Dowell SF, Ling AE, Humphrey CD, Shieh WJ, Guarner J, Paddock CD, Rota P, Fields B, DeRisi J, Yang JY, Cox N, Hughes JM, LeDuc JW, Bellini WJ, Anderson LJ. A novel coronavirus associated with severe acute respiratory syndrome. *N Engl J Med* 2003; **348**: 1953-1966
- 3 **Drosten C**, Gunther S, Preiser W, van der Werf S, Brodt HR, Becker S, Rabenau H, Panning M, Kolesnikova L, Fouchier RA, Berger A, Burguiere AM, Cinatl J, Eickmann M, Escriou N, Grywna K, Kramme S, Manuguerra JC, Muller S, Rickerts V, Sturmer M, Vieth S, Klenk HD, Osterhaus AD, Schmitz H, Doerr HW. Identification of a novel coronavirus in patients with severe acute respiratory syndrome. *N Engl J Med* 2003; **348**: 1967-1976
- 4 **Lee N**, Hui D, Wu A, Chan P, Cameron P, Joynt GM, Ahuja A, Yung MY, Leung CB, To KF, Lui SF, Szeto CC, Chung S, Sung JJ. A major outbreak of severe acute respiratory syndrome in Hong Kong. *N Engl J Med* 2003; **348**: 1986-1994
- 5 **Tsang KW**, Ho PL, Ooi GC, Yee WK, Wang T, Chan-Yeung M, Lam WK, Seto WH, Yam LY, Cheung TM, Wong PC, Lam B, Ip MS, Chan J, Yuen KY, Lai KN. A cluster of cases of severe acute respiratory syndrome in Hong Kong. *N Engl J Med* 2003; **348**: 1977-1985
- 6 **Booth CM**, Matukas LM, Tomlinson GA, Rachlis AR, Rose DB, Dwosh HA, Walmsley SL, Mazzulli T, Avendano M, Derkach P, Ephtimios IE, Kitai I, Mederski BD, Shadowitz SB, Gold WL, Hawryluck LA, Rea E, Chenkin JS, Cescon DW, Poutanen SM, Detsky AS. Clinical features and short-term outcomes of 144 patients with SARS in the greater Toronto area. *JAMA* 2003; **289**: 2801-2809
- 7 **Poutanen SM**, Low DE, Henry B, Finkelstein S, Rose D, Green K, Tellier R, Draker R, Adachi D, Ayers M, Chan AK, Skowronski DM, Salit I, Simor AE, Slutsky AS, Doyle PW, Krajden M, Petric M, Brunham RC, McGeer AJ. Identification of severe acute respiratory syndrome in Canada. *N Engl J Med* 2003; **348**: 1995-2005
- 8 **Lu HY**, Huo N, Wang GF, Li HC, Nie LG, Que CL, Li J, Li YH, Gao XM, Zhang ZD, Zhuang H, Xu XY. The factors affecting on the produce of IgG antibody in SARS patients. *Shijie Huaren Xiaohua Zazhi* 2004; **12**: 723-725
- 9 **National Research Project for SARS, Beijing Group**. Serum antibodies detection for serological diagnosis of severe acute respiratory syndrome. *Zhonghua Jiehe he Huxi Zazhi* 2003; **26**: 339-342
- 10 **World Health Organization**. SARS: availability and use of laboratory testing, 2003/04/24
- 11 **World Health Organization**. Update 71 Status of diagnostic tests, training course in China, 2003/06/02
- 12 **Li TS**, Qiu ZF, Han Y, Zhang HW, Wang Z, Liu ZY, Fan HW, Lv W, Yu Y, Wang HL, Zhang HY, Xie J, Zhou BT, Ma XJ, Ni AP, Wang AX, Deng GH. The alterations of T cell subsets of severe acute respiratory syndrome during acute stage. *Zhonghua Jianshan Yixue Zazhi* 2003; **26**: 297-299
- 13 **Yin CB**, Zhang FC, Tang XP, Chen WL, Chen YQ, Wang J, Jia WD. Measurement of subsets of blood T lymphocyte in 93 patients with severe acute respiratory syndrome and its clinical significance. *Zhonghua Jiehe He Huxi Zazhi* 2003; **26**: 343-346
- 14 **Zeng QS**, Chen L, Cai X, Chen RC, Xie NW, Zhong NS. Chest Xray and CT in the diagnosis of SARS. *Zhonghua Fangshexue Zazhi* 2003; **37**: 601-603
- 15 **Du XK**, Yu WJ, Wang SL, Zhu QJ, Hong N. Preliminary analysis of clinical images of SARS. *Zhonghua Fangshexue Zazhi* 2003; **37**: 780-783
- 16 **Wang W**, Ma DQ, Zhao DW, Chao CH, Guo YB, Wu H, Yuan CW, Duan Y, Lang ZW. CT appearances and dynamic changes in severe acute respiratory syndrome. *Zhonghua Fangshexue Zazhi* 2003; **37**: 686-689
- 17 **Zhao DW**, Ma DQ, Wang W, Wu H, Yuan CW, Jia CY, He W, Chen JH. Early Xray and CT manifestations of SARS. *Zhonghua Fangshexue Zazhi* 2003; **37**: 597-599
- 18 **Lai RQ**, Feng XD, Wang ZC, Lai HW, Tian Y, Zhang W, Yang CH. Clinicopathological and ultramicrostructural changes of tissue in a patient with severe acute respiratory syndrome. *Zhonghua Binglixue Zazhi* 2003; **32**: 205-208
- 19 **Chen J**, Xie YQ, Zhang HT, Wan JW, Wang DT, Hu CH, Wang QC, Xue XH, Si WX, Luo RF, Qiu HM. Lung pathology of severe acute respiratory syndrome. *Acta Acad Med Sin* 2003; **25**: 336-360

• BRIEF REPORTS •

Syndecan-1 and E-cadherin expression in differentiated type of early gastric cancer

Mei-Fang Huang, You-Qing Zhu, Zhi-Fen Chen, Jun Xiao, Xin Huang, Yong-Yan Xiong, Gui-Fang Yang

Mei-Fang Huang, You-Qing Zhu, Zhi-Fen Chen, Jun Xiao, Xin Huang, Department of Digestive Disease, Zhongnan Hospital of Wuhan University, Wuhan 430071, Hubei Province, China
Yong-Yan Xiong, Gui-Fang Yang, Department of Pathology, Zhongnan Hospital of Wuhan University, Wuhan 430071, Hubei Province, China

Supported by the Medical Science Research Foundation of Hubei Province, No. 101130780

Co-first-authors: Mei-Fang Huang and You-Qing Zhu

Co-correspondents: Mei-Fang Huang

Correspondence to: You-Qing Zhu, Department of Digestive Disease, Zhongnan Hospital of Wuhan University, Wuhan 430071, Hubei Province, China. uqing-zhu@sina.com

Telephone: +86-27-67813275 Fax: +86-27-87307622

Received: 2004-07-12 Accepted: 2004-11-04

Key words: Gastric cancer; Cellular phenotype; Syndecan-1

Huang MF, Zhu YQ, Chen ZF, Xiao J, Huang X, Xiong YY, Yang GF. Syndecan-1 and E-cadherin expression in differentiated type of early gastric cancer. *World J Gastroenterol* 2005; 11(19): 2975-2980

<http://www.wjgnet.com/1007-9327/11/2975.asp>

Abstract

AIM: To elucidate the role and alterations of syndecan-1 and E-cadherin expression in different cellular phenotypes of differentiated-type gastric cancers (DGCs).

METHODS: A total of 120 DGCs at an early stage, and their adjacent mucosa, were studied both by immunohistochemistry. Syndecan-1 and E-cadherin were assessed by immunohistochemical staining with anti-syndecan-1 and anti-E-cadherin antibodies, respectively. Based on immunohistochemistry, DGCs and their surrounding mucosa were divided into four types: gastric type (G-type), ordinary type (O-type), complete-intestinal type (CI-type), and null type (N-type).

RESULTS: Syndecan-1 expression was significantly lower in G-type cancers (29.4%) than in O-type (79.6%) and CI-type cancers (90%) ($P < 0.05$, respectively), but E-cadherin did not show this result. In addition, syndecan-1 expression was significantly reduced in DGCs comprised partly of poorly differentiated adenocarcinoma or signet-ring cell carcinoma, compared to DGCs demonstrating papillary and/or tubular adenocarcinoma ($P < 0.05$). G-type intestinal metaplasia (IM) surrounding the tumors was observed in 23.8% of G-type, 4.9% of O-type, and 6.7% of CI-type cancers ($P < 0.05$; G-type vs O-type). Reduction of syndecan-1 expression was significant in G-type IM (25%) compared to non-G-type IM (75%; $P < 0.05$).

CONCLUSION: Loss of syndecan-1 plays a role in the growth of G-type cancers of DGCs at an early stage, and the reduction of syndecan-1 expression in IM surrounding the tumors may influence the growth of G-type cancer.

INTRODUCTION

Gastric cancer is one of the most common malignant tumors of the gastrointestinal tract worldwide. In the past decade, infection with *Helicobacter pylori* has received wide attention for its potential role in the induction and progression of gastric cancer. However, the molecular pathways involved in gastric carcinogenesis are still poorly understood. Basic research has produced remarkable advances in our understanding of cancer biology. Among the most important of these advances was the recognition that syndecan-1 plays a role as a cell adhesion molecule, similar to E-cadherin, and is associated with the maintenance of epithelial morphology. However, the expression of syndecan-1 was augmented during epithelial regeneration and rearrangement in the stomach and other tissues^[1-3]. E-cadherin is a member of the transmembrane glycoprotein family and is responsible for the epithelial cell-cell adhesion molecule expressed by epithelial cells. Inactivation of the E-cadherin gene and abnormal expression of its protein are considered to be correlated with the dedifferentiation of gastric cancer cells with gastric phenotype^[4-8], but not the intestinal phenotype.

Gastric cancers with gastric phenotype have a poor outcome^[9] and higher malignant potential in the incipient phase of invasion and metastasis compared to those with other phenotypes. Differentiated-type gastric cancers (DGCs) with gastric phenotype are likely to change to undifferentiated-type adenocarcinomas in the invasive portion of the tumor. Phenotypic classification may be useful for predicting the biologic behavior and choosing the therapeutic strategy^[10]. To our knowledge, however, there are no data that compare the expression of syndecan-1 and E-cadherin in human gastric cancer. The aim of this study was to clarify the role and alterations of syndecan-1 expression in comparison with those of E-cadherin in different cellular phenotypes of DGCs, by using immunohistochemical staining.

MATERIALS AND METHODS

Specimens

One hundred and sixty patients (86 men, 74 women, average

age 52 years, range 21-60 years) with early gastric cancer were included in this study. DGC specimens were randomly selected from the histopathology files of our hospital between 2000 and 2003. Written informed consent was obtained from the patients before the interview for this study. Pathologic findings such as tumor size, depth of invasion, lymphatic invasion, blood vessel invasion, and lymph node metastasis were found from surgical files.

Early gastric cancers were defined as cancers with invasion limited to the submucosal layer. These tumors had been treated by surgical operation, all of which included the adjacent normal mucosa. The specimens were fixed in 40 g/L formaldehyde and embedded in paraffin wax, and 4- μ m consecutive sections were used for histologic examination by hematoxylin-eosin (H&E) staining and immunohistochemistry.

Histologic classification of the intramucosal lesions was carried out according to the general rules established by the Padova classification^[11]. DGCs were divided into two types, as follows, according to Koseki's classification^[12]: solely differentiated type, composed of DGCs demonstrating papillary and/or tubular adenocarcinoma; and complex type, comprised predominantly of DGCs and partly of poorly differentiated adenocarcinoma or signet-ring cell carcinoma.

Immunohistochemistry and classification of phenotypic expression

Fresh 4- μ m-thick serial sections were cut from routinely fixed, paraffin-embedded blocks and placed on poly-L-lysine-coated slides (Sigma Chemical, Poole, UK). One slide of each specimen was stained with hematoxylin-eosin and used to confirm the recorded histological classification. Immunohistochemical staining of syndecan-1 and E-cadherin was performed in accordance with standard procedures on 4- μ m-thick sections of formalin-fixed, paraffin-embedded sequential tissue sections^[13]. Antigen retrieval was performed by boiling for 12 min in an aluminum pressure cooker (Prestige, UK) at 103 kPa in pre-heated 10 mol/L sodium citrate buffer (pH 6.0). After cooling in running tap water, the slides were rinsed in 0.1 mol/L phosphate-buffered saline (PBS; pH 7.4). Nonspecific staining was blocked by incubation of the sections in normal horse serum for 30 min, prior to application of the primary monoclonal antibody to syndecan-1 (Serotec, Kidlington, UK) at a concentration of 0.001 mg/mL. This is an IgG1 antibody which reacts specifically with syndecan-1, as revealed by molecular cloning. After incubation in a moist chamber overnight at room temperature, the slides were washed in PBS and incubated for 30 min with biotinylated horse antimouse IgG (Vectastain Elite ABC kit; Vector Laboratories, Burlingame, CA). Slides were washed and then incubated for 30 min with avidin-biotin complex (Vectastain Elite ABC kit), according to the manufacturer's recommendations. Staining was performed by incubation with 3-3 diaminobenzidine (DAB; Sigma) activated with hydrogen peroxide. Slides were counter-stained with Mayer's hematoxylin. Negative controls were obtained by replacing primary antibody with PBS.

The avidin-biotin peroxidase complex method was employed for the detection of human gastric mucin (HGM; Novocastra Laboratories, Newcastle, UK), MUC2 (Novocastra Laboratories), CD10 (Novocastra Laboratories). Paradoxical

concanavalin A (Con A) staining, identifying class III mucins in mucous neck and pyloric gland cells, was employed, according to the method of Katsuyama and Spicer^[14]. HGM staining the surface of normal gastric epithelium and Con A were defined as gastric phenotype markers. MUC2 is a glycoprotein expressed predominantly in goblet cells, and CD10 expression is seen at the brush border on the luminal surface of epithelial cells. MUC2 and CD10 were defined as intestinal phenotype markers.

Classification of tissues

DGCs and normal mucosa surrounding the tumors were classified into four types based on the mucin phenotype, according to a modification of the classification of Ohmura^[15]: gastric type (G-type), ordinary type (O-type), complete-intestinal type (CI-type), and null type (N-type). The criteria for each phenotype are shown in Table 1.

These cellular phenotypes were evaluated both in tumor cells and in the background normal mucosa surrounding the tumors.

Table 1 Criteria for cellular phenotype

	HGM expression	Con A expression	MUC2 expression	CD10 expression
G-type	(+)	(+)	(-)	(-)
O-type	(+)	(+)	(+)	(+)
CI-type	(-)	(-)	(+)	(+)
N-type	(-)	(-)	(-)	(-)

G-type, gastric type; O-type, ordinary type; CI-type, complete-intestinal type; N-type, null type.

Grading of intestinal metaplasia (IM)

Intestinal metaplasia (IM) in the surrounding mucosa within 1 cm of the cancer was classified according to the classification of Egashira *et al*^[16]: negative, slight (with scattered IM); moderate (with continuous IM but scattered nonmetaplastic glands in between); and severe (with continuous IM). In this study, IM was divided into two groups based on the classification of Egashira *et al*^[16], for cellular phenotype: (1) that showing G-type expression (G-type IM); and (2) that not showing G-type mucin (non-G-type IM).

Evaluation of syndecan-1 and E-cadherin immunostaining

The results of immunohistochemical staining were evaluated independently by two observers. Immunohistochemical reaction intensities of syndecan-1 were classified into four grades. Briefly, -, no staining; \pm , weak staining or strong staining in fewer than 25% of tumor cells; +, moderate staining or strong staining in only 25-75% of tumor cells; and ++, strong staining of more than 75% of tumor cells. The sections for syndecan-1 were judged positive when more than 25% of cancer cells (+ or ++) were stained; others were judged negative. Concerning E-cadherin staining, its expression was demonstrated not only in the plasma membranes but also in the cytoplasm of tumor cells. The latter staining pattern of E-cadherin was suggested to reflect dysfunction of the cadherin cell adhesion system^[17]. Therefore, reduced expression and cytoplasmic localization

of E-cadherin in more than 20% of tumor cells was defined as abnormal expression^[17]. Staining of syndecan-1 and E-cadherin in IM was compared with that in foveolar epithelium. Sections were regarded as negative when the staining intensities of IM showed weak expression compared to those of foveolar epithelium; sections were regarded as positive when the staining intensities of IM were similar to those of foveolar epithelium. Normal gastric foveolar epithelium was used as an internal positive control.

Statistics

Statistical analysis was performed by the Mann-Whitney *U*-test between two independent groups, and by the χ^2 test and Fisher's exact probability test between two proportions. Statistical significance was defined as $P < 0.05$.

RESULTS

Mucin phenotype and pathological factors

The results are summarized in Table 2. There was no significant difference in the tumor size among the phenotypes. Forty-one surgically resected specimens had submucosal invasion. Of the 120 gastric cancers evaluated, 12 (10%) did not express any cellular phenotype (N-type). In the remaining 108 cases, G-type was observed in 34 cases (28.3%), O-type in 54 cases (45%), and CI-type in 20 cases (16.7%). The frequency of complex type was significantly higher in G-type (52.9%, 18 of 34) and N-type (75%, 9 of 12) compared with O-type (11.1%, 6 of 54) and CI-type cancers (10%, 2 of 20), as shown in Table 2. The G-type and N-type cancers were associated with a higher rate of lymphatic/venous invasion than O-type and CI-type cancers, although no significant differences were found in lymph node metastasis among the cellular phenotypes.

Syndecan-1 immunohistochemistry

Syndecan-1 protein was mainly stained at the basolateral surfaces of the foveolar epithelium, IM (Figure 1A), and tumor cells (Figure 1B). Stromal plasma cells were also stained for syndecan-1.

Table 2 Correlation of pathological factors and expression of syndecan-1 and E-cadherin in each mucin phenotype

	G-type (n = 34)	O-type (n = 54)	CI-type (n = 20)	N-type (n = 12)	P
Tumor size (cm, mean±SD)	3.5±0.9	2.9±0.7	3.1±0.6	2.7±0.4	NS
Histology					
Solely differentiated type	16	45	18	3	<0.05 ^{a,c}
Complex type	18	9	2	9	<0.05 ^{a,c}
Lymphatic and/or venous invasion ¹	17	14	5	5	<0.05 ^{a,g}
Lymph node metastasis	7	8	1	4	NS
Syndecan-1 expression	10	43	18	8	<0.05 ^{a,c}
E-cadherin expression	22	32	15	8	NS
IM	21	41	15	8	NS
IM with G-type ²	5	2	1	0	<0.05 ^a

^a $P < 0.05$ vs O-type; ^c $P < 0.05$ vs CI-type; ^a $P < 0.05$ vs O-type; ^g $P < 0.05$ vs CI-type G-type, gastric type; O-type, ordinary type; CI-type, complete-intestinal type; N-type, null type; NS, not significant. ¹Evaluated in 41 surgically resected specimens with submucosal invasion. ²Evaluated in 85 cases with positive for IM.

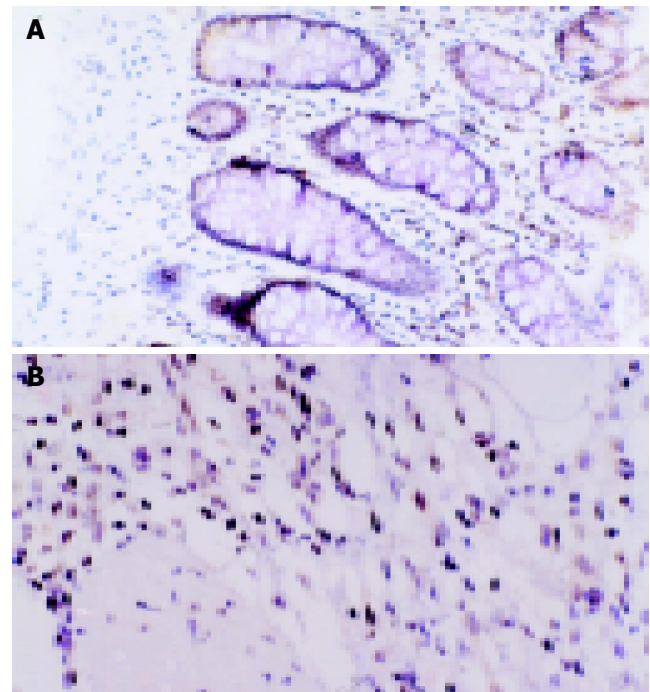


Figure 1 Expression of syndecan-1 in gastric mucosa on semi-serial sections. A: Positive staining with anti-syndecan-1 antibody is found at the basolateral surfaces of foveolar epithelial cells, IM and at the cell surfaces of stromal plasma cells. B: Positive staining is noted at the basolateral surfaces of cancer cells and at the cell surfaces of stromal plasma cells.

Correlation of syndecan-1 and E-cadherin expression with cellular phenotype and pathological factors

The expression of syndecan-1 protein was seen in 10 (29.4%) G-type, 43 (79.6%) O-type, 18 (90%) CI-type, and 8 (66%) N-type, and was significantly lower in G-type than in O-type and CI-type cancers ($P < 0.05$, respectively). However, there was no significant correlation between the expression of E-cadherin and any cellular phenotype (Table 2). Complex-type cancer showed a significant reduction or loss of syndecan-1 expression compared with the solely differentiated-type cancer ($P < 0.05$). Moreover, the expression of syndecan-1 was markedly decreased in poorly differentiated-type cancer cells, and was sparse in DGCs, whereas E-cadherin expression was not reduced in cancer cells. Lymphatic and/or venous invasion tended to be correlated with syndecan-1 expression ($P > 0.05$), whereas, with regard to lymph node metastasis, a significant correlation was noticed for E-cadherin ($P < 0.05$), but not for syndecan-1 (Tables 3 and 4).

Correlation of syndecan-1 and E-cadherin with cellular phenotype and intestinal metaplasia (IM)

IM in the surrounding mucosa was observed in 21 (61.8%) G-type cancers, in 41 (75.9%) O-type, in 15 (75%) CI-type, and in 8 (66.7%) N-type cancers, none of these differences being statistically significant (Table 2). IM with gastric phenotype was seen in only 9.4% of IM (8 of 85). The remaining 90.5% of IM (77 of 85) did not show G-type. Interestingly, G-type IM in the surrounding mucosa was observed in 5 cases (23.8%) of G-type cancers, but in 2 (4.9%) of O-type cancers, only 1 (6.7%) of CI-type, and

Table 3 Correlation of pathological factors and expression of syndecan-1

	Syndecan-1 expression		P
	Positive (n = 80)	Negative (n = 40)	
Histology			
Solely differentiated type	66	16	<0.05
Complex type	14	24	<0.05
Lymphatic and/or venous invasion ¹	28	13	NS
Lymph node metastasis	12	8	NS
IM with G-type ²	2	6	<0.05

G-type, gastric type; NS, not significant. ¹Evaluated in 41 surgically resected specimens with submucosal invasion. ²Evaluated in 85 cases with positive for IM.

none (0%) of N-type cancers (Table 4). Therefore, G-type IM was accompanied significantly more often by G-type cancers than by non-G-type, including O-type and CI-type cancers ($P < 0.05$; Table 4). In addition, G-type IM was observed significantly more often in cancers with negative expression of syndecan-1 (75%) than in those with positive expression (25%; $P < 0.05$), although there was no such relation for E-cadherin expression (Table 4). Reduction or loss of syndecan-1 expression and abnormal expression of E-cadherin were not seen in foveolar epithelium.

DISCUSSION

Syndecans are a family of cell-surface transmembrane heparan-sulfate proteoglycans. The sugar side chains of syndecan are structurally related to heparin and have functional cytoplasmic and extracellular domains that are thought to participate in both cell-cell and cell-extracellular matrix adhesion^[18-21]. Syndecan-1 is expressed not only in epithelial tissue but also in fibroblasts and plasma cells^[22-24]. Studies of the role of syndecan-1 in malignant transformation have revealed that syndecan-1 expression is associated with the maintenance of epithelial morphology and inhibition of invasion^[25,26]. Reduced expression of syndecan-1 was associated with malignant transformation in hepatocellular carcinoma^[27] and with poor prognosis in colorectal carcinoma^[28]. Furthermore, the expression of syndecan-1 was augmented during epithelial regeneration and rearrangement in the stomach^[29]. Syndecan-1 plays an important role in cell-cell adhesion, and many studies have examined the role of syndecan-1 in oncogenesis^[22-28].

A number of authors have reported about an association between E-cadherin expression and gastric cancers^[17,30]. However, there are few studies evaluating syndecan-1 in comparison with other adherent molecules, including E-cadherin, in other malignancies^[31,32]. And there are no data that compare syndecan-1 and E-cadherin expression in each cellular phenotype in early gastric cancers. In the present study, we found that syndecan-1 expression was significantly reduced in G-type cancers and G-type IM compared with the other phenotypes of cancers and IM. Furthermore, G-type IM was accompanied significantly more often by G-type cancers than by O-type and CI-type cancers. These data suggest that the reduction of syndecan-1 may play a role in the growth of both G-type gastric cancer and G-type IM. G-type cancers are considered to have a more

Table 4 Correlation of pathological factors and E-cadherin

	E-cadherin expression		P
	Positive (n = 77)	Abnormal (n = 43)	
Histology			
Solely differentiated type	57	29	NS
Complex type	20	14	NS
Lymphatic and/or venous invasion ¹	23	18	NS
Lymph node metastasis	7	13	<0.05
IM with G-type ²	4	4	NS

G-type, gastric type; NS, not significant. ¹Evaluated in 41 surgically resected specimens with submucosal invasion. ²Evaluated in 85 cases with positive for IM.

aggressive nature when compared with cancers of other cellular phenotypes^[9,10]. Therefore, the altered expression of syndecan-1 in early-stage gastric cancers may alter the biological behavior of the transformed epithelial cells and affect the invasive characteristics. In addition, assessment of the expression level of syndecan-1 may serve as a novel biomarker for predicting the malignant potential of cancers.

Human gastric foveolar epithelium, IM, and most DGC cells expressed syndecan-1 protein and mRNA, as reported previously^[29]. Syndecan-1 was mainly localized at the basolateral surfaces of the cells, implying that it participates in cell-cell and cell-extracellular matrix adhesion^[17-21]. The expression of syndecan-1 was lost or reduced in G-type cancers, which were significantly associated with complex type cancers, comprised predominantly of DGCs and partly of poorly differentiated adenocarcinoma or signet-ring cell carcinoma. It is reported that DGCs with gastric phenotype tend to change to undifferentiated-type adenocarcinomas^[33]. Therefore, the reduction of syndecan-1 might affect dedifferentiation, which appears as the loss of tumor glandular formation. Previous report indicates that the detachment of invading cancer cells from the nests was more frequently observed in syndecan-1-negative colorectal cancers^[28]. As for E-cadherin, however, its expression did not relate to cellular phenotype or to histologically complex type cancer. A report by Koseki *et al*^[12], showed that G-type cancer frequently demonstrated the abnormal expression of E-cadherin. Blok *et al*^[34], speculated that a reduction or loss of E-cadherin expression, with the concomitant acquisition of a morphologically diffuse growth pattern, might be responsible for the development of poorly differentiated and/or dedifferentiated cells in intestinal-type gastric cancer (which corresponds to our complex type cancer). The reasons for the discrepancy in these results are considered to be the differences of patient numbers examined and of the incidence of complex type in G-type cancers. Another explanation might be a defect in the catenin part of E-cadherin/catenin complex^[34]. Day *et al*^[31], reported that a greater reduction of syndecan-1 expression than of E-cadherin expression was seen in the transition from moderate to severe dysplasia in colon tumors. This result suggests that the changes in the expression of syndecan-1 probably occur before those in E-cadherin, perhaps influencing the expression of the latter adhesion molecule^[32]. Thus, our data are in agreement with their results. IM is generally known to be a precursor of DGC^[35,36]. In this study, we

focused on IM with different cellular phenotypes in the development of DGCs. Similar to our current finding, Egashira *et al.*^[6], have described that the IM surrounding G-type cancers showed gastric phenotype at a significantly higher incidence than it showed intestinal phenotype. The reduction of syndecan-1 expression was seen in IM alone, but not in gastric foveolar epithelium. Syndecan-1 expressed in IM was observed in both complete-type and incomplete-type IM, implying that syndecan-1 expression is not associated with cell differentiation in IM. The mechanism by which the functional loss of syndecan-1 contributes to the phenotypic expression of G-type IM is unclear. However, tumor phenotype in the early stage is widely thought to resemble that of the tissue of origin. It is, therefore, probable that the histogenesis of G-type cancer occurs in the pathway through which IM exhibits gastric phenotype, with functional loss of syndecan-1.

The present study showed that the immunoreactivity of E-cadherin appeared to be a more useful predictor of lymph node metastasis than syndecan-1, although many investigations of the relationship between E-cadherin and lymph node and/or vascular invasion have had controversial findings^[1,2,5,6,8,30,34]. We find here that the expression of syndecan-1 was not associated with lymph node metastasis, although lymphatic and/or venous invasion tended to be higher in cancers with a reduction or loss of syndecan-1 expression than in those with positive expression. Further studies are necessary to clarify the value of syndecan-1 compared with that of E-cadherin for predicting metastasis.

In conclusion, the present study shows that syndecan-1 may play a role in gastric cellular phenotyping and dedifferentiation in DGCs at an early stage, and it also shows that the reduction of syndecan-1 expression in the mucosa surrounding the tumors may influence the growth of gastric phenotype cancer. In the current study, the number of cancers analyzed may be small, particularly considering that four different categories of cellular phenotypes were compared. Thus, further investigations will be required with a larger sample size in order to confirm more clearly the expression of syndecan-1 and E-cadherin in various cellular phenotypes of gastric cancers and the background mucosa.

REFERENCES

- 1 Seagal J, Leider N, Wildbaum G, Karin N, Melamed D. Increased plasma cell frequency and accumulation of abnormal syndecan-1plus T-cells in Igmu-deficient/lpr mice. *Int Immunol* 2003; **15**: 1045-1052
- 2 Dull RO, Dinavahi R, Schwartz L, Humphries DE, Berry D, Sasisekharan R, Garcia JG. Lung endothelial heparan sulfates mediate cationic peptide-induced barrier dysfunction: a new role for the glycocalyx. *Am J Physiol Lung Cell Mol Physiol* 2003; **285**: L986-L995
- 3 Tanabe H, Yokota K, Kohgo Y. Localization of syndecan-1 in human gastric mucosa associated with ulceration. *J Pathol* 1999; **187**: 338-344
- 4 Takeichi M. Cadherin cell adhesion receptors as a morphogenetic regulator. *Science* 1991; **251**: 1451-1455
- 5 Becker KF, Atkinson MJ, Reich U, Becker I, Nekarda H, Siewert JR, Hofler H. E-cadherin gene mutations provide clues to diffuse type gastric carcinomas. *Cancer Res* 1994; **54**: 3845-3852
- 6 Shino Y, Watanabe A, Yamada Y, Tanase M, Yamada T, Matsuda M, Yamashita J, Tatsumi M, Miwa T, Nakano H. Clinicopathologic evaluation of immunohistochemical E-cadherin expression in human gastric carcinomas. *Cancer* 1995; **76**: 2193-2201
- 7 Tamura G, Sakata K, Nishizuka S, Maesawa C, Suzuki Y, Iwaya T, Terashima M, Saito K, Satodate R. Inactivation of the E-cadherin gene in primary gastric carcinomas and gastric carcinoma cell lines. *Jpn J Cancer Res* 1996; **87**: 1153-1159
- 8 Jawhari A, Jordan S, Poole S, Browne P, Pignatelli M, Farthing MJ. Abnormal immunoreactivity of the E-cadherin-catenin complex in gastric carcinoma: relationship with patient survival. *Gastroenterology* 1997; **112**: 46-54
- 9 Tajima Y, Shimoda T, Nakanishi Y, Yokoyama N, Tanaka T, Shimizu K, Saito T, Kawamura M, Kusano M, Kumagai K. Gastric and intestinal phenotypic marker expression in gastric carcinomas and its prognostic significance: immunohistochemical analysis of 136 lesions. *Oncology* 2001; **61**: 212-220
- 10 Koseki K, Takizawa T, Koike M, Ito M, Nihei Z, Sugihara K. Distinction of differentiated type early gastric carcinoma with gastric type mucin expression. *Cancer* 2000; **89**: 724-732
- 11 Rugge M, Correa P, Dixon MF, Hattori T, Leandro G, Lewin K, Riddell RH, Sipponen P, Watanabe H. Gastric dysplasia: the Padova international classification. *Am J Surg Pathol* 2000; **24**: 167-176
- 12 Koseki K, Takizawa T, Koike M, Ito M, Nihei Z, Sugihara K. Distinction of differentiated type early gastric carcinoma with gastric type mucin expression. *Cancer* 2000; **89**: 724-732
- 13 Adams JC, Kureishy N, Taylor AL. A role for syndecan-1 in coupling fascin spike formation by thrombospondin-1. *J Cell Biol* 2001; **152**: 1169-1182
- 14 Katsuyama T, Spicer SS. Histochemical differentiation of complex carbohydrates with variants of the concanavalin A-horse-radish peroxidase method. *J Histochem Cytochem* 1978; **26**: 233-250
- 15 Ohmura K, Tamura G, Endoh Y, Sakata K, Takahashi T, Motoyama T. Microsatellite alterations in differentiated-type adenocarcinomas and precancerous lesions of the stomach with special reference to cellular phenotype. *Hum Pathol* 2000; **31**: 1031-1035
- 16 Egashira Y, Shimoda T, Ikegami M. Mucin histochemical analysis of minute gastric differentiated adenocarcinoma. *Pathol Int* 1999; **49**: 55-61
- 17 Shiozaki H, Tahara H, Oka H, Miyata M, Kobayashi K, Tamura S, Iihara K, Doki Y, Hirano S, Takeichi M. Expression of immunoreactive E-cadherin adhesion molecules in human cancers. *Am J Pathol* 1991; **139**: 17-23
- 18 Mali M, Jaakkola P, Arvilommi AM, Jalkanen M. Sequence of human syndecan indicates a novel gene family of integral membrane proteoglycans. *J Biol Chem* 1990; **265**: 6884-6889
- 19 Bernfield M, Kokenyesi R, Kato M, Hinkes MT, Spring J, Gallo RL, Lise EJ. Biology of the syndecans: a family of transmembrane heparan sulfate proteoglycans. *Annu Rev Cell Biol* 1992; **8**: 365-393
- 20 Elenius K, Jalkanen M. Function of the syndecans-a family of cell surface proteoglycans. *J Cell Sci* 1994; **107(Pt 11)**: 2975-2982
- 21 Saunders S, Jalkanen M, O'Farrell S, Bernfield M. Molecular cloning of syndecan, an integral membrane proteoglycan. *J Cell Biol* 1989; **108**: 1547-1556
- 22 Hayashi K, Hayashi M, Jalkanen M, Firestone JH, Trelstad RL, Bernfield M. Immunocytochemistry of cell surface heparan sulfate proteoglycan in mouse tissues. A light and electron microscopic study. *J Histochem Cytochem* 1987; **35**: 1079-1088
- 23 Ito Y, Yoshida H, Nakano K, Takamura Y, Miya A, Kobayashi K, Yokozawa T, Matsuzuka F, Matsuura N, Kuma K, Miyauchi A. Syndecan-1 expression in thyroid carcinoma: stromal expression followed by epithelial expression is significantly correlated with dedifferentiation. *Histopathology* 2003; **43**: 157-164
- 24 Sanderson RD, Lalor P, Bernfield M. B lymphocytes express and lose syndecan at specific stages of differentiation. *Cell Regul* 1989; **1**: 27-35

- 25 **Dhodapkar MV**, Abe E, Theus A, Lacy M, Langford JK, Barlogie B, Sanderson RD. Syndecan-1 is a multifunctional regulator of myeloma pathobiology: control of tumor cell survival, growth, and bone cell differentiation. *Blood* 1998; **91**: 2679-2688
- 26 **Rapraeger AC**, Ott VL. Molecular interactions of the syndecan core proteins. *Curr Opin Cell Biol* 1998; **10**: 620-628
- 27 **Matsumoto A**, Ono M, Fujimoto Y, Gallo RL, Bernfield M, Kohgo Y. Reduced expression of syndecan-1 in human hepatocellular carcinoma with high metastatic potential. *Int J Cancer* 1997; **74**: 482-491
- 28 **Fujiya M**, Watari J, Ashida T, Honda M, Tanabe H, Fujiki T, Saitoh Y, Kohgo Y. Reduced expression of syndecan-1 affects metastatic potential and clinical outcome in patients with colorectal cancer. *Jpn J Cancer Res* 2001; **92**: 1074-1081
- 29 **Park PW**, Pier GB, Hinkes MT, Bernfield M. Exploitation of syndecan-1 shedding by *Pseudomonas aeruginosa* enhances virulence. *Nature* 2001; **411**: 98-102
- 30 **Gabbert HE**, Mueller W, Schneiders A, Meier S, Moll R, Birchmeier W, Hommel G. Prognostic value of E-cadherin expression in 413 gastric carcinomas. *Int J Cancer* 1996; **69**: 184-189
- 31 **Day RM**, Hao X, Ilyas M, Daszak P, Talbot IC, Forbes A. Changes in the expression of syndecan-1 in the colorectal adenoma-carcinoma sequence. *Virchows Arch* 1999; **434**: 121-125
- 32 **Barbareschi M**, Maisonneuve P, Aldovini D, Cangi MG, Pecciarini L, Angelo Mauri F, Veronese S, Caffo O, Lucenti A, Palma PD, Galligioni E, Doglioni C. High syndecan-1 expression in breast carcinoma is related to an aggressive phenotype and to poorer prognosis. *Cancer* 2003; **98**: 474-483
- 33 **Egashira Y**. Mucin histochemical study of differentiated adenocarcinoma of stomach. *Nihon Shokakibyo Gakkai Zasshi* 1994; **91**: 839-848
- 34 **Blok P**, Craanen ME, Dekker W, Tytgat GN. Loss of E-cadherin expression in early gastric cancer. *Histopathology* 1999; **34**: 410-415
- 35 **Filipe MI**, Munoz N, Matko I, Kato I, Pompe-Kirn V, Jutersek A, Teuchmann S, Benz M, Prijon T. Intestinal metaplasia types and the risk of gastric cancer: a cohort study in Slovenia. *Int J Cancer* 1994; **57**: 324-329
- 36 **Takahashi H**, Endo T, Yamashita K, Arimura Y, Yamamoto H, Sasaki S, Itoh F, Hirata K, Imamura A, Kondo M, Sato T, Imai K. Mucin phenotype and microsatellite instability in early multiple gastric cancers. *Int J Cancer* 2002; **100**: 419-424

Science Editor Zhu LH and Guo SY Language Editor Elsevier HK

• BRIEF REPORTS •

Combined human growth hormone and lactulose for prevention and treatment of multiple organ dysfunction in patients with severe chronic hepatitis B

Hui-Guo Ding, Jing Shan, Bin Zhang, Hong-Bo Ma, Li Zhou, Rui Jin, Yu-Fen Tan, Li-Xiang He

Hui-Guo Ding, Jing Shan, Bin Zhang, Hong-Bo Ma, Li Zhou, Rui Jin, Yu-Fen Tan, Li-Xiang He, Department of Gastroenterology and Hepatology, Beijing Youan Hospital, Capital University of Medical Sciences, Beijing 100054, China

Supported by the Foundation of Beijing Science and Technology Commission, No. H010210110129

Correspondence to: Dr. Hui-Guo Ding, Department of Gastroenterology and Hepatology, Beijing Youan Hospital, Capital University of Medical Sciences, Beijing 100054, China. dinghuiguo@medmail.com.cn

Telephone: +86-10-63292211-2718 Fax: +86-10-63295525

Received: 2004-03-05 Accepted: 2004-04-13

Key words: Chronic severe hepatitis B; Multiple organ dysfunction; Human growth hormone; Insulin-like growth factor-1; Lactulose

Ding HG, Shan J, Zhang B, Ma HB, Zhou L, Jin R, Tan YF, He LX. Combined human growth hormone and lactulose for prevention and treatment of multiple organ dysfunction in patients with severe chronic hepatitis B. *World J Gastroenterol* 2005; 11(19): 2981-2983

<http://www.wjgnet.com/1007-9327/11/2981.asp>

Abstract

AIM: To evaluate the efficiency and safety of combined recombinant human growth hormone (rhGH) and lactulose for treatment and/or prevention of multiple organ dysfunction in patients with chronic severe hepatitis B.

METHODS: Forty-eight inpatients with chronic severe hepatitis B were randomly divided into rhGH group ($n = 28$) and control group ($n = 20$). In rhGH group, 4-4.5 IU of rhGH was injected intramuscularly once daily for 2-4 wk, and 100 mL of enema containing 30 mL of lactulose, 2 g of metronidazole and 0.9% saline was administered every 2 d for 2-4 wk. Their symptoms and complications were noted. Liver and kidney functions were analyzed by an Olympus analyzer. Serum GH, IGF-1, IGFBP1 and IGFBP3 were measured by ELISA.

RESULTS: Clinical symptoms of 90% of these patients in rhGH group were obviously improved. The total effectiveness in rhGH group was better than that in control group (75% vs 40%, $P < 0.05$). After 2- and 4-wk treatment of rhGH respectively, serum albumin (26.1 ± 4.1 vs 30.2 ± 5.3 , 31.9 ± 5.1 g/L), prealbumin (79.6 ± 28.0 vs 106.6 ± 54.4 , 108.4 ± 55.0 g/L), cholesterol (76.3 ± 16.7 vs 85.6 ± 32.3 , 96.1 ± 38.7 mg/dL), and IGFBP1 (56.8 ± 47.2 vs 89.7 ± 50.3 ng/mL after 2 wk) were significantly increased compared to control group ($P < 0.05$). However, serum GH was decreased. The increase of serum IGF1 and IGFBP3 after rhGH treatment was also observed.

CONCLUSION: rhGH in combination with lactulose may be beneficial to the prevention and treatment of multiple organ dysfunction in patients with chronic severe hepatitis.

INTRODUCTION

Severe viral hepatitis, namely severe acute or chronic liver failure, develops quickly with an extremely dangerous prognosis. Its mortality rate is between 60% and 90%^[1] and there is still no breakthrough in medical treatment. It has been proved that multiple organ dysfunction is the main cause of death of these patients^[2,3]. Therefore, it is very important to treat effectively severe hepatitis patients with multiple organ dysfunction. The mortality would fall significantly if patients with multiple organ dysfunction are properly treated. The aim of our study was to evaluate the efficacy and safety of recombinant human growth hormone (rhGH) in combination with lactulose for treatment and/or prevention of chronic severe hepatitis B with multiple organ dysfunction. The mechanism of these drugs was also studied.

MATERIALS AND METHODS

Patients and controls

Forty-eight patients with chronic severe hepatitis B from January 1999 to February 2002 were enrolled. Chronic severe hepatitis was previously defined during the National Conference of Xi'an in 2002. In brief, inclusion criteria were as follows: a history of chronic hepatitis or liver cirrhosis; severe asthenia, serum total bilirubin more than $171 \mu\text{mol/L}$; prothrombin time activity (PTA) less than 40%. Of those patients, 28 were in treatment group (23 males and 5 females, average age of 42.6 years), 20 were in control group (17 males and 3 females, average age of 41.5 years). Their clinical data, such as liver and kidney biochemical parameters, were comparable.

Protocol of study

Treatment methods All patients in treatment group received standard treatment: rhGH 4-4.5 IU im injection once daily

for 2-4 wk, enema containing 0.9% normal saline 100 mL plus lactulose 30 mL and metronidazole 2.0 g once every 2 d for 2-4 wk. Patients in control group only received standard treatment.

Sample collection Venous blood 3 mL was collected at 6:00-7:00 a.m., and centrifuged at 4 °C, stored at -20 °C. Clinical symptoms and complications were recorded and the patients were followed-up for at least 6 mo according to CRF.

Biochemical tests Serum growth hormone (GH), insulin-like growth factor-1 (IGF-1), insulin-like growth factor binding proteins 1, 3 (IGFBP1, IGFBP3) were respectively measured by ELISA. All the test kits were purchased from DSL Corporation, and used according to their manufacturer's instructions.

Efficacy endpoints Clinical symptoms were completely improved and complications were controlled in 4 wk, and no new complications occurred. Liver functions were markedly improved in 3 mo, the total bilirubin decreased by 30-60%. PTA value was increased. All patients were followed-up for 6 mo.

Statistical analysis

Statistical evaluations were performed using SPSS 10.0 statistical software. Clinical effects of the two groups were compared by χ^2 test, quantitative data were expressed as mean \pm SD and analyzed with two-way variance test. *P* less than 0.05 was considered statistically significant.

RESULTS

The results of this study indicated that the clinical symptoms of 90% of the patients were markedly improved. The total effective rate was 75% in treatment group and 40% in control group. There was a significant difference between the two groups (*P*<0.05).

In treatment group, serum prealbumin, cholesterol and total protein in 60% of the patients were significantly increased (*P*<0.05, Table 1). The albumin level could maintain for 2-4 wk after rhGH was stopped. In contrast, prealbumin, cholesterol and albumin in 60% of the patients in control group were consistently decreased.

Table 1 Effects of rhGH on liver function of patients with severe chronic hepatitis B (mean \pm SD)

Marker of liver function	Pretreatment <i>n</i> = 28	2-wk treatment <i>n</i> = 28	4-wk treatment <i>n</i> = 16
Total protein (g/L)	51.6 \pm 4.3	67.8 \pm 8.4 ^a	69.2 \pm 7.8
Prealbumin (g/L)	80 \pm 28	107 \pm 54 ^a	108 \pm 55
Albumin (g/L)	26.1 \pm 4.1	30.2 \pm 5.3 ^a	31.9 \pm 5.1 ^b
Cholesterol (mg/dL)	76 \pm 17	86 \pm 32 ^a	96 \pm 39
Total bilirubin (mg/dL)	15 \pm 14	20 \pm 16	12 \pm 13
PTA (%)	21.3 \pm 5.5	24.7 \pm 12.2	36.8 \pm 7.9
ALT (IU/L)	117 \pm 210	83 \pm 77	59 \pm 43
AST (IU/L)	171 \pm 243	104 \pm 79	76 \pm 56

^a*P*<0.05, ^b*P*<0.01 vs pretreatment.

The level of serum GH in chronic severe hepatitis patients was relatively higher than that in normal subjects. But it decreased after rhGH was used for 2-4 wk. The level

of IGF-1 and IGFBP3 had a trend increase, but there was no statistical difference. The serum IGFBP1 level was markedly increased (Table 2). The mortality rate of the patients with high serum GH level after treatment was nearly 100%.

Table 2 Effects of rhGH on GH-IGF axis in patients with severe chronic hepatitis B (mean \pm SD)

Marker of GH-IGF axis	Pretreatment (<i>n</i> = 15)	2-wk treatment (<i>n</i> = 15)
GH (ng/mL)	10.4 \pm 7.6	6.2 \pm 8.1 ^a
IGF-1 (μ g/mL)	6.3 \pm 4.5	8.8 \pm 6.7
IGFBP1 (ng/mL)	56.8 \pm 47.2	89.7 \pm 50.3 ^a
IGFBP3 (μ g/mL)	3.5 \pm 1.7	5.1 \pm 3.4

^a*P*<0.05 vs pretreatment.

DISCUSSION

Up to now, there has been no ideal treatment for severe hepatitis. It was reported that the mortality rate of severe hepatitis was more than 80% if liver transplantation was not performed^[4]. Liver transplantation is the optimal choice for treatment of liver failure. Therefore, the fundamental purpose of internal medical treatment is to make the state of illness stable and to wait for appropriate liver donor for liver transplantation^[4]. Many complications in severe hepatitis patients had a close relation to the prognosis^[1,2]. It was found in our previous study that the mortality rate of severe hepatitis patients with more than two complications was 72.8% and nearly 100% of those with more than four complications. The pathophysiological mechanism of multiple organ dysfunction in severe hepatitis patients is still not clear^[1,3]. At present, it is considered that infection and severe endotoxemia could play an important role in severe hepatitis with multiple organ dysfunction^[1-3]. Malnutrition of severe hepatitis patients, especially chronic severe hepatitis patients, was the leading cause of accompanying infections^[1,5]. Therefore, if infection is controlled effectively and endotoxin is removed, malnutrition may improve, and the multiple organ dysfunction of severe hepatitis patients may be prevented and cured effectively. According to this hypothesis, we designed a new therapy method for chronic severe hepatitis: human GH combined with lactulose enema.

GH, composed of 191 amino acids, is a sort of single chain polypeptide secreted by adenohipophyseal acidophils. It is well known that GH not only promote growth and development but also has comprehensive biological functions, concerning cell multiplication and differentiation. GH could also regulate immunity and metabolism^[6]. Furthermore, liver is the main target organ of GH *in vivo*, and the center of GH-IGF axis^[7,8]. It has been found that decreased serum IGF-1, IGFBP3 and ALS had a close relation to liver reserve function and the prognoses of liver cirrhosis patients^[9]. It was also found^[10] that serum IGF-1 and IGFBP3 were decreased in severe viral hepatitis patients while IGFBP1 was increased. The decrease of IGF-1 also had a close relation to the prognosis of severe hepatitis patients. Assy *et al*^[9], performed hypodermic injection in liver cirrhosis patients with rhGH 0.4 U/kg, and measured serum IGF-1 24 h later with RIA. If IGF-1 <10 nmol/L, the prognosis was bad, the 1-year survival rate was only 15%; if IGF-1

>10 nmol/L, the 1- and 2-year survival rates of liver cirrhosis patients were both 100%; indicating that IGF-1 could be used to forecast the prognosis of liver cirrhosis patients^[11,12]. Our study showed that the GH level of chronic severe hepatitis patients was high, exogenous human GH could increase IGFBP1, IGF-1 and IGFBP3, while serum GH level was decreased. These results indicated that exogenous GH might improve GH resistance state of chronic severe hepatitis^[10-12]. GH resistance is related to metabolic disturbances, such as malnutrition, energy metabolism abnormality, both of which play an important part in secondary hepatocyte damage and multiple organ dysfunction of severe hepatitis. On the other hand, the prognoses of severe hepatitis patients depend on the balance between necrosis and regeneration of liver. Many cell factors (such as HGF, HSGF) can stimulate the proliferation of hepatic cells, but the clinical curative effect is not satisfactory. It has been found that epidermal growth factor could significantly alleviate the multiple organ failure due to thioacetamide. Our study also showed that the use of human GH for 2-4 wk in treating chronic severe hepatitis patients could reduce the occurrence and development of complications, prolong the survival and improve the life-quality of patients. Serum prealbumin, albumin level increased and the overall effective rate was 75% without any obvious side effect^[13].

It has been proved that toxic substances (such as endotoxin, NH_3 , γ -GABA, *etc.*) and high level of inflammatory cell factors in the serum of severe hepatitis patients could lead to fever, hypotension, ARDS, and eventually multiple organ dysfunction^[1]. Besides, these substances may affect the regeneration capacity of liver. Therefore, it is important to look for an effective method to reduce endotoxin and inflammatory cell factors. Biological and non-biological artificial livers could be used to treat severe hepatitis, through reducing the toxic substances in serum, such as endotoxin and bilirubin. However, most of the toxic substances could combine with proteins into large molecules and could not be filtered through, so treatment should be conducted repeatedly. Some useful cell factors were also filtered. Meanwhile there were some complications, such as secondary bacterial or virus infections. For this reason, the long-term treatment of severe hepatitis with artificial liver should be further explored, and at present it has been only used as the transient therapy before liver transplantation^[3]. Professor Fan (Hong Kong University) *et al.*, used selective filtration to remove toxic substances, and retained some liver growth factors meanwhile. They achieved perfect results in animal experiments, but there has been no clinical experiment^[3]. Some scholars utilized tumor necrosis factor antibody to treat experimental hepatic failure animals, and also obtained good results, but there is no clinical experiment report, either.

Lactulose can be decomposed into lactic acid and acetic acid by enteric bacteria. Both of them can acidify the intestinal tract, and restrain the production and absorption of toxic substances, such as endotoxin, NH_3 , *etc.*, so that they can remove endotoxin perfectly without severe side effects. It has been proved by clinical researches that

lactulose can remove endotoxin and decrease the generation of endotoxin. In this study, we preliminarily observed the curative effects of human GH associated with lactulose in treating chronic severe hepatitis, and achieved satisfactory results. In treatment group, the clinical symptoms of most of the patients were improved evidently. According to the modified criteria of therapeutical effect, the markedly effective rate was 21.4% (6/28), the effective rate was 53.5% (15/28), the overall effective rate was 75%, and there was a significant difference compared to the control group. This result indicated that human GH combined with lactulose could effectively prevent exacerbation of severe hepatitis, and prevent and cure its complications. Its mechanisms may lie in the following factors: preventing the generation and absorption of intestinal endotoxin, curing endotoxemia; improving GH resistance of chronic severe hepatitis patients and abnormal metabolic status, and increasing serum prealbumin, albumin and cholesterol level. It is preliminarily concluded that human GH combined with lactulose could prevent and cure severe hepatitis complicated by multiple organ dysfunction.

REFERENCES

- 1 **Riordan SM**, Williams R. Acute liver failure: targeted artificial and hepatocyte-based support of liver regeneration and reversal of multiorgan failure. *J Hepatol* 2000; **32**: 63-76
- 2 **Ding HG**, Gao GJ, Chen T, Jin R. Analysis of prognostic factor of severe hepatitis. *Linchuang Gandanbing Zazhi* 2002; **6**: 124-126
- 3 **Zimmerman JE**, Knaus WA, Sun X, Wagner DP. Severity stratification and outcome prediction for multisystem organ failure and dysfunction. *World J Surg* 1996; **20**: 401-405
- 4 **Ho DW**, Fan ST, To J, Woo YH, Zhang Z, Lau C, Wong J. Selective plasma filtration for treatment of fulminant hepatic failure induced by D-galactosamine in a pig model. *Gut* 2002; **50**: 869-876
- 5 **Qiu JG**, Delany HM, Teh EL, Freundlich L, Gliedman ML, Steinberg JJ, Chang CJ, Levenson SM. Contrasting effects of identical nutrients given parenterally or enterally after 70% hepatectomy: bacterial translocation. *Nutrition* 1997; **13**: 431-437
- 6 **Huang C**, Ding HG, Wang JT. Change of growth hormone and insulin like growth factor-1 axis in liver diseases. *Zhonghua Ganzhangbing Zazhi* 2001; **9**(Suppl): 118-119
- 7 **Sass DA**, Shakil AO. Fulminant hepatic failure. *Gastroenterol Clin North Am* 2003; **32**: 1195-1211
- 8 **Donaghy A**, Ross R, Gimson A, Hughes SC, Holly J, Williams R. Growth hormone, insulinlike growth factor-1, and insulinlike growth factor binding proteins 1 and 3 in chronic liver disease. *Hepatology* 1995; **21**: 680-688
- 9 **Assy N**, Hochberg Z, Enat R, Baruch Y. Prognostic value of generation of growth hormone-stimulated insulin-like growth factor-I (IGF-I) and its binding protein-3 in patients with compensated and decompensated liver cirrhosis. *Dig Dis Sci* 1998; **43**: 1317-1321
- 10 **Min J**, Yu H, Yan H, He L, Liu H, Zhao C. The growth hormone and insulin-like growth factors axis in liver failure patients. *Zhonghua Ganzhangbing Zazhi* 2001; **9** Suppl: 76-78
- 11 **Donaghy A**, Ross R, Wicks C, Hughes SC, Holly J, Gimson A, Williams R. Growth hormone therapy in patients with cirrhosis: a pilot study of efficacy and safety. *Gastroenterology* 1997; **113**: 1617-1622
- 12 **Wallace JD**, Abbott-Johnson WJ, Crawford DH, Barnard R, Potter JM, Cuneo RC. GH treatment in adults with chronic liver disease: a randomized, double-blind, placebo-controlled, cross-over study. *J Clin Endocrinol Metab* 2002; **87**: 2751-2759
- 13 **Rodeck B**, Kardorff R, Melter M, Ehrich JH. Improvement of growth after growth hormone treatment in children who undergo liver transplantation. *J Pediatr Gastroenterol Nutr* 2000; **31**: 286-290

• BRIEF REPORTS •

Protective effect of *fufanghuangqiduogan* against acute liver injury in mice

Shuang-Ying Gui, Wei Wei, Hua Wang, Li Wu, Wu-Yi Sun, Cheng-Yi Wu

Shuang-Ying Gui, Wei Wei, Hua Wang, Li Wu, Wu-Yi Sun
Cheng-Yi Wu, Institute of Clinical Pharmacology, Anhui Medical
University, Hefei 230032, Anhui Province, China
Shuang-Ying Gui, Department of Pharmacy, Anhui College of
TCM, Hefei 230031, Anhui Province, China
Supported by the State High Technology Research and Development
Program of China (863 Program), No. 2002AA2Z3235
Correspondence to: Professor Wei Wei, Institute of Clinical
Pharmacology, Anhui Medical University, Hefei 230032, Anhui
Province, China. wwei@ahmu.edu.cn
Telephone: +86-551-5161208 Fax: +86-551-5161208
Received: 2004-07-19 Accepted: 2004-09-04

© 2005 The WJG Press and Elsevier Inc. All rights reserved.

Key words: Fufanghuangqiduogan; *Radix Paeonia Pall*;
Radix Astragali; Acute liver injury

Gui SY, Wei W, Wang H, Wu L, Sun WY, Wu CY. Protective
effect of *fufanghuangqiduogan* against acute liver injury in
mice. *World J Gastroenterol* 2005; 11(19): 2984-2989
<http://www.wjgnet.com/1007-9327/11/2984.asp>

Abstract

AIM: To study the effects and possible mechanisms of *fufanghuangqiduogan* (FFHQ) in mice with acute liver injury (ALI).

METHODS: ALI was successfully induced by injecting carbon tetrachloride (CCl₄) intraperitoneally and by tail vein injection of *Bacillus Calmette Guerin* (BCG) and lipopolysaccharide (LPS) in mice, respectively. Each of the two model groups was divided into normal group, model group, FFHQ (60, 120 and 240 mg/kg) treatment groups, and bifendate treatment group. At the end of the experiment, levels of alanine aminotransferase (ALT) and aspartate aminotransferase (AST), content of malondialdehyde (MDA), activities of superoxide dismutase (SOD) and glutathione peroxidase (GSH-px) in liver homogenate were measured by biochemical methods. The activities of tumor necrosis factor- α (TNF- α) and interleukin-1 (IL-1) were determined by radio-immunoassay. Hepatic tissue sections were stained with hematoxylin and eosin and examined under a light microscope.

RESULTS: In the two models of ALI, FFHQ (60, 120, 240 mg/kg) was found to significantly decrease the serum transaminase (ALT, AST) activities. Meanwhile, FFHQ decreased MDA contents and upregulated the lower SOD and GSH-px levels in liver homogenate. Furthermore, in immunologic liver injury model, FFHQ decreased levels of TNF- α and IL-1 in serum. Histologic examination showed that FFHQ could attenuate the area and extent of necrosis, reduce the immigration of inflammatory cells.

CONCLUSION: FFHQ had protective effect on liver injury induced by either CCl₄ or BCG+LPS in mice, and its mechanisms were related to free radical scavenging, increasing SOD and GSH-px activities and inhibiting the production of proinflammatory mediators.

INTRODUCTION

Acute liver injury (ALI) is a co-operative consequence of endotoxemia, microcirculation dysfunction as well as inflammatory cells (such as macrophage, lymphocyte) that release inflammatory mediators and cytokines (such as tumor necrosis factor- α (TNF- α), interleukin-1 (IL-1)) when stimulated. ALI is mostly induced by viral hepatitis, alcoholism, iron overload, or drug toxicity. It has a very high morbidity and mortality. The treatment might be anti-inflammatory or antioxidant action. Many modern Western medicines have been used to remedy ALI, but strategies are difficult to achieve satisfied outcomes due to their side effects. However, some traditional Chinese herbs (such as *Radix Paeonia Pall*, *Radix Astragali*, *Radix Salviae Miltiorrhizae*, *Cordycep sinensis*, *Ginkgo biloba*, *Picrorhiza scrophulariiflora*) have been found to have particular advantages in therapeutic research of ALI and other liver disease for their definite effectiveness, cheap prices and negligible side effects^[1-6]. Traditional Chinese medicine (TCM) treatment is based on overall analysis of symptoms and signs, and the physical condition of the patient^[7]. *Fufanghuangqiduogan* (FFHQ) is an extract of prescription TCM consisting of *Radix Astragali*, *Radix Paeonia lactiflora*, etc. The present study aims at exploring the effects of FFHQ on the prevention of immunologic ALI induced by *Bacillus Calmette Guerin* (BCG)+ lipopolysaccharide (LPS) in mice and chemical ALI induced by CCl₄ in mice, and the content of malondialdehyde (MDA) and the activities of superoxide dismutase (SOD) and glutathione peroxidase (GSH-px) in mice liver homogenate were determined in order to investigate its possible mechanisms.

MATERIALS AND METHODS

Drugs and materials

CCl₄, purchased from Beijing Chemical Factory, was diluted to 0.1% in vegetable oil. LPS from *Escherichia coli* was obtained from Sigma Chemical Co. (St. Louis, MO, USA). BCG was purchased from Institute of Shanghai Biological Products. FFHQ is an extract of traditional Chinese herbs

consisting of *Radix Astragali*, *Radix Paeonia lactiflora* and *Radix Glycyrrhizae* purchased from Anhui Heyitang Pharmacy, China. These herbs mixed up in specified ratio (1:4:0.8) were boiled with water and extracted by alcohol: 95% alcohol in liquid of these herbs by the volume proportion of 2:1 was mixed and stored at 0–4 °C for 24 h, then the sediments were filtered and the suspension including the protein and amylum was finally heated at 90–95 °C to evaporate the remaining alcohol and to obtain yellow brown powders. FFHQ was mainly composed of the total glucosides of *Paeony* (TGP), the total astragalosides (TAS), the total flavonoids of *astragalus* (TFA), *astragalus* polysaccharides and so on. TGP and TAS, accounting for 59.3%, were main effective components of FFHQ. FFHQ was dissolved into 0.5% sodium carboxymethylcellulose (CMC-Na) solutions before use. Commercial kits used for determining lipid peroxidation and SOD activity were obtained from the Jiancheng Institute of Biotechnology (Nanjing, China). Other chemicals used in these experiments were of analytical grade from commercial sources.

Animals

Male Kunming mice (20±2 g) were obtained from the Animal Department of Anhui Medical University. Mice were maintained on 12-h light/dark cycles. Animals were allowed free access to food and water. All mice were fasted for 16 h prior to blood/tissue sampling. All experiments were performed in accordance with the institutional ethical guideline.

Establishment of chemical liver injury model^[8–10]

A CCl₄ 0.1% vegetable oil solution was injected intraperitoneally into each animal in a dose of 10 mL/kg body weight. All the mice were anesthetized with ether, then killed by cervical dislocation 16 h after CCl₄ injection and trunk blood was collected into heparinized tubes (50 U/mL) and centrifuged (1 500 r/min, 10 min, 4 °C). Serum was aspirated and stored at -70 °C until assayed as described below. The liver was also removed and stored at -70 °C until use.

Establishment of immunological liver injury model^[11]

A 2.5 mg dose of BCG (viable bacilli) suspended in 0.2 mL saline was injected via the tail vein into each animal, and 10 d later, injected with 7.5 µg LPS dissolved in 0.2 mL saline. The mice were anesthetized with ether, and then killed by cervical dislocation 16 h after LPS injection. The other method adopted in the case of pretreatment studies was the same as in CCl₄-induced liver injury mentioned above.

Drug treatment

In the two model experiments, the animals were equally divided into six groups randomly which included normal, model control, FFHQ groups (three different doses) and bifendate. The mice in FFHQ groups received daily doses of 60, 120 or 240 mg/kg b.w. of FFHQ using an 18-gauge stainless steel animal feeding needle for 10 d prior to LPS injection and for 7 d prior to CCl₄ injection, respectively. Mice in normal and model control group in the two model experiments were fed only with the same volume of vehicle.

Measurement of serum ALT, AST, TNF-α and IL-1

Serum alanine aminotransferase (ALT) and aspartate aminot-

ransferase (AST) were determined using commercial kits produced by Jiancheng Institute of Biotechnology (Nanjing, China). The activities of ALT and AST were expressed as an international unit (U/L). Serum TNF-α and IL-1 were measured using commercial kits produced by Beijing Biotechnology Co., Ltd, and their levels were expressed as nanogram per milliliter.

Measurement of MDA, SOD and GSH-px in liver homogenate

Liver was thawed, weighed and homogenized in Tris-HCl (5 mmol/L containing 2 mmol/L EDTA, pH 7.4). Homogenates were centrifuged (1 000 r/min, 10 min, 4 °C) and the supernatant was used immediately for the assays of MDA and SOD. MDA, SOD and GSH-px were determined following the instructions on the kit. In brief, MDA in liver tissue was determined by the thiobarbituric acid method. All samples were assayed in triplicates. The content of MDA was expressed as nanomole per gram liver tissue. The assay for total SOD was based on its ability to inhibit the oxidation of oxyamine by the xanthine-xanthine oxidase system. The red product (nitrite) produced by the oxidation of oxyamine had an absorbance at 550 nm. One unit (U) of SOD activity was defined as the amount that reduced the absorbance at 550 nm by 50%. All samples were assayed in triplicates. Results were expressed as unit per gram liver tissue. GSH-px was measured by the DTNB method, and its content was expressed as unit per milligram protein.

Histologic analysis

Formalin-fixed specimens were embedded in paraffin and stained with hematoxylin and eosin for conventional morphologic evaluation. After decapitation of rats, small liver specimens were placed in 100 mL/L formalin solution and processed routinely by embedding in paraffin. Tissue sections (4–5 µm) were stained with hematoxylin and eosin and examined under light microscope (Olympus, Japan). An experienced histologist who was unaware of the treatment conditions made histologic assessments.

Statistical analysis

All values were presented as mean±SD. Statistical analysis of the data for multiple comparisons was performed by one-way analysis of variance followed by Duncan's test. For a single comparison, the significance of differences between means was determined by Student's *t*-test. A level of *P*<0.05 was taken as statistically significant.

RESULTS

Effect of FFHQ on serum ALT, AST, TNF-α and IL-1

Activities of both serum AST and ALT, indices of hepatic cell damage, were significantly higher in BCG+LPS-induced group and CCl₄ group than in the control group in the two models. FFHQ (60, 120, 240 mg/kg b.w.) significantly reduced the activities of serum AST and ALT. Levels of TNF-α and IL-1 in serum were significantly higher in BCG+LPS-induced group than in the control group in the immunologic mice model. FFHQ (60, 120, 240 mg/kg b.w.) significantly reduced the levels of serum TNF-α and IL-1 in the immunologic mice model (Tables 1 and 2).

Table 1 Effects of FFHQ on serum ALT, AST, TNF- α and IL-1 in immunologic liver injury in mice ($n = 10$, mean \pm SD)

Group	Dose (mg/kg b.w.)	ALT (U/L)	AST (U/L)	TNF- α (ng/mL)	IL-1 ng/mL
Normal	---	22.3 \pm 6.1	31.5 \pm 8.5	1.29 \pm 0.41	0.157 \pm 0.054
Model	---	204.3 \pm 49.6 ^d	197.6 \pm 42.3 ^d	3.95 \pm 1.24 ^d	0.341 \pm 0.101 ^d
FFHQ	60	171.6 \pm 33.7 ^a	172.0 \pm 35.8 ^a	3.00 \pm 0.98 ^a	0.289 \pm 0.068 ^a
	120	131.1 \pm 24.8 ^b	151.2 \pm 39.8 ^b	2.76 \pm 0.63 ^b	0.244 \pm 0.049 ^b
	240	129.7 \pm 26.5 ^b	143.5 \pm 30.9 ^b	2.61 \pm 0.55 ^b	0.273 \pm 0.051 ^b
Bifendate	100	89.6 \pm 21.3 ^b	95.4 \pm 28.3 ^b	2.89 \pm 0.92 ^a	0.279 \pm 0.046 ^a

^a $P < 0.05$, ^b $P < 0.01$ vs model group; ^d $P < 0.01$ vs normal group.

Table 2 Effects of FFHQ on serum ALT and AST in chemical ALI in mice ($n = 10$, mean \pm SD)

Group	Dose (mg/kg b.w.)	ALT (U/L)	AST (U/L)
Normal	---	26.4 \pm 8.2	34.1 \pm 9.3
Model	---	222.4 \pm 35.9 ^d	231.8 \pm 40.0 ^d
FFHQ	60	181.6 \pm 30.7 ^a	182.0 \pm 35.8 ^a
	120	153.1 \pm 34.8 ^b	161.2 \pm 39.8 ^b
	240	144.7 \pm 46.5 ^b	153.5 \pm 30.9 ^b
Bifendate	100	103.5 \pm 29.8 ^b	139.3 \pm 31.6 ^b

^d $P < 0.01$ vs normal group; ^a $P < 0.05$, ^b $P < 0.01$ vs model group.

Effect of FFHQ on liver homogenate MDA, total SOD and GSH-px

Liver homogenate MDA content in BCG+LPS-induced group and CCl₄ group was significantly higher than that in the control group in the two models, while liver homogenate total SOD activity and the GSH-px level were sharply decreased. FFHQ (60, 120, 240 mg/kg b.w.) could not only significantly attenuate MDA generation, but evidently increased the liver total SOD activity and the GSH-px level in the two mice models (Tables 3 and 4).

Table 3 Effects of FFHQ on MDA, SOD and GSH-px of immunologic ALI mice's liver homogenate ($n = 10$, mean \pm SD)

Group	Dose (mg/kg b.w.)	MDA (nmol/g tissue)	SOD (U/g tissue)	GSH-px (U/mg protein)
Normal	---	6.54 \pm 1.82	396.6 \pm 60.6	141.4 \pm 27.5
Model	---	15.18 \pm 3.57 ^d	181.3 \pm 40.7 ^d	97.9 \pm 24.7 ^d
FFHQ	60	12.57 \pm 3.15 ^a	212.3 \pm 39.8 ^a	116.5 \pm 29.1 ^a
	120	10.74 \pm 2.34 ^b	252.1 \pm 42.0 ^b	129.5 \pm 30.5 ^b
	240	10.08 \pm 2.28 ^b	269.0 \pm 52.7 ^b	133.1 \pm 34.1 ^b
Bifendate	100	12.03 \pm 3.21 ^a	193.8 \pm 40.5	107.6 \pm 30.5

^a $P < 0.05$, ^b $P < 0.01$ vs model group; ^d $P < 0.01$ vs normal group.

Table 4 Effects of FFHQ on MDA, SOD and GSH-px of chemical ALI mice's liver homogenate ($n = 10$, mean \pm SD)

Group	Dose (mg/kg b.w.)	MDA (nmol/g tissue)	SOD (U/g tissue)	GSH-px (U/mg protein)
Normal	---	6.76 \pm 2.3	440.5 \pm 51.8	136.4 \pm 24.5
Model	---	18.68 \pm 4.72 ^d	204.3 \pm 34.1 ^d	91.9 \pm 21.2 ^d
FFHQ	60	13.21 \pm 2.88 ^b	310.1 \pm 35.5 ^b	105.5 \pm 23.6 ^a
	120	12.36 \pm 3.19 ^b	321.3 \pm 39.2 ^b	121.1 \pm 24.6 ^b
	240	12.08 \pm 3.28 ^b	337.0 \pm 35.1 ^b	124.3 \pm 27.9 ^b
Bifendate	100	12.29 \pm 2.67 ^b	221.6 \pm 38.5	98.3 \pm 22.5

^a $P < 0.05$, ^b $P < 0.01$ vs model group; ^d $P < 0.01$ vs normal group.

Histologic results

In the two models, normal mice had no pathologic abnormality. Liver parenchyma was in good morphology and hepatocytes were arranged around the central vein. No congestion and inflammation were noticed in the sinusoids (Figures 1A and 2A). In the two models, model group mice had severe pathologic abnormality. Hepatocytes were prominent with marked vacuolization; moreover, hepatocytes necrosis, striped necrosis, bridging necrosis appeared and inflammatory cells were arranged around the necrotic tissue. Congestions in liver sinusoids were significant with scattering immersion of inflammatory cells (Figures 1B and 2B). In the two models, the area and extent of necrosis in FFHQ-treated groups attenuated and the immigration of inflammatory cells reduced. Liver parenchyma was well preserved with radially arranged hepatocytes around the central vein. Regular sinusoidal structures were noticed without congestion (Figures 1C and 2C).

DISCUSSION

FFHQ was an extract of Chinese herbs prescription that has various kinds of pharmacologic actions. In the prescription, the main Chinese herbs such as *Radix Astragali* and *Radix Paeonia lactiflora* have been used to relieve the pain and be an effective prescription for treatment of liver disease and other diseases^[1,2,7,12,13]. FFHQ has some active compounds, such as TGP (consist of paeoniflorin, albiflorin, benzoylpaeoniflorin, oxypaeoniflorin, paeonin, etc.), TAS (consist of astragaloside I-VI, soyasaponin, etc.), TFA, *astragalus* polysaccharides and so on. The previous results from our laboratory showed that TGP was effective against ALI induced by CCl₄, D-galactosamine (D-GalN) and BCG+LPS in mice and chronic liver^[1]. *In vivo* and *in vitro*, TGP showed obvious anti-inflammatory and antioxidative activities in other diseases besides in liver disease. For example, it was found that treatment of AA rats with TGP (50 mg/kg, ig (14-28 d)) could inhibit the elevated level of MDA and NO, and upregulated the lowered activities of SOD and GSH-px^[14,15]. *In vitro*, TGP could scavenge OH \cdot and O₂^[16,17]. It was reported^[13] that TAS could protect liver from chemical injury induced by CCl₄, D-GalN and acetaminophen in mice. TAS could impede the elevation of ALT level, decrease the MDA content and increase the GSH concentration in mice liver homogenate. Obvious improvements of histologic changes were also observed. *In vitro*, TAS (0.75 μ mol/L-0.18 mmol/L) could decrease elevated ALT level in hepatocytes separated from rats. Previous studies of our institute showed that TAS had an antinociceptive effect on formalin test in mice that related to its inhibitory effect on the production of NO. Besides, *astragalus* polysaccharide was found to have immunoregulatory

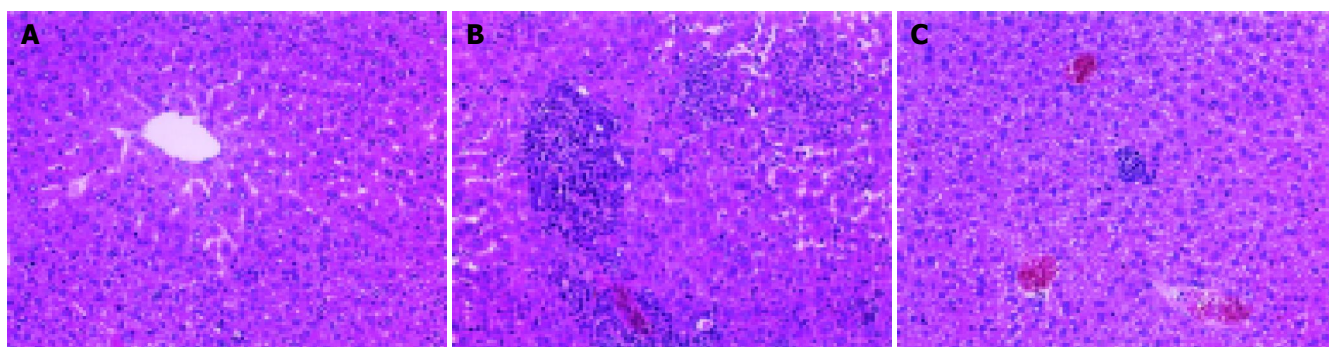


Figure 1 Histologic results of tissues stained with hematoxylin and eosin under light microscope in immunologic ALI mice. **A:** Normal control group; **B:** model

group; **C:** FFHQ-treated group.

activity and was used in various kinds of immunologic diseases^[17]. In our previous study, the optimum proportion of herbs in FFHQ prescription was obtained by uniform design in ALI mice. On the basis of the optimum proportion, FFHQ extracts were produced with the method stated in the part of “Drugs and materials”. In the present study, the two kinds of ALI models in mice were successfully established, namely immunologic ALI model induced by BCG+LPS and chemical ALI model induced by CCl₄ to observe the protective effects and its probable mechanisms of FFHQ.

CCl₄ is a well-known hepatotoxic chemical^[8,10,18,19]. The main cause of ALI by CCl₄ is free radicals of its metabolites. By the activation of liver cytochrome P-450, CCl₄ generates methyltrichloride radicals (CCl₃), which are highly unstable and immediately react with membrane components. They form covalent bonds with unsaturated fatty acids, or take a hydrogen atom from the unsaturated fatty acids of membrane lipids, resulting in the production of chloroform and lipid radicals. The lipid radicals react with molecular oxygen, which initiates peroxidative decomposition of phospholipids in the endoplasmic reticulum. The peroxidation process results in the release of soluble products that may affect cell membrane. Cell membrane integrity is broken and the enzymes (such as ALT, AST, *etc.*) in cell plasma leak out. The free radicals and its triggered lipid peroxidation were involved in the main mechanisms by which CCl₄ induced ALI^[20-25]. MDA was one of the main lipid peroxidation products, its elevated levels could reflect the degrees of lipid peroxidation injury in hepatocytes.

However, SOD is a scavenger of peroxide anion radicals^[26], which could inhibit the initiation of lipid peroxidation by free radicals; GSH-px could particularly catalyze the reductive action of GSH to H₂O₂ to protect the integrity of plasma membrane and functions. The present study showed that level of serum ALT, AST and the content of MDA in liver homogenate increased in the model group mice and the activities of SOD and GSH-px decreased correspondingly. FFHQ decreased the elevated level of ALT and AST, markedly inhibited the increase of MDA level and upregulated lower level of the activities of SOD and GSH-px in different extents, in a dose-dependent manner. These results indicated that median and high doses of FFHQ had potential action against lipid peroxidation, and this effect perhaps is the main mechanism of protection on ALI. The results were consistent with that TGP and TAS showed anti-inflammatory and antioxidant activities in our previous and in the studies of others.

Injection of BCG followed by LPS is useful for the creation of experimental models of immunologic ALI^[11,27,28]. In the present study, immunologic ALI in mice was successfully induced by BCG+LPS. On this basis, administration of FFHQ *in vivo* resulted in marked reduction of liver injury, as demonstrated by significant reduction of the serum transaminase concentration and amelioration of the severe hepatic pathologic abnormalities. Meanwhile, FFHQ decreased MDA content and increased GSH-px and total SOD activities in liver homogenate, in a dose-dependent manner. Furthermore, FFHQ significantly reduced TNF- α and IL-1 production in

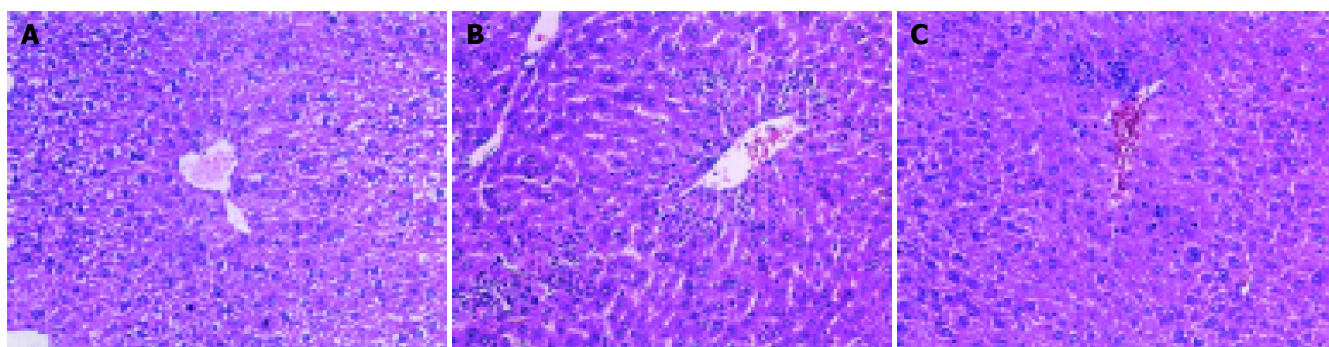


Figure 2 Histologic results of tissues stained with hematoxylin and eosin under light microscope in chemical ALI in mice. **A:** Normal control group; **B:** model

group; **C:** FFHQ-treated group.

serum, in a dose-dependent manner. In the present study, the effects of FFHQ on two models in mice were investigated first. The results showed that FFHQ decreased MDA content in liver homogenate, meanwhile, SOD and GSH-px activities rose significantly. Those results are in accordance with the findings of FFHQ's antioxidant properties.

TNF- α is a multifunctional cytokine mostly secreted by inflammatory cells and has been implicated in a number of liver diseases. TNF- α has been proven to be the key mediator and cytokine in the destruction of hepatocyte in human liver diseases^[29,30]. Many previous studies have showed that TNF- α could mediate cell injuries in liver caused by alcoholism, endotoxin, reperfusion, primary graft nonfunctional and graft rejection and so on, and the activity of TNF- α was positively related with the extent of liver necrosis^[28-31]. At the same time, TNF- α can activate nuclear transcription factor-kappa B of hepatocytes, Kupffer cells and endotheliocyte, which increases expression of intercellular adhesion molecule-1, vascular-cell adhesion molecule-1 and selection, these inflammatory factors further impel the inflammatory injury of hepatocytes^[32,33]. The present study is in accordance with the reported results. In the two ALI models in mice, serum TNF- α level in model groups was significantly higher than that in control groups. IL-1 is another critical inflammatory mediator and cytokine in ALI. Although IL-1 itself has no damage on liver, its elevation could stimulate inflammatory cells to excrete many other cytokines including TNF- α , IL-6 and IL-8, which contribute to ALI^[34]. Our data provided further evidence for the role of cytokines including TNF- α and IL-1 during ALI. Serum level of TNF- α and IL-1 elevated significantly in model group in immunologic ALI mice model. Median and high doses of FFHQ significantly reduced the elevated level of TNF- α and IL-1 in mice serum. Therefore, inhibition of pro-inflammatory mediator and cytokines is partly the mechanisms of FFHQ protective effect on ALI.

In the two model experiments, histologic changes, such as hemorrhage and necrosis in hepatic lobules, inflammatory infiltration of lymphocytes and Kupffer cells around the central vein, were simultaneously improved in FFHQ treatment groups. All results mentioned above suggested that FFHQ may not only be an anti-inflammatory agent, but also be used as an antioxidative therapy for ALI in mice.

In summary, the present study further demonstrated that inflammatory reaction, free radicals and its triggered lipid peroxidation are main pathologic characteristics of ALI. FFHQ has protective effect either on chemical ALI in mice or on immunologic ALI in mice. The mechanisms of FFHQ on ALI may be related to its immunoregulatory properties and antioxidant, such as free radical scavenging, increased SOD, GSH-px activities and proinflammatory mediators. To conform to the modernization of TCM, the study on active components about the prescription of FFHQ needs to be developed further. Both experiments to extract, isolate and identify the active components about the prescription of FFHQ and studies on the mechanisms involved are now in progress.

REFERENCES

- Dai LM, Chen XG, Xu SY. Protective effects of total glucosides of paeony on experimental hepatitis. *Zhongguo Yaolixue Tongbao* 1993; **9**: 449-453
- Shen WM, Wang CB, Wang DQ, Tian YP, Yan GT, Hao XH. The protective effects of TFA on reperfusion induced hepatic injury in hemorrhagic shock. *Zhongguo Yaolixue Tongbao* 1997; **13**: 532-534
- Singh AK, Mani H, Seth P, Gaddipati JP, Kumari R, Banuadha KK, Sharma SC, Kulshreshtha DK, Maheshwari RK. Picroliv preconditioning protects the rat liver against ischemia-reperfusion injury. *Eur J Pharmacol* 2000; **395**: 229-239
- McKenna DJ, Jones K, Hughes K. Efficacy, safety, and use of ginkgo biloba in clinical and preclinical applications. *Altern Ther Health Med* 2001; **7**: 70-86, 88-90
- Diamond BJ, Shiflett SC, Feiwei N, Matheis RJ, Noskin O, Richards JA, Schoenberger NE. Ginkgo biloba extract: mechanisms and clinical indications. *Arch Phys Med Rehabil* 2000; **81**: 668-678
- Hase K, Kasimu R, Basnet P, Kadota S, Namba T. Preventive effect of lithospermate B from *Salvia miltiorhiza* on experimental hepatitis induced by carbon tetrachloride or D-galactosamine/lipopolysaccharide. *Planta Med* 1997; **63**: 22-26
- Lin KJ, Chen JC, Tsauer W, Lin CC, Lin JG, Tsai CC. Prophylactic effect of four prescriptions of traditional Chinese medicine on alpha-naphthylisothiocyanate and carbon tetrachloride induced toxicity in rats. *Acta Pharmacol Sin* 2001; **22**: 1159-1167
- Mansour MA, Ginawi OT, El-Hadiyeh T, El-Khatib AS, Al-Shabanah OA, Al-Sawaf HA. Effects of volatile oil constituents of *Nigella sativa* on carbon tetrachloride-induced hepatotoxicity in mice: evidence for antioxidant effects of thymoquinone. *Res Commun Mol Pathol Pharmacol* 2001; **110**: 239-251
- Santra A, Das S, Maity A, Rao SB, Mazumder DN. Prevention of carbon tetrachloride-induced hepatic injury in mice by *Picrorhiza kurroo*. *Indian J Gastroenterol* 1998; **17**: 6-9
- Murakami T, Nagamura Y, Hirano K. The recovering effect of betaine on carbon tetrachloride-induced liver injury. *J Nutr Sci Vitaminol (Tokyo)* 1998; **44**: 249-255
- Ferluga J. Tuberculin hypersensitivity hepatitis in mice infected with *Mycobacterium bovis* (BCG). *Am J Pathol* 1981; **105**: 82-90
- Yang Q, Lu JT, Zhou AW, Wang B, He GW, Chen MZ. Antinociceptive effect of astragalosides and its mechanism of action. *Acta Pharmacol Sin* 2001; **22**: 809-812
- Zhang YD, Shen JP, Zhu SH, Huang DK, Ding Y, Zhang XL. Effects of astragalus (ASI, SK) on experimental liver injury. *Yaoxue Xuebao* 1992; **27**: 401-406
- Li J, Tang XL, Chen MZ, Xu SY. Immunoregulatory mechanisms of total glucosides of paeony in adjuvant arthritic rats. *Zhongguo Yaolixue Tongbao* 1995; **11**: 475-478
- Ge ZD, Wei W, Shen YX, Wang B, Ding CH, Zhou AW, Zhang AP, Xu SY. Effects of paeoniflorin, total glucosides of paeony removed paeoniflorin on interleukin 2 production by splenic lymphocytes from adjuvant arthritic rats. *Anhui Yike Daxue Xuebao* 1996; **31**: 4-6
- Gao BB, Dai LM, Xu SY. The scavenging activities of TGM and TGP on free radicals. *Wuifang Yixueyuan Xuebao* 1996; **18**: 43-46
- Xu DJ, Chen MZ. Effect of astragalus polysaccharide on immunologic function in mice. *Anhui Yiyao* 2003; **7**: 418-419
- Yu C, Wang F, Jin C, Wu X, Chan WK, McKeehan WL. Increased carbon tetrachloride-induced liver injury and fibrosis in FGFR4-deficient mice. *Am J Pathol* 2002; **161**: 2003-2010
- Marucci L, Alpini G, Glaser SS, Alvaro D, Benedetti A, Francis H, Phinzy JL, Marziani M, Mauldin J, Venter J, Baumann B, Ugili L, LeSage G. Taurocholate feeding prevents CCl4-induced damage of large cholangiocytes through PI3-kinase-dependent mechanism. *Am J Physiol Gastrointest Liver Physiol* 2003; **284**: G290-G301
- Marathe GK, Harrison KA, Roberts LJ, Morrow JD, Murphy RC, Tjoelker LW, Prescott SM, Zimmerman GA, McIntyre TM. Identification of platelet-activating factor as the inflammatory lipid mediator in CCl4-metabolizing rat liver. *J Lipid Res* 2001; **42**: 587-596

- 21 **Terao J**, Asano I, Matsushita S. High-performance liquid chromatographic determination of phospholipid peroxidation products of rat liver after carbon tetrachloride administration. *Arch Biochem Biophys* 1984; **235**: 326-333
- 22 **elSisi AE**, Earnest DL, Sipes IG. Vitamin A potentiation of carbon tetrachloride hepatotoxicity: enhanced lipid peroxidation without enhanced biotransformation. *Toxicol Appl Pharmacol* 1993; **119**: 289-294
- 23 **elSisi AE**, Earnest DL, Sipes IG. Vitamin A potentiation of carbon tetrachloride hepatotoxicity: role of liver macrophages and active oxygen species. *Toxicol Appl Pharmacol* 1993; **119**: 295-301
- 24 **Bruckner JV**, Ramanathan R, Lee KM, Muralidhara S. Mechanisms of circadian rhythmicity of carbon tetrachloride hepatotoxicity. *J Pharmacol Exp Ther* 2002; **300**: 273-281
- 25 **Badger DA**, Sauer JM, Hoglen NC, Jolley CS, Sipes IG. The role of inflammatory cells and cytochrome P450 in the potentiation of CCl₄-induced liver injury by a single dose of retinol. *Toxicol Appl Pharmacol* 1996; **141**: 507-519
- 26 **Hsu CT**. The role of the autonomic nervous system in chemically-induced liver damage and repair-using the essential hypertensive animal model (SHR). *J Auton Nerv Syst* 1995; **51**: 135-142
- 27 **Shands JW**, Senterfitt VC. Endotoxin-induced hepatic damage in BCG-infected mice. *Am J Pathol* 1972; **67**: 23-40
- 28 **Nagai H**, Yakuo I, Yamada H, Shimazawa T, Koda A, Niu K, Asano K, Shimizu T, Kasahara M. Liver injury model in mice for immunopharmacological study. *Jpn J Pharmacol* 1988; **46**: 247-254
- 29 **Streetz K**, Leifeld L, Grundmann D, Ramakers J, Eckert K, Spengler U, Brenner D, Manns M, Trautwein C. Tumor necrosis factor alpha in the pathogenesis of human and murine fulminant hepatic failure. *Gastroenterology* 2000; **119**: 446-460
- 30 **Crespo J**, Cayon A, Fernandez-Gil P, Hernandez-Guerra M, Mayorga M, Dominguez-Diez A, Fernandez-Escalante JC, Pons-Romero F. Gene expression of tumor necrosis factor alpha and TNF-receptors, p55 and p75, in nonalcoholic steatohepatitis patients. *Hepatology* 2001; **34**: 1158-1163
- 31 **Colletti LM**, Cortis A, Lukacs N, Kunkel SL, Green M, Strieter RM. Tumor necrosis factor up-regulates intercellular adhesion molecule 1, which is important in the neutrophil-dependent lung and liver injury associated with hepatic ischemia and reperfusion in the rat. *Shock* 1998; **10**: 182-191
- 32 **Issekutz TB**. Effects of six different cytokines on lymphocyte adherence to microvascular endothelium and *in vivo* lymphocyte migration in the rat. *J Immunol* 1990; **144**: 2140-2146
- 33 **Essani NA**, McGuire GM, Manning AM, Jaeschke H. Endotoxin-induced activation of the nuclear transcription factor kappa B and expression of E-selectin messenger RNA in hepatocytes, Kupffer cells, and endothelial cells *in vivo*. *J Immunol* 1996; **156**: 2956-2963
- 34 **Muto Y**, Nouri-Aria KT, Meager A, Alexander GJ, Eddleston AL, Williams R. Enhanced tumour necrosis factor and interleukin-1 in fulminant hepatic failure. *Lancet* 1988; **2**: 72-74

Science Editor Guo SY Language Editor Elsevier HK

• BRIEF REPORTS •

Docetaxel shows radiosensitization in human hepatocellular carcinoma cells

Chang-Xin Geng, Zhao-Chong Zeng, Ji-Yao Wang, Shi-Ying Xuan, Chong-Mao Lin

Chang-Xin Geng, Shi-Ying Xuan, Chong-Mao Lin, Department of Gastroenterology, Qingdao Municipal Hospital, Qingdao University, Qingdao 266071, Shandong Province, China
Zhao-Chong Zeng, Department of Radiation Oncology, Zhongshan Hospital, Fudan University, Shanghai 200032, China
Ji-Yao Wang, Department of Gastroenterology, Zhongshan Hospital, Fudan University, Shanghai 200032, China
Correspondence to: Dr. Chang-Xin Geng, Department of Gastroenterology, Qingdao Municipal Hospital, Qingdao 266071, Shandong Province, China. changxin_geng@hotmail.com
Telephone: +86-532-5937758
Received: 2004-06-08 Accepted: 2004-08-05

Abstract

AIM: To determine the radiosensitizing potential of docetaxel in human hepatocellular carcinoma SMMC-7721 cells and its mechanisms.

METHODS: SMMC-7721 cells were incubated with docetaxel at 0.125, 0.25, and 0.5 nmol/L for 24 h and at 0.125 and 0.25 nmol/L for 48 h before irradiation. Radiation doses were given from 0 to 10 Gy. Cell survival was measured by a standard clonogenic assay after a 9-d incubation. The reactive oxygen species (ROS) and glutathione (GSH) are detected after being given the same dose of docetaxel for the same time.

RESULTS: The sensitization enhancement ratios (SER) for SMMC-7721 cells determined at the 50% survival level were 1.15, 1.21 and 1.49 at 0.125, 0.25, and 0.5 nmol/L for pre-incubation of 24 h, respectively; the SER were 1.42, 1.67 at 0.125 and 0.25 nmol/L, for pre-incubation of 48 h, respectively. The ROS of SMMC-7721 cells increased and GSH decreased after pretreatment with the same doses of docetaxel for 24 or 48 h.

CONCLUSION: A radiosensitizing effect of docetaxel could be demonstrated unambiguously in this cell line used. In addition, our data showed that the mechanism of radiopotential by docetaxel probably does not involve a G2/M block in SMMC-7721 cells, and ROS generation and GSH deletion may play a key role in the radiosensitizing effect of docetaxel.

© 2005 The WJG Press and Elsevier Inc. All rights reserved.

Key words: Docetaxel; Hepatocellular carcinoma; SMMC-7721 cell line; Radiosensitization; Reactive oxygen species

Geng CX, Zeng ZC, Wang JY, Xuan SY, Lin CM. Docetaxel

shows radiosensitization in human hepatocellular carcinoma cells. *World J Gastroenterol* 2005; 11(19): 2990-2993
<http://www.wjgnet.com/1007-9327/11/2990.asp>

INTRODUCTION

Human hepatocellular carcinoma (HCC) is one of the major causes of death worldwide, and surgical resection is the only curative therapy, the resection rate is only 10-30%, the remaining patients are subjected to various forms of non-surgical therapy. Searching for effective chemotherapeutic agents is important to improve the survival rate of patients with advanced or recurrent HCC after surgical treatment. HCC is well known for its expression of multidrug resistance gene and its poor response to chemotherapeutic agents, thus is usually insensitive to chemotherapeutic drugs currently used in clinical setting and there is thus an urgent need for the evaluation of new options against HCC. External-beam radiation is one of the options employed currently in clinical practice. It has been recommended that a dosage greater than 50 Gy be used to kill HCC cells, however, this dose is associated with radiation-induced hepatitis and liver failure when the whole liver is treated, therefore, if radiation is used, the delivered dose should be limited to 30-35 Gy over 3-4 wk^[1,2].

Docetaxel is a new taxoid structurally similar to paclitaxel, a semisynthetic product of a renewable resource, the needles of the European yew, *Taxus baccata* L. In comparison to paclitaxel, docetaxel is more potent as an inhibitor of microtubule depolymerization, and a less efflux of docetaxel from tumor cells was observed. Docetaxel has been assessed in various cancers, and has shown an active effect against lung cancers, breast carcinoma, the carcinoma of the head and neck^[3-5].

In vitro studies provided ample evidence that docetaxel can enhance radiation sensitivity of tumor cells; treatment regimens consisting of docetaxel combined with radiotherapy have undergone extensive preclinical investigation. The focus was primarily on cell radiosensitization because docetaxel arrests cells in the radiosensitive G2/M phase of the cell cycle. In contrast with paclitaxel, docetaxel seems to be a better radiosensitizer than paclitaxel.

Studies have shown that combination therapy of docetaxel with radiation has higher efficacy and reduced effects in patients with lung cancer, head and neck cancer^[6,7].

Docetaxel and agent combination with radiotherapy was also feasible and, a high complete response rate could be observed. But the related information about HCC is hardly

reported and needs investigation, and the mechanism of docetaxel underlying its radioenhancing effect remains to be elucidated further. This study is to investigate the radiosensitizing effect of docetaxel and its mechanism in SMMC-7721 human HCC cells *in vitro* and to provide the basis for clinical application study in patients with HCC.

MATERIALS AND METHODS

Reagents

Docetaxel (Rhone-Poulenc Rorer Pharmaceuticals Inc.) was stored as 100 $\mu\text{mol/L}$ stock solution in absolute ethanol at -80°C . This solution was further diluted in the medium and used in the cell culture immediately before each experiment.

Cell cultures

Human HCC SMMC-7721 cell line was obtained from Liver Cancer Institute of Fudan University. The cells were cultured in flasks with RPMI1640 (Gibco BRL, Grand Island, NY) medium supplemented with 100 IU/mL penicillin, 100 $\mu\text{g/mL}$ streptomycin and 10% new-born bovine serum (Hyclone, Logan, UT) and maintained at 37°C in a humidified atmosphere containing 50 mL/L CO_2 .

Colony forming assay

Exponentially growing SMMC-7721 cells were trypsinized and seeded on the basis of different density in a 60-mm culture plate (Corning, NY) with 4 mL of medium, and allowed to bind. Twenty-four hours later, the medium was discarded and replaced by different concentrations of docetaxel containing medium. The cells were incubated for 24 and 48 h and then irradiated at room temperature with an Oris $^{137}\text{Cesium}$ source at doses ranging from 0 to 10 Gy. For 24 h group, docetaxel was added at 0.125, 0.25, 0.5 nmol/L and for 48 h group docetaxel was added at 0.125 and 0.25 nmol/L, respectively. For each radiation dose, four dishes were irradiated control and drug-treated cells. After irradiation, the docetaxel containing medium was replaced with equal volume of fresh medium without drug. The dishes were incubated at 37°C in air and 50 mL/L CO_2 for 9 d. The cells were fixed in ethanol, and stained with Giemsa, and manually counted. Colonies of >50 cells were considered as survivors. For all of the data obtained by cologenic assays, drug toxicity was adjusted for the surviving fraction of drug-treated cells to yield corrected survivals of 100% for non-irradiated but docetaxel-treated cells. The effect shown is therefore the sensitizing action, after the subtraction of the direct cytotoxic effect of docetaxel.

Reactive oxygen species measurement

After logarithmic growth phase SMMC-7721 cells were treated with 0.125, 0.25, and 0.5 nmol/L docetaxel for 24 h, 0.125 and 0.25 nmol/L docetaxel for 48 h, the cells were incubated with 2',7'-dichlorofluorescein diacetate (DCF/DA; 5 $\mu\text{mol/L}$; Sigma) at 37°C for 50 min to estimate the reactive oxygen species (ROS) level. The cells were harvested and detected immediately for fluorescence intensity detection on Becton Dickinson FACSCalibur flow cytometer and data were acquired and analyzed using FACS/CELLQuest software (San Jose, CA) on a Power Macintosh

7 600/120 computer (Apple Computers, Cupertino, CA)^[8], three independent experiments were repeated in each drug treated group and the control group was not given docetaxel and incubated with DCF/DA. All experiments were conducted in triplicate.

Determination of intracellular glutathione content

The determination of intracellular glutathione (GSH) content was conducted according to Shen *et al*^[9], with modification. Briefly after logarithmic growth phase SMMC-7721 cells ($\geq 10^6$) were treated with different doses of docetaxel (0.25, 0.5, 10 nmol/L) for 24 h, harvested by trypsination, washed, resuspended in PBS and counted under phase contrast microscope. The cells suspension was centrifuged at 300 r/min for 5 min, the cell pellets were added with 0.75 mL distilled water and 0.25 mL thiosalicylic acid to precipitate protein. After centrifugation at 12 000 g for 5 min at 4°C , the supernatant was used for GSH assay. The control group was not given docetaxel. All experiments were conducted in triplicate.

Statistical analysis

The intracellular GSH content was expressed as mean \pm SD. Their differences between drug treated groups and the control group were analyzed with Student's *t*-test.

RESULTS

The radiopotentiating effect of docetaxel on SMMC-7721 cells

Different doses of docetaxel incubated with SMMC-7721 cells both for 24 and 48 h show radiopotentiating effect: SERs for SMMC-7721 cells determined at the 50% survival level were 1.15, 1.21, 1.49 at 0.125, 0.25, 0.5 nmol/L for pre-incubation 24 h, respectively; SERs were 1.42, 1.67 at 0.125 and 0.25 nmol/L, for pre-incubation of 48 h, respectively. The surviving fraction of drug-treated cells was adjusted drug toxicity to yield corrected survivals of 100% for non-irradiated but docetaxel-treated cells. The effect shown is therefore the sensitizing action, after the subtraction of the direct cytotoxic effect of docetaxel (Figures 1 and 2).

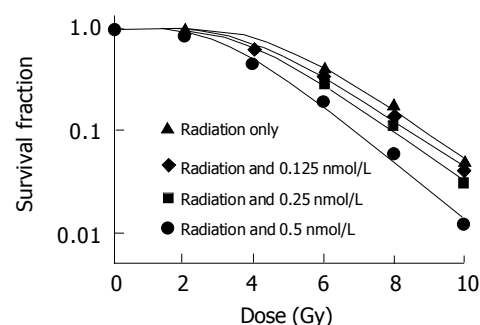


Figure 1 Dose response to radiation incubated with or without docetaxel for 24 h.

Effect of docetaxel on intracellular ROS

As demonstrated in Figure 3, The SMMC-7721 cells ROS level (corresponding to the fluorescence intensity) increased

significantly after treatment with 0.125, 0.25, and 0.5 nmol/L docetaxel for 24 h and 0.125 and 0.25 nmol/L docetaxel for 48 h. In comparison with that of the control group, the ROS level increased by 1.61, 1.69, 1.72, 1.33 and 1.38 times, respectively.

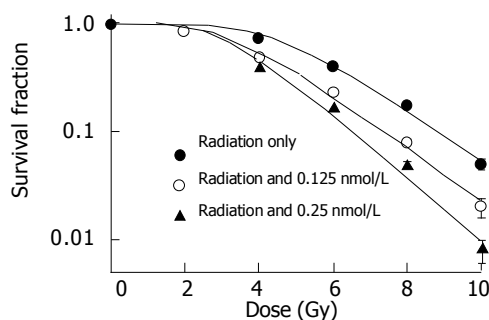


Figure 2 Dose response to radiation incubated with or without docetaxel for 48 h.

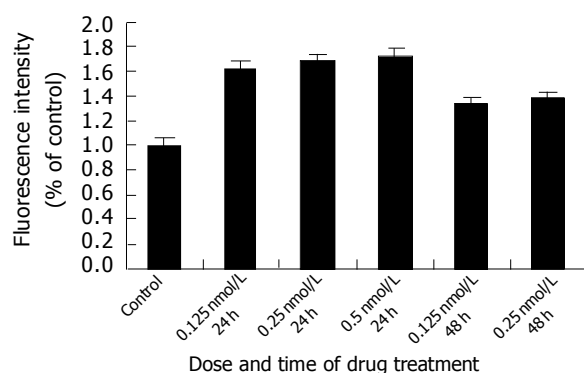


Figure 3 Effect of docetaxel on ROS generation of SMMC-7721 cells. Data were from three independent experiments.

Effect of docetaxel on intracellular GSH

Intracellular GSH decreased significantly after treatment with 0.125, 0.25, and 0.5 nmol/L docetaxel for 24 h and 0.125 and 0.25 nmol/L docetaxel for 48 h, in comparison with that of the control group ($P < 0.05$) (Figure 4), and on a dose- and time-dependent basis.

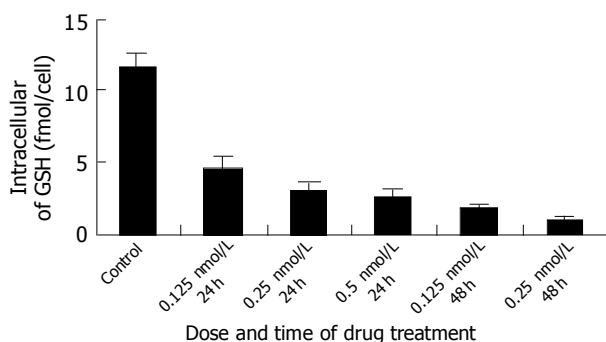


Figure 4 Changes of intracellular GSH content induced by different doses of docetaxel. The data were from three independent experiments.

DISCUSSION

Docetaxel is a new taxoid cytotoxic agent which promotes tubulin assembly into microtubules and inhibits their depolymerization, in comparison to paclitaxel, docetaxel is a more active tubulin assembly promoter and microtubule stabilizer.

It has been demonstrated that docetaxel can enhance radiation sensitivity of tumor cells, potentiate tumor response, and increase the therapeutic ratio of radiotherapy, compared with tumor radioresponse, normal tissue radioresponse was much less affected by docetaxel^[10]. In contrast to previously published results with paclitaxel, docetaxel seems to be a better radiosensitizer than paclitaxel.

Our results demonstrated that several doses of docetaxel incubated with SMMC-7721 cells for both 24 and 48 h shows radiosensitizing effect on this cell line, and on dose- and time-dependent basis. It is suggested that radiosensitization by paclitaxel require progression of cells through the cycle and accumulation in G2/M phase. But the colony forming assay and flow cytometric analysis of SMMC-7721 cells after treatment with different concentrations of docetaxel show that docetaxel at radiopotentiating doses did not cause any cell cycle redistribution, and the G2/M phase arrest gets apparent at a much higher dose (10 nmol/L), but the survival fraction decreases to 0 (data not shown here) at this dose of docetaxel, and this high dose docetaxel cannot be applied to radiation sensitizing study any further. So we speculate that the radiopotentiating effect of docetaxel on SMMC-7721 cells probably does not involve a G2/M arrest, and the mechanism underlying this phenomenon remains to be investigated. This is in agreement with results showing that docetaxel radiopotentiated human lung cancer cell line H460 cells, but did not cause any cell cycle redistribution and G2/M phase block. It is reported that reoxygenation of radioresistant hypoxic cells could account for radioenhancement by taxanes. Whether reoxygenation of SMMC-7721 cells by docetaxel occurred and is involved in radioenhancement needs investigation.

In order to investigate the mechanisms underlying the radioenhancement of docetaxel in SMMC-7721 cells, after SMMC-7721 cells were treated with different doses of docetaxel for 24 or 48 h, the ROS and GSH levels were determined. Our results demonstrated that the drug-treated SMMC-7721 cells ROS increased and GSH decreased significantly compared with that of the control group ($P < 0.05$), suggesting that intracellular oxidative stress and GSH deletion occurred after docetaxel treatment, and increased ROS and GSH deletion may be involved in the radioenhancement of docetaxel in SMMC-7721 cells. According to radiation biology, radiation in the presence of oxygen caused generation of peroxide, and peroxide could damage DNA, prevent DNA from repairing, thus enhancing the radiosensitivity of DNA, potentiating the radiosensitizing effect. ROS has been found to regulate translocation of NF- κ B as well as translocation of p53 and the p53-mediated apoptosis pathway^[11,12]. Also it has been found that induction of apoptosis was accompanied by the generation of intracellular ROS prior to the activation of caspase-3. Recently it was reported that arsenic trioxide and L-S, R-buthionine sulfoximine (BSO) combination treatment

enhanced HCC cells apoptosis through increased production of ROS^[13], modulation of the ROS production inside and outside of cells may influence the cell survival during oxidative insults. Oxidative stress can occur in irradiated human leukemia “blasts”, and may play a direct role in radiation-induced apoptosis. Early studies have also demonstrated that the onset of apoptosis is associated with a fall of intracellular GSH in different cellular systems and GSH could significantly reduce apoptosis mediated by a monoclonal antibody directed to Fas antigen, and apoptosis could be almost prevented by GSH. GSH is an important cellular thiol which is regarded as the major determinant of the intracellular redox potential; on the other hand, apoptosis may be regulated by the redox status within the cells. Loss of GSH was shown to be tightly coupled with a number of downstream events in apoptosis, in caspase activation and events in chromatin, and GSH depletion may act as a link between oxidative stress and ceramide-mediated apoptosis^[14]. Also it was found that decreased cells proliferation associated with decreased levels of intracellular GSH, and blockade of GSH synthesis enhanced ROS production and suppressed cells proliferation, cells with compromised cellular GSH were susceptible to redox imbalance-induced inhibition of proliferation^[15]. But if there is GSH in the cells, the peroxide can be cleared and DNA damage can be repaired. Depleting the intracellular GSH by specific inhibitor BSO could increase cellular radiosensitivity. GSH plays a critical protective role in maintaining nuclear and mitochondrial DNA functional integrity, determining the intrinsic radiosensitivity of Hep G2 cells, the protective role of GSH may relate to modification of DNA damage dependent signaling.

It was reported that buthionine sulfoximine-mediated GSH depletion increased radiation-induced chromosome aberrations, apart from exchange aberrations, this could be due to reduction in the free-radical scavenging effect of GSH, a failure in rejoining of DNA double-strand breaks, or induction of apoptosis. Induction of endogenous GSH in living cells following low-dose gamma-ray irradiation is partially responsible for the appearance of radioresistance to a subsequent lethal dose of radiation, and may make it possible to use higher doses of radiation in radiotherapy for tumor patients. Radiation-induced apoptosis in radiation-resistant murine lymphoma cell line (LY-ar) cells was restored by pretreatment with paclitaxel, was correlated with lowered levels of intracellular GSH^[16].

In summary, the present study demonstrates that docetaxel shows radiosensitizing effect on SMMC-7721 HCC cells *in vitro*. It leads to ROS generation and GSH deletion, subsequently results in redox imbalance in SMMC-7721 cells, and it is speculated that the redox imbalance caused by docetaxel may play an important role in the radioenhancement in SMMC-7721 cells. As far as we know, this is the first report concerning radiosensitization and of docetaxel and liver carcinoma the role of redox imbalance

by docetaxel in the radiosensitization so far. Our results not only provide the basis for further *in vivo* and clinical studies in HCC but also contribute to understanding the pharmacology of docetaxel further.

REFERENCES

- 1 **Guo WJ**, Yu EX. Evaluation of combined therapy with chemoembolization and irradiation for large hepatocellular carcinoma. *Br J Radiol* 2000; **73**: 1091-1097
- 2 **Aguayo A**, Patt YZ. Nonsurgical treatment of hepatocellular carcinoma. *Semin Oncol* 2001; **28**: 503-513
- 3 **Petrioli R**, Pozzessere D, Messinese S, Sabatino M, Ceciarini F, Marsili S, Correale P, Fiaschi AI, Voltolini L, Gotti G, Francini G. Weekly low-dose docetaxel in advanced non-small cell lung cancer previously treated with two chemotherapy regimens. *Lung Cancer* 2003; **39**: 85-89
- 4 **Coleman RE**, Howell A, Eggleton SP, Maling SJ, Miles DW. Phase II study of docetaxel in patients with liver metastases from breast cancer. UK study group. *Ann Oncol* 2000; **11**: 541-546
- 5 **Glisson BS**, Murphy BA, Frenette G, Khuri FR, Forastiere AA. Phase II Trial of docetaxel and cisplatin combination chemotherapy in patients with squamous cell carcinoma of the head and neck. *J Clin Oncol* 2002; **20**: 1593-1599
- 6 **Wu HG**, Bang YJ, Choi EK, Ahn YC, Kim YW, Lim TH, Suh C, Park K, Park CI. Phase I study of weekly docetaxel and cisplatin concurrent with thoracic radiotherapy in Stage III non-small-cell lung cancer. *Int J Radiat Oncol Biol Phys* 2002; **52**: 75-80
- 7 **Pradier O**, Rave-Frank M, Lehmann J, Lucke E, Boghun O, Hess CF, Schmidberger H. Effects of docetaxel in combination with radiation on human head and neck cancer cells (ZMK-1) and cervical squamous cell carcinoma cells (CaSki). *Int J Cancer* 2001; **91**: 840-845
- 8 **Lin HL**, Liu TY, Chau GY, Lui WY, Chi CW. Comparison of 2-methoxyestradiol-induced, docetaxel-induced, and paclitaxel-induced apoptosis in hepatoma cells and its correlation with reactive oxygen species. *Cancer* 2000; **89**: 983-994
- 9 **Shen HM**, Yang CF, Ong CN. Sodium selenite-induced oxidative stress and apoptosis in human hepatoma HepG2 cells. *Int J Cancer* 1999; **81**: 820-828
- 10 **Creane M**, Seymour CB, Colucci S, Mothersill C. Radiobiological effects of docetaxel (Taxotere): a potential radiation sensitizer. *Int J Radiat Biol* 1999; **75**: 731-737
- 11 **Kheradmand F**, Werner E, Tremble P, Symons M, Werb Z. Role of Rac1 and oxygen radicals in collagenase-1 expression induced by cell shape change. *Science* 1998; **280**: 898-902
- 12 **Martinez JD**, Pennington ME, Craven MT, Warters RL, Cress AE. Free radicals generated by ionizing radiation signal nuclear translocation of p53. *Cell Growth Differ* 1997; **8**: 941-949
- 13 **Kito M**, Akao Y, Ohishi N, Yagi K, Nozawa Y. Arsenic trioxide-induced apoptosis and its enhancement by buthionine sulfoximine in hepatocellular carcinoma cell lines. *Biochem Biophys Res Commun* 2002; **291**: 861-867
- 14 **Lavrentiadou SN**, Chan C, Kawcak T, Ravid T, Tsaba A, van der Vliet A, Rasooly R, Goldkorn T. Ceramide-mediated apoptosis in lung epithelial cells is regulated by glutathione. *Am J Respir Cell Mol Biol* 2001; **25**: 676-684
- 15 **Noda T**, Iwakiri R, Fujimoto K, Aw TY. Induction of mild intracellular redox imbalance inhibits proliferation of CaCo-2 cells. *FASEB J* 2001; **15**: 2131-2139
- 16 **Nguyen LN**, Munshi A, Hobbs ML, Story MD, Meyn RD. Paclitaxel restores radiation-induced apoptosis in a bcl-2-expressing, radiation-resistant lymphoma cell line. *Int J Radiat Oncol Biol Phys* 2001; **49**: 1127-1132

• BRIEF REPORTS •

Protective effect of L-arginine preconditioning on ischemia and reperfusion injury associated with rat small bowel transplantation

Bin Cao, Ning Li, Yong Wang, Jie-Shou Li

Bin Cao, Department of Surgery, Nanjing University Medical School, The First Affiliated Hospital of Nanjing Medical University, Nanjing 210029, Jiangsu Province, China
Ning Li, Yong Wang, Jie-Shou Li, Department of Surgery, Nanjing University Medical School, Nanjing 210002, Jiangsu Province, China
Correspondence to: Bin Cao, The First Affiliated Hospital of Nanjing Medical University, Nanjing 210029, Jiangsu Province, China. caobin3333@sina.com.cn
Telephone: +86-25-83918293 Fax: +86-25-4803956
Received: 2004-02-28 Accepted: 2004-04-16

© 2005 The WJG Press and Elsevier Inc. All rights reserved.

Key words: L-arginine; Small bowel transplantation

Cao B, Li N, Wang Y, Li JS. Protective effect of L-arginine preconditioning on ischemia and reperfusion injury associated with rat small bowel transplantation. *World J Gastroenterol* 2005; 11(19): 2994-2997
<http://www.wjgnet.com/1007-9327/11/2994.asp>

Abstract

AIM: To investigate the protective effect and possible mechanism of L-arginine preconditioning on ischemia and reperfusion injury associated with small bowel transplantation (SBT).

METHODS: Male inbred Wistar rats weighting between 180 and 250 g were used as donors and recipients in the study. Heterotopic rat SBT was performed according to the techniques of Li and Wu. During the experiment, intestinal grafts were preserved in 4 °C Ringer's solution for 8 h before being transplanted. Animals were divided into three groups. In group 1, donors received intravenous L-arginine (50 mg/kg, 1 mL) injection 90 min before graft harvesting. However, donors in control group were given normal saline (NS) instead. In group 3, six rats were used as sham-operated control. Specimens were taken from intestinal grafts 15 min after reperfusion. Histological grading, tissue malondialdehyde (MDA) and myeloperoxidase (MPO) levels were assessed. The graft survival of each group was monitored daily until 14 d after transplantation.

RESULTS: Levels of MDA and MPO in intestine of sham-operated rats were 2.0 ± 0.22 mmol/g and 0.66 ± 0.105 U/g. Eight hours of cold preservation followed by 15 min of reperfusion resulted in significant increases in tissue MDA and MPO levels. Pretreatment with L-arginine before graft harvesting resulted in lower enhancement of tissue levels of MDA and MPO and the differences were significant (4.71 ± 1.02 mmol/g vs 8.02 ± 3.49 mmol/g, 1.03 ± 0.095 U/g vs 1.53 ± 0.068 U/g, $P < 0.05$). Besides, animals in L-arginine pretreated group had better histological structures and higher 2-wk graft survival rates comparing with that in NS treated group (3.3 ± 0.52 vs 6 ± 0.1 , 0/6 vs 6/6, $P < 0.05$ or 0.01).

CONCLUSION: L-arginine preconditioning attenuates ischemia and reperfusion injury in the rat SBT model, which was due to antioxidant activities partially.

INTRODUCTION

Small bowel transplantation (SBT) has become an accepted therapy for intestinal disease in patients who require total parenteral nutrition. Although the results of SBT have dramatically improved during the past few years, ischemia-reperfusion injury (IRI), rejection and infection continues to be a major obstacle.

Ischemic preconditioning is the process in which one or more brief periods of ischemia with intermittent reperfusion confer a state of protection against subsequent long-term IRI. This phenomenon has been reported in small intestine^[1]. During the study an increase in NO synthesis was detected after intestinal preconditioning, and the protection induced by this process could be partly inhibited by the addition of the NO synthesis inhibitor L-NAME, so the preconditioning response might depend on the release of endogenous protective substances such as NO. Further investigation confirmed the protective effect of ischemic preconditioning on cold preservation and reperfusion injury in SBT^[2].

L-arginine is the substrate of NO *in vivo*. Studies showed L-arginine application could improve graft morphology, mucosal structure and mucosal barrier function after SBT^[3,4]. Another report^[5] confirmed sustained NO production via L-arginine administration ameliorated effects of intestinal IRI. In the studies mentioned above L-arginine was given to recipients before reperfusion, it is uncertain whether the administration of L-arginine to donor has the same effect, so the purpose of this study was to investigate the effect of L-arginine preconditioning on graft IRI.

MATERIALS AND METHODS

Animal protocols

Male inbred Wistar rats weighting between 180 and 250 g (Shanghai Laboratory Animal Center of the Chinese Academy of Sciences) were used as donors and recipients. Housed and fed at the Animal Center of Jinling Hospital, the rats were made to get accustomed to the environment

for at least 7 d before experiment. The donor and recipient were paired according to similar body weight.

Rat SBT was performed according to the techniques of Li and Wu. Briefly, the total length of intestinal graft was harvested with the vessel pedicle composed of superior mesenteric artery (SMA) and portal vein (PV). The graft intestine was preserved in Ringer's solution at 4 °C for 8 h before being transplanted heterotopically. In recipient the graft SMA and PV were anastomosed to the abdominal aorta and left renal vein respectively.

Animals were randomly assigned to the following groups. In group 1 (L-arginine), the donors were infused with L-arginine (50 mg/kg, 1 mL) 90 min before graft harvesting. In group 2 (control), donor animals received normal saline (NS), 1 mL injection instead of L-arginine. In group 3 (sham-operated), six rats were used as sham-operated control, of which the intestine was mobilized without enterectomy to exclude the influence of operation.

Measurement of MDA and MPO contents

Tissue malondialdehyde (MDA) and myeloperoxidase (MPO) activities were determined as indexes of tissue antioxidant status and neutrophils accumulation. The samples were obtained after 15 min of reperfusion and stored at -70 °C. Tissue MDA activity was determined by thiobarbituric acid test^[6]. To measure tissue MPO activity, frozen intestine was thawed and extracted for MPO, following the homogenization and sonication procedure as described by Krawisz^[7]. MPO activity in supernatant was measured and calculated from the absorbance (at 460 nm) changes that resulted from decomposition of H₂O₂ in the presence of O-dianisidine.

Histology

Full-thickness graft specimens for histological examination were fixed in 10% buffered formalin and processed for H&E light microscopy. The sections were graded for tissue injury using a scale of 0 (none) to 8 (severe)^[8] based on the following criteria: (0) normal mucosa; (1) development of subepithelial (Gruenhagen's) spaces at villus tips; (2) extension of the subepithelial space with moderate epithelial cell lifting from the lamina propria; (3) massive lifting down sides of villi, some denuded tips; (4) denuded villi, dilated capillaries; (5) disintegration of the lamina propria; (6) crypt layer injury; (7) transmucosal infarction. All histological analyses were performed in a blinded fashion so as to avoid bias.

Two-week graft survival rate

After operation the graft survival of each group was monitored daily until 14 d after transplantation.

Statistical analysis

All results were expressed as mean±SD. Significance was determined using one-way analysis of variance (ANOVA) for repeated measures followed by Newman-Keuls correction where appropriate. For comparison of graft survival, Mann-Whitney *U* test was used. All the changes and differences were considered statistically significant when the *P* value was less than 0.05.

RESULTS

Tissue MDA and MPO contents of intestinal grafts

The results of tissue MDA and MPO contents are shown in Table 1. The tissue concentrations of MDA and MPO in intestine of sham-operated rats were 2.0±0.22 mmol/g and 0.66±0.105 U/g. Eight hours of cold preservation followed by 15 min of reperfusion resulted in significant increases in tissue MDA and MPO levels. But the increases of MDA and MPO activities were significantly lower in L-arginine group than in control group.

Table 1 MDA and MPO levels after heterotopic SBT with or without L-arginine treatment

	Sham-operated	Control	L-arginine
MDA	2.0±0.22 mmol/g	8.02±3.49 mmol/g ^a	4.71±1.02 mmol/g ^c
MPO	0.66±0.105 U/g	1.53±0.068 U/g ^a	1.03±0.095 U/g ^c

^a*P*<0.05 vs sham-operated. ^c*P*<0.05 vs control.

Histology

After 15 min of reperfusion, grafts in control group showed moderate to severe histological changes of IRI. A significant decrease in extent of IRI-related changes was observed in grafts of recipients treated with L-arginine 90 min before graft harvesting (Figure 1 and Table 2).

Two-week graft survival rate of intestinal grafts

The results of this experiment demonstrated that 8 h of preservation induced severe IRI with none surviving for

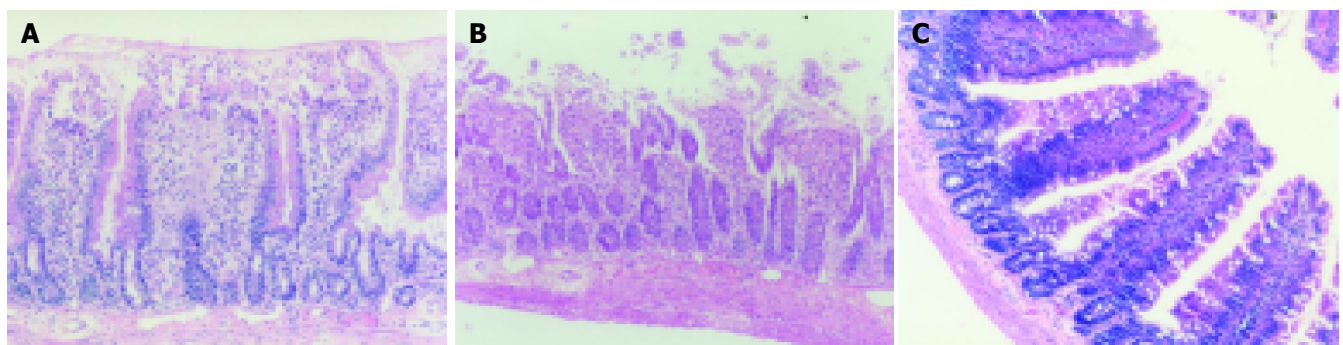


Figure 1 Small intestine underwent 8-h cold preservation and 15-min reperfusion, A: with L-arginine preconditioning; B: without L-arginine preconditioning; C:

normal small intestine.

Table 2 Histologic grading of graft with or without L-arginine treatment

Control	L-arginine
6±0.1	3.3±0.52 ^a

^aP<0.05 vs control.

more than 2 wk in control group. The longest survival time of graft in control group was 36 h. On the other hand, all grafts in L-arginine-treated group survived for more than 2 wk (Table 3).

DISCUSSION

Improvements in immunosuppression and the decrease in severe acute rejection after clinical SBT have allowed us to focus on issues other than the aforementioned complications. SBT is considered not optimal (including the preservation solution, preservation temperature and the mechanical and technical aspects). There has been increasing evidence that small bowel IRI will cause postoperative complications such as initial graft dysfunction, endotoxemia, peritonitis and an increased risk for the development of acute and chronic rejection. To efficiently improve the result of SBT, further investigations into the prevention and treatment of IRI are necessary.

Although the exact mechanism of IRI is still unknown, studies have shown that the effects of IRI are mediated partially by reactive oxygen metabolites and abnormal recruitment of activated polymorphonuclear neutrophils (PMN). This complex process can be modulated by numerous factors such as luminal pancreatic proteases^[9], phospholipase A2 (PLA-2)^[10], nitric oxide (NO)^[11], diamines^[12], regulators of calcium influx^[13], adenosine^[14], and other processes associated with PMN activation in the gut^[15].

Studies of intestinal IRI linking the local process to the resulting systemic changes have identified NO as a potential mediator. Although some studies showed NO was detrimental^[16,17] to IRI, the majority of studies demonstrated NO was beneficial to IRI^[18-20]. NO was considered to have a potent vasodilative action and a strong anti-platelet effect, in addition to prevention of neutrophil-endothelial cell interaction.

The substrate for NO synthesis is the amino acid, L-arginine, which combines with molecular oxygen in the presence of cofactors flavin mononucleotide and heme, a process that is catalyzed by NO synthase. Arginine is oxidized to produce an NO molecule and L-citrulline, which can be recycled through two intermediates back to L-arginine. Supplementation with L-arginine has been used in animal models to reduce the reperfusion injury to the heart or liver^[21-23]. In SBT, L-arginine has been proved effective on improving mucosal structure and barrier function when infused intravenously before reperfusion^[3,4].

As we all know, L-arginine can stimulate the immune function, so it may affect the immunosuppression treatment when given to the recipient. Therefore in our study we gave L-arginine to the donor before graft harvesting, hoping it could protect the graft from IRI without affecting anti-

Table 3 Effect of L-arginine on 2-wk graft survival rate of intestinal graft

Group	2-wk survival	Longest survival time
Control	0/6	36 h
L-arginine	6/6 ^b	8 mo

^bP<0.01 vs control.

rejection treatment. The present study demonstrated that the graft survival rate significantly improved after a relatively low dose of L-arginine was given to donor animals 90 min before harvesting. A concomitant lower increase of tissue MDA and MPO activities were also observed. The change of MDA and MPO activities indicated L-arginine preconditioning alleviated IRI partially through attenuating the oxidative stress.

We did examine the NO activity in graft after 15 min of reperfusion. The result suggested IRI induced a marked increase in graft NO level compared with normal intestine, which accorded with other studies^[24]. But the difference of NO activity between control and L-arginine group was not significant. The possible reasons may be as follows: At the time of graft harvesting, the vessel was irrigated with Ringer's solution, so the concentration of L-arginine in graft might be very low. Low concentration of L-arginine together with the short half-life of NO and long period of preservation might explain the similar changes of NO level between the two groups. It strongly suggests that alternative cytoprotective mechanisms of L-arginine should be involved in the attenuation of IRI instead of direct vasodilative and anti-platelet effects of NO.

In conclusion, the result of this study demonstrates that L-arginine preconditioning attenuates ischemia and reperfusion injury in the rat SBT model, which was due to antioxidant activities partially. The exact role of NO in it needs further investigation.

REFERENCES

- Hotter G, Closa D, Prados M, Fernandez-Cruz L, Prats N, Gelpi E, Rosello-Catafau J. Intestinal preconditioning is mediated by a transient increase in nitric oxide. *Biochem Biophys Res Commun* 1996; **222**: 27-32
- Sola A, De Oca J, Gonzalez R, Prats N, Rosello-Catafau J, Gelpi E, Jaurrieta E, Hotter G. Protective effect of ischemic preconditioning on cold preservation and reperfusion injury associated with rat intestinal transplantation. *Ann Surg* 2001; **234**: 98-106
- Mueller AR, Platz KP, Heckert C, Hausler M, Radke C, Neuhaus P. L-Arginine application improves mucosal structure after small bowel transplantation. *Transplant Proc* 1998; **30**: 2336-2338
- Mueller AR, Platz KP, Schirmeier A, Nussler NC, Seehofer D, Schmitz V, Nussler AK, Radke C, Neuhaus P. L-arginine application improves graft morphology and mucosal barrier function after small bowel transplantation. *Transplant Proc* 2000; **32**: 1275-1277
- Ward DT, Lawson SA, Gallagher CM, Conner WC, Shea-Donohue T. Sustained nitric oxide production via l-arginine administration ameliorates effects of intestinal ischemia-reperfusion. *J Surg Res* 2000; **89**: 13-19
- Mihara M, Uchiyama M. Determination of malonaldehyde precursor in tissues by thiobarbituric acid test. *Anal Biochem* 1978; **86**: 271-278

- 7 **Krawisz JE**, Sharon P, Stenson WF. Quantitative assay for acute intestinal inflammation based on myeloperoxidase activity. Assessment of inflammation in rat and hamster models. *Gastroenterology* 1984; **87**: 1344-1350
- 8 **Chiu CJ**, McArdle AH, Brown R, Scott HJ, Gurd FN. Intestinal mucosal lesion in low-flow states. I. A morphological, hemodynamic, and metabolic reappraisal. *Arch Surg* 1970; **101**: 478-483
- 9 **Montgomery A**, Borgstrom A, Haglund U. Pancreatic proteases and intestinal mucosal injury after ischemia and reperfusion in the pig. *Gastroenterology* 1992; **102**: 216-222
- 10 **Siems WG**, Grune T, Esterbauer H. 4-Hydroxynonenal formation during ischemia and reperfusion of rat small intestine. *Life Sci* 1995; **57**: 785-789
- 11 **Payne D**, Kubes P. Nitric oxide donors reduce the rise in reperfusion-induced intestinal mucosal permeability. *Am J Physiol* 1993; **265**: G189-G195
- 12 **Koshi S**, Inoue M, Obayashi H, Miyauchi Y. Inhibition of post-ischemic reperfusion injury of the small intestine by diamine oxidase. *Biochim Biophys Acta* 1991; **1075**: 231-236
- 13 **Mustafa NA**, Yandi M, Turgutalp H, Ovali E, Aydemir V, Albayrak L. Role of diltiazem in ischemia-reperfusion injury of the intestine. *Eur Surg Res* 1994; **26**: 335-341
- 14 **Schoenberg MH**, Poch B, Moch D, Marzinzig M, Marzinzig E, Mattfeldt T, Gruber H, Beger HG. Effect of acadesine treatment on postischemic damage to small intestine. *Am J Physiol* 1995; **269**: H1752-H1759
- 15 **Weixiong H**, Aneman A, Nilsson U, Lundgren O. Quantification of tissue damage in the feline small intestine during ischaemia-reperfusion: the importance of free radicals. *Acta Physiol Scand* 1994; **150**: 241-250
- 16 **Ialenti A**, Iannaro A, Moncada S, Di Rosa M. Modulation of acute inflammation by endogenous nitric oxide. *Eur J Pharmacol* 1992; **211**: 177-182
- 17 **Miura M**, Ichinose M, Kageyama N, Tomaki M, Takahashi T, Ishikawa J, Ohuchi Y, Oyake T, Endoh N, Shirato K. Endogenous nitric oxide modifies antigen-induced microvascular leakage in sensitized guinea pig airways. *J Allergy Clin Immunol* 1996; **98**: 144-151
- 18 **Kubes P**, Granger DN. Nitric oxide modulates microvascular permeability. *Am J Physiol* 1992; **262**: H611-H615
- 19 **Poss WB**, Timmons OD, Farrukh IS, Hoidal JR, Michael JR. Inhaled nitric oxide prevents the increase in pulmonary vascular permeability caused by hydrogen peroxide. *J Appl Physiol* (1985) 1995; **79**: 886-891
- 20 **Guidot DM**, Repine MJ, Hybertson BM, Repine JE. Inhaled nitric oxide prevents neutrophil-mediated, oxygen radical-dependent leak in isolated rat lungs. *Am J Physiol* 1995; **269**: L2-L5
- 21 **Li SQ**, Liang LJ. Protective mechanism of L-arginine against liver ischemic-reperfusion injury in rats. *Hepatobiliary Pancreat Dis Int* 2003; **2**: 549-552
- 22 **Yagnik GP**, Takahashi Y, Tsoulfas G, Reid K, Murase N, Geller DA. Blockade of the L-arginine/NO synthase pathway worsens hepatic apoptosis and liver transplant preservation injury. *Hepatology* 2002; **36**: 573-581
- 23 **Okonski P**, Szram S, Banach M, Fila M, Bielaski K, Mussur M, Zaslonka J. Effect of L-arginine on overhydration and ultrastructure preservation of rat's heart exposed to cold cardioplegic ischaemia. *Ann Transplant* 2003; **8**: 57-62
- 24 **Platz KP**, Mueller AR, Heckert C, Hausler M, Guckelberger O, Lobeck H, Neuhaus P. Nitric oxide production after syngeneic and allogeneic small bowel transplantation. *Transplant Proc* 1998; **30**: 2662-2664

Science Editor Zhu LH Language Editor Elsevier HK

• BRIEF REPORTS •

Mutations of p53 gene exons 4-8 in human esophageal cancer

Li-Ya Li, Jin-Tian Tang, Li-Qun Jia, Pei-Wen Li

Li-Ya Li, Li-Qun Jia, Pei-Wen Li, Department of Oncology, China-Japan Friendship Hospital, Beijing 100029, China
Jin-Tian Tang, Institute of Medical Physics and Engineering, Tsinghua University, Beijing 100084, China
Supported by Ministry of Science and Technology of the People's Republic of China grants, No. 2003CA04200 and 2004CB720301; National Natural Science Foundation of China grant, No.10490195 and 30271465; Beijing Municipal Science & Technology Commission grant, No. H030230160130 and in part by a grant from Tsinghua University YUYUAN foundation
Co-first-authors: Li-Ya Li and Jin-Tian Tang
Correspondence to: Dr. Li-Ya Li, Department of Oncology, China-Japan Friendship Hospital, Beijing 100029, China. tjt@263.net
Telephone: +86-10-64480373
Received: 2004-05-29 Accepted: 2004-07-06

Abstract

AIM: To characterize the tumor suppressor gene p53 mutations in exon 4, esophageal cancer and adjacent non-cancerous tissues.

METHODS: We performed p53 (exons 4-8) gene mutation analysis on 24 surgically resected human esophageal cancer specimens by PCR, single-strand conformation polymorphism, and DNA sequencing.

RESULTS: p53 gene mutations were detected in 9 of 22 (40.9%) esophageal cancer specimens and 10 of 17 (58.8%) adjacent non-cancerous tissues. Eight of sixteen (50.0%) point mutations detected were G→A transitions and 9 of 18 (50.0%) p53 gene mutations occurred in exon 4 in esophageal cancer specimens. Only 1 of 11 mutations detected was G→A transition and 4 of 11 (36.4%) p53 gene mutations occurred in exon 4 in adjacent non-cancerous tissues.

CONCLUSION: Mutation of p53 gene in exon 4 may play an important role in development of esophageal cancer. The observation of p53 gene mutation in adjacent non-cancerous tissues suggests that p53 gene mutation may be an early event in esophageal carcinogenesis. Some clinical factors, including age, sex, pre-operation therapy and location of tumors, do not influence p53 gene mutation rates.

© 2005 The WJG Press and Elsevier Inc. All rights reserved.

Key words: Gene p53; Esophageal cancer

Li LY, Tang JT, Jia LQ, Li PW. Mutations of p53 gene exons 4-8 in human esophageal cancer. *World J Gastroenterol* 2005; 11(19): 2998-3001
<http://www.wjgnet.com/1007-9327/11/2998.asp>

INTRODUCTION

Esophageal cancer is one of the most fatal cancers both in China and in the rest of the world^[1]. The p53 tumor suppressor gene, located in chromosome 17p13, is a well-known transcription factor of cell cycle regulation and mutation of p53 gene is the most common phenomenon in carcinogenesis and tumor progression^[2,3].

We investigated p53 (exons 4-8) gene mutations in esophageal cancer and adjacent non-cancerous tissues by PCR and single-strand conformation polymorphism (SSCP) analysis to evaluate p53 mutation correlation and to compare the relationship between p53 (exons 4-8) gene mutations and some clinical factors.

MATERIALS AND METHODS

Specimens

Twenty-two esophageal cancer tissue specimens and 17 non-cancerous tissue specimens, from a high-incidence area of Linxian County in Henan Province, China, were selected for this study. Patients were admitted to hospitals during 1997-1999 (Table 1) and underwent radical surgery for thoracic esophageal carcinoma. The resected specimens were embedded in paraffin and subjected to subsequent molecular analysis after the pathological findings were confirmed as squamous cell carcinoma.

DNA extraction

DNA was extracted using chelating resin for PCR amplification. In brief, three 10-μm-thick paraffin sections were cut, transferred into sterile distilled water containing 20% chelating resin iminodiacetic acid (Sigma, St. Louis, MO), and boiled for 30 min. After centrifugation, the supernatant was transferred to a sterile 500-μL tube and stored at -20 °C.

PCR amplification

The primers used for PCR amplification of the p53 (exons 4-8) gene were as follows: 5'-TTT TCA CCC ATC TAC AGT CC-3', 5'-CAA GAA GCC CAG ACG GAA AC-3', 5'-CCT GGC CCC TGT CAT CTT CT-3' and 5'-AAG AAA TGC AGG GGG ATA CG-3' for exon 4; 5'-TCT GTC TCC TTC CTC TTC CTA-3', 5'-CAT GTG CTG TGA CTG CTT GT-3', 5'-TGT GCA GCT GTG GGT TGAT TC-3' and 5'-CAG CCC TGT CGT CTC TCC AG-3' for exon 5; 5'-TTG CTC TTA GGT CTG GCC CC-3' and 5'-CAG ACC TCA GGC GGC TCA TA-3' for exon 6; 5'-TAG GTT GGC TCT GAC TGT ACC-3' and 5'-TGA CCT GGA GTC TTC CAG TGT-3' for exon 7; 5'-AGT GGT AAT CTA CTG GGA CGG-3' and 5'-ACC TCG CTT AGT GCT CCC TG-3' for exon 8.

Hot start PCR was performed as follows: 45 cycles of

Table 1 Characteristics of patients with squamous cell esophageal cancer

Patient No.	Age(yr)	Sex	Location of tumor	Therapy of preoperation	Time of operation	Sample	
						Tumor	Adjacent tissue
1	65	M	Upper	Radiotherapy	1997	+	-
2	48	M	Upper		1997	+	+
3	39	M	Lower		1998	+	-
4	61	F	Lower		1998	+	+
5	40	M	Lower		1998	+	+
6	70	F	Mid		1998	-	+
7	54	M	Mid		1998	-	+
8	70	F	Lower		1999	+	+
9	50	M	Mid		1999	+	+
10	66	M	Upper		1999	+	+
11	43	M	Mid	Radiotherapy	1999	+	+
12	60	M	Upper		1999	+	+
13	62	M	Upper		1999	+	+
14	60	F	Upper		1999	+	+
15	51	M	Upper		1999	+	+
16	67	M	Upper		1999	+	+
17	53	F	Mid		1999	+	+
18	49	M	Upper		1999	+	-
19	57	F	Lower		1999	+	-
20	61	M	Lower	Chemotherapy	1999	+	+
21	63	M	Lower		1999	+	-
22	65	F	Mid	Radiotherapy	1999	+	-
23	60	M	Mid		1999	+	+
24	54	M	-		1999	+	-

Upper: upper thoracic esophageal cancer, Mid: mid-thoracic esophageal cancer, Lower: lower thoracic esophageal cancer.

denaturation at 95 °C for 30 s; annealing at 58 °C, at 62 °C, at 60 °C and at 60 °C for 30 s for exons 4-8; extension at 72 °C for 1 min, and final extension at 72 °C for 7 min. The amplified products were subjected to electrophoresis in 1.5% agarose gel containing 2 µg/mL ethidium bromide in TBE buffer. After electrophoresis the gels were examined under an ultraviolet light transilluminator.

SSCP analysis

Nonradioactive SSCP was performed as previously reported^[25]. Twenty microliters of reaction mixtures containing 52 µL of PCR product (20-200 ng of DNA), 0.2 µL of 1 mol/L methylmercury hydroxide, 3 µL of loading buffer (15% Ficoll, 0.25% bromophenol blue, 0.25% xylene cyanol), and TBE buffer were heated to 90 °C for 4 min, then put on ice and electrophoresed in 18% polyacrylamide TBE gel at 300 V, while the temperature was maintained at 20 °C for exon 4, at 35 °C for exon 5, at 5 °C for exon 6, and at 25 °C for exons 7 and 8. The gels were stained with 0.5 µg/mL ethidium bromide in TBE buffer for 20 min at room temperature. The bands migrated apart from that of wild type were determined as SSCP positive. The bands possibly mutated by SSCP were extracted from the gels and amplified by 25 cycles of PCR to enrich the mutated alleles.

DNA sequencing

Sequencing was carried out on PCR products of SSCP positive cases. To purify single- or double-stranded PCR products with a range of 100 bp, the PCR products were processed using the QIAquick PCR purification kit (QIAGEN Inc., Valencia, CA, USA) according to the manufacturer's protocol. Sequencing was performed by the dideoxy chain termination

method using a big dye terminator cycle-sequencing kit (Perkin-Elmer Corporation, Foster City, CA, USA). The same primers were as used for PCR. Cycle sequencing was performed following the protocol, i.e., 30 cycles of denaturation at 95 °C for 20 s, annealing at 54 °C for 30 s, and extension at 72 °C for 3 min. After ethanol precipitation, the samples were analyzed by a genetic analyzer (ABI Prism 310, Perkin-Elmer Corporation). PCR-SSCP analysis and sequencing of the possible positive cases were repeated thrice to rule out contamination and artifacts.

Statistical analysis

Results among p53 exon 4-8 mutations and clinical factors were analyzed using χ^2 test and Fisher's exact test. $P < 0.05$ was considered statistically significant.

RESULTS

p53 gene mutations in esophageal carcinomas

We found p53 gene mutations in 9 of 22 specimens of esophageal carcinomas (40.9%). Sixteen of eighteen mutations were caused by single-nucleotide substitutions, among them, nine were missense mutations leading to amino acid substitution, and the other five were silent mutations without any amino acid change. Two of eighteen mutations were caused by deletions (Table 2). Eight of sixteen point mutations detected were G-A transitions at various codons. Nine of eighteen (50.0%) p53 gene mutations occurred in exon 4 at codons 102, 107, 111, 131, 135.

p53 gene mutations in adjacent non-cancerous tissues

We found p53 gene mutations in 10 of 17 specimens of adjacent non-cancerous tissues (58.8%). All mutations were

caused by single-nucleotide substitutions, among them, seven were missense mutations leading to amino acid substitution, and the other four were silent mutations without any amino acid change. Only 1 of 11 mutations detected was G-A transitions at codon 145. No deletion was found (Table 3). Four of eleven (36.4%) p53 gene mutations occurred in exon 4 at codons 58, 107, 111, and 141.

Table 2 p53 gene mutations in tumor tissue from esophageal cancer patients

No.	Exon	Codon	Nucleotide	Amino acid
1	None			
2	4	111	CTG-CTA	Leu-Leu
	4	131	GGG-GAG	Gly-Glu
3	None			
4	5	179	CCA-CTA	Pro-Leu
5	None			
6	-	-	-	-
7	-	-	-	-
8	4	107	TAC-TAT	Tyr-Tyr
9	None			
10	None			
11	4	102	ACC-ACT	Thr-Thr
	4	135	CAT-TAT	His-Tyr
	5		16 bp deletion	
12	None			
13	None			
14	4	131	GGG-GAG	Gly-Glu
	6	196	CGA-TGA	Arg-stop
15	None			
16	None			
17	None			
18	7i	242	CTG-CCG	Leu-Pro
19	None			
20	4	111	CTG-CTA	Leu-Leu
	4	131	GGG-GAG	Gly-Glu
	5	152	CCG-CCA	Pro-Pro
	6	208	GAC-AAC	Asp-Asn
	7i	250	CCC-TCC	Pro-Ser
21	6	208	GAC-AAC	Asp-Asn
	7i	248	CGG-TGG	Arg-Trp
22	None			
23	None			
24	4		6 bp deletion	

Table 3 p53 mutation in adjacent non-cancer tissue from esophageal cancer patients

No.	Exon	Codon	Nucleotide	Amino acid
1	-			
2	7i	256	ACA-GCA	Thr-Ala
3	-			
4	5	144	CAG-CCG	Gln-Arg
5	None			
6	5	145	CTG-CTA	Leu-Leu
7	4	111	CTG-CAG	Leu-Gln
8	4	141	TGC-TGT	Gys-Cys
	7i	256	ACA-GCA	Thr-Ala
9	None			
10	None			
11	4	107	TAC-TAT	Tyr-Tyr
12	None			
13	4	58	TTG-TGG	Leu-Trp
14	None			
15	None			
16	None			
17	5	144	CAG-CCG	Gln-Arg
18	-			
19	-			
20	None			
21	-			
22	-			
23	7i	267	CCT-TCT	Pro-Ser
24	8	282	CGG-CGC	Arg-Arg

p53 gene mutations and their correlation with clinical factors

40.9% and 58.8% of p53 gene mutations occurred in esophageal carcinoma specimens and adjacent non-cancerous tissue specimens. A comparison of p53 gene mutations in esophageal carcinoma specimens and adjacent non-cancerous tissue specimens with other clinical factors, including age, sex, pre-operation therapy and location of tumors, showed no clear correlation between two kinds of specimens ($P>0.05$).

DISCUSSION

The wild-type p53 protein has an inhibitory effect on cell proliferation and transformation and this effect has been believed to be mediated by its ability to arrest cells in G₁ phase of the cell cycle^[2]. Recent studies also reported that p53 gene mutation was correlated with an increased risk of developing human papilloma virus-associated cancers^[4]. In addition to its role in cell regulation, p53 has been implicated in DNA synthesis and repair^[5], maintenance of genomic stability^[6], cell differentiation and apoptosis^[7]. Point mutational damage to p53 could significantly alter regulatory tumor suppressor activity of this gene^[8].

In the worldwide, esophageal cancer is the fourth most common malignancy, after gastric, colorectal and hepatocellular malignancies^[9]. It has been reported that squamous cell carcinoma accounts for 70% of esophageal cancers^[10]. During the last 30 years, an increased incidence of 350%, particularly of adenocarcinoma has been described in population of USA, Western Europe and Sweden^[11-13]. Because surgical resection alone could rarely result in long-term survival, efforts are focused now on combined modality therapy in an attempt to improve its local control and to eliminate micrometastatic diseases present at the time of resection.

We found p53 tumor-suppressor gene mutations in 9 of 22 (40.9%) esophageal carcinoma specimens examined and 10 of 17 (58.8%) adjacent non-cancerous tissue specimens examined from Linxian County, China. Gao *et al*^[14], detected p53 gene mutations in normal epithelia (33.3%), basal cell hyperplasia (13.0%, BCH), and dysphasia (36.4%, Dys). Shi *et al*^[15], showed that p53 gene mutations were detected in 70% of 43 surgically resected esophageal cancer specimens and in p53 positive immunostaining non-cancerous lesions adjacent to cancer containing BCH (47%) and Dys (67%). Fujiki *et al*^[16], reported that the p53 gene mutation rates were 28.6% in esophageal cancer specimens, 20% in Dys, and 50% in BCHs. The observation of p53 gene mutation in adjacent non-cancerous tissues suggests that such mutations may occur even before morphological changes can be observed. The different p53 gene mutation rates were also reported from other esophageal carcinoma high-incidence areas, ranging 30-75%^[17-20]. The mutation frequency was significantly different. The difference may be due to different exons examined or due to different tumor samples, which contained inflammatory and stromal cells. A mutation might be hidden by the wild-type sequence of the gene in normal cells and was not detectable by screening procedures or there were differences in areas where specimens were collected and in examination methods.

Most point mutations of p53 gene have been known to

occur at codons 97-292^[21]. Greenblatt *et al*^[22], reported that p53 played an important role in transcription of target genes in a sequence-specific manner. Our study showed that, except one mutation in codon 58, 28 of 29 identified point mutations were involved in Linxian County, a highly conserved region. It is worth noting that 8 of 16 point mutations detected were G-A transitions and 2 of 18 mutations were caused by deletions in esophageal carcinoma tissues, but only 1 of 11 mutations detected was G-A transition and no deletion was found in adjacent non-cancerous tissues. G-A transitions may be a result of carcinogen-induced alkylations of DNA. The formation of O⁶-methylguanine may cause a mispair for thymine in DNA replication. In the subsequent round of DNA replication, an adenine would replace the original guanine and result in G-A transitions^[23].

It has been reported that mutations have rarely been found outside exons 5-8 of the p53 gene^[24]. Shi *et al*^[15], reported the exon distributions of p53 mutations in Henan Province, China. The exon 4 mutation was not found both in esophageal carcinoma and in adjacent non-cancerous tissue specimens. But in our study, 9 of 18 (50.0%) p53 gene mutations occurred in exon 4 in esophageal carcinoma tissues and 4 of 11 (36.4%) p53 gene mutations occurred in exon 4 in adjacent non-cancerous tissues. The results may be due to the differences the methods we used contributed to the higher detection rate of genetic alteration.

Our findings indicate that the mutation of p53 gene in exon 4 may play an important role in the development of esophageal cancer. The observation of p53 gene mutation in adjacent non-cancerous tissues suggests that p53 gene mutation may be an early event in esophageal carcinogenesis.

REFERENCES

- 1 Li JY. Epidemiology of esophageal cancer in China. *Natl Cancer Inst Monogr* 1982; **62**: 113-120
- 2 Finlay CA, Hinds PW, Levine AJ. The p53 proto-oncogene can act as a suppressor of transformation. *Cell* 1989; **57**: 1083-1093
- 3 Hollstein M, Sidransky D, Vogelstein B, Harris CC. p53 mutations in human cancers. *Science* 1991; **253**: 49-53
- 4 Vos M, Adams CH, Victor TC, van Helden PD. Polymorphisms and mutations found in the regions flanking exons 5 to 8 of the TP53 gene in a population at high risk for esophageal cancer in South Africa. *Cancer Genet Cytogenet* 2003; **140**: 23-30
- 5 Kastan MB, Onyekwere O, Sidransky D, Vogelstein B, Craig RW. Participation of p53 protein in the cellular response to DNA damage. *Cancer Res* 1991; **51**: 6304-6311
- 6 Lane DP. Cancer. p53, guardian of the genome. *Nature* 1992; **358**: 15-16
- 7 Oren M. Relationship of p53 to the control of apoptotic cell death. *Semin Cancer Biol* 1994; **5**: 221-227
- 8 Nigro JM, Baker SJ, Preisinger AC, Jessup JM, Hostetter R, Cleary K, Bigner SH, Davidson N, Baylin S, Devilee P. Mutations in the p53 gene occur in diverse human tumour types. *Nature* 1989; **342**: 705-708
- 9 Alidina A, Siddiqui T, Burney I, Jafri W, Hussain F, Ahmed M. Esophageal cancer--a review. *J Pak Med Assoc* 2004; **54**: 136-141
- 10 Gamliel Z. Incidence, epidemiology, and etiology of esophageal cancer. *Chest Surg Clin N Am* 2000; **10**: 441-450
- 11 Blot WJ, Devesa SS, Kneller RW, Fraumeni JF. Rising incidence of adenocarcinoma of the esophagus and gastric cardia. *JAMA* 1991; **265**: 1287-1289
- 12 Devesa SS, Blot WJ, Fraumeni JF. Changing patterns in the incidence of esophageal and gastric carcinoma in the United States. *Cancer* 1998; **83**: 2049-2053
- 13 Heitmiller RF, Sharma RR. Comparison of prevalence and resection rates in patients with esophageal squamous cell carcinoma and adenocarcinoma. *J Thorac Cardiovasc Surg* 1996; **112**: 130-136
- 14 Gao H, Wang LD, Zhou Q, Hong JY, Huang TY, Yang CS. p53 tumor suppressor gene mutation in early esophageal precancerous lesions and carcinoma among high-risk populations in Henan, China. *Cancer Res* 1994; **54**: 4342-4346
- 15 Shi ST, Yang GY, Wang LD, Xue Z, Feng B, Ding W, Xing EP, Yang CS. Role of p53 gene mutations in human esophageal carcinogenesis: results from immunohistochemical and mutation analyses of carcinomas and nearby non-cancerous lesions. *Carcinogenesis* 1999; **20**: 591-597
- 16 Fujiki T, Haraoka S, Yoshioka S, Ohshima K, Iwashita A, Kikuchi M. p53 Gene mutation and genetic instability in superficial multifocal esophageal squamous cell carcinoma. *Int J Oncol* 2002; **20**: 669-679
- 17 Putz A, Hartmann AA, Fontes PR, Alexandre CO, Silveira DA, Klug SJ, Rabes HM. TP53 mutation pattern of esophageal squamous cell carcinomas in a high risk area (Southern Brazil): role of life style factors. *Int J Cancer* 2002; **98**: 99-105
- 18 Sepehr A, Taniere P, Martel-Planche G, Zia'ee AA, Rastgar-Jazii F, Yazdanbod M, Etemad-Moghadam G, Kamangar F, Saidi F, Hainaut P. Distinct pattern of TP53 mutations in squamous cell carcinoma of the esophagus in Iran. *Oncogene* 2001; **20**: 7368-7374
- 19 Kihara C, Seki T, Furukawa Y, Yamana H, Kimura Y, van Schaardenburgh P, Hirata K, Nakamura Y. Mutations in zinc-binding domains of p53 as a prognostic marker of esophageal-cancer patients. *Jpn J Cancer Res* 2000; **91**: 190-198
- 20 Wang LS, Chow KC, Liu CC, Chiu JH. p53 gene alternation in squamous cell carcinoma of the esophagus detected by PCR-cold SSCP analysis. *Proc Natl Sci Counc Repub China B* 1998; **22**: 114-121
- 21 Ireland AP, Clark GW, DeMeester TR. Barrett's esophagus. The significance of p53 in clinical practice. *Ann Surg* 1997; **225**: 17-30
- 22 Greenblatt MS, Bennett WP, Hollstein M, Harris CC. Mutations in the p53 tumor suppressor gene: clues to cancer etiology and molecular pathogenesis. *Cancer Res* 1994; **54**: 4855-4878
- 23 Mitra G, Pauly GT, Kumar R, Pei GK, Hughes SH, Moschel RC, Barbacid M. Molecular analysis of O6-substituted guanine-induced mutagenesis of ras oncogenes. *Proc Natl Acad Sci USA* 1989; **86**: 8650-8654
- 24 Montesano R, Hollstein M, Hainaut P. Genetic alterations in esophageal cancer and their relevance to etiology and pathogenesis: a review. *Int J Cancer* 1996; **69**: 225-235
- 25 Hongyo T, Buzard GS, Palli D, Weghorst CM, Amorosi A, Galli M, Caporaso NE, Fraumeni JF, Rice JM. Mutations of the K-ras and p53 genes in gastric adenocarcinomas from a high-incidence region around Florence, Italy. *Cancer Res* 1995; **55**: 2665-2672

Recurrent acute pancreatitis and its relative factors

Wei Zhang, Hong-Chao Shan, Yan Gu

Wei Zhang, Hong-Chao Shan, Yan Gu, Department of Surgery, Ninth Affiliated People's Hospital, Shanghai Second Medical University, Shanghai 200011, China

Correspondence to: Wei Zhang, Department of Surgery, Ninth Affiliated People's Hospital, Shanghai Second Medical University, Shanghai 200011, China. weizh1518@hotmail.com

Telephone: +86-21-53591134

Received: 2004-06-29 Accepted: 2004-08-05

Abstract

AIM: To evaluate the causes and the relative factors of recurrent acute pancreatitis.

METHODS: From 1997 to 2000, acute pancreatitis relapsed in 77 of 245 acute pancreatitis patients. By reviewing the clinical treatment results and the follow-up data, we analyzed the recurrent factors of acute pancreatitis using univariate analysis and multivariate analysis.

RESULTS: Of the 245 acute pancreatitis patients, 77 were patients with recurrent acute pancreatitis. Of them, 56 patients relapsed two times, 19 relapsed three times, each patient relapsed three and four times. Forty-seven patients relapsed in hospital and the other 30 patients relapsed after discharge. Eighteen patients relapsed in 1 year, eight relapsed in 1-3 years, and four relapsed after 3 years. There were 48 cases of biliary pancreatitis, 3 of alcohol pancreatitis, 5 of hyperlipidemia pancreatitis, 21 of idiopathic pancreatitis. Univariate analysis showed that the patients with local complications of pancreas, obstructive jaundice and hepatic function injury were easy to recur during the treatment period of acute pancreatitis ($P = 0.022 < 0.05$, $P = 0.012 < 0.05$ and $P = 0.002 < 0.05$, respectively). Multivariate analysis showed that there was no single factor related to recurrence. Of the 47 patients who had recurrence in hospital, 16 had recurrence in a fast period, 31 after refeeding.

CONCLUSION: Acute pancreatitis is easy to recur even during treatment. The factors such as changes of pancreas structure and uncontrolled systemic inflammatory reaction are responsible for the recurrence of acute pancreatitis. Early refeeding increases the recurrence of acute pancreatitis. Defining the etiology is essential for reducing the recurrence of acute pancreatitis.

its relative factors. *World J Gastroenterol* 2005; 11(19): 3002-3004

<http://www.wjgnet.com/1007-9327/11/3002.asp>

INTRODUCTION

With the knowledge of progress and prognosis for acute pancreatitis, the diagnosis and treatment of acute pancreatitis are more and rational. But some acute pancreatitis patients have frequent occurrence in hospital or after discharge. These patients obviously had increased hospital-stay and cost, and their quality of life decreased. About 25% patients with acute pancreatitis had recurrence^[1]. We reviewed the clinical data of acute pancreatitis patients in our hospital for 3 years, and evaluated the relative factors that affected the recurrence in 77 patients.

MATERIALS AND METHODS

Clinical data

From 1997 to 2000, 245 acute pancreatitis patients (based on clinical diagnosis and classification standard of pancreatitis, 1997, Chinese Medical Association^[2]) were admitted to our hospital. According to the different causes, classification and clinical stages, the patients received different treatments. Routing treatments included: intravenous fluid resuscitation, anti-shock, water maintenance, electrolyte and acid-base balances, fluid replenishment, fast, naso-gastric decompressing, using somatostatin, parenteral nutrition, pain relief, using wide-spectrum antibiotics and serum albumin. In clinical observations and follow-up, 77 acute pancreatitis patients had recurrence. Of them, 32 were men and 45 were women, and the average was 58.04 ± 15.43 years. The average follow-up time was 26 mo (12-60 mo).

Diagnosis standard of recurrent acute pancreatitis

After conservative or operative treatment, the clinical syndromes and signs of acute pancreatitis disappeared, serum and uric amylase returned to normal. Other laboratory tests such as blood leukocyte counting, liver functions, renal functions, blood sugar, etc., were normal, and there were no uncomfortable complaints after refeeding. After that, if the patients had acute pancreatitis syndromes or signs with elevating serum and uric amylase again, they were diagnosed as recurrent acute pancreatitis.

Classification of recurrent acute pancreatitis

Biliary pancreatitis: Clinical jaundice with elevated serum bilirubin, direct bilirubin/total bilirubin > 50%, the dilation of intra-hepatic and extra-hepatic bile duct (the diameter more than 1 cm) by image examinations such as B-ultrasound,

computer tomography (CT), endoscope retrograde cholangiopancreatography (ERCP), magnetic resonance cholangiopancreatography (MRCP).

Alcohol-induced pancreatitis: An average of 80 g alcohol taken daily for more than 5 years or an excess alcohol taken immediately before the acute attack.

Hyperlipidemia pancreatitis: The levels of serum lipid, especially the triglyceride was obviously elevated.

Idiopathy pancreatitis: No remarkable findings in his or her disease history, clinical manifestations, laboratory and image examinations.

Refeeding recovery

The naso-gastric tube was removed when clinical syndromes and signs were disappeared. Then the patients were allowed to drink water for 1-3 d. If there were no discomforts, the patients were told to eat non-fat fluid and non-fat semi-fluid diets gradually, and at last to eat low-fat semi-fluid diets. The total calorie of non-fat fluid diets was 510 kcal/d, containing 2.7% protein, 0.6% lipid, 96.7% carbon hydrate. The total calorie of non-fat semi-fluid diets was 1 500 kcal/d, containing 8.2% protein, 1.6% lipid, 90.2% carbohydrate. The total calorie of low-fat semi-fluid diets was 1 600-1 800 kcal/d, containing 15.5% protein, 17.6% lipid and 66.9% carbohydrate respectively.

Analysis of relative factors

The clinical data of each patient were recorded in detail. The possible factors related to recurrent acute pancreatitis were calculated, including age more than and equal 60 years or less than 60 years; etiology, biliary pancreatitis; bile duct obstruction; levels of serum amylase, three times more than normal values; acute hepatic function injury manifested as high levels of serum glutamic-pyruvic or serum glutamic-oxalacetic transaminase with or without elevated serum bilirubin; severe systemic infection; local complications of acute pancreatitis such as acute fluid accumulation, necrosis, pseudocyst, abscess formation.

Statistical analysis

χ^2 test was used for univariate analysis, and logistic regression for multivariate analysis by SPSS. $P < 0.05$ was considered statistically significant.

RESULTS

Status of recurrent acute pancreatitis

The recurrent rate of acute pancreatitis in this study was 31.43% (77/245). Of the 77 relapsed patients, 56 (72.73%) had two relapses, 19 (24.67%) had three relapses, and each one (2.60%) had four and five relapses. Forty-seven (61.04%) had their recurrence in hospital, and 30 (38.96%) after discharge. Seventeen had recurrence in 1 year after discharge, nine in 1-3 years, and four 3 years after discharge.

Etiology and classification of recurrent acute pancreatitis

Of the 77 recurrent acute pancreatitis patients, 48 had biliary pancreatitis, 3 had alcohol-induced pancreatitis, 3 had hyperlipidemic pancreatitis, and 21 had idiopathy pancreatitis. No trauma, post-operative and drug-induced

pancreatitis were found. With the clinical diagnosis and classification standard by Chinese Medicine Association, 13 patients were confirmed to have severe acute pancreatitis in 77 recurrent acute pancreatitis patients. Of them, five had pancreas necrosis, five pseudocyst, one pancreatogenic encephalopathy and two respiratory failure.

Laboratory tests of recurrent acute pancreatitis patients

Of the 77 recurrent patients, 61 had their serum or uric amylase three times higher than the values of upper limit of normal. Fifty-three had the leukocyte counting more than 10.0×10^9 , 47 the glucemia more than 6.1 mmol/L, 37 with acute hepatic function injury, and 32 the serum calculi less than 2.2 mmol/L.

Analysis of relative factors of recurrent acute pancreatitis

The univariate analysis indicated that the recurrence of acute pancreatitis in treatment period was associated with local complications of pancreas, obstructive jaundice and hepatic function injury ($P = 0.022 < 0.05$, $P = 0.012 < 0.05$ and $P = 0.002 < 0.05$, respectively). Multivariate analysis showed that there was no single factor related to recurrent acute pancreatitis (Table 1).

Table 1 Relative factors of recurrent acute pancreatitis

Relative factors	Total cases (n)	Recurrent (%)	Univariate analysis P	Multivariate analysis P
Age ≥ 60	101	37 (36.63)	0.142	0.423
Male	109	32 (29.36)	0.532	0.569
Biliary	162	48 (29.36)	0.397	0.215
Obstructive jaundice	58	26 (44.83)	0.012	0.144
Amylase elevation	167	48 (28.74)	0.185	0.194
Liver injury	127	51 (40.16)	0.002	0.257
Systemic infection	12	5 (41.67)	0.642	0.082
Local complication	18	10 (55.66)	0.022	0.091

DISCUSSION

Recurrent acute pancreatitis represents a challenging clinical problem because of its high recurrent rate^[1,3]. Of the 245 patients with acute pancreatitis in this study, 77 (31.43%) had relapses. Of the 77 recurrent patients 47 (61.04%) had relapse in hospital, suggesting that acute pancreatitis is easy to relapse. Gullo *et al*^[1], reported that 288 (27%) had recurrence in the total of 1 068 acute pancreatitis patients, and alcohol was the most frequent factor. Pelli *et al*^[4], found that 46% alcohol-induced acute pancreatitis patients had recurrence, 80% of them had relapses during the first 4 years. We analyzed 30 recurrent acute pancreatitis patients after discharge by follow-up, 50% patients had recurrence in 1 year after discharge, one-third patients in 1-3 years and 13% patients 3 years after their discharge.

Some factors were probably related to recurrent acute pancreatitis^[4-6]. Theoretically, if the causes of acute pancreatitis existed, they could make the acute pancreatitis to relapse repeatedly. For example, biliary pancreatitis could recur, while the choledocholithiasis was existed or small gallstones went to the common bile duct from cholecyst duct^[7-9]. In

hyperlipidemia pancreatitis a high level blood viscosity in patients would make the pancreas microcirculation abnormal and acute pancreatitis could relapse. Somogyi *et al*^[3], suggested the causes of recurrent acute pancreatitis could be categorized into: (1) toxic-metabolic acute pancreatitis such as alcohol, hypertriglyceridemia, hypercalcemia and medications; (2) mechanical obstructive acute pancreatitis such as choledocholithiasis (microlithiasis), peripapillary/ampullary obstruction (diverticulum, cyst, polypus, tumor, stenosis and infection), pancreatic duct obstruction (tumor, non-neoplastic stricture), congenital malformations (annular pancreas); and (3) miscellaneous acute pancreatitis such as vascular (hypotension, vasculitis, hypercoagulable state, embolism), infections (cytomegalovirus, tuberculosis, Coxsackie virus, mumps, human immunodeficiency virus, parasites), tropical pancreatitis, cystic fibrosis. Of the 77 recurrent acute pancreatitis patients in this paper, 8 (10.39%) belonged to toxic-metabolic pancreatitis, 48 (62.34%) mechanical pancreatitis, and 21 (27.27%) miscellaneous pancreatitis. In our country, alcohol-induced pancreatitis was fewer. Although a lot of drugs could induce acute pancreatitis, but it was mainly limited in case reports. Recent years, hyperlipidemia pancreatitis was emphasized^[10]. Therefore, it is suggested that acute pancreatitis patients should do serum lipid tests routinely in order to find their causes and reduce relapse. Biliary pancreatitis could be properly diagnosed by using B-ultrasound, CT, ERCP and MRCP. But for idiopathy pancreatitis, the causes were difficult to find and it could have a higher recurrent rate^[11-13].

Univariate analysis indicated that patients with local complications such as acute fluid accumulation, necrosis, pseudocyst, abscess formation had a tendency to recur, which should be responsible for the changed pancreas structure. Levy *et al*^[14], reported that patients with higher Balthazar's CT scores had abdominal pain recurrence more often than the others^[14], indicating that the acute pancreatitis patients with obstructive jaundice and hepatic function injury are easy to relapse. We previously studied acute pancreatitis patients with hepatic function injury and found that the liver was a common organ that could be affected by acute pancreatitis. It is known that acute pancreatitis is a systemic disease. Patients with obstructive jaundice and hepatic function injury meant that the systemic infection was uncontrolled, and so it was easy to relapse^[15]. Multivariate analysis showed that there was no single factor related to recurrence during treatment, indicating that the recurrence of acute pancreatitis probably is a result of multiple factors acting together.

In our study, the symptoms and signs, serum amylase, blood glucose, blood calculi, liver function tests, local and systemic complications and mortality of recurrent acute pancreatitis patients were not different from those of primary acute pancreatitis^[1].

So far there is no report that the refeeding in acute pancreatitis patients was associated with their relapsing. Naso-gastric decompression, parental nutrition, using

histamine H₂-receptor antagonists and somatostatin were not found to have any relations with relapsing of acute pancreatitis^[14]. But in our studies two-thirds of the patients relapsing in hospital were associated with refeeding, and the most were after refeeding of non-fat fluid diets. To prolong the fast time properly by using parenteral or enteral nutritional support therapies and to pay attention to the levels of serum amylase and lipase of patients can decrease the risk of recurrence after refeeding in patients with acute pancreatitis.

REFERENCES

- 1 **Gullo L**, Migliori M, Pezzilli R, Olah A, Farkas G, Levy P, Arvanitakis C, Lankisch P, Beger H. An update on recurrent acute pancreatitis: data from five European countries. *Am J Gastroenterol* 2002; **97**: 1959-1962
- 2 **Pancreatic Group, Chinese Medical Association**. Clinical diagnosis and classification standard of acute pancreatitis. *Zhonghua Waikao Zazhi* 1997; **35**: 773-775
- 3 **Somogyi L**, Martin SP, Venkatesan T, Ulrich CD. Recurrent acute pancreatitis: an algorithmic approach to identification and elimination of inciting factors. *Gastroenterology* 2001; **120**: 708-717
- 4 **Pelli H**, Sand J, Laippala P, Nordback I. Long-term follow-up after the first episode of acute alcoholic pancreatitis: time course and risk factors for recurrence. *Scand J Gastroenterol* 2000; **35**: 552-555
- 5 **Gloor B**, Stahel PF, Muller CA, Worni M, Buchler MW, Uhl W. Incidence and management of biliary pancreatitis in cholecystectomized patients. Results of a 7-year study. *J Gastrointest Surg* 2003; **7**: 372-377
- 6 **Jackson WD**. Pancreatitis: etiology, diagnosis, and management. *Curr Opin Pediatr* 2001; **13**: 447-451
- 7 **Werner J**, Uhl W, Buchler MW. Surgical Treatment of Acute Pancreatitis. *Curr Treat Options Gastroenterol* 2003; **6**: 359-367
- 8 **Alimoglu O**, Ozkan OV, Sahin M, Akcakaya A, Eryilmaz R, Bas G. Timing of cholecystectomy for acute biliary pancreatitis: outcomes of cholecystectomy on first admission and after recurrent biliary pancreatitis. *World J Surg* 2003; **27**: 256-259
- 9 **Kaw M**, Al-Antably Y, Kaw P. Management of gallstone pancreatitis: cholecystectomy or ERCP and endoscopic sphincterotomy. *Gastrointest Endosc* 2002; **56**: 61-65
- 10 **Yadav D**, Pitchumoni CS. Issues in hyperlipidemic pancreatitis. *J Clin Gastroenterol* 2003; **36**: 54-62
- 11 **van Brummelen SE**, Venneman NG, van Erpecum KJ, VanBerge-Henegouwen GP. Acute idiopathic pancreatitis: does it really exist or is it a myth? *Scand J Gastroenterol Suppl* 2003; **239**: 117-122
- 12 **Lehman GA**. Acute recurrent pancreatitis. *Can J Gastroenterol* 2003; **17**: 381-383
- 13 **Billi P**, Barakat B, D'Imperio N, Pezzilli R. Relapses of biliary acute pancreatitis in patients with previous attack of biliary pancreatitis and gallbladder *in situ*. *Dig Liver Dis* 2003; **35**: 653-655
- 14 **Levy P**, Heresbach D, Pariente EA, Boruchowicz A, Delcenserie R, Millat B, Moreau J, Le Bodic L, de Calan L, Barthet M, Sauvanet A, Bernades P. Frequency and risk factors of recurrent pain during refeeding in patients with acute pancreatitis: a multivariate multicentre prospective study of 116 patients. *Gut* 1997; **40**: 262-266
- 15 **Zhang W**, Shan HC, Guo SY. Acute liver damage in patients with acute pancreatitis. *Zhonghua Gandan Waikao Zazhi* 2004; **10**: 225-227

• BRIEF REPORTS •

Mild hypothermia protects liver against ischemia and reperfusion injury

Cheng-You Wang, Yong Ni, Yan Liu, Zhi-Heng Huang, Min-Jie Zhang, Yong-Qiang Zhan, Hai-Bin Gao

Cheng-You Wang, Yong Ni, Yan Liu, Zhi-Heng Huang, Min-Jie Zhang, Yong-Qiang Zhan, Hai-Bin Gao, Department of Hepatobiliary Surgery, Shenzhen Second People's Hospital, Shenzhen 518035, Guangdong Province, China
Supported by the Health Committee of Guangdong Province, No. A1998550

Correspondence to: Dr. Cheng-You Wang, Department of Hepatobiliary Surgery, Shenzhen Second People's Hospital, Shenzhen 518029, Guangdong Province, China. chengyouw@163.com
Telephone: +86-755-26106138 Fax: +86-755-83356952
Received: 2002-10-09 Accepted: 2002-11-13

Abstract

AIM: To determine whether mild hypothermia could protect liver against ischemia and reperfusion injury in pigs.

METHODS: Twenty-four healthy pigs were randomly divided into normothermia, mild hypothermia and normal control groups. The experimental procedure consisted of temporary interruption of blood flow to total hepatic lobe for different lengths of time and subsequent reperfusion. Hepatic tissue oxygen pressure (P_{iO_2}) and aspartate aminotransferase (AST) values were evaluated, and ultrastructural analysis was carried out for all samples.

RESULTS: Serum AST was significantly lower, and hepatic P_{iO_2} values were significantly higher in the mild hypothermia group than in the normothermia group during liver ischemia-reperfusion periods ($P = 0.032$, $P = 0.028$). Meanwhile, the histopathologic injury of liver induced by ischemia-reperfusion was significantly improved in the mild hypothermia group, compared with that in the normothermia group.

CONCLUSION: Mild hypothermia can protect the liver from ischemia-reperfusion injury in pigs.

© 2005 The WJG Press and Elsevier Inc. All rights reserved.

Key words: Ischemia-reperfusion injury; Hypothermia; Liver; Pathophysiology

Wang CY, Ni Y, Liu Y, Huang ZH, Zhang MJ, Zhan YQ, Gao HB. Mild hypothermia protects liver against ischemia and reperfusion injury. *World J Gastroenterol* 2005; 11(19): 3005-3007
<http://www.wjgnet.com/1007-9327/11/3005.asp>

INTRODUCTION

Hepatic vascular exclusion is a major performance of hepatic

resection with minimal intraoperative blood loss. Interruption of hepatic inflow is required during extension liver resection. Temporary vascular inflow occlusion by clamping of the hepatic pedicle (Pringle maneuver) is an effective measure to control blood loss during the operative procedure because it is associated with the least hemodynamic consequences and side effects. However, liver dysfunction is still a relatively frequent complication of clinical surgeries as a result of liver ischemic reperfusion^[1,2]. Therefore, the ability to improve liver tolerance to ischemia is clinically important.

Several pathways for ischemic reperfusion injury have been postulated, such as oxygen-derived free radicals^[3], calcium influx^[4], adenosine triphosphate depletion, mitochondrion dysfunction, activation of lysosomal enzymes and disturbance of microcirculation^[5,6]. However, the precise mechanisms of hepatic injury remain obscure. It has been shown that ischemic reperfusion injury in the liver first becomes evident in microvascular system particularly in sinusoidal endothelial cells of the liver. Because intrahepatic tissue oxygenation depends on delivery of oxygen by the liver microvasculature, microcirculatory disturbances due to ischemia-reperfusion injury will result in tissue oxygen changes in the liver parenchyma^[7]. The partial pressure of oxygen (the P_{iO_2}), which is physically dissolved in interstitial fluid, corresponds to the availability of oxygen at cellular level. The P_{iO_2} value not only follows metabolic rate, perfusion and microcirculation, but also reflects the functional number of capillaries per tissue volume, the highly variable O_2 diffusion in capillary wall, parenchyma and intercellular substance.

The experimental and clinical findings suggest that hypothermic perfusion technique and topical cooling of liver in hepatic resection may be very useful in preserving hepatocytes and sinusoidal endothelial cells and in maintaining stability of the systemic or hepatic circulation after reperfusion^[8,9]. In recent years, mild hypothermia has been proved to be of protective role in brain injury with few systemic side-effects. In this study, we evaluated the role of mild hypothermia in liver ischemia-reperfusion injury.

MATERIALS AND METHODS

Animals

Twenty-four healthy pigs weighing 30-35 kg with male/female ratio of 1:1 (kindly provided by Experimental Animal Center, Sun Yat-Sen University of Medical Sciences, Guangzhou, China) were included in the study. All pigs were acclimatized for at least 7 d before the experiment and allowed free access to food and water. The animals were randomly divided into three experimental groups: normothermia, mild hypothermia, and normal control groups.

Surgical procedures

All surgical procedures were carried out under intravenous anesthesia. The pigs underwent laparotomy with a median incision, and the inflow of liver blood was occluded by the Pringle's method, i.e., the liver was exposed after supra-median incision into the abdomen, and the hepatic artery, portal vein and common bile duct in the hepato-duodenal ligament were clamped off with non-injury clamps. When the clamps were taken away, the inflow of liver blood was resumed, which is termed as reperfusion. In group A (normothermia group), the inflow of liver blood was occluded for 30 min at normothermia (normal body temperature), and reperfusion was performed for 60 min. In group B (mild hypothermia group), the liver and rectal temperatures were lowered down to 33-35 °C with cooling blanket before liver ischemia, while other treatments were the same as for group A. In group C (controlled group), the liver and hepato-duodenal ligament was exposed at normothermia without interruption of the inflow of liver blood.

Establishment of mild hypothermia

The pigs were cooled with cooling blankets (Kangnuo Tech Co. Ltd, Beijing, China) for 1-2 h to reach a temperature in rectal and liver of 34-35 °C (± 0.2 °C) with subsequent use of light flash to maintain the temperature.

Detection of hepatic tissue oxygen pressure ($P_{ti}O_2$)

$P_{ti}O_2$ was measured in each animal by LICOX CMP monitors (Kiel-Mielkendorf Co. Ltd, Germany) with a polarographic microcatheter $P_{ti}O_2$ probe and a micromputer^[10]. After calibration in a saline bath, the $P_{ti}O_2$ probe was inserted into the hepatic parenchyma of the middle lobe using an 18-gauge venous cannula. $P_{ti}O_2$ was measured serially before and during the ischemia period (at 10, 20, and 30 min) and after reperfusion at two different points (30 and 60 min).

Detection of serum aspartate aminotransferase (AST)

The serum levels of aspartate aminotransferase (AST) were determined by an autonomic-physiotechnic monitor. Venous blood samples for AST were drawn before ischemia, 30 min after ischemia and 60 min after reperfusion.

Histopathological examination of liver

Liver tissues were collected before ischemia, 30 min after ischemia and 60 min after reperfusion from the left and right of the liver, and fixed in 10% neutral buffered formalin, embedded in paraffin, sectioned at 5 μ m, and stained with hematoxylin and eosin. They were observed under a light microscope to examine histopathological changes.

Ultrastructural investigation

To study the ultrastructural changes of hepatocytes, liver tissues from all groups were fixed for observation under transmission electron microscope (TEM). The cut samples for TEM underwent technical procedures as previously described^[11]. Thin sections were observed under HITACH-H600 electron microscope.

Statistical analysis

The data were presented as mean \pm SE, the differences of these

groups were compared by a *t*-test. $P < 0.05$ was considered statistically significant.

RESULTS

Changes of liver $P_{ti}O_2$

The hepatic $P_{ti}O_2$ values of three groups before ischemia were 43.3 ± 6.9 , 42.7 ± 9.5 , and 41.9 ± 8.2 mmHg (1 mmHg = 0.133 kPa) respectively. There were no significant differences among these groups ($P > 0.05$). The liver $P_{ti}O_2$ value declined to 18.6 ± 2.8 mmHg at 30 min after ischemia in group A, but increased slowly to 30.9 ± 2.6 mmHg 60 min after reperfusion. There were significant differences between the ischemic and non-ischemic periods ($P < 0.05$). In group B, the hepatic $P_{ti}O_2$ value was 28.7 ± 1.9 mmHg 30 min after ischemia and 37.9 ± 5 mmHg 60 min after reperfusion. There were significant differences between the groups in pre-ischemia and reperfusion periods ($P < 0.05$). Meanwhile, there were significant differences in each stage of ischemia-reperfusion of pig livers between groups A and B ($P < 0.05$, Figure 1).

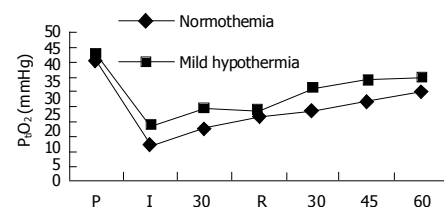


Figure 1 Changes of intrahepatic $P_{ti}O_2$. P: pre-ischemia; I: ischemia; R: reperfusion.

Changes in serum AST

Serum AST values are shown in Figure 2. AST values were 42.6 ± 5.7 , 46.2 ± 3.9 , and 49.0 ± 6.8 U/L, respectively, before ischemia in groups A, B, and C. There were no significant differences between the groups ($P > 0.05$). However, AST values at 30 min after ischemia, 30 and 60 min after reperfusion were significantly different between groups A and B ($P < 0.05$).

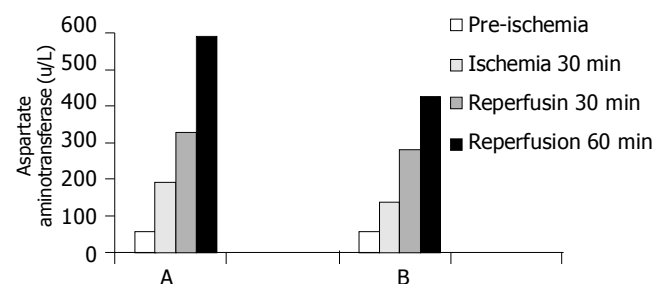


Figure 2 The changes in serum AST. AST values at 30 min after ischemia, 30 and 60 min after reperfusion were significant differences between normothermia group and mild hypothermia. $P < 0.05$.

Histopathological examination of liver

Before ischemia, the histopathological structures were normal in three groups. In the ischemic group of normothermia, light

microscopy showed swelling of hepatocytes, stenosis of hepatic sinus, infiltration of inflammatory cells in the interstitial tissue and dotted necrosis of hepatocytes after 30 min of ischemia. The swelling of hepatocytes was even worse and local necrosis of hepatocytes could be observed 60 min after reperfusion. In the mild hypothermia group, the pathological changes of liver were significantly lighter compared to the normothermia group during the periods of ischemia and reperfusion.

Ultramicrostructural analysis

Under electromicroscope, swelling of mitochondria and enlargement of endoplasm were observed 30 min after ischemia, even worse swelling, destruction, bubble-degeneration of mitochondria, and degranulation of rough endoplasm were found 60 min after reperfusion. However, the mild hypothermia group only showed widening and swelling of mitochondria with complete membrane and few changes in nuclear membrane and nucleoli.

DISCUSSION

The induction of hepatic hypothermia began with whole-body cooling in experimental models in 1953 and clinically in 1961. It was designed to minimize the ischemia-reperfusion injury associated with hepatic inflow occlusion. Body surface cooling and cooling via an extracorporeal circuit, however, are not widely accepted for hepatic surgery because of the adverse effects on extrahepatic organs^[12-15]. In this study, we found that hypothermia had a protective effect against hepatic ischemia-reperfusion injury in pigs. Our study showed that the P_aO_2 values during ischemia and reperfusion in group B were significantly higher than those in group A. It has been previously shown that intrahepatic P_aO_2 as an indicator of microvascular perfusion is a parameter of early ischemia-reperfusion injury^[6,16-18]. Microcirculatory disturbances during ischemia and reperfusion period might induce local hypoxia in the liver, thereby causing liver damage. We postulate that mild hypothermia might decrease hepatic oxygen consumption during ischemic and attenuate endothelial injury and microcirculatory dysfunction in reperfusion period, and then increase hepatic tissue oxygenation and reduce liver damage.

Liver damage associated with different models of ischemia-reperfusion injury is most commonly characterized by the release of hepatocellular enzymes into extracellular fluids. AST is a comparatively sensible parameter reflecting the injury of liver cells, and serum AST values reflect the extent of injury in liver cells. Mild hypothermia is associated with reduction in serum AST after reperfusion. This means that a relatively well maintained state of hepatic cells by mild hypothermia during ischemia leads to a lesser degree of liver cell injury following reperfusion. The data indicate that the decrease in mitochondria destruction, hepatocyte degeneration and necrosis due to mild hypothermia also presumably contributes to an increase in hepatic tissue P_aO_2 , resulting in attenuation of tissue damage following hepatic injury.

In conclusion, mild hypothermia prevents hepatic injury

after ischemia-reperfusion in pigs, and may play a crucial role in clinical situations associated with liver dysfunction after ischemia-reperfusion.

REFERENCES

- 1 St Peter SD, Post DJ, Rodriguez-Davalos MI, Douglas DD, Moss AA, Mulligan DC. Tacrolimus as a liver flush solution to ameliorate the effects of ischemia/reperfusion injury following liver transplantation. *Liver Transpl* 2003; **9**: 144-149
- 2 Takahashi Y, Ganster RW, Gambotto A, Shao L, Kaizu T, Wu T, Yagnik GP, Nakao A, Tsoulfas G, Ishikawa T, Okuda T, Geller DA, Murase N. Role of NF-kappaB on liver cold ischemia-reperfusion injury. *Am J Physiol Gastrointest Liver Physiol* 2002; **283**: G1175-G1184
- 3 Jin MB, Todo S. The role of endothelin-1 in hepatic ischemia and reperfusion injury. *J Gastroenterol* 2002; **37**: 763-765
- 4 Khandoga A, Biberthaler P, Enders G, Axmann S, Hutter J, Messmer K, Krombach F. Platelet adhesion mediated by fibrinogen-intercellular adhesion molecule-1 binding induces tissue injury in the postischemic liver *in vivo*. *Transplantation* 2002; **74**: 681-688
- 5 Khandoga A, Enders G, Biberthaler P, Krombach F. Poly(ADP-ribose) polymerase triggers the microvascular mechanisms of hepatic ischemia-reperfusion injury. *Am J Physiol Gastrointest Liver Physiol* 2002; **283**: G553-G560
- 6 Pannen BH. New insights into the regulation of hepatic blood flow after ischemia and reperfusion. *Anesth Analg* 2002; **94**: 1448-1457
- 7 Serafin A, Rosello-Catafau J, Prats N, Xaus C, Gelpi E, Peralta C. Ischemic preconditioning increases the tolerance of fatty liver to hepatic ischemia-reperfusion injury in the rat. *Am J Pathol* 2002; **161**: 587-601
- 8 Heijnen BH, Elkhouloufi Y, Straatsburg IH, Van Gulik TM. Influence of acidosis and hypoxia on liver ischemia and reperfusion injury in an *in vivo* rat model. *J Appl Physiol* (1985) 2002; **93**: 319-323
- 9 Biberthaler P, Luchting B, Massberg S, Teupser D, Langer S, Leiderer R, Messmer K, Krombach F. The influence of organ temperature on hepatic ischemia-reperfusion injury: a systematic analysis. *Transplantation* 2001; **72**: 1486-1490
- 10 van Wagenveld BA, van Gulik TM, Gelderblom HC, Scheepers JJ, Bosma A, Endert E, Gouma DJ. Prolonged continuous or intermittent vascular inflow occlusion during hemihepatectomy in pigs. *Ann Surg* 1999; **229**: 376-384
- 11 Atila K, Coker A, Sagol O, Coker I, Topalak O, Astarcioglu H, Karademir S, Astarcioglu I. Protective effects of carnitine in an experimental ischemia-reperfusion injury. *Clin Nutr* 2002; **21**: 309-313
- 12 Imber CJ, St Peter SD, Lopez de Cenarruzabeitia I, Pigott D, James T, Taylor R, McGuire J, Hughes D, Butler A, Rees M, Friend PJ. Advantages of normothermic perfusion over cold storage in liver preservation. *Transplantation* 2002; **73**: 701-709
- 13 Kato A, Singh S, McLeish KR, Edwards MJ, Lentsch AB. Mechanisms of hypothermic protection against ischemic liver injury in mice. *Am J Physiol Gastrointest Liver Physiol* 2002; **282**: G608-G616
- 14 Zhang Y, Zhang B, Pan R. Protective effect of ischemic preconditioning on liver. *Chin J Traumatol* 2001; **4**: 123-125
- 15 Ricciardi R, Veal TM, Anwaruddin S, Wheeler SM, Foley DP, Donohue SE, Quarfordt SH, Meyers WC. Porcine hepatic phospholipid efflux during reperfusion after cold ischemia. *J Surg Res* 2002; **103**: 79-88
- 16 Poggetti RS, Moore EE, Moore FA, Koike K, Banerjee A. Gut ischemia/reperfusion-induced liver dysfunction occurs despite sustained oxygen consumption. *J Surg Res* 1992; **52**: 436-442
- 17 Vollmar B, Glasz J, Post S, Menger MD. Role of microcirculatory derangements in manifestation of portal triad cross-clamping-induced hepatic reperfusion injury. *J Surg Res* 1996; **60**: 49-54
- 18 Vollmar B, Glasz J, Leiderer R, Post S, Menger MD. Hepatic microcirculatory perfusion failure is a determinant of liver dysfunction in warm ischemia-reperfusion. *Am J Pathol* 1994; **145**: 1421-1431

• CASE REPORT •

The right hepatic artery syndrome

Kazumi Miyashita, Katsuya Shiraki, Takeshi Ito, Hiroki Taoka, Takeshi Nakano

Kazumi Miyashita, Katsuya Shiraki, Takeshi Ito, Takeshi Nakano, First Department of Internal Medicine, Mie University School of Medicine, Tsu, Mie 514-8507, Japan

Hiroki Taoka, First Department of Surgery, Mie University School of Medicine, Tsu, Mie 514-8507, Japan

Correspondence to: Katsuya Shiraki, MD, PhD, First Department of Internal Medicine, Mie University School of Medicine, 2-174 Edobashi, Tsu, Mie 514-8507, Japan. katsuyas@clin.medic.mie-u.ac.jp
Telephone: +81-59-231-5015 Fax: +81-59-231-5201

Received: 2004-06-29 Accepted: 2004-08-12

Abstract

Various benign and malignant conditions could cause biliary obstruction. Compression of extrahepatic bile duct (EBD) by right hepatic artery was reported as a right hepatic artery syndrome but all cases were compressed EBD from stomach side. Our case compressed from dorsum was not yet reported, so it was thought to be a very rare case. We present here the first case of bile duct obstruction due to the compression of EBD from dorsum by right hepatic artery.

© 2005 The WJG Press and Elsevier Inc. All rights reserved.

Key words: Right hepatic artery syndrome; Obstructive jaundice; Extrahepatic bile duct; Right hepatic artery; Endoscopic retrograde cholangiography; Cholangioenterostomy

Miyashita K, Shiraki K, Ito T, Taoka H, Nakano T. The right hepatic artery syndrome. *World J Gastroenterol* 2005; 11 (19): 3008-3009

<http://www.wjgnet.com/1007-9327/11/3008.asp>

INTRODUCTION

In the biliary legion, anatomic variation is relatively common. Arterial anomalies are not infrequent findings during biliary surgery and variations in the positions of hepatic arteries^[1-5] are well known. However, it has been rarely reported that the extrahepatic bile duct (EBD) is compressed by the vessels of hepatobiliary lesion.

CASE REPORT

A 55-year-old Japanese man with an unremarkable medical and family history was admitted for fever and body weight loss. On laboratory examination, alkaline phosphatase was 1 403 IU/L (normal range: 120-340 IU/L) and gamma-glutamyl transpeptidase was 130 IU/L (normal range: 8-60 IU/L). An abdominal computed tomography

(CT) showed compression from the dorsum and stenosis of the EBD (Figure 1: thick arrow head, EBD; Figure 3) by the right hepatic artery (Figure 1: thin arrow head, anterior branch and posterior branch), but did not reveal a mass or lymph node swelling around the EBD. Endoscopic retrograde cholangiography (ERC) showed a stenotic lesion of the common hepatic duct (Figure 2). An intraductal ultrasonography and biopsy were performed transpapillary, but no malignant finding was reported. Drainage of the bile duct using an endoscopic nasobiliary drainage tube improved fever and normalized enzymes. The resultant diagnosis was cholangitis due to compression of the EBD by the right hepatic artery from the posterior side. As a treatment, the stenotic site of the common hepatic duct was removed and end-to-side hepaticojejunostomy was performed. The operation showed that the right hepatic artery had crossed EBD from posterior side of EBD and compressed it. Pathologic examination showed no malignancy or inflammatory cell invasion, but demonstrated sclerosis and severe tortuosity of right hepatic artery. The post-operative course was uneventful and the patient has been well for 1 year after the operation.



Figure 1 An abdominal CT showed compression from the dorsum and stenosis of the EBD (thick arrow head: EBD) by right hepatic artery (thin arrow head: anterior branch and posterior branch), but did not reveal a mass or lymph node swelling around the EBD.



Figure 2 3D CT showed compression from the dorsum of the EBD (arrows).



Figure 3 ERC showed a stenotic lesion of the common hepatic duct (arrow). An intraductal ultrasonography and biopsy were performed transpapillary, but no malignant finding was reported.

DISCUSSION

Compression of the EBD by the right hepatic artery has been reported as a right hepatic artery syndrome, but in all six cases reported, the EBD was compressed from the stomach side. In particular in this patient, the right hepatic artery ran across the back of the bile duct, which is a standard variation. It is possible that the etiology of the obstructive jaundice in this patient was that the common hepatic artery

was short and proximal ramification of the right hepatic artery of the anterior segment branch and posterior segment branch or severe tortuosity of the right hepatic artery by arterial sclerosis.

REFERENCES

- 1 **Chung JP**, Kim KW, Chi HS, Lee SI, Shin ET, Cho JH, Lee HW, Kang JK, Park IS. Obstructive jaundice due to compression of the common hepatic duct by right hepatic artery--a case associated with the absence of the lateral segment of the left hepatic lobe. *Yonsei Med J* 1994; **35**: 231-238
- 2 **Tsuchiya R**, Eto T, Harada N, Yamamoto K, Matsumoto T, Tsunoda T, Yamaguchi T, Noda T, Izawa K. Compression of the common hepatic duct by the right hepatic artery in intra-hepatic gallstones. *World J Surg* 1984; **8**: 321-326
- 3 **Kumada S**, Nakano H, Kitamura K, Watahiki H, Takeda I, Ozawa H, Hachisuga K. A case of the obstructive jaundice due to compression of the common hepatic duct by right hepatic artery (right hepatic artery syndrome) (in Japanese). *Biliary Tract Pancreas* 1981; **2**: 533
- 4 **Luttwak EM**, Schwartz A. Jaundice due to obstruction of the common duct by aberrant artery: demonstration of celiac anomaly by translumbar aortography and simultaneous choledochogram. *Ann Surg* 1961; **153**: 134
- 5 **Hunt AH**. Compression of the common bile duct by an enlarging collateral vein in a case of portal hypertension. *Br J Surg* 1965; **52**: 636-637

Science Editor Guo SY Language Editor Elsevier HK

• ACKNOWLEDGEMENTS •

Acknowledgements to Reviewers of *World Journal of Gastroenterology*

Many reviewers have contributed their expertise and time to the peer review, a critical process to ensure the quality of *World Journal of Gastroenterology*. The editors and authors of the articles submitted to the journal are grateful to the following reviewers for evaluating the articles (including those were published and those were rejected in this issue) during the last editing period of time.

Constantine Arvanitakis, Professor and Chairman

Fourth Department of Medicine, Aristotle University of Thessaloniki, Hippokraton General Hospital, 49, Konstantinoupoleos str., Thessaloniki 54642, Greece

Zong-Jie Cui, Professor

Institute of Cell Biology, Beijing Normal University, Beijing 100875, China

Xue-Gong Fan, Professor

Xiangya Hospital, Changsha 410008, Hunan Province, China

Michael W Fried, Professor

Department of Gastroenterology and Hepatology, Division of Digestive Diseases, University NC, Division of Gastroenterology, University Hospital Zurich, Raemistrasse 100, Zurich CH- 8091, Switzerland

De-Wu Han, Professor

Shanxi Medical University, 86 Xinjian South Road, Taiyuan 030001, Shanxi Province, China

Hong-Xiang Liu, PhD

Department of Pathology, Division of Molecular Histopathology, University of Cambridge, Box 231, Level 3, Lab Block, Addenbrooke's Hospital, Hills Road, Cambridge CB2 2QQ, United Kingdom

Reza Malekzadeh, Professor

Director, Digestive Disease Research Center, Tehran University of Medical Sciences, Shariati Hospital, Kargar Shomali Avenue, 19119 Tehran, Iran

Simon Bar-Meir, M.D.

President of the Israeli Gastroenterological Society Professor of Medicine and Director, Department of Medicine Chaim Sheba Medical Center, Tel Hashomer, Israel

Jae-Gahb Park, Professor

Seoul National University College of Medicine, 28 Yongon-dong, Chongno-gu, Seoul 110-744, Korea

Zhiheng Pei, Assistant Professor

Department of Pathology and Medicine, New York University

School of Medicine, Department of Veterans Affairs, New York Harbor Healthcare System, 6001W, 423 East 23rd street, New York NY 10010, United States

Lun-Xiu Qin, Professor

Liver Cancer Institute and Zhongshan Hospital, Fudan University, 180 Feng Lin Road, Shanghai 200032, China

Christian Rabe, M.D.

Resident, Department of Medicine 1, University of Bonn Sigumund-Freud-Strasse 25 D 53105 Bonn, Germany

Michael Steer, Professor

Department of Surgery, Tufts-Nemc, 860 Washington St, Boston, Ma 02111, United States

Qin Su, Professor

Department of Pathology, Cancer Hospital and Cancer Institute, Chinese Academy of Medical Sciences and Peking Medical College, PO Box 2258, Beijing 100021, China

Hong-Yang Wan, M.D.

International Co-operation Laboratory on Signal Transduction Eastern Hepatobiliary Surgery Institute, SMMU, 225 Changhai Road, Shanghai 200438, China

Yuan Wang, Professor

Institute of Biochemistry and Cell Biology, Shanghai Institutes for Biological Sciences, Chinese Academy of Sciences, Shanghai 200031, China

Harry H-X Xia, M.D.

Department of Medicine, The University of Hong Kong, Pokfulam Road, Hong Kong, China

Jian-Zhong Zhang, Professor

Department of Pathology and Laboratory Medicine, Beijing 306 Hospital, 9 North Anxiang Road, PO Box 9720, Beijing 100101, China

Zhi-Rong Zhang, Professor

West China School of Pharmacy, Sichuan University, 17 South Renmin Road, Chengdu 610041, Sichuan Province, China

Mu-Jun Zhao, M.D.

Institute of Biochemistry and Cell Biology, Chinese Academy of Sciences, 320 Yueyang Road, Shanghai 200031, China

Xiao-Hang Zhao, Professor

State Key Laboratory of Molecular Oncology, Cancer Institute of Chinese Academy of Medical Sciences, 17 Panjiayuan, Chaoyangqu, Beijing 100021, China

Meetings

Major meetings coming up

**Digestive Disease Week
106th Annual Meeting of AGA, The
American Gastroenterology Association**
May 14-19, 2005
www.ddw.org/
Chicago, Illinois

13th World Congress of Gastroenterology
September 10-14, 2005
www.wcog2005.org/
Montreal, Canada

**13th United European Gastroenterology
Week, UEGW**
October 15-20, 2005
www.uegf.org/
Copenhagen, Denmark

**American College of Gastroenterology
Annual Scientific Meeting**
October 28-November 2, 2005
www.acg.gi.org/
Honolulu Convention Center, Honolulu,
Hawaii

Events and Meetings in the upcoming 6 months

**World Congress on Gastrointestinal
Cancer**
June 15-18, 2005
Barcelona

Events and meetings in 2005

**Canadian Digestive Disease Week
Conference**
February 26-March 6, 2005
www.cag-acg.org
Banff, AB

2005 World Congress of Gastroenterology
September 12-14, 2005
Montreal, Canada

**International Colorectal Disease
Symposium 2005**
February 3-5, 2005
Hong Kong

**13th UEGW meeting *United European
Gastroenterology Week***
October 15-20, 2005
www.webasistent.cz/guarant/uegw2005/
Copenhagen-Malmoe

**7th International Workshop on Thera-
peutic Endoscopy**
September 10-12, 2005
www.alfamedical.com
Theodor Bilharz Research Institute

EASL 2005 the 40th annual meeting
April 13-17, 2005
www.easl.ch/easl2005/
Paris, France

**Pediatric Gastroenterology, Hepatology
and Nutrition**
March 13, 2005
Jakarta, Indonesia

**21st annual international congress of
*Pakistan society of Gastroenterology &
GI Endoscopy***
March 25-27, 2005
www.psgc2005.com
Peshawar

**8th Congress of the Asian Society of
HepatoBiliary Pancreatic Surgery**
February 10-13, 2005
Mandaluyong, Philippines

**APDW 2005 - Asia Pacific Digestive
Week 2005**
September 25-28, 2005
www.apdw2005.org
Seoul, Korea

World Congress on Gastrointestinal Cancer
June 15-18, 2005
Barcelona

**British Society of Gastroenterology
Conference (BSG)**
March 14-17, 2005

www.bsg.org.uk
Birmingham

**Digestive Disease Week DDW 106th
Annual Meeting**
May 15-18, 2005
www.ddw.org
Chicago, Illinois

**70th ACG Annual Scientific Meeting
and Postgraduate Course**
October 28-November 2, 2005
Honolulu Convention Center, Honolulu,
Hawaii

Events and Meetings in 2006

**EASL 2006 - THE 41ST ANNUAL
MEETING**
April 26-30, 2006
Vienna, Austria

**Canadian Digestive Disease Week
Conference**
March 4-12, 2006
www.cag-acg.org
Quebec City

**XXX pan-american congress of digestive
diseases XXX congreso panamericano de
enfermedades digestivas**
November 25-December 1, 2006
www.gastro.org.mx
Cancun

**World Congress on Gastrointestinal
Cancer**
June 14-17, 2006
Barcelona, Spain

**7th World Congress of the International
Hepato-Pancreato-Biliary Association**
September 3-7, 2006
www.edinburgh.org/conference
Edinburgh

**71st ACG Annual Scientific Meeting
and Postgraduate Course**
October 20-25, 2006
Venetian Hotel, Las Vegas, Nevada

Instructions to authors

GENERAL INFORMATION

World Journal of Gastroenterology (WJG, ISSN 1007-9327 CN 14-1219/R) is a weekly journal of more than 48 000 circulation, published on the 7th, 14th, 21st and 28th of every month.

Original Research, Clinical Trials, Reviews, Comments, and Case Reports in esophageal cancer, gastric cancer, colon cancer, liver cancer, viral liver diseases, *etc.*, from all over the world are welcome on the condition that they have not been published previously and have not been submitted simultaneously elsewhere.

Published jointly by

The WJG Press and Elsevier Inc.

SUBMISSION OF MANUSCRIPTS

Manuscripts should be typed double-spaced on A4 (297×210 mm) white paper with outer margins of 2.5 cm. Number all pages consecutively, and start each of the following sections on a new page: Title Page, Abstract, Introduction, Materials and Methods, Results, Discussion, Acknowledgements, References, Tables, Figures and Figure Legends. Neither the Editors nor the Publisher is responsible for the opinions expressed by contributors. Manuscripts formally accepted for publication become the permanent property of The WJG Press and Elsevier Inc., and may not be reproduced by any means, in whole or in part without the written permission of both the Authors and the Publisher. We reserve the right to put onto our website and copy-edit accepted manuscripts. Authors should also follow the guidelines for the care and use of laboratory animals of their institution or national animal welfare committee.

Authors should retain one copy of the text, tables, photographs and illustrations, as rejected manuscripts will not be returned to the author(s) and the editors will not be responsible for the loss or damage to photographs and illustrations.

Online submission

Online submission is strongly advised. Manuscripts should be submitted through the Online Submission System at: <http://www.wjgnet.com/index.jsp>. Authors are highly recommended to consult the ONLINE INSTRUCTIONS TO AUTHORS (<http://www.wjgnet.com/wjg/help/instructions.jsp>) before attempting to submit online. Authors encountering problems with the Online Submission System may send an email describing the problem to wjg@wjgnet.com for assistance. If you submit manuscript online, do not make a postal contribution. A repeated online submission for the same manuscript is strictly prohibited.

Postal submission

Send 3 duplicate hard copies of the full-text manuscript typed double-spaced on A4(297×210 mm) white paper together with any original photographs or illustrations and a 3.5 inch computer diskette or CD-ROM containing an electronic copy of the manuscript including all the figures, graphs and tables in native Microsoft Word format or *.rtf format to:

World Journal of Gastroenterology

Apartment 1066 Yishou Garden,
58 North Langxinzhuang Road,
PO Box 2345, Beijing 100023, China
E-mail: wjg@wjgnet.com
<http://www.wjgnet.com>

MANUSCRIPT PREPARATION

All contributions should be written in English. All articles must be submitted using a word-processing software. All submissions must be typed in 1.5 line spacing and in word size 12 with ample margins. The letter font is Tahoma. For authors originating from China, one copy of the Chinese translation of the manuscript is also required (excluding references). Style should conform to our house format. Required information for each of the manuscript sections is as follows:

Title page

Full manuscript title, running title, all author(s) name(s), affiliations, institution(s) and/or department(s) where the work was accomplished, disclosure of any financial support for the research, and the name, full address, telephone and fax numbers and email address of the corresponding author should be involved. Titles should be concise and informative (removing all unnecessary words), emphasize what is NEW, and avoid abbreviations. A short running title of less than 40 letters should be provided. List the author(s)' name(s) as follows: initials and/or first name, middle name or initial(s) and full family name.

Abstract

An informative, structured abstract of no more than 250 words should accompany each manuscript. Abstracts for original contributions should be structured into the following sections: AIM: Only the purpose should be included. METHODS: The materials, techniques, instruments and equipments, and the experimental procedures should be included. RESULTS: The observatory and experimental results, including data, effects, outcome, *etc.* should be included. Authors should present *P* value where necessary, and the significant data should accompany. CONCLUSION: Accurate view and the value of the results should be included.

The format of structured abstracts is at: <http://www.wjgnet.com/wjg/help/11.doc>

Key words

Please list 3-10 key words that could reflect content of the study.

Text

For most article types, the main text should be structured into the following sections: INTRODUCTION, MATERIALS AND METHODS, RESULTS AND DISCUSSION, and should include appropriate Figures and Tables. Data should be presented in the body text or Figures and Tables, not both.

Illustrations

Figures should be numbered as 1, 2, 3 and so on, and mentioned clearly in the main text. Provide a brief title for each figure on a separate page. No detailed legend should be involved under the figures. This part should add into the text where the figures are applicable. Digital images: black and white photographs should be scanned and saved in TIFF format at a resolution of 300 dpi; color images should be saved as CMYK (print files) and not RGB (screen-viewing files). Place each photograph in a separate file. Print images: supply images of size no smaller than 126×76 mm printed on smooth surface paper; label the image by writing the Figure number and orientation using an arrow. Photomicrographs: indicate the original magnification and stain in the legend. Digital Drawings: supply files in EPS if created by Freehand and Illustrator, or TIFF from Photoshop. EPS files must be accompanied by a version in native file format for editing purposes. Scans of existing line drawings should be scanned at a resolution of 1200 dpi and as close as possible to the size at which they will appear when printed, not smaller. Please use uniform legends for the same subjects. For example: Figure 1 Pathological changes of atrophic gastritis after treatment. A: ...; B: ...; C: ...; D: ...; E: ...; F: ...; G: ...

Tables

Three-line tables should be numbered as 1, 2, 3 and so on, and mentioned clearly in the main text. Provide a brief title for each table. No detailed legend should be involved under the tables. This part should add into the text where the tables are applicable. The information should complement but not duplicate that contained in the text. Use one horizontal line under the title, a second under the column heads, and a third below the Table, above any footnotes. Vertical and italic lines should be omitted.

Notes in tables and illustrations

Data which is not statistically significant should not be noted. ^a*P*<0.05, ^b*P*<0.01 (*P*>0.05 should not be noted). If there are other series of *P* values, ^c*P*<0.05 and ^d*P*<0.01 are used; Third series of *P* values can be expressed as ^e*P*<0.05 and ^f*P*<0.01. Other notes in tables or under

illustrations should be expressed as 1F , 2F , 3F ; or some other symbols with a superscript (Arabic numerals) in the upper left corner. In a multi-curve illustration, each curve should be labeled with ●, ○, ■, □, ▲, △, etc. in a certain sequence.

Acknowledgments

Brief acknowledgments of persons who have made genuine contributions to the manuscripts and who endorse the data and conclusions are included. Authors are responsible for obtaining written permission to use any copyrighted text and/or illustrations.

References

Cited references should mainly be drawn from journals covered in the Science Citation Index (<http://www.isinet.com>) and/or Index Medicus (<http://www.ncbi.nlm.nih.gov/PubMed>) databases. Mention all references in the text, tables and figure legends, and set off by consecutive, superscripted Arabic numerals. References should be numbered consecutively in the order in which they appear in the text. Abbreviate journal title names according to the Index Medicus style (<http://www.ncbi.nlm.nih.gov/entrez/query.fcgi?db=journals>). Unpublished observations and personal communications are not listed as references. The style and punctuation of the references conform to ISO standard and the Vancouver style (5th edition); see examples below. Reference lists not conforming to this style could lead to delayed or even rejected publication status. Examples:

Standard journal article (list all authors and include the PubMed ID [PMID] where applicable)

- 1 **Das KM**, Farag SA. Current medical therapy of inflammatory bowel disease. *World J Gastroenterol* 2000; 6: 483-489 [PMID: 11819634]
- 2 **Pan BR**, Hodgson HJF, Kalsi J. Hyperglobulinemia in chronic liver disease: Relationships between *in vitro* immunoglobulin synthesis, short lived suppressor cell activity and serum immunoglobulin levels. *Clin Exp Immunol* 1984; 55: 546-551 [PMID: 6231144]
- 3 **Lin GZ**, Wang XZ, Wang P, Lin J, Yang FD. Immunologic effect of Jianpi Yishen decoction in treatment of Pixu-diarrhoea. *Shijie Huaren Xiaohua Zazhi* 1999; 7: 285-287 [CMFAID:1082371101835979]

Books and other monographs (list all authors)

- 4 **Sherlock S**, Dooley J. Diseases of the liver and biliary system. 9th ed. Oxford: Blackwell Sci Pub, 1993: 258-296

Chapter in a book (list all authors)

- 5 **Lam SK**. Academic investigator's perspectives of medical treatment for peptic ulcer. In: Swabb EA, Azabo S. Ulcer disease: investigation and basis for therapy. New York: Marcel Dekker, 1991: 431-450

Electronic journal (list all authors)

- 6 **Morse SS**. Factors in the emergence of infectious diseases. *Emerg Infect Dis serial online*, 1995-01-03, cited 1996-06-05; 1(1):24 screens. Available from: URL: <http://www.cdc.gov/ncidod/EID/eid.htm>

PMID requirement

From the full reference list, please submit a separate list of those references embodied in PubMed, keeping the same order as in the full reference list, with the following information only: (1) abbreviated journal name and citation (e.g. *World J Gastroenterol* 2003;9(11): 2400-2403; (2) article title (e.g. Epidemiology of gastroenterologic cancer in Henan Province, China); (3) full author list (e.g. Lu JB, Sun XB, Dai DX, Zhu SK, Chang QL, Liu SZ, Duan WJ); (4) PMID (e.g. 14606064). Provide the full abstracts of these references, as quoted from PubMed on a 3.5 inch disk or CD-ROM in Microsoft Word format and send by post to The WJG Press. For those references taken from journals not indexed by *Index Medicus*, a printed copy of the first page of the full reference should be submitted. Attach these references to the end of the manuscript in their order of appearance in the text.

Inappropriate references

Authors should always cite references that are relevant to their article, and avoid any inappropriate references. Inappropriate references include those that are linked with a hyphen and the difference between the two numbers at two sides of the hyphen is more than 5. For example, [1-6], [2-14] and [1,3,4-10,22] are all considered as inappropriate references. Authors should not cite their own unrelated published articles.

Statistical data

Present as mean±SD and mean±SE.

Statistical expression

Express *t* test as *t*(in italics), *F* test as *F*(in italics), chi square test as χ^2 (in Greek), related coefficient as *r*(in italics), degree of freedom as γ (in Greek), sample number as *n*(in italics), and probability as *P*(in italics).

Units

Use SI units. For example: body mass, *m*(B) = 78 kg; blood pressure, *p* (B)=16.2/12.3 kPa; incubation time, *t*(incubation)=96 h, blood glucose concentration, *c*(glucose) 6.4±2.1 mmol/L; blood CEA mass concentration, *p*(CEA) = 8.6 24.5 μg/L; CO₂ volume fraction, 50 mL/L CO₂ not 5% CO₂; likewise for 40 g/L formaldehyde, not 10% formalin; and mass fraction, 8 ng/g, etc. Arabic numerals such as 23,243,641 should be read 23 243 641.

The format about how to accurately write common units and quantum is at: <http://www.wjgnet.com/wjg/help/15.doc>

Abbreviations

Standard abbreviations should be defined in the abstract and on first mention in the text. In general, terms should not be abbreviated unless they are used repeatedly and the abbreviation is helpful to the reader. Permissible abbreviations are listed in Units, Symbols and Abbreviations: A Guide for Biological and Medical Editors and Authors (Ed. Baron DN, 1988) published by The Royal Society of Medicine, London. Certain commonly used abbreviations, such as DNA, RNA, HIV, LD50, PCR, HBV, ECG, WBC, RBC, CT, ESR, CSF, IgG, ELISA, PBS, ATP, EDTA, mAb, can be used directly without further mention.

Italicization

Quantities: *t* time or temperature, *c* concentration, *A* area, *l* length, *m* mass, *V* volume.

Genotypes: *gyrA*, *arg 1*, *c myc*, *c fos*, etc.

Restriction enzymes: *EcoRI*, *HindI*, *BamHI*, *Kbo I*, *Kpn I*, etc.

Biology: *Helicobacter pylori*, *H pylori*, *E coli*, etc.

SUBMISSION OF THE REVISED MANUSCRIPTS AFTER ACCEPTED

Please revise your article according to the revision policies of WJG. The revised version including manuscript and high-resolution image figures (if any) should be copied on a floppy or compact disk. Author should send the revised manuscript, along with printed high-resolution color or black and white photos, copyright transfer letter, the final check list for authors, and responses to reviewers by a courier (such as EMS) (submission of revised manuscript by e-mail or on the WJG Editorial Office Online System is NOT available at present).

Language evaluation

The language of a manuscript will be graded before sending for revision. (1) Grade A: priority publishing; (2) Grade B: minor language polishing; (3) Grade C: a great deal of language polishing; (4) Grade D: rejected. The revised articles should be in grade B or grade A.

Copyright assignment form

It is the policy of WJG to acquire copyright in all contributions. Papers accepted for publication become the copyright of WJG and authors will be asked to sign a transfer of copyright form. All authors must read and agree to the conditions outlined in the Copyright Assignment Form (which can be downloaded from <http://www.wjgnet.com/wjg/help/9.doc>).

Final check list for authors

The format is at: <http://www.wjgnet.com/wjg/help/13.doc>

Responses to reviewers

Please revise your article according to the comments/suggestions of reviewers. The format for responses to the reviewers' comments is at: <http://www.wjgnet.com/wjg/help/10.doc>

Proof of financial support

For paper supported by a foundation, authors should provide a copy of the document and serial number of the foundation.

Publication fee

Authors of accepted articles must pay publication fee.

World Journal of Gastroenterology standard of quantities and units

Number	Nonstandard	Standard	Notice
1	4 days	4 d	In figures, tables and numerical narration
2	4 days	four days	In text narration
3	day	d	After Arabic numerals
4	Four d	Four days	At the beginning of a sentence
5	2 hours	2 h	After Arabic numerals
6	2 hs	2 h	After Arabic numerals
7	hr, hrs,	h	After Arabic numerals
8	10 seconds	10 s	After Arabic numerals
9	10 year	10 years	In text narration
10	Ten yr	Ten years	At the beginning of a sentence
11	0,1,2 years	0,1,2 yr	In figures and tables
12	0,1,2 year	0,1,2 yr	In figures and tables
13	4 weeks	4 wk	
14	Four wk	Four weeks	At the beginning of a sentence
15	2 months	2 mo	In figures and tables
16	Two mo	Two months	At the beginning of a sentence
17	10 minutes	10 min	
18	Ten min	Ten minutes	At the beginning of a sentence
19	50% (V/V)	500 mL/L	
20	50% (m/V)	500 g/L	
21	1 M	1 mol/L	
22	10 μM	10 μmol/L	
23	1NHCl	1 mol/L HCl	
24	1NH ₂ SO ₄	0.5 mol/L H ₂ SO ₄	
25	4rd edition	4 th edition	
26	15 year experience	15- year experience	
27	18.5 kDa	18.5 ku, 18 500u or M _r 18 500	
28	25 g·kg ⁻¹ /d ⁻¹	25 g/(kg·d) or 25 g/kg per day	
29	6900	6 900	
30	1000 rpm	1 000 r/min	
31	sec	s	After Arabic numerals
32	1 pg·L ⁻¹	1 pg/L	
33	10 kilograms	10 kg	
34	13 000 rpm	13 000 g	High speed; g should be in italic and suitable conversion.
35	1000 g	1 000 r/min	Low speed. g cannot be used.
36	Gene bank	GeneBank	International classified genetic materials collection bank
37	Ten L	Ten liters	At the beginning of a sentence
38	Ten mL	Ten milliliters	At the beginning of a sentence
39	umol	μmol	
40	30 sec	30 s	
41	1 g/dl	10 g/L	10-fold conversion
42	OD ₂₆₀	A ₂₆₀	"OD" has been abandoned.
43	Oneg/L	One microgram per liter	At the beginning of a sentence
44	A ₂₆₀ nm ^b P<0.05	A ₂₆₀ nm ^a P<0.05	A should be in italic. In Table, no note is needed if there is no significance in statistics: ^a P<0.05, ^b P<0.01 (no note if P>0.05). If there is a second set of P value in the same table, ^c P<0.05 and ^d P<0.01 are used for a third set: ^e P<0.05, ^f P<0.01.
45	*F=9.87, [§] F=25.9, [#] F=67.4	¹ F=9.87, ² F=25.9, ³ F=67.4	Notices in or under a table
46	KM	km	kilometer
47	CM	cm	centimeter
48	MM	mm	millimeter
49	Kg, KG	kg	kilogram
50	Gm, gr	g	gram
51	nt	N	newton
52	l	L	liter
53	db	dB	decibel
54	rpm	r/min	rotation per minute
55	bq	Bq	becquerel, a unit symbol
56	amp	A	ampere
57	coul	C	coulomb
58	HZ	Hz	
59	w	W	watt
60	KPa	kPa	kilo-pascal
61	p	Pa	pascal
62	ev	EV	volt (electronic unit)
63	Jonle	J	joule
64	J/mmol	kJ/mol	kilojoule per mole
65	10×10×10cm ³	10 cm×10 cm×10 cm	
66	N·km	KN·m	moment
67	$\bar{x} \pm s$	mean±SD	In figures, tables or text narration
68	Mean±SEM	mean±SE	In figures, tables or text narration
69	im	im	intramuscular injection
70	iv	iv	intravenous injection
71	Wang et al	Wang et al.	
72	EcoRI	EcoRI	Eco in italic and RI in positive. Restriction endonuclease has its prescript form of writing.
73	Ecoli	E.coli	Bacteria and other biologic terms have their specific expression.
74	Hp	H pylori	
75	Iga	Iga	writing form of genes
76	igA	IgA	writing form of proteins
77	~70 kDa	~70 ku	